

Rafat Siddique

Waste Materials and By-Products in Concrete

With 151 Figures and 174 Tables

 Springer

Rafat Siddique
Professor
Department of Civil Engineering,
Thapar University
(Formerly, Thapar Institute of
Engineering & Technology)
Patiala (Punjab) 147 004
India

ISBN: 978-3-540-74293-7

e-ISBN: 978-3-540-74294-4

ISSN: 1612-1317

Library of Congress Control Number: 2007933830

© 2008 Springer-Verlag Berlin Heidelberg

This work is subject to copyright. All rights are reserved, whether the whole or part of the material is concerned, specifically the rights of translation, reprinting, reuse of illustrations, recitation, broadcasting, reproduction on microfilm or in any other way, and storage in data banks. Duplication of this publication or parts thereof is permitted only under the provisions of the German Copyright Law of September 9, 1965, in its current version, and permission for use must always be obtained from Springer. Violations are liable to prosecution under the German Copyright Law.

The use of general descriptive names, registered names, trademarks, etc. in this publication does not imply, even in the absence of a specific statement, that such names are exempt from the relevant protective laws and regulations and therefore free for general use.

Cover Design: deblik, Berlin

Printed on acid-free paper

9 8 7 6 5 4 3 2 1

springer.com

*To my father – the man who illuminated my
path and inspired me throughout my life,
I gratefully dedicate this book*

Preface

Large quantities of waste materials and by-products are generated from manufacturing processes, service industries and municipal solid wastes, etc. As a result, solid waste management has become one of the major environmental concerns in the world. With the increasing awareness about the environment, scarcity of land-fill space and due to its ever increasing cost, waste materials and by-products utilization has become an attractive alternative to disposal. High consumption of natural sources, high amount production of industrial wastes and environmental pollution require obtaining new solutions for a sustainable development.

During recent years there has been a growing emphasis on the utilization of waste materials and by-products in construction materials. Utilization of waste materials and by-products is a partial solution to environmental and ecological problems. Use of these materials not only helps in getting them utilized in cement, concrete, and other construction materials, it helps in reducing the cost of cement and concrete manufacturing, but also has numerous indirect benefits such as reduction in land-fill cost, saving in energy, and protecting the environment from possible pollution effects. Further, their utilization may improve the microstructure, mechanical and durability properties of mortar and concrete, which are difficult to achieve by the use of only ordinary Portland cement.

Significant research has been going-on in various parts of the world on the subject. Some waste materials and by-products have established their credentials in their usage in cement-based materials and for others research is in progress for exploring the potential applications.

This book is a small step forward in bringing the research related to the use of waste materials and by-products in cement-based materials. Chapters have not been made too lengthy, though the author is fully aware that there could be a book separately on each of these topics. This book is intended to cater to the needs of graduate students, researchers, and concrete technologist and practicing engineers in the field.

The book has twelve chapters. Each chapter is devoted to a particular waste material/by-product. It is based on the literature/research findings published in journals/conference proceeding, etc. Waste materials/by-products covered in the book are; granulated blast furnace slag, metakaolin, waste/recycled plastics, scrap-tire, waste glass, coal fly ash, rice husk ash, municipal solid waste ash, wood ash,

volcanic ash, cement kiln dust and foundry sand. Each chapter contains introduction, properties of the waste material/by-product, its usage potential, and its effect on the properties of fresh and hardened concrete and other cement based materials. References have been put at the end of each of the chapters for the convenience of the readers.

I would like to place on record my immense sense of gratitude to professors, scientists, concrete technologists, and my colleagues and friends world-wide who have contributed significantly in the broader area of concrete technology, and my sincere appreciation and acknowledgement to the published work of the researchers on the subject, which has been referred in this book.

I am extremely grateful to **Springer** for bringing out the book in excellent form and in the shortest possible time.

Lastly, I really find myself wanting in appropriate words to express my irrepayable gratitude to my father, brothers, sisters and friends whose consistent encouragement and love have been a tremendous impetus to the completion of this book.

Patiala, India

Rafat Siddique

Contents

1	Ground Granulated Blast Furnace Slag	1
	Introduction	1
	Advantages of Using GGBS	1
1.1	Properties of GGBS	2
1.1.1	Physical Properties	2
1.1.2	Chemical Composition	3
1.1.3	Particle Size Distribution	3
1.2	Fresh Properties of Mortar/Paste/Concrete Containing GGBS	4
1.2.1	Bleeding Characteristics	4
1.2.2	Workability	5
1.2.3	Setting Times	6
1.3	Properties of Hardened Concrete Containing GGBS	7
1.3.1	Microstructure	7
1.3.2	Compressive Strength	11
1.3.3	Tensile and Flexural Strength	17
1.4	Durability Properties of Concrete Containing GGBS	21
1.4.1	Creep and Shrinkage	21
1.4.2	Chloride Binding Capacity/Resistance	22
1.4.3	Sulfate Resistance	25
1.4.4	Alkali Silica Reaction	30
1.4.5	Freezing and Thawing Resistance	30
1.4.6	Corrosion Resistance	31
1.4.7	Carbonation	35
	References	36
2	Metakaolin	41
	Introduction	41
	Uses of Metakaolin	42
	Advantages of Using Metakaolin	42
2.1	Properties of Metakaolin	42
2.1.1	Physical Properties	42
2.1.2	Chemical Composition	42
2.2	Hydration Reaction Mechanism	43

2.2.1	Temperature Effect	50
2.2.2	Alkaline Activation	53
2.2.3	Effect of Dehydroxylation	55
2.2.4	Dilatency	56
2.3	Fresh Properties of Mortar/Concrete Containing Metakaolin	56
2.4	Properties of Hardened Mortar/Concrete Containing Metakaolin	58
2.4.1	Pore Size Distribution	58
2.4.2	Water Absorption and Sorptivity	61
2.4.3	Compressive Strength	64
2.4.4	Tensile Strength	70
2.4.5	Bending Strength	71
2.4.6	Micro-Hardness	71
2.4.7	Relative Strength	75
2.5	Durability Properties of Concrete Containing Metakaolin	76
2.5.1	Alkali-Silica Reaction	76
2.5.2	Chloride-Ion Diffusion	77
2.5.3	Hydroxide Ion Diffusion	81
2.5.4	Sulfate Resistance	82
2.5.5	Corrosion Resistance	87
2.5.6	Creep and Shrinkage	87
	References	89
3	Recycled/Waste Plastic	93
	Introduction	93
3.1	Types of Plastic and Plastic Waste	94
3.1.1	Benefits/Advantages of Plastics	94
3.1.2	Disadvantages of Plastics	96
3.2	Utilization of Waste/Recycled Plastics	96
3.2.1	Advantages of Waste/Recycled Plastic	96
3.2.2	Classification of Recycled Plastic in Concrete	97
3.3	Management Options	97
3.3.1	Collection	98
3.3.2	Landfilling Plastics	99
3.3.3	Incineration of Plastics	100
3.3.4	Plastics Recycling	100
3.4	Recycling Methods	101
3.4.1	Mechanical Recycling	101
3.4.2	Chemical or Feedstock Recycling	102
3.5	Fresh Properties of Concrete Containing Recycled/Waste Plastic	104
3.5.1	Bulk Density	104
3.5.2	Air Content	105
3.5.3	Slump	106
3.6	Properties of Hardened Concrete Containing Recycled/Waste Plastic	108
3.6.1	Compressive Strength	108
3.6.2	Splitting Tensile Strength	112

3.6.3	Modulus of Elasticity	113
3.6.4	Time and Temperature Dependent Properties	113
3.6.5	Impact Resistance	116
3.6.6	Permeability	116
3.6.7	Abrasion Resistance	118
3.7	Uses of Recycled Plastic in Concrete	118
	References	119
4	Scrap Tires	121
	Introduction	121
4.1	Classification of Scrap Tires	122
4.1.1	Scrap Tires	122
4.1.2	Slit Tires	123
4.1.3	Shredded/Chipped Tires	123
4.1.4	Ground Rubber	123
4.1.5	Crumb Rubber	123
4.2	Management Options	124
4.2.1	Disposal	124
4.2.2	Recycling	124
4.3	Fresh Properties of Concrete Containing Scrap Tires	124
4.3.1	Slump	124
4.3.2	Air Content	126
4.3.3	Unit Weight and Density	127
4.4	Properties of Hardened Concrete Containing Scrap Tires	127
4.4.1	Compressive Strength	127
4.4.2	Tensile Strength	132
4.4.3	Abrasion Resistance	134
4.4.4	Shrinkage	135
4.4.5	Fatigue, Toughness, and Impact Resistance	135
4.4.6	Freezing and Thawing Resistance	137
4.5	Use of Scrap Tire Ash in Mortar	138
4.6	Use of Scrap Tire Steel Beads in Concrete	138
4.7	Fire-Performance of Concrete with Rubber	139
4.8	Use of Scrap Tire Rubber in Flowable Fill	140
4.9	Environmental Studies of Recycled Rubber	142
4.10	Uses of Rubber Concrete (Rubcrete)	142
	References	143
5	Waste Glass	147
	Introduction	147
5.1	Properties of Waste Glass	148
5.1.1	Physical Properties	148
5.1.2	Chemical Composition	148
5.1.3	Mechanical Properties	149
5.1.4	Other Properties (Thermal, Reflection, and Glare)	150

5.2	Management Options	151
5.2.1	Disposal	151
5.2.2	Recycling	151
5.2.3	Uses of Waste Glass	152
5.3	Fresh Properties of Concrete Containing Waste Glass	153
5.3.1	Unit Weight, Air Content	153
5.3.2	Slump	154
5.3.3	VeBe Time	154
5.3.4	Flow Table	155
5.3.5	Compaction Factor	155
5.4	Properties of Hardened Concrete Containing Waste Glass	155
5.4.1	Compressive Strength	155
5.4.2	Tensile Strength	162
5.4.3	Flexural Strength	163
5.4.4	Dynamic Modulus of Elasticity	164
5.4.5	Alkali-Silica Reaction	165
5.5	Use of Waste Glass in Asphalt Concrete	171
5.5.1	Mix Design	171
5.6	Use of Waste Glass in Granular Base	172
5.6.1	Mix Design	172
	References	173
6	Coal Fly Ash	177
	Introduction	177
6.1	Classification of Fly Ash	178
6.2	Properties of Fly Ash	179
6.2.1	Physical Properties	179
6.2.2	Chemical Composition	180
6.2.3	Mineralogical Characteristics	181
6.3	Utilization of Fly Ash in Cement and Concrete	183
6.3.1	High Volume Uses	183
6.3.2	Medium Volume Uses	183
6.3.3	Low Volume Uses	183
6.3.4	Miscellaneous Uses	183
6.4	Fresh Properties of Concrete Containing Fly Ash	184
6.4.1	Water Requirement and Workability	184
6.4.2	Segregation and Bleeding	185
6.4.3	Time of Setting	185
6.4.4	Air Entrainment	187
6.4.5	Temperature Rise	188
6.5	Properties of Hardened Concrete Containing Fly Ash	190
6.5.1	Strength Development	190
6.5.2	Elastic Properties	201
6.5.3	Porosity	202
6.5.4	Sorptivity	204

6.5.5	Creep	205
6.5.6	Drying Shrinkage	206
6.5.7	Thermal Conductivity	207
6.6	Durability Properties of Concrete Containing Fly Ash	208
6.6.1	Permeability	208
6.6.2	Freezing and Thawing Resistance	213
6.6.3	Resistance to Aggressive Chemicals	214
6.6.4	Alkali-Silica Reaction	221
6.6.5	Carbonation	223
6.6.6	Corrosion Resistance	224
6.6.7	Abrasion Resistance	227
	References	229
7	Rice Husk Ash	235
	Introduction	235
7.1	Properties of RHA	236
7.1.1	Physical Properties	236
7.1.2	Chemical Composition	236
7.1.3	Pozzolanic Activity	237
7.2	Fresh Properties of Paste/Concrete Containing RHA	239
7.2.1	Workability	239
7.2.2	Air-Entrainment	240
7.2.3	Consistency and Setting Times	241
7.3	Properties of Hardened Concrete Containing RHA	243
7.3.1	Porosity and Water Absorption Capacity	243
7.3.2	Compressive and Tensile Properties	243
7.3.3	Drying Shrinkage	252
7.4	Durability Properties of Concrete Containing RHA	253
7.4.1	Permeability	253
7.4.2	Corrosion Resistance	257
7.4.3	Carbonation	258
7.4.4	Freezing and Thawing Resistance	259
7.4.5	Sulfate Resistance	259
7.4.6	Deicing Salt Scaling Resistance	261
7.4.7	Alkali-Silica Reaction	262
	References	262
8	Municipal Solid Waste Ash	265
	Introduction	265
8.1	Properties of MSW Ash	266
8.1.1	Physical Properties	266
8.1.2	Chemical Composition	268
8.1.3	Elemental Analysis	271
8.1.4	Hydration Characteristics of MSW Ash with C_3S and C_2S ..	274
8.2	Utilization of MSW Ash	276

8.2.1	Cement Production	276
8.2.2	Concrete	276
8.2.3	Ceramics	277
8.2.4	Glass and Glass-Ceramics	277
8.2.5	Road Pavement	277
8.2.6	Embankment	278
8.3	Properties of Cement Containing MSW Ash	278
8.3.1	Compositional Effects	278
8.3.2	Degree of Hydration	281
8.3.3	Consistency and Setting Times	283
8.3.4	Compressive Strength	285
8.3.5	Pore Size Distribution	288
8.3.6	Shrinkage/Expansion Characteristics	290
8.4	Properties of Concrete Containing MSW Ash	292
8.4.1	Compressive Strength	293
8.4.2	Chloride Penetration/Resistance	294
8.4.3	Shrinkage	296
8.5	Leachate Analysis	297
8.6	Use of MSW Bottom Ash in Road Base	299
	References	300
9	Wood Ash	303
	Introduction	303
9.1	Properties of Wood Ash	305
9.1.1	Physical Properties	305
9.1.2	Chemical Composition	307
9.1.3	Elemental Analysis	308
9.1.4	Mineralogical Analysis	309
9.2	Uses of Wood Ash	310
9.2.1	Land Application	311
9.2.2	Pollution Control	312
9.2.3	Construction Materials	313
9.3	Properties of Concrete Containing Wood Ash	313
9.3.1	Batch Leaching of WWA	313
9.3.2	Slump	314
9.3.3	Water Absorption Capacity	314
9.3.4	Compressive Strength	315
9.3.5	Splitting Tensile Strength	316
9.3.6	Flexural Strength	317
9.3.7	Drying Shrinkage	318
9.3.8	Freezing and Thawing Resistance	319
	References	320
10	Volcanic Ash	323
	Introduction	323

10.1 Volcanic Ash Particles Component	324
10.1.1 Volcanic Glass	324
10.1.2 Minerals or Crystals (Phenocrysts)	324
10.1.3 Other Rocks (Often Called Lithics)	325
10.2 Properties of Volcanic Ash	326
10.2.1 Density	326
10.2.2 Hardness	326
10.2.3 Chemical Composition	327
10.3 Uses of Volcanic Ash	329
10.3.1 As Abrasive	329
10.3.2 In Ceramics	330
10.3.3 In Ceramics Glazes and Bodies	330
10.3.4 In Glass and Vitreous Enamels	330
10.3.5 In Light Weight Aggregates, Cellular Blocks, and Concrete	330
10.3.6 Miscellaneous Uses	331
10.4 Effect of Volcanic Ash on Soil Properties	331
10.4.1 Maximum Dry Density	331
10.4.2 Deformation Properties	332
10.4.3 Compressive Strength Characteristics	332
10.5 Properties of Blended Cement Containing Volcanic Ash	336
10.5.1 Consistency and Setting Times	336
10.5.2 Compressive Strength	337
10.5.3 Microstructure of Hydration Products	338
10.5.4 Alkali-Silica Reaction and Autoclave Expansion	339
10.5.5 Electrical Resistivity	340
10.5.6 Total Pore Volume (TPA)	341
10.6 Properties of Concrete Containing Volcanic Ash	342
10.6.1 Compressive Strength	342
10.6.2 Chloride-Ion Resistance and Porosity	344
10.6.3 Sulfate Resistance	346
References	348
11 Cement Kiln Dust	351
Introduction	351
11.1 Properties of Cement Kiln Dust (CKD)	351
11.1.1 Physical Properties	351
11.1.2 Chemical Composition	352
11.2 Uses of CKD	352
11.2.1 Soil Stabilization	353
11.2.2 Waste Treatment	353
11.2.3 Cement Replacement	353
11.2.4 Highway Uses	353
11.3 Properties of Cement Mortar/Concrete Containing CKD	354
11.3.1 Compressive Strength	354

11.3.2 Tensile Strength Properties	361
11.3.3 Hydration Properties	363
11.3.4 Setting Times	365
11.3.5 Sorptivity	366
11.3.6 Electrical Conductivity	366
11.3.7 Durability Properties	368
11.3.8 Alkali-Silica Reaction (ASR)	368
11.4 Properties of Controlled Low-Strength Materials Containing CKD ..	370
11.5 Use of CKD as Soil Stabilizer	372
11.6 Use of CKD in Asphalt Pavement/Concrete	373
11.7 Leachate Analysis	375
References	378
12 Foundry Sand	381
Introduction	381
12.1 Types of Foundry Sands	382
12.1.1 Green Sand	382
12.1.2 Chemically-Bonded Sand	383
12.2 Properties of Foundry Sand	383
12.2.1 Physical Characteristics	383
12.2.2 Chemical Composition	385
12.2.3 Mechanical Properties	386
12.2.4 Potential Contaminants	387
12.3 Management Options	388
12.3.1 Recycling	388
12.3.2 Disposal	388
12.3.3 Uses of Foundry Sand	388
12.4 Properties of Controlled Low Strength-Materials (CLSM)	
Containing Foundry Sand	393
12.4.1 Plastic Properties	393
12.4.2 Compressive Strength	394
12.4.3 Permeability	395
12.4.4 Leachate Analysis	396
12.5 Properties of Concrete Containing Foundry Sand	398
12.5.1 Compressive Strength	398
12.5.2 Splitting Tensile Strength and Modulus of Elasticity	402
12.5.3 Freezing and Thawing Resistance	402
12.5.4 Drying Shrinkage	404
References	405
Index	407

Chapter 1

Ground Granulated Blast Furnace Slag

Introduction

Ground Granulated Blast Furnace Slag (GGBS) is a by-product of the manufacturing of iron in a blast furnace where iron ore, limestone and coke are heated up to 1500°C. When these materials melt in the blast furnace, two products are produced – molten iron, and molten slag. The molten slag is lighter and floats on the top of the molten iron. The molten slag comprises mostly silicates and alumina from the original iron ore, combined with some oxides from the limestone. The process of granulating the slag involves cooling the molten slag through high-pressure water jets. This rapidly quenches the slag and forms granular particles generally no larger than 5 mm in diameter. The rapid cooling prevents the formation of larger crystals, and the resulting granular material comprises some 95% non-crystalline calcium-aluminosilicates. The granulated slag is further processed by drying and then ground to a very fine powder, which is GGBS (ground granulated blast furnace slag) cement. Grinding of the granulated slag is carried out in a rotating ball mill.

Different forms of slag product are produced depending on the method used to cool the molten slag. These products include air-cooled blast furnace slag (ACBFS), expanded or foamed slag, palletized slag, and granulated blast furnace slag.

Advantages of Using GGBS

Utilization of GGBS in cement and concrete results in

- Improved workability, pumpability and compaction characteristics for concrete placement
- Increased strength and durability
- Reduced permeability
- High resistance to chloride penetration
- High resistance to sulfate attack
- High resistance to ASR
- Very low heat of hydration
- More chemically stable

- Improved surface finish
- Enhanced architectural appearance
- Lighter and more even color
- Enhanced reflectivity for greater visibility and safety
- Suppresses efflorescence
- Enhancement of the life cycle of concrete structures
- Reduction in maintenance and repair costs
- Slashes lifetime construction costs
- Production of GGBS involves virtually zero CO₂ emissions, and no emissions of SO₂ and NO_x

1.1 Properties of GGBS

1.1.1 Physical Properties

GGBS cement is a near-white powder. It imparts a lighter, brighter color to concrete, in contrast to the stony grey of concrete made with Portland cement. Figure 1.1 shows the GGBS and OPC color difference. The color of the finished concrete is lighter; the concrete has a smoother surface finish. Typical physical properties of GGBS as reported by Tasong et al. (1999) are given in Table 1.1.

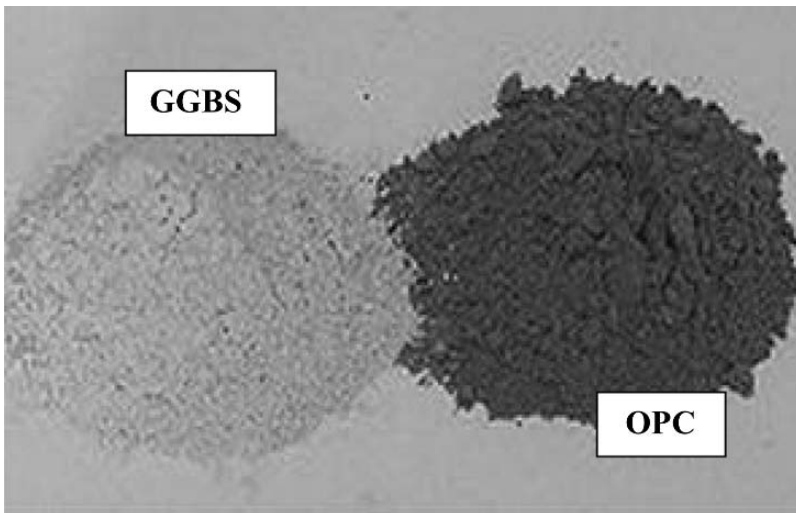


Fig. 1.1 GGBS and OPC, significant color difference between two

Table 1.1 Physical properties of GGBS (Tasong et al., 1999)

Property	Value
Physical form	Off white powder
Bulk density (kg/m ³)	1200
Specific gravity	2.9
Specific surface (m ² /kg)	425–470

1.1.2 Chemical Composition

GGBS comprises mainly of CaO, SiO₂, Al₂O₃, MgO. It has the same main chemical constituents as ordinary Portland cement, but in different proportions. Typical Chemical Composition of GGBS as reported by Tasong et al. (1999) is given in Table 1.2.

1.1.3 Particle Size Distribution

Wan et al. (2004) studied the shape and particle size distribution (PSD) of different ground granulated blast furnace slag (GGBS). Samples (A, B, C, and D) of GGBS were prepared by using four processing approaches, a ball mill, steel balls as grinding medium, an airflow mill and a vibro-mill, respectively. The surface area of GGBS were determined by the Blaine air permeability method, the PSD of GGBS was analyzed with LPA (Malvern Mastersizer, 2000) and the morphology with SEM. Results of surface area and diameter of GGBS are given in Table 1.3 and particle size distribution in Table 1.4. They concluded that: (i) even though the surface areas of GGBS were almost similar, both the geometric characteristics and the PDS could be different due to different grinding techniques. The PDS of GGBS processed by a ball mill was the widest, while that by an airflow mill was the narrowest. The shape of GGBS processed by a vibro-mill was predominantly spherical with a smooth surface, while that by a ball mill and an airflow mill appeared to have similar edges.

Table 1.2 Chemical composition of GGBS (Tasong et al., 1999)

Composition	%
SiO ₂	35.34
Al ₂ O ₃	11.59
Fe ₂ O ₃	0.35
CaO	41.99
MgO	8.04
MnO	0.45
S ₂	1.18
SO ₃	0.23

Table 1.3 Surface area and average diameter of GGBS (Wan et al., 2004)

Samples	A	B	C	D
Surface area (m ² /kg)	510	685	515	512
Diameter (μm)	13.69	9.12	11.72	13.15

Table 1.4 Particle size distribution (PSDs) of GGBS (Wan et al., 2004)

Samples	Range of particle size (μm)						
	<3.0	3.0–5.0	5.0–10.0	10.0–20.0	20.0–40.0	40.0–60.0	>60.0
A	5.26	3.80	14.35	25.03	32.52	18.11	0.93
B	8.35	6.14	28.44	36.80	18.69	1.58	0
C	3.56	3.04	23.02	48.36	18.02	0	0
D	3.18	2.96	15.78	27.24	35.45	15.39	0

1.2 Fresh Properties of Mortar/Paste/Concrete Containing GGBS

1.2.1 Bleeding Characteristics

Bleeding is the term used to describe the movement of water to the surface of the freshly placed concrete. All concrete bleeds to some extent but bleed water is only observed on the surface when the rate of bleeding exceeds the rate of evaporation. Immediately after compaction there is a short dormant period which is followed by a period in which the rate of bleeding is almost uniform. Bleeding will end when the movement of water is blocked by the growth of the hydration products or by the solids effectively coming into contact with each other or by a combination of both. Bleeding results in a variation in the effective water content throughout the concrete element which produces corresponding changes in the concrete properties.

Wainwright and Ait-Aider (1995) examined the influence of the composition of OPC and the addition of up to 70% GGBS on the bleed characteristics of concrete. Five series of concrete mixes were made with cement contents ranging from 200 kg/m³ to 400 kg/m³ and slag replacement levels of 40% and 70%. The bleed water was drawn at 10 minute intervals during the first 40 minutes and at 30 minute intervals thereafter until cessation of bleeding. They concluded that the partial replacement of OPC with 40% and 70% of GGBS led to increases in the bleeding of the concretes, these increases were more pronounced at the higher replacement levels.

Olorunsogo (1998) investigated the effect of particle size distribution (PSD) of GGBS on the bleeding rate and bleeding capacity of mortar mixes containing 30% and 70% slag. Retained water on the surface of the mortar mixes was collected at intervals of 10 min. within the first 40 min., and 30 min. intervals thereafter until cessation of bleeding. They concluded that: (i) on the basis of equal w/c, bleeding rate and capacity increased significantly with increase in the amount of the slag included except for the 30% slag mortar mix, which had the lowest bleed capacity at 0.45 w/c; and (ii) when PSD of slag was varied by altering slope (n) at constant position parameter (x₀) no specific relationship between bleeding characteristics and

PSD was observed. However, the highest value of bleeding rate and capacity were exhibited by mixes in which the slag with intermediate value of slope was included. Also, the slag samples with similar size range distribution (having a constant slope, n) the bleeding rate increased with the increase in x_0 , except the 30% slag mixes that were made to 0.35 w/c. Changing the w/c from 0.35 to 0.45 resulted in increase of 86, 83, and 71 % in bleeding rate of the OPC, 30%, and 70% slag mixes respectively.

Wainwright and Rey (2000) studied the influence of GGBS additions on the bleeding of concrete. GGBS from four different sources (S1–S4) and Portland cement from one source were used. One basic mix with a nominal cement content of 300 kg/m^3 was used in mix proportion of 1:2.5:3.6 with water/binder ratio of 0.56. Slag replacement levels of 55 and 85% by weight of cement were used. Bleed tests were performed in accordance with ASTM C 232 (1992). Bleed tests were performed starting 30, 75 and 120 min after completion of mixing for each of the mixes. Bleeding rate is defined as the volume of water collected per second during the first 40 min of the test. The volume is expressed in ml/cm^2 of exposed surface. Bleed capacity is defined as the fraction of the initial volume of the concrete that has separated out as bleed water during the entire course of the test. Bleed capacity and bleed rate results of concrete mixes are shown in Table 1.5. They concluded that: (i) addition of 55% slag increased the bleed capacity by 30% (compared to the plain Portland cement (OPC) mix) but had little effect on bleed rate; (ii) Increasing the slag content to 85% had no further significant effect on bleeding; (iii) source of slag was also found to have little effect on the bleeding; and (iv) delaying the start of the bleed tests from 30 to 120 min reduced the bleed capacity of the OPC mix by more than 55% compared with 32% for the slag mixes. The reduction in bleed rate was similar for all mixes at about 45%.

1.2.2 Workability

Wainwright and Rey (2000) reported the influence of GGBS additions on the slump of concrete. GGBS from four different sources (S1 to S4) and Portland cement from one source were used. One basic mix with a nominal cement content of 300 kg/m^3 was used in mix proportion of 1:2.5:3.6 with water/binder ratio of 0.56. Slag replacement levels of 55 and 85% by weight of cement were used. Mixture proportions and slump results are given in Table 1.6.

Table 1.5 Influence of test start time on bleed capacity and rate (Wainwright and Rey, 2000)

	Bleed capacity (ml/ml)			Bleed rate ($\text{ml/cm}^2/\text{s}$) $\times 10^{-6}$		
	30 min	75 min	120 min	30 min	75 min	120 min
OPC	8	8.1 [1.3%]	7.9 [1.3%]	17.8	10.5 [41%]	9.0 [49%]
55% GGBS	10.7	7.7 [28%]	6.7 [36%]	18.5	11.5 [38%]	9.8 [47%]
85% GGBS	11.1	4.2 [62%]	3.5 [68%]	16.5	14.5 [12%]	10.5 [36%]

Note: Values in bracket represent % change from 30 minute reading.

Table 1.6 Mix proportions and workability (Wainwright and Rey, 2000)

Mix		Mix proportions (kg/m ³)					Water/binder	Slump (mm)
		OPC	GGBS	Fines	Coarse	Water		
OPC		300	–	750	1080	168	0.56	15
55% GGBS	Source 1	135	165	750	1080	168	0.56	30
	Source 2	135	165	750	1080	168	0.56	20
	Source 3	135	165	750	1080	168	0.56	25
	Source 4	135	165	750	1080	168	0.56	45
85% GGBS	Source 1	45	255	750	1080	168	0.56	30
	Source 2	45	255	750	1080	168	0.56	40
	Source 3	45	255	750	1080	168	0.56	25
	Source 4	45	255	750	1080	168	0.56	20

Wan et al. (2004) concluded that workability of mortar increased with the increase of the surface area of GGBS. Four samples (A, B, C, and D) of GGBS were used. Fluidity ratio was determined of the samples. The influence of GGBS on the fluidity of mortar is shown in Table 1.7. The fluidity of sample B and D was much better than that of sample A. The fluidity of mortar was associated with the morphological characteristics of the GGBS particles. The smoother the surface of particles, the better was the fluidity of mortar.

1.2.3 Setting Times

The setting time of concrete with GGBS is generally greater than that of similar concrete with Portland cement only. Setting time increased with the increase in GGBS content as shown in Fig. 1.2.

Wainwright and Ait-Aider (1995) investigated the effect of GGBS additions on the setting times and consistency of cements. Cement from three different sources and GGBS from one source was used. Cements were partially replaced with 40 and 70% of GGBS. Table 1.8 gives the results of setting times and consistency of OPC and blended cements with GGBS. They concluded that: (i) consistency and setting times results were almost similar for all the three sources of cements; (ii) inclusion of GGBS affected the consistency of cements, and it was reduced with the increase in GGBS content; and (iii) Setting time of cements was increased with the increase in GGBS content.

Table 1.7 Test results of fluidity ratio for different surface area and particle sizes of GGBS (Wan et al., 2004)

Sample	Surface area (m ² /kg)	Average diameter (μm)	Fluidity ratio (%)
Sample A	510	13.69	1.02
Sample B	685	9.12	1.06
Sample C	515	11.72	1.03
Sample D	512	13.15	1.06

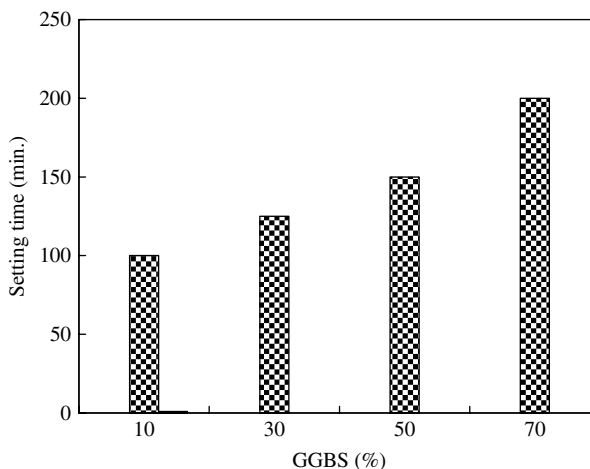


Fig. 1.2 Effect of GGBS on setting time (www.ecocem.ie)

Table 1.8 Setting times and consistency of cements (Wainwright and Ait-Aider, 1995)

Cement type	GGBS (% by wt)	Consistency (%)	Initial setting (min)	Final setting (min)
Source 1	0	31.2	108	182
Source 1	40	29.0	164	224
Source 1	70	26.5	241	318
Source 2	0	30.6	105	171
Source 2	40	28.2	153	219
Source 2	70	26.8	248	322
Source 2	0	30.4	118	169
Source 2	40	30.1	170	213
Source 2	70	27.0	249	310

1.3 Properties of Hardened Concrete Containing GGBS

1.3.1 Microstructure

GGBS can be effectively used in concrete to reduce the pore sizes and cumulative (Basheer et al., 2002). It appears that higher GGBS replacement percentage has denser structure and prevents concrete from water penetration. The GGBS reacts with water in alkali environment and then with calcium hydroxide to form cement hydration product through pozzolanic reaction to form extra C–S–H gel in the paste and slow down the strength development at early age. Denser microstructure or lower porosity results from higher C–S–H content that represents higher GGBFS replacement percentage and higher durability of concrete. SEM micrographs (Fig. 1.3) by Daube and Bakker (1983) indicated that the addition of GGBFS modifies the products and the pore structure in a hardened cementitious material. It was found that a great number of calcium hydroxide and large capillary pores (0.05–60 μm) were found in OPC specimens. But few needle shape ettringite existed in GGBFS

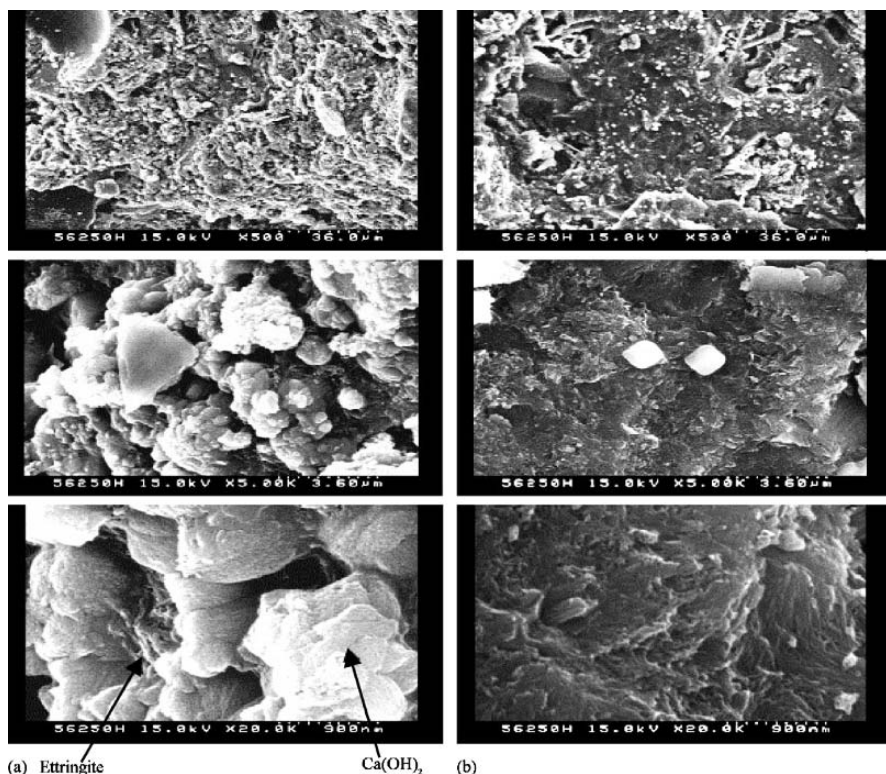


Fig. 1.3 SEM micrograph of: (a) ordinary Portland cement concrete; and (b) GGBFS (60%) concrete (Daube and Bakker, 1983)

concrete specimens and the capillary pores were less than ($10\text{--}50\mu\text{m}$) which could be filled up with pozzolanic reaction product such as low density C–S–H gel.

Hydration product; $\text{Ca}(\text{OH})_2$ activates the slag hydration to form a mixture of low CaO/SiO_2 (C/S) ratio $\text{CaO}\text{--}\text{SiO}_2\text{--}\text{H}_2\text{O}$ (C–S–H) and AFm (cementitious product from the reaction of reactive alumina and calcium hydroxide) phases. Pozzolanic reaction is also found to increase the C/S ratio to a value of about 1.7 in slag-cement blends due to unstable low calcium C–S–H and $\text{Ca}(\text{OH})_2$ mixture. When supplementary cementitious material like GGBFS are used in concrete, they do not only reduce the porosity but also the pores become finer and the change in mineralogy of the cement hydrates leads to the reduction in mobility of chloride ions.

Luo et al. (2003) studied the pore structure of three types of concretes made with OPC, OPC/70% GGBS and OPC/65% GGBS/5% gypsum. The mix ratio for the three kinds of concretes was 1:1.7:3.29 with water-binder ratio of 0.34. Regarding pore structure, they reported that coarse pores of GGBS concrete were much less and the pore structure of OPC concrete was improved greatly when 70% GGBS was added, especially for the pore structure for the time of 60 days. But sulfates did not

improve the pore structure of GGBS as expected, and it surely showed that some other causes, except the expanding reaction between sulfates and C3A, influence the pore structure of concretes. Thus, it is not right to improve the pore structure of GGBS concrete with sulfates.

Li and Zhao (2003) investigated the effect of combination of ground granulated blast furnace slag (GGBS) and fly ash (FA) on the microstructure of concretes. Three types of concretes viz GGFAC (concrete incorporating GGBS and FA), HFAC (high-volume fly ash concrete), and PCC (control Portland cement concrete) were made. PCC had 500 kg/m^3 of cement content, HFAC had 300 kg/m^3 of cement & 200 kg/m^3 FA, GGFAC had 300 kg/m^3 of cement & 125 kg/m^3 FA and 75 kg/m^3 of GGBS. Microstructure of concretes was studied at the age of 7 and 360 days using scanning electron microscope.

The image characteristics (SEM) of concretes at 7 days are shown in Figs. 1.4(a)–1.6(a). As can be seen from Fig. 1.4(a), there were great deals of needle-shaped ettringite and plated-shaped calcium hydroxide in PCC, and large pores could also be observed. Figure 1.6(a) shows that there are numerous un-hydrated FA particles in HFAC. However, SEM observation of GGFAC (Fig. 1.5(a)) shows that microstructure changed greatly with the incorporation of GGBS, and no FA particles can be observed. The main hydration products were cotton-shaped C–S–H gel and a certain amount of needle-shaped ettringite.

The characteristics of concretes at 360 days are shown in Figs. 1.4(b)–1.6(b). It is seen from Fig. 1.4(b) that though the microstructure of PCC was very compact, there were great deals of plated-shaped calcium hydroxide in it. The microstructures

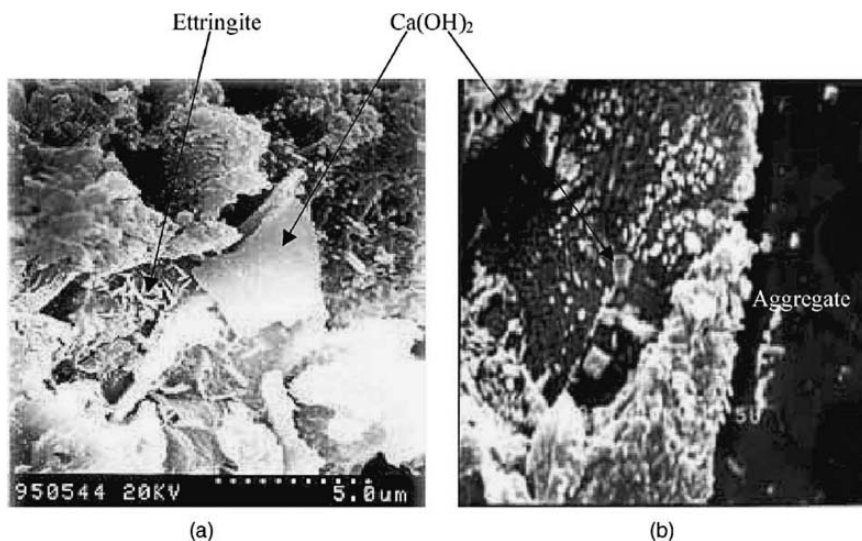


Fig. 1.4 SEM micrograph of PCC; (a) at the age of 7 days, (b) at the age of 360 days (Li and Zhao, 2003)

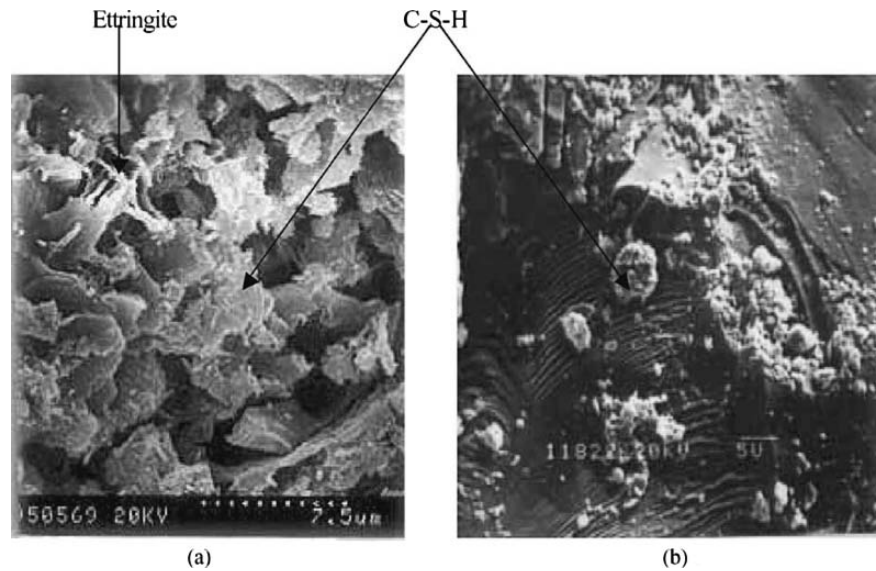


Fig. 1.5 SEM micrograph of GGFAC; (a) at the age of 7 days, (b) at the age of 360 days (Li and Zhao, 2003)

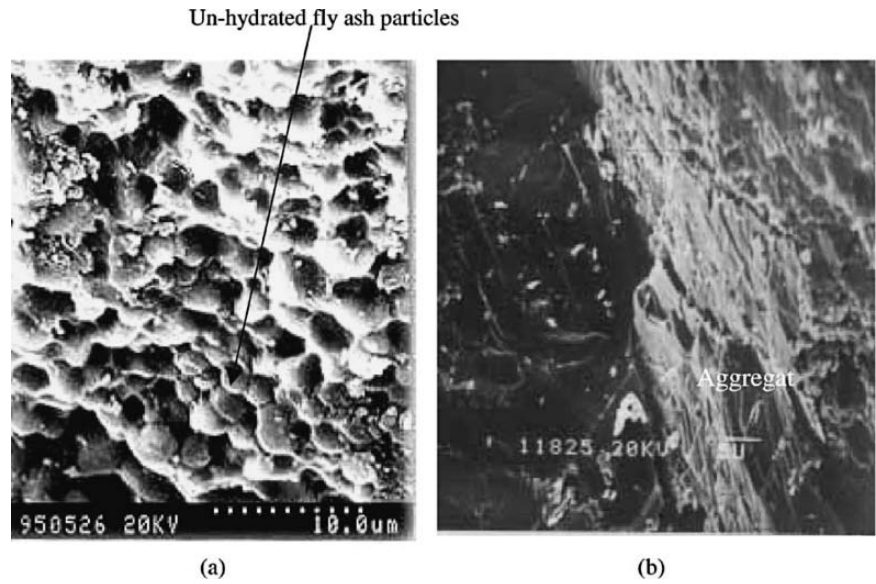


Fig. 1.6 SEM micrograph of HFAC; (a) at the age of 7 days, (b) at the age of 360 days (Li and Zhao, 2003)

of HFAC and GGFAC were also very compact, and no needle-shaped ettringite or plated shaped calcium hydroxide was observed.

Gao et al. (2005) studied the interfacial transition zone (ITZ) of aggregate–cement paste and the morphology of hydrates in concrete made with ground granulated blast-furnace slag (GGBS) using XRD, SEM and micro-hardness measurements. Specific surface area of cement, GGBS (slag 1), GGBS (slag 2) was 361, 425, 600 m²/kg, respectively. They concluded that: (i) pozzolanic reaction of GGBS started at very early age. The reaction became more discernible at the curing ages of 7–28 days. The pozzolanic reaction rate was in direct proportion to the specific surface area of GGBS; (ii) GGBS significantly decreased the content of Ca(OH)₂ crystals in the aggregate–mortar ITZ. Moreover, it reduced the mean size of Ca(OH)₂ crystals, which made the microstructure of ITZ more dense; and (iii) weak zone at the coarse aggregate–mortar interface almost vanished in concrete with 40% GGBS of specific surface area 425 m²/kg. And weak zone completely vanished when GGBS with a specific surface area of 600 m²/kg replaced 20% of the Portland cement. Meanwhile, the cementitious matrix was strengthened.

1.3.2 Compressive Strength

Hogan and Meusel (1981) found that compressive strength development was slow during the first three days of hydration for concrete containing 40–65% GGBS as Portland cement (PC) replacement. However, after three days of hydration, the strength of GGBS concrete was higher than that of normal concrete especially at 40% replacement. Roy and Idorn (1982) also reported similar results. However, it was reported that the benefit in strength of concrete containing 20–60% GGBS did not occur until after 28 days of curing, where similar or higher long term strength was obtained as compared with that of normal PC concrete (Aldea et al., 2000; Hwang and Lin, 1986; Miura and Iwaki, 2000).

Douglas et al. (1991) investigated the compressive strength development of alkali activated ground granulated blast-furnace slag concretes. These concretes incorporated sodium silicate as an activator but did not contain any Portland cement. Five alkali activated slag concrete mixtures were made. The first three mixtures were made using a sodium silicate solution having a silicate modulus ($M_s = 1.47$) and low water-to-binder ratios ranging from 0.34 to 0.39. Two other mixtures incorporated a sodium silicate solution of silicate modulus ($M_s = 1.36$) and higher water-to-binder ratios of 0.50 and 0.46. One of these mixtures was air-entrained. Cylinders of size 102 × 203 mm were cast to determine compressive strengths up to one year. Compressive strength test results are given in Table 1.9. They reported that: (i) strength of all the mixtures increased with age; (ii) 28-day strength ranged from 46.3 MPa to 59.6 MPa, where as 91-day strength was between 48.5 MPa and 62.8 MPa; (iii) ground granulated blast-furnace slag activated with sodium silicate can be used to make slag concretes with satisfactory workability and strength properties as measured at ages up to 91 days; and (iv) air can be entrained in activated slag concrete in order to improve workability and durability.

Table 1.9 Properties of hardened concretes (Douglas et al., 1991)

Mix No.	w/b	Density of cylinders (kg/m ³)	Compressive strength (MPa)					
			1d	3d	7d	14d	28d	91d
1	0.39	2373	28.1	38.2	41.6	43.4	46.3	48.5
2	0.34	2387	37.5	41.8	44.6	48.3	51.0	52.6
3	0.35	2464	38.9	49.4	54.5	—	59.6	62.8
4	0.50	2435	23.2	33.7	41.0	43.1	45.4	50.2
5	0.46	2415	20.4	35.0	41.5	44.3	46.8	51.0

Ujhelyi and Ibrahim (1991) studied the effect of hot weather on the compressive strength of concrete made with various percentages of granulated blast furnace slag and ground rhyolite tuff as partial replacement of cement. The cement content in control mix was 350 kg/m³ with water-to-cement ratio 0.531. Two series of mixes were made: the materials of the first were stored in laboratory room (temperature: 20°C ± 3°C, relative humidity: 20–35%), that of the second in special room (temperature: 42°C ± 1°C, relative humidity: 20%). Compressive strength was determined at 7, 28 and 90 day. Based on the investigation, following conclusions were drawn: (i) concretes containing slag as a partial replacement of cement (up to 40 pct) had higher compressive strengths casting and curing at +42°C than that of concretes made with Portland cement alone; (ii) Compressive strengths of 7 day in concretes made with additives were less than that of concretes made with Portland cement; (iii) compressive strength in 28 and 90 day of concretes made with slag or pozzolana reached that of concretes made with pure Portland cement; and (iv) in spite of reducing Portland cement content with increasing ratio of additive, compressive strengths remain unchanged after casting and curing at high air temperature comparing with that of Portland cement concretes because the active SiO₂ of additives reacts at high temperature with CaOH₂ of cement in the early period.

Wainwright and Rey (2000) studied the influence of GGBS on the compressive strength of concrete. GGBS from four different sources (S1 to S4) and Portland cement from one source were used. One basic mix with a nominal cement content of 300 kg/m³ was used in mix proportion of 1:2.5:3.6 with water/binder ratio of 0.56. Slag replacement levels of 55 and 85% by weight of cement were used. Compressive strength results for all mixes up to 28 days are shown in Table 1.10. It can be seen from the table that source of the slag appeared to have little influence on strength development, and strength of OPC concrete and those containing GGBS increased with age.

Babu and Kumar (2000) determined the cementitious efficiency of GGBS in concrete at various replacement percentages (10–80%) through the efficiency concept by establishing the variation of strength to water-to-cementitious materials ratio relations of the GGBS concretes from the normal concretes at the age of 28 days. The 28-day compressive strength of concretes containing GGBS up to 30% replacement were all slightly above that of normal concretes, and at all other percentages, the relationships were below that of normal concretes. It was also observed that the variations due to the different percentages of slag replacement were smaller

Table 1.10 Compressive strength results (Wainwright and Rey, 2000)

Mix code	Compressive strength (MPa)		
	7 days	14 days	28 days
OPC	39.5	45.3	53.1
55% GGBS Source 1	18.5	28.5	42.5
55% GGBS Source 2	26.0	38.5	50.5
55% GGBS Source 3	22.5	36.0	50.5
55% GGBS Source 4	25.0	41.5	51.5
85% GGBS Source 1	17.5	28.0	33.5
85% GGBS Source 2	21.5	33.5	41.0
85% GGBS Source 3	17.5	25.5	29.5
85% GGBS Source 4	19.0	26.5	32.5

than the corresponding variations in the case of fly ash. The result showed that the slag concretes based on overall efficiency factor (k), will need an increase of 8.6% for 50% replacement and 19.5% for 65% replacement in the total cementitious materials for achieving strength equivalent to that of normal concrete at 28 days.

Quillin et al. (2001) studied the early strength development of ‘BRECEM’ concretes, made from 50:50 mixtures of calcium aluminate cement (CAC) and ground granulated blast furnace slag (GGBS), using 100 mm cubes at w/c ratios of 0.35 and 0.45. Concrete were both air-cured and water cured. Tests were conducted up to the age of 90 days and compressive strength results are shown in Fig. 1.7. They concluded that: (i) BRECEM concrete with w/c ratio of 0.35 developed strength more rapidly than those made using w/c ratio of 0.45. The 90-day strength was also higher than those made using a w/c ratio of 0.45, although for water stored concretes, strengths were still increasing in both cases; and (ii) BRECEM concretes stored in air initially developed strength more rapidly than equivalent concretes stored in water. The initial strength development was predominantly due to the hydration of the more reactive CAC component. However, the compressive strength of

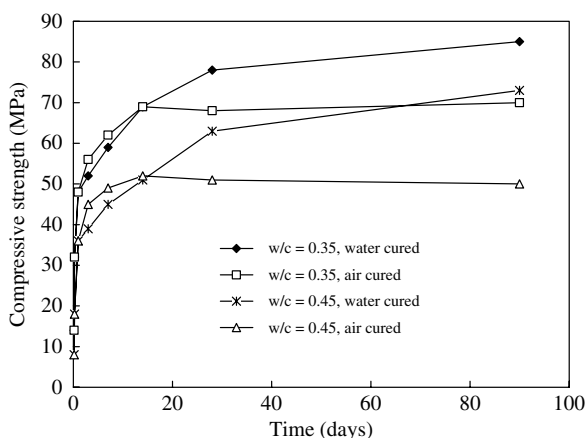


Fig. 1.7 Compressive strength development in BRECEM concretes (Quillin et al., 2001)

air-stored concretes rapidly leveled out after 14 days and at later test age's water-stored concretes had a higher compressive strength than air stored ones. The continuing increase in compressive strength with time for water-stored samples after 14 days will have risen due to the ongoing hydration of the GGBS and any remaining CAC.

Jianyong and Yan (2001) reported the 28-day compressive strength of three high-performance concrete (HPC) mixtures. Mix proportions and compressive strength results are given in Table 1.11. As shown in this table, Concrete B and C acquired much higher compressive strength than Concrete A at each testing age. At the age of 3 days, the compressive strengths of concrete A, B and C were 63.8, 69.3 and 69.3 MPa, respectively. At 28 days of age, the compressive strengths of Concrete B and C increased greatly to 100.4 and 104.0 MPa, respectively, compared with 81.1 MPa of Concrete A. The development of compressive strength reflected the strengthening effect of ultra-fine GGBS and SF on mechanical properties of concrete.

Li and Zhao (2003) studied the influence of combination of ground granulated blast furnace slag (GGBS) and fly ash (FA) on the compressive strength of high-strength concrete. Three types of concretes; GGFAC (concrete incorporating GGBS and FA), HFAC (high-volume fly ash concrete), and PCC (control Portland cement concrete) were made and their strength was determined up to the age of 360 days. PCC had 500 kg/m³ of cement content, HFAC had 300 kg/m³ of cement & 200 kg/m³ FA, GGFAC had 300 kg/m³ of cement & 125 kg/m³ FA and 75 kg/m³ of GGBS. Table 1.12 gives the strength development of PCC, HFAC (containing 40% of FA) and the concrete (GGFAC) incorporating a combination of 25% FA and 15% GGBS. It can be seen that there is a general trend of increasing strength with age up to 1 year for all concretes. As expected, the behavior of HFAC at early ages is different from that of PCC and GGFAC. Though it had the highest strength at the end test age, its strength was the lowest before 56 days. The strength development of GGFAC is similar to that of PCC, only with slightly lower values before 28 days. This indicates that GGFAC can achieve adequate early compressive strength, while maintaining a high long-term strength.

Wan et al. (2004) reported the effect of GGBS on compressive strength and activity index of compressive strength of mortars up to the age of 28 days. Four samples (A, B, C, and D) of GGBS were used. The weight proportion of reference sample (with out GGBS) was: Portland cement/standard sand/water = 540:1350:238, whereas for samples containing GGBS, it was: Portland cement/GGBS/standard sand/water = 270:270:1350:238. Results of compressive strength and activity index

Table 1.11 Mix proportions (kg/m³) and compressive strength of HPC (Jianyong and Yan, 2001)

Mix	Mix proportions							Compressive strength (MPa)		
	OPC	GGBS	SF	SP (%)	Fine Agg.	Coarse Agg.	Water	3 days	7 days	28 days
A	600	–	–	1.6	610	1134	156	63.8	71.2	81.1
B	420	180	–	1.6	610	1134	156	69.3	83.2	100.4
C	360	180	60	1.6	610	1134	156	69.3	97.0	104.0

Table 1.12 Compressive strength gain of concretes (Li and Zhao, 2003)

Binder combination	Cube compressive strength (MPa)							Strength gain from 28 day to 1-year (%)
	1 day	3 day	7 day	28 day	56 day	112 day	360 day	
PCC	40.5	51.2	66.8	81.1	87.9	91.2	96.3	18.7
HFAC	21.7	32.6	43	65.2	86.7	97.5	107.1	64.3
GGFAC	35.1	49.3	65.4	80.6	89.8	93.7	99.4	23.3

of compressive strength are given in Table 1.13. They concluded that strength of mortar incorporating GGBS is both related to the surface area and particle size distribution (PSD) of GGBS. When GGBS had the same surface area, the more the mortar contained fine particles ($< 3 \mu\text{m}$) of GGBS, the higher its early strength was. The mortars containing $3\text{--}20 \mu\text{m}$ particles of GGBS, the higher was its long-term strength; and (ii) compressive strengths increased with the increase of the surface area of GGBS.

Cheng et al. (2005) reported the effect of GGBS on the compressive strength of concrete. They made three concrete mixes (A, B, and C). Mix A was control one with mixture proportion 1:1.82:1.97 with water-binder ratio of 0.55. Mixes B and C were made by replacing cement with 40 and 60% of GGBS, respectively. Compressive strength was determined according to ASTM C39/C39M, (2004). At the age of 91 days, the compressive strength of specimens was 42.4, 45.3 and 48.6 MPa for mix A, mix B and mix C, respectively. Compressive strength developments depend upon the GGBS replacement percentage and the concrete age. The glassy compounds in GGBS react slowly with water and it takes time to obtain hydroxyl ions from the hydration product of Portland cement to breakdown the glassy slag parcels at early age. However, GGBS concrete had higher compressive strength than ordinary Portland cement concrete (OPC) after GGBS hydration and pozzolanic reaction was almost accomplished. Higher GGBS replacement percentage had higher ultimate strength.

Khatib and Hibbert (2005) investigated the influence of incorporating ground granulated blast furnace slag (GGBS) and metakaolin (MK) on the compressive strength of concrete. Portland cement (PC) was partially replaced with 0–80% GGBS and 0–20% MK. Twelve different mixes were made. First mix was control (M1) having a proportion of 1 (PC): 2 (fine aggregate): 4 (coarse aggregate). In

Table 1.13 Results of compressive strength and activity index (Wan et al., 2004)

Sample	Surface area (m^2/kg)	Average dia (μm)	Compressive strength (MPa)		Activity index (%)	
			7 days	28 days	7 days	28 days
Reference (OPC)	–	–	43.4	54.3	–	–
Sample A	510	13.69	35.6	55.4	82	102
Sample B	685	9.12	42.5	63.0	98	116
Sample C	515	11.72	35.2	58.4	81	108
Sample D	512	13.15	34.9	56.5	80	104

the next three mixes (M2, M3 and M4), PC was partially replaced with 40, 60 and 80% GGBS (by mass). Mixes (M5, M6, M7 and M8) contained 0, 30, 50 and 70% GGBS as partial replacement of PC, and 10% MK as partial substitution of the total cementitious material (CM). Mixes (M9, M10, M11 and M12) contained 0, 20, 40 and 60% GGBS as partial replacement of PC, and 20% MK as partial substitution of the total cementitious material (CM). Tests were conducted at the age of 1, 7, 14, 28, and 90 days.

The compressive strength development for concretes containing 0, 40, 60 and 80% GGBS (mixes M1–M4) is presented in Fig. 1.8. There was a systematic decrease in compressive strength with the increase in GGBS content during the early stages of hydration. Beyond 28 days and up to at least 90 days, the presence of GGBS was highly beneficial at 40 and 60% replacement with a strength exceeding that of the control. A noticeable strength reduction at all ages is observed at 80% GGBS. This figure shows GGBS content required to give maximum compressive strength at varying MK contents. The incorporation of MK caused an increase in strength, especially during the early ages of curing. However, the use of GGBS in concrete reduced the strength during the first 28 days (Figs. 1.9–1.12). Beyond 28 days, the strength increased with the presence of GGBS up to 60% replacement. The decrease in compressive strength during the early ages of curing of GGBS concrete was compensated by the inclusion of MK. The presence of MK in concrete containing GGBS did not cause a decrease in the long-term strength. The incorporation of up to 60% GGBS to partially replace PC in concrete caused an increase in long-term compressive strength. An increase in MK content up to 20% as partial substitution of PC increased the strength, especially during the early ages of hydration. The inclusion of more than 10% MK in concretes containing GGBS did not contribute to further increase in compressive strength.

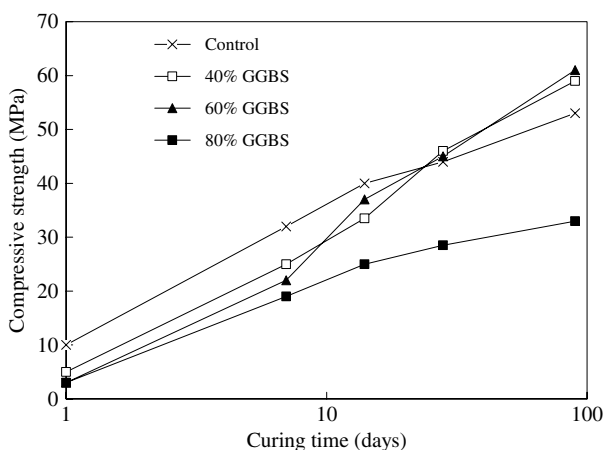
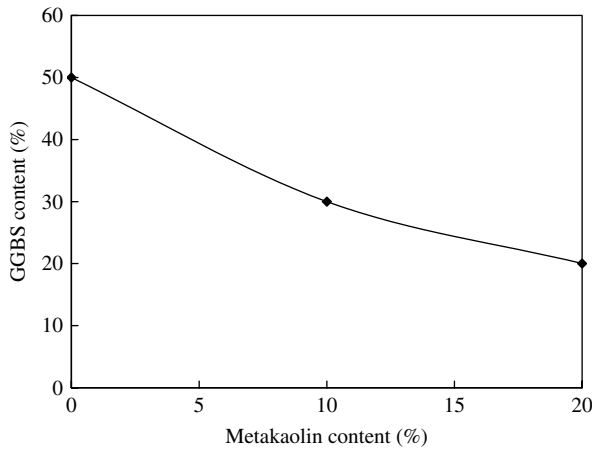


Fig. 1.8 Effect of GGBS on compressive strength development (Khatib and Hibbert, 2005)

Fig. 1.9 GGBS content required to give maximum compressive strength at varying MK contents (Khatib and Hibbert, 2005)



1.3.3 Tensile and Flexural Strength

Ujhelyi and Ibrahim (1991) investigated the effect of hot weather on the flexural strength of concrete containing various percentages of granulated blast furnace slag and ground rhyolite tuff as partial replacement of cement. The cement content in control mix was 350kg/m³ with water-to-cement ratio 0.531. Two series of mixes were made: the materials of the first were stored in laboratory room (temperature: +20°C ± 3°C, relative humidity: 20–35%), that of the second in special room (temperature: +42°C ± 1°C, relative humidity: 20%). Following conclusions were drawn: (i) Concretes containing slag as a partial replacement of cement (up to 40%) had higher flexural strengths casting and curing at +42°C than that of concretes made with Portland cement alone; (ii) flexural strength of concretes made with slag was equal (or higher) comparing to Portland cement concrete cast and cured

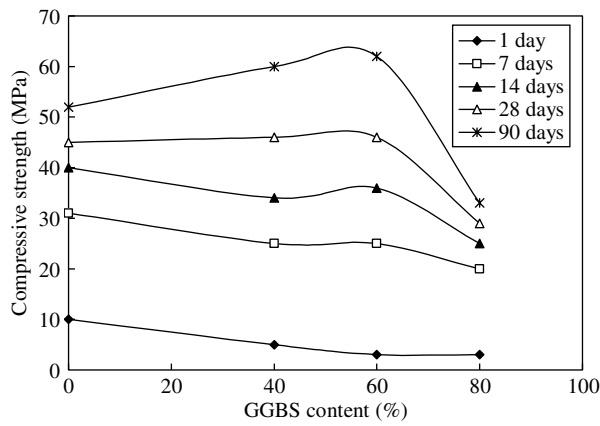
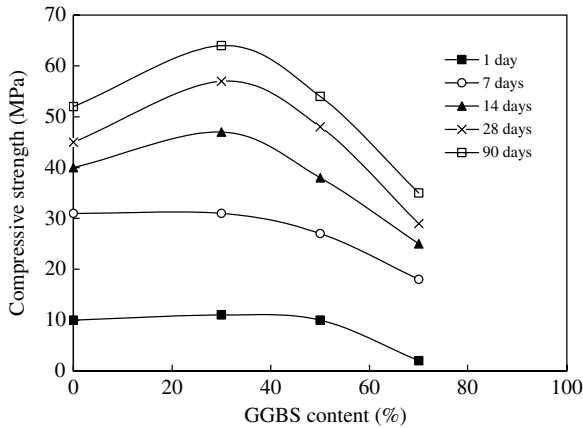


Fig. 1.10 Influence of varying GGBS contents at 0% MK (Khatib and Hibbert, 2005)

Fig. 1.11 Influence of varying GGBS contents at 10% MK (Khatib and Hibbert, 2005)



in high temperature; and (iii) flexural strengths remain unchanged despite reduction in cement content and with increasing ratio of additive, curing at high air temperature comparing with that of Portland cement concretes because the active SiO_2 of additives reacts at high temperature with Ca(OH)_2 of cement in the early period.

Jianyong and Yan (2001) reported the 28-day compressive strength of three high-performance concrete (HPC) mixtures. Concrete A was made of OPC (600 kg/m^3). Concrete B had (420 kg/m^3 of OPC and 180 kg/m^3 GGBS), and concrete C had (360 kg/m^3 of OPC and 180 kg/m^3 GGBS, 60 kg/m^3 of Silica fume). Splitting tensile strength results are given in Table 1.14. It is evident that Concrete B and C acquired much splitting tensile strength than Concrete A at each testing age. The development of splitting tensile strength showed the same tendency as that of compressive strength. Such a tendency reflects the strengthening effect of ultra-fine GGBS and SF on mechanical properties of concrete.

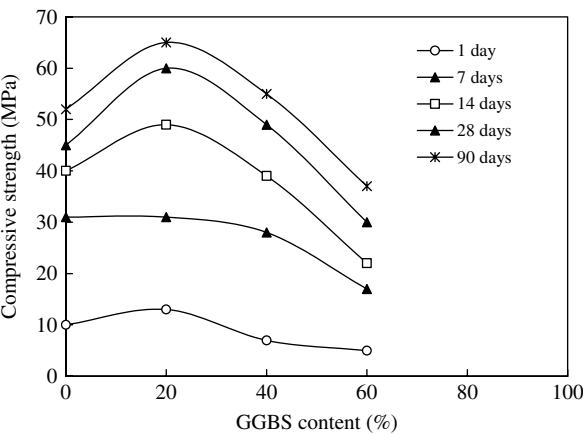


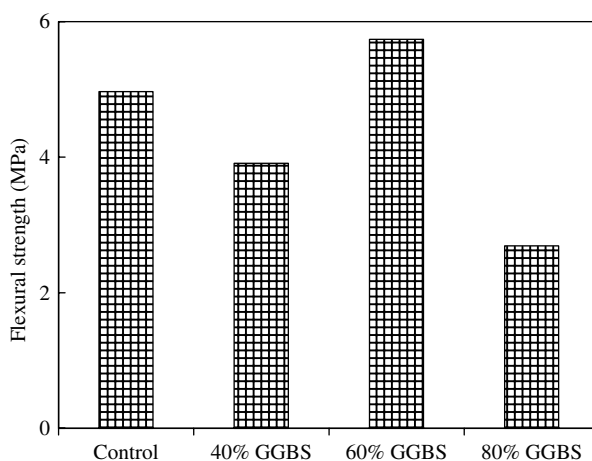
Fig. 1.12 Influence of varying GGBS contents at 20% MK (Khatib and Hibbert, 2005)

Table 1.14 Test results of splitting tensile strength (Jianyong and Yan, 2001)

Mix	Cementitious materials (kg/m ³)			Splitting tensile strength (MPa)		
	OPC	GGBS	SF	3 days	7 days	28 days
A	600	–	–	3.8	4.54	5.54
B	420	180	–	4.06	5.03	5.91
C	360	180	60	5.2	5.44	6.14

Khatib and Hibbert (2005) studied the effect of ground granulated blast furnace slag (GGBS) and metakaolin (MK) on the flexural strength of concrete. Portland cement (PC) was partially replaced with 0–80% GGBS and 0–20% MK. Twelve different mixes were made. First mix was control (M1) having a proportion of 1 (PC): 2 (fine aggregate): 4 (coarse aggregate). In the next three mixes (M2, M3 and M4), PC was partially replaced with 40, 60 and 80% GGBS (by mass). Mixes (M5, M6, M7 and M8) contained 0, 30, 50 and 70% GGBS as partial replacement of PC, and 10% MK as partial substitution of the total cementitious material (CM). Mixes (M9, M10, M11 and M12) contained 0, 20, 40 and 60% GGBS as partial replacement of PC, and 20% MK as partial substitution of the total cementitious material (CM). Flexural strength was determined at the age of 90 days. Figure 1.13 shows 90-day flexural strength values for mixes containing 0, 40, 60, and 80% GGBS. The flexural strength of concrete containing 60% GGBS was noticeably higher than the control, whereas a slight decrease at 40% and marked decrease at 80% replacement were observed.

At the age of 90 days, Flexural strength of concrete mixes containing 30, 50, and 70% GGBS along with 10% Metakaolin (MK) are shown in Fig. 1.14. The incorporation of 30% and 50% GGBS at 10% MK increased the flexural strength and even at high GGBS content (i.e., 70%), the flexural strength was similar to that

**Fig. 1.13** Effect of GGBS on flexural strength (Khatib and Hibbert, 2005)

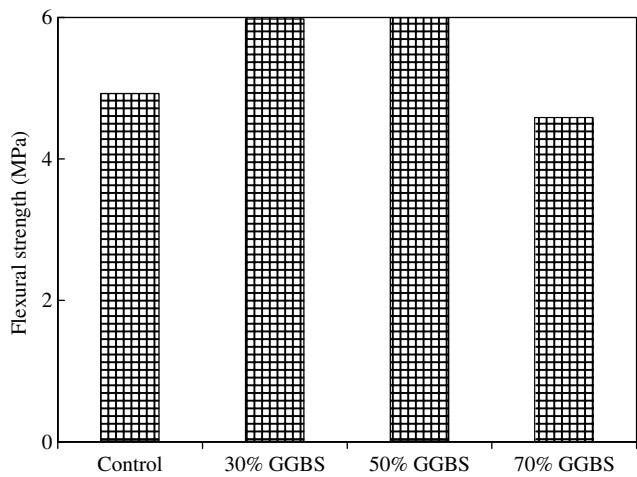


Fig. 1.14 Effect of GGBS content on flexural strength at 10% MK (Khatib and Hibbert, 2005)

of the control. This could be due to improvement of the interfacial zone between the paste and the aggregate in the presence of both GGBS and MK.

Figure 1.15 shows the flexural strength at 90 days of concrete mixes containing 40, 60, and 80% GGBS along with 20% Metakaolin (MK). The flexural strengths for all GGBS mixes containing 20% MK at 90 days of curing, were higher than that of the control even at high GGBS replacement level of 60%. This suggested that the interfacial zone between the paste and the aggregate was improved in the presence of GGBS and MK. MK level above 10% is quite advantageous in increasing the flexural strength.

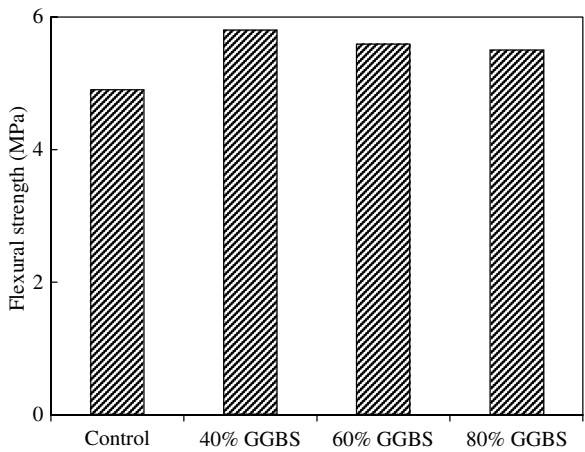


Fig. 1.15 Effect of GGBS content on flexural strength at 20% MK (Khatib and Hibbert, 2005)

1.4 Durability Properties of Concrete Containing GGBS

1.4.1 Creep and Shrinkage

The creep of concrete is the deformation of hardened concrete caused by a long-lasting constant load applied on it. Drying shrinkage of concrete is the shrinkage caused by evaporation of internal water in hardened concrete. Creep and drying shrinkage are very important time-dependent properties of high-performance concrete (HPC).

Jianyong and Yan (2001) studied the creep and drying shrinkage results of three high-performance concrete (HPC) mixtures. Concrete A was made of OPC (600 kg/m^3). Concrete B had (420 kg/m^3 of OPC and 180 kg/m^3 GGBS), and concrete C had (360 kg/m^3 of OPC and 180 kg/m^3 GGBS, 60 kg/m^3 of Silica fume). Specimens for creep and shrinkage were of size $100 \times 100 \times 300 \text{ mm}$ and $100 \times 100 \times 500$, respectively. The creep and shrinkage tests were conducted up to the age of 180 and 210 days, respectively. Creep and shrinkage results are shown in Figs. 1.16 and 1.17, respectively.

It is evident from this figure that up to 180-days of testing, Concrete B and C always obtained much smaller creep value than Portland cement concrete A. When ultra-fine GGBS and SF were used at the same time (Concrete C), the creep value was the lowest, which is in accordance with the development trend of mechanical strengths. At test age of 180 days, the creep value for Concrete A, B and C was 1293×10^{-6} , 623×10^{-6} and 450×10^{-6} , respectively. According to creep rate, three groups of concrete tested were all subject to a faster development of creep at early ages than at late ages, and the age of 60 days was the turning point. For the individual concrete, the value of creep rate was different. Before 60 days, Concrete A was much greater than B and C, and C was the lowest. After 60 days, the creep

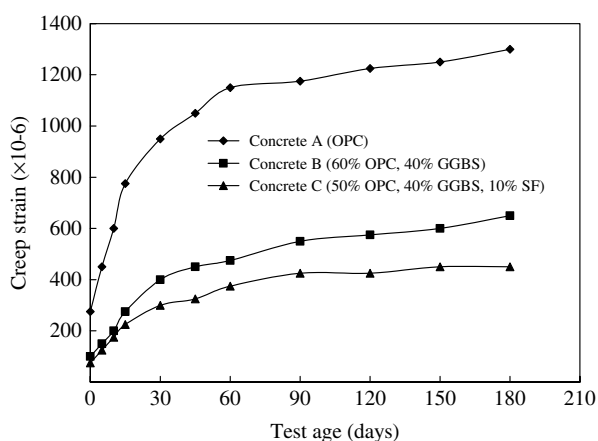
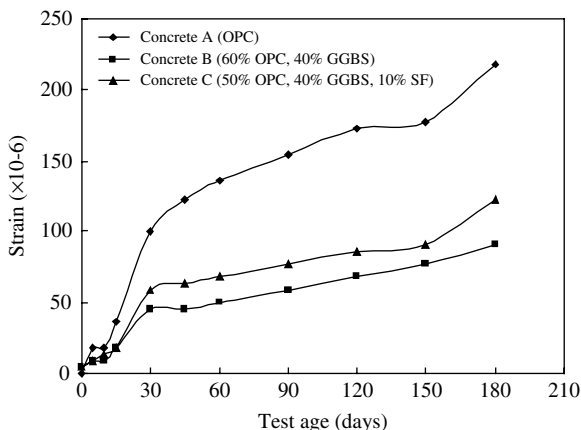


Fig. 1.16 Development of creep of concrete (Jianyong and Yan, 2001)

Fig. 1.17 Test results of drying shrinkage of concrete (Jianyong and Yan, 2001)



rates of A, B and C became similar while Concrete B and C can be thought to have equal creep rate.

Figure 1.17 shows the drying shrinkage of concretes. It can be seen that at early test ages the difference between amounts of drying shrinkage of Concrete A, B and C was small. After 28 days, Concrete A obtained substantially greater amount of drying shrinkage than Concrete B and C, while the latter two always had similar shrinkage amount. At age of 180 days, the amount of shrinkage for Concrete A, B and C was 220×10^{-6} , 96×10^{-6} and 127×10^{-6} , respectively.

1.4.2 Chloride Binding Capacity/Resistance

Dhir et al. (1996) determined the chloride binding capacity of paste samples containing Portland cement (PC) alone, and blends of PC and GGBS. GGBS was added as 0, 33.3, 50 and 66.7% of the total binder. The water-binder ratio was kept constant at 0.55. They concluded that: (i) with the increase in GGBS percentage, the chloride binding capacity increased for all chloride concentrations. For a GGBS replacement level of 66.7%, the chloride binding capacity was around 5 times that of the PC control for the case of 5 mole/liter exposure concentrations; and (ii) as the chloride concentration increased, the binding capacity increased for all GGBS contents. The chloride binding capacity appeared to be directly proportional to the exposure concentration. This could be attributed to the sensitivity of the chloride binding capacity to the ratio of Cl^-/OH^- ions in the cement pore solutions, (in this case, the chloride solutions to which the pastes were exposed). As the Cl^-/OH^- ratio increased chloride binding capacity increased.

Dhir et al. (1996) determined the strength and intrinsic permeability of concrete mixes. Four concrete mixes were made. All the mixes had the same total binder content of 300 kg/m^3 with GGBS replacement levels of 0, 33.3, 50 and 66.7%. 100 mm cubes, were cast for strength and intrinsic permeability tests, and 100 mm diameter \times 300 mm high cylinders, for chloride diffusion measurements. Air permeability

testing was conducted at ages of 28 days and 90 days, whilst chloride diffusion testing was carried out at 28 days. Strength and intrinsic permeability results of PC and GGBS concrete are given in Table 1.15. It is evident from this table that: (i) 28 day cube strength decreased with the increase in GGBS replacement level; (ii) however, at 90 days, the strengths of GGBS and PC concrete mixes were much closer; (iii) at 28 days, despite the lower compressive strengths of the GGBS concrete, compared to the control, the intrinsic permeabilities were similar. At 90 days, the intrinsic permeability of the GGBS became much better; and (iv) GGBS enhanced the protection against chloride ingress and with the increase in GGBS replacement level, the coefficient of chloride diffusion steeply decreased.

Xu (1997) investigated the chloride binding properties and the concentrations of chloride and hydroxyl ions in the pore solutions of Ordinary Portland cement (OPC) and blended (35% OPC, 65% GGBS) cements, containing 2.0–9.0% sulfates derived from sodium sulfate and calcium sulfate. Chlorides derived from sodium and calcium chlorides were introduced at the time of mixing. The results indicated that calcium sulfate had a different effect on chloride binding and the pore solution chemistry than sodium sulfate. The slag cement had higher chloride binding capacities as a result of simple replacement for OPC, but at the same sulfate contents, the slag cement did not give the expected higher binding capacities, suggesting that the difference in sulfate content between the two cements may be the main reason for their different chloride binding behavior.

Huang and Yeih (1997) studied the diffusivity of chloride ions through high strength concrete containing slag. Numerical methods were used to compute the diffusion coefficients of chloride ions in concrete, and were found to be $2.53 \times 10^{-14} \text{m}^2/\text{s}$ to $9.84 \times 10^{-4} \text{m}^2/\text{s}$ for compressive strengths between 62.5MPa and 91.1MPa.

Luo et al. (2003) measured the chloride diffusion coefficients and chloride-binding capacity of the three kinds of concretes made with OPC, OPC/70% GGBS and OPC/65% GGBS/5% gypsum. The mix ratio for the three kinds of concretes was 1:1.7:3.29 with water-binder ratio of 0.34. Both the total chloride diffusion coefficient and the free chloride diffusion coefficient were determined. The total chloride diffusion coefficient is the coefficient for all the diffused chlorides including the bound chloride by the concrete, and the free chloride diffusion coefficient

Table 1.15 PC and GGBS concrete details (Dhir et al., 1996)

GGBS (%)	Mix details			Cube strength (N/mm ²)		Intrinsic permeability (m ²) $\times 10^{-17}$		Coefficient of chloride diffusion (cm ² /s) $\times 10^{-9}$ at 28-day
	PC (C) Kg/m ³	GGBS (G) Kg/m ³	W/(C+G)	28 day	90 day	28 day	90 day	
0	300	–	0.55	45.0	51.0	2.08	1.85	10.90
33.3	200	100	0.55	41.0	51.5	1.97	1.61	0.873
50.0	150	150	0.55	34.0	47.0	2.06	1.72	0.329
66.7	100	200	0.55	32.0	45.0	2.31	1.93	0.100

is only the unbound chloride diffused to the concrete. Results of chloride diffusion coefficients are given in Table 1.16. They concluded that: (i) GGBS decreased the chloride diffusion coefficient greatly; (ii) both the total chloride diffusion coefficient and the free chloride diffusion coefficient decreased greatly when 70% GGBS was added; (iii) but chloride diffusion coefficient increased greatly when 5% gypsum was added; and (iv) GGBS increased the chloride-binding capability greatly, especially the chemical chloride-binding capability, but sulfates and alkalinity decrease the chloride-binding capability greatly.

Cheng et al. (2005) studied the influence of GGBS on the rapid chloride permeability (RCPT) and water permeability of concrete. Three concrete mixes (A, B, and C). Mix A was control one with mixture proportion 1:1.82:1.97 and water-binder ratio of 0.55. Mixes B and C were made by replacing cement with 40 and 60% of GGBS, respectively. ASTM C1202-97 procedure was followed for carrying out RCPT test. For each mix, cylindrical specimens ($\varnothing 100\text{ mm} \times 200\text{ mm}$) were cast and moist-cured for 91 days. 50 mm-thick samples were cut from the middle portion of each cylinder. For measuring water permeability $100 \times 200\text{ mm}$ cylinders were cast. Based on the results obtained they reported that: (i) water permeability was 2.56×10^{-13} , 1.52×10^{-13} , and $1.32 \times 10^{-13}\text{ m/s}$ for mix A, mix B, and mix C, respectively. It appeared that higher GGBS replacement percentage made structure denser and prevented concrete from water penetration; and (ii) RCPT results indicated the highest total charge-passed (10271 C) obtained in mix A specimen and the lowest total charge passed (1864 C) in mix C specimen, which represented highest chloride-ion penetration resistance. The reaction products were very efficient to fill up the large capillary pores and refine the pore system in concrete thereby enhancing its permeability resistance.

Hooton and Titherington (2004) investigated the strength and chloride penetration resistance of high-performance concretes after curing either at 23°C or accelerated by heating to 65°C . Six air-entrained concrete mixtures with different cement replacement levels of slag (25–27%) and silica fume (4–8%) (by mass) were made. The water to cementitious materials ratio (w/cm) was kept constant, at 0.30. The total cementing materials content was 460 kg/m^3 for all mixtures. They measured chloride penetration resistance of a series of high-performance concretes after curing either at 23°C or accelerated by heating to 65°C . According to ASTM C 1202, (1997), very low permeability concretes have RCPT values below 1000 coulombs (C), while moderate permeability concretes have an RCPT value between 2000 and 4000. Coulomb values above 4000 indicate high-permeability concrete. They concluded that: (i) concretes containing silica fume (SF) or ternary blends of SF and ground granulated blast-furnace slag (GGBFS) exhibited improved chloride penetration resistance compared to those of plain Portland cement concretes; (ii) all

Table 1.16 Chloride diffusion coefficient of concrete ($10^{-8}\text{ cm}^2/\text{s}$) (Luo et al., 2003)

	OPC concrete	GGBS concrete	Concrete with gypsum
Total chloride	3.02	1.95	2.44
Free chloride	2.65	1.58	2.14

concretes recorded are below 4000 Coulombs, which was also possible because of water/cement ratio, 0.30. The 100% OPC mixture, whether accelerated or ambient cured, was in the moderate permeability category (between 2000 and 4000 C). All mixtures containing supplementary cementing materials, for both accelerated and ambient curing conditions, were in the very low permeability category of less than 1000 C; and (iv) chloride penetration resistance of Portland cement concrete was adversely affected by accelerated curing.

Roy et al. (2000) studied the characteristics and performance of alkali-activated cementitious materials (AAC) whose properties equal or exceed those of normal Portland cement-based materials. The materials activated included: ground granulated blast furnace slag, fly ash, silica fume, and other pozzolans whether alone or when combined with Portland cement. The activators used were NaOH, KOH, Na_2SO_4 , Na_2CO_3 , CaSO_4 , and soluble silicates of sodium and potassium. Steady state chloride diffusion studies were conducted of pastes of Type I Portland cement, and its blends with different proportions of ground granulated blast-furnace slag. Very substantial reductions in diffusion rates have been found with the increased proportion of slag. In addition, alkali activation has been shown to reduce the diffusion rate by at least a factor or two.

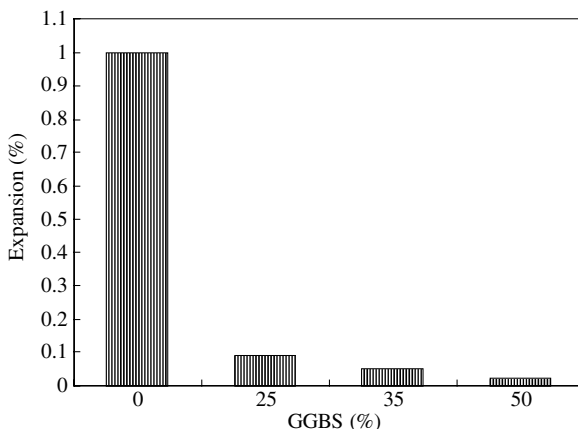
1.4.3 Sulfate Resistance

Solution of sulfate can attack the hardened cement paste in the concrete causing deterioration. The precise chemical reaction will depend on the nature of the sulfate present and the type of cement. In some clay soils the ground water is a solution of magnesium and calcium sulfates. These salts react with the $\text{Ca}(\text{OH})_2$ and the calcium aluminate hydrate in the concrete to produce gypsum and calcium sulphoaluminate. These products have considerably greater volume than the compounds they replace, leading to expansion and disruption of the concrete. The rate and extent of sulfate attack depends upon the ease with which sulfate ions are able to penetrate the concrete and upon the chemical resistance of the cement paste. The effect of GGBS in limiting the impact of sulfate attack, as measured from the expansion it produces in concrete, is shown in Fig. 1.18.

Sulfate resisting Portland cements (SRPC), with low C_3A content, are much less effective in combating sulfate attack than GGBS. GGBS counters sulfate attack in three ways: (i) GGBS does not contain any C_3A , and its inclusion in concrete reduces the overall proportion of C_3A in the mix; (ii) GGBS reacts with $\text{Ca}(\text{OH})_2$ to substantially reduce its presence in the concrete, leaving significantly less $\text{Ca}(\text{OH})_2$ to react to form ettringite. No such effect takes place with SRPC; and (iii) greatly reduced permeability of GGBS concrete, over concrete made with SRPC, limits the penetration of sulfates into the set concrete.

Mangat and El-Khatib (1992) investigated the effect of initial curing conditions on the sulfate resistance of concrete made with ordinary Portland cement and using PFA, silica fume and ground granulated blast furnace slag as partial

Fig. 1.18 Effect of GGBS on sulfate resistance
(www.ecocem.ie)



replacement of cement. Five different concrete mixes were used. First was control mix having proportions 1:2:3.4 with water/cement ratio of 0.45. The cement content was 350 kg/m^3 . In the remaining mixes, cement was partially replaced by 22% PFA, 9% silica fume, 40% and 80% GGBS respectively, by weight. $100 \times 100 \times 250 \text{ mm}$ prism specimens were used. Three different initial curing conditions were adopted, namely: AI (Air 45°C , 25% RH); CH (Wet/Air 45°C , 25% RH); AL (Air 20°C , 55% RH). After the initial curing period of 28 days under the three curing regimes CH, AI and AL, specimens were immersed in fresh water for another 28 days. The temperature of the fresh water was 20°C for specimens cured initially at 20°C and 45°C for specimens cured initially at 45°C . After soaking the specimens for 28 days, extensometer measurements were taken for the specimens across each face. These initial measurements were considered as datum for sulfate attack studies. After that, specimens were immersed in a sulfate solution (7% Na_2SO_4 + 3% MgSO_4 by weight). The temperature of the sulfate solution was 20°C for specimens cured initially at 20°C and 45°C for specimens cured initially at 45°C . Expansion measurements across the demec points to measure the change in length were taken after 47, 83, 152, 207, 337, 502 and 660 days of immersion in the sulfate solution. Based on the results, following conclusions were drawn: (i) initial moist curing of concrete (at 45°C) followed by dry curing at 45°C , 25% RH resulted in lower sulfate resistance than initial air curing at low relative humidity (25% and 55% RH); (ii) sulfate resistance of concrete increased with the replacement of cement with 22% PFA, 9% silica fume, 80% GGBF slag. The sulfate resistance also increased due to drying out of concrete during early curing at low relative humidity and due to carbonation; and (iii) the use of PFA (22%), silica fume (9%) and GGBS (80%), for partial replacement of OPC, resulted in higher sulfate resistance than for plain concrete under curing conditions.

Gollop and Taylor (1996) examined the cubes of a blended cement paste stored for 6 months in solutions of Na_2SO_4 or MgSO_4 by scanning electron microscopy. The blend of cement contained 31% of PC and 69% of blast furnace slag (GGBS). They concluded that: (i) tendency of the materials made with slag cements to soften

and disintegrate as a result of sulfate attack rather than to expand; (ii) when a blend containing 69% of blast furnace slag was stored in $0.25 \text{ mol l}^{-1} \text{ Na}_2\text{SO}_4$ solution, the principal chemical reaction resulted in partial decalcification of the C-S-H and replacement of an AFm phase, loosely described as mono-sulfate, by ettringite. The results suggested that neither Al^{+3} substituted in the C-S-H, nor that present in hydrotalcite, was available for reaction with sulfate; (iii) storage in $0.25 \text{ mol l}^{-1} \text{ MgSO}_4$ solution produced the same reaction, but the dominant effects in this case were decomposition of the C-S-H and formation of brucite and gypsum in the surface regions below the cube faces and of magnesium silicate hydrate and gypsum at the cube edges; (iv) SO_4^{2-} ions penetrated to a depth of about 1 mm below the cube faces and probably more deeply at the edges. These results were similar to those observed with a sulfate-resisting PC under similar conditions; (v) the micro-structural features of the deposits of gypsum, and of the brucite formed on reaction with MgSO_4 differed from those observed with the plain PC. The quantity of gypsum formed in the paste stored in Na_2SO_4 solution was probably less for the slag blend; (vi) damage from sulfate attack was attributed partly to decalcification, which weakened the C-S-H matrix, and partly to ettringite formation, which caused expansion and cracking; and (vi) In typical cases of blends high in slag, at least as much sulfur entered the hydration products in sulfide as in sulfate.

El-Darwish et al. (1997) studied the replacement of OPC by ground steel slag up to 30% volume replacement in concrete. Concrete specimens exposed to sodium and magnesium sulfate solutions containing 3.5% SO_3 and seawater were monitored for expansion, loss of strength and stiffness up to one year. Samples in seawater and sodium sulfate solutions performed satisfactorily. However, C-S-H gel transformed into M-S-H in magnesium sulfate solution.

Cao et al. (1997) investigated the sulfate resistance of Portland cements and blended cements. Four Portland cements of different characteristics and blended cements containing fly ash, ground granulated blast furnace slag and silica fume were used. Mortar cubes were made with water-to-binder ratio of 0.6, sand-to-binder ratio of 2.75 and cured for 7 days prior to immersion in sulfate solutions. Three sulfate solutions were: (i) 5% Na_2SO_4 solution having pH 12; and (ii) 5% Na_2SO_4 and maintained at nominal pHs of 7 and 3 by automatic titration with 10% H_2SO_4 at regular set intervals. ASTM C 1012-95a, (1995) procedure was followed to evaluate the performances of binders in sulfate solutions maintained at different pH levels ranging from 3 to 12 using expansion of mortar prisms (ASTM C 1012) and strength development of mortar cubes. The results indicated that sulfate resistance of cementitious materials was dependent on its composition and on the pH of the environment. Portland cement with low C_3A and low C_2S performed well in all sulfate solutions. Blended cements containing silica fume and fly ash (particularly at 40% replacement) showed a much superior performance than any of the Portland cements used. For slag blended cement, this can be achieved when the replacement percentage was higher than 60%. The selection of the mineral admixture and its replacement dosage became more critical as the pH of the sulfate solution decreased. It was found that 40% fly ash blend, 5% silica fume blend or a high slag blend

(80%) provided a good overall performance related to resistance to sulfate attack over a wide pH range.

Higgins (2003) studied the influence of addition of a small percentage of calcium carbonate or calcium sulfate on the sulfate resistance of concrete containing ground granulated blast furnace slag. Six concrete mixtures were made having water/cementitious ratio of 0.5 and total cementitious content of 350 kg/m³. Three test methods were employed to assess sulfate resistance at 20°C: (i) 100-mm cubes were immersed in magnesium (containing 1.5% SO₃) and sodium sulfate solutions (containing 1.5 and 2.4% SO₃) and monitored for corner-loss and strength-loss, over six years; and (ii) 20 × 20 × 160 mm prisms made of mortar were immersed in magnesium and sodium sulfate solutions and their expansions monitored for up to six years.

Compressive strength of the cubes stored in water and in the sulfate solutions are given in Table 1.17. The strengths in the sulfate solutions are expressed as a percentage of the strength of equivalent concretes stored in water for the same age. Table 1.18 shows the ‘wear ratings’ of the cubes, measured annually. ‘Wear rating’ is taken as the measure of the attack on the corners of a cube. It is the average depth of erosion or damage for one corner (in mm).

In sodium sulfate solution, the PC concrete had almost completely disintegrated by 6 years, while the GGBS concretes showed minor strength- and corner-loss. As would be expected, 70% GGBS concrete was more resistant to attack than 60% GGBS concrete. The lower level of addition of calcium sulfate (to increase the SO₃ level of the cementitious to 2%), significantly increased the degree of attack. However at the higher level of addition of calcium sulfate (to increase the SO₃ level of the cementitious to 3%) the degree of attack was reduced, as was also the case with the addition of calcium carbonate.

In magnesium sulfate solution, the PC concrete performed somewhat better, whereas the GGBS concretes performed distinctly less well in the magnesium than the sodium solution. This is what is normally observed (Osborne, 1990) with GGBS concrete generally more susceptible to attack by magnesium sulfate than sodium sulfate. Once again 70% GGBS concretes were more resistant than 60% and the

Table 1.17 Compressive strength in water and in sulfate solutions (Higgins, 2003)

	Compressive strength in water (N/mm ²)						% strength in Na ₂ SO ₄			% strength in MgSO ₄		
	3- day	7- day	28- day	1- year	2- year	6- year	1- year	2- year	6- year	1- year	2- year	6- year
Portland cement	34	41	53	66	68	69	97	87	0	85	74	28
60% GGBS	17	31	48	65	69	73	106	97	62	95	75	18
70% GGBS	13	28	49	63	66	71	105	89	90	94	77	28
60% GGBS + CaCO ₃	15	28	45	67	69	76	99	97	84	96	83	41
60% GGBS 2% SO ₃	19	29	47	68	67	72	97	99	33	94	81	19
60% GGBS 3% SO ₃	18	32	50	62	69	75	102	99	80	94	88	50

Table 1.18 Wear rating in sulfate solutions (Higgins, 2003)

	Wear rating in Na ₂ SO ₄ solution						Wear rating in MgSO ₄ solution					
	1- year	2- year	3- year	4- year	5- year	6- year	1- year	2- year	3- year	4- year	5- year	6- year
Portland cement	1	1	1	3	10	71	1	1	1	0	0	2
60% GGBS	2	2	3	5	9	12	4	6	7	10	15	23
70% GGBS	2	3	3	3	2	3	5	4	6	6	7	6
60% GGBS + CaCO ₃	0	2	2	2	2	3	1	2	4	4	7	9
60% GGBS 2% SO ₃	1	4	12	11	15	22	1	4	8	9	14	20
60% GGBS 3% SO ₃	1	2	2	1	1	3	1	2	4	2	2	5

lower level of addition of calcium sulfate gave no advantage. The higher level of addition of calcium sulfate and the addition of calcium carbonate both reduced the degree of attack.

For PC concrete, the expansion was rapid, reaching 1% after about 9 months in all solutions. In sulfate solutions the 60% GGBS specimens disintegrated at a relatively low expansion of less than 0.1%. The 70% GGBS and the specimens with additions of calcium sulfate or carbonate, all survived with low expansions, although the lower level of calcium sulfate addition showed signs of more rapid expansion at 72 months. In magnesium sulfate, expansion is more rapid and severe. All the specimens had disintegrated by 48 months. Once again the higher level of addition of calcium sulfate and the addition of calcium carbonate, proved particularly beneficial.

Higgins and Crammond (2003) investigated how cement-type, aggregate-type and curing, affect the susceptibility of concrete to the thaumasite form of sulfate attack (TSA). The cements were Portland cement (PC), sulfate-resisting Portland cement (SRPC) and a combination of 70% ground granulated blast furnace slag (GGBS) with 30% PC. These were combined with various carbonate aggregates or a non-carbonate control. Initial curing was either in water or in air. Concrete cubes were immersed in four strengths of sulfate solution at 5 and 20°C up to six years. They concluded that: (i) Deterioration, consistent with TSA was found to occur on all of the PC and SRPC concretes made with carbonate aggregate and stored in sulfate solutions at 5°C; (ii) degree of TSA increased with the sulfate concentration of the test solution and with time; (iii) at 5°C, there was no discernible difference between the performance of SRPC concretes containing carbonate aggregates and those made with PC; (iv) concretes made with 70%GGBS/30%PC and normal quality carbonate aggregates performed extremely well and showed no evidence of TSA in any of the solutions, with either normal or high-alumina GGBS. However concretes made with 70%GGBS/30%PC and inferior quality carbonate aggregates did not perform well at either 5 or 20°C; (v) an initial air-cure proved beneficial against both conventional sulfate attack and TSA. After six years, the air-cured 70% GGBS concretes showed no evidence of attack, even in

the strongest sulfate solution; (vi) presence of carbonate in the mix substantially improved the resistance of 70%GGBS/30%PC concretes to conventional sulfate attack; and (vii) overall, the worst performers were concretes made with PC. However, the concretes made with PC, appeared slightly less susceptible to conventional sulfate attack than those made with 70%GGBS/30% PC and it would appear that the low C_3A PC used in the present study, had some sulfate-resisting properties.

1.4.4 Alkali Silica Reaction

Alkali Silica Reaction (ASR) is a chemical reaction between alkalis in Portland cement and certain types of silica in aggregates. It results in the formation of expansive gels, which lead to cracking of the concrete. The cycle continues until the concrete is no longer serviceable. The presence of ASR will initially produce an expansion of the concrete that can be measured. GGBS could be very effective in controlling ASR because: (i) GGBS reduces the alkalinity of the concrete, and thus the alkali-silica ratio; (ii) GGBS reduces mobility of alkalis in the concrete; and (iii) GGBS reduces free lime in the concrete which is regarded as an important factor for alkali silica reaction.

Hester et al. (2005) made a comparative assessment of the effects of alkali-level of GGBS on potential alkali-silica reactivity of concrete. Expansion tests were performed on a matrix of concrete mixes using Irish normal Portland cement, two slags of differing alkali content (less than 1% and more than 1%), three aggregates and alkali loads of 5 and 6 kg Na_2O_{eq}/m^3 . Cement was replaced with 50% slag. They concluded that: (i) partial replacement of Portland cement with slag at a replacement level of 50% significantly reduced the expansion of the concrete in expansion tests; and (ii) no significant difference in behavior was observed, irrespective of aggregate type or alkali load, indicating that the alkali level of the slag was is not a contributory factor at the 50% replacement level.

These trends are supported by Arano and Kawamura (2000). They carried out similar tests to those described on one aggregate combination at replacement levels of 5, 10, 20, 30, and 60%. The degree of expansion decreased as the replacement level increased. Expansion percentage was 0.18, 0.17, 0.08, 0.02, and 0.0% at 0, 5, 20, 30, and 60% slag replacement level, respectively.

1.4.5 Freezing and Thawing Resistance

Stark (1997) studied the frost resistance and deicing salt resistance of slag cement using dynamic modulus of elasticity and RILEM CDF (Capillary suction of deicing solution and Freeze-thaw) test for deicing salt resistance. Frost resistance of slag concrete was highly dependent on the degree of hydration. Carbonation was more important than the degree of hydration on resistance to deicing salt.

Stark and Ludwig (1997) discussed the improved freeze-thaw performance of concrete made with a high content of blast furnace slag (more than 60%). The freeze-deicing salt resistance of blast furnace cement concrete was related to the carbonation of the surface which increases the capillary porosity and leads to metastable calcium carbonates that are soluble in NaCl. The degree of hydration at the beginning of freezing determines the pore size distribution and the strength of the structure.

Knaack and Stark (1997) studied the super-sulfated cements containing 75–85% of highly basic slag with alumina content greater than 15%. Compared to conventional slag cements, these systems are mainly activated by a high amount of gypsum with only a small amount of Portland cement. Super-sulfated cements displayed lower performances in scaling and freeze-thaw tests due to a lower degree of hydration at age of 28 days.

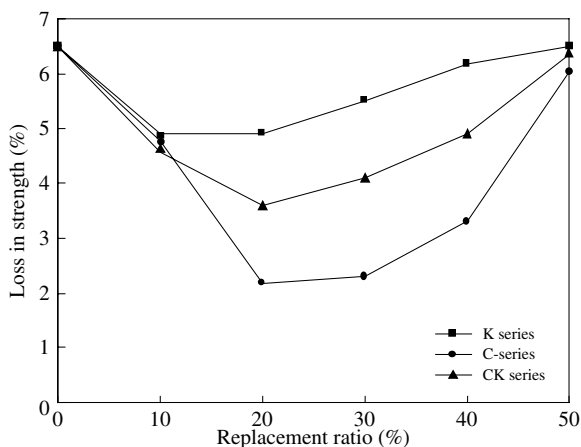
Nanaumi et al. (1997) discussed the difficulty of generating a suitable air-void system in concrete with anti-washout admixtures. They studied the frost resistance of blast furnace slag concrete (with 30–60% per cement unit addition) and plastic micro-spheres using cellulose ether as anti-washout admixture. At 60% addition of slag and 2% (per cement unit) addition of micro-spheres, scaling resistance was improved.

Yuksel et al. (2007) investigated the usage of granulated blast furnace slag (GBFS), bottom ash (BA), and combination of both as partial replacement of fine aggregate on the concrete durability. Three series concrete were produced i.e., of GBFS, BA and GBFS+BA, which were coded as C, K, and CK, respectively. Five test groups were constituted with the replacement percentages as 10, 20, 30, 40, and 50% in each series. 70 mm cubes specimens were made. Freezing–thawing resistance was measured by freezing and thawing the specimens in water. Specimens were settled completely under water in a tray. The specimens in the tray were freeze at -20°C for 18 h. After 18 h, the tray was placed in 20°C water pool and specimens were thawed for 6 h. These cycles were repeated 50 times. Then, weight losses of the specimens were determined and compressive strength tests were conducted. The 90-day's compressive strength values are used as reference values to compare the strength of specimens after the freeze–thaw cycles. Compressive strength losses of the specimens with respect to by-product replacement ratios are given in Fig. 1.19. For three series, resistance to freeze–thaw increased up to 20% replacement. However, it decreased again for the replacement level above 20%. C-series gave the best performance among the three series. For all the series, the loss in strength was below the loss in strength value for reference concrete.

1.4.6 Corrosion Resistance

Corrosion of reinforcements embedded in concrete is the most common cause of deterioration of concrete structures. Corrosion of steel reinforcement leads to cracking and eventually spalling of concrete. Due to the high alkalinity of concrete pore fluid, steel in concrete initially and, in most cases, for sustained long periods of

Fig. 1.19 Freezing-thawing test results (Yüksel et al., 2007)



time, remains in a passive state. Initiation of corrosion is either due to reduction in alkalinity arising from carbonation or the breakdown of the passive layer by the attack of chloride ions. The time to initiation of corrosion is determined largely by the thickness and the quality of concrete cover as well as the permeability of concrete.

Good quality durable concrete reduces the rapid deterioration of concrete under severe environmental conditions. For making good quality durable concrete, use of GGBS is very advantageous. It not only reduces the porosity but also the pores become finer and the change in mineralogy of the cement hydrates leads to a reduction in the mobility of chloride ions (Li and Roy, 1986). Torii et al. (1995) reported that the resistance to chloride ion penetration of 50% GGBFS concrete was almost the same as that of 10% silica fume concrete.

Mangat and Molloy (1991) studied the corrosion of steel reinforcement electrodes embedded in different matrices of concrete which were exposed to simulated marine splash zone exposure for about 600 days (1200 cycles) after initial curing in air for 14 days. The corrosion potentials and polarization resistance were monitored at regular intervals to determine the state and rate of corrosion. The control mix had proportions by weight 1:2.5:1.2 with a water/cement ratio of 0.58. The cement content was 430 kg/m³. The concrete matrices included different cement replacement levels of PFA (15, 20, and 25%), GGBS (20, 40, and 60%) and (5, 10, and 5%) micro-silica, at a water/ (cement + blend) ratio of 0.58. The results showed that: (i) replacement of cement by 15% PFA had no significant influence on corrosion rates of rebar in concrete. At higher PFA contents (up to 25%), corrosion rates increased after long-term exposure to a chloride environment; (ii) replacement of cement by up to 40% GGBFS had no significant influence on rebar corrosion. At 60% GGBFS content the corrosion rate of reinforcement was significantly reduced; (iii) Corrosion rates of rebar in concrete were significantly reduced at 10 and 15% replacement of cement by micro-silica solids; (iv) Cl⁻ concentrations in micro-silica concrete were greatly reduced while Cl⁻/OH⁻ ratios increased due to a reduction in alkalinity with

increasing micro-silica content; (v) The corrosion process of reinforcement in plain concrete, PFA concrete and concrete with low contents of GGBS was similar and was anodically controlled. In microsilica and GGBFS (60% replacement) concretes the cathodic polarization increased greatly although control of corrosion remained principally anodic; and (vi) Chloride concentration of the pore fluid gave a more reliable indication of corrosivity of a matrix than Cl^-/OH^- ratio, especially when comparing concretes with different types and contents of replacement materials.

Al-Amoudi et al. (1993) investigated the long-term corrosion resistance of steel rebars in 5% sodium chloride solution. The results of regression analyses indicated excellent correlation between corrosion resistance and porosity for both plain and blended cement concretes. It was found that the corrosion rate of the steel rebar in GGBFS containing concrete specimens was about between one-half and one-twelfth of those in plain concrete specimens.

Jau and Tsay (1998) evaluated the slag cement subjected to seawater corrosion by conducting various investigations such as compressive strength, permeability, electrical resistance, concentration of chloride ions corrosion potential and pore size distribution at various ages and concluded that slag concrete with 20–30% substitution has the best corrosion resistance properties.

Pal et al. (2002) studied the corrosion behavior of embedded reinforcement under different proportions of slag. In the study corrosion of steel was examined electrochemically and also by an accelerated carbonation test. Table 1.19 shows the results obtained from the study. It can be seen from this table that as the slag content increased, the corrosion rate, weight loss, half cell potentials and the carbonation depth were found to be decreasing.

Yeau and Kim (2005) investigated the role of ground granulated blast-furnace slag (GGBS) on the corrosion resistance of concrete. Concrete mixtures were made with two types of cements (ASTM Type I or ASTM Type V) and varying percentages (0, 25, 40, and 55%) of GGBS. These concrete mixtures were proportioned to have the 28-day strength of 35 MPa. Accelerated steel corrosion (ASC) test was conducted to measure half-cell potential and the surface areas of steel bars corroded. $150 \times 150 \times 500$ mm concrete specimens with three different covers, 10, 20, and 30 mm. were prepared. Repeated wetting and drying method was used to accelerate steel corrosion. After curing the concrete specimens in water for three different numbers of days, 28 days, 56 days, and 91 days, these tests were conducted up to 30 cycles. For each wetting–drying cycle, test specimens were wetted in 3% NaCl

Table 1.19 Comparison of weight loss, icorr, half-cell potential and carbonation depth for different slag replaced concrete (Pal et al., 2002)

Concrete	Weight loss (mg)	Icorr (A/m^2)	Half-cell potential (mV)	Carbonation depth (m)
Reference concrete	0.33	0.1169	−503	2.0
30% slag concrete	0.27	0.0823	−108	2.0
50% slag concrete	0.29	0.1239	−176	1.0
70% slag concrete	0.26	0.0842	−31	1.0

solution for 3 days and then dried at 60 8C for 4 days. After 30 weeks, the specimens were crushed out and the surface area corroded was calculated as a percentage to the total area of steel embedded in concrete. Figure 1.20 presents the test results obtained from the measurements of the surface area corroded from steel bars after concrete specimens were cured for 56 days in water and then the accelerated corrosion tests were carried out by 30 wetting–drying cycles. The results showed that the corroded surface area (%) depended on the thickness of the concrete cover, as well as the amount of GGBS mixed. The corroded areas of steel embedded in control concrete mixtures were about 2 times and 3 times larger than those of steel involved in 40% GGBS concrete mixture and 55% GGBS concrete mixture, respectively. Upon comparison of the corroded surface areas, the proportion of corroded areas in Type I cement was lower than that of the corroded areas in Type V cement. These results suggested that the resistance to steel corrosion can be superior, since not only Type I cement was used, but also the amount of GGBS was increased.

Cheng et al. (2005) studied the influence of GGBS on corrosion behavior of reinforced concrete beams (150 mm × 150 mm × 900 mm) under various loading ratios (37 and 75% of the ultimate load) and exposed to 3.5% NaCl solution. Beams were made of three concrete mixes (A, B, and C). Mix A was control one with mixture proportion 1:1.82:1.97 with water-binder ratio of 0.55. Mixes B and C were made by replacing cement with 40 and 60% of GGBS, respectively. A direct current (1mAcm^{-2}) was applied to accelerate the corrosion process. Open circuit potential (OCP) and direct current polarization resistance were obtained to evaluate the rebar corrosion. As per ASTM C 876, (1991), when OCP is higher than -127mV (SCE), there is only 10% probability that the reinforcement may corrode. If the potential is from -127 to -276mV (SCE), corrosion probability is uncertain. Corrosion probability may be higher than 90% for OCP between -276 and -427mV (SCE). Corrosion test results indicated that: (i) without sustained loading, mixes with 40% and 60% GGBS significantly increased the exposure time span to severe corrosion in comparison with control mix; (ii) GGBS replacement for cement refined the pore

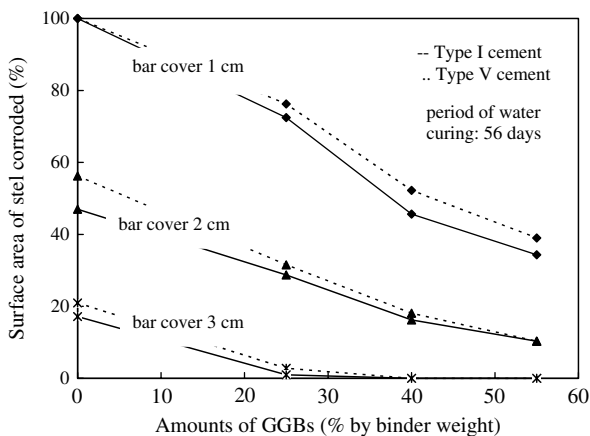
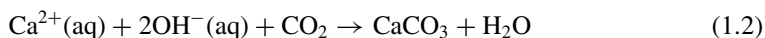


Fig. 1.20 Surface area (%) corroded from steel bars in concrete specimens (Yeau and Kim, 2005)

structure and reduced the corrosion probability of reinforcing steel; (iii) although, the pH value was 13.2 for control concrete, 12.8 for 40% GGBS replacement concrete and 12.4 for 60% GGBS replacement concrete, respectively. There seemed no prominent negative effect on the corrosion behavior due to decreasing alkalinity in pore solution; (iv) with 37% loading ratio, the OCP of control specimen dropped from -75 to -427mV (SCE) after 4-day accelerated exposure. Mix (40% GGBS) specimen and mix (60% GGBS) specimen reach severe corrosion condition after 6–8-day exposure, which revealed that sustained loading or cracks plays paramount role in the corrosion process of reinforcing steel in concrete.; (v) for the control specimen men with 75% sustained loading, the potential dropped below -427mV (SCE) even after 2-day accelerated corrosion process and GGBS concretes having cracks wider than 0.02mm had no better corrosion resistance; and (vi) at higher sustained loading ratio, OCP did not significantly vary among the three mixes, and the corrosion process was controlled by the pre-determined cracks.

1.4.7 Carbonation

Carbonation is a slow process under natural conditions. Although the concentration of carbon dioxide (CO_2) present in the atmosphere is between $0.03\text{--}0.10\%$ by volume, it is highly reactive with cement hydrates such as calcium hydroxide [$\text{Ca}(\text{OH})_2$] and calcium silicate hydrate (C-S-H or $3\text{CaO} \cdot 2\text{SiO}_2 \cdot 3\text{H}_2\text{O}$), as well as non-hydrated cement phases such as tricalcium silicate (C_3S or $3\text{CaO} \cdot \text{SiO}_2$) and dicalcium silicate (C_2S or $2\text{CaO} \cdot \text{SiO}_2$). Among these phases, CO_2 has a greater affinity for reaction with $\text{Ca}(\text{OH})_2$. The overall reactions can be represented as shown by the following irreversible reactions (Leberand and Blakey 1956; Papadakis et al. 1989).



Steel embedded in concrete is usually protected from corrosion by a thin oxide layer that is formed and maintained on the surface due to the highly alkaline environment of the surrounding concrete (pH value around 13). However, due to the reactions in (1.1–1.5), the pH of pore water drops to a value as low as 8.5 in the case of severe carbonation (Gjorv, 1989). The passive layer on the steel surface will no longer remain stable when the alkalinity of the concrete surrounding the steel drops to approximately 11.5.

Sulapha et al. (2003) studied the carbonation of concrete incorporating ground granulated blast-furnace slag, fly ash and silica fume. In the concrete mixtures, OPC was partially replaced with GGBS, FA and SF. The replacement percentages of

GGBS (having $4,500\text{ cm}^2/\text{g}$ fineness) were 30, 50, and 65%; the replacement level of GGBS (with $6,000$ or $8,000\text{ cm}^2/\text{g}$ fineness) was 65%. Only two replacement percentages were used for FA (15 and 30%) and SF (5 and 10%). Prisms of size $100 \times 100 \times 400\text{ mm}$ were cast. The carbonation depth of the specimens was monitored every two weeks in the first two months, and thereafter once a month up to 12 months. After a certain exposure period, the specimens were split and freshly broken surfaces were sprayed with a standard solution of 1% phenolphthalein in 70% ethyl alcohol. In the noncarbonated region with pH values above 9.2, the indicator turned purple-red; in the carbonated portion with pH less than 9.2, the solution remained colorless. The distance between the color change boundary and the concrete surface was measured as the carbonation depth. Based on the results obtained, they concluded that: (i) lower w/b (0.3–0.6) and a prolonged curing age in water (from one to 28 days) generally led to a slower rate of carbonation, possibly due to pore structure densification; (ii) carbonation rate of low fineness GGBS ($4,500\text{ cm}^2/\text{g}$) and FA concrete increased with an increase in OPC replacement level. In the case of SF, both replacement percentages (5 and 10%) led to a lower carbonation rate compared to that of OPC. However, 5% replacement showed a better performance than 10% replacement; (iii) concrete containing low fineness GGBS ($4,500\text{ cm}^2/\text{g}$) and FA exhibited higher rates of carbonation than plain OPC concrete. The reduction in Ca(OH)_2 content seemed to have more influence over pore refinement, and hence led to faster rates of carbonation; (iv) concrete incorporating GGBS of higher fineness ($6,000$ and $8,000\text{ cm}^2/\text{g}$) and silica fume, the carbonation rates were lower than that of plain OPC concrete. The pore modification, being more dominant than the change in Ca(OH)_2 content, appeared to control the carbonation rate; (v) ternary blended concrete containing 35% OPC, 55% GGBS, and 10% SF showed a higher carbonation rate than the plain OPC mixture and 10% SF concrete. Compared to 65% GGBS concrete, the ternary blended concrete exhibited a lower rate of carbonation; and (vi) the Ca(OH)_2 content of concrete decreased with an increased OPC replacement percentage by GGBS (30–65%), FA (15–30%), or SF (5–10%), due to the pozzolanic reaction. As compared to GGBS or FA concrete, the reduction in Ca(OH)_2 was much smaller for SF concrete due to its lower replacement levels. Hence, SF concrete generally showed higher carbonation resistance, since pore refinement was likely to dominate over the change in Ca(OH)_2 content.

References

- ASTM C 876 (1991) Standard test method for half-cell potentials of uncoated reinforcing steel in concrete, Annual Book of ASTM Standards, American Society for Testing and Materials.
- ASTM C 232 (1992) Standard test methods for bleeding of concrete. ASTM Standards, Vol. 4.02:13942, Annual Book of ASTM Standards, American Society for Testing and Materials.
- ASTM C 1012-95a (1995) Standard test method for length change of hydraulic cement mortars exposed to a sulfate solution. Annual book of ASTM Standards, Sect. 1.4 – Construction, Vol. 4.01, Cement; lime; gypsum pp. 450–456.

- ASTM C 1202 (1997) Standard test method for electrical indication of concrete's ability to resist chloride ion penetration, Vol. 4.02, Annual Book of ASTM Standards, American Society for Testing and Materials.
- ASTM C39/C39M (2004) Standard test method for compressive strength of cylindrical concrete specimens, Vol. 4.02, Annual Book of ASTM Standards, American Society for Testing and Materials.
- Al-Amoudi OSB, Rasheeduzzafar MM, Al-Mana AI (1993) Prediction of long-term corrosion resistance of plain and blended cement concretes. *ACI Materials Journal* 90 (6): 564–570.
- Aldea C, Young F, Wang K, Shah SP (2000) Effect of curing conditions on properties of concrete using slag replacement. *Cement Concrete Research* 30: 465–72.
- Arano N, Kawamura M (2000) Comparative consideration on the mechanisms of ASR suppression due to different mineral admixtures. In: Be'rube' MA, Fournier B, Durand B, (Eds.), *Proceedings of the 11th International Conference on Alkali-Aggregate Reaction in Concrete*, Quebec, pp. 553–62.
- Babu KG, Kumar VSR (2000) Efficiency of GGBS in concrete. *Cement and Concrete Research* 30: 1031–1036.
- Basheer PAM, Gilleece PRV, Long AE, McCarter WJ (2002) Monitoring electrical resistance of concretes containing alternative cementitious materials to assess their resistance to chloride penetration. *Cement and Concrete Composites* 24: 437–449.
- Cao HT, Bucea L, Ray A, Yozghatlian S (1997) The effect of cement composition and pH of environment on sulfate resistance of Portland cements and blended cements. *Cement and Concrete Composites* 19: 161–171.
- Cheng A, Huang R, Wu JK, Chen CH (2005) Influence of GGBS on durability and corrosion behavior of reinforced concrete. *Materials Chemistry and Physics* 93: 404–411.
- Daube J, Bakker R (1983) Portland blast-furnace slag cement: a review. *Blended Cement ASTM-STP 897*, 5 pp.
- Dhir RK, El-Mohr MAK, Dyer TD (1996) Chloride binding in GGBS concrete. *Cement and Concrete Research* 26 (12): 1767–1773.
- Douglas E, Bilodeau A, Brandstetr J (1991) Alkali activated ground granulated blast-furnace slag concrete: Preliminary investigation. *Cement and Concrete Research* 21: 101–108.
- El-Darwish I, Kurdi A, Mahmoud H, El-Kair HA (1997) Mechanical properties and durability of Portland cement concrete incorporating ground steel making slag. *AEJ Alexandria Engineering Journal* 36, Alexandria University Alexandria.
- Gao JM, Qian CX, Liu HF, Wang B, Li L (2005) ITZ microstructure of concrete containing GGBS. *Cement and Concrete Research* 35 (7): 1299–1304.
- Gjovr OE (1989) Mechanism of corrosion of steel in concrete structures. *Proceedings International Conference on Evaluation of Materials Performance in Severe Environment (EVALMAT 89)*. The Iron and Steel Institute of Japan, Kobe, Japan pp. 565–578.
- Gollop RS, Taylor HFW (1996) Micro structural and micro analytical studies of sulfate attack. IV. Reactions of a slag cement paste with sodium and magnesium sulfate solutions. *Cement and Concrete Research* 26 (7): 1013–1028.
- Hester D, McNally C, Richardson M (2005) A study of the influence of slag alkali level on the alkali-silica reactivity of slag concrete. *Construction and Building Materials* 19: 661–665.
- Higgins DD (2003) Increased sulfate resistance of GGBS concrete in the presence of carbonate. *Cement and Concrete Composites* 25: 913–919.
- Higgins DD, Crammond NJ (2003) Resistance of concrete containing GGBS to the thaumasite form of sulfate attack. *Cement and Concrete Composites* 25: 921–929.
- Hogan FJ, Meusel JW (1981). Evaluation for durability and strength development of a ground granulated blast furnace slag. *Cement Concrete Aggregate* 3 (1): 40–52.
- Hooton RD, Titherington MP (2004) Chloride resistance of high-performance concretes subjected to accelerated curing. *Cement and Concrete Research* 34: 1561–1567.
- Huang R, Yeih W-C (1997) Assessment of chloride diffusion in high strength concrete using the accelerated ionic migration test. *Journal of the Chinese Institute of Engineers, Taipei Taiwan, Series A/Chung-kuo Kung Ch'eng Hsueh K'an* 20: 39–45.

- Hwang CL, Lin CY (1986) Strength development of blended blast furnace slag cement mortars. *ACI SP 91*: 1323–40.
- Jau WC, Tsay DS (1998) A study of the basic engineering properties of slag cement concrete and its resistance to sea water corrosion. *Cement and Concrete Research* 28 (10): 1363–1371.
- Jianyong L, Yan Y (2001) A study on creep and drying shrinkage of high performance concrete. *Cement and Concrete Research* 31: 1203–1206.
- Khatib JM, Hibbert JJ (2005) Selected engineering properties of concrete incorporating slag and metakaolin. *Construction and Building Materials* 19: 460–472.
- Knaack U, Stark J (1997) Frost and frost-deicing salt resistance of super-sulfated cement concrete, Frost Resistance of Concrete. Proceedings of the International RILEM Workshop on Resistance of Concrete to Freezing and Thawing with or Without De-icing Chemicals, Essen, Germany, pp. 139–146.
- Leberand I, Blakey FA (1956) Some effects of carbon dioxide on mortar and concrete. *ACI Materials Journal* 28: 295–308.
- Li S, Roy DM (1986) Investigation of relations between porosity, pore structure and chloride diffusion of fly ash blended cement pastes. *Cement and Concrete Research* 16: 749–759.
- Li G, Zhao X (2003) Properties of concrete incorporating fly ash and ground granulated blast-furnace slag. *Cement and Concrete Composites* 25: 293–299.
- Luo R, Cai Y, Wang C, Huang X (2003) Study of chloride binding and diffusion in GGBS concrete. *Cement and Concrete Research* 33: 1–7.
- Malvern Mastersizer (2000) Particle size analyser. Malvern Instruments Ltd., Worcestershire, U.K.
- Mangat PS, El-Khatib JM (1992) Influence of initial curing on sulfate resistance of blended cement concrete. *Cement and Concrete Research* 22: 1089–1100.
- Mangat PS, Molloy BT (1991) Influence of PFA, slag and microsilica on chloride induced corrosion of reinforcement in concrete. *Cement and Concrete Research* 21: 819–834.
- Miura T, Iwaki I (2000) Strength development of concrete incorporating high levels of ground granulated blast-furnace slag at low temperatures. *ACI Materials Journal* 97 (1): 66–70.
- Nanaumi T, Ayuta K, Yamakawa T (1997) Frost resistance of antiwashout underwater concrete containing expanded plastic micro-spheres and blast-furnace slag. *Semento Konkurito Ronbunshu* 51: 90–95 (Chem. Abstr. 128, 208152).
- Olorunsogo FT (1998) Particle size distribution of GGBS and bleeding characteristics of slag cement mortars. *Cement and Concrete Research* 28 (6): 907–919.
- Osborne GJ (1990) The effectiveness of a carbonated outer layer to concrete in the prevention of sulfate attack. Proceedings of International Conference on the Protection of Concrete, University of Dundee, UK.
- Pal SC, Mukherjee A, Pathak SR (2002) Corrosion behavior of reinforcement in slag concrete. *ACI Materials Journal* 99 (6): 1–7.
- Papadakis VG, Vayenas CG, Fardis M N (1989) A reaction engineering approach to the problem of concrete carbonation. *AIChE Journal* 35 (10): 1639–1650.
- Quillin K, Osborne G, Majumdar A, Singh B (2001) Effects of w/c ratio and curing conditions on strength development in BRECEM concretes. *Cement and Concrete Research* 31: 627–632.
- Roy DM, Idorn GM (1982) Hydration, structure, and properties of blast furnace slag cement, mortars, and concrete. *American Concrete Institute Journal* 79: 444–457.
- Roy DM, Jiang W, Silsbee MR (2000) Chloride diffusion in ordinary, blended, and alkali-activated cement pastes and its relation to other properties. *Cement and Concrete Research* 30: 1879–1884.
- Stark J (1997) Frost resistance with and without deicing salt – a purely physical problem, Frost Resistance of Concrete. Proceedings of the International RILEM Workshop on Resistance of Concrete to Freezing and Thawing with or Without De-icing Chemicals, Essen, Germany, pp. 83–99.
- Stark J, Ludwig HM (1997) Freeze-thaw and freeze-deicing salt resistance of concretes containing cement rich in granulated blast furnace slag. *ACI Materials Journal* 94: 47–55.

- Sulapha P, Wong SF, Wee TH, Swaddiwudhipong S (2003) Carbonation of concrete containing mineral admixtures. *Journal of Materials in Civil Engineering* 15: 134–143.
- Tasong WA, Wild S, Tilley RJD (1999) Mechanism by which ground granulated blast furnace slag prevents sulfate attack of lime stabilized kaolinite. *Cement and Concrete Research* 29: 975–982.
- Torii K, Sasatani T, Kawamura M (1995) Effects of fly ash, blast furnace slag, and silica fume on resistance of mortar to calcium chloride attack. *Proceedings of 5th International Conference on Fly Ash, Silica Fume, Slag, and Natural Pozzolans in Concrete, SP-153, Vol. 2, American Concrete Institute*, pp. 931–949.
- Ujhelyi JE, Ibrahim AJ (1991) Hot weather concreting with hydraulic additives. *Cement and Concrete Research* 21: 345–354.
- Wainwright PJ, Ait-Aider H (1995) The influence of cement source and slag additions on the bleeding of concrete. *Cement and Concrete Research* 25 (7): 1445–1456.
- Wainwright PJ, Rey N (2000) The influence of ground granulated blast furnace slag (GGBS) additions and time delay on the bleeding of concrete. *Cement and Concrete Composites* 22: 253–257.
- Wan H, Shui Z, Lin Z (2004) Analysis of geometric characteristics of GGBS particles and their influences on cement properties. *Cement and Concrete Research* 34: 133–137.
- www.ecocem.ie Concrete mix design using GGBS. Ecocem Ireland Ltd., 56 Tritonville Road, Sandymount, Dublin 4, Ireland.
- Xu Y (1997) The influence of sulfates on chloride binding and pore solution chemistry. *Cement and Concrete Research* 27 (12): 1841–1850.
- Yeau KY, Kim EK (2005) An experimental study on corrosion resistance of concrete with ground granulate blast-furnace slag. *Cement and Concrete Research* 35: 1391–1399.
- Yuksel I, Bilir T, Ozkan O (2007) Durability of concrete incorporating non-ground blast furnace slag and bottom ash as fine aggregate. *Building and Environment* 42 (7): 2651–2659.

Chapter 2

Metakaolin

Introduction

Metakaolin (MK) is a pozzolanic material. It is obtained by calcination of kaolinitic clay at a temperature between 500°C and 800°C. The raw material input in the manufacture of metakaolin ($\text{Al}_2\text{Si}_2\text{O}_7$) is kaolin clay. Kaolin is a fine, white, clay mineral that has been traditionally used in the manufacture of porcelain. Kaolinite is the mineralogical term that is applicable to kaolin clays. Kaolinite is defined as a common mineral, hydrated aluminum disilicate, the most common constituent of kaolin. The meta prefix in the term is used to denote change. In the case of metakaolin, the change that is taking place is dehydroxylation, brought on by the application of heat over a defined period of time.

The behavior of clay minerals on heating depends on their structure, crystal size and degree of crystallinity. At just above 100°C, clay minerals lose most of their adsorbed water. The temperature at which kaolinite loses water by dehydroxylation is in the range of 500–800°C. This thermal activation of a mineral is also referred to as calcining. Beyond the temperature of dehydroxylation, kaolinite retains two-dimensional order in the crystal structure and the product is termed metakaolin. The key in producing metakaolin for use as a supplementary cementing material, or pozzolans is to achieve as near as possible complete dehydroxylation without over-heating. Successful processing of kaolinite results in a disordered, amorphous state, which is highly pozzolanic. Thermal exposure beyond a defined point will result in sintering and the formation of mullite, which is dead burnt and not reactive. In other words, kaolinite, to be optimally altered to a metakaolin state, requires that it is thoroughly roasted but never burnt.

Metakaolin is a silica-based product that, on reaction with $\text{Ca}(\text{OH})_2$, produces CSH gel at ambient temperature. Metakaolin also contains alumina that reacts with CH to produce additional alumina-containing phases, including C_4AH_{13} , C_2ASH_8 , and C_3AH_6 (Changling et al., 1995; Zhang and Malhotra, 1995).

Uses of Metakaolin

Metakaolin finds its usage in many aspects of concrete:

- High performance, high strength and lightweight concrete
- Precast concrete for architectural, civil, industrial, and structural purposes
- Fiber cement and ferrocement products
- Glass fiber reinforced concrete
- Mortars, stuccos, repair material, pool plasters
- Improved finishability, color & appearance.

Advantages of Using Metakaolin

- Increased compressive and flexural strengths
- Reduced permeability
- Increased resistance to chemical attack
- Increased durability
- Reduced effects of alkali-silica reactivity (ASR)
- Reduced shrinkage due to particle packing, making concrete denser
- Enhanced workability and finishing of concrete
- Reduced potential for efflorescence.

2.1 Properties of Metakaolin

2.1.1 Physical Properties

Metakaolin is 99.9% finer than 16 μm , and has a mean particle size of 3 μm (as measured by MicroTrac laser diffraction granulometer method (www.metakaolin.com)). Some physical properties of metakaolin are given in Table 2.1.

2.1.2 Chemical Composition

Major constituents of metakaolin are SiO_2 and Al_2O_3 . Typical chemical composition as reported by (Ambrose et al., 1994) is given in Table 2.2.

Metakaolin must meet the requirements of ASTM “C 618, Standard Specification for Coal Fly Ash and Raw or Calcined Natural Pozzolan for Use as a Mineral Admixture in Concrete,” Class N, with the following modifications as given in Table 2.3.

Table 2.1 Physical properties of metakaolin (www.metakaolin.com)

Property	Value
Specific gravity	2.60
Bulk density (g/cm ³)	0.3–0.4
Physical form	Powder
Color	Off-White
GE Brightness	79–82

Table 2.2 Typical chemical composition of metakaolin (Ambroise et al., 1994)

Ingredients	% by weight
SiO ₂	51.52
Al ₂ O ₃	40.18
Fe ₂ O ₃	1.23
CaO	2.0
MgO	0.12
K ₂ O	0.53
SO ₃	0.0
TiO ₂	2.27
Na ₂ O	0.08
L.O.I	2.01

Table 2.3 Requirements of metakaolin (ASTM C 618)

Modified specification requirements	Limit
Item	
Silicon dioxide (SiO ₂) plus aluminum oxide (Al ₂ O ₃) plus iron oxide (Fe ₂ O ₃)	Min 85%
Available alkalies	Max 1.0%
Loss on Ignition	Max 3.0%
Fineness: amount retained when wet-sieved on 45 μ m sieve	Max 1.0%
Strength activity index at 7 days (% of control)	85
Increase of drying shrinkage of mortar bars at 28 days	Max 0.03%

2.2 Hydration Reaction Mechanism

Ambroise et al. (1986) and Sayanam et al. (1989) demonstrated that thermal activation of clay minerals between temperatures of 600–900°C by dehydroxylation leads to breaking down or partial break down of crystal lattice structure forming a transition phase with high reactivity. One such example is the production of metakaolin (Al₂O₃.2SiO₂) or AS₂ by the calcinations of clay or lattice soils rich in kaolinite (Pera et al., 1998). The principal reaction is between AS₂ and CH derived from cement hydration, in the presence of water. This reaction forms additional cementitious C-S-H gel, together with crystalline products, which include calcium aluminate hydrates and aluminosilicate hydrates (C₂ASH₈, C₄AH₁₃ and C₃AH₆). The crystalline products depend principally on the AS₂/CH ratio and reaction temperature (Murat, 1983; Kinuthia et al., 2000; Wild et al., 1998).

The optimum replacement percentage of cement with MK is associated with the changes in the nature and proportion of the different reaction products, temperature

and reaction time. Hydration reaction depends upon the level of reactivity of MK in terms of the processing conditions and purity of feed clay. The feed clay (kaolin) should be either naturally pure or refined by standard mineral processing techniques, otherwise the impurities would act as diluents (Kostuch et al., 1993). Reactivity level of MK can be determined by Chapelle test (Kostuch et al., 1993; Asbridge et al., 1994). Table 2.4 presents the comparison of reactivity level of MK with silica fume (SF) and fly ash (FA). It is expressed as consumption rate of CH per gram of pozzolans. The amount of CH in hardened concrete can be determined by thermogravimetric analysis (TG) and differential thermal analysis (DTA). Besides this, the reactivity of pozzolans can also be assessed by chemical determination of unreacted pozzolan in hydrated PC-pozzolan pastes. Kostuch et al. (1993) have reported that: (i) CH was significantly reduced with age for all replacement levels (0, 10, and 20%); and (ii) 20% replacement of cement by MK was required to fully remove all the CH in concrete at 28 days where as Oriol and Pera (1995) reported that between 30 to 40% MK is required to remove all the CH in MK-PC paste at a water-binder ratio of 0.5 when cured in lime-saturated water for 28 days.

Ambroise et al. (1994) studied the early hydration period of pastes containing metakaolin using isothermal calorimetry and conductivity. Differential thermal analysis, X-ray diffraction, and Fourier transform infrared spectrometry were used to follow the consumption of calcium hydroxide (CH) and identify the products of reaction. The results showed that CH was quickly consumed, the microstructure was rich CSH and stratlingite (C_2ASH_8), and the pore size distribution displaced toward smaller values. At up to 30% replacement, MK acted as an accelerating agent, the pore size distribution was displaced toward small values, and the CH content was considerably reduced.

Klimesch and Ray (1998a) investigated autoclaved metakaolin-lime-quartz slurries with Ca/ (Si + Al) composition of 0.8 and Al/ (Si+Al) ratios between 0.03 and 0.38. Hydrogarnet (C_3ASH_6) was always among the first phases formed and invariably appeared before 11 Å tobermorite. With increasing reaction time for Al/(Si+Al) ratios ≤ 0.13 , the amount of hydrogarnet decreased and finally disappeared while 11 Å tobermorite increased concurrently. For Al/(Si+Al) ratios > 0.13 , hydrogarnet coexisted with 11 Å tobermorite after 4 h and beyond. Thus, in the presence of aluminous additives, hydrogarnet formation appeared to play a more significant role in relation to 11 Å tobermorite formations than was thought. Increasing addition of metakaolin retarded the lime-quartz reaction, while enhancing the initial C-S-H formation. At low MK additions, where Al/(Si + Al) ratios were 0.03 and 0.13, the amount of hydrogarnet decreased with the increasing reaction time and was not detected after 4 and 23 h of autoclaving, respectively. 11 Å tobermorite increased concurrently after 4 h. At higher MK additions, for autoclaving periods of up to 4 h, the amount of hydrogarnet remained essentially constant if the Al/(Si + Al) ratio

Table 2.4 Pozzolanic activity of various pozzolans (Asbridge et al., 1994)

Pozzolan	SF	FA	MK
Reactivity (mg) Ca (OH) ₂ /g pozzolan	427	875	1050

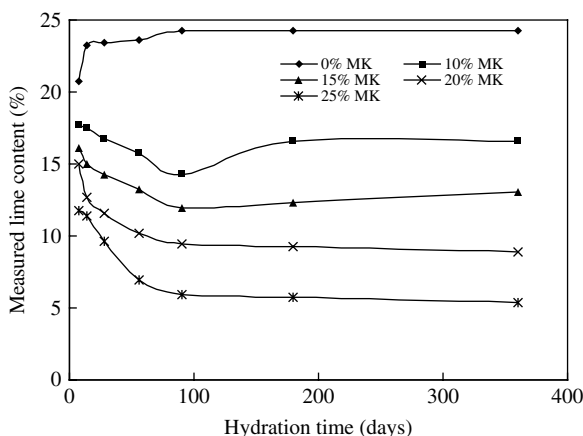
was 0.23, and increased if this ratio was 0.38. Hydrogarnet remained and coexisted with 11 Å tobermorite at these Al/(Si + Al) ratios, after 4 h autoclaving and beyond.

Klimesch and Ray (1998b) studied the effect of metakaolin (MK) additions on binding material and physical properties of cement-quartz pastes autoclaved at 180°C. For this purpose, a control cement-quartz mixture was prepared using 61.5% OPC and 38.5% quartz with the bulk C/S molar ratio (0.83) equivalent to that of C₅S₆H₅. MK was introduced at 6, 12, 18.25, 24, and 30.5% as a quartz replacement (constant % cement) in one series and as a cement replacement (constant % quartz) in another series. Water (deionized) to total solids ratio was 0.46 for all mixtures. They concluded that: (i) for MK additions of up to 12%, the amount of tobermorite formation decreased when cement was partially replaced, whereas the opposite effect was observed in the case of partial replacement of quartz. An overall decrease in both compressive strength and drying shrinkage occurred with MK additions. In autoclaved systems, MK provided a source of silica that was more reactive than ground quartz; (ii) when added as a quartz replacement, the amount of tobermorite decreased while hydrogarnet (C₃ASH₆) increased concurrently with increasing amount of MK, indicating that hydrogarnet may prevail upon tobermorite by competing with it for Al₂O₃ and possibly SiO₂. In contrast, when MK was added as a cement replacement, an increase in the tobermorite content was noted up to 12% addition followed by a sharp decrease at greater addition; and (iii) MK addition, as either quartz or a cement replacement, also indicated that unreacted MK will be present if the bulk Ca/Al molar ratio is less than 3. The decrease in these physical properties can be attributed mainly to increasing amounts of both hydrogarnet and α-C₂SH, and a general decrease in the C-S-H type binding phases.

Frías and Cabrera (2000) determined the degree of hydration of metakaolin (MK) and cement pastes. Cement was partially replaced with 0, 10, 15, 20 and 25% of MK. The water/binder was 0.55 by weight. In order to determine the degree of hydration of MK pastes, it is necessary to know the total amount of calcium present in the hydrated MK/OPC systems. The total calcium hydroxide was calculated taking into account the weight loss due to the dehydroxylation of Ca(OH)₂ and the decomposition of CaCO₃. Figure 2.1 shows the percentage of calcium hydroxide with the curing time up to 360 days. They concluded that: (i) calcium hydroxide contents of MK/OPC samples increased with age until 3±7 days. Subsequently, the values start decreasing, more or less depending on MK content; and (ii) in the cases of mixtures with 10 and 15% of MK, an inflexion point at 56 and 90 days, respectively was observed. Beyond this point, the calcium hydroxide content achieved a progressive increase. This behavior of calcium hydroxide content was due to different hydration mechanisms: the increase in the Ca(OH)₂ amounts are due to the OPC hydration, while the decrease in the values is related with the pozzolanic reaction of MK. The inflexion points (for 10% and 15% of MK) represent the end of the pozzolanic reaction, due to the total consumption of MK.

Cabrera and Rojas (2001) studied the reaction kinetics of a mixture of metakaolin and lime in water at 60°C using thermal analysis. The numerical results have been used to determine the nature of the reaction. It was shown that, on the whole, this pozzolanic reaction is diffusion controlled and can be represented by the Jander

Fig. 2.1 Evolution of calcium hydroxide with time (Frías and Cabrera, 2000)



diffusion equation. They presented a new rapid method for monitoring the reaction, utilizing a microwave oven to stop it at any desired reaction time. They determined nature and quantity of the reaction products by differential thermal analysis (DTA), thermogravimetry (TG) and X-ray diffraction (XRD). Based on the experimentation, they concluded that: (i) microwave drying to stop the hydration process was found to be a very practical and useful method that does not alter the nature of the reaction products. A drying time of 9 min was found to be adequate to drive off the free water from the metakaolin-lime-water mixture; (ii) lime was consumed at a very rapid rate in the initial period of reaction (up to 50 h). The reaction mechanism was consistent with diffusion control for the first 120 h; the calculated rate of reaction constant from the Jander equation showed that the metakaolin was very reactive and comparable in reactivity to silica fume; and (iii) the reaction products detected from 2 h up to 9 days indicated that C_2ASH_8 and C_4AH_{13} phases were meta-stable for up to 9 days at $60^\circ C$ under the circumstances studied, notwithstanding the fact that hydrogarnet (C_3ASH_6) was also present from 30 h up to 9 days. This might be an indication that hydrogarnet is not formed from a transformation reaction, but results from direct reaction between metakaolin and lime.

Frías and Cabrera (2001) examined metakaolin/lime and MK-blended cement pastes samples stored and cured at $20^\circ C$ and up to 360 days of hydration. The nature of the reaction products and their sequence of appearance were obtained from differential thermal analysis (DTA) and X-ray diffraction (XRD) techniques. The results showed a different behavior of the pozzolanic reaction in both pastes. The mechanism of hydration of the pozzolanic reaction was closely related with the matrix used. XRD data revealed the absence of crystalline phases in MK-blended cements up to 360 days of curing. MK showed high pozzolanic activity, which provided the quick formation of CSH, C_2ASH_8 (stratlingite), and C_4AH_{13} in MK/lime systems. The CSH was detected at 2 days of hydration time, followed by C_2ASH_8 and C_4AH_{13} . These two phases were detected at the same time. In an MK/cement system (up to 25% of MK), the development of the hydrated phases presented a

different behavior to the MK/lime system. The C_2ASH_8 was detected between 3 and 7 days of curing time and it depends on MK contents. Subsequently, the C_4AH_{13} was possibly formed between 180 and 360 days. This phase was only detected with high MK contents, mainly with 25% MK. Below 20% MK, this phase was not identified. In the XRD patterns for the MK/lime systems, the C_2ASH_8 was only identified as a crystalline hydrated phase, but not the C_4AH_{13} . This fact indicated very low crystallinity of the C_4AH_{13} with respect to the C_2ASH_8 phase. In MK-blended cement, XRD showed that the C_2ASH_8 formed during the pozzolanic reaction is an amorphous compound and on prolonged hydration it was possible to identify a very weak peak with high MK contents. The pozzolanic reaction in a blended cement matrix is more complex than in an MK/lime matrix, because of the presence of different ions (CO_3^{2-} , SO_4^{2-} , alkalis, chlorides), which could alter the kinetics as well as the development and crystallinity of the hydrates phases. It was due to the changes in solubility and evolution of the concentrations of the majority compounds (CaO , Al_2O_3 , and SiO_2). These findings indicated that there was no formation of the C_4AH_{13} up to 180 days and the formation of an amorphous C_2ASH_8 .

Poon et al. (2001) reported the degree of pozzolanic reactions of high-performance cement paste blended with metakaolin, and compared them with silica fume (SF) or fly ash (FA) blended cement pastes. The cement pastes prepared were: MK blended pastes with MK contents of 5, 10, and 20%, SF-blended pastes with SF contents of 5% and 10%, an FA blended paste with a FA content of 20%, and a control PC paste without any pozzolanic replacement. The results of the pozzolanic reaction of the pastes at different ages are given in Table 2.5, which are presented as the percentage values of the reacted pozzolan relative to the initial amount of the pozzolan in the paste. Based on the test results they concluded that: (i) degree of pozzolanic reaction of MK at each age was higher at a replacement level of 5% than at the replacement levels of 10 and 20%. The higher rate of pozzolanic reaction in cement pastes with a lower replacement level can be attributed to the higher concentration of CH available for the pozzolan to react with; (ii) comparing the different pozzolanic materials, initially, the rate of pozzolanic reaction of MK was greater than that of SF. At 3 days, the degree of pozzolanic reaction of MK in the pastes at the MK replacement levels of 5 and 10% was 20.6% and 15.3%, which were 30% and 49% higher than that of SF in the corresponding blended cement pastes; (iii) for longer curing times, the reaction rate was reduced for both MK and SF, but the reduction was greater for

Table 2.5 Degree of reaction of blended cement pastes (Poon et al., 2001)

Mix	Degree of reaction of pozzolans (%)			
	3 days	7 days	28 days	90 days
5% MK	20.56	29.52	39.44	56.28
10% MK	15.34	26.98	36.28	50.96
20% MK	9.38	18.64	30.82	41.29
5% SF	15.86	24.64	38.53	54.85
10% SF	10.32	21.25	35.38	52.06
20% FA	3.98	7.29	17.54	28.59

the MK; (iv) the higher initial reactivity of MK can be attributed to its Al_2O_3 phases (Curcio et al., 1998), which are involved in the formation of gehlenite (C_2ASH_8) and a small amount of crystalline C_4AH_{13} phase (Murat, 1983); (v) the higher initial reactivity of MK compared to SF may also be related to its fineness; and (vi) although the rate of MK reaction became slower after prolonged curing, there was still a considerable increase in the degree of pozzolanic reaction of MK from 28 to 90 days. For cement paste with 10% MK, the degree of pozzolanic reaction of MK was 36.3% at 28 days and 51.0% at 90 days. The reaction of MK was not completed at the age of 90 days and about half of the MK remained unreacted.

Saikia et al. (2002a) investigated the hydration behavior of lime–metakaolin mixtures produced in the presence of the sludge. Petroleum effluent treatment plant (ETP) sludge contains hydrocarbons and its ash is pozzolanic in character. The hydrocarbon may be utilized in the calcination of clay. The hydration products were characterized by using FTIR, TG, DTA and XRD methods. Use of sludge in metakaolin preparation increased the initial hydration rate, enhanced the production of C–S–H or C–A–S–H gel, and improved the pozzolanic activity of metakaolin. Presence of relatively high amount of alkali metal oxides, alumina and free lime in the sludge enhanced the hydration reaction with increased formation of C–S–H, C–A–S–H gels.

Saikia et al. (2002b) presented the physicochemical characteristics of cocalcined kaolin and petroleum effluent treatment plant (ETP) sludge and its effect on the technological and hydration characteristics of cement. Conductivity measurements indicated that both the sludge ash (SA) and cocalcined kaolin–sludge mixtures in aqueous medium were reactive in nature. The rate of hydration was investigated by determining the combined water (CW) and $\text{Ca}(\text{OH})_2$ content in the hydration products. The hydration products were characterized by FTIR spectrophotometric method and XRD analysis technique. They concluded that: (i) kaolin calcined in the presence of a limited amount of petroleum ETP sludge when used as a mineral admixture enhanced the rate of hydration of cement; (ii) cocalcined kaolin–sludge mixtures increased the water requirements and decreased the setting times of the cements; and (iii) blended cements with improved technological properties may be prepared by replacing 20% cement with cocalcined kaolin–sludge compositions containing up to 30% sludge.

Sun et al. (2004) quantitatively studied the hydration process of K-PS geopolymer cement under an 80% RH environment using environmental scanning electron microscope (ESEM). An energy dispersion X-ray analysis (EDXA) was also employed to distinguish the chemical composition of hydration product. The ESEM micrographs showed that metakaolin particles pack loosely at 10 min after mixing, resulting in the existence of many large voids. As hydration proceeded, a lot of gels were seen and gradually precipitated on the surfaces of these particles. At later stage, these particles were wrapped by thick gel layers and their interspaces were almost completely filled. The corresponding EDXA results illustrated that the molar ratios of K/Al increased while Si/Al decreased with the development of hydration. As a result, the molar ratios of K/Al and Si/Al of hydration products at an age of 4 h amounted to 0.99 and 1.49, respectively, which were close to the theoretical values

(K/Al = 1.0, Si/Al = 1.0 for K-PS geopolymer cement paste). In addition, well-developed crystals could not be found at any ages; instead, sponge like amorphous gels were always observed.

Badogiannis et al. (2005) investigated the hydration rate of metakaolin pastes. The metakaolinite content in metakaolin (MK4, derived from poor Greek kaolins) was 49%, where as it was 95% in a commercial metakaolin (MKC) of high purity. Cement was replaced with 0, 10, and 20% metakaolin. Pastes of PC, MK4-10, MK4-20, MKC-10 and MKC-20 were studied by means of a TG analyzer. The weight loss up to 550°C, which corresponds to the total water incorporated in the cement paste (total combined water), was determined. The Ca(OH)_2 content, which for PC is directly related to the hydration of silicate compounds, was also measured. When pozzolanic materials were combined with PC, the Ca(OH)_2 content (when compared to that of PC alone) also provided an indication of the pozzolanic reaction. The weight loss in the range 600–700°C, if any, corresponds to the decomposition of CaCO_3 and it has to be converted to the equivalent Ca(OH)_2 . The carbonation of the pastes may take place during the preparation of the paste or during the grinding of the paste prior to the TG measurement. The water combined in the hydration products (other than calcium hydroxide) corresponds to the weight loss up to 300°C. Any changes of this value indicated that the quantity, type and relative proportions of the hydration products are changing. Figure 2.2 shows the calcium hydroxide content, total combined water and water in the hydration products at 7 days. There was significant decrease of calcium hydroxide content in samples containing metakaolin, relative to the PC control, due to the pozzolanic reaction. Also the pozzolanic reaction was more rapid in samples containing the commercial metakaolin MKC. This phenomenon is related to the higher fineness of MKC as well as to its higher metakaolinite content (95%). In contrast, pastes containing MK4 exhibited higher values of total combined water and water in the hydration products than the MKC pastes, probably due to the different hydration products.

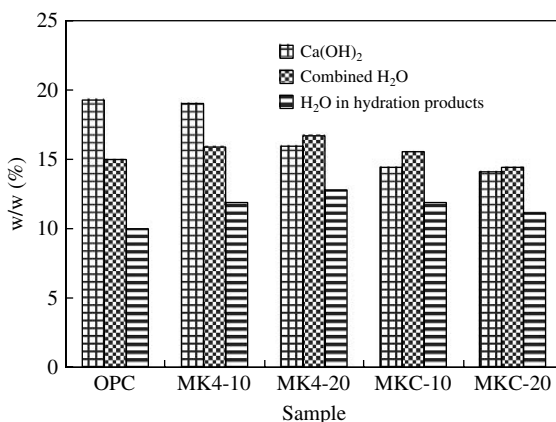


Fig. 2.2 Calcium hydroxide, total combined water and water in the hydration products for a hydration age of 7 days (Badogiannis et al., 2005)

Fig. 2.3 Calcium hydroxide, total compound water and water in the hydration products in relation to the hydration age for the sample MK4-20, 20% MK content (Badogiannis et al., 2005)

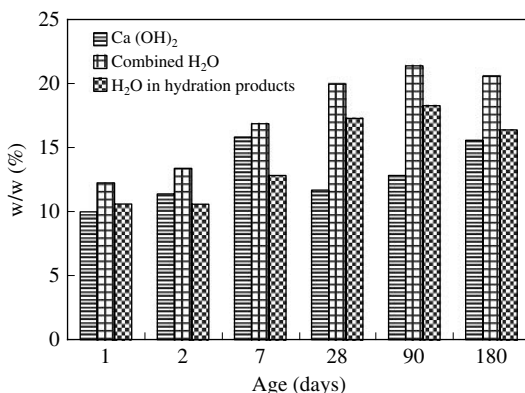


Figure 2.3 shows the calcium hydroxide content, total combined water and water in the hydration products for the sample MK4-20 in relation to the hydration age. A steep decrease of $\text{Ca}(\text{OH})_2$ content was observed between 7 and 28 days, due to the acceleration of the pozzolanic reaction. At the same period, the change of the water combined in the hydration products (other than calcium hydroxide) could be attributed to the change of the quantity, type and relative proportions of the hydration products.

Wong and Razak (2005) gave an alternative approach for the evaluation of efficiency factor (k) of a pozzolanic material. The cementing efficiency factor (k) of a pozzolan is defined as the number of parts of cement in a concrete mixture that could be replaced by one part of pozzolan without changing the property. The method, developed following Abram's strength–W/C ratio rule, calculates efficiency in terms of relative strength and cementitious materials content. The advantage of this method is that only two mixtures are required to determine the k -factor of a specific mixture. A laboratory investigation on silica fume (SF) and metakaolin (MK) concrete found that the computed efficiency factors varied with pozzolan type, replacement level and age. At 28 days, the k values ranged from 1.6 to 2.3 for MK and 2.1 to 3.1 for SF mixtures, while at 180 days, the k values varied from 1.8 to 4.0 for MK and 2.4 to 3.3 for SF mixtures. Generally, the k factors increased with age but declined with higher pozzolanic content. It was also observed that change in W/CM ratio from 0.33 to 0.27 did not significantly affect the resultant efficiency factors. Based on the obtained results, it was concluded that a single k value for a pozzolan does not exist, even for specific cement–pozzolan content.

2.2.1 Temperature Effect

Oriol and Pera (1995) investigated the effect of a microwave curing on lime consumption in metakaolin blended cements. The microwave treatment conditions were assessed for plain Portland cement pastes, and then the lime consumption for various metakaolin contents was evaluated by Fourier transform infra-red spectrometry and

differential thermal analysis. The results were compared with those obtained for room temperature curing. It was concluded that pozzolanic reaction of metakaolin could be consequently promoted by microwave heating. As heat is generated quickly inside the cementitious material, thermal acceleration of the reaction was more efficient, allowing both reduction of the necessary amount of metakaolin (15% instead of 30–40% in normal conditions) and of the water: cement ratio (0.4 instead of 0.5). These results are quite interesting for the development of fiber-reinforced cement composites, in which microwave heating allows the reduction of the curing period.

Frías et al. (2000) discussed the effect that the pozzolanic reaction of metakaolin has on the heat evolution in metakaolin-cement mortars in comparison to the behavior of other traditional pozzolanic materials such as fly ash and silica fume. The results revealed that MK mortars produced a slight heating increase when compared to a 100% Portland cement mortar, due to the high pozzolanic activity of MK. With respect to the hydration heat, MK-blended mortar showed closer behavior to silica fume than to fly ash. The results obtained for pozzolanic activity are shown in Fig. 2.4. After 2 hours, both the SF and MK showed pozzolanic activity, since the samples had fixed significant amounts of calcium ions (lime), while the FA, due to its lesser activity at early stages, hardly showed any reaction with lime before day 28.

Bai and Wild (2002) investigated temperature change and heat evolution of mortar incorporating PFA and metakaolin. They determined temperature-time profiles of mortar cubes using a semi-adiabatic curing method for curing times of 160hr. The binders employed were metakaolin-Portland cement (MK-PC), fly ash-Portland cement (PFA-PC) and MK-PFA-PC blends, with a maximum PC replacement level of 40% and MK levels of up to 15%. Relative to PC mortar, MK-PC mortars showed an enhanced temperature-rise whereas in PFA-PC mortars the temperature-rise was depressed. In ternary mortars MK and PFA had a compensatory effect. Both MK

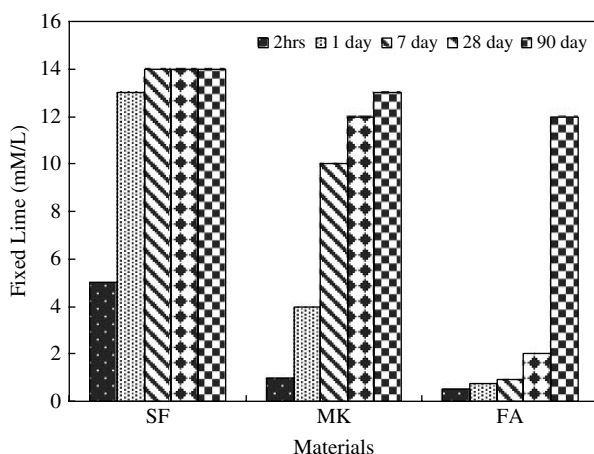


Fig. 2.4 Variation of pozzolanic activity: Fixed lime over time (Frías et al., 2000)

and PFA delayed the time taken to reach the peak temperature with MK producing the greatest delay. Partial substitution of MK for PC had only a minor influence on the total heat evolved by the mortar whereas partial substitution of PC with PFA produced a marked fall in the heat evolved. The temperature-rise of MK-PC mortars with respect to PC-mortar showed two distinct peaks, which are attributed to a two-stage hydration effect.

Ramlochan et al. (2004) analyzed the microstructural and microchemical development of heat-cured Portland cement mortars containing silica fume, metakaolin, blast furnace slag, and fly ash using pore solution analysis, X-ray diffraction (XRD) and scanning electron microscopy (SEM) with energy-dispersive X-ray analysis (EDX). Incorporation of these materials into the mixture modified the composition of the C-S-H gel, the quantities of the hydration products, and the microstructure. Ettringite was formed during moist storage in all specimens, but was not accompanied by expansion where a sufficient amount of metakaolin, blast-furnace slag, or a suitable fly ash replaced a proportion of the Portland cement.

Rojas (2006) determined the effect of curing temperature on the reaction kinetics in a metakaolin/lime mixture cured at 60°C and after 60 months of hydration. The stability of hydrated phases formed during the pozzolanic reaction in these working conditions was evaluated. The results exhibited that metastable hexagonal phases (C_2ASH_8 and probably C_4AH_{13}) coexist with stable cubic phase (hydrogarnet) in the absence of lime. Also, there was evidence of the possible presence of a calcium aluminum silicate hydroxide hydrate (vermugite). DTA curve showed the presence of CSH and the coexistence of metastable and stable phases in a MK/lime system cured at 60°C for 60 months of hydration. The metastable phase was assigned to stratlingite (C_2ASH_8) and probably to C_4AH_{13} . The stable phase was attributed to katoite, a hydrogarnet structured phase. XRD pattern confirmed the presence of stratlingite and katoite as main crystalline compounds present under tested conditions.

Rojas and Sánchez de Rojas (2003) showed the results of an experimental study on kinetics of pozzolanic reaction in MK/lime binder as well as MK-blended cement at 60°C. The sequence, development and crystallinity of hydrated phases up to 123 days of curing time were studied by means of DTA and XRD techniques. It is well known that the pozzolanic reaction between metakaolin (MK) and calcium hydroxide produce CSH, stratlingite (C_2ASH_8), C_4AH_{13} and hydrogarnet (C_3ASH_6). However, the presence or absence of these hydrated phases depends on different parameters, such as curing temperature, matrix used, etc. They concluded that: (i) the sequence and formation of the hydrated phases was different in both matrices cured at 60°C; (ii) in an MK/lime system (1:1 in weight), hydrated phases formed at high temperature (from DTA data) were essentially CSH, C_2ASH_8 , C_4AH_{13} and C_3ASH_6 . CSH was detected at 6 hours of hydration time, followed by C_2ASH_8 and C_4AH_{13} at 12 hours of curing and finally C_3ASH_6 at 30 hours of age; (iii) In a MK-blended cement system (10%, 20% and 25% of MK), the development of hydrated phases presented a different behavior from the MK/lime system. Stratlingite was detected in all cases as the sole reaction product from pozzolanic reaction. There was no evidence of formation of C_4AH_{13} and

hydrogarnet (only traces); (iv) XRD patterns for the MK/lime systems, stralingite and hydrogarnet were identified as crystalline hydrated phases but not C_4AH_{13} ; and (v) In MK-blended cement at 60°C, XRD showed important changes with respect to the crystallinity of hydrated phases. Stralingite did not appear as a crystalline phase, indicating a very low crystallinity of this compound in blended cements. At 20% and 25% of MK, the presence of hydrogarnet traces was observed.

2.2.2 Alkaline Activation

Palomo et al. (1999) investigated the MK when exposed to aggressive solutions. The alkali activation of metakaolin is a way of producing high strength cementitious materials. Prisms of mortar made of sand and alkali-activated metakaolin were immersed in deionized water, ASTM sea water, sodium sulfate solution (4.4% wt), and sulfuric acid solution (0.001 M). The prisms were removed from the solutions at 7, 28, 56, 90, 180, and 270 days. Their microstructure was characterized and their physical, mechanical, and microstructural properties were measured. It was observed that: (i) the nature of the aggressive solution had little negative effect on the evolution of microstructure and the strength of these materials; (ii) 90-day and older samples experienced a slight increase in their flexural strengths with time. This tendency was most pronounced in samples cured in sodium sulfate solutions. This behavior may be related to the change in microstructure of the cementitious matrix of the mortars cured longer than 90 days; (iii) some of the amorphous material present had crystallized to a zeolite-like material belonging to the faujasite family of zeolites. The alkaline activation of metakaolin with concentrated NaOH solutions produced an amorphous material—a zeolitic precursor with excellent cementing properties in terms of mechanical strength; and (iv) the resultant hydroceramic demonstrated good stability for up to 270 days when submerged in aggressive liquids of various types. The time that the sample spends in solution is responsible for a certain degree of transformation of the amorphous aluminosilicate network structure into a crystalline one. Faujasite crystals act as reinforcement of the cement matrix.

Alonso and Palomo (2001a) studied the influence of temperature, activator concentration and solids ratio on alkaline activation of metakaolin and calcium hydroxide mixtures. They found that: (i) when metakaolin activation was carried out with highly concentrated alkaline solutions in the presence of calcium hydroxide, the main reaction product was sodium aluminosilicate similar to the one obtained when metakaolin was activated in the absence of calcium hydroxide. Additionally, there was formation of CSH gel as a secondary product; and (ii) the rate of polymer formation was influenced by parameters such as curing temperature, alkali concentration, initial solids content, etc. When the activator concentration increased, a delay in polymer formation was noticed, whereas temperature accelerated its formation. The solids ratio (metakaolin/ $Ca(OH)_2$) did not influence the rate of aluminosilicate

formation, but larger product precipitation was produced when the solids ratio increased.

Alonso and Palomo (2001b) did the calorimetric study of alkaline activation of calcium hydroxide-metakaolin solid mixtures. A series of MK + calcium hydroxide mixes were activated in 1:1 proportion, with different sodium hydroxide concentrations: 5, 10, 12, 15 and 18 M at 45°C during 24 h. The activation steps were examined through isothermal conduction calorimetry and the reaction products characterization was carried out by means of chemical analysis and instrumental techniques (XRD, FTIR and nuclear magnetic resonance (NMR)). Based on the investigation, they concluded that: (i) when sodium hydroxide concentration was 5 M or lower in the MK activation in calcium hydroxide presence, the main product formed was CSH gel; (ii) when the activation was carried out with 10 M or higher NaOH concentrations, the main reaction product was the alkaline aluminosilicate, with polymeric character, similar to the one obtained in the MK activation with the same activator but in calcium hydroxide absence. As secondary reaction product (between 20% and 30%), CSH gel was obtained; (iii) a threshold OH^- concentration existed above which, the alkaline polymer was mainly formed, and beneath which, the CSH gel was the main reaction product; and (iv) a high hydroxyl group concentration impeded the calcium hydroxide dissolution, Ca^{2+} concentration was small and the dissolved silicates were fixed as sodium aluminosilicate. when $[\text{OH}^-]$ was not so high, $[\text{Ca}^{2+}]$ in solution increased and it precipitated as hydrated calcium silicate.

Rojas and Cabrera (2002) investigated the influence of curing temperature on the kinetics of reaction of a metakaolin (MK)/lime mixture. MK and analytical grade $\text{Ca}(\text{OH})_2$ were mixed in a ratio of 1:1 by weight with a water/binder ratio of 2.37. Specimens were cured at 20 and 60°C. In the first case, the curing time varied from 2 h up to 180 days and, in the second case, from 2 h up to 123 days. A mathematical model was applied to calculate the rate constant for the hydration reaction. The identity and the amount of the phases present were determined from thermal analysis (TG and DTA) data. Based on the results, they concluded that: (i) for the same curing period (9 days), the samples cured at 60°C showed 82% of reacted lime, while for the sample cured at 20°C, it was only 18%. In the later case, the $\text{Ca}(\text{OH})_2$ content disappeared at 180 days. However, the specimens cured at 60°C showed 6% lime left at 123 days; (ii) rate constant obtained by Jander model at 60°C and up to 5 days of curing was 68 times higher than that obtained at 20°C; (iii) at early stages of the reaction, the C-S-H was the main phase for both temperatures. Subsequently, stratlingite (C_2ASH_8) and C_4AH_{13} appeared, and finally the C_3ASH_6 (hydrogarnet) was the predominant phase in the samples cured at 60°C. No hydrogarnet formation was detected at 20°C; (iv) at 60°C of curing temperature, there was no clear evidence of a transformation of metastable phases (C_2ASH_8 and C_4AH_{13}) into hydrogarnet up to 123 days. C_2ASH_8 , C_4AH_{13} and C_3ASH_6 amounts increased with curing time. This indicates the fact that hydrogarnet was produced as a result of the pozzolanic reaction between MK and lime and not through a transformation reaction; and (v) at 20°C, there was clear evidence of the existence of C_4AH_{13} in the absence of calcium hydroxide.

2.2.3 Effect of Dehydroxylation

Salvador (1995) studied to reduce the calcination time to a few seconds using flash-calcination processes on fine products. Flash-calcination enables the dehydroxylation of powdered kaolinite clay within several tenths of a second, when traditional soak-calcinations require minutes at least. The pozzolanic properties of the metakaolin produced from two different kaolinites, using two different flash calciners increased with the dehydroxylation rate, and rapidly decreased at the occurrence of recrystallization for temperatures above 900°C. Flash-calcined products revealed structural properties different from soak-calcined products. Two different lime reactivity tests were thus done to assess the pozzolanic properties of products: the compressive strengths of mini cylinders of metakaolin + lime + water after solidification, and the Chapelle test. Processing flash-calcination in a temperature range with a sufficient residence time, led to metakaolins with lime reactivity similar or better than reactivity of standard metakaolin obtained by soak-calcination. By measuring compressive strength of mini cylinders they verified that, after a flash-calcination, the quality of the pozzolana increased with α (degree of dehydroxylation) values. During the few seconds or tenths of seconds of flash-calcination, temperatures above 950°C induced recrystallization from the amorphous phase. Recrystallization was accompanied, as with a soak-calcination, by a rapid drop of lime reactivity. This performance drop was correlated with the decrease of the exothermic band surface area on D.T.A. traces.

Shvarzman et al. (2003) investigated the effect of heat treatment parameters on the dehydroxylation/ amorphization process of the kaolinite-based materials such as natural and artificial kaolin clays with different amounts of amorphous phase (metakaolin). The process of dehydroxylation/amorphization of kaolinite was characterized by DTA/TGA with mass-spectrometry and X-ray powder diffraction. Based on the study, they concluded that: (i) at the calcinations temperatures below 450°C, kaolin clays showed relatively low level of the dehydroxylation degree, less than 0.18. In the range from 450 to 570°C, the degree of dehydroxylation sharply increased to 0.95, and finally at the temperatures between 570 and 700°C the kaolinite was fully dehydroxylated since the only moderate change of degree of dehydroxylation was observed in this range (from 0.95 to 1.0); (ii) the dehydroxylation was accompanied by kaolinite amorphization, which affected the activity of additives. A method of qualitative evaluation of amorphous phase content (APC) in treated materials was developed and applied for characterization of the investigated samples; (iii) pastes containing less than 20% of amorphous phase can be considered as inert materials from the standpoint of pozzolanic activity. It was shown that chemical activity is a linear function of APC in its range of 50–100%; and (iv) activity strength index (ASI) of mature mixes (7, 28 and 90 days) depends significantly on APC, as well as the degree of dehydroxylation. In contrast to the chemical activity, the increase of APC by over 55% did not lead to additional growth in ASI. Therefore, even with the partial dehydroxylation of kaolinite accompanied with ~55% amorphization the material may be considered as very active pozzolanic admixture (according to ASTM 618).

2.2.4 Dilatency

Curcio and DeAngelis (1998) evaluated the cement pastes containing metakaolin with a coaxial cylinder rotational viscometer. Dilatancy is caused by the angular and plate like shape of metakaolin particles. A sample with silica fume was included for comparison. Dilatancy is heavily influenced by the water/binder ratio, by the amount of metakaolin and by its fineness. The thixotropy of the pastes was somewhat decreased by metakaolin, and increased by silica fume. The dilatant properties, which are a consequence of the attrition generated in the contact of moving solid particles in sheared suspensions, can be explained by considering the angular and plate like shape of metakaolin particles.

2.3 Fresh Properties of Mortar/Concrete Containing Metakaolin

Wild et al. (1996) studied the workability of metakaolin concretes. Replacement levels of ordinary Portland cement (OPC) by metakaolin (MK) were 0, 5, 10, 15, 20, 25, and 30% and water-binder ratio (w/b) was 0.45. OPC concrete mixture proportion was 1:2.3:3.4. Workability results (slump, compacting factor and vebe time) are given in Table 2.6.

Brooks and Johari (2001) reported the slump and setting times of concretes containing 0, 5, 10, and 15% metakaolin (MK). Control concrete mixture proportion was 1:1.5:2.5 with water-binder ratio of 0.28. Slump and setting times results are given in Table 2.7. It can be seen that slump decreased and setting times increased with the increase in MK content.

Li and Ding (2003) investigated the fluidity of Portland cement containing metakaolin (MK) and ultra-fine slag (S). Four series of pastes were made. First series contained 100% cement, 0% MK, and 0% slag; second had 90% cement and 10% MK, 0% slag; third had 70% cement, 10% MK, and 20% slag, and the fourth series had 60% cement, 10% MK, and 30% slag. Based on the test results, they concluded that: (i) after incorporation of MK into PC, the fluidity of MK blended cement became poorer than that of PC at the same dosage of superplasticizer and the same water/binder ratio; (ii) when both MK (10%) and ultra-fine slag (20% or 30%) were incorporated into PC together, fluidity of the blended cement paste was

Table 2.6 Workability of metakaolin concretes (Wild et al., 1996)

Metakaolin (MK) (%)	Superplasticizer (%)	Slump (mm)	Compacting factor	Vebe time (Sec)
0	0	5	0.81	26
5	0.6	10	0.84	15
10	1.2	15	0.88	10
15	1.8	25	0.89	9
20	2.4	75	0.89	7
25	3.0	75	0.89	4
30	3.6	90	0.90	5

Table 2.7 Workability, setting times of MK concretes (Brooks and Johari, 2001)

Concrete mixes	Slump (mm)	Initial setting time (hours)	Final setting time (hours)
OPC	100	5	7.7
MK5	30	6.42	8.82
MK10	20	6.98	9.42
MK15	5	6.45	9.31

improved comparing to MK blended cement. This indicated that ultra-fine slag can improve the physical properties of MK blended cement: (iii) incorporation of 10% MK and 20% or 30% ultra-fine slag jointly into PC, improved the fluidity of blended cements, also the 28-day compressive strength; (iv) both MK and slag can react with CH released by cement clinker hydration to produce secondary C-S-H gel inside the cement paste. The secondary formed C-S-H gel improved the microstructure of cement paste matrix; and (v) XRD analysis indicated that more $\text{Ca}(\text{OH})_2$ was consumed after adding both mineral admixtures.

Bai et al. (2003a) used neural networks to predict workability of concrete incorporating metakaolin and fly ash. The predictions reflected the effect of graduated variations in pozzolanic replacement in Portland cement (PC) up to 15% MK and 40% FA. The results showed that the models are reliable and accurate and illustrate how neural networks can be used to beneficially predict the workability parameters of slump, compacting factor and Vebe time across a wide range of PC–FA–MK compositions. On the basis of the models developed, effects of MK and FA on workability were analyzed and iso-slump maps were plotted for w/b 0.25, 0.4 and 0.5. Through this, it is possible for the designer to produce mixtures with various blend compositions for a given range of slumps.

Li and Ding (2003) investigated the consistency and setting times of Portland cement containing metakaolin (MK) and ultra-fine slag (S). Four series of pastes were made. First series contained 100% cement, 0% MK, and 0% slag; second had 90% cement and 10% MK, 0% slag; third had 70% cement, 10% MK, and 20% slag, and the fourth series had 60% cement, 10% MK, and 30% slag. Test results of water consistency and setting times are presented in Table 2.8. They concluded that: (i) standard consistency of cement paste was in the range of 26.3–29.1%. Mixture PO had the lowest water requirement, but MK blended cement M1 had the highest water requirement. After the slag was mixed with MK blended cement, the water

Table 2.8 Physical properties of cement paste (Li and Ding, 2003)

Mixture type	Composition (%)			Water required for standard consistency (%)	Setting times (Hours: mins)	
	Cement	MK	Slag		Initial	Final
PO	100	0	0	26.3	1:36	3:27
M1	90	10	0	29.1	1:11	2:12
S2	70	10	20	28.4	1:55	4:34
S3	60	10	30	28.0	2:19	6:15

Table 2.9 Properties of metakaolin cements (Badogiannis et al., 2005)

Sample	Metakaolin (% w/w)	Water demand (% w/w)	Setting time (min)	
			Initial	Final
PC	–	27.5	105	140
MK1-10	10	29.0	75	130
MK2-10	10	29.0	85	130
MK3-10	10	32.0	105	160
MK4-10	10	32.5	155	180
MKC-10	10	31.0	95	130
MK1-20	20	32.0	105	160
MK2-20	20	31.5	110	165
MK3-20	20	38.5	120	160
MK4-20	20	41.0	205	230
MKC-20	20	37.5	140	170

requirement of cement mixture S2 and S3 was reduced, but it was still higher than that of PC; and (ii) initial and final setting times of the cement incorporating 10% MK were shorter than those of PC, while the initial and final times of S2 and S3 cements were longer than those of PC.

Badogiannis et al. (2005) reported the results of water demand and setting times of cements containing five metakaolins. The metakaolinite contents in metakaolins MK1, MK2, MK3, and MK4 (derived from poor Greek kaolins) were 36, 37, 71, and 49%, respectively, where as it was 95% in a commercial metakaolin (MKC) of high purity. Cement was replaced with 0, 10, and 20% metakaolin. Results of water demand and setting times of cement pastes are given in Table 2.9. They concluded that: (i) blended cements demanded significantly more water than the relatively pure cement. With a metakaolin content of 10%, the water demand varied from 29.0% to 32.5%, while the PC had a water demand of 27.5%. With a metakaolin content of 20%, the water demand varied from 31.5% to 41.5%. Metakaolins MK1 and MK2 showed the best behavior and increase in water demand was less. The increase in water demand could be attributed to the high fineness of metakaolin as well as to their narrow particle size distribution; and (ii) the initial and final setting time of metakaolin cements was affected by the metakaolin content. Cements with 10% metakaolin, generally, exhibited similar setting times to that of PC, while for 20% metakaolin content there was a delay in the setting. MK4 showed the greatest effect on the setting delay of the cements.

2.4 Properties of Hardened Mortar/Concrete Containing Metakaolin

2.4.1 Pore Size Distribution

Bredy et al. (1989) conducted study on porosity and pore size distribution of pastes containing MK. Pastes were prepared with MK content of 0–50% at different

water-to-binder (w/b) ratios to maintain the same consistency. They concluded that when the MK content was below 20%, the total porosity of paste decreased. Beyond 30%, an increase in porosity was found. Larbi and Bijen (1992) reported that at 100 days of curing, the pore volume of mortar and the threshold diameter decreased in the presence of MK.

Khatib and Wild (1996) determined the porosity and pore size distribution of cured OPC-metakaolin paste. Pastes containing 0, 5, 10 and 15% metakaolin were prepared at a constant water/binder (w/b) ratio of 0.55. Specimens were moist cured for periods from 3 to 365 days. The intruded pore volume and the pore structure were measured by mercury intrusion proximity. Pore volume of pastes containing metakaolin (MK) and proportion of pores with radii smaller than $20\mu\text{m}$ are given in Table 2.10. For the control paste, there was a continuous reduction in total pore volume with age and also the rate of reduction declined with age. It can be seen from this table that total pore volume decreased with an increasing rate up to 14 days. Between 14 and 28 days, pore volume increased. Beyond 28 days, pore volume again continued to decrease with age, but at a decreasing rate. This trend indicated that there was a clearly defined minimum point at around 14 days for pastes containing metakaolin. Also these pastes possessed a greater total pore volume than the control paste. Thus, the increase in pore volume between 14 and 28 days appeared to be associated with a renewed increase in CH content and a decline in relative strength. The proportion of pores with radii smaller than $20\mu\text{m}$ was increased with the increase in metakaolin content.

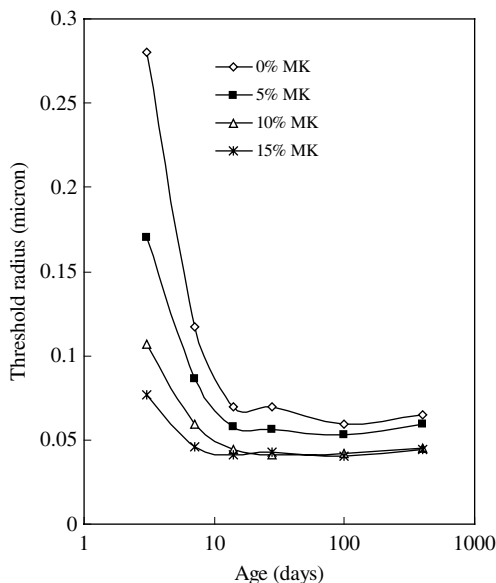
Threshold value for paste decreased with the increase in metakaolin content. Figure 2.5 shows the threshold radius for pastes with and without metakaolin at different curing periods. The threshold radius is taken as the radius before which the cumulative pore volume rises sharply. Incorporation of metakaolin in cement paste led to refinement of the pore structure. The threshold value for paste decreased as the metakaolin content in the paste increased.

Frías and Cabrera (2000) studied effect of metakaolin on the pore size distribution of cement pastes. Ordinary Portland cement (OPC) was partially replaced with 0, 10, 15, 20 and 25% of MK. Surface area of metakaolin was $15.5\text{ m}^2/\text{g}$, and water/binder ratio was 0.55. The mixtures were placed in plastic airtight containers and then left in a curing room at 100% RH. After the predetermined curing time (1, 3, 7, 14, 28, 56, 90, 180 and 360 days), the hydration reaction was stopped

Table 2.10 Pore volume and % of pores of pastes containing MK (Khatib and Wild, 1996)

Age (days)	Pore volume (mm^3/g)				% of small pores (radii $< 20\mu\text{m}$)			
	Metakaolin (MK) (%)				Metakaolin (MK) (%)			
	0	5	10	15	0	5	10	15
3	262.0	257.6	284.1	277.6	22.2	28.3	31.0	39.9
7	229.6	261.7	268.8	251.6	26.5	32.1	41.0	50.4
14	209.9	203.4	221.0	212.1	30.3	43.0	53.9	55.7
28	189.1	205.3	237.1	222.7	33.7	43.5	48.7	54.9
90	181.4	180.8	219.6	198.9	37.3	44.7	49.9	57.6

Fig. 2.5 Variation of threshold radius with age and varying MK content (Khatib and Wild, 1996)



using two different ways, depending on the parameter studied: (a) Vacuum oven method: the samples were left at 50°C and 1 bar. After 3 days, a constant mass was detected; and (b) Microwave method: this procedure was good and quick to dry the samples. Total, capillary, and gel porosity and pore size distribution measurements were carried out using mercury intrusion porosimeter (MIP). They reported that: (i) at 24 hours, pastes showed almost similar total porosity (between $49 \pm 50\%$) in all cases. Subsequently, there was a continuous reduction in porosity with hydration time up to 28 days. Beyond this age, the total porosity was practically constant and a clear difference between OPC and MK mixes could be observed; (ii) MK mixes showed a greater total porosity than the OPC paste and an increase of about 16% was obtained. MK contents did not have significant effect on the total porosity. This fact can probably be related to the high water/binder ratio used; (iii) a clear difference was observed for the capillary porosity ($5 \pm 0.01 \mu\text{m}$). During the first 7 days, an important difference between pastes with or without MK contents was not detected. However, at 14 days, the capillary porosity from OPC paste and paste containing a 10% of MK showed a slight increase with respect to the other MK pastes. However, there was no difference of capillary porosity in pastes containing 15 and 25% of MK with longer hydration time; (iv) incorporation of MK in the elaboration of blended pastes reduced the pore size to less 100 \AA . Gradual increase in the very fine pores was observed with age. There were two important moments on the evolution of the porosity at 7 and 90 days, respectively. This period of time corresponded with the start and the end of the pozzolanic reaction; and (v) a strong reduction on the average pore diameter was observed in the first days. Depending on MK contents, the evolution of this parameter was different. In the case of OPC paste, the average pore diameter decreased from 40 to $14.5 \mu\text{m}$ for a hydration time between 1 and 56

days. Subsequently, the average pore diameter was almost a constant value. In paste with 10% of MK, the reduction of average pore diameter finished at 28 days while for the 15, 20, and 25% MK pastes, this phenomenon occurred at 14 days. Above 10% of MK, the average pore diameter curves did not show any difference.

Poon et al. (2001) investigated the porosity and pore size distribution of high-performance cement paste blended with metakaolin, and compared them with silica fume (SF) or fly ash (FA) blended cement pastes. The cement pastes prepared were: MK blended pastes with MK contents of 5, 10, and 20%, SF-blended pastes with SF contents of 5 and 10%, an FA blended paste with a FA content of 20%, and a control PC paste without any pozzolanic replacement. The w/b ratio for all the pastes was 0.3. Pore size and porosity were measured by MIP, and results are given in Tables 2.11 and 2.12. The results showed that for all the pastes, the porosity and average pore size decreased as the curing age increased. The pastes containing MK had lower porosity and smaller average pore diameters than the control paste and the SF pastes with the same percentages of replacement at all the tested ages. This indicated that the MK was more effective than the SF in the refinement of the pore structure of the blended cement system, although they both reduced the porosity and pore sizes of the cement pastes. In comparison, the cement paste containing 20% FA showed higher total porosity than the control until the age of 28 days, indicating the lower pozzolanic activity of this type of material.

2.4.2 Water Absorption and Sorptivity

Khatib and Mangat (1995) exhibited that sorptivity values determined on concrete taken from the top surface of a concrete cube can be several times greater than those for concrete taken from the bottom surface of the cube. In addition, carbonation influenced sorptivity. Dias (2000) observed that air-cured concrete, over a 4-year period, undergoes an increase in weight and a reduction in sorptivity as a result of carbonation of the surface zone. Also, the greater the initial (6 months) sorptivity, the greater was the reduction in sorptivity (at 4 years) due to carbonation. Equivalent water-cured concrete did not show any drop in sorptivity from carbonation, although sorptivity did decrease with time as a result of continued hydration.

Table 2.11 Average pore diameter of blended cement pastes (Poon et al., 2001)

Mix	Average pore diameter (μm)			
	3 days	7 days	28 days	90 days
Control	0.0380	0.0371	0.0362	0.0348
5% MK	0.0357	0.0279	0.0257	0.0243
10% MK	0.0287	0.0251	0.0197	0.0186
20% MK	0.0204	0.0143	0.0122	0.0114
5% SF	0.0366	0.0370	0.0367	0.0349
10% SF	0.0353	0.0341	0.0325	0.0306
20% FA	0.0368	0.0356	0.0347	0.0339

Table 2.12 Total porosity of blended cement pastes (Poon et al., 2001)

Mix	Total porosity (% v/v)			
	3 days	7 days	28 days	90 days
Control	20.11	17.99	15.58	14.04
5% MK	18.17	15.36	13.82	12.51
10% MK	16.84	15.18	12.37	11.68
20% MK	16.30	12.85	10.73	9.21
5% SF	18.72	16.83	14.53	13.84
10% SF	16.97	15.49	14.23	13.42
20% FA	22.35	18.59	15.62	13.82

Bai et al. (2002) reported the influence of the composition of Portland cement–pulverized fuel ash–metakaolin (PC–PFA–MK) binders on the sorptivity and carbonation of PC–PFA–MK concrete cured both in air and in water. Concrete mixtures were made with four different cement replacement levels (10, 20, 30 and 40%) for PC–PFA–MK concrete with various MK/PFA proportions, and water and air cured for up to 18 months. Based on the test results, they concluded that: (i) increasing the MK content of water-cured PC–PFA–MK concrete reduced the sorptivity values below that of the control, whereas the sorptivities of PC–PFA concrete exceed that of the control; (ii) air-cured concrete showed higher sorptivity than equivalent water-cured concrete, and this difference was substantial both for PC concrete and PC–PFA concrete. In contrast, for PC–PFA–MK concrete, the difference reduced as the MK content increased, such that at high MK levels, the air cured and water-cured concrete sorptivities were similar; (iii) increasing replacement of PC with PFA in PC–PFA air (CO₂ enriched)-cured concrete increased carbonation depth whereas systematically replacing the PFA with MK in PC–PFA–MK concrete reduced carbonation depth; and (iv) there was a strong correlation between carbonation depth and sorptivity as the binder composition of PC–PFA–MK concrete was varied. However, other than for concrete with high MK contents, concrete containing blended binders showed greater carbonation depths than that of the PC concrete but lower sorptivities. This anomaly was attributed to a much reduced CH content in the blended binder concretes coupled with reduced sorptivity deriving from surface layer carbonation over a prolonged period.

Courard et al. (2003) investigated the water absorption of mortars. Cement was partially replaced by metakaolin. Replacement percentages were 0, 10, 15, and 20%. One mixture with natural kaolin was also made. The specimens were made with 3 parts of sand, 1 part of cement and 0.5 part of water) in which cement was OPC (CEM I 42.5). Water absorption, measured by total immersion, was performed after 28 days and 14 months, and results are given in Table 2.13.

Razak et al. (2004) determined the effect of metakaolin and silica fume on the near surface properties of concrete. Metakaolin and silica fume mixtures, each with 10% replacement, were tested for initial surface absorption, water absorption and sorptivity. Metakaolin and silica fume were found to enhance the overall near surface characteristics of the concrete. The inclusion of metakaolin and silica fume

Table 2.13 Water absorption for mortars with cement CEM I 42.5, metakaolin and kaolin (Courard et al., 2003)

Material	Water absorption (% in mass)		Decrease ratio
	After 28 days	After 14 months	
CEM I 42.5	8.16	7.82	4.1
5% Metakaolin	8.39	8.04	4.1
10% Metakaolin	8.78	8.44	3.9
15% Metakaolin	9.71	8.77	9.7
20% Metakaolin	9.70	8.97	7.5
10% Kaolin	9.51	7.90	16.9

greatly reduced the initial surface absorption, water absorption and sorptivity of concrete when compared with concrete made with OPC.

Khatib and Clay (2004) studied water absorption characteristics of metakaolin concrete. Water absorption (WA) was measured by total immersion of concrete containing metakaolin (MK). Five concrete mixes were made. The control mix (0% MK) contained only Portland cement (OPC). The mix had a proportion of 1 (binder):2.3 (fine aggregate):3.4 (coarse aggregate). In the other four mixes, the OPC was partially replaced with 5, 10, 15 and 20% MK, respectively. The w/b ratio was kept constant at 0.45 for all mixes. Concrete cubes of 100 mm in size were cast, and testing was conducted at 1, 7, 14, 28 and 90 days from the time of casting. Water absorption (WA) by total immersion for all mixes versus curing time is shown in Fig. 2.6. There tends to be a small systematic increase in WA with the increase in MK contents at all curing times. WA values for all mixes ranged between 4.2% and 5.4% by dry mass. The WA values for the control mix decreased with the increase in curing period. The decrease in WA was noticeable during the first 7 days. After 14 days, there was little decrease in WA. A decrease in WA with curing time was

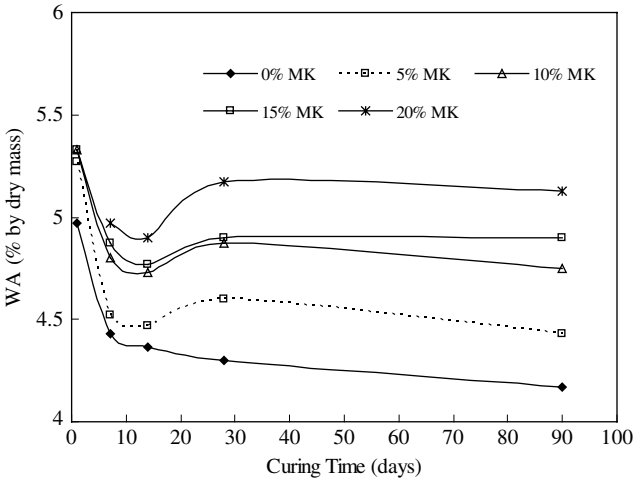


Fig. 2.6 Variation of WA with curing time for concrete containing MK (Khatib and Clay, 2004)

obtained for all MK mixes up to about 14 days. Between 14 and 28 days curing period, there was a slight increase in WA caused by the presence of MK. This might be due to the formation of a denser hydration phase. After 28 days, 5% and 10% MK mixes showed a slight decrease in WA, whereas at higher MK replacement levels (15% and 20%), there was little change in WA.

2.4.3 Compressive Strength

Wild et al. (1996) investigated the effect of varying percentages of metakaolin on the compressive strength of concrete mixtures. Replacement levels of ordinary Portland cement (OPC) by metakaolin (MK) were 0, 5, 10, 15, 20, 25, and 30% and water-binder ratio (w/b) was 0.45. OPC concrete mixture proportion was 1:2.3:3.4. Compressive strength tests were conducted up to the age of 90 days, and results are presented in Table 2.14. They concluded that inclusion of MK as partial replacement of cement enhanced the compressive strength of concrete at all ages, but the optimum replacement level of OPC by MK to give maximum long term strength enhancement was about 20%.

Curcio et al. (1998) examined the role of metakaolin as pozzolanic microfiller for high-performance mortars. They characterized superplasticized mortars containing metakaolin (MK) as 15% replacement of cement and with a water/binder ratio of 0.33. Four commercially available MK samples and one silica fume sample were studied for comparison. They concluded that: (i) specimens containing three of the four metakaolin samples had a higher rate of compressive strength development as compared to that of the control at ages below 28 days, a consequence of the higher hydration rate. Silica fume and the fourth and coarser metakaolin had a less pronounced effect; (ii) at 90 and 180 days metakaolin and silica fume specimens gave similar strengths. The difference in the compressive strength between the specimens with microfillers and the control decreased after 28 days, because of a smaller slowdown of the hydration rate in the control; (iii) extent of strength enhancement at short curing ages was influenced by the type of cement; it was lower for early strength Portland as compared to ordinary Portland; and (iv) DTA calcium hydroxide peak heights on mortars and the pozzolanic activity test on mixtures of

Table 2.14 Compressive strengths and densities of metakaolin concretes (Wild et al., 1996)

(MK) (%)	Density (kg/m ³)	Compressive strength (MPa)				
		1-day	7 days	14 days	28 days	90 days
0	2490	19.07	50.23	57.10	62.60	72.43
5	2440	21.50	53.80	58.97	63.50	71.63
10	2460	22.43	62.30	69.23	71.00	80.07
15	2470	20.23	64.80	74.67	76.00	83.70
20	2480	19.33	66.47	75.73	82.47	85.13
25	2470	15.73	62.50	69.77	73.93	82.23
30	2480	14.53	60.53	72.33	76.73	81.80

80% cement and 20% microfiller showed that three of the four metakaolins had a remarkable pozzolanic activity comparable to that of silica fume, even if slightly lower at longer ages. The fourth and coarser metakaolin sample was less reactive. The amount of water that was lost after 24 h at 90°C was different for all types of specimens and was dependent on the differences of the hydration products formed and on the permeability of the materials. It can be related to the fineness of the microfiller in the specimens with metakaolin.

Brooks and Johari (2001) determined the compressive strength of concretes containing 0, 5, 10, and 15% metakaolin (MK). Mixture proportion of OPC concrete was 1:1.5:2.5 with a water-to-cement ratio of 0.28. 28-day Compressive strength results of MK concretes are given in Table 2.15. It is evident from the table that compressive strength increased with the increase in the metakaolin content.

Poon et al. (2001) showed that the cement pastes containing 5%–20% MK had higher compressive strengths than the control at all ages from 3 to 90 days, with the paste containing 10% MK performing the best. The cement pastes containing SF or FA had lower compressive strength than the control at early ages. The SF replacements resulted in higher compressive strengths than the control at 28 and 90 days, while the FA replacement resulted in a higher compressive strength than the control only at 90 days. The above results indicated that at early ages, the MK contributed better to the compressive strength development of high-performance cement pastes than the SF.

Roy et al. (2001) studied the effect of silica fume (SF), metakaolin (MK), and low-calcium fly ash on compressive strength of concrete. They reported that compressive strength increased on addition of MK. SF also increased compressive strength but lesser than MK. Similarly, FA also increased compressive strength but to a lesser magnitude. No significant change in compressive strength was found as a function of replacement level for SF and MK series. However, the compressive strength decreased as the FA replacement level increased. This clearly showed that low-calcium fly ash is less reactive than SF and MK and needs an external activation.

Bai et al. (2002) reported the influence of the composition of Portland cement–pulverized fuel ash–metakaolin binders on strength development of PC–PFA–MK concrete cured both in air and water. Concrete mixtures were made with four different total cement replacement levels (10, 20, 30 and 40%) for PC–PFA–MK concrete with various MK/PFA proportions and cured in water and air up to 18 months. In water-cured concrete made with PC–PFA–MK binder, the MK enhanced early (28 days) strength, and PFA retarded early strength. Air-cured concrete showed a loss in strength relative to equivalent concrete that was water cured and the strength

Table 2.15 Workability, setting times of MK concretes (Brooks and Johari, 2001)

Concrete mixes	Compressive strength (MPa)
OPC	87.0
MK5	91.5
MK10	104.0
MK15	103.5

difference increased with curing period. The difference was enhanced in concrete made with PC–PFA binder at high replacement levels, which showed a much reduced strength gain with time when air cured, whereas for PC–PFA–MK concrete, this difference was reduced as the MK content increases.

Jin and Li (2003) investigated the effect of mineral admixtures such as silica fume, slag, fly ash, and metakaolin on the mechanical behavior of young concrete under either uniaxial compression or tension. Tests were conducted at ages of 1/2, 1, 2, 3, 7, and 28 days. They reported that: (i) stress-strain (deformation) curves for young concretes were different from mature concretes in their capability in resisting the deformation. More ductile behavior was observed for a young concrete. However, the complete stress-deformation curves for young concrete under uniaxial tension showed less ductility as compared to those under uniaxial compression; (ii) incorporation of metakaolin, silica fume, and slag into concrete can prompt both the strength and modulus of elasticity development of a young concrete; and (iii) metakaolin showed the best enhancement on the mechanical properties of young concrete. The reactivity of slag modified concrete was speeded up after one day. They also proposed an empirical formula for evaluating compressive strength of young concrete.

Li and Ding (2003) determined 28-day compressive strength of cement mortars containing metakaolin (MK) or combination of MK and slag as partial replacement of Portland cement. Four series of cement mortars pastes were made. First series (PO) contained 100% cement, 0% MK, and 0% slag; second (M1) had 90% cement and 10% MK, 0% slag; third (S2) had 70% cement, 10% MK, and 20% slag, and the fourth series (S3) had 60% cement, 10% MK, and 30% slag. Cement-to-sand ratio was 1:2.5, and water-to-binder ratio was 0.44. Compressive strength results of cement mortar are shown in Fig. 2.7. They showed that MK enhanced the compressive strength of cement mortar. Compressive strength of cement mortar M1 was about 8 MPa higher than that of PC mortar. Concrete achieved the best compressive strength

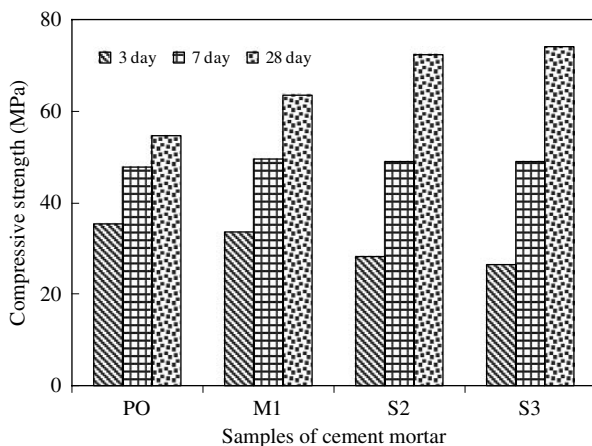


Fig. 2.7 The compressive strength of cement mortars (Li and Ding, 2003)

when PC was replaced by 10% MK. When PC was mixed with MK and ultra-fine slag at the same time, the 3-day compressive strength of S2 and S3 cement mortars was lower than that of PC and cement mortar M1. However, after 7 days, the strengths of S2 and S3 were higher than that of the M1 and PC mortars. After 28 days, the strength of S2 and S3 had greatly surpassed that of the two former cement mortars. Both MK and slag can react with CH release by cement clinker hydration to produce secondary C-S-H gel inside the cement paste. The secondary formed C-S-H gel improved the microstructure of cement paste matrix; therefore, the macroscopic property of cement was also improved. XRD analysis indicated that more $\text{Ca}(\text{OH})_2$ was consumed after adding both mineral admixtures.

Poon et al. (2003) studied the performance of metakaolin concrete at elevated temperatures up to 800°C. They prepared eight normal and high strength concrete (HSC) mixes incorporating 0, 5, 10 and 20% MK. They found that after an increase in compressive strength at 200°C, the MK concrete suffered a more severe loss of compressive strength. MK concrete showed a distinct pattern of strength gain and loss at elevated temperatures. After gaining an increase in compressive strength at 200°C, it maintained higher strengths as compared to the corresponding SF, FA and pure OPC concretes up to 400°C. A sharp reduction in compressive strength was observed for all HSC after 400°C followed by severe cracking and explosive spalling. Within the range 400–800°C, MK concretes suffered more loss and possessed lower residual strengths than the other concretes.

Poon et al. (2004) discussed the effect of elevated temperatures on the compressive strength, stress–strain relationship (stiffness) and energy absorption capacities of high-performance concretes (HPC). High-performance concretes (HPCs) were prepared in three series, with different cementitious material constitutions using plain ordinary Portland cement (PC), with and without metakaolin (MK) and silica fume (SF). Each series comprised a concrete mix, prepared without any fibers, and concrete mixes reinforced with either or both steel fibers and polypropylene (PP) fibers. The results showed that: (i) after exposure to 600°C and 800°C, the concrete mixes retained 45% and 23% of their compressive strength, respectively; (ii) at elevated temperatures, the loss of stiffness was much quicker than the loss in compressive strength, but the loss of energy absorption capacity was relatively slower; (iii) at 20% replacement of the cement by MK resulted in a higher compressive strength but a lower specific toughness, as compared with the concrete prepared with 10% replacement of cement by SF; (iv) MK concrete also showed quicker losses in the compressive strength, elastic modulus and energy absorption capacity after exposure to the elevated temperatures; (v) steel fibers approximately doubled the energy absorption capacity of the unheated concrete. The steel-fiber-reinforced concretes also showed the highest energy absorption capacity after the high-temperature exposure, although they suffered a quick loss of this capacity. In comparison, using PP fibers reduced the energy absorption capacity of the concrete after exposure to 800°C, although it had a minor beneficial effect on the energy absorption capacity of the concrete before heating; and (vi) for the unheated concretes, the use of MK at a replacement level of 20% of cement resulted in higher compressive strength than the use of SF at the level of 10%. In addition, the use of MK resulted in a

quicker degradation of the compressive strength of the concrete after exposure to the elevated temperatures.

Badogiannis et al. (2004) investigated the effect of metakaolin on the compressive strength of concrete. Poor Greek kaolin (C) was thermally treated and the produced metakaolin (MK) was superfine ground. In addition, a commercial metakaolin (MKC) of high purity was used. Eight mixture proportions were used to produce high-performance concrete, where metakaolin replaced either cement or sand in percentages of 10% or 20% by weight of the control cement content. The strength development of metakaolin concrete was evaluated using the efficiency factor (k value). The produced metakaolin (MK) as well as the commercial one (MKC) imparted a similar behavior with respect to the concrete strength. Both metakaolins exhibited very high k -values (close to 3.0 at 28 days) and were characterized as highly reactive pozzolanic materials that can lead to concrete production with an excellent performance. When metakaolin replaced sand, higher strengths than the OPC concrete were obtained at all ages up to 90 days. When metakaolin replaced cement, its positive effect on concrete strength generally started after 2 days.

Badogiannis et al. (2005) studied the compressive strength of cement containing five metakaolins upto the age of 180 days. The metakaolinite contents in metakaolins MK1, MK2, MK3, and MK4 (derived from poor Greek kaolins) were 36, 37, 71, and 49%, respectively, whereas it was 95% in a commercial metakaolin (MKC) of high purity. Cement was replaced with 0, 10, and 20% metakaolins. They concluded that metakaolin had a very positive effect on the cement strength after 2 days and specifically at 28 and 180 days (Table 2.16). The produced metakaolins as well as the commercial one gave similar hydration products after 28 days and the pozzolanic reaction was accelerated between 7 and 28 days, accompanied by a steep decrease of $\text{Ca}(\text{OH})_2$ content. Finally, it was concluded that a 10% metakaolin content seemed to be, generally, more favorable than 20%. The produced metakaolins, derived from poor Greek kaolins, as well as the commercial one imparted similar properties with respect to the cement strength development, the setting and the hydration.

Fortes-Revilla et al. (2006) determined the effect of factors such as dosage, curing conditions and use of a superplasticizer admixture on the porosity, mechanical strength and composition of slaked lime (SL)–metakaolin (MK) mortars. Statistical correlations were established to describe the mechanical properties as well as poros-

Table 2.16 Compressive strength of concrete containing metakaolins (Badogiannis et al., 2005)

Age (days)	Compressive strength (MPa)											
	PC		MK1		MK2		MK3		MK4		MKC	
	10%	20%	10%	20%	10%	20%	10%	20%	10%	20%	10%	20%
1	17	18	17	16	18	16	21	19	20	18	20	19
2	30	30	28	23	30	24	33	29	32	28	33	29
7	44	44	45	44	48	45	50	50	51	50	54	50
28	57	57	64	68	65	67	66	69	68	65	72	70
180	70	70	79	77	80	75	74	72	80	78	76	76

ity and composition of the slaked lime–metakaolin mortars. They concluded that: (i) SL/MK ratio had a moderate effect on mortar flexural and compressive strengths; (ii) SL + MK/sand ratio is the factor with the highest impact on all the properties studied: strength, porosity and mortar composition. As this ratio increased, strength, porosity and amount of hydration and carbonation products formed in the samples also rose; (iii) next factor in order of importance was the presence of a superplasticizer admixture, which affected porosity, strength and the amount of calcite in the sample. The presence of this superplasticizer admixture increased strength, raised the percentage of calcite in the mortars and reduced porosity; and (iv) neither curing nor open air carbonation time (in the range studied) had any significant effect on the composition or porosity of the SL–MK mortars studied, although they had a moderate effect on mechanical strength.

Fraire-Luna et al. (2006) investigated the hydration and properties of composite cementitious pastes with 75% fluorgypsum. Blast furnace slag and metakaolin were the complementary cementitious materials. The pastes were cured under water at 20°C for 360 days. All pastes developed and maintained strength under water, except those of commercial gypsum. The addition of metakaolin had a positive effect, after 360 days, compressive strengths of 13.4, 13.8 and 14.6 MPa were achieved for systems with 0%, 5% and 10% of metakaolin, respectively. The microstructure of the composite pastes was formed of a framework of gypsum crystals, which formed in the initial stages; the matrix was later densified by the formation of C–S–H and ettringite, as a result of the slag and metakaolin reactions. The fluorgypsum reacted rapidly in the initial days, however it was still present after one year; the slag reacted in a slower fashion, and the metakaolin was very reactive and contributed to the ettringite since the early ages, which enhanced the strength. Secondary electron images showed that the amount of ettringite increased with the MK contents and the curing time. The formation of ettringite in the empty spaces left by the gypsum crystals formation, resulted in a positive effect without the expansion and cracking typically observed when ettringite formed in consolidated cementitious microstructures. The incorporation of the reaction products of BFS and MK in the microstructure of the structure of the gypsum provided an acceptable mechanical strength and water resistance, obtaining a material that can be used under conditions where commercial plaster is not advisable, and also for other construction uses.

Razak and Wong (2005) presented a mathematical model for estimating compressive strength of high-strength concrete incorporating pozzolanic materials, based on the strength of a control ordinary Portland cement (OPC) concrete made with similar mixture characteristics and curing history. In this study, metakaolin (MK) and silica fume (SF) were used as cement replacement materials at 5, 10, and 15% by mass. Water/cementitious materials (w/cm) ratios varied from 0.27 to 0.33, and strength testing was conducted up to an age of 180 days. It was found that the strength of a pozzolanic mixture could be related to the strength of its equivalent control by a linear function. Key parameters involved in the model were the pozzolanic and dilution factors, which can be correlated to the pozzolan content in the mixture. The study concluded that the accuracy of the model increased with concrete's age. At 28 days and above, 97% of the estimated strengths were within

$\pm 5\%$ of the actual value. It has been demonstrated that the strength of a concrete mixture made with MK or SF can be related to the strength of an OPC control mixture. This relationship is described by using a linear equation in the form of $S_p = \alpha S_c + \beta$, where α and β are factors related to the pozzolanic and dilution effects of the particular pozzolan. The pozzolanic factor α and the dilution factor β can be represented by a three parameter hyperbolic function and a quadratic function of the pozzolan content, respectively.

Potgieter-Vermaak and Potgieter (2006) studied the compressive strength enhancement up to the age of 28 days, in mortars containing metakaolin additions between 10 and 30%. Activation temperature of MK ranged from 550 to 850°C for durations of 30 and 60 min. Cement mixes containing various replacement levels of MK from 10 to 30% by mass were prepared. These mixed cements were used to prepare mortars with a small sand/cementitious proportion of 3:1 by mass and water: cementitious material ratio of 0.375. Based on the results, they concluded that: (i) best activation temperature to produce metakaolin from kaolin is $> 700^\circ\text{C}$, and should preferably be at least 750°C ; (ii) compressive strengths increased with increased curing times and depended strongly on the activation temperature used. Strength enhancements did not depend significantly on the concentration of metakaolin addition; and (iii) longer activation time resulted in marginally higher compressive strengths in the mortars containing MK heated for 60 min compared to those having material heated for 30 min.

2.4.4 Tensile Strength

Qian and Li (2001) investigated the tensile strength of concrete incorporating 0, 5, 10, and 15% metakaolin as partial replacement of cement. Metakaolin had specific surface area $12000 \text{ m}^2/\text{kg}$, and its average particle diameter was $2.23 \mu\text{m}$. $300 \times 100 \times 20 \text{ mm}$ samples were tested under direct tension. Tests were conducted at the age of 28 days. Tensile strength test results are presented in Table 2.17. The results showed that tensile strength of concrete increased systematically with increasing metakaolin replacement level. The average tensile strength increases were 7% (5% metakaolin), 16% (10% metakaolin), and 28% (15% metakaolin), and the average ultimate strain increases were 3% (5% metakaolin), 19% (10% metakaolin), and 27% (15% metakaolin). The descending area of over-peak stress was less steep when metakaolin replacement was 5% and 10% whereas with 15% metakaolin it was similar to that for concrete without metakaolin. The tensile elasticity modulus for these specimens is in the range from 26 to 27 GPa.

Table 2.17 Tensile strength of concrete with different metakaolin replacement (Qian and Li, 2001)

Age (days)	Tensile strength (MPa)			
	MK (0%)	MK (5%)	MK (10%)	MK (15%)
28	3.35	3.58	3.88	4.29

2.4.5 Bending Strength

Qian and Li (2001) investigated the bending strength of concrete incorporating 0, 5, 10, and 15% metakaolin as partial replacement of cement. Metakaolin had specific surface area 12000 m²/kg, with average particle diameter being 2.23 μ m. 400 \times 100 \times 100 mm beam specimens were tested under four-point bend on a span of 300 mm. Tests were conducted up to the age of 80 days. Bending test results are presented in Table 2.18. They concluded that: (i) metakaolin replacement level of 5% had little effect on the bend strength of the concrete; and (ii) at 10 and 15% replacement, the 28-day bend strength increased by 32% and 38%, respectively. At 80 days of testing, increase in bending strength was 13 and 24% for 10 and 15% replacement, respectively. Therefore, significant improvement in bend strength of concrete can be achieved for replacement levels of 10–15% metakaolin.

Courard et al. (2003) determined the effect of metakaolin additions on the bending strength of mortar. Cement was replaced on a mass basis of 5–20% for metakaolin. The specimens were made with 3 parts of sand, 1 part of cement and 0.5 part of water) in which cement was OPC (CEM I 42.5). The first series of specimens was prepared from a mixture in which cement was replaced by metakaolin. Four different replacements, varying from 5% to 20% on a cement mass basis, were mixed with the cement. One mix was made with 10% by mass of natural kaolin. 40 \times 400 \times 160 mm specimens were cast and tested up to the age of 28 days. Bending strength results are shown in Fig. 2.8. They concluded that replacement of cement by metakaolin decreased the bending strength during the first days but achieved almost equal strength at 28 days.

2.4.6 Micro-Hardness

Micro-hardness testing provides a tool for quantifying micro-structural gradients across the interfacial transition zone (ITZ). Micro-hardness measurements can contribute to characterization of the properties of the ITZ relative to the bulk cement paste matrix and also provide one means of estimating the width of the ITZ. Lyubimova and Pinus (1962) evaluated micro-hardness gradients across aggregate–paste interfaces and observed, over a range of water/binder ratios, that measured micro-hardness decreased within 100 μ m of the aggregate surface. Whilst reductions in micro-hardness for the ITZ relative to the bulk regions are consistent with the hypothesis that the ITZ is a region of higher than average porosity, such observations

Table 2.18 Bending strength of concrete with different metakaolin replacement (Qian and Li, 2001)

Age (days)	Bending strength (MPa)			
	MK (0%)	MK (5%)	MK (10%)	MK (15%)
28	4.65	4.74	6.16	6.40
80	5.70	5.81	6.46	7.06

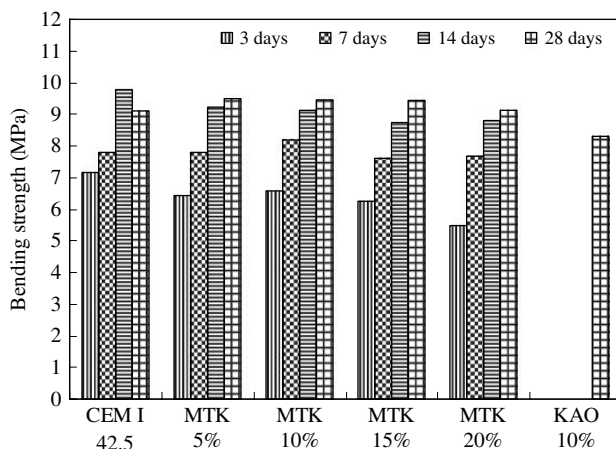


Fig. 2.8 Bending strength of mortars with CEM I 42.5, metakaolin and kaolin (Courard et al., 2003)

are not universal. Increases in micro-hardness within $50\text{ }\mu\text{m}$ of the aggregate surface have been reported (Saito and Kawamura, 1986), and Igurashi et al. (1996) suggested four ITZ/bulk region micro-hardness profiles. For example, in specimens where the microstructure of the ITZ is similar to the bulk region, the close proximity of the aggregate surface can increase micro-hardness values above those recorded for the bulk region by impeding the displacement of material from the indentation site. In contrast, where the ITZ microstructure is weaker than the bulk region, a depression in the micro-hardness profile is expected within the zone of influence of the aggregate, the profile at the aggregate surface also being influenced by the strength of the paste–aggregate bond.

Asbridge et al. (2002) determined the variations in the micro-hardness of the hydrated cement matrix component as functions of the distance from the aggregate surfaces for specimens in which the binder was Portland cement or a blend of Portland cement and metakaolin. Cement matrix of mortars were prepared with an aggregate content of 35% by volume. Water/binder ratios were 0.4, 0.5 and 0.6. Metakaolin was used as partial substitute (10% by mass) of Portland cement. Micro-hardness measurements were made using a Buehler Micromet Hardness Tester fitted with a Knoop indenter. Measurements were obtained using a 25 g load. Micro-hardness measurements were made up to distances of $120\text{ }\mu\text{m}$ from the aggregate. Variations in micro-hardness of bulk paste/ITZ are shown in Figs. 2.9–2.12. From Fig. 2.9, it appears that in Portland cement specimens, the ITZ was softer (more porous) than the bulk matrix at lower water/binder ratios. The micro-hardness of the ITZ was 22% lower than the bulk matrix at a water/binder ratio of 0.4 and was 18% lower at a water/binder ratio of 0.5. Figure 2.10 indicates that in the specimens prepared with Portland cement and 10% metakaolin as binder (metakaolin samples), the micro-hardness of the ITZ was similar to that of the bulk matrix. From Figs. 2.11 and 2.12, it is evident that the micro-hardness of the bulk matrix and, to a greater

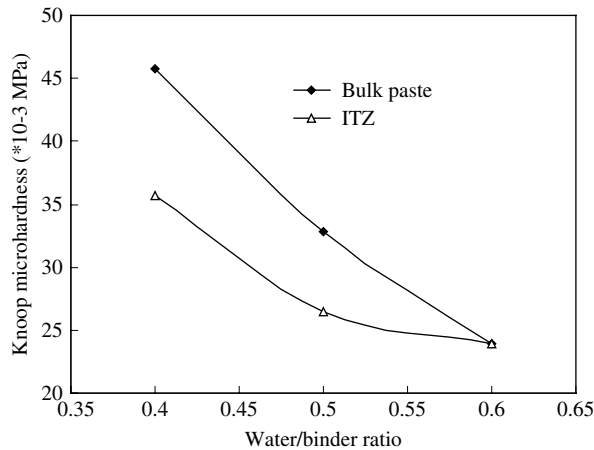


Fig. 2.9 Variation in micro-hardness of bulk paste and ITZ with water/binder ratio (Portland cement binder) (Asbridge et al., 2002)

degree, the ITZ was increased when metakaolin was used as a partial replacement for Portland cement. Based on the results, they concluded that: (i) micro-hardness of the paste–aggregate interfacial transition zones (ITZs) were found to be between 14% and 22% lower than those of the corresponding bulk cement pastes at the lower water/binder ratios (0.4 and 0.5) for samples prepared with Portland cement, and 0.4 for samples prepared with a binder comprising Portland cement and metakaolin; and (ii) metakaolin increased the mean micro-hardness of specimens prepared at the higher water/binder ratios of 0.5 and 0.6 by 13% and 54%, respectively.

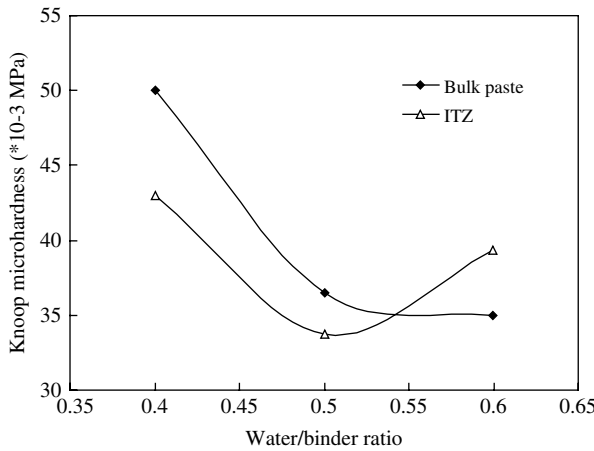


Fig. 2.10 Variation in micro-hardness of bulk paste and ITZ with water/binder ratio (Portland cement/metakaolin binder) (Asbridge et al., 2002)

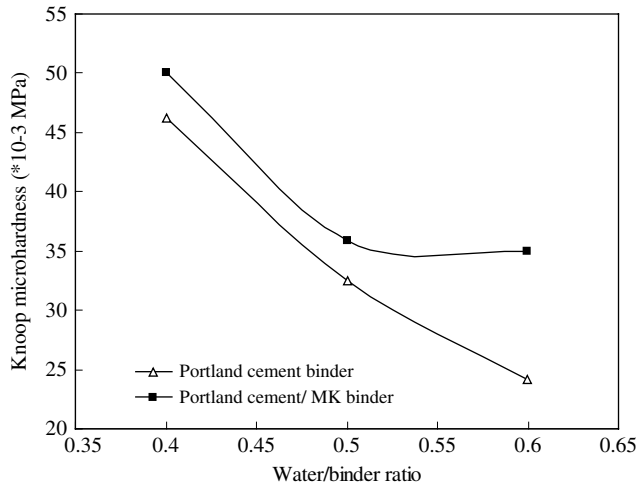


Fig. 2.11 Variation in micro-hardness of bulk paste with water/binder ratio and binder composition (Asbridge et al., 2002)

Glinicki and Zielinski (2004) described an application of a depth-sensing indentation (DSI) system to characterize properties of hardened cement paste. The test method developed, based on the micro-hardness testing concept, was implemented on a universal testing frame. Preliminary experiments were dedicated to evaluate efficiency of mineral additives in cement paste from Vickers hardness data. A suitable method of specimen preparation for micro-hardness tests was elaborated and successfully applied. The investigation revealed a clearly linear correlation between

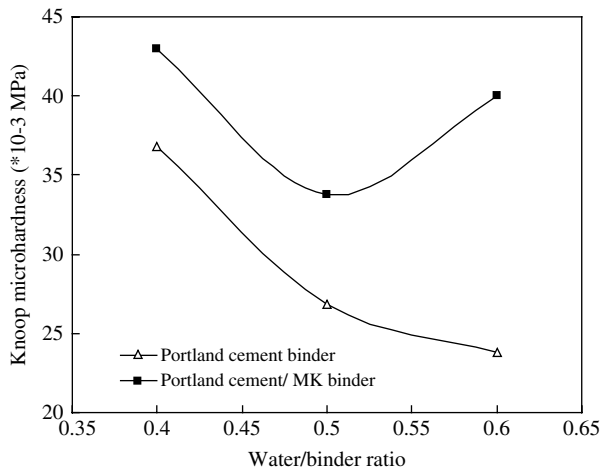


Fig. 2.12 Variation in micro-hardness of ITZ with water/binder ratio and binder composition (Asbridge et al., 2002)

Vickers hardness and water-to-cement (w/c) ratio. An evaluation of the efficiency of mineral additives in cement paste was possible assuming a criterion of equal Vickers hardness. The tests revealed a clearly linear correlation between Vickers hardness and w/c ratio of hardened cement pastes, both pure and modified with the addition of high reactivity metakaolin.

2.4.7 Relative Strength

Wild et al. (1996) investigated the role of metakaolin (MK) in enhancing the strength of concrete and identified the principal mechanisms. They cured metakaolin concretes with a range of MK contents (0–30%) for periods of 1–90 days. The change in relative strength with both curing time and metakaolin content was analyzed in relation to the ‘filler effect’, acceleration in OPC hydration and the pozzolanic reaction. Based on the investigation, they concluded that: (i) there are three elementary factors which influence the contribution that metakaolin makes to concrete strength when it partially replaced cement in concrete. These are the filler effect, the acceleration of OPC hydration, and the pozzolanic reaction of MK with CH; (ii) the filler effect was immediate, the acceleration of OPC had its major impact within the first 24 hours and the maximum effect of the pozzolanic reaction occurred at between 7 and 14 days; (iii) the optimum replacement level of OPC by MK to give maximum long term strength enhancement was about 20%. This differed from silica fume which continuously enhanced strength at extended ages up to replacement levels of at least 28%; and (iv) the positive contribution which metakaolin made to strength enhancement of concrete did not continue beyond about 14 days irrespective of the replacement level. This was a result of an elementary change in the MK-CH reaction beyond 14 days.

Wild and Khatib (1997) discussed about portlandite (CH) consumption in metakaolin cement pastes and mortars. Cement mortars and pastes containing 0, 5, 10 and 15% replacement of cement with metakaolin and with a water/binder (w/b) ratio of 0.55 were cured for periods from 3 to 365 days. The Portlandite content at different ages was determined by thermogravimetric analysis and was related to changes in relative strength. They concluded that: (i) the amounts of CH detected in young mortar pastes (both with and without metakaolin) were less than those detected in the equivalent aggregate free pastes. This was explained in terms of reduced initial hydration in the mortar pastes due to the formation of a denser bulk cement paste matrix of lower w/c ratio than the cement paste in the equivalent aggregate free pastes. This might have been due to the better compaction of the paste matrix in the mortar and greater loss of water due to bleeding, relative to the neat paste; (ii) the CH contents of both metakaolin mortar pastes and their equivalent standard pastes showed a minimum at about 14 days which coincided with a maximum in relative strength. This was attributed to a peak in pozzolanic activity for which more CH was being removed from the paste than was being generated by cement hydration; (iii) reaction of metakaolin with lime between 14 and 28 days

appeared to be severely retarded, with further sharp increase in CH content. This retardation could be explained in terms of formation of an inhibiting layer of reaction product on the metakaolin particles; (iv) beyond 28 days, there was evidence of further secondary reaction of metakaolin with CH particularly for the aggregate free pastes, although this is not reflected in any additional enhancement of relative strength; and (v) at the age of one year for paste with 15% replacement of cement by metakaolin, the amount of CH present relative to the cement is still 50% of that present in the equivalent metakaolin free paste. This suggests that replacement levels considerably in excess of 15% would be required to fully consume all the CH.

2.5 Durability Properties of Concrete Containing Metakaolin

2.5.1 Alkali-Silica Reaction

Ramlochan et al. (2000) evaluated the efficacy of high-reactivity metakaolin (HRM) in controlling expansion due to **alkali-silica reaction (ASR)**. Expansion of concretes and mortars containing 0–20% HRM as a partial replacement for OPC was determined. Concrete prisms ($75 \times 75 \times 300$ mm) were cast with two alkali-silica reactive aggregates: a siliceous limestone (Spratt) and greywacke-argillite gravel (Sudbury). Prisms containing the Spratt aggregate were cast with 0, 5, 10, 15, and 20% HRM as a partial cement replacement, and prisms containing the Sudbury aggregate were cast with 0, 10, and 15% HRM replacement levels. Concrete mixes were proportioned to have a total cementitious material (C+HRM) content of 420 kg/m^3 and a water-cementitious material ratio $W/(C+HRM)$ between 0.42 and 0.45. In concrete mixes containing 10% or more HRM, a calcium based high-range water-reducer was used to maintain workability. Mortar bars ($25 \times 25 \times 285$ mm) were cast with each reactive aggregate. Mortar mixes were proportioned to have an aggregate-cementitious material ratio of 2.25 and a water-cementitious material ratio of 0.5. The accelerated mortar bar method (CAN/CSA A23.2-25A or ASTM C 1260), modified for testing mineral admixtures was used. Tests were conducted up to 2 years. Based on the results obtained, they concluded that: (i) incorporation of HRM as a partial cement replacement between 10 and 15% may be sufficient to control deleterious expansion due to alkali-silica reaction in concrete, depending on the nature of the aggregate; (ii) amount of HRM required to control the expansion to $< 0.04\%$ at 2 years was found to be between 10 and 15% depending on the aggregate; (iii) the mechanism by which HRM may suppress expansion due to alkali-silica reaction appeared to be entrapment of alkalis by the supplementary hydrates and a consequent decrease in the pH of pore solutions; and (iv) alkali concentration of pore solutions expressed from pastes was significantly reduced when HRM was used to replace up to 20% of the OPC. The long-term hydroxyl ion concentration was reduced to less than 0.2 mol/l for both moderate-alkali cement and high-alkali cement.

2.5.2 Chloride-Ion Diffusion

Zhang and Malhotra (1995) measured the resistance to chloride penetration of PC concrete and PC–10% MK concrete. The concrete of w/b ratio 0.4 was moist-cured for 28 and 91 days prior to being subjected to electrical conductivity measurements in compliance with the ASTM C1202 test. The PC–MK concrete showed significantly lower conductivity values than the PC concrete. Thomas et al. (1997) and Hooton et al. (1997) determined the chloride penetration resistance of concrete of w/b ratios 0.3 and 0.4 containing 0, 8 and 12% replacement of PC with ‘high-reactivity MK’ (HRM). Data were presented in the form of ‘apparent diffusion coefficients’ calculated using Fick’s second law of diffusion from chloride concentration–depth profiles after 28, 90 and 140 days exposure to 1.0 mol/l NaCl solution. Cabrera and Nwaubani (1998) measured the effective chloride diffusion coefficients of PC, PC–15% PFA and PC–15% MK (for two different MKs) pastes using a chloride diffusion cell. The pastes of water/binder (w/b) ratio 0.4 were moist-cured (100% RH) for 60 days before being placed in the cell. Both the PC–MK and the PC–PFA pastes gave lower chloride diffusion coefficients than the PC paste, and the former gave particularly low values.

Boddy et al. (2001) and Gruber et al. (2001) determined the chloride diffusion up to 365 and 1095 days. The apparent diffusion coefficients were reduced on increasing the exposure time and on decreasing the w/b ratio, and showed marked decreases with increasing HRM content. Thomas et al. (1997) determined the chloride binding capacity of cement paste with and without 8% HRM by exposing dried paste samples to various concentrations of NaCl solution and determining the amount of chloride removed from solution on establishment of equilibrium. For up to a 1-M solution concentration, the binding capacities of the two pastes were similar but above this concentration, the binding capacity of the HRM paste increased at a much greater rate with increased solution concentration than did the pure PC paste.

Asbridge et al. (2001) studied the effect of metakaolin and variations in aggregate volume content on the diffusion kinetics of chloride ions in hydrated Portland cement model mortars. Chloride diffusion was monitored under both steady- and non-steady-state conditions, and capillary porosity data were obtained. 10% metakaolin was used as partial replacement for Portland cement. The compositions of pastes and mortars are given in Table 2.19.

Based on the tests results, they concluded that: (i) the steady-state diffusivity of chloride ions in mortar pastes incorporating metakaolin did not vary significantly with aggregate volume fractions. Mortar-paste capillary porosity data only showed some increases at aggregate volume fractions greater than 40%; (ii) non-steady-state

Table 2.19 Composition of pastes and mortars (Asbridge et al., 2001)

	Steady state	Non-steady state
Binder	PC/MK	PC, PC/MK
Water/binder ratio	0.35	0.40
Aggregate contents (% vol)	0, 15, 30, 40, 50, 55	0, 15, 35, 55

chloride diffusivities of mortar pastes increased with aggregate volume content in samples with only Portland cement as binder; (iii) The capillary porosity of the mortar paste increased with aggregate volume, indicating that the ITZ had a higher overall porosity than the bulk paste. The chloride diffusivity increased relatively sharply at aggregate volume fractions above 35%, whereas capillary porosities increased broadly linearly with aggregate content. This is suggestive of some interconnection of higher porosity ITZ regions results in percolation, thus, facilitating chloride diffusion; and (iv) the use of 10% metakaolin as a partial replacement for Portland cement reduced non-steady-state chloride diffusivities by approximately one-order of magnitude relative to those of samples with only Portland cement as binder. Mortar-paste diffusivities did not vary significantly with variations in aggregate content. Relative to control samples, metakaolin reduced mortar-paste capillary porosities although the latter still increased with increasing aggregate volumes. The lack of variation in mortar-paste diffusivity and rising capillary porosity with increasing aggregate content supports the hypothesis that the use of metakaolin increases permeation path tortuosity and inhibits percolation.

Bai et al. (2003b) reported the influence of the composition of Portland cement (PC)–pulverized fuel ash (PFA)–metakaolin (MK) binders on chloride ingress of PC–PFA–MK concrete exposed to synthetic seawater. Eleven mixes, with a binder (PC–PFA–MK) content of 390 kg/m^3 , w/b ratio of 0.5 and a wide range of MK–PFA combinations, were used. PC–PFA–MK concrete covering four different total cement replacement levels (10, 20, 30 and 40%) and with various MK: PFA proportions were exposed to synthetic seawater for up to 1.5 years. The chloride concentration–penetration depth profiles were compared with those of the control PC concrete. Table 2.20 gives an example of chloride concentration–penetration depth data for 30% total replacement. They concluded that: (i) blending the binders in PC concrete and PC–PFA concrete with MK produced concrete with good resistance to chloride penetration when exposed to seawater; (ii) significant reductions in chloride penetration depths occurred when PC was partially replaced with PFA and MK. These reductions increased with both increasing total replacement level and increasing exposure time. This was attributed to the relative changes in intrinsic diffusivity and chloride binding capacity with age exhibited by the different binder compositions; (iii) in ternary PC–PFA–MK blends, MK had a significant beneficial effect on both the chloride concentration and penetration depth. At short exposure duration (2 and 4 months) increasing MK content generally led to reduced concentration and penetration depth. A 30% PC replacement by PFA was particularly effective in decreasing both the chloride concentration and penetration depth, especially at long exposure times; and (iv) in the case of binary blends, substantial enhancement with MK and reduction with PFA in early compressive strength (28 days) of the water-cured specimens occurred. At long curing times (18 months) both MK and PFA enhanced strength. Both binary (PC–PFA) and ternary blends caused significant improvement in compressive strength of concrete exposed to seawater compared to that of the control concrete.

Courard et al. (2003) studied the effect of metakaolin additions on the chloride diffusion rates of mortars. Cement was partially replaced with metakaolin. Replace-

Table 2.20 Chloride concentration (ppm) – penetration depth (mm) data for 30% total replacement (Bai et al., 2003b)

Mixes	Depth (mm)											
	1	2.75	4.5	6.25	8	9.75	12	14.3	16.5	18.8	21	23.3
2 months												
Control	25.5	9.8	4.5	2.1	0	–	–	–	–	–	–	–
0% MK-30% PFA	3	1	0.77	0.72	0	–	–	–	–	–	–	–
7.5% MK-22.5% PFA	2	0.5	0	–	–	–	–	–	–	–	–	–
4 months												
Control	38	19	10.5	5.5	2.3	0	–	–	–	–	–	–
0% MK-30% PFA	10	2.5	1	0.8	0	–	–	–	–	–	–	–
7.5% MK-22.5% PFA	3.5	0.67	0	–	–	–	–	–	–	–	–	–
10 months												
Control	45	37	29	20	15	9	5	2	0	–	–	–
0% MK-30% PFA	35	14	7	2.93	1	0	–	–	–	–	–	–
7.5% MK-22.5% PFA	30	16.6	7	3.36	2	0	–	–	–	–	–	–
18 months												
Control	51.7	43	35	26.4	23	19.5	16.5	10.8	7.6	4	2.5	0
0% MK-30% PFA	50.1	18.7	11	7.86	2	0.78	0	–	–	–	–	–
7.5% MK-22.5% PFA	42.5	30.6	15	5.48	3	1	0	–	–	–	–	–

ment percentages were 0, 10, 15, and 20%. One mixture with natural kaolin was also made. The specimens were made with 3 parts of sand, 1 part of cement and 0.5 part of water) in which cement was OPC (CEM I 42.5). Specimens of 100 mm diameter and 150 mm height were made for chloride diffusion tests. Rates of diffusion of Cl^- and Na^+ ions into cement mortars were monitored using two-compartment diffusion cells. The cells were filled at one side with $\text{Ca}(\text{OH})_2$ solution and at the other side with 1 M NaCl in saturated $\text{Ca}(\text{OH})_2$ solution. At periodic intervals, chloride concentration was determined by titration from a 20 cm^3 sample of the solution. The evolution of chloride diffusion was measured for 314 days for cement, metakaolin and kaolin (Table 2.21). The occurrence time (breakthrough time) was calculated from the intercept of the concentration versus time date. Transport through OPC mortar specimens was observed after only 13 days, with an apparent diffusion coefficient of $1.29 \times 10^{-12} \text{ m}^2/\text{s}$. Occurrence time (breakthrough time) represents the time necessary for the initiation of Cl^- ion transfer through the sample. It gives, consequently, a view of the porous skeleton. The best results were obtained for a

Table 2.21 Chloride diffusion rates for mortars with CEM I 42.5, metakaolin and kaolin (Courard et al., 2003)

Material	Breakthrough time (days)	Apparent diffusion coefficient (m^2/s)
CEM I 42.5	13	1.29×10^{-12}
5% Metakaolin	45	4.71×10^{-12}
10% Metakaolin	82	3.31×10^{-12}
15% Metakaolin	203	1.23×10^{-12}
20% Metakaolin	Not after one year	–
10% Kaolin	4	1.81×10^{-12}

metakaolin content of 20% because after about 1 year test no diffusion was observed. An increase from 10% to 15% metakaolin content seemed to induce an increase of 150% of occurrence time and a decrease of 170% for diffusion coefficient. Kaolin had no effect and seemed on the contrary to accelerate the phenomenon of diffusion in comparison with the reference mix.

Poon et al. (2006) determined the chloride penetrability of the concrete mixes incorporating metakaolin (MK) or silica fume (SF) at water-to-binder (w/b) ratios of 0.3 and 0.5. Two series of concrete mixes were prepared at the w/b ratios of 0.3 and 0.5. Each series included three MK mixes with 5, 10, and 20% metakaolin and two SF mixes with 5 and 10% silica fume; and a control mix without any mineral admixture. MK or SF was used as a replacement of cement on a weight to weight basis. The maximum nominal size of the coarse aggregate was 10 mm for the concrete with a w/b of 0.3 and 20 mm for the concrete with a w/b of 0.5. For the concrete at a w/b of 0.3, the superplasticizer was used to achieve a slump of not less than 100 mm. The chloride penetrability of concrete was determined following the procedures of ASTM C1202-94 using the 50 mm thick portions as sample obtained from the 100 by 200 mm concrete cylinders. Chloride permeability tests were conducted up to the age of 90 days and results are presented in Table 2.22. They concluded that: (i) both the MK and SF concretes showed lower total charges passed than the control. At the w/b of 0.3, concrete with a 10% MK replacement showed the best performance, while at the w/b of 0.5, concrete with a 20% replacement was the best; (ii) when comparing the MK and SF concretes, 5% SF replacement in concrete resulted in a lower total charge passed than a 5% MK replacement, but a 10% MK replacement resulted in a lower total charge passed than a 10% SF replacement, at both w/b of 0.3 and 0.5. The difference in the total charge passed between the MK concrete and the SF concrete with a 10% replacement level is particularly significant when they were prepared at the w/b of 0.5; and (iii) this indicated that at a higher w/b ratio and percentage of replacement the use of MK is more effective than SF in improving the resistance of concretes to chloride ion penetration.

Table 2.22 Chloride permeability of control and blended concretes (Poon et al., 2006)

Series	w/b ratio	Mix	Total charge passed (Coulombs)			
			3 days	7 days	28 days	90 days
1	0.30	Control	2461	2151	1035	931
		5% MK	1327	1244	862	646
		10% MK	417	347	199	135
		20% MK	406	395	240	124
		5% SF	1060	945	665	426
		10% SF	567	445	360	336
2	0.50	Control	5312	4054	2971	2789
		5% MK	4215	3765	2079	1065
		10% MK	1580	1247	918	752
		20% MK	751	740	640	580
		5% SF	3156	2047	1641	1235
		10% SF	3140	1877	1223	1053

2.5.3 Hydroxide Ion Diffusion

Coleman and Page (1997) determined the hydroxide ion concentrations of expressed pore solutions of Ordinary Portland cement pastes containing 0, 10 and 20% of metakaolin by weight of cement at various stages of hydration. Blended cements were prepared from OPC and two grades of metakaolin, labeled as MK501 (major elements; SiO₂ 54.2%; Al₂O₃ 40.8%) and MK505 (major elements; SiO₂ 52.1%; Al₂O₃ 41%), of differing composition with respect to minor contaminants. All cement paste samples were prepared in duplicate with distilled water at a water/solids ratio of 0.5. Blended cement pastes were produced by partial replacement of the OPC with metakaolin. Samples containing chloride ions were prepared by dissolution of the required quantities of sodium chloride in the water prior to mixing. The specimens were cast into plastic cylinders (80 mm × 49 mm diameter), and stored for periods of 1, 7, 36 and 100 days. Pore solutions were expressed from duplicate paste specimens for each level of metakaolin replacement and maturity. The determination of hydroxide and chloride ion concentrations was carried out in triplicate for each pore solution. Hydroxide concentrations were obtained by titration with nitric acid in the presence of phenolphthalein and chloride concentrations were measured by a spectrophotometric method. The effects of replacement additions of metakaolin on the pore solution chloride ion concentrations for samples containing 1.0% of internal chloride ions are shown in Figs. 2.13 and 2.14. It is clear from these that both grades of metakaolin caused a substantial reduction in the concentrations of free chloride ions that were retained in the pore solution phase of paste specimens in which 1% chloride (by weight of total solids) had been included as a mix contaminant. This effect was also observed for specimens made from the 501 grade of metakaolin with 0.4% chloride. In specimens with only 0.1% chloride as a mix contaminant, the capacity of the cement hydration products to bind chloride ions was such that

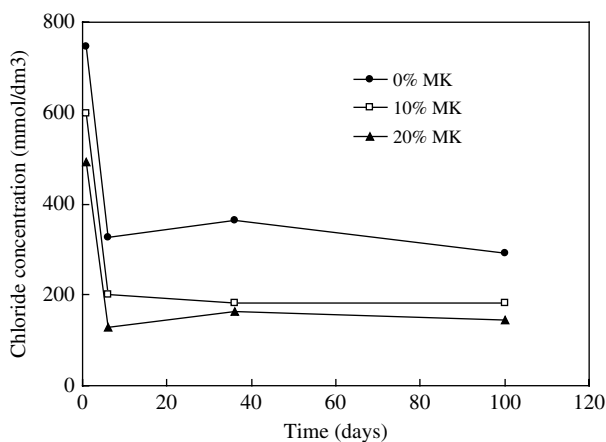
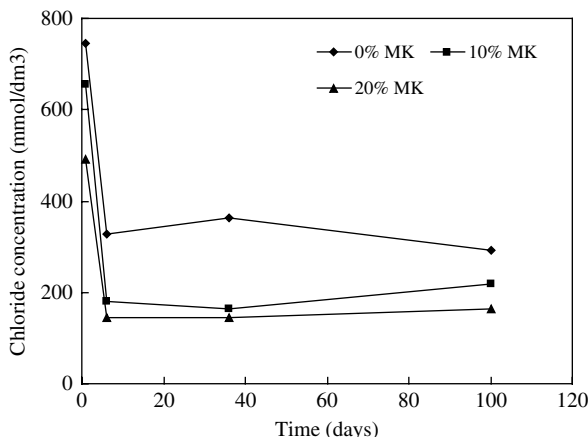


Fig. 2.13 Effect of additions of MK501 on pore solution chloride ion concentration for samples containing 1.0% internal chloride ions (by weight of total solids) (Coleman and Page, 1997)

Fig. 2.14 Effect of additions of MK505 on pore solution chloride ion concentration for samples containing 1.0% internal chloride ions (by weight of total solids) (Coleman and Page, 1997)



the concentrations of chloride remaining in the pore solution at ages of 36 days or longer had fallen to around 10 mmol dm^{-3} , irrespective of whether the material contained 0, 10 or 20% metakaolin.

2.5.4 Sulfate Resistance

Sulfate attack is one of the most aggressive environmental deteriorations that affect the long-term durability of concrete structures. The sulfate attack on concrete leads to expansion, cracking, and deterioration of many civil engineering structures exposed to sulfate environment such as piers, bridges, foundations, concrete pipes, etc. The sulfate ions in solution, which come from the soil, ground water, and seawater, are found in combination with other ions such as sodium, potassium, magnesium and calcium ions. The sulfate attack is generally attributed to the reaction of sulfate ions with calcium hydroxide and calcium aluminate hydrate to form gypsum and ettringite. The gypsum and ettringite formed as a result of sulfate attack is significantly more voluminous (1.2–2.2 times) than the initial reactants. The formation of gypsum and ettringite leads to expansion, cracking, deterioration, and disruption of concrete structures. In addition to the formation of ettringite and gypsum and its subsequent expansion, the deterioration due to sulfate attack is partially caused by the degradation of calcium silicate hydrate (C–S–H) gel through leaching of the calcium compounds. This process leads to loss of C–S–H gel stiffness and overall deterioration of the cement paste matrix.

Khatib and Wild (1998) evaluated the effect of metakaolin on the sulfate resistance of mortar. Two types of cements were used; high C_3A and intermediate C_3A content. Cement was replaced with 0, 5, 10, 15, 20, and 25% of metakaolin (MK). Specimens of size $25 \times 25 \times 285 \text{ mm}$ were moist-cured in air for 14 days, and their length was measured before immersing in 5% Na_2SO_4 solution. Test results demonstrated that: (i) expansion decreased systematically with the increase in MK

content for both types of cement; (ii) for mortars containing high C_3A cement, the control mortar and mortars containing 5% and 10% MK showed rapid expansion and deterioration between 40 and 70 days exposure to sulfate solution. Mortars containing 15% and 20% MK showed small but quite sharp expansions also between 40 and 70 days, but subsequently stabilized. By 520 days, mortar containing 20% and 25% MK showed no significant changes in length; and (iii) with intermediate C_3A content in cement, trend was similar to the mortars made with high C_3A content. The control mortar (0% MK) showed significant expansion followed by 5% MK mortar. Mortar containing 10% MK exhibited little expansion and other mortar specimens containing 15, 20 and 25% were found to be extremely stable, showing little overall change and no sign of deterioration after 520 days of exposure in sodium sulfate solution.

Lee et al. (2005) reported an experimental study on the magnesium sulfate resistance of mortar and paste specimens incorporating varying percentages of metakaolin (MK). The resistance of mortar specimens was evaluated by expansion measurements. Four different mortar mixtures were prepared. Cement was partially replaced with 0, 5, 10 and 15% of MK by mass. The water–cementitious material ratio (w/cm) was fixed at 0.45 by mass. The cementitious material/fine aggregate was invariant at 2.0 in all mortar mixtures. Prisms ($25 \times 25 \times 285$ mm) were cast for expansion measurements. All mortar and paste samples were immersed in magnesium sulfate solution ($MgSO_4$) for 360 days. Sulfate solution concentrations used were 0.42% (3380 ppm of SO_4^{2-}), 1.27% (10,140 ppm of SO_4^{2-}) and 4.24% (33,800 ppm of SO_4^{2-}), respectively. Test results of expansion of mortars at 360 days are shown in Fig. 2.15. They concluded that: (i) at low solution concentration (0.42%) of magnesium sulfate ($MgSO_4$), only the MK5 mortar specimen showed an expansion value of over 0.1%; (ii) at magnesium sulfate solution concentration of 1.27%, the mortar specimens with 5% to 15% replacement levels of MK exhibited poor resistance to magnesium sulfate attack. After 360 days of

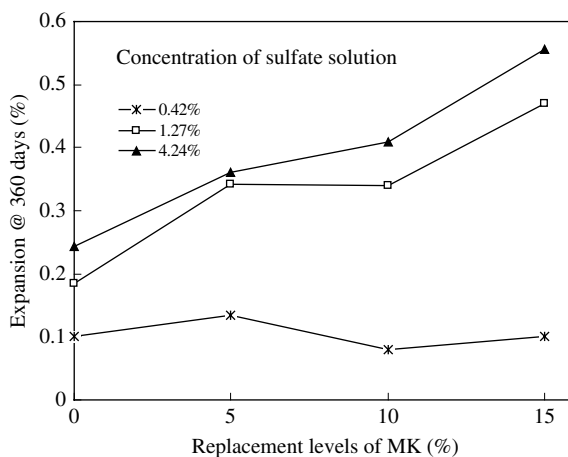


Fig. 2.15 Effect of solution concentrations and MK replacement levels on the expansion of mortar specimens exposed to magnesium sulfate solution (Lee et al., 2005)

exposure, expansion values were 0.343, 0.339 and 0.469% for MK5, MK10 and MK15 mortar specimens, respectively, whereas the MK0 mortar specimens exhibited about 0.185% expansion after the same period of exposure; and (iii) at high solution concentration of magnesium sulfate (4.24% MgSO_4), the expansion values for the MK0 mortar was about 0.244% after 360 days of exposure, whereas mortar specimens with partial replacement levels of MK showed expansions of 0.360%, 0.410% and 0.556% for MK5, MK10 and MK15 mortar mixtures, respectively.

Al-Akhras (2006) investigated the effect of metakaolin (MK) as replacement of cement on the durability of concrete to subjected sulfate attack. Three MK replacement levels 5, 10, and 15% by weight of cement were used. The other experimental parameters were: water to binder ratio (0.5 and 0.6), initial moist curing period (3, 7, and 28 days), curing type (moist and autoclaving), and air content (1.5% and 5%). The degree of sulfate attack was evaluated by measuring expansion of concrete prisms ($75 \times 75 \times 300$ mm). The sulfate exposure testing procedure was conducted by immersing concrete specimens after the specified initial curing in a water tank containing 5% sodium sulfate solution for a total period of 18 month (ASTM C1012-04). The effect of MK replacement level on the variation of sulfate expansion exposure is shown in Figs. 2.16 and 2.17. Based on the results, they concluded that: (i) the sulfate resistance of MK concrete was higher than that of plain concrete (without MK replacement). Sulfate resistance of MK concrete increased with increasing the MK replacement levels. Plain concrete was not durable to sulfate attack reaching maximum sulfate expansion values of 0.4% and 0.45% after 18 months at w/b ratios of 0.5 and 0.6, respectively; (ii) the 10% and 15% MK concrete at both w/b ratios used (0.5 and 0.6) showed excellent durability to sulfate attack and sulfate expansion was 0.10% and 0.07% for concrete at w/b ratio of 0.5, and 0.13% and 0.10% for concrete specimens at w/b ratio of 0.6, respectively; and (iii) The 5% MK concrete showed intermediate durability to sulfate attack reaching maximum sulfate expansion values of 0.17% and 0.2% for concrete at w/b ratios of 0.5 and 0.6, respectively.

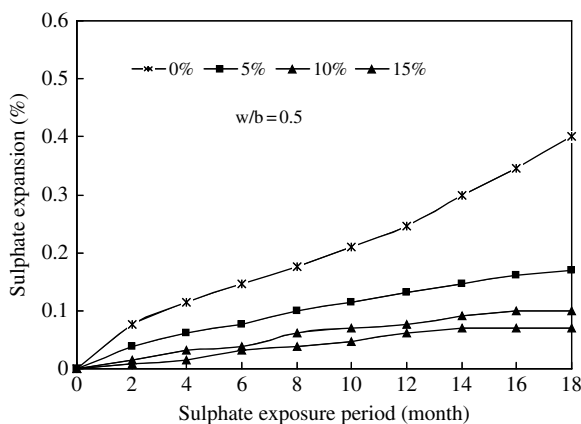
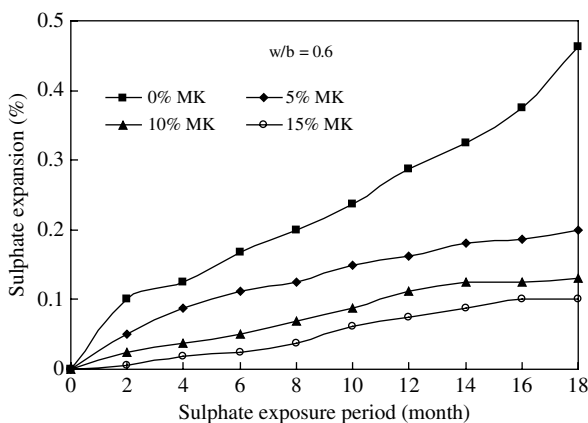


Fig. 2.16 Effect of metakaolin replacement level on the variation of sulfate expansion with sulfate exposure period at w/b ratio of 0.5 (Al-Akhras, 2006)

Fig. 2.17 Effect of metakaolin replacement level on the variation of sulfate expansion with sulfate exposure period at w/b ratio of 0.6 (Al-Akhras, 2006)



The increase in the sulfate resistance of MK concrete with increase in MK replacement level can be explained by the following mechanisms. First, the replacement of a portion of Portland cement with MK reduces the total amount of tricalcium aluminate hydrate in the cement paste matrix of concrete. The second mechanism is through the pozzolanic reaction between the MK and calcium hydroxide released during the hydration of cement, which consumes part of the calcium hydroxides. Thus, the quantity of expansive gypsum formed by the reaction of calcium hydroxide will be less in MK concrete than in plain concrete. Furthermore, the formation of secondary C–S–H by the pozzolanic reaction, although less dense than the primary C–S–H gel, is effective in filling and segmenting large capillary pores into small, discontinuous capillary pores through pore size refinement, decreasing the total permeability of concrete. In addition to the pozzolanic reaction, the filler action of MK due to the fine particle size of MK (1 μm) compared to the particle size of cement (12 μm) further densifies the pore structure of MK concrete to enhance the resistance of MK concrete to sulfate attack.

Smallwood et al. (2003) studied the resistance of metakaolin (MK)–Portland cement (PC) concrete to thaumasite-type of sulfate attack (TSA). The thaumasite form of sulfate attack is a deleterious physico-chemical attack of the calcium silicate hydrate (C–S–H), binding phase of concrete. Water/binder ratios (w/b) are known to control ingress of potentially deleterious ions by pore structure refinement at low (0.40) values. Equally, a physical-chemical barrier exists at about w/b ratio of 0.45 regardless of the binder type. The inclusion of metakaolin in the binder has been shown to impart such properties through densification of the matrix and removal of calcium hydroxide. Results were found for concrete incorporating dolomitic limestone aggregate and with 0% and 7% metakaolin replacement of a high-C₃A PC binder at w/b ratios to 0.40 and 0.46. Exposure to three environments containing a sulfatic clay, sulfate solution and water produced evidence of deleterious reactions within these samples. Visual data were quantified by a wear rating up to 280 days of exposure. These results confirmed the importance of low water binder ratios in the resistance of ion ingress and gave an early indication of

the desirable durability-enhancing properties of MK replacement of PC. Finally, the results also showed that the two sulfatic environments of exposure produce marked differences in the degradation modes. They concluded that: (i) expansion of concrete exposed to sulfate solution at 5°C was reduced by reducing the w/b ratio and by partially replacing the binder with 7% MK. The expansion of the concrete was accompanied by corresponding reductions in concrete compressive strength; (ii) concrete with low w/b ratio (0.40) at 5°C experienced initial autogenous shrinkage followed by marked expansion, whereas concrete at the higher w/b ratio (0.46) showed negligible shrinkage and reduced expansion. Replacing the binder with 7% MK tends to delay these processes; and (iii) the form of degradation of the concrete exposed to sulfate solution at 5°C was very different from that exposed to sulfatic clay at 5°C. In the former case, material resulting from chemical reaction continually spalled away from the outer surfaces leaving them continuously exposed to the aggressive solution. Clearly diffusion rates and concentration gradients of aggressive species at the concrete – exposure-medium interface are going to be very different in the two different exposure environments and the former may not be appropriate for investigating reaction mechanisms under field conditions. The preliminary evidence confirmed that MK inhibited TSA in the short term and may therefore have potential application for preventing TSA in concrete. In addition the observation of extrusion of gel, particularly extreme for the concrete with w/b ratio 0.40 and with 7% MK, suggested that alkali carbonate reaction may be associated with the TSA in the particular system under investigation.

Tsivilis et al. (2003) reported the results relating to the effect of a second mineral addition on the sulfate resistance of limestone cement. Limestone cement mortars containing natural pozzolana, blast furnace slag, fly ash or metakaolin were exposed to sulfate solution at low and room temperature and their performance was studied for over a year. Concrete made from limestone cement may exhibit a lack of durability due to the formation of thaumasite. The addition of minerals that improved the concrete durability is expected to slow down the formation of thaumasite. Limestone cement containing 15% w/w limestone was used. Mortar specimens were prepared by replacing a varying part of the limestone cement with the above minerals. Siliceous and calcareous sand was used in order to study the effect of the sand type on the thaumasite formation. The specimens were immersed in a 1.8% MgSO_4 solution and cured at 5 and 25°C. The formation of thaumasite was checked and confirmed by visual inspection, strength tests, ultrasonic pulse velocity measurements, XRD and TGA. It was concluded that the use of specific minerals, as partial replacement of cement, inhibited the thaumasite formation in limestone cement mortar. Limestone cement mortar is susceptible to the thaumasite-kind of sulfate attack at low temperature. The use of specific mineral replacements retards the thaumasite formation in limestone cement mortar. Incorporation of metakaolin and GGBS substantially improve the resistance of the limestone cements against sulfate attack. The use of fly ash seemed to retard sulfate attack. The effectiveness of natural pozzolans against sulfate attack very much depends on their rate of reaction. Slowly reacting pozzolans appear to be unable to provide effective resistance against

sulfate attack, if the concrete is exposed to sulfates before the pozzolanic reaction begins to act.

Roy et al. (2001) studied the effect of silica fume, metakaolin, and low-calcium fly ash on chemical resistance of concrete. Effects of aggressive chemical environments were evaluated on the mortars prepared with OPC and silica fume (SF)/metakaolin (MK)/low-calcium fly ash at various replacement levels. The natural adverse chemical environmental conditions were simulated using sulfuric acid, hydrochloric acid, nitric acid, acetic acid, phosphoric acid, and a mixture of sodium and magnesium sulfates. Chemical resistance information was used in conjunction with compressive strength measurements to propose realistic OPC/mineral admixture proportions. Substitution of SF, MK, or FA under certain conditions increased the chemical resistance of such mortars over those made with plain Portland cement. Mortars were relatively little affected by 1% hydrochloric acid, 1% sulfuric acid, and 1% nitric acid environments, but those mortars made from all three series showed poor resistance to higher acid concentrations: 5% sulfuric acid, 5% acetic acid, and 5% phosphoric acid environments. Chemical resistance increased in the order of SF to MK to FA series and decreased as the replacement level is increased from 0–10 wt. % replacement level to 15–30 wt. % level. Contrary to expectation, chemical resistance increased with change from 0.36 to 0.40 W/S ratios.

2.5.5 Corrosion Resistance

Batis et al. (2005) studied the effect of metakaolin on the corrosion resistance of cement mortar. A poor Greek kaolin with low kaolinite content was thermally treated and the produced metakaolin (MK) was ground to the appropriate fineness. In addition, a commercial metakaolin (MKC) of high purity was used. Several mixture proportions were used to produce mortar specimens, where metakaolin replaced either sand or cement. Mortar specimens were then exposed to the corrosive environment of either partial or total immersion in 3.5% w/w NaCl solution. For evaluation of the performance of metakaolin, the following criteria considered: compressive strength, corrosion potential, mass loss, electrochemical measurements of the corrosion rate by the Linear Polarization method, carbonation depth and porosity. They concluded that: (i) metakaolin improved the compressive strength and the 10% addition showed the optimum contribution to the strength development and (ii) the use of metakaolin, either as a sand replacement up to 20%, or as a cement replacement up to 10% w/w, improved the corrosion behavior of mortar specimens, while there is no positive effect when metakaolin was added in greater percentages.

2.5.6 Creep and Shrinkage

Brooks and Johari (2001) studied the effect of metakaolin (Mk) on creep and shrinkage of concrete mixtures containing 0, 5, 10, and to 15% of MK. Control mixtures

Table 2.23 Results for the 200-day total and autogenous shrinkage of concrete (Brooks and Johari, 2001)

Item/Concrete mixtures	OPC	MK5	MK10	MK15
Total shrinkage from initial set (10^{-6})	861	713	618	516
Total shrinkage from 24 hour (10^{-6})	558	499	455	410
Total autogenous shrinkage from initial set (10^{-6})	445	485	419	327
Autogenous shrinkage 24 hours (10^{-6})	142	271	256	221
% of A.S. – T.S. from initial set	52	68	68	63
% of A.S. – T.S. from 24 hour	25	54	56	54
Weight loss of the exposed specimens (%)	0.85	0.67	0.73	0.76

were made with OPC, whereas the other mixtures were prepared by replacing cement partially with 5, 10, and 15% MK. Mixture proportion of OPC concrete was 1:1.5:2.5 with a water-to-cement ratio of 0.28. Cylindrical concrete specimens of 267 x 76 mm diameter were cast for autogenous shrinkage and creep tests. Autogenous was measured from the time of initial set to 24 hours and from 24 hours till 200 days. Total shrinkage consists of autogenous shrinkage from 24 hours and drying shrinkage due to water loss to environment. The results of autogenous, total shrinkage and creep are given in Tables 2.23 and 2.24. Based on the test results they concluded that: (i) at early days, autogenous shrinkage was reduced with the increase in MK content. The autogenous shrinkage after 24 hours for MK15 concrete was reduced by 65% compared with OPC concrete. The reduction of autogenous shrinkage could be due to the dilution effect which is caused by reduction in cement content; (ii) at long-term, autogenous shrinkage increased with the increase in MK content. The 200 day autogenous shrinkage increased by 91%, 80%, and 56% for MK5, MK10, and MK15, respectively; and (iii) inclusion of MK reduced both total and basic creep of concrete, with a greater reduction in creep at higher replacement levels. The reduction in creep could be attributed to a denser pore structure, stronger paste matrix and improved paste aggregate interface of MK concrete mixtures as a result of the formation of additional hydrate phases from secondary pozzolanic reaction of MK and its filler effect. The 200-day specific drying creep which is taken as the difference between the specific total creep and basic creep was also reduced for MK concretes.

Table 2.24 Results of creep after 200 days (Brooks and Johari, 2001)

Concrete mixture	Creep (10^{-6})		Stress (MPa)	Specific Creep (10^{-6} /MPa)		Drying creep (10^{-6} /MPa)
	Dry	Sealed		Dry	Sealed	
OPC	358	285	13.9	25.8	20.5	5.3
MK5	312	235	16.8	18.5	14.0	4.5
MK10	201	126	17.7	11.3	7.2	4.1
MK15	171	115	17.9	9.5	6.4	3.1

References

- Al-Akhras NM (2006) Durability of metakaolin to sulfate attack. *Cement and Concrete Research* 36 (9): 1727–1734.
- Alonso S, Palomo A (2001a) Alkaline activation of metakaolin and calcium hydroxide mixtures: influence of temperature, activator concentration and solids ratio. *Materials Letters* 47: 55–62.
- Alonso S, Palomo A (2001b) Calorimetric study of alkaline activation of calcium hydroxide + metakaolin solid mixtures. *Cement and Concrete Research* 31: 25–30.
- Ambroise J, Maximilien S, Pera J (1994) Properties of metakaolin blended cements. *Advanced Cement Based Materials* 1: 161–168.
- Ambroise J, Murat M, Pera J (1986) Investigations on synthetic binders obtained by middle-temperature thermal dissociation of clay minerals. *Silicates Industries* 7 (8): 99–107.
- Asbridge AH, Chadbourne GA, Page CL (2001) Effects of metakaolin and the interfacial transition zone on the diffusion of chloride ions through cement mortars. *Cement and Concrete Research* 31: 1567–1572.
- Asbridge AH, Page CL, Page MM (2002) Effects of metakaolin, water/binder ratio and interfacial transition zones on the micro hardness of cement mortars. *Cement and Concrete Research* 32: 1365–1369.
- Asbridge AH, Walters GV, Jones TR (1994) Ternary blended concretes- OPC/GGBFS/metakaolin. Denmark: Concrete Across Borders, pp. 547–557.
- Badogiannis E, Kakali G, Dimopoulou G, Chaniotakis E, Tsivilis S (2005) Metakaolin as a main cement constituent: Exploitation of poor Greek kaolins. *Cement & Concrete Composites* 27: 197–203.
- Badogiannis E, Papadakis VG, Chaniotakis E, Tsivilis S (2004) Exploitation of poor Greek kaolins: strength development of metakaolin concrete and evaluation by means of k-value. *Cement and Concrete Research* 34: 1035–1041.
- Bai J, Wild S (2002) Investigation of the temperature change and heat evolution of mortar incorporating PFA and metakaolin. *Cement & Concrete Composites* 24: 201–209.
- Bai J, Wild S, Sabir BB (2002) Sorptivity and strength of air-cured and water-cured PC–PFA–MK concrete and the influence of binder composition on carbonation depth. *Cement and Concrete Research* 32: 1813–1821.
- Bai J, Wild S, Sabir BB (2003b) Chloride ingress and strength loss in concrete with different PC–PFA–MK binder compositions exposed to synthetic seawater. *Cement and Concrete Research* 33: 353–362.
- Bai J, Wild S, Ware JA, Sabir BB (2003a) Using neural networks to predict workability of concrete incorporating metakaolin and fly ash. *Advances in Engineering Software* 34: 663–669.
- Batis G, Pantazopoulou P, Tsivilis S, Badogiannis E (2005) The effect of metakaolin on the corrosion behavior of cement mortars. *Cement & Concrete Composites* 27: 125–130.
- Boddy A, Hooton RD, Gruber KA (2001) Long-term testing of the chloride-penetration resistance of concrete containing high-reactivity metakaolin. *Cement and Concrete Research* 31 (5): 759–765.
- Bredy P, Chabannet M, Pera J (1989) Microstructural and porosity of metakaolin blended cements. *Material Research Society Symposium* 137: 431–436.
- Brooks JJ, Johari MMA (2001) Effect of metakaolin on creep and shrinkage of concrete. *Cement & Concrete Composites* 23: 495–502.
- Cabrera JG, Nwaubani SO (1998) The microstructure and chloride ion diffusion characteristics of cements containing metakaolin and fly ash. In: V.M. Malhotra (Eds.), *Sixth CANMET/ACI/JCI International Conference on Fly Ash, Silica Fume, Slag and Natural Pozzolans in Concrete*, Bangkok, Thailand, 1: 385–400.
- Cabrera J, Rojas MF (2001) Mechanism of hydration of the metakaolin-lime-water system. *Cement and Concrete Research* 31: 177–182.
- Changling H, Osbaeck B, Makovicky E (1995) Pozzolanic reaction of six principal clay minerals: Activation reactivity assessments and technological effects. *Cement and Concrete Research* 25 (8): 1691–1702.

- Coleman NJ, Page CL (1997) Aspects of the pore solution chemistry of hydrated cement pastes containing metakaolin. *Cement and Concrete Research* 27 (1): 147–154.
- Courard L, Darimont A, Schouterden M, Ferauche F, Willem X, Degeimbre R. (2003) Durability of mortars modified with metakaolin. *Cement and Concrete Research* 33: 473–1479.
- Curcio F, DeAngelis BA (1998) Dilatant behavior of superplasticized cement pastes containing metakaolin. *Cement and Concrete Research* 28 (5): 629–634.
- Curcio F, Deangelis BA, Pagliolico S (1998) Metakaolin as pozzolanic micro filler for high-performance mortars. *Cement and Concrete Research* 28 (6): 803–809.
- Dias WPS (2000) Reduction of concrete sorptivity with age through carbonation. *Cement and Concrete Research* 30 (8): 1255–1261.
- Fortes-Revilla C, Martínez-Ramírez S, Blanco-Varela MT (2006). Modeling of slaked lime–metakaolin mortar engineering characteristics in terms of process variables. *Cement & Concrete Composites* 28: 458–467.
- Fraire-Luna PE, Escalante-Garcia JI, Gorokhovskiy A (2006) Composite systems fluorgypsum–blast furnace slag–metakaolin, strength and microstructures. *Cement and Concrete Research* 36: 1048–1055.
- Frías M, Cabrera J (2000) Pore size distribution and degree of hydration of MK-Cement pastes. *Cement and Concrete Research* 30: 561–569.
- Frías M, Cabrera J (2001) Influence of MK on the reaction kinetics in MK/lime and MK-blended cement systems at 20°C. *Cement and Concrete Research* 31: 519–527.
- Frías M, Sánchez de Rojas MI, Cabrera J (2000) The effect that the pozzolanic reaction of metakaolin has on the heat evolution in metakaolin-cement mortars. *Cement and Concrete Research* 30: 209–216.
- Glinicki MA, Zielinski M (2004) Depth-sensing indentation method for evaluation of efficiency of secondary cementitious materials. *Cement and Concrete Research* 34: 721–724.
- Gruber KA, Ramlochan T, Boddy A, Hooton, RD, Thomas MDA (2001) Increasing concrete durability with high-reactivity metakaolin. *Cement and Concrete Research* 23 (6): 479–484.
- Hooton RD, Gruber KA, Boddy A (1997) The chloride penetration resistance of concrete containing high reactivity metakaolin. *Proceedings of the PCI/FHWA International Symposium on High Performance Concrete*, New Orleans, LA, pp. 172–183.
- Igurashi S, Bentur A, Mindess S (1996) Micro-hardness testing of cementitious materials. *Advanced Cement Based Materials* 4: 48–57.
- Jin X, Li Z (2003) Effects of mineral admixture on properties of young concrete. *Journal of Materials in Civil Engineering* 15 (5): 435–442.
- Khatib JM, Clay RM (2004) Absorption characteristics of metakaolin concrete. *Cement and Concrete Research*. 34 (1): 19–29.
- Khatib JM, Mangat PS (1995) Absorption characteristics of concrete as a function of location relative to casting position. *Cement and Concrete Research* 25 (5): 999–1010.
- Khatib JM, Wild S (1996) Pore size distribution of metakaolin paste. *Cement and Concrete Research* 26 (10): 1545–1553.
- Khatib JM, Wild S (1998) Sulfate resistance of metakaolin mortar. *Cement and Concrete Research* 28 (1): 83–92.
- Kinuthia JM, Wild S, Sabir BB, Bai J (2000) Self-compensating autogenous shrinkage in Portland cement-metakaolin-fly ash pastes. *Advance Cement Research* 12 (1): 35–43.
- Klimesch DS, Ray A (1998a) Hydrogarnet formation during autoclaving at 180°C in unstirred metakaolin-lime-quartz slurries. *Cement and Concrete Research* 28 (8): 1109–1117.
- Klimesch DS, Ray A (1998b) Autoclaved cement-quartz pastes with metakaolin additions. *Advanced Cement Based Materials* 7: 109–117.
- Kostuch JA, Walters GV, Jones TR (1993) High performance concrete incorporating metakaolin – a review. *Concrete* 2000, University of Dundee, pp. 1799–1811.
- Larbi JA, Bijen JM (1992) Influence of pozzolans on the Portland cement paste – aggregate interface in relation to diffusion of ions and water absorption in concrete. *Cement and Concrete Research* 22: 551–562.

- Lee ST, Moon HY, Hooton RD, Kim JP (2005) Effect of solution concentrations and replacement levels of metakaolin on the resistance of mortars exposed to magnesium sulfate solutions. *Cement and Concrete Research* 35: 1314–1323.
- Li Z, Ding Z (2003) Property improvement of Portland cement by incorporating with metakaolin and slag. *Cement and Concrete Research* 33: 579–584.
- Lyubimova TY, Pinus ER (1962) Crystallization structure in the contact zone between aggregate and cement. *Concr. Kolloidn. Z. (USSR)* 24 (5): 578–587.
- Murat M (1983) Hydration reaction and hardening of calcined clays and related minerals. *Cement and Concrete Research* 13: 259–266.
- Oriol M, Pera J (1995) Pozzolanic activity of metakaolin under microwave treatment. *Cement and Concrete Research* 25 (2): 265–270.
- Palomo A, Blanco-Varela MT, Granizo ML, Puertas F, Vazquez T, Grutzeck MW (1999) Chemical stability of cementitious materials based on metakaolin. *Cement and Concrete Research* 29: 997–1004.
- Pera J, Ambroise J, Messi, A (1998) A pozzolanic activity of calcined laterite. *Silicates Industries, Ceram Sci Technol* 63 (7–8): 107–111.
- Poon CS, Azhar S, Anson M, Wong YL (2003) Performance of metakaolin concrete at elevated temperatures. *Cement & Concrete Composites* 25: 83–89.
- Poon CS, Kou SC, Lam L (2006) Compressive strength, chloride diffusivity and pore structure of high performance metakaolin and silica fume concrete. *Construction and Building Materials* 20: 858–865.
- Poon CS, Lam L, Kou SC, Wong YL, Wong R (2001) Rate of pozzolanic reaction of metakaolin in high-performance cement pastes. *Cement and Concrete Research* 31: 1301–1306.
- Poon CS, Shui ZH, Lam L (2004) Compressive behavior of fiber reinforced high-performance concrete subjected to elevated temperatures. *Cement and Concrete Research* 34: 2215–2222.
- Potgieter-Vermaak SS, Potgieter JH (2006) Metakaolin as an extender in South African cement. *Journal of Materials in Civil Engineering* 18 (4): 619–623.
- Qian X, Li Z (2001) The relationships between stress and strain for high-performance concrete with metakaolin. *Cement and Concrete Research* 31: 1607–1611.
- Ramlochan T, Thomas M, Gruber KA (2000) The effect of metakaolin on alkali-silica reaction in concrete. *Cement and Concrete Research* 30: 339–344.
- Ramlochan T, Zacarias P, Thomas MDA, Hooton RD (2004) The effect of pozzolans and slag on the expansion of mortars cured at elevated temperature Part II: Microstructural and microchemical investigations. *Cement and Concrete Research* 34: 1341–1356.
- Razak HA, Chai HK, Wong HS (2004) Near surface characteristics of concrete containing supplementary cementing materials. *Cement & Concrete Composites* 26: 883–889.
- Razak HA, Wong HS (2005) Strength estimation model for high-strength concrete incorporating metakaolin and silica fume. *Cement and Concrete Research* 35: 688–695.
- Rojas MF (2006) Study of hydrated phases present in a MK–lime system cured at 60°C and 60 months of reaction. *Cement and Concrete Research* 36: 827–831.
- Rojas MF, Cabrera J (2002) The effect of temperature on the hydration rate and stability of the hydration phases of metakaolin–lime–water systems. *Cement and Concrete Research* 32: 133–138.
- Rojas MF, Sánchez de Rojas MI (2003) The effect of high curing temperature on the reaction kinetics in MK/lime and MK-blended cement matrices at 60°C. *Cement and Concrete Research* 33: 643–649.
- Roy DM, Arjunan P, Silsbee MR (2001) Effect of silica fume, metakaolin, and low-calcium fly ash on chemical resistance of concrete. *Cement and Concrete Research* 31: 1809–1813.
- Saikia NJ, Sengupta P, Gogoi PK, Borthakur PC (2002a) Cementitious properties of metakaolin–normal Portland cement mixture in the presence of petroleum effluent treatment plant sludge. *Cement and Concrete Research* 32: 1717–1724.
- Saikia NJ, Sengupta P, Gogoi PK, Borthakur PC (2002b) Hydration behavior of lime–co-calcined kaolin–petroleum effluent treatment plant sludge. *Cement and Concrete Research* 32: 297–302.

- Saito M, Kawamura M (1986) Resistance of the cement – aggregate interfacial zone to the propagation of cracks. *Cement and Concrete Research* 16 (5): 653–661.
- Salvador S (1995) Pozzolanic properties of flash-calcined kaolinite: A comparative study with soak-calcined products. *Cement and Concrete Research* 25 (1): 102–112.
- Sayanam RA, Kalsotra AK, Mehta SK, Singh RS, Mandal G (1989) Studies on thermal transformations and pozzolanic activities of clay from Jamu region (India). *Journal of Thermal Analysis* 35: 99–106.
- Shvarzman A, Kovler K, Grader GS, Shter GE (2003) The effect of dehydroxylation/ amorphization degree on pozzolanic activity of kaolinite. *Cement and Concrete Research* 33: 405–416.
- Smallwood I, Wild S, Morgan E (2003) The resistance of metakaolin (MK)–Portland cement (PC) concrete to the thaumasite-type of sulfate attack (TSA)—Programme of research and preliminary results. *Cement & Concrete Composites* 25: 931–938.
- Sun W, Zhang Y-S, Lin W, Liu Z-Y (2004) In situ monitoring of the hydration process of K-PS geopolymer cement with ESEM. *Cement and Concrete Research* 34: 935–940.
- Thomas MDA, Gruber KA, Hooton RD (1997) The use of high reactivity metakaolin in high performance concrete, 1st Engineering Foundation Conference on High Strength Concrete, Hawaii, pp. 517–530.
- Tsivilis S, Kakali G, Skaropoulou A, Sharp JH, Swamy RN (2003) Use of mineral admixtures to prevent thaumasite formation in limestone cement mortar. *Cement & Concrete Composites* 25: 969–976.
- Wild S, Khatib JM (1997) Portlandite Consumption in metakaolin cement pastes and mortars. *Cement and Concrete Research* 27 (1): 137–146.
- Wild S, Khatib JM, Jones A (1996) Relative strength, pozzolanic activity and cement hydration in superplasticised metakaolin concrete. *Cement and Concrete Research* 26 (10): 1537–1544.
- Wild S, Khatib J, Roose JL (1998) Chemical and autogenous shrinkage of Portland cement-metakaolin pastes. *Advanced Cement Research* 10 (3): 109–119.
- Wong HS, Razak HA (2005) Efficiency of calcined kaolin and silica fume as cement replacement material for strength performance. *Cement and Concrete Research* 35: 696–702.
- Zhang MH, Malhotra VM (1995) Characteristics of a thermally activated aluminosilicate pozzolanic material and its use in concrete. *Cement and Concrete Research* 25 (8): 1713–1725.

Chapter 3

Recycled/Waste Plastic

Introduction

Plastics have become an inseparable and integral part of our lives. The amount of plastics consumed annually has been growing steadily. Its low density, strength, user-friendly designs, fabrication capabilities, long life, light weight, and low cost are the factors behind such phenomenal growth. Plastics have been used in packaging, automotive and industrial applications, medical delivery systems, artificial implants, other healthcare applications, water desalination, land/soil conservation, flood prevention, preservation and distribution of food, housing, communication materials, security systems, and other uses. With so large and varying applications, plastics contribute to an ever increasing volume in the solid waste stream. In the United States, approximately 13.5 billion kg of plastic wastes is produced each year, which represents about 8%, by weight, of the total solid wastes (Office of Solid Waste and Emergency Response, 1990). Plastic wastes are very visible as they contribute to a large volume of the total solid wastes. Current data estimate that plastics represent 14–21% by volume of the US solid waste stream (Environmental Protection Agency, 1991). Precisely because of their large visibility, plastic wastes (and particularly non-sustainable plastic products) have been viewed as a serious solid waste problem. In the year 1996, in the MSW, plastics amounted to about 12%, by weight in United States (Franklin Associates Ltd., 1998). The waste plastics collected from the solid wastes stream is a contaminated, assorted mixture of a variety of plastics. This makes their identification, segregation, and purification very challenging. In the plastics waste stream, polyethylene forms the largest fraction, which is followed by PET. Lesser amounts of a variety of other plastics can also be found in the plastics waste stream as given in Table 3.1 (Subramanian, 2000).

World's annual consumption of plastic materials has increased from around 5 million tons in the 1950s to nearly 100 million tons in 2001. In the UK, a total of approximately 4.7 million tons of plastic products were used in various economic sectors in 2001. The amount of plastic waste generated annually in the UK is estimated to be nearly 3 million tons. An estimated 56% of all plastics waste is used packaging, three-quarters of which is from households. It is estimated that only 7% of total plastic waste arising are currently being recycled. According to

Table 3.1 Types and quantities of plastics in municipal solid waste in USA (Subramanian, 2000)

Type of plastic	Quantity (t) \times 1000
Polyethyleneterephthalate (PET)	1700
High density polyethylene (HDPE)	4120
Low density polyethylene (LDPE)	5010
Polypropylene (PP)	2580
Polystyrene (PS)	1990
Other	3130

a 2003 Environment Agency report, 80% of post-consumer plastic waste is sent to landfill, 8% is incinerated and only 7% is recycled. In addition to reducing the amount of plastics waste requiring disposal, recycling plastic can have several other advantages. In the United States, approximately 11 million tons of plastic wastes are produced each year, which represents about 11.1% of total MSW generation (EPA, 2003). Plastic wastes are very visible as they contribute to a large volume of the total solid wastes. Precisely because of their large visibility, plastic wastes (and particularly non-sustainable plastic products) have been viewed as a serious solid waste problem.

The largest component of the plastic waste is low density polyethylene/linear low density polyethylene (LDPE) at about 23%, followed by 17.3% of high density polyethylene, 18.5% of polypropylene, 12.3% of polystyrene (PS/extended PS), 10.7% polyvinyl chloride, 8.5% polyethylene terephthalate and 9.7% of other types (Association of Plastics Manufactures in Europe, 2004).

3.1 Types of Plastic and Plastic Waste

The quantity of plastics consumed annually all over the world has been growing phenomenally. Its exceptionally user-friendly, characteristics/features, unique flexibility, fabricatability and processability coupled with immense cost-effectiveness and longevity are the main reasons for such astronomical growth. Besides its wide use in packaging, automotive and industrial applications, these are also extensively used in medical delivery systems, artificial implants and other healthcare applications, water desalination and bacteria removal of, preservation and distribution of food, housing appliances, communication and electronics industry etc. Table 3.2 details the uses of plastics and recycled plastics (Recycling and Resource Recovery Council, Australia, 1994).

3.1.1 Benefits/Advantages of Plastics

The growth in the use of plastic is due to its beneficial properties, which include:

- Extreme versatility and ability to be tailored to meet specific technical needs
- Lighter weight than competing materials reducing fuel consumption during transportation

Table 3.2 Uses of plastics and recycled plastics (Recycling and Resource Recovery Council, Australia, 1994)

Name of plastic	Description	Some uses for virgin plastic	Some uses for plastic made from recycled waste plastic
Polyethylene terephthalate (PET)	Clear tough plastic, may be used as a fiber.	Soft drink and mineral water bottles, filling for sleeping bags and pillows, textile fibers.	Soft drink bottles, (multi-layer) detergent bottles, clear film for packaging, carpet fibers, and fleecy jackets.
High density polyethylene (HDPE)	Very common plastic, usually white or colored.	Crinkly shopping bags, freezer bags, milk and cream bottles, bottles for shampoo and cleaners, milk crates.	Compost bins, detergent bottles, crates, mobile rubbish bins, agricultural pipes, pallets, kerbside recycling crates.
Unplasticised polyvinyl chloride (UPVC)	Hard rigid plastic.	Clear cordial and juice bottles, blister packs, plumbing pipes and fittings.	Detergent bottles, tiles, plumbing pipe fittings.
Plasticized polyvinyl chloride (PPVC)	Flexible, clear, elastic plastic.	Garden hose, shoe soles, blood bags and tubing.	Hose inner core, industrial flooring.
Low density polyethylene (LDPE)	Soft, flexible plastic.	Lids of ice-cream containers, garbage bags, garbage bins, black plastic sheet.	Film for builders, industry, packaging and plant nurseries, bags.
Polypropylene (PP)	Hard, but flexible plastic – many uses.	Ice-cream containers, potato crisp bags, drinking straws, hinged lunch boxes.	Compost bins, kerbside recycling crates, worm factories.
Polystyrene (PS)	Rigid, brittle plastic. May be clear, glassy.	Yoghurt containers, plastic cutlery, imitation crystal “glassware”.	Clothes pegs, coat hangers, office accessories, spools, rulers, video/CD boxes.
Expanded polystyrene (EPS)	Foamed, lightweight, energy absorbing, thermal insulation.	Hot drink cups, takeaway food containers, meat trays, packaging.	

- Good safety and hygiene properties for food packaging
- Durability and longevity
- Resistance to chemicals, water and impact
- Excellent thermal and electrical insulation properties
- Comparatively lesser production cost
- Unique ability to combine with other materials like aluminum foil, paper, adhesives
- Far superior aesthetic appeal
- Material of choice – Human life style & plastic inseparable
- Intelligent features, smart materials & smart systems

3.1.2 Disadvantages of Plastics

Plastics production also involves the use of potentially harmful chemicals, which are added as stabilizers or colorants. Many of these have not undergone environmental risk assessment and their impact on human health and the environment is currently uncertain. Such an example is phthalates, which are used in the manufacture of PVC. PVC has in the past been used in toys for young children and there have been concerns that phthalates may be released when these toys are sucked (come into contact with saliva). Risk assessments of the effects of phthalates on the environment are currently being carried out. The disposal of plastics products also contributes significantly to their environmental impact. Most plastics are non-degradable, and they may take a long time to break down once they are landfilled. With more and more plastics products, particularly plastics packaging, being disposed of soon after their purchase, the landfill space required by plastics waste is a growing concern.

3.2 Utilization of Waste/Recycled Plastics

Applications of plastic usage are wide-ranging. Some plastic items such as food packaging, become waste only a short time after purchase. Other plastic items lend themselves to be reused many times over. Reusing plastic is preferable to recycling as it consumes lesser amounts of energy and resources. Long life, multi-trip plastics packaging has become more widespread in recent years, replacing less durable and single-trip alternatives, thereby reducing waste. In United States, 80% of post-consumer plastic waste is sent to landfill, 8% is incinerated and only 7% is recycled (EPA, 2003). In addition to reducing the amount of plastic waste requiring disposal, recycling plastic can have several other advantages:

- Conservation of non-renewable fossil fuels – plastic production uses 8% of the world's oil production, 4% as feedstock and 4% during manufacture
- Reduced consumption of energy
- Reduced amounts of solid waste going to landfill
- Reduced emissions of carbon-dioxide (CO₂), nitrogen-oxide (NO) and sulfur dioxide (SO₂)

3.2.1 Advantages of Waste/Recycled Plastic

Advantages of using waste/recycled plastics are: (i) reduction of municipal solid wastes being land filled; and (ii) an alternative to pressure-treated lumber that leaches toxic chemicals into water.

3.2.2 Classification of Recycled Plastic in Concrete

3.2.2.1 Virgin Polypropylene

The virgin polypropylene fibers are 19 mm long fibrillated fibers. These are in slender fiber-form.

3.2.2.2 Recycled Plastic (Melted Processed)

The recycled plastic (melted processed) is produced by drawing molten automobile bumpers into long strands, which are cut, to 28 mm length. It is in slender fiber-form.

3.2.2.3 Recycled Plastic (Automobile Shredded Residue)

Automobile shredded residue comprised mainly mixed plastics and some rubber, with a maximum particle dimension of 19 mm. It is in flake form.

3.2.2.4 Recycled Plastic (Shredded)

The recycled plastic (shredded) is produced by shredding plastics that is obtained from a mixed plastic stream; the process yielded plastic flakes with a maximum planar dimension of 25. It is in flake form.

Zoorob and Suparma (2000) reported the physical properties of recycled plastic (low density polyethylene, LDPE), and the same are given in Table 3.3. Details of the properties of virgin and recycled discrete reinforcement system used in concrete by Soroushian et al. (2003) are given in Table 3.4.

3.3 Management Options

An integrated approach is required in an attempt to manage such large quantities of a diverse, contaminated mixture of plastics in an energy efficient and environmentally benign manner. This would require examining critically various steps in the life of the plastics such as the raw materials for their manufacture, the manufacturing processes, design and fabrication of the finished products, possible reuse of those items, and the proper disposal of the wastes etc., in totality. Such an integrated

Table 3.3 Physical properties of recycled plastics (Zoorob and Suparma, 2000)

Properties	Low density polyethylene (LDPE)
Granulate shape	Pellet
Size (mm)	5.00–2.36
Specific gravity	0.92
Softening point (°C)	120
Melting point (°C)	140

Table 3.4 Properties of virgin and recycled discrete reinforcement system (Soroushian et al., 2003)

Discrete reinforcement	Aspect ratio	Specific gravity	Dosage in concrete (kg/m ³)	Volume (%)
Virgin polypropylene	150	1.2	0.9 1.8	0.075 0.15
Recycled plastic (melt-processed)	11.1	0.8	0.9 1.5	0.1 0.19
Recycled plastic (automotive shredded residue)	1.65	1.0	20	2.0
Recycled plastic (shredded)	3.70	1.0	10 20	1 2
Discrete reinforcement			Mixture identification	
Virgin polypropylene			poly1.5 & poly3.0	
Recycled plastic (melt-processed)			plmp1.5 & plmp2.5	
Recycled plastic (automotive shredded residue)			plsr34	
Recycled(shredded)			plsh17 & plsh34	

waste management concept comprises: (i) source reduction; (ii) reuse; (iii) recycling; (iv) landfill; and (v) waste-to-energy conversion.

The flow chart of a plastic waste management operation system is schematically shown in Fig. 3.1 The major operations involved in a waste management process include the collection of the plastic waste outside or inside the municipal waste stream, its disposal in landfills, its energy recovery, recycling into useful products, and the establishment of markets for the recycled products (Rebeiz and Craft, 1995).

3.3.1 Collection

Plastic wastes could be retrieved in two ways; first method consists of collecting plastics after they enter the municipal waste stream, and second method involves collection of plastics before they enter the municipal waste stream. Most post-consumer wastes end up in the municipal waste stream. Curlee (1986) reported that these plastic wastes are usually very contaminated and are difficult to recycle economically. Therefore, the wastes are either disposed in landfills or incinerated to reduce their volume and to recover their energy content. Conversely, plastic wastes collected outside the municipal waste stream are relatively clean and can be recycled after undergoing some separation and purification processes.

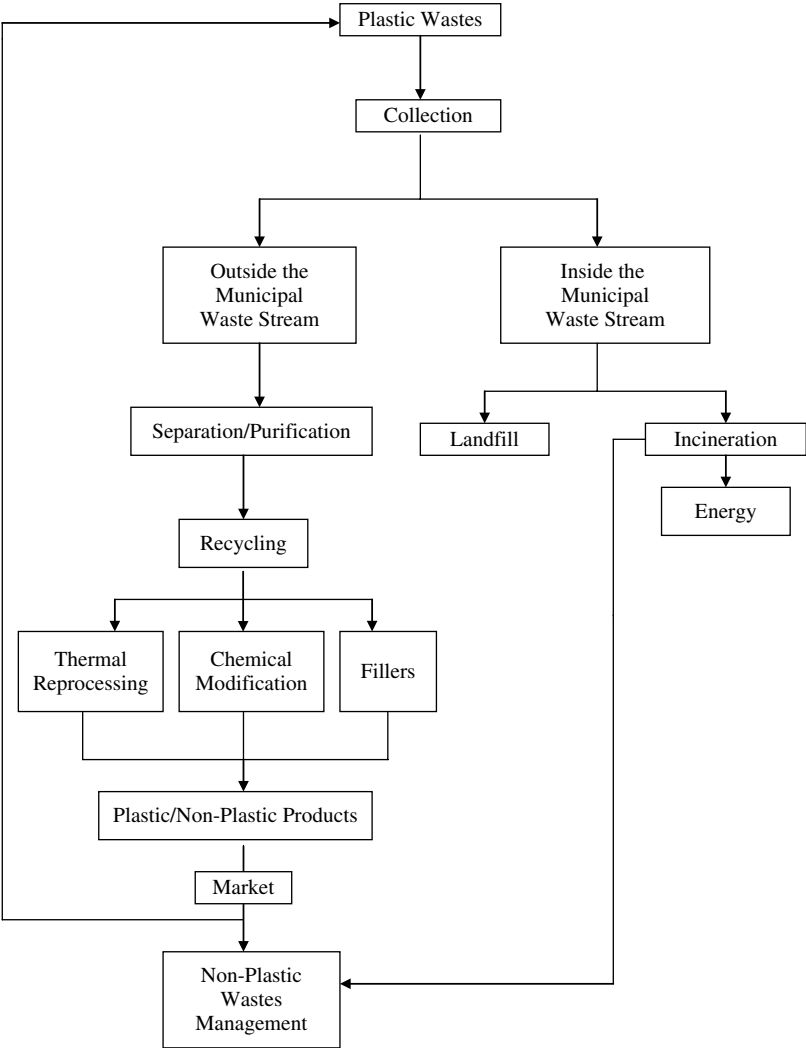


Fig. 3.1 Plastic waste management process (Rebeiz and Craft, 1995)

3.3.2 Landfilling Plastics

The disposal of plastics in landfills raises some concerns since the material degrades very slowly. Wastes such as paper and food wastes, are equally very slow to degrade in landfills. Therefore, the degradation of plastics and other wastes should not be made an issue since it has little effect on landfill capacity. Plastic wastes do not create difficulties in landfill operations and also do not contribute to the toxicity of leachate from the landfills (Environmental Protection Agency, 1991; Office of Solid Waste and Office of Water, 1990). Biodegradation (such as incorporating

starch additives to the plastic) and photo degradation (such as incorporating photo-sensitive additives to the plastic) are the two technologies that are being explored for commercial applications. Light and air must be present for these materials to decompose, along with sufficient moisture and nutrients to sustain microbial action (Alter, 1993; Boettcher, 1992). These requirements are not met for materials buried in landfills. Accordingly, the EPA does not believe that the use of degradable plastics will help solve landfill capacity problems. Furthermore, the environmental impact of degradable residues is still not well understood (Environmental Protection Agency, 1991; Office of Solid Waste and Office of Water, 1990). Moreover, making plastics degradable would lower the quality and performance of the material and therefore would mitigate some of its major desirable features in various applications.

3.3.3 Incineration of Plastics

The heat content of plastic wastes can be recovered by incineration. Plastic wastes are a good fuel source because most resins have a heating value almost equivalent to that of the coal. In addition to providing an attractive source of alternative energy, preserving natural resources and minimizing the impact of dependency on energy, incineration also greatly reduces the volume of garbage by about 90–95%. But, there is always public resistance emerging against incineration because of the emission of some toxic fumes. However, current technology makes it possible to operate incineration plants in a way that emissions would not be a problem and, therefore, would conform to the Clean Air Act Amendments of 1990 (Alter, 1993; Yakowitz, 1990).

Two types of ashes are produced by incineration process; fly ash (the very fine particles entrained in incinerator exhaust gases) and bottom ash (the large and heavy particles removed from the bed of the incinerator), which require disposal. Landfilling these ash residues may not always be acceptable because of the potential for groundwater and soil pollution due to leachate carrying heavy metals such as lead and cadmium. Methods of protecting groundwater and soil from leachate such as lining the landfill can be expensive and are not always effective from an environmental standpoint. Accordingly, some research is being undertaken to effectively stabilize and recycle incineration residue in construction applications (Goumans et al., 1991).

3.3.4 Plastics Recycling

Plastics recycling aspect has to be taken into consideration in any plastic waste management program. In addition to reducing the amount of waste disposed in landfills, it can also significantly contribute to the conservation of raw petrochemical products and energy saving (Environmental Protection Agency, 1991; Office of Solid Waste and Office of Water, 1990) Rebeiz and Craft (1995) have reported that there are few technological and economical constraints that currently limit the full and efficient

recycling of plastic wastes into useful products, and these are: (i) contamination of plastic wastes with other materials such as dirt and metals that can damage the equipment used in the reprocessing of the waste; (ii) plastics are not homogeneous materials like aluminum or paper, but consist of a large number of grades with different molecular structures and properties. Each plastic component in a mixed waste has a different melting behavior, rheology, and thermal stability; (iii) plastic mixtures are usually insoluble and form discrete phases within a continuous phase; (iv) plastic waste feedstock is not usually uniform over time; and (v) plastic wastes have a relatively low density. Therefore, they are usually compacted or ground-up before transportation to reduce shipping costs.

3.4 Recycling Methods

3.4.1 Mechanical Recycling

Mechanical recycling of plastics refers to processes which involve melting, shredding or granulation of waste plastics. Plastics must be sorted prior to mechanical recycling. Technology is being introduced to sort plastics automatically using various techniques such as X-ray fluorescence, infrared and near infrared spectroscopy, electrostatics and flotation. Following sorting, the plastic is either melted down directly and molded into a new shape, or melted down after being shredded into flakes, and then processed into granules called regranulate.

Zhang and Forssberg (1999) studied the liberation and its impact on the separation of personal computer (PC) scrap and printed circuit board (PCB) scrap. Special equipment functioning as a shape separator and an aspirator was used for the classification of electronic scrap. Yarahmadi et al. (2001) reported that retained properties and durability are among the most important tasks when evaluating the possibility of mechanical recycling of plastic waste of (rigid PVC).

Ambrose et al. (2002) performed the mechanical recycling of 100% post-consumer plastic waste into high-quality products. The chemical and physical properties of these recycled materials were compared with similar products manufactured from virgin resins. The properties of a blow-molded bottle prepared from 100% post-consumer high-density polyethylene (HDPE) showed that this recycled polymer exceeded the materials specifications for virgin plastics designs. Similarly, a sample of thermoplastic polyolefin (TPO, 100% polypropylene), obtained entirely from shredder residue (SR) displayed sufficient material strength for future separation and reprocessing.

Avila and Duarte (2003) did the thermo-mechanical recycling of post-consumed plastic bottles, especially the ones made of polyethylene terephthalate (PET), and its use as composite materials for engineering applications. Yarahmadi et al. (2003) reported that PVC floorings as plastic waste can be mechanically recycled in the form in which they were recovered without upgrading, and without the addition of new plasticizer. Paula et al. (2005) prepared polymeric blends by mechanical

recycling and characterized LDPE/Al residues from cartooned packaging with recycled HDPE/LDPE and virgin PE resins. It was observed that processability, mechanical properties, chemical resistance and water absorption are dependent on the blend compositions.

Dodbiba et al. (In Press) compared the two treatment options, i.e., energy recovery recycling and mechanical recycling of plastic wastes from discarded TV sets in the context of life cycle assessment (LCA) methodology. They concluded that mechanical recycling of plastics is more attractive treatment option in environmental terms than incineration for energy recovery, which generates a larger environmental burden. Eswaraiyah et al. (In Press) reported that air classification is one among the clean mechanical separation methods that can achieve reasonably good separation of metals and plastics from the PCB stuff.

3.4.2 Chemical or Feedstock Recycling

Feedstock recycling describes a range of plastic recovery techniques to make plastics, which break down polymers into their constituent monomers, which in turn can be used again in refineries or petrochemical and chemical production. A range of feedstock recycling technologies is currently being explored. These include: pyrolysis, hydrogenation, gasification and thermal-cracking. Feedstock recycling has a greater flexibility over composition and is more tolerant to impurities than mechanical recycling, although it is capital-intensive and requires very large quantities of used plastic for reprocessing to be economically viable.

3.4.2.1 Chemical Modification

Plastic can be recycled by chemical modification or depolymerization. The two ways to achieve depolymerization are hydrolysis (chemical decomposition) and pyrolysis (thermal decomposition). For example, PET (polyethylene terephthalate) can be chemically modified to produce unsaturated polyester, thermoset polyester typically used in bathtubs, boat hulls, and automobile exterior panels. Another example is the thermal decomposition of acrylic wastes into methyl methacrylate (MMA); a monomer typically used in aircraft windows and neon signs. The technology of depolymerizing single condensation polymers such as urethanes, PET, nylon, and polymethyl methacrylates is relatively easy. However, it is much more complicated to chemically modify mixed plastics to produce useful and economical chemical feedstocks. (Rebeiz and Craft, 1995).

3.4.2.2 Thermal Reprocessing

Thermal reprocessing consists of heating a thermoplastic at very high temperatures, thus making the plastic flow. The plastic is then converted into a new product as it cools. This method does not involve the modification of the chemical composition of the plastics. For example, PET being thermoplastic polyester, can be heated and

reprocessed into building panels, fence posts, or fibers for carpeting. This process cannot be repeated indefinitely since repeated thermal reprocessing may eventually adversely affect the plastic properties. Thermal reprocessing is quite straightforward if it is applied to relatively pure thermoplastics. However, thermal reprocessing could not be applied to thermosets (such as cross-linked polyesters) because they cannot soften at high temperatures without degrading. Thermal reprocessing becomes much more involved if various thermoplastics are mixed together. One way of doing is to separate the various plastics. Separation of various plastics can be easy or complicated depending on the source of the waste. The other way to thermally reprocess mixed plastics is to use special equipment that takes into account the different thermal properties or makes few demands on the melting behavior of the plastic wastes (i.e., compression molding or melting in salt bath) and does not require meticulous removal of non-plastic wastes. Systems/Mechanisms have been developed to reprocess mixed or commingled plastic wastes where plastics with lower melting point act as a matrix that carries other plastics and contaminants into the mold. Chemical agents, called compatibilizers, could be used to improve the adherence between different polymer phases (Barlow and Paul, 1987; Stein, 1992). Plastics are currently being recycled with some success into wood products replacement (Barlaz et al., 1993; Ehrig, 1992). These materials can be cut, sawn, and nailed like wood. They are more resistant to moisture but more sensitive to temperature variations than wood. Such construction products include fence posts, large cable reels, park benches, railroad ties, boat docks, breakwaters, auto curb stops and traffic posts. However, these products cost about 2–4 times more than the same product made from wood. There are many commercially available machines that could handle certain commingled plastic wastes of varying compositions (Barlaz et al., 1993; Ehrig, 1992).

3.4.2.3 Fillers

Plastic waste can also be used as fillers with virgin resins or other materials like concretes or as fill material in road construction. In such applications, chemical composition of the plastics is generally not very significant. This is an easy way to recycle thermosets or contaminated plastics in second grade applications. One such use is thermoplastic wastes that are melted and co-extruded or co-injected into moldings with virgin resins. These virgin resins with superior properties are forced into the perimeter of the mold while the recycled plastics, with inferior properties, are injected in the center of the mould (Curlee, 1986). Plastic wastes may also be used with some effectiveness as a partial replacement of inorganic aggregates in concrete applications to decrease the dead weight of structures. Similarly, recycled rubber can be used in asphaltic concrete mixes (McQuillen et al., 1998) or as a fill material in road construction (Eldin and Senouci, 1992). The advantages of adding recycled rubber to the asphalt mix include increased skid resistance under icy conditions, improved flexibility and crack resistance, and reduced traffic noise.

Remias et al. (2000) developed a system which utilizes nitrogen oxides and dioxygen to break down and oxidize polyethene. The principal nongaseous products

are α,ω -diacids, mainly succinic, glutaric, adipic and pimelic acids. Ernst et al. (2000) have used electrochemical applications for quantification of heavy metals for the recycling of waste plastics.

Masuda et al. (2001) developed a new reactor system for recovery fuels from the waste plastic mixture in steam atmosphere. This system was composed of three kinds of reactors connected in series. One was a reactor filled with stirred heat medium particles, which enabled the high heat transfer rate, the high holdup and the good contact of the melted plastics with steam. The second was a tank reactor. The last one was a fixed bed reactor with FeOH catalyst particles, which showed the catalysis in steam for the decomposition both of a wax and sublimate materials generated by the degradation of plastics.

Cavalieri and Padella (2002) reported that a polymer milling process with liquid CO₂ was applied to polymeric mixed waste, obtaining a powder material which was successfully utilized as a matrix for a new composite material. Developed materials have interesting mechanical properties and material performance can easily be improved. Investigations on selected mixtures of PP and PE clearly showed evidence of chemical compatibilization.

Shen et al. (2002) investigated the floatability of seven plastics (POM, PVC, PET, PMMA, PC, PS and ABS) in the presence of methyl cellulose (MC) and separation of plastics mixtures. It was found that the seven plastics can be separated into three groups by using the wetting agent MC. In addition, flotation selectivity for the plastics is dominated not only by wettability of plastics, but also by particle size, density and shape.

Miskolczi et al. (2004) reported that fuel-like utilization is one way of the chemical recycling of liquids from waste polymers. Hall and Williams (2007) investigated three plastic fractions from a commercial waste electrical and electronic equipment (WEEE) processing plant for the possibility of recycling them by batch pyrolysis.

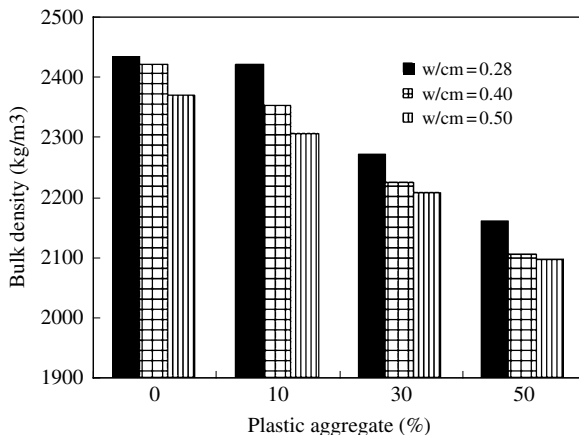
3.5 Fresh Properties of Concrete Containing Recycled/Waste Plastic

3.5.1 Bulk Density

Al-Manaseer and Dalal (1997) investigated the effect of plastic aggregates on the bulk density of concrete. For this purpose, they made twelve concrete mixes with different w/cm containing varying percentages (0, 10, 30, and 50%) of plastic aggregates. They concluded that: (i) bulk density of concrete decreased with the increase in plastic aggregates content (Fig. 3.2); (ii) reduction in bulk density was directly proportional to the plastic aggregates content; and (iii) density of concrete was reduced by 2.5, 6, and 13% for concrete containing 10, 30, and 50% plastic aggregates, respectively. Reduction in density was attributed to the lower unit weight of the plastics.

Choi et al. (2005) studied the influence of polyethylene terephthalate (PET) bottles lightweight aggregate (WPLA) on the density of concrete. Mixture proportions

Fig. 3.2 Bulk density versus plastic aggregates percentage (Al-Manaseer and Dalal, 1997)



of concrete were planned so that the water–cement ratios were 45%, 49%, and 53%, and the replacement ratios of WPLA were 0%, 25%, 50%, and 75% by volume of fine aggregate. Density of concrete mixtures decreased with the increase in WPLA content.

3.5.2 Air Content

Bayasi and Zeng (1993) examined the effect of polypropylene fibers on the air content of concrete. For the purpose, seven mixtures of polypropylene fibers reinforced concrete were made. Mixture proportions and details (length and percentages) of polypropylene fibers are given in Table 3.5. They reported that air content increased with the inclusion of polypropylene fibers, and there was no detectable effect on air content of fresh concrete at volume below 0.3%.

Table 3.5 Fresh concrete properties of polypropylene reinforced concrete (Bayasi and Zeng, 1993)

Mix No.	Fiber length (mm)	Fiber volume fraction (%)	Air content (%)	Slump (mm)	Inverted slump cone (sec)
1*	–	0	2.0	216	–
2	12.7	0.1	1.5	241	–
3	12.7	0.3	2.5	203	–
4	12.7	0.5	4.5	191	14
5	19.0	0.1	1.5	267	–
6	19.0	0.3	3.5	241	–
7	19.0	0.5	5.0	25	18

* Mix 1 is the control mix in which there are no fibers (consists of cement content 424 kg/m³, water-cement ratio = 0.41, aggregate-cement = 4.0, dry aggregate content = 1696 kg/m³, Superplasticizer-cement ratio = 0.01).

Soroushian et al. (2003) reported that inclusion of recycled plastic in concrete resulted in the reduction of air content. The dosages of various virgin and recycled discrete reinforcement systems considered in the investigation are given in Table 3.4. Figure 3.3 shows the effects of recycled plastic (fibers) on air content of concrete. Discrete reinforcement systems caused a significant loss (approximately 1%) in air content. Mehta and Monteiro (1993) also reported that slump loss reduced the efficiency of air entrainment in the fresh concrete.

3.5.3 Slump

Bayasi and Zeng (1993) investigated the effect of polypropylene fibers on the slump and inverted slump cone time of concrete mixes. Test results are given in Table 3.5. They reported: (i) increase in inverted slump cone time; (ii) for fiber volume fractions less than or equal to 0.3%, fiber effect on fresh mix workability appeared insignificant and rather inconsistent; and (iii) for fiber volume of 0.5%, however, fibers appeared to adversely affect fresh mix workability, more evident by the increase in inverted slump cone time with 19 mm fibers with a more pronounced effect than 12.7 mm fibers.

Al-Manaseer and Dalal (1997) determined the slump of concrete mixes made with plastic aggregates. Table 3.6 shows the cone and K-slump data for all mixes. They reported that: (i) there was increase in slump when plastic aggregates were incorporated in concrete. The concrete containing 50% plastic aggregates had a slightly higher cone slump than the concrete without plastic aggregates; and (ii) K-slump consistency results showed a similar pattern to that obtained from the cone slump. Plastic aggregates neither absorbed nor added any water to the concrete mix. Due to this non-absorptive characteristic, concrete mixes containing plastic aggregates will have more free water. Consequently, the slump increased.

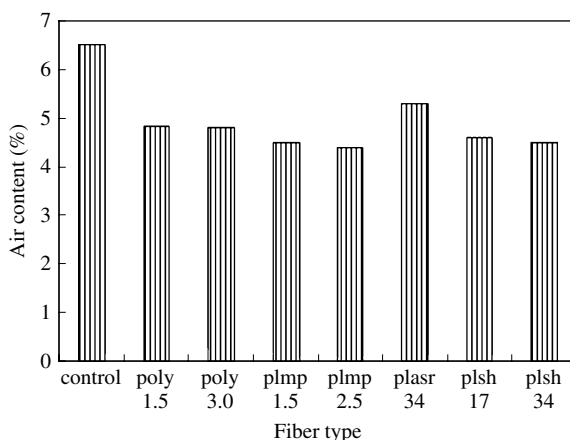


Fig. 3.3 Air content versus plastic fiber type (Soroushian et al., 2003)

Table 3.6 Cone and K-slump data (Al-Manaseer and Dalal, 1997)

Plastic aggregate (%)	Consistency (mm)			Workability (mm)			Cone slump (mm)		
	W/Cm	W/Cm	W/Cm	W/Cm	W/Cm	W/Cm	W/Cm	W/Cm	W/Cm
	0.28	0.40	0.50	0.28	0.40	0.50	0.28	0.40	0.50
0	65	70	70	50	55	55	178	190	—
10	60	73	65	55	60	45	—	190	—
30	75	70	75	60	45	50	178	—	—
50	73	83	80	55	60	50	206	216	—

Soroushian et al. (2003) reported reduction in slump with the use of recycled plastic in concrete. Slump test results are shown in Fig. 3.4. It is evident that the addition of any discrete reinforcement caused slump loss. While non-slender plastic particles, automobile shredded residue, and flakes were used at dosages that were in order of magnitude of those of slender fibers, their effects on fresh mixture properties were comparable. This could be attributed to the pronounced adverse effects of highly slender fibers on fresh mixture workability. Mehta and Monteiro (1993) concluded that slump loss reduced the efficiency of air entrainment in the fresh concrete.

Choi et al. (2005) investigated the influence of polyethylene terephthalate (PET) bottles lightweight aggregate (WPLA) on the workability (slump) of concrete. Mixture proportions of concrete were planned so that the water–cement ratios were 45, 49, and 53%, and the replacement ratios of WPLA were 0, 25, 50, and 75% by volume of fine aggregate. They reported that slump value of waste PET bottles lightweight aggregate concrete (WPLAC) increased with the increase in water–cement ratio and the replacement ratio. The improvement ratios of workability represent 52%, 104%, and 123% in comparison with that of normal concrete at the water–cement ratio 45%, 49%, and 53%, respectively. This may be attributed to not only the spherical and smooth shape but also to the absorption of WPLA.

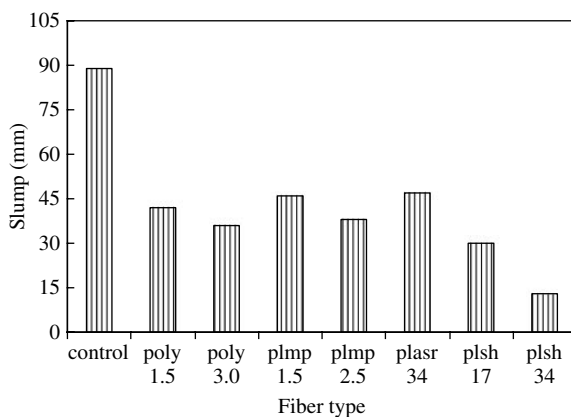


Fig. 3.4 Slump test versus plastic fiber type (Soroushian et al., 2003)

Table 3.7 Mix proportions and fresh concrete properties (Batayneh et al., In Press)

Plastic (%)	Mix proportions (kg/m ³)					w/c ratio	Slump (mm)
	Water	Cement	CA	FA	Plastic		
0	252	446	961	585	0	0.56	78
5	252	446	961	555.7	17.8	0.56	73
10	252	446	961	526.5	35.5	0.56	69
15	252	446	961	497.2	53.2	0.56	63
20	252	446	961	468.0	71.0	0.56	57

Batayneh et al. (In Press) studied the effect of ground plastic on the slump of concrete. Concrete mixes of up to 20% of plastic particles are proportioned to partially replace the fine aggregates. Details of mixture proportions and slump test results are given in Table 3.7. It can be seen from these results that: (i) there was a decrease in the slump with the increase in the plastic particle content; and (ii) for a 20% replacement, the slump decreased to 25% of the original slump value with 0% plastic particle content. This decrease in the slump value is due to the shape of plastic particles, i.e., the plastic particles have sharper edges than the fine aggregate. Since the slump value at 20% plastic particle content is 58 mm, this value can be considered acceptable and the mix can be considered workable.

3.6 Properties of Hardened Concrete Containing Recycled/Waste Plastic

3.6.1 Compressive Strength

Bayasi and Zeng (1993) reported the effect of polypropylene fibers on the compressive strength of concrete. Compressive behavior characteristics are given in Table 3.8, and it includes compressive strength strain at peak stress and compressive toughness index. Compressive toughness index is defined as the total compressive energy absorbed (total area under compressive stress-strain curve) divided by the pre-peak compressive energy absorbed (area under the stress-strain diagram up to peak stress). From the compressive test results, they concluded that 19 mm fibrillated polypropylene fibers had no obvious effect on the compressive strength of concrete. However, 19 mm fibrillated polypropylene fibers enhanced the energy absorption and toughness characteristics of concrete under compression. This was evidenced by the increase in compressive toughness index of concrete as a result of fiber addition. From Table 3.8, it may also be concluded that 12.7 mm long polypropylene fibers improved the compressive strength of concrete when used at volumes that do not cause adverse effects on the workability (less than 0.5%).

Al-Manaseer and Dalal (1997) investigated the influence of inclusion of plastic aggregates on the compressive strength of concrete. Concrete mixtures were made with different w/cm and varying percentages of plastic aggregates. Test results are shown in Fig. 3.5. Compressive strength decreased with increase in aggregates

Table 3.8 Hardened concrete properties of polypropylene fiber reinforced concrete (Bayasi and Zeng, 1993)

Mix No.	Fiber length (mm)	Fiber volume fraction (%)	Compressive behavior characteristics			Impact strength (No of blows)		Permeability (coulombs)	Permeable voids (%)
			Strength (MPa)	Strain at peak	Toughness index	At first crack	At failure		
1	—	0	39.3	0.0016	1.167	5	5	3678	15.3
2	12.7	0.1	46.9	0.0019	1.173	17	28	6770	15.0
3	12.7	0.3	46.9	0.0017	2.031	186	201	4830	14.4
4	12.7	0.5	38.3	0.0022	1.243	50	71	6796	13.0
5	19.0	0.1	37.2	0.0017	1.451	11	20	8614	14.4
6	19.0	0.3	40.0	0.0021	1.440	19	42	11905	17.1
7	19.0	0.5	38.6	0.0017	1.600	34	72	8332	12.1

content. At any given plastic aggregates content, the compressive strength was found to decrease when the w/cm was increased. Figure 3.6 shows the percentage reduction in the compressive strength due to the addition of plastic aggregates. In general, the rate of reduction in strength was found to decrease with the increase in plastic aggregates content. There were 34, 51, and 67% reduction in the compressive strength for concrete containing 10, 30, and 50% plastic aggregates. The reduction in the compressive strength due to the addition of plastic aggregates might be due to either poor bond between the cement paste and the plastic aggregates or to the low strength that is characteristic of plastic aggregates. Fractured surface of concrete cylinder showed that most of the plastic aggregates pulled out rather than splitting apart. The failure of the concrete specimens containing plastic aggregates under compression load did not exhibit the typical brittle type of failure normally obtained for conventional concrete. The observed failure was more of a gradual failure, depending on the plastic aggregates content. As the plastic aggregates content was

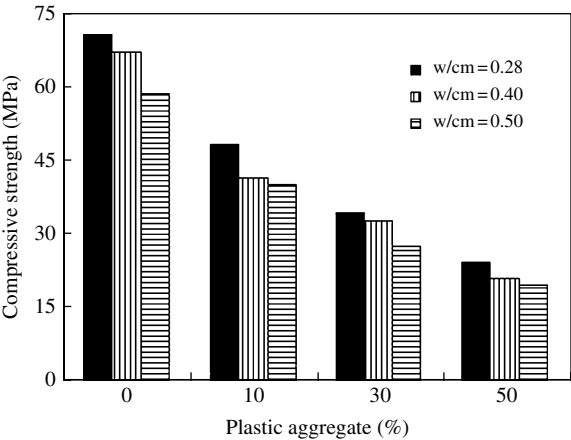
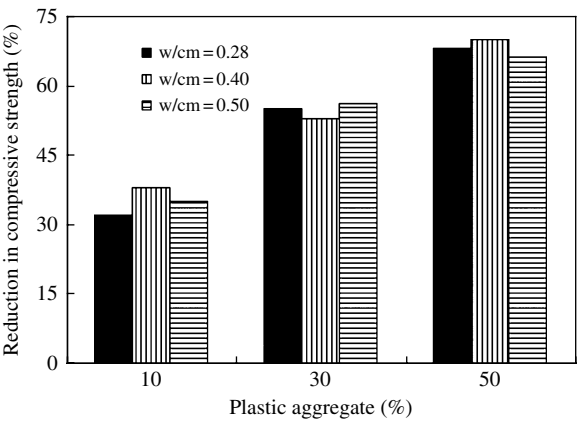


Fig. 3.5 Compressive strength versus plastic fiber percentage (Al-Manaseer and Dalal, 1997)

Fig. 3.6 Percentage reduction in compressive strength versus plastic fiber percentage (Al-Manaseer and Dalal, 1997)



increased, the failure type became more ductile. The specimens containing plastic aggregates were capable of resisting the load for a few minutes after failure without full disintegration. This trend was found to be more obvious as the percent age of plastic aggregates was increased.

Soroushian et al. (2003) demonstrated that compressive strength of concrete decreased with the inclusion of recycled plastic in it. The compressive strength test results are shown in Fig. 3.7. The mean values and 95% confidence intervals were derived based on nine test specimens (three specimens per mixture, three replications of each mixture). All mixtures containing slender fibers (poly, and plmp in Table 3.4) showed a slight increase in compressive strength. The mixtures containing non-slender fibers (plasr and plsh in Table 3.4) showed a relatively small (approximately 5%) loss in compressive strength, which could be attributed to the relatively low elastic modulus of these non-slender fibers.

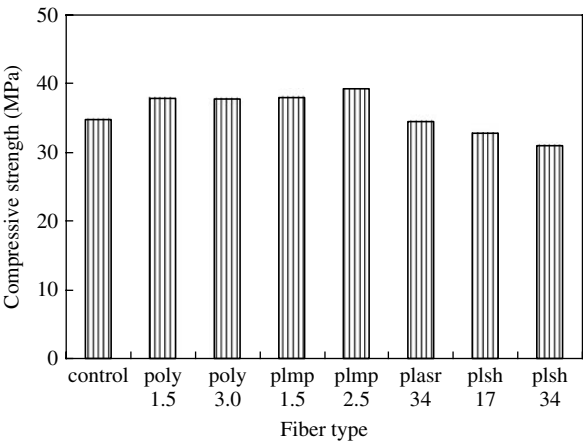


Fig. 3.7 Compressive strength versus plastic fiber type (Soroushian et al., 2003)

Choi et al. (2005) examined the role of polyethylene terephthalate (PET) bottles lightweight aggregate (WPLA) on the compressive strength of concrete. Mixture proportions of concrete were planned so that the water–cement ratios were 45%, 49%, and 53%, and the replacement ratios of WPLA were 0%, 25%, 50%, and 75% by volume of fine aggregate. Compressive strength test results are given in Table 3.9. It can be seen that: (i) compressive strength of concrete mixtures decreased with the increase in PET aggregates; and (ii) for a particular PET aggregate content, compressive strength increased with the reduction in w/c ratio.

Batayneh et al. (In Press) investigated the effect of ground plastic on the compressive strength of concrete. Concrete mixes of up to 20% of plastic particles are proportioned to partially replace the fine aggregates. Details of mixture proportions are given in Table 3.7. They concluded that: (i) addition of the plastic particles led to a reduction in the strength properties. For a 20% replacement, the compressive strength exhibited a sharp reduction up to 72% of the original strength. With 5% replacement the compressive strength showed a 23% reduction; (ii) similar behavior, but in a lower effect, was observed in both the splitting and flexural strengths of the tested samples; and (iii) this reduction in strength was due to the fact that the strength of the plastic particles is lower than that of the aggregate. Therefore, both the use of concrete with plastic particles and the percentage of replacement should be controlled, according to the allowable strength of the structural element to be constructed.

Marzouk et al. (2007) studied the innovative use of consumed plastic bottle waste as sand-substitution aggregate within composite materials for building application. Bottles made of polyethylene terephthalate (PET) were used as partial and complete substitutes for sand in concrete composites. Various volume fractions of sand varying from 2% to 100% were substituted by the same volume of granulated plastic, and various sizes of PET aggregates. They concluded that: (i) substituting sand at

Table 3.9 Hardened concrete properties (Choi et al., 2005)

W/C ratio	PET aggregate (%)	Compressive strength (MPa)			Splitting tensile strength (MPa)	Modulus of elasticity (MPa $\times 10^3$)
		3 days	7 days	28 days		
53	0	18.4	24.0	31.5	3.27	23.5
	25	17.6	23.4	29.7	2.65	23.0
	50	17.1	21.5	26.3	2.25	21.2
	75	14.8	19.2	21.8	2.04	18.5
49	0	19.0	27.8	34.6	3.27	23.3
	25	18.8	26.7	33.7	2.76	22.8
	50	18.6	24.3	29.1	2.35	18.1
	75	15.8	21.6	23.2	1.94	16.7
45	0	24.8	31.3	37.2	3.32	25.5
	25	23.2	27.4	33.8	2.80	18.7
	50	22.0	26.5	31.8	2.55	17.3
	75	20.7	24.8	24.9	2.04	15.6

a level below 50% by volume with granulated PET, whose upper granular limit equals 5 mm, affected neither the compressive strength nor the flexural strength of composites; and (ii) plastic bottles shredded into small PET particles may be used successfully as sand-substitution aggregates in cementitious concrete composites. These composites appeared to offer an attractive low-cost material with consistent properties; moreover, they would help in resolving some of the solid waste problems created by plastics production and in saving energy.

3.6.2 Splitting Tensile Strength

Al-Manaseer and Dalal (1997) studied the effect of plastic aggregates on the splitting tensile strength of concrete. The splitting tensile strength of concrete made with different w/cm and various percentages of plastic aggregates is shown in Fig. 3.8. They concluded that: (i) splitting tensile strength decreased with the increase in plastic aggregates percentage. The splitting tensile strength was found to decrease by 17% for concrete containing 10% plastic aggregates; (ii) for a given plastic aggregate content, the splitting tensile strength was found to decrease when w/cm was increased; and (iii) splitting failure of concrete specimens containing plastic aggregates did not exhibit the typical brittle failure observed in case of conventional concrete. The splitting tensile failure was more of a gradual failure as was the case for specimens tested under compression load. In general, specimens containing plastic aggregates were found more capable of resisting the splitting load after failure without full disintegration. The failure was found to be more ductile in nature when the percentage of plastic aggregates was increased.

Choi et al. (2005) investigated the influence of polyethylene terephthalate (PET) bottles lightweight aggregate (WPLA) on the splitting tensile strength of concrete. Mixture proportions of concrete were planned so that the water–cement ratios were 45%, 49%, and 53%, and the replacement ratios of WPLA were 0%, 25%, 50%,

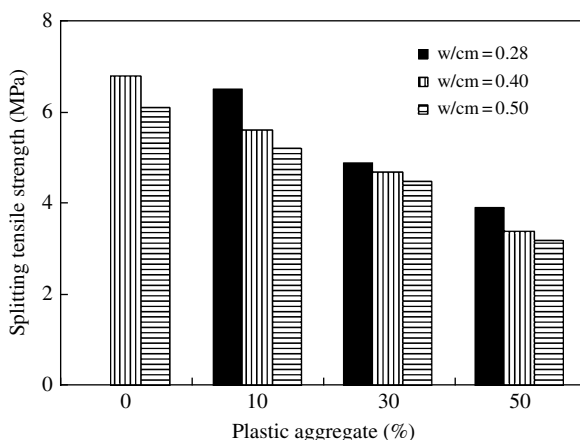


Fig. 3.8 Splitting tensile strength versus plastic aggregate percentage (Al-Manaseer and Dalal, 1997)

and 75% by volume of fine aggregate. Splitting tensile strength test results are given in Table 3.9. It is clear from this table that: (i) splitting tensile strength of concrete mixtures decreased with the increase in PET aggregates; and (ii) for a particular PET aggregate content, splitting tensile strength increased with the reduction in w/c ratio.

3.6.3 Modulus of Elasticity

Al-Manaseer and Dalal (1997) reported the effect of plastic aggregates on the modulus of elasticity of concrete. Figure 3.9 shows the results of modulus of elasticity of concrete containing different percentages of plastic aggregates. They concluded that: (i) modulus of elasticity decreased with the increase in plastic aggregate content; (ii) depending upon w/cm, modulus of elasticity varied between 24.3 GPa for concrete containing no aggregates (w/cm = 0.28) to 8.6 GPa for concrete containing 50% plastic aggregates (w/cm = 0.50); and (iii) in general, increase in w/cm ratio decreased the modulus of elasticity of concrete.

Choi et al. (2005) investigated the effect of polyethylene terephthalate (PET) bottles lightweight aggregate (WPLA) on the modulus of elasticity of concrete. Mixture proportions of concrete were planned so that the water–cement ratios were 45%, 49%, and 53%, and the replacement ratios of WPLA were 0%, 25%, 50%, and 75% by volume of fine aggregate. Modulus of elasticity test results is given in Table 3.9. It is clear from this table that modulus of elasticity of concrete mixtures decreased with the increase in PET aggregates.

3.6.4 Time and Temperature Dependent Properties

Rebeiz (1995) concluded that compressive strength increased with age and decreased with the increase in temperature when recycled polyethylene terephthalate

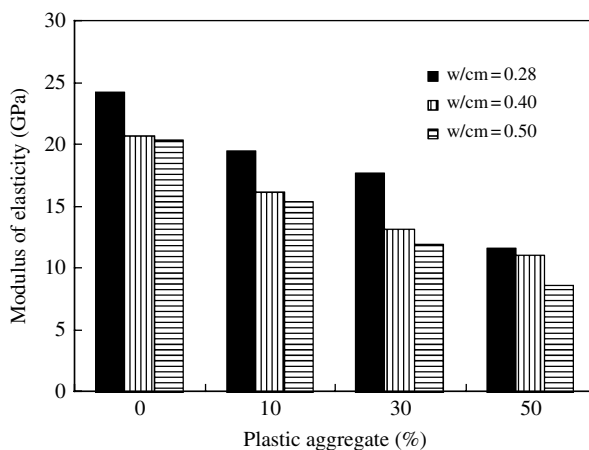


Fig. 3.9 Modulus of elasticity versus plastic fiber percentage (Al-Manaseer and Dalal, 1997)

(PET) was used. The production of the unsaturated polyester resin based on recycled PET was done in two steps (Rebeiz et al., 1991). The first step consisted of digesting the PET molecules by charging the PET scrap and a glycol into a reactor and heating for several hours in the presence of a transesterification catalyst. The second step consisted of adding dibasic acids to the solution to produce the polyester resin. The unsaturated polyester was then diluted with styrene to reduce its viscosity and allowed it to further cure to a solid (polymer) upon the addition of suitable free radical initiators and promoters. Curing took place because the styrene combined with the reactive double bonds of the polyester chains, thus linking them together and forming a strong three-dimensional polymer network (Rebeiz et al., 1991). The unsaturated polyester resin used in this study had a low viscosity of 110 cps at 25°C. The excellent wetting properties of the resin made it possible to formulate a PC system with a high aggregate-resin ratio. About 25%, by weight, of recycled PET was used in the production of the final resin. The resin was dark in color since the recycled PET used in its production was not purified to the same extent as the recycled PET used in other applications, which could facilitate the proper recycling operation and minimize its cost. It should be noted that the most expensive part of the PET bottles recycling process is the removal of aluminum and paper impurities, and green and brown colors. The PC mixing procedure followed 'Polymer Concrete Test Method 1.0', of the Society of Plastics Industry; referred to as SPI 1.0 (Composite Institute, 1987). The optimum mix design, proportioned by weight, was: 10% resin, 45% oven-dried coarse aggregates, 32% oven-dried sand and 13% fly ash. One percent (by weight of resin) of 9% active oxygen methylethyl ketone peroxide initiator and 0.1% (by weight of resin) of 12% solution cobalt naphthenate (CoNp) promoter (used as an accelerator) were added to the resin immediately prior to its mixing with the inorganic aggregates to start the curing process.

The effect of age on the compressive strength of polymer concrete (PC) is shown in Fig. 3.10. Polymer concrete (PC) achieved more than 80% of its final strength in one day. Conversely, normal cement concrete usually achieves about 20% of its

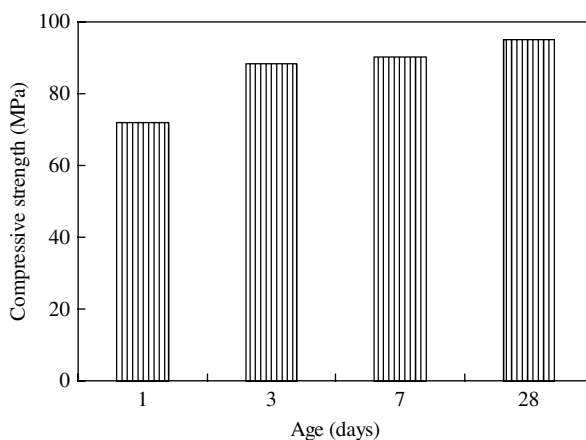


Fig. 3.10 Compressive strength versus age (Rebeiz, 1995)

final strength in one day. The early strength gain is important in precast applications because it permits the structures to resist large stresses early due to transportation and erection operations. The good compressive strength of PC allows the use of thinner sections in precast components, thus reducing dead loads in structures and minimizing transportation and erection costs. The effect of temperature on the compressive strength of PC is shown in Fig. 3.11. It is evident from which that increase in temperature resulted in strength loss in PC because the resin binder decreases in strength with an increase in temperature. For example, an increase in temperature from 25 to 60°C decreased the compressive strength by about 40%. The same kind of behavior was observed when PC using 100% virgin resin was tested (Okada et al., 1975). PC is much more susceptible to high temperatures than normal cement concrete because the synthetic visco-elastic resin binder used in producing PC is more temperature-sensitive than the inorganic cement binder used in producing normal cement concrete.

Hayashi et al. (1996) examined the thermal and temperature-dependent mechanical properties of resin concrete (REC). Resin concrete (REC) is a concrete in which aggregates are bonded with synthetic resin instead of cement hydrates in ordinary cement concrete. RECs with various resin contents were prepared by using two kinds of unsaturated polyester resins and two kinds of epoxy resins with different heat distortion temperatures (HDT) and glass transition temperatures ($T[g]$), and tested for thermal properties such as specific heat, thermal conductivity and coefficient of thermal expansion, and temperature-dependent mechanical properties such as dynamic Young's modulus, logarithmic decrement, creep coefficient and compressive and flexural strengths. Based on the test results, they concluded that: (i) thermal properties of RECs were very similar to those of ordinary cement concrete; (ii) deformation and strength properties of RECs were temperature-dependent, and showed distinct inflection points in temperature in the respective properties where temperature-dependence became dominant; and (iii) the inflection points were related to the HDT of the resins used rather than $T[g]$, and were not affected by the resin content. The points can be defined as heat distortion temperatures of RECs.

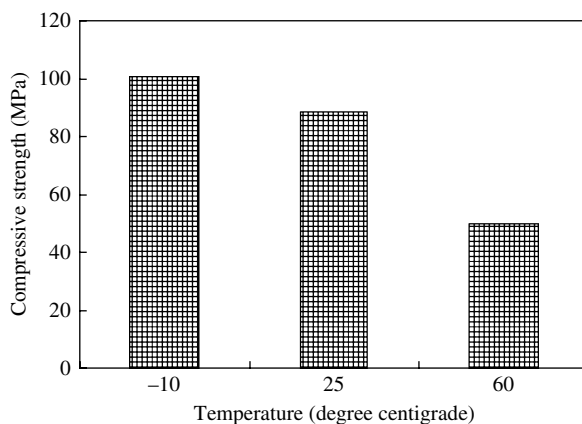


Fig. 3.11 Temperature effect on compressive strength (Rebeiz, 1995)

The maximum ambient temperature must be limited to these points or lower for the structural use of RECs. Consequently, the high HDT of the resins is preferable for structural RECs.

Byung-Wan et al. (2006) determined the mechanical properties such as the compressive strength, the splitting tensile strength, and the flexural strength of polymer concrete using an unsaturated polyester resin based on recycled PET. They concluded that at the age of 7 days, polymer concrete using resin based on recycled PET achieved compressive strength of 73.7 MPa, flexural strength of 22.4 MPa, splitting tensile strength of 7.85 MPa, and elastic modulus of 27.9 GPa. Some relationships exist between the compressive strength of polymer concrete and other properties (elastic modulus, flexural strength, and splitting tensile strength). The use of recycled PET in polymer concrete helps in reducing the cost of the material, solving some of the solid waste problems posed by plastics, and saving energy.

3.6.5 Impact Resistance

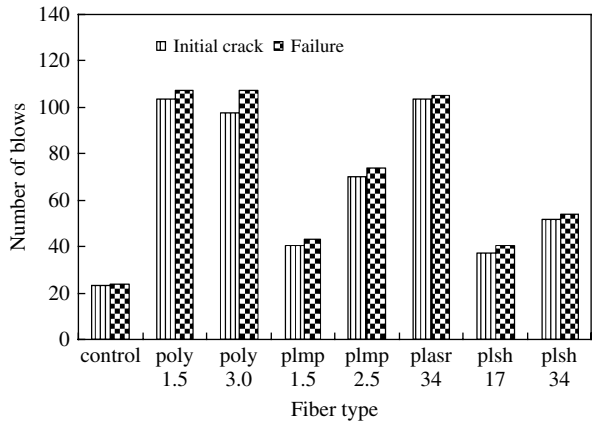
Bayasi and Zeng (1993) investigated the influence of polypropylene fibers on the impact resistance of concrete. Impact resistance results are given in Table 3.8. Based on the test results, they concluded that polypropylene fiber enhanced the impact resistance of concrete significantly. This was especially true for 12.7 mm long fibers. These fibers significantly increased the impact resistance of concrete for volumes that do not affect mix workability (less than 0.5%), while, at higher volume contents, impact resistance may tend to decrease.

Soroushian et al. (2003) studied the effect recycled plastic on the impact resistance of concrete. The impact test involved repeated dropping of a standard hammer from a particular height until a 63.5 mm concrete cylinder with a 152.4 mm diameter exhibited failure (Balaguru and Shah, 1992). The specimens were moist-cured for 28 days, and then allowed to air dry in the laboratory at 50% relative humidity and 22°C for an additional 3 months. The mean values and 95% confidence intervals were derived using nine specimens (from three replicated mixtures) for each concrete material. It is evident that all discrete reinforcement systems considered herein yielded important gains in the impact resistance as shown in Fig. 3.12. Different fibers provided different geometric, bond, and stiffness characteristics, which explains rather significant differences observed in the improvements in impact resistance brought about by different fiber reinforcement systems.

3.6.6 Permeability

Bayasi and Zeng (1993) investigated the effect of recycled plastic on the permeability of concrete. Test results of permeability and permeable void volume are given in Table 3.8. They concluded that 19 mm polypropylene fibers significantly increased the permeability of concrete with an inconsistent effect on the volume fraction of

Fig. 3.12 Impact resistance versus fiber type (Soroushian et al., 2003)



permeable voids. 12.7 mm long fibers somewhat increased the permeability of concrete and tend to decrease the volume of permeable voids.

Soroushian et al. (2003) demonstrated that there was decrease in air permeability with the inclusion of discrete reinforcement in concrete. The specimens were allowed to air dry in a laboratory at 59% relative humidity and 22°C before testing. This test involved attachment of a vacuum pump to the surface of the specimen, with the rate of airflow under vacuum measured. Figure 3.13 depicts the air permeability test results that were performed on impact test specimens prior to the performance of impact test. Lower airflow rates are preferable, indicating lower permeability. Discrete reinforcement systems were used in the project to reduce permeability of concrete, which could be attributed to reduced shrinkage micro-cracking. Reduced permeability favors long-term durability of concrete systems incorporating discrete reinforcement.

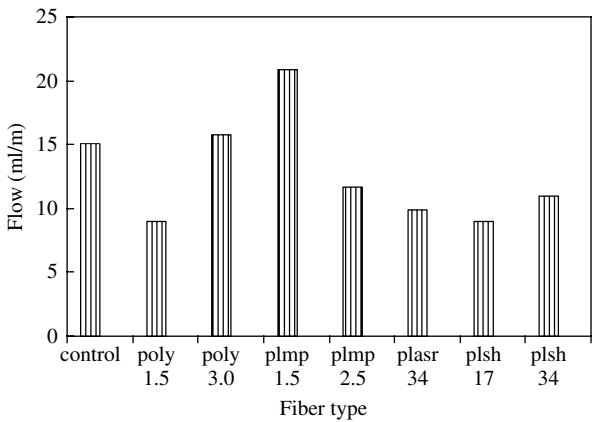
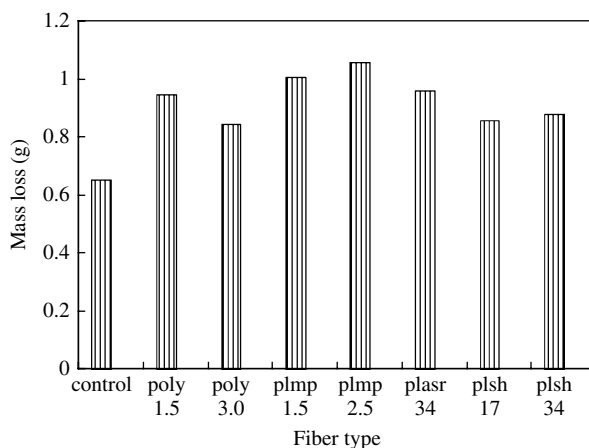


Fig. 3.13 Air permeability versus fiber type (Soroushian et al., 2003)

Fig. 3.14 Abrasion resistance versus fiber type (Soroushian et al., 2003)



3.6.7 Abrasion Resistance

Soroushian et al. (2003) investigated the influence of recycled plastic on the abrasion resistance of concrete as per ASTM C 779. The abrasion test results are shown in Fig. 3.14. Most discrete reinforcement systems were observed to cause some reduction of the abrasion resistance of concrete (reflected in increased mass loss in the presence of fibers). This effect could result from the fact that fibers occurring near the surface could debond under abrasion effects, thereby contributing to mass loss; change in the bleeding characteristics of concrete in the presence of fibers could also modify surface characteristics of concrete and thus its abrasion resistance.

3.7 Uses of Recycled Plastic in Concrete

1. Recycled plastic can be effectively used in the repair and overlay of damaged cement concrete surfaces in pavements, bridges, floors, and dams.
2. It is also used in a variety of precast applications such as utility components (e.g., drains for acid wastes, underground vaults and junction boxes, sewer pipes, power line transmission poles).
3. It is used in transportation related components (e.g., median barriers, bridge panels, railroad ties).
4. The available types of recycled plastics can be used to fabricate marine construction materials that are economically competitive and environmentally superior to conventional marine construction products.

References

- Al-Manaseer AA, Dalal TR (1997) Concrete containing plastic aggregates. *Concrete International* 19 (8): 47–52.
- Alter H (1993) The origins of municipal solid waste: II. Policy options for plastics waste management. *Waste Management Research* 11: 319–332.
- Ambrose CA, Hooper R, Potter AK, Singh MM (2002) Diversion from landfills: quality products from valuable plastics. *Resources, Conservation and Recycling* 36 (4): 309–318.
- Association of Plastics Manufactures in Europe (APME) (2004) Plastic recovery in perspective: plastics consumption and recovery in Western Europe.
- Avila AF, Duarte MVA (2003) Mechanical analysis on recycled PET/HDPE composites. *Polymer Degradation and Stability* 80 (2): 373–382.
- Balaguru PN, Shah SP (1992) Fiber reinforced cement composites. McGraw-Hill, Inc., 530 pp.
- Barlaz MA, Haynie FH, Overcash MF (1993) Framework for assessment of recycle potential applied to plastics. *Journal of Environmental Engineering, ASCE* 119 (5): 798–810.
- Barlow JW, Paul DR (1987) The compatibility of mixed plastic scrap. Reclamation of Plastic Waste Research Report – Phase I, Plastic Institute of America, Lowell, Massachusetts, USA, pp. 137–148.
- Batayneh M, Marie I, Asi I (In Press) Use of selected waste materials in concrete mixes. *Waste Management*.
- Bayasi Z, Zeng J (1993) Properties of polypropylene fiber reinforced concrete. *ACI Materials Journal* 90 (6): 605–610.
- Boettcher FP (1992) Environmental compatibility of polymers – emerging technologies in plastics recycling. ACS Symposium Series 513, American Chemical Society, pp. 16–25.
- Byung-Wan JO, Seung-Kook P, Cheol-Hwan K (2006) Mechanical properties of polyester polymer concrete using recycled polyethylene terephthalate. *ACI Structural Journal* 103 (2): 219–225.
- Cavalieri F, Padella F (2002) Development of composite materials by mechanochemical treatment of post-consumer plastic waste. *Waste Management* 22 (8): 913–916.
- Choi Y-W, Moon D-J, Chung J-S, Cho S-K (2005) Effects of waste PET bottles aggregate on the properties of concrete. *Cement and Concrete Research* 35: 776–781.
- Composite Institute (1987) Polymer concrete test methods. The Society of Plastics Industry, Washington DC, USA.
- Curlee TR (1986) The economic feasibility of recycling: a case study of plastic wastes. Praeger, New York.
- Dodbiba G, Takahashi K, Sadaki J, Fujita T (In Press) The recycling of plastic wastes from discarded TV sets: comparing energy recovery with mechanical recycling in the context of life cycle assessment. *Journal of Cleaner Production*.
- Ehrig RJ (1992) Plastics recycling: products and processes. Oxford University Press, New York.
- Eldin NN, Senouci AB (1992) Use of scrap tires in road construction. *Construction Engineering Management, ASCE* 118 (3): 561–576.
- Environmental Protection Agency (1991) Plastic wastes: Management, control, recycling and disposal. Pollution Technology Review No. 201, Noyes Data Corporation, Park Ridge, NJ.
- Environmental Protection Agency (2003) Report on Plastics, USA.
- Ernst T, Popp R, Eldik RV (2000). Quantification of heavy metals for the recycling of waste plastic from electrotechnical applications. *Talanta* 53 (2): 347–357.
- Eswaraiah C, Kavitha T, Vidyasagar S, Narayan SS (In Press) Classification of metals and plastics from printed circuit boards (PCB) using air classifier. *Chemical Engineering and Processing*.
- Franklin Associates Ltd. (1998) Characterization of municipal solid waste – 1997 Update. (Prepared for the USEPA) Prairie Village, KS.
- Goumans J, Van der Sloot H, Aalbers T (1991) Waste materials in construction. *Studies in Environmental Science*, 48, Elsevier Science Publishing Company Inc., New York, 672 pp.
- Hall WJ, Williams PT (2007) Analysis of products from the pyrolysis of plastics recovered from the commercial scale recycling of waste electrical and electronic equipment. *Journal of Analytical and Applied Pyrolysis* 79 (1–2): 375–386.

- Hayashi F, Oshima M, Koyanagi W (1996) Thermal properties and temperature dependence of mechanical properties of resin concretes for structural use. *Structural Materials* 45 (9): 1014–1020.
- Marzouk OY, Dheilily RM, Queneudec M (2007) Valorization of post-consumer waste plastic in cementitious concrete composites. *Waste Management* 27(2): 310–318.
- Masuda T, Kushino T, Matsuda T, Mukai SR, Hashimoto K, Yoshida Shu-ichi (2001) Chemical recycling of mixture of waste plastics using a new reactor system with stirred heat medium particles in steam atmosphere. *Chemical Engineering Journal* 82 (1–3):173–181.
- McQuillen JL, Takallou HB, Hicks RG, Esch, D (1998) Economic analysis of rubber modified asphalt mixes. *Journal of Transportation Engineering, ASCE* 114 (3): 259–277.
- Mehta PK, Monteiro PM (1993) *Concrete: structure, properties, and materials*. Prentice Hall, Englewood Cliffs, NJ, USA 549 pp.
- Miskolczi N, Bartha L, Deák G, Jóver B (2004) Thermal degradation of municipal plastic waste for production of fuel-like hydrocarbons . *Polymer Degradation and Stability* 86 (2): 357–366.
- Office of Solid Waste and Emergency Response (1990) Characterization of municipal solid waste in the United States. 1990 Update (EPA/530-SW-90–042).
- Office of Solid Waste and Office of Water (1990) Methods to manage and control plastic wastes. Report to Congress (EPA/530-XW-89-051).
- Okada K, Koyanagi W, Yonezawa T (1975) Thermo dependent properties of polyester resin concrete. *Proceedings of the 5th International Congress on Polymer Concrete*, Lancaster, UK, 210–215.
- Paula M M da S, Rodrigues FBBM, Bernardin AM, Fiori MA, Angioletto E (2005) Characterization of aluminized polyethylene blends via mechanical recycling. *Material Science and Engineering* 403 (1–2): 37–41.
- Rebeiz KS (1995) Time-temperature properties of polymer concrete using recycled PET. *Cement and Concrete Composites* 17: 119–124.
- Rebeiz KS, Craft AP (1995) Plastic waste management in construction: technological and institutional issues. *Resources, Conservation and Recycling* 15: 245–257.
- Rebeiz KS, Fowler DW, Paul DR (1991) Formulating and evaluating unsaturated polyester composite made with recycled PET. *Journal of Material Education* 13: 441–454.
- Recycling and Resource Recovery Council (1994) *Uses of plastics and recycled plastics*. Australia.
- Remias JE, Pavlosky TA, Sen A (2000) Oxidative chemical recycling of polyethene. *Comptes Rendus de l'Académie des Sciences – Series IIC – Chemistry* 3 (7): 627–629.
- Shen H, Forssberg E, Pugh RJ (2002) Selective flotation separation of plastics by chemical conditioning with methyl cellulose. *Resources, Conservation and Recycling* 35 (4): 229–241.
- Soroshian P, Plasencia J, Ravanbakhsh S (2003) Assessment of reinforcing effects of recycled plastic and paper in concrete. *ACI Materials Journal* 100 (3): 203–207.
- Stein RS (1992) Miscibility in polymer recycling. *Emerging technologies in plastics recycling*. ACS Symposium Series 513, American Chemical Society, Westerville, Ohio, USA pp. 39–48.
- Subramanian PM (2000) Plastics recycling and waste management in the US. *Resource, Conservation and Recycling* 28: 253–263.
- Yakowitz H (1990) Incineration of municipal solid waste: Scientific and technical evaluation of the state-of-the art by an expert panel. *Resources, Conservation and Recycling* 4: 241–252.
- Yarahmadi N, Jakubowicz I, Gevert T (2001) Effects of repeated extrusion on the properties and durability of rigid PVC scrap. *Polymer Degradation and Stability* 73 (1): 93–99.
- Yarahmadi N, Jakubowicz I, Martnsson L (2003) PVC floorings as post-consumer products for mechanical recycling and energy recovery. *Polymer Degradation and Stability* 79 (3): 439–448.
- Zhang S, Forssberg E (1999) Intelligent liberation and classification of electronic scrap. *Powder Technology* 105 (1–3): 295–301.
- Zoorob SE, Suparna LB (2000) Laboratory design and investigation of the properties of continuously graded asphaltic concrete containing recycled plastics aggregate replacement (Plasphalt). *Cement & Concrete Composites* 22: 233–242.

Chapter 4

Scrap Tires

Introduction

Large quantities of scrap tires are generated each year globally. For example, in United States more than 270 million scrap-tires are produced each year (Rubber Manufacturer's Association, 2000). In addition to this, more than 300 million tires are currently stockpiled throughout the United States (Rubber Manufacturer's Association, 2000). These stockpiles are dangerous not only due to potential environmental threat, but also from fire hazards and provide breeding grounds for rats, mice, vermines and mosquitoes (Naik and Singh, 1991; Singh, 1993). Over the years, disposal of tires has become one of the serious problems in environments. Landfilling is becoming unacceptable because of the rapid depletion of available sites for waste disposal. For example France, which produces over 10 million scrap-tires per year, has dwindling supply of landfills due to a new law that forbids any new landfill in the country. Used tire are required to be shredded before landfilling. Innovative solutions to meet the challenge of tire disposal-problem have long been in development. The promising options are: (1) use of tire rubber in asphaltic concrete mixtures; (2) incineration of tires for the production of steam; and (3) reuse of ground tire rubber in a number of plastic and rubber products. In addition, scrap-tires have been used as a fuel for cement kiln, as feedstock for making carbon black, and as artificial reefs in marine environment (Paul, 1985). Because of high capital investment involved in it, using tires as a fuel is technically feasible but economically not very attractive. The use of rubber-tires in making carbon black eliminates shredding and grinding costs, but carbon black from tire pyrolysis is more expensive, and has lower quality than that from petroleum oils (Paul, 1985). Table 4.1 shows some of the fact and figures as reported by the Rubber Manufacturer's Association (2000).

A tire is a composite of complex elastomer formulations, fibers, and steel/fiber cord. Tires are made of plies of reinforcing cords extending transversely from bead to bead, on top of which a belt is located below the thread. Table 4.2 lists typical types of materials used to manufacture tires.

Table 4.1 Some facts and figure concerning tires in USA (Rubber Manufacturer's Association, 2000)

Facts	Figures
Number of scrap-tires generated annually	270 million
Approximate weight of scrap-tires	3.6 million tons
Number of scrap-tires in stock piles	300 million
Number of tires processing facilities	498
Scrap tires used in Civil Engineering applications	30 million
Scrap tires processed into ground rubber	18 million
Scrap tires used for fuel	125 million
Number of states with scrap-tires legislation/regulations	48

Table 4.2 Typical materials used in manufacturing tire (Rubber Manufacturer's Association, 2000)

1. Synthetic Rubber
2. Natural Rubber
3. Sulfur and sulfur compounds
4. Phenolic resin
5. Oil
 - (i) Aromatic
 - (ii) Naphthenic
 - (iii) Paraffinic
6. Fabric
 - (i) Polyester
 - (ii) Nylon
7. Petroleum waxes
8. Pigments
 - (i) Zinc oxide
 - (ii) Titanium dioxide
9. Carbon black
10. Fatty acids
11. Inert materials
12. Steel wires

4.1 Classification of Scrap Tires

4.1.1 Scrap Tires

They can be managed as a whole tire, as slit tire, as shredded or chopped tire, as ground rubber, or as a crumb rubber product. A typical automobile tire weighs approximately 9 kg whereas a truck tire weighs about 44–45 kg. Table 4.3 gives the major materials used to manufacture tires by percentage of total weight of the finished tire that each material represents.

Table 4.3 Typical composition of manufactured tires by weight (Rubber Manufacturer's Association, 2000)

Composition (% by weight)	Automobile tire	Truck tire
Natural rubber	14	27
Synthetic Rubber	27	14
Carbon black	28	28
Steel	14–15	14–15
Fabric, filler, accelerators, antiozonants	16–17	16–17

4.1.2 *Slit Tires*

These are produced in tire cutting machines. These machines can slit the tire into two halves or can separate the sidewalls from the tread of the tires.

4.1.3 *Shredded/Chipped Tires*

Tire shreds or chips involve primary, secondary, or both shredding operations. The size of the tire shreds produced in the primary shredding process can vary from as large as 300–460 mm long by 100–230 mm wide, down to as small as 100–50 mm in length, depending on the manufacturer's shredder model and the condition of the cutting edges. Production of tire chips, normally sized from 76 mm to 13 mm, requires both primary and secondary shredding to achieve adequate volume (quantity) reduction (Read et al., 1991).

4.1.4 *Ground Rubber*

Ground rubber for commercial applications may be nominally sized as large as 19 mm (or $\frac{3}{4}$ inch) to as small as 0.15 mm (No. 100 sieve). It depends upon the type of size reduction equipment and intended applications. The processed used tires in ground rubber applications are typically subjected to two stages of magnetic separation and to screening. Various size fractions of rubber are recovered (Heitzman, 1992). Some processes/markets term 30 mesh rubber as crumb rubber.

4.1.5 *Crumb Rubber*

Crumb rubber consists of particles ranging in size from 4.75 mm (No. 4 Sieve) to less than 0.075 mm (No. 200 Sieve). Generally, the following methods are used to convert scrap tires into crumb rubber. These methods are: (i) cracker mill process; (ii) granular process; and (iii) micro-mill process. The cracker mill process tears apart or reduces the size of tire rubber by passing the material between rotating corrugated steel drums. This process produces an irregularly shaped torn particles

having large surface area. The size of these particles varies from 5 mm to 0.5 mm (No. 4 to No. 40 Sieve), and is commonly known as crumb rubber.

Granular process shears apart the rubber with revolving steel plates, producing granulated crumb rubber particles, ranging in size from 9.5 mm (3/8 inch) to 0.5 mm (No. 40 Sieve) (Heitzman, 1992).

4.2 Management Options

4.2.1 Disposal

Disposing of scrap-tires in landfills is becoming unacceptable because of rapid depletion of available sites for waste disposal. For example, in US, approximately 45% of 270 million tires are disposed of in landfills, stockpiles, or illegal dumps. As of the year 2000, 48 states of the 50 United States have legislation/regulations related to land filling. Thirty-three states ban whole tires from disposal in landfills. Twelve states ban all forms of scrap-tires from being disposed of in landfills. Five states have no landfill restrictions on disposal of tires. Thirty states charge for land filling tires, whereas seven states allow monofills (Rubber Manufacturer's Association, 2000).

4.2.2 Recycling

According to the data available for the year 2000 for US, about 15 million of the 270 million scrap-tires generated yearly are exported, 10 million are recycled into new products, 20 million are processed into ground rubber, 125 million are used as tired-derived fuel, and 30 million in civil engineering applications (Rubber Manufacturer's Association, 2000). Ground rubber is used in making rubber products such as floor mats, carpet padding, vehicles mudguards, plastic products, and as a fine aggregate addition (dry process) in asphalt courses. Crumb rubber is also used as an asphalt binder modifier (wet process) in hot mix asphalt pavements (Naik and Singh, 1995; Naik et al., 1995). Over 30 million tires go to the retreaders, who re-tread about one-third of the tires received (Scrap Tire Management Council, 1998).

4.3 Fresh Properties of Concrete Containing Scrap Tires

4.3.1 Slump

Raghvan et al. (1998) determined the workability (slump) of mortar containing shredded automobile and truck tires. They used two different shapes of rubber particles as constituents of mortar: (i) granules about 2 mm in diameter; and (ii) shreds having two sizes; 5.5 mm × 1.2 mm and 10.8 mm × 1.8 mm (length × diameter). Based on their investigation, they reported that mortars incorporating rubber shreds

achieved workability (defined as the ease with which mortar/concrete can be mixed, transported and placed) comparable to or better than a control mortar without rubber particles.

Khatib and Bayomy (1999) studied the use of recycled tire rubber in a Portland cement concrete (PCC) mixture, and reported the workability of rubcrete. For this purpose, they used two types of tire rubber (fine crumb rubber and coarse tire chips) in PCC mixtures. A control PCC mixture with 38 MPa targeted compressive strength was designed. The mixture was made with 0.48 water-to-cement ratio. Details of the mix design are given in Table 4.4. In rubberized mixtures, all mix design parameters (cement content, water-cement ratio, and aggregate volume) were kept constant except for the aggregate constituents. Three groups (A, B, and C) of rubberized PCC mixtures were developed by partially replacing the aggregate with rubber. Details of the rubber contents for rubberized mixtures are given in Table 4.5. Based on the test results, they reported that slump values for all the three group mixtures were around 76 mm at 0% rubber content. There was decrease in slump with the increase in rubber content as a percentage of total aggregate volume. At rubber contents of 80% or higher (40% by total aggregate volume), the slump was near zero and the mix was not workable by hand mixing. It was also observed that mixtures made with fine crumb rubber were more workable than those with coarse tire chips or a combination of tire chips and crumb rubber.

Albano et al. (2005) reported the slump values of concrete containing automobile-tire treads as partial replacement of fine aggregate. The weight percentage of rubber used was 5 and 10%, with particle sizes of 0.29 mm and 0.59 mm. Scrap rubber used was untreated and treated with a solution of sodium hydroxide (NaOH) and with a coupling agent silane A-174, with the purpose of improving the interfacial adhesion between concrete and rubber. Slump values for traditional concrete mix and concrete-scrap rubber mix are given in Table 4.6. It can be seen from the table that slump decreased from a value of 8 cm for the traditional composite to a value of 1 cm for the blends with 5% rubbers of 0.29 and 0.59 mm particle sizes. When rubber content was increased to 10%, it decreased to a value of 0.5. Similar decreasing trend was observed when rubber was treated. When comparing traditional concrete mixes with concrete-scrap rubber mixes, slump reduced 88%, due to the decrease

Table 4.4 Properties of materials and mix design of PCC control mixture (Khatib and Bayomy, 1999)

Materials	Specific gravity	Weight (kg/m ³)	Volume (m ³ /m ³)
Coarse aggregate (gravel)	2.650	1024.0	0.386
Fine aggregate (Sand)	2.670	786.0	0.294
Portland cement	3.150	388.0	0.123
Water	1.000	186.0	0.186
Crumb rubber	1.180	—	—
Tire chips	—	—	—

Table 4.5 Designated rubber contents for rubberized mixtures (Khatib and Bayomy, 1999)

Materials	Rubber content (%) by total aggregate volume		
	Group A*	Group B**	Group C***
Control mixture	0.00	0.00	0.00
5	2.16	2.84	2.50
10	4.32	5.68	5.00
15	6.49	8.51	7.50
20	8.65	11.35	10.00
40	17.30	22.70	20.00
60	25.95	34.05	30.00
80	34.59	45.41	40.00
100	43.24	56.76	50.00

*Crumb rubber replaced the fine aggregate.

**Tire chips replaced coarse aggregate in this group.

***Criteria to replace sand by crumb and the coarse aggregates by chips, was divided equally.

on blend flow, because of the presence of a high portion of fine aggregates (rubber particles), which have a very low density, hence greater volume.

4.3.2 Air Content

Fedroff et al. (1996) concluded that rubcrete mixtures had higher air content than control mixtures even without the use of air-entraining admixture (AEA). Khatib and Bayomy (1999) also reported that high values of air content were obtained at high rubber contents (details of the mixture and rubber contents are given in Tables 4.4 and 4.5). The rate of increase in air content was almost the same for the three groups when rubber content was <30% of total aggregate volume. Interestingly, Group B (mixes with tire chips only) had a lower air content than Group A (mixes with crumb rubber only) for rubber contents >30%. It is believed that this was result of the extra compaction effort required for the Group B samples at high rubber contents. This may be due to the non-polar nature of rubber particles and their tendency to entrap air in their rough surfaces. Also when rubber was added to a concrete mixture, it might attract air as it has the tendency to repel water, and then air may adhere to the rubber particles.

Table 4.6 Slump results obtained for traditional concrete (TC) and concrete-crap rubber (Albano et al., 2005)

Rubber (%)	Particle size (mm)	TC (%)		CSRM untreated (%)		CSRM treated (NaOH) (%)		CSRM treated (silane) (%)	
		0	5	10	5	10	5	10	5
Slump	0.59	8	1	0.5	0.5	0.5	2	0.5	
(cm)	0.29	8	1	0.5	1	0	1	0.5	

Table 4.7 Density values for traditional concrete (TC) and concrete-crap rubber mix (Albano et al., 2005)

Rubber (%)	Particle size (mm)	TC (%)	CSRM untreated (%)			CSRM treated (NaOH) (%)		CSRM treated (silane) (%)	
			0	5	10	5	10	5	10
Density	0.59	2887	2300	2033	2248	1981	2218	2021	
(kg/m ³)	0.29	2887	2237	1784	2218	1780	2189	1971	

4.3.3 Unit Weight and Density

Because of low specific gravity of rubber particles, unit weight of mixtures containing rubber decreased with the increase in the percentage of rubber content. Moreover, increase in rubber content increased the air content, which in turn reduces the unit weight of the mixtures. The decrease in unit weight of rubcrete was negligible when rubber content was lower than 10–20% of the total aggregate volume, but with further increase in rubber content, it could be as low as 75% of the normal weight concrete (Khatib and Bayomy, 1999).

Albano et al. (2005) investigated the effect of automobile-tire treads on the density of traditional concrete. They used them as partial replacement of fine aggregate. Particle sizes of tire-treads were 0.29 mm and 0.59 mm. The weight percentage of rubber used was 5 and 10%. Scrap rubber used was untreated and treated with a solution of sodium hydroxide (NaOH) and with a coupling agent silane A-174, with the purpose of improving the interfacial adhesion between concrete and rubber. Table 4.7 shows density values for concrete without rubber and with rubber of different particle size treated and untreated. When comparing traditional concrete mix with concrete–scrap rubber mix (particle size 0.59 mm) it can be seen that density diminishes (20–29%), being this effect more significant when rubber percentage was 10% by weight. On the other hand, surface treatments done to rubber did not affect significantly the relation weight/volume of the composites. Also, density was lower for composites based on smaller particle size (22–38%). However, when particle size and percentage were compared, results showed that the influence of percentage on density was more noticeable for bigger size particle. This behavior is due to the physical properties of rubber, since it has lower density than sand, hence it occupies greater volume. This effect was more pronounced for smaller rubber particles, due to the greater porosity of the composite obtained; this means greater quantity of spaces filled with water within the interface rubber–concrete.

4.4 Properties of Hardened Concrete Containing Scrap Tires

4.4.1 Compressive Strength

Several authors (Ali et al., 1993; Eldin and Senouci, 1993; Khatib and Bayomy, 1999; Rostami et al., 1993; Topcu, 1995) reported the compressive strength results

of rubberized concrete. Results of various studies indicate that the size, proportions, and surface texture of rubber particles noticeably affect the compressive strength of rubcrete mixtures.

Eldin and Senouci (1993) studied the influence of rubber-tire particles on the compressive strength of concrete. They prepared a 35 MPa non-air-entrained control concrete using Portland cement (Type-I), 38 mm crushed stone aggregate (2.65 specific gravity), sand of 2.4 fineness modulus, and water cement ratio of 0.48. One cubic meter of concrete mixture contained 1116 kg of coarse aggregate, 629 kg of sand, 447 kg of cement, and 214 kg of water. They prepared two groups of concrete mixtures containing rubber particles. In the first group of mixtures, only the coarse aggregate of the control mix was replaced by rubber aggregate (group 1). In the second, only the sand was replaced by crumb rubber (group 2). In each of the group, consisting of several batches, mineral aggregate (fine or coarse) was replaced by the rubber aggregate in increments of 25% by volume. Two types of tire chips were used as coarse aggregate. One was obtained by mechanical grinding (Edgar chips) and the other by cryogenic grinding (Preston rubber). Edgar chips were then sieved in three groups of 38, 25, and 19 mm maximum sizes. Preston rubber particles were of 6 mm maximum size. The crumb rubber used as fine aggregate was also obtained by cryogenic grinding (Preston rubber). It was ground to pass a 2.00 mm sieve. Compressive strength of concrete mixtures (group 1) containing tire-chips as coarse aggregate replacement recorded losses up to 85% of the compressive strength, depending on the percentage of rubber. There was almost no increase in compressive strengths between the 7th and the 28th day; the least increase was seen for the specimens containing 75% and 100% tire chips, whereas for concrete mixtures (group 2) containing crumb rubber as fine aggregate replacement, In this case also, reduction in compressive strength was observed with increase in the crumb-rubber content. However, specimens lost up to 65% of their compressive strength.

Rubber-containing concrete did not exhibit brittle failure under compression and split tension. The specimens exhibited high capacity for absorbing plastic energy under both compression and tension loadings. The failure of group 1 specimens containing Edgar chips was a gradual splitting failure, whereas the failure of group 1 specimens containing Preston rubber and group 2 specimens was a gradual shearing failure. They also presented a mathematical model which quite accurately describes the effects of rubber aggregates on the compressive and tensile strengths of concrete. The strength reduction can be attributed both to a reduction of the quantity of the solid load-carrying material and to stress concentrations (tensile and compressive) in the paste at the boundaries of the rubber aggregate.

Topcu (1995) also showed that the addition of coarse rubber-chips in concrete lowered the compressive strength more than the addition of fine crumb rubber. However, results reported by Ali et al. (1993); Fattuhi and Clark (1996) indicated the opposite trend.

Biel and Lee (1996) concluded that the type of cement noticeably affects the compressive strength of rubcrete. They used two types of cement, magnesium oxy-chloride cement and Portland cement in making rubcrete. The percentage of fine aggregate substitution varied from 0 to 90% by weight. It was observed that 90%

loss in compressive strength occurred for both Portland cement rubber concrete (PCRC) and magnesium oxychloride cement rubber concrete (MOCRC) when aggregates (90% of fine aggregate and 25% of total aggregate) were replaced by untreated rubber. Magnesium oxychloride cement concrete exhibited approximately 2.5 times the compressive strength of Portland cement concrete for both with and without rubber in the concrete. In terms of splitting tensile strength, Portland cement concrete specimens made with 25% of rubber by total aggregate volume retained 20% of their splitting tensile strength after initial failure, whereas the magnesium oxychloride cement concrete specimens with the same rubber content retained 34% of their splitting tensile strength. They further noted that use of magnesium oxychloride cement may provide high-strength and better bonding characteristics to rubber concrete, and rubber concrete made with magnesium oxychloride cement could possibly be used in structural applications if rubber content is limited to 17% of the total volume of the aggregate.

Khatib and Bayomy (1999) investigated the compressive strength of Portland cement concrete (PCC) mixture containing recycled tire rubber. For this purpose, they used fine crumb rubber and coarse tire chips. A control PCC mixture with 38 MPa targeted compressive strength was designed. The mixture required 0.48 water-to-cement ratio. Details of the mix design have already mentioned Table 4.4. Three groups (A, B, and C) of rubberized PCC mixtures were developed by partially replacing the aggregate with rubber. In rubberized mixture, all mix design parameters (cement content, water-cement ratio, and aggregate volume) were kept constant except for the aggregate constituents. Details of the rubber contents for rubberized mixtures are given in Table 4.5. Based on the test results, they reported: (i) there was systematic reduction in concrete compressive strength with the increase of rubber content. The initial 28-day compressive strength of about 38 MPa decreased to almost 3 MPa when full replacement of coarse aggregate by rubber chips was made; (ii) for the mixture with crumb rubber replacement, the strength decreased to about 3.6 and 3.2 MPa for mixtures with crumb and chip rubber replacement, respectively. There was approximately 90% reduction in the 28-day strength when 100% of the aggregate volume was replaced by rubber; and (iii) as rubber content increased, specimens tend to fail gradually in either conical or columnar shape failure mode. The specimens sustained a much higher deformation than the control mixture. With rubber content near 60%, the specimens exhibited significant elastic deformation, which was retained on unloading, thereby significantly enhancing the flexibility and ability to deform elastically.

They also gave the possible reasons for reduction in strength with the inclusion of rubber in concrete mixtures. First, because the rubber particles are much softer (elastically deformable) than the surrounding cement paste, on loading, cracks are initiated quickly around the rubber particles in the mix, which accelerated the failure of the rubber-cement matrix. Secondly, due to the lack of adhesion between rubber particles and the paste, soft rubber particles may be viewed as voids in the concrete matrix. The assumed increase in void content would certainly cause a reduction in strength. Eldin and Senouci (1993) discussed the latter assumption, where they resembled the rubber content to the air content in its effect on the concrete strength.

They developed a model based on an early analysis by Goodier (1933) to quantify the effect of voids or flaws on the strength of the rubberized PCC mixtures. The third possible reason for strength reduction is the fact that PCC strength is dependent greatly on the coarse aggregate, density, size, and hardness (Mehta and Monteiro, 1993). Because the aggregates are partially replaced by rubber, the reduction in strength is anticipated.

Studies have indicated that if the rubber particles have rougher surface or given a pretreatment, then better and improved bonding may develop with the surrounding matrix, and, therefore, that may result in higher compressive strength. Pretreatments may vary from washing rubber particles with water to acid etching, plasma pretreatment, and various coupling agents (Naik and Singh, 1991). In acid pretreatment, rubber particles are soaked in an alkaline solution (NaOH) for 5 minutes, and then rinsed with water. This treatment enhances the strength of concrete containing rubber particles through a microscopic (a very small) increase in the surface texture of the rubber particles. Eldin and Senouci (1993) soaked and thoroughly washed rubber aggregates with water to remove contaminants, while Rostami et al. (1993) used water, water and carbon tetrachloride solvent, and water and a latex admixture cleaner. Results showed that concrete containing water-washed rubber particles achieved about 16% higher compressive strength than concrete containing untreated rubber aggregates, whereas this improvement in compressive strength was 57% when rubber aggregates treated with carbon tetrachloride were used.

Segre and Joekes (2000) studied the use of tire rubber particles as addition to cement paste and reported the compressive strength tests results. In their work, the surface of powdered tire rubber (particles of maximum size 35 mesh, 500 μm) was modified to increase its adhesion with cement paste. Low-cost procedures and reagents were used in the surface treatment to minimize the final cost of the modified material. Among the surface treatments tested to enhance the hydrophilicity of the rubber surface, a sodium hydroxide (NaOH) solution gave the best result. The tire rubber particles were surface-treated with saturated NaOH aqueous solutions for 20 min, at room temperature, with stirring. The mixture was filtered and the rubber was washed with water and dried at ambient temperature. Cement paste test specimens were prepared (water/cement ratio = 0.36) with the addition of 10% by mass of as-received or 10% by mass of NaOH-treated rubber. When sodium silicate was added, the water was substituted by a 10% volume aqueous solution of this reagent. Compressive strength results are given in Table 4.8. The test results showed that the NaOH treatment enhanced the adhesion of tire rubber particles to cement paste. The addition of rubber particles reduced the compressive strength of

Table 4.8 Compressive strengths for cement test specimens rubber (Segre and Joekes, 2000)

Specimen	Compressive strength (MPa)
Control	43.1 \pm 3.2
With as-received rubber	29.4 \pm 3.1
With NaOH-treated rubber	28.1 \pm 3.5

the specimens. However, a reduction of 33% in compressive strength was observed, a value significantly lower than the 60% as reported by Lee et al. (1993).

Hernandez-Olivares et al. (2002) investigated the compressive strength of concrete filled with small volumetric fractions of crushed tire rubber up to the age of 28 days. Two percentages of crumb rubber (3.5 and 5%) by volume were used. Rubber crumbed fibers were obtained from used truck tires. Strip process produced short fibers between 0.85 and 2.15 cm long, with an average of 1.25 cm. Their surfaces were rough and damaged due to the cutting process. They contained 4% of fine dust particles, retained by the 1.6 mm sieve that acted as airing particles. The apparent density of rubber fiber was 0.84 g/cm^3 and they had a water absorption coefficient of 25%, with a natural humidity of 6.25%. Based on the results, they concluded that rubber fiber-filled concrete achieved a characteristic compressive strength 23 MPa, while for plain concrete it was 36 MPa. The average compression values were 29 and 40 MPa, respectively.

Huang et al. (2004) reported the 28-compressive strength results of concrete mixture made with rubber chips. They used chips of size $25.4 \times 25.4 \times 5 \text{ mm}$ dimensions and 15% by volume of gravel (coarse aggregate) were replaced by rubber chips. Control concrete achieved a strength of 40.61 MPa, whereas rubberized concrete could achieve only 22.33 MPa; loss of 45%.

Albano et al. (2005) determined 28-day compressive strength of concrete made with automobile-tire treads as partial replacement of fine aggregate. The weight percentage of rubber used was 5 and 10%, with particle sizes of 0.29 mm and 0.59 mm. Scrap rubber was untreated and treated with a solution of sodium hydroxide (NaOH) and with a coupling agent silane A-174, with the purpose of improving the interfacial adhesion between concrete and rubber. Table 4.9 shows compressive strength values obtained for concrete mixtures with and without rubber of different particle sizes, percentages and surface treatments. It can be observed that there was a drastic decrease in the compressive strength of concrete made with scrap rubber compared to traditional concrete mixtures. In particular, concrete mixtures with 5% rubber of 0.59 mm particle size, approximately 60% reduction in compressive strength was observed. When rubber content increased to 10%, the reduction in compressive strength reached 88%. On the other hand, when rubber particle size was 0.29 mm, the same tendency was observed; however, compressive strength values were even lower. The same behavior was obtained for mixtures when treated-rubber was used. From these results it can be inferred that particle size exerts an important effect on

Table 4.9 Compressive strength values for traditional concrete (TC) and concrete-crap rubber mix (Albano et al., 2005)

Rubber (%)	Particle size (mm)	TC (%)	CSRM untreated (%)		CSRM treated (NaOH) (%)		CSRM treated (silane) (%)	
			5	10	5	10	5	10
Compressive strength (MPa)	0.59	30.32	11.66	3.49	12.19	4.00	11.56	4.94
	0.29	30.32	8.80	0.78	9.19	1.70	8.83	0.78

compressive strength, since small rubber particles originate greater interstitial voids, probably filled with water, so a low aggregate-concrete interaction is achieved, with subsequent loss in compressive strength. Besides, physical and mechanical properties of rubber also contribute to the behavior observed.

4.4.2 Tensile Strength

Eldin and Senouci (1993) investigated the influence of rubber-tire particles on the splitting tensile strength of concrete. A non-air-entrained control concrete using Portland cement was designed. Besides control mixture, they also prepared two groups of concrete mixtures containing rubber particles. In the first group of mixture, only the coarse aggregate of the control mix was replaced by rubber aggregate (group 1). In the second, only the sand was replaced by crumb rubber (group 2). In each of the group, consisting of several batches, mineral aggregate (fine or coarse) was replaced by the rubber aggregate in increments of 25% by volume. Two types of tire chips were used as coarse aggregate. One was obtained by mechanical grinding (Edgar chips) and the other by cryogenic grinding (Preston rubber). Edgar chips were then sieved in three groups of 38, 25, and 19 mm maximum sizes. Preston rubber particles were of 6 mm maximum size. The crumb rubber used as fine aggregate was also obtained by cryogenic grinding (Preston rubber). It was ground to pass a 2.00 mm sieve. Tensile strength of concrete mixtures (group 1) containing tire-chips as coarse aggregate replacement recorded losses up to 50% of the tensile strength, depending on the percentage of rubber were measured. There was almost no increase in tensile strengths between the 7th and the 28th day; the least increase was seen for the specimens containing 75% and 100% tire chips. In case of concrete mixtures (group 2) containing crumb rubber as fine aggregate replacement, reduction in tensile strength was observed with increase in the crumb-rubber content. However, specimens lost up to 50% of their tensile strength.

Khatib and Bayomy (1999) reported the flexural strength of Portland cement concrete (PCC) mixture containing recycled tire rubber (fine crumb rubber and coarse tire chips). Control PCC mixture had a flexural strength of 11 MPa at the age of 28 days. Details of the mix design and that of the mixtures containing tire-chips, and crumb rubber have already been given in Table 4.4 and 4.5. They reported that flexural strength decreased with the increase of the rubber content in similar fashion to that observed in case of compressive strength. However, it was noticed that the initial rate of strength reduction was steeper than that of the compressive strength. For the mixture with crumb rubber replacement, the strength decreased to about 1.2 and 0.6–0.8 MPa for mixtures with crumb and chip rubber replacement, respectively. This was approximately 90% reduction in the 28-day strength when 100% of the aggregate volume was replaced by rubber. The reduction in strength was due to the weak bond between cement paste and rubber particles. When analyzing the failed samples visually, it was observed that rubber particles could be removed from the cement paste by fingers. Furthermore, visual observations during testing indicated

that beam samples of the rubberized mixtures had much higher deflections before failure than beam samples of the control mixture.

Segre and Joekes (2000) investigated the flexural strength, and modulus of elasticity of cement paste containing surface-modified tire rubber particles. Surface of powdered tire rubber (particles of maximum size 35 mesh, 500 μm) was modified to increase its adhesion to cement paste. The tire rubber particles were surface-treated with saturated NaOH aqueous solutions for 20 min, at room temperature, with stirring. The mixture was filtered and the rubber was washed with water and dried at ambient temperature. Cement paste specimens were prepared (water/cement ratio = 0.36) with the addition of 10% by mass of as-received or 10% by mass of NaOH-treated rubber. When sodium silicate was added, the water was substituted by a 10% volume aqueous solution of this reagent. Results of flexural strength, modulus of elasticity and fracture energy are presented in Table 4.10. It can be seen that for flexural strength, the specimens with NaOH-treated rubber and with as-received rubber, without silicate solution, showed higher values than the control specimens. The inclusion of tire rubber increased the fracture energy by a factor of four, indicating that specimens containing rubber exhibited higher toughness, as compared to the control. No differences were observed for the modulus of elasticity.

Lee et al. (1998) developed “tire-added latex concrete” to incorporate recycled tire rubber as a part of concrete. Crumb rubber from used tires was used in TALC (Tire-added latex concrete) as a substitute for fine aggregates or styrene-butadiene rubber (SBR) latex while maintaining the same water-cementitious materials ratio. TALC showed higher flexural and impact strengths than those of Portland cement, latex modified concrete, and rubber-added concrete. Pictures taken using the scanning electron microscopy (SEM) seem to support that there was better bonding between crumb rubber and Portland cement paste due to latex. TALC showed potential as a viable construction material that is less brittle than other types of concrete.

Hernandez-Olivares et al. (2002) reported that addition of crumb tire rubber volume fractions up to 5% in a cement matrix did not have a significant effect on the splitting tensile strength and bending strength of concrete. They concluded that: (i) splitting tensile strength of rubber filled concrete was 2.3 MPa at the age of 28 days,

Table 4.10 Flexural strength, modulus of elasticity and fracture energy of cement specimens (Segre and Joekes, 2000)

Specimen	Flexural strength (MPa)	Modulus of elasticity (GPa)	Fracture toughness (Jm^{-2})
Control	5.6 ± 3.1	5.9 ± 1.9	6.3 ± 0.9
With NaOH-treated rubber	9.9 ± 1.2	6.2 ± 0.3	22.0 ± 1.4
With as-received rubber	10.9 ± 2.0	7.3 ± 0.5	25.9 ± 3.5
With NaOH-treated + silicate solution	4.6 ± 0.5	3.9 ± 0.7	25.4 ± 2.6
With as-received rubber + silicate solution	5.9 ± 1.1	5.2 ± 1.2	25.7 ± 3.1
Cement + silicate solution	7.2 ± 1.2	6.4 ± 0.8	

whereas it was 2.8 MPa for control concrete; and (ii) bending strength of rubber filled concrete was 4 MPa at the age of 28 days, whereas it was 5.4 MPa for control concrete.

Huang et al. (2004) conducted tests for splitting tensile strength and modulus of elasticity at the age of 28 days for concrete mixture made with rubber chips. They used chips of size $25.4 \times 25.4 \times 5$ mm dimension, and 15% by volume of gravel (coarse aggregate) was replaced by rubber chips. They reported that control concrete achieved splitting tensile strength of 3.01 MPa, and modulus of elasticity of 35.13 GPa, whereas rubberized concrete achieved splitting tensile strength of 2.34 MPa and modulus of elasticity of 28.89 GPa.

4.4.3 Abrasion Resistance

Segre and Joekes (2000) studied the abrasion resistance of cement paste containing surface-modified tire rubber particles. Surface of powdered tire rubber (particles of maximum size 35 mesh, $500 \mu\text{m}$) was modified to increase its adhesion to cement paste. The tire rubber particles were surface-treated with saturated NaOH aqueous solutions, and then mixture was filtered and rubber was washed with water and dried at ambient temperature. For measuring the abrasion resistance, layer of cement paste (water/cement ratio of 0.36) with the addition of 10% by mass of as-received or 10% by mass of NaOH-treated rubber was spread over an asbestos–cement support. After curing, the support was cut into specimens measuring $100 \times 100 \times 3$ mm. The wearing was followed gravimetrically after each 100-abrasion cycle, up to 1000 cycles. Figure 4.1 shows the mass loss as a function of number of abrasive cycles. The mass loss of specimens containing NaOH-treated rubber was significantly lower than that of the specimens containing as-received rubber. These results are

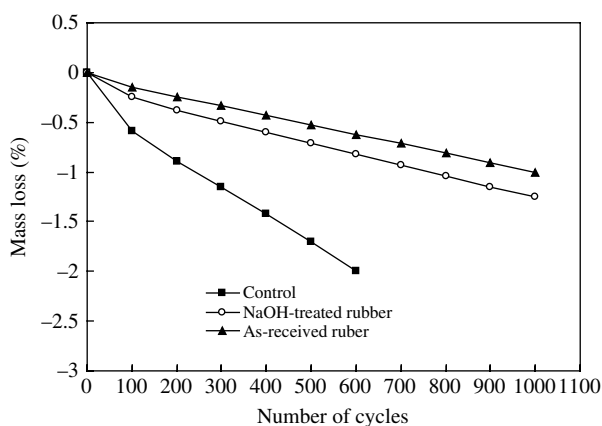


Fig. 4.1 Mass loss for cement test specimens with 10% by mass of tire rubber (Segre and Joekes, 2000)

fundamental to show the increased adhesion obtained by treatment of the rubber particles, since the pull-out force expresses the magnitude of the adhesion strength between the rubber and the cement matrix.

4.4.4 Shrinkage

Limited amount of literature is available concerning the plastic shrinkage of concrete containing rubber particles. Preliminary results reported by Raghvan et al. (1998) suggest that incorporation of rubber shreds (two different shapes of rubber particles) as constituents of mortar: (i) granules about 2 mm in diameter; and (ii) shreds having two sizes; 5.5 mm \times 1.2 mm and 10.8 mm \times 1.8 mm (length \times diameter) help in reducing plastic shrinkage cracking in comparison to control mortar. They further reported that control specimens developed cracks having an average width of about 0.9 mm, while the average crack width for specimens with a mass fraction of 5% rubber shreds was about 0.4–0.6 mm. It was also reported that onset time of cracking was delayed by the addition of 5% rubber shreds. Mortar without rubber shreds cracked within 30 minutes, while mortar with 15% fraction by mass cracked after one hour. It was further indicated that the higher the content of rubber shreds, the smaller the crack length and width, and the onset time of cracking was more delayed.

4.4.5 Fatigue, Toughness, and Impact Resistance

Eldin and Senouci (1993) demonstrated that the failure mode of specimens containing rubber particles was gradual as opposed to brittle. Biel and Lee (1996) reported that failure of concrete specimens with 30, 45, and 60% replacement of fine aggregate with rubber particles occurred as a gradual shear that resulted in a diagonal failure, whereas failure of plain (control) concrete specimens was explosive, leaving specimens in several pieces.

Tantala et al. (1996) investigated the toughness (toughness is also known as energy absorption capacity, and is generally defined as the area under load-deflection curve of a flexural specimen) of a control concrete mixture and rubcrete mixtures with 5 and 10% buff rubber by volume of coarse aggregate. They reported that toughness of both rubcrete mixtures was higher than the control concrete mixture. However, the toughness of rubcrete mixture with 10% buff rubber (2–6 mm) was lower than that of rubcrete with 5% buff rubber because of the decrease in compressive strength.

Based on their investigations on use of rubber shreds (having two sizes which were, nominally, 5.5 mm \times 1.2 mm and 10.8 mm \times 1.8 mm) and granular (about 2 mm in diameter) rubber in mortar, Raghvan et al. (1998) reported that mortar specimens with rubber shreds were able to withstand additional load after peak load. The specimens were not separated into two pieces under the failure flexural load

because of bridging of cracks by rubber shreds, but specimens made with granular rubber particles broke into two pieces at the failure load. This indicated that post-crack strength seemed to have enhanced when rubber shreds were used instead of granular rubber.

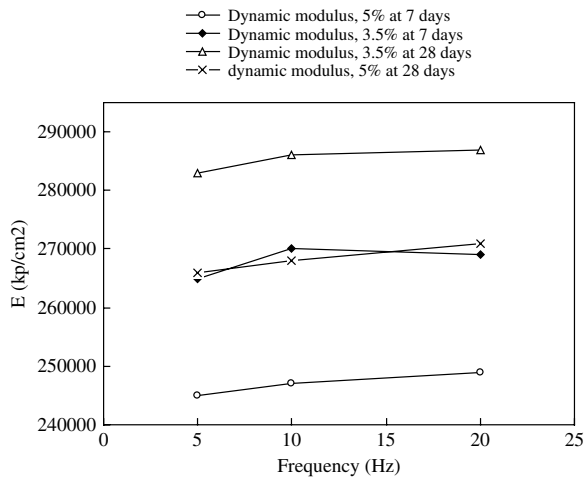
Goulias and Ali (1997) found that the dynamic modulus of elasticity and rigidity decreased with an increase in the rubber content, indicating a less stiff and less brittle material. They further reported that dampening capacity of concrete (a measure of the ability of the material to decrease the amplitude of free vibrations in its body) seemed to decrease with an increase in rubber content. However, Topcu and Avcular (1997a) have recommended the use of rubberized concrete in circumstances where vibration damping is required, and reported that the impact resistance of concrete increased when rubber aggregates were incorporated into the concrete mixtures. The increase in resistance was derived from the enhanced ability of the material to absorb energy. Eldin and Senouci (1993); Fattuhi and Clark (1996) and Topcu (1995) also reported similar results.

Khatib and Bayomy (1999) reported that as the rubber content is increased, rubcrete specimens tend to fail gradually, and failure mode shape of the test specimen is either a conical or columnar (conical failure is gradual, whereas columnar is more of shreds having two sizes which were, nominally, $5.5 \text{ mm} \times 1.2 \text{ mm}$ and $10.8 \text{ mm} \times 1.8 \text{ mm}$ (length \times diameter sudden failure). At a rubber content of 60%, by total aggregate volume, the specimens exhibited elastic deformations, which the specimens retained after unloading.

Hernandez-Olivares et al. (2002) studied the dynamic modulus of concrete filled with small volumetric fractions (3.5 and 5% by volume) of crushed tire rubber up to the age of 28 days. Figure 4.2 shows the variation of young's dynamic modulus corresponding with 5, 10 and 20 Hz frequencies. Based on the results obtained they reported that: (i) a clear dependence can be observed, either the specimen characteristics or the test frequencies; (ii) dynamic modulus were lower at 7 days than at 28 days, which is, in principle, obvious due to the endurance process of the concrete matrix, enlarging the stiffness of the material. Concrete with 5% of rubber recorded a lower dynamic modulus than 3.5% rubber fiber concrete. This trend was maintained with age (7 and 28 days); and (iii) young dynamic modulus was sensitive to the load application frequency. It increased slightly with the increase in frequency.

Hernandez-Olivares et al. (2007) presented the results of fatigue laboratory tests on prismatic samples of rubber-filled concrete cut off from slabs of $90 \times 60 \times 5 \text{ cm}$, after a long term exposition to natural weathering (one year ageing). They used different volume fractions of rubber (0, 3.5 and 5%). From these experimental results, an analytical model based on classical Westergaard well known equations was developed to calculate the minimum thickness of RRFC for rigid pavements subjected to high density traffic, in order to assess the durability of this rigid pavements under 10^6 cycles of 13 tons axle load, as per design rules based on AASHTO test. The results of recycled tire rubber-filled concrete (RRFC) under fatigue loads and the analytical study presented in this paper show the feasibility of using this cement based composite material as a rigid pavement for roads on elastic sub grade.

Fig. 4.2 Young dynamic modulus as a function of frequency, age and fraction of crumb rubber (Hernandez-Olivares et al., 2002)



4.4.6 Freezing and Thawing Resistance

Savas et al. (1996) carried out investigations to study the rapid freezing and thawing (ASTM C 666, Procedure A) durability of rubber concrete. Various mixtures were made by incorporating 10, 15, 20, and 30% ground rubber by weight of cement. Based on their studies, they concluded that: (i) rubcrete mixtures with 10 and 15% ground rubber (2–6 mm in size) exhibited durability factors higher than 60% after 300 freezing and thawing cycles, but mixtures with 20 and 30% ground rubber by weight of cement could not meet the ASTM standards (durability factor); (ii) air-entrainment did not provide improvements in freezing and thawing durability for concrete mixtures with 10, 20, and 30% ground tire rubber; and (iii) increase in scaling (scaling gives an evaluation of the surface exposed to freezing and thawing cycles as measured by the loss of weight) increased with the increase in freezing and thawing cycles.

Benazzouk and Queneudec (2002) studied the freeze-thaw durability of cement-rubber composites through the use of two types of rubber aggregate. The types of the aggregates were: Compact Rubber Aggregate (CRA) and Expanded Rubber Aggregates (ERA). Volume-ratio of the aggregates ranged from 9 to 40%. The results showed improvements in the durability of the composite containing 30 and 40% rubber by volume. Improvement in the durability of the composite containing ERA type aggregates was better than composite made with CRA aggregates. The finding was more distinct for ERA type.

Paine et al. (2002) investigated the use of crumb rubber as an alternative to air-entrainment for providing freeze-thaw resisting concrete. Three sizes of crumb rubber 0.5–1.5 mm, 2–8 mm, and 5–25 mm were used. Test results showed that there is potential for using crumb rubber as a freeze-thaw resisting agent in concrete. The crumb rubber concrete performed significantly better under freeze-thaw conditions than plain concrete, and the performance of crumb rubber concrete in terms of scaling was similar to that of air-entrained concrete.

4.5 Use of Scrap Tire Ash in Mortar

Al-Akhras and Smadi (2002) studied the properties of tire-rubber ash (TRA) mortar. Tire rubber chips were obtained and burned at a controlled temperature of 850°C for 72 hours. The residue of tire-rubber chips (ash) was collected. TRA was utilized as partial replacement of sand in five percentages ranging from 0 to 10% with an increment of 2.5% by weight of sand. Based on the test results, they concluded that: (i) as the TRA content increased, workability of the fresh mortar decreased. This behavior was due to the increase in the cementitious materials in the mortar mix, particularly due to the large surface area of the TRA; (ii) both initial and final setting time increased with the increase in TRA content. The initial setting time increased from 145 minutes for the control paste mix to 220 minutes for 10% TRA paste mix. The final setting time increased from 270 minutes for control paste mix to 390 minutes for 10% TRA paste mix; and (iii) TRA specimens showed higher compressive strengths at various curing periods up to 90 days compared with those of the control specimens. Also the tensile and flexural strengths of the TRA mortar specimens were higher than those of the control specimens.

4.6 Use of Scrap Tire Steel Beads in Concrete

The beads in the passenger tires are made of high tensile strength steel wires (1500–1900 MPa) and are used to secure the tire in the rim. The recycled steel beads, being products of the magnetic separation, include short steel wires as well as wires covered by or embedded in rubber pieces. The difference between the tire chips and the steel beads is that the steel beads contain a much smaller quantity and size of rubber pieces and larger quantity of steel wires, as indicated by the rubber and steel volume fractions shown in Table 4.11.

Papakonstantinou and Tobolski (2006) investigated the use of steel beads, a by-product of tire-recycling process in concrete mixtures. Control concrete mixture was designed to have 28-day compressive strength of 40.92 MPa. The steel beads consisted of steel wires of varying lengths (20–60 mm) and diameters (0.3–1.3 mm) as well as rubber particles bonded to the wires. Their cross section was typically circular. The density of the steel beads was 1.6 g/cm³. The maximum size of the rubber particles was 12.5 mm (0.5 in.), while the volumetric percentage of the steel wires in steel beads was approximately 30%. The steel beads were substituted into the concrete mix in volumetric percentages of 2, 4, 6, and 8%. They conducted

Table 4.11 Properties of recycled tire materials Papakonstantinou and Tobolski (2006)

	Tire chips	Crumb rubber	Steel beads
Volume rubber (%)	95–99	99–100	30–70
Volume steel (%)	1–5	0	30–70
Density (g/cm ³)	0.9–1.5	0.8–1.2	1.6–3.8

Table 4.12 Experimental results of concrete mixtures containing steel beads Papakonstantinou and Tobolski (2006)

Steel bead (%)	Slump (cm)	Air content (%)	Density (kg/m ³)	Compressive strength (MPa)	Modulus of elasticity (GPa)	Splitting tensile strength (MPa)
0	17.8	1.7	2387	40.92	29.23	2.82
2	16.5	1.6	2373	40.13	25.86	2.75
4	15.3	1.6	2355	35.39	25.44	2.64
6	14.0	1.9	2325	33.43	25.99	2.55
8	11.4	2.1	2310	30.07	22.06	2.47

tests for slump, air-content, density, compressive strength, splitting tensile strength and modulus of elasticity. The experimental results of various properties are given in Table 4.12. Based on the results, they concluded that: (i) slump decreased at a constant rate as steel bead content increased. However, the mix remained workable (slump higher than 100 mm) at all steel bead contents. The steel wires had a tendency to interlock during the mixing process, leaving localized areas of high steel and rubber; (ii) the air content for the control mix was 1.7%. It decreased to 1.6% when 2 and 4% steel beads were used. Beyond 6% content, air content began to slightly increase with an increase in steel bead content. In all cases, the air content was kept less than 2.1%; (iii) density of the concrete mixtures was not significantly affected by steel bead content. The density for the control mix was 2387 kg/m³ while the mix containing 4% steel beads had a density of 2310 kg/m³; and (iv) compressive strength, modulus of elasticity and splitting tensile strength decreased with the increase in steel bead contents as evident from the results given in Table 4.12.

4.7 Fire-Performance of Concrete with Rubber

Hernandez-Olivares and Barluenga (2004) investigated the fire performance of high-strength concrete (HSC) filled with recycled rubber. For the purpose, they made HSC with silica fume, and then included rubber in 3, 5, and 8% volumetric fractions (25.2 kg/m³, 42 kg/m³ and 67.2 kg/m³, respectively). The solid fiber-shaped particles of recycled tire rubber were taken from truck tires. The length of the fibers was between 0.85 and 2.15 cm, with an average value of 1.25 cm. Its density was 0.84 g/cm³ and water absorption rate of 25%. A softening temperature of 175°C and a combustion temperature of 200°C have been determined. Prismatic specimens (20 × 30 × 5 cm) were subjected to a temperature up to 1000°C. Based on the observations, they concluded that fire tests have shown a reduction of curvature and risk of explosive spalling when HSC was filled with rubber. The depth of damage (temperature over 500°C for reinforced concrete structures) was also reduced. This could mean a reduction of the reinforcement covering in structural elements or an increase of safety in HSC structural elements against fire.

4.8 Use of Scrap Tire Rubber in Flowable Fill

Pierce and Blackwell (2003) studied the use of crumb rubber as aggregate in flowable fill also known as controlled low-strength material. They used No. 30 mesh rubber which was finer than standard concrete sand, with only the lower 10% of particles approaching the acceptable limits for sand. Absorption capacity of crumb rubber was 2.4% of its dry weight in the saturated-surface dry condition. This absorption capacity was relatively higher when compared with sand, which normally has an absorption capacity of 0.5% or less. The bulk specific gravity of crumb rubber samples was between 0.53 and 0.60, which is nearly five times less than that of sand. Nine series of mixtures were developed. Mixture details including their designation are given in Table 4.13. The first part of the mixture designation provides the w/c ratio; the second part identifies the percentage of crumb rubber by the total weight of ingredients. The letter F in the designation indicated that a small amount of fluidizing agent (0.5% by weight) was added.

Flowability, volume stability (bleeding), setting time, density, and compressive strength of flowable fill were investigated. Flowability was measured as per ASTM D 6103-97 (2002) standard test, and results are given in Table 4.14. The ACI criterion for high flowability is a spread diameter of 20–30 cm (ACI, 1999). Only two mixtures met this criterion. Both of these mixtures contained fluidizing agent. It is evident from the results that flowability increased by 40% when fluidizing agent was added to Mixture 2-22.

Bleeding results are shown in Table 4.14. According to ACI Committee 229 (1999), 2% bleeding is the limit for an acceptable amount of consolidation. Bleeding increased substantially with increasing w/c ratio. For the seven mixtures at the same crumb rubber-to-cement ratio of 1.3, the trend suggested that the w/c ratio was a critical factor and must be properly designed to effectively control bleeding. Initial hardening results are given in Table 4.14. To meet initial load bearing capacity requirements, ASTM C403/C403M-99 (2002) recommends a minimum equivalent strength of 140 kPa (20 psi) after three days of curing. Results indicated that all but three of the nine mixtures reached this strength within one day. Only one mixture did not meet the three-day recommendation; Mixture 2-22-F needed six days to reach strength of 140 kPa (20 psi).

Table 4.13 Mixtures of flowable fill incorporating crumb rubber (Pierce and Blackwell, 2003)

Mixture designation	w/c ratio	w/cm ratio	Crumb rubber	
			% by weight	% by volume
1.5-24-F	1.5	0.6	24.3	48
1.75-23-F	1.75	0.7	23.2	46
2-22-F ^a	2	0.8	22.2	44
2.5-21	2.5	1.0	20.5	40
3-19	3	1.2	19.0	37
3-29	3	1.6	28.5	48
3-38	3	2.4	38.0	57
4-17	4	1.6	16.6	32

Table 4.14 Flowability, bleeding and initial hardening time of flowable fill mixtures (Pierce and Blackwell, 2003)

Mixture designation	Flowability (cm)	Bleeding (% volume)	Time to reach 140 kPa (days)
1.5-24-F	0	1.3	1
1.75-23-F	20.3	1.9	2
2-22-F ^a	23.9	3.7	6
2-22	16.8	4.3	1
2.5-21	35	10.1	1
3-19	36.3	13.8	1
3-29	31.8	9.5	1
3-38	16.8	4.6	2
4-17	> 60	29.9	1

Unconfined compressive strength of flowable fill mixtures was determined at the age of 7, 14, and 28 days, and results have been given in Table 4.15. Results show that the measured unconfined compressive strengths for these eight mixtures generally varied between 210 and 2070 kPa (30 and 300 psi), which are common for most standard flowable fills. Using the mean 28-day strengths, seven of the mixtures fall below the 1380 kPa (200 psi) maximum strength criterion for excavatability (ACI, 1999). It was recognized that some, but not all, of these mixtures may develop strengths exceeding 1380 kPa (200 psi) at curing times beyond 28 days.

Based on the experimental results, Pierce and Blackwell (2003) concluded that: (i) crumb rubber can be used as a complete replacement for concrete sand in flowable fill. Crumb rubber contents as high as 38% by weight (57% by volume) can be mixed in flowable fill without noticeable segregation of the rubber, although there was measurable bleeding in some cases. No admixtures are required to coat the rubber particles; (ii) flowable fills mixed with crumb rubber produced bulk densities that were 60–80% of the typical bulk density of standard flowable fills mixed with sand. A lightweight flowable fill produced with crumb rubber provides the construction industry with a material that imparts less stress on the soil beneath it, thus

Table 4.15 Unconfined compressive strength measured (Pierce and Blackwell, 2003)

Mixture designation	Average compressive strength (kPa)		
	7-day	14-day	28-day
3-38	179	228	269
3-29	—	566	766
3-19	331	359	483
2.5-21	932	1449	2601
2-22	—	897	1021
2-22-F ^a	97	469	676
1.75-23-F	718	897	1194
1.5-24-F	114	1525	—

mitigating the potential for soil settlement, especially when constructing on soft and compressible soils; (iii) reduction in bulk density from using crumb rubber did not adversely impact the strength of flowable fill; and (iv) crumb rubber offers other benefits when used in flowable fill, such as improved ductility and higher thermal insulation. These and other technical benefits need to be explored further.

4.9 Environmental Studies of Recycled Rubber

Recycling materials conserve valuable natural resources and reduces the amount of waste entering landfills. One issue to consider, however, is the suitability of using recycled materials in subsurface applications. ASTM D 6270-98 (2002) provides guidelines for using scrap tires in civil engineering applications. Acceptable limits for metals and organics in leachate from shredded tires are discussed there.

According to several studies, Toxicity Characteristics Leaching Procedure (TCLP) test results show that tire shreds are not a hazard to human health (Downs et al., 1997; Ealding, 1992; Zelibor, 1991). Laboratory test results (Downs et al., 1997) have shown that metals are leached at low pH and that organics are leached at high pH. This indicates that unbound shredded tires should be used in environments where the soil and groundwater are at a fairly neutral pH.

Downs et al. (1997); Humphrey et al. (1997) and Edil and Bosscher (1992) have carried out field studies to investigate leachate from tire shreds placed above and below the water table. Concentrations of iron and manganese exceeded secondary drinking water standards in both cases. Since secondary standards apply to the aesthetic, not health, quality of water, this is a minor concern unless state or local regulations require leachate to meet more stringent concentration levels. Levels of organic compounds in the leachate from tire shreds located above the water table were below detection limits, but those below the water table were detectable (Downs et al., 1997; Humphrey et al., 1997). ASTM D 6270-98 (2002) specifies that applications involving tire shreds should be confined to locations above the water table until it is determined that these detectable levels are not a threat to human health.

Groenevelt and Grunthal (1998) and Reddy and Quinn (1997) conducted studies on leachate from crumb rubber and reported no deleterious effects to the environment. Al-Tabbaa and Aravinthan (1998) have shown that scrap tire rubber can absorb and retain volatile organic compounds (VOCs). Park et al. (1997) conducted laboratory-scale column tests on a slurry cutoff wall backfill material that contained 15% ground tires by weight. The authors reported a 10-fold increase in breakthrough time for the VOCs in the slurry amended with ground tires when compared to that of standard soil-bentonite slurry.

4.10 Uses of Rubber Concrete (Rubcrete)

Fattuhi and Clark (1996) have suggested that rubcrete could possibly be used in the following areas:

- (i) where vibration damping is needed, such as in foundation pad for rotating machinery and in railway stations;
- (ii) for trench filling and pipe bedding, pile heads, and paving slabs; and,
- (iii) where resistance to impact or blast is required such as in railway buffers, jersey barriers (A protective concrete barrier used as a highway divider and a means of preventing access to a prohibited area) and bunkers.

Rubcrete because of its light unit weight (density ranges from 900 to 1600 kg/m³) may also be suitable for architectural applications such as: (i) nailing concrete; (ii) false facades; (iii) stone backing; and (iv) interior construction.

Topcu and Avcular (1997b) have suggested that rubber-concrete may be used in highway construction as a (i) shock absorber, in sound barriers; (ii) sound booster (which controls the sound effectively); and (iii) in buildings as an earthquake shock-wave absorber. However, research is needed before definite recommendations can be made.

Eldin and Senouci (1993) recommended that concrete with rubber aggregate is suitable for: (1) Architectural applications such as nailing concrete, false facades, stone backing, and interior construction because of its light unit weight; (2) low-strength-concrete applications such as sidewalks, driveways, and selected road construction applications; and (3) crash barriers around bridges and similar structures because of its high toughness (high plastic energy absorption). It is also speculated that the material can be used in sound barriers and vibration-control applications because of its apparent high sound attenuation and vibration absorbency. However, more research is needed before one can draw a conclusion regarding recommended applications.

References

- ACI Committee 229 (1999) Controlled low-strength materials (CLSM). American Concrete Institute, Farmington Hills, MI, USA
- Al-Akhras NM, Smadi MM (2002) Properties of tire rubber ash mortar. Dhir RK et al. (Eds.), *Proceedings of the International Conference on Sustainable Concrete Construction*. University of Dundee, Scotland, UK pp. 805–814.
- Albano C, Camacho N, Reyes J, Feliu JL, Hernandez M (2005) Influence of scrap rubber addition to Portland Concrete Composites: Destructive and non-destructive testing. *Composite Structures* 71: 439–446.
- Ali NA, Amos AD, Roberts M (1993) Use of ground rubber tires in Portland cement concrete. Dhir RK (Ed.), *Proceedings of the International Conference on Concrete 2000*, University of Dundee, Scotland, UK pp. 379–390.
- Al-Tabbaa A, Aravinthan A (1998) Natural clay-shredded tire mixtures as landfill barrier materials. *Waste Management* 18 (1): 9–16.
- ASTM C403/C403M-99 (2002) Standard test method for time of setting of concrete mixtures by penetration resistance. *Annual Book of ASTM Standard: Concrete and Aggregates*, Vol. 04.02, West Conshohocken, PA.
- ASTM D 6103-97 (2002) Standard test method for flow consistency of controlled low strength material (CLSM). *Annual Book of ASTM Standards: Soil and Rock (II)*, Vol. 04.09, West Conshohocken, PA.

- ASTM D 6270-98 (2002) Standard practice for use of scrap tires in civil engineering applications. Annual Book of ASTM Standards: Environmental Assessment; Hazardous Substances and Oil Spill Responses; Waste Management, Vol. 11.04, West Conshohocken, PA.
- Benazzouk A, Queneudec M (2002) Durability of cement rubber-composites under freeze thaw cycles. Dhir RK et al. (Eds.), Proceedings of the International Conference on Sustainable Concrete Construction. University of Dundee, Scotland, UK, pp. 356–362.
- Biel TD, Lee H (1996) Magnesium oxychloride cement concrete with recycled tire rubber. Transportation Research Record No. 1561, Transportation Research Board, Washington, DC, pp. 6–12.
- Downs LA, Humphrey DN, Katz LE, Blumenthal M (1997) Water quality effects of using tire chips below the groundwater table. Report Prepared by the Department of Civil and Environmental Engineering, University of Maine, Maine for the Maine Department of Transportation, Orono.
- Ealding W (1992) Leachable metals in scrap tires. Final Report submitted to Virginia Department of Transportation Materials Division, Virginia Department of Transportation Scrap Tire Task Force, Richmond, Virginia, USA.
- Edil TB, Bosscher PJ (1992) Development of engineering criteria for shredded or whole tires in highway applications. Report No. WI 14-92, Department of Civil and Environmental Engineering, University of Wisconsin, Madison, WI.
- Eldin NN, Senouci AB (1993) Rubber-tire particles as concrete aggregates. *ASCE Journal of Materials in Civil Engineering* 5 (4): 478–496.
- Fattuhi NI, Clark NA (1996) Cement-based materials containing tire rubber. *Journal of Construction and Building Materials* 10 (4): 229–236.
- Fedroff D, Ahmad S, Savas BZ (1996) Mechanical properties of concrete with ground waste tire rubber. Transportation Research Board, Report No. 1532, Transportation Research Board, Washington, DC, pp. 66–72.
- Goodier JN (1933) Concentration of stress around spherical and cylindrical inclusions and flaws. *Trans., ASME* 55: 39–44.
- Goulias DG, Ali AH (1997) Non-destructive evaluation of rubber-modified concrete. Proceedings of a Special Conference, ASCE, New York, pp. 111–120.
- Groenevelt PH, Grunthal PE (1998) Utilization of crumb rubber as a soil amendment for sports turf. *Soil and Tillage Research* 47 (1–2): 169–172.
- Heitzman M (1992) Design and construction of asphalt paving materials with crumb rubber. Transportation Research Record No. 1339, Transportation Research Board, Washington DC.
- Hernandez-Olivares F, Barluenga G (2004) Fire Performance of recycled rubber-filled high-strength concrete. *Cement and Concrete Research* 34 (10): 109–117.
- Hernandez-Olivares F, Barluenga G, Bollati M, Witoszek B (2002) Static and dynamic behavior of recycled tire rubber-filled concrete. *Cement and Concrete Research* 32 (10): 1587–1596.
- Hernandez-Olivares F, Barluenga G, Parge-Lunda B, Bollati M, Witoszek B (2007) Fatigue behaviour of recycled tyre rubber-filled concrete and its implications in the design of rigid pavements. *Construction and Building Materials* 21 (10):1918–1927.
- Huang B, Li G, Pang S-S, Eggers J (2004) Investigation into tire rubber-filled concrete. *ASCE Materials Journal* 16 (3): 187–194.
- Humphrey DN, Katz LE, Blumenthal M (1997) Water quality effects of tire chip fills placed above the groundwater table. Testing Soil Mixed with Waste or Recycled Materials, ASTM STP 1275: 453–464.
- Khatib ZK, Bayomy FM (1999) Rubberized Portland cement concrete. *ASCE Journal of Materials in Civil Engineering* 11 (3): 206–213.
- Lee BI, Burnett L, Miller T, Postage B, Cuneo J (1993) Tyre rubber/cement matrix composites. *Journal of Material Science Letter* 12 (13): 967–968.
- Lee HS, Lee H, Moon JS, Jung HW (1998) Development of tire-added latex concrete. *ACI Materials Journal* 95 (4): 356–364.
- Mehta PK, Monteiro PJM (1993) Concrete structure, properties, and materials. Second Edition, Prentice-Hall, Englewood Cliffs, New Jersey, USA.

- Naik TR, Singh SS (1991) Utilization of discarded tires as construction materials for transportation facilities. Report No. CBU-1991-02, UWM center for by-products utilization. University of Wisconsin-Milwaukee, Milwaukee, 16 pages.
- Naik TR, Singh SS (1995) Effects of scrap-tire rubber on properties of hot-mix asphaltic concrete – a laboratory investigation. Report No. CBU-1995-02, UWM center for by-products utilization. University of Wisconsin-Milwaukee, Milwaukee, 93 pages.
- Naik TR, Singh SS, Wendorf RB (1995) Applications of scrap-tire rubber in asphaltic materials: state of the art assessment. Report No. CBU-1995-02, UWM center for by-products utilization. University of Wisconsin-Milwaukee, Milwaukee, 49 pages.
- Paine KA, Dhir RK, Moroney R, Kopasakis K (2002) Use of crumb rubber to achieve freeze thaw resisting concrete. Dhir RK et al., (Eds.), Proceedings of the International Conference on Concrete for extreme Conditions. University of Dundee, Scotland, UK pp. 486–498.
- Papakonstantinou CG, Tobolski MJ (2006) Use of waste tire beads in Portland cement concrete. *Cement and Concrete Research* 36: 1686–1691.
- Park JK, Kim JY, Madsen CD, Edil T.B (1997) Retardation of volatile organic compound movement by a soil-bentonite slurry cutoff wall amended with ground tires. *Water Environment Research* 69 (5) 1022–1031.
- Paul J (1985) Encyclopedia of polymer science and engineering. 14 :787–802.
- Pierce CE, Blackwell MC (2003) Potential of scrap tire rubber as lightweight aggregate in flowable fill. *Waste Management* 23 (3): 197–208.
- Raghvan D, Huynh H, Ferraris CF (1998) Workability, mechanical properties and chemical stability of a recycled tire rubber-filled cementitious composite. *Journal of Materials Science* 33 (7): 1745–1752.
- Read J, Dodson T, Thomas J (1991) Experimental project – use of shredded tires for lightweight fill. Oregon Department of Transportation, post construction report for project No. DTFH -71-90-501-OR-11, Salem, OR, USA.
- Reddy CM, Quinn JG (1997) Environmental chemistry of benzothiazoles derived from rubber. *Environmental Science and Technology* 31 (10): 2847–2853.
- Rostami H, Lepore J, Silverstraim T, Zundi I (1993) Use of recycled rubber tires in concrete. Dhir RK (Ed.), Proceedings of the International Conference on Concrete 2000, University of Dundee, Scotland, UK pp. 391–399.
- Rubber Manufacturer's Association (2000). Washington, DC.
- Savas BZ, Ahmad S, Fedroff D (1996) Freeze-thaw durability of concrete with ground waste tire rubber. Transportation Research Record No. 1574, Transportation Research Board, Washington, DC, pp. 80–88.
- Scrap Tire Management Council (1998) Scrap tires use. Washington, DC, USA
- Segre N, Joekes I (2000) Use of tire rubber particles as addition to cement paste. *Cement and Concrete Research* 30 (9): 1421–1425.
- Singh SS (1993) Innovative applications of scrap-tires. Wisconsin Professional Engineer, pp. 14–17.
- Tantala MW, Lepore JA, Zandi I (1996) Quasi-elastic behavior of rubber included concrete. Mersky R (Ed.), Proceedings of the 12th International Conference on Solid Waste Technology and Management, Philadelphia, PA..
- Topcu IB (1995) The properties of rubberized concrete. *Cement and Concrete Research* 25 (2): 304–310.
- Topcu IB, Avcular N (1997a) Collision behaviors of rubberized concrete. *Cement and Concrete Research* 27 (12): 1893–1898.
- Topcu IB, Avcular N (1997b) Analysis of rubberized concrete as a composite material. *Cement and Concrete Research* 27 (8): 1135–1139.
- Zelibor JL (1991) Leachate from scrap tires: RMA TCLP report. Education Seminar on Scrap Tire Management. Scrap Tire Management Council, Washington, DC, September, pp. 382–391.

Chapter 5

Waste Glass

Introduction

Glass is a transparent material formed by melting a mixture of materials such as silica, soda ash, and CaCO_3 at high temperature followed by cooling during which solidification occurs without crystallization. When waste glass is crushed to sand-like particle sizes, similar to that of natural sand, it exhibits properties of an aggregate material. Glass is produced in many forms, including packing or container glass, flat glass, bulb glass and cathode ray tube glass. Table 5.1 gives types of glass, and their main uses. The uses of glass products have increased tremendously resulting in large amounts of waste glass. United Nations estimates the volume of yearly disposed solid waste to be 200 million tons, 7% of which is made up of glass the world over (Topcu and Canbaz, 2004).

There are two types of waste glasses; colored and colorless. Most colorless waste glasses are recycled effectively. Colored waste glasses with their low recycling rate are generally dumped into landfill sites. However, with the shortage of landfill sites, land filling is becoming more and more difficult. Since the glass is not biodegradable, landfills do not provide an environment-friendly solution. Therefore, there is strong need to utilize waste glasses.

Table 5.1 Types of glass and their main uses

Type of glass	Main products
Soda lime glass	Bottles and jars
	Tableware
	Flat glass
Lead glasses	Crystal tableware
	Television screens and
	display screen equipment
Borosilicate glasses	Glass fiber
	Wool insulation
	Ovenware
Technical glasses e.g.	Scientific
Alumino-silicate,	Frits
Alkali-barium	Optical

5.1 Properties of Waste Glass

5.1.1 Physical Properties

Crushed glass (cullet) particles are generally angular in shape and may contain some elongated and flat particles. The degree of angularity and the quantity of flat and elongated particles depends on the degree of processing (crushing). Smaller particles, resulting from extra crushing, will exhibit somewhat less angularity and reduced quantities of flat and elongated particles.

Uncontaminated or clean glass itself exhibits consistent properties; however, the properties of waste glass from Material Recovery Facilities (MRFs) are much more variable due to the presence of non-glass debris present in the waste stream. Table 5.2 gives some typical physical properties of waste glass collected from a number of MRF facilities (WSDTED, 1993).

Glass collected from MRF facilities can be expected to exhibit a specific gravity of approximately 2.5. The degree of variability in this value depends on the degree of sample contamination and is reflected in the range of specific gravity data shown in Table 5.2. Crushed glass, which exhibits coefficients of permeability ranging from 10^{-1} to 10^{-2} cm/sec, is a highly permeable material, similar to coarse sand. The actual coefficient of permeability depends on the gradation of the glass, which, in turn, depends on the degree of processing (crushing and screening) to which the glass is subjected. The particle size distribution of glass received from MRF facilities can vary greatly. Table 5.3 details the typical glass gradation values for crushed glass received from a New York City MRF (Chesner, 1992).

5.1.2 Chemical Composition

Glass-formers are those elements that can be converted into glass when combined with oxygen. Silicon dioxide (SiO_2), used in the form of sand, is the most common

Table 5.2 Selected physical properties of waste glass (WSDTED, 1993)

Test	Glass samples ^a		ASTM test method
	Coarse	Fine	
Particle shape angularity	Angular	Angular	ASTM D2488
Flat (%)	20–30	1	
Flat/Elongated (%)	1–2	1	
Specific gravity ^b	1.96–2.41	2.49–2.52	ASTM D854 ^c
			ASTM C127 ^c
Permeability (cm/sec)	$\sim 2 \times 10^{-1}$	$\sim 6 \times 10^{-2}$	ASTM D2434

^a Coarse and Fine glass samples represent minus 19 mm (3/4 in) and minus 6.4 mm (1/4 in) samples, respectively, collected from several MRF facilities unless otherwise indicated.

^b Coarse specific gravity samples represent glass fraction greater than 4.75 mm (No. 4 sieve); fine samples represent glass fraction less than 4.75 mm (No. 4 sieve).

^c ASTM D 854 and C127 procedures were used for coarse and fine fractions respectively.

Table 5.3 Waste glass gradation results (Chesner, 1992)

Standard sieve size	Average % finer
25.4 mm (1 in)	100.0
12.7 mm (1/2 in)	98.7
6.35 mm (1/4 in)	86.0
3.18 mm (1/8 in)	32.6
0.84 mm (No. 20)	6.4
0.42 mm (No. 40)	3.2
0.21 mm (No. 80)	1.5
0.075 mm (No. 200)	0.6

glass-former. Common glass contains about 70% SiO₂. Soda ash (anhydrous sodium carbonate, Na₂CO₃) acts as a fluxing agent in the melt. It lowers the melting point and the viscosity of the formed glass, releases carbon dioxide, and helps stir the melt.

Glass bottles and window glasses are generally made from soda-lime glass. Lead-alkali-silicate glasses are used in the manufacture of light bulbs, neon signs, and crystal and optical glassware. Borosilicate glasses, which have extraordinary chemical resistance and high temperature softening points are used in the manufacture of cooking and laboratory ware (Samtur, 1974). Table 5.4 lists the typical chemical compositions of these glasses as reported by Ahmed (1991) of soda-lime and Lead glasses, and by Phillips et al. (1972) of borosilicate glass.

5.1.3 Mechanical Properties

Typical mechanical properties of waste glasses are given in Table 5.5.

Table 5.4 Typical chemical composition of glass types

Constituent	Soda-lime (Ahmed, 1991)	Lead (Ahmed, 1991)	Borosilicate (Phillips et al., 1972)
SiO ₂	70–73	60–70	60–80
Al ₂ O ₃ ^a	1.7–2.0	–	1–4
Fe ₂ O ₃	0.06–0.24	–	–
Cr ₂ O ₃ ^b	0.1	–	–
CaO	9.1–9.8	1	–
MgO	1.1–1.7	–	–
BaO	0.14–0.18	–	–
Na ₂ O	13.8–14.4	7–10	45
K ₂ O	0.55–0.68	7	–
PbO	–	15–25	–
B ₂ O ₃	–	–	10–25

^a Higher levels for amber-colored glass.

^b Only present in green glass.

Table 5.5 Typical mechanical properties of waste glass

Test	Results	Test method
Los Angeles abrasion (%)	3042	ASTM C131
Maximum dry density (kg/m ³)	1800–1900	ASTM D1557
Optimum moisture (%)	5.7–7.5	ASTM D1557
Angle of internal friction (deg)	51–53	ASTM D3080
California bearing ratio (%)		
15% glass	132	ASTM D1883
50% glass	42–125	
Hardness (measured by Moh's Scale of Mineral Hardness)	5.5	

5.1.4 Other Properties (Thermal, Reflection, and Glare)

Glass is known for its low thermal conductivity. Aggregates and aggregate mixtures with low thermal conductivity can help to decrease the depth of frost penetration. Dickson (1973) reported the studies conducted at the Colorado School of Mines in the early 1970's that glass aggregate pavements take a longer time to cool down to the lower thermal conductivity of glass, when compared to natural aggregates. WSDTED (1993) reported thermal conductivity test results as per ASTM C518 for mixed-colored crushed glass, and the same are presented in Table 5.6. Comparison of the results for crushed glass with those for a natural gravelly sand aggregate mix show that glass can be expected to exhibit higher heat retention than natural aggregate materials.

The high reflective properties of glass can be a desirable property in highway construction if they are able to assist in delineating the roadway surface from the surrounding environments. Excessive reflection could, however, result in glare that could adversely affect roadway visibility. There are no documented studies on the quantities of size fractions of glass in pavements that are likely to produce excessive glare. There is, however, a noticeable glass reflection in pavements with glass fractions exceeding 15% by weight.

Table 5.6 Thermal conductivity test results (WSDTED, 1993)

Material	Apparent thermal conductivity watts/meter – °K	
	Sample 1	Sample 2
Crushed Glass	0.315	0.260
Gravelly Sand	0.463	0.638

5.2 Management Options

5.2.1 Disposal

Most of waste glass that is produced is dumped into landfill sites or roadways sites. However, with the increasing scarcity of landfill sites and the fact that glass is not biodegradable, landfills do not provide an environmental friendly solution. Reindl (1998) reported many non-container uses of glass which included road construction aggregate asphalt paving, concrete aggregates, building applications (such as glass tiles and bricks, wall panels, etc.), fiber glass insulation, glass fiber, abrasive, art glass, agricultural fertilizer, landscaping, reflective beads, tableware, hydraulic cement, etc. Aggregates, building application (glass tiles & bricks, wall panels etc.)

5.2.2 Recycling

Over the past decade, there have been widespread efforts to recover post-consumer glass. Generally, glass recovery and recycling have been attempted through the collection of waste glass at recycling centers or Material Recovery Facilities (MRFs). MRFs are facilities that are designed to sort, store, and market municipal solid waste recyclables that are collected at the curb (source-separated materials). Curbside separation of glass involves homeowner or apartment dweller separation of container glass (or glass commingled with other recyclables such as ferrous and aluminum cans and plastic containers) in preparation for the transport of these materials to the MRF. At most MRFs, waste glass is hand-sorted by color (white, amber, and green), and crushed for size reduction (generally to less than 50 mm in size). Crushed (color-sorted) glass, which is commonly known as cullet, is marketed in most locales as a raw material for use in the manufacture of new glass containers.

Traditionally, glass recycling has involved the collection and sorting of glass by color for use in the manufacture of new glass containers. Recycling post-consumer glass from the municipal solid waste stream for use as a raw material in new glass products is limited because of the high cost of collection and processing (hand sorting) of waste glass (Chesner and Petrarca, 1988; WSDTED, 1993) and specifications that limit impurities (e.g., ceramics, ferrous metal, paper, plastics and mixed-colored cullet) in the glass production process. In addition, during collection and handling of glass, high percentages of glass breakage (30–60%) (Egosi, 1992) limit the quantity of glass that can actually be recovered using hand-sorting practices. Given these limitations, traditional glass recycling rates have been relatively low.

Glass can be recycled indefinitely as part of a simple but hugely beneficial process, as its structure does not deteriorate when reprocessed. Most of glass produced is in the form of containers and the bulk of it is collected again (post consumer), recycled and is used for making new containers/products. The efficiency of this process depends on the method of collection and sorting glass of different colors. If different color glasses (Clear, Green and Amber) could be separated, then they

could be used for manufacturing similar color glass containers. However, when the glasses of different colors get mixed, they become unsuitable for recycling and are used for other purposes or sent to landfill sites.

In the case of bottles and jars, up to 80% of the total mixture can be made from reclaimed scrap glass, called “cullet”. Cullet from a factory has a known composition and is recognized as domestic cullet. If recycled glass is used to make new bottles and jars, the energy needed in the furnace is greatly reduced. In addition, recycling (i) reduces the demand for raw materials; (ii) reduces the amount of waste glass which needs to be landfilled; (iii) taking part in recycling the waste we produce makes us think about the effect we are having on our environment and enables us to contribute towards a greater level of sustainability.

There is significant interest in the development of concrete with waste glass. Recycling waste glass as an aggregate is effective for environment and economical advantage. Therefore, the most common flint, amber, and emerald green bottles can be used as aggregate in concrete. Figure 5.1 provides a schematic representation of the flow of container glass in the United States along with potential recycling options.

5.2.3 Uses of Waste Glass

- Asphalt Concrete Aggregate
- Granular Base or Fill
- In Cement mortar and Concrete
- As Aggregate in recycled asphalt pavement (RAP)

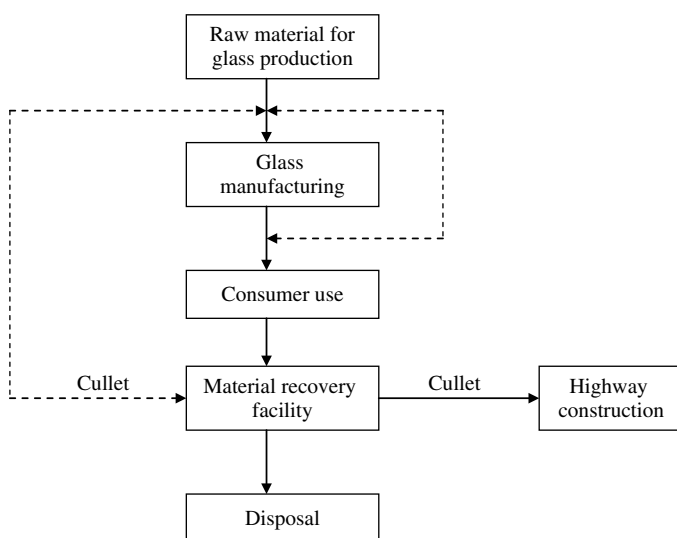


Fig. 5.1 General overview of glass cycle in the United States

5.3 Fresh Properties of Concrete Containing Waste Glass

5.3.1 Unit Weight, Air Content

Park et al. (2004) used waste glasses from soda-lime series. Waste glasses were collected and sorted into three different colors – amber (A), emerald (EG), and flint (F). They were crushed into fragments of 6–20 mm in size, and then were used as fine aggregate for concrete. The fineness modulus of amber, emerald green, and flint glasses were 3.49, 3.48, and 3.48, respectively. The specific gravity of amber, emerald green, and flint glasses were 2.52, 2.50, and 2.50, respectively. The chemical composition of amber glass was SiO_2 (72.1%), Al_2O_3 (1.74%), $\text{Na}_2\text{O}+\text{K}_2\text{O}$ (14.11%), $\text{CaO}+\text{MgO}$ (11.52%), SO_3 (0.13%), Fe_2O_3 (0.31%), Cr_2O_3 (0.01%). The chemical composition of emerald green glass was SiO_2 (71.3%), Al_2O_3 (2.18%), $\text{Na}_2\text{O}+\text{K}_2\text{O}$ (13.0%), $\text{CaO}+\text{MgO}$ (12.18%), SO_3 (0.05%), Fe_2O_3 (0.59%), Cr_2O_3 (0.44%), and the composition of flint glass was SiO_2 (73.04%), Al_2O_3 (1.81%), $\text{Na}_2\text{O}+\text{K}_2\text{O}$ (13.94%), $\text{CaO}+\text{MgO}$ (10.75%), SO_3 (0.22%), Fe_2O_3 (0.04%). They prepared concrete mixtures with water-cement ratio of 0.50, sand-coarse aggregate ratio of 0.47. Fine aggregate were replaced at 30, 50, and 70% with waste glass aggregates.

Park et al. (2004) reported the air content of concrete containing waste glass aggregates, regardless of their color with an input ratio of 30, 50 and 70%. There was increase of 12.2–21.6%, 23.71–30.4% and 30.6–41.4% in air content, respectively, compared to the plain (control) concrete containing no waste glass. This tendency of air content increase may be due to the fact that there were more waste glass aggregates that were larger than 0.6 mm in particle size than sand, and also that they had an irregular shape, which resulted in a larger relative surface area that maintained more air.

Topcu and Canbaz (2004) used crushed green soda glass as coarse aggregate in concrete. Unit weight and specific gravity of the waste glass were 1493 kg/m^3 and 2400 kg/m^3 , respectively. Waste glass (WG) was used as 0, 15, 30, 45 and 60% of the aggregate mixtures in place of calcareous crushed stone aggregates to a fineness of 4–16 mm. Results of unit weight and air content are given in Table 5.7. Unit weight of the concrete with out WG was 2340 kg/m^3 . With the addition of WG, there was linear decrease of 0.3% in unit weight. This difference in unit weight was attributed to the fact that the specific gravity of WG is much lower than that of the calcareous crushed aggregate produced with general rock. They further reported that the air content of the concretes containing waste glass up to 60% was 0.4–0.7%, while a high proportion of waste glass addition unevenly decreased the air content by as much as 27%. The reason for such a discrepancy was thought to result from the poor geometry of waste glass, as a result of which water and air voids occur in particularly lower parts. Further more, low air content in concrete containing a high proportion of waste glass was thought to be connected to the smooth surface of waste glass, which helps decrease porosity between waste glass and cement paste.

Table 5.7 Fresh concrete properties of concrete with WG (Topcu and Canbaz, 2004)

Waste glass (%)	Unit weight (kg/m ³)	Air content (%)	Slump (mm)	VeBe time (sec)	Flow able (mm)
0	2340	0.5	95	6.5	350
15	2335	0.7	100	4.5	375
30	2340	0.5	80	6.3	360
45	2330	0.4	90	6.1	370
60	2335	0.45	80	7.0	370

5.3.2 Slump

Park et al. (2004) reported slump test results of concrete containing waste glass. They concluded that there was a tendency for the slump to decrease as the mixing ratio of waste glass aggregate increased regardless of their color. Reduction in slump was between 19.6 and 26.9%, 30.1 and 34.6% and 38.5 and 44.3% for waste glass aggregates content of 30, 50 and 70%, respectively, compared to the plain concrete containing no waste glass. This tendency may be due to (i) as the mixing ratio of waste glass aggregate increased, additional cement paste attached to the surface of the waste glass, which resulted in less available cement paste necessary for the fluidity of the concrete; (ii) waste glass aggregates had sharper and more angular grain shapes and were larger than sands, which resulted in less fluidity. However, the color of waste glass aggregate did not severely affect the slump.

Topcu and Canbaz (2004) observed slump values to be between 80 and 100 mm. Using a high proportion of waste glass decreased the slump value by as much as 0.2% due to the fact that waste glass has poor geometry, which is also supported by Kisacik (2002) investigation which found this amount to be 2%.

Terro (2006) investigated the effect of replacement of fine and coarse aggregates with recycled glass on the slump of cement concrete. Percentages of replacement of 10, 25, 50, and 100% of aggregates with fine waste glass (FWG), coarse waste glass (CWG), and fine and coarse waste glass (FCWG) were used. Soda-lime glass used for bottles was washed and crushed to fine and coarse aggregate sizes for use in the concrete mixes. He concluded that slump seemed to increase with higher percentages of waste glass. This may be attributed to the poorer cohesion between the glass aggregates, having smooth impermeable surfaces, and the cement paste. It was also observed that concrete made with FWG had, in general, lower slump values than that made with CWG and FCWG. The latter exhibited very high slump values. This could be due to the lower specific surface and smooth surface of the coarse glass, which reduces the inter-particle friction.

5.3.3 VeBe Time

Topcu and Canbaz (2004) observed that the VeBe time ranged from 4.5 to 7.0 seconds (Table 5.7), and 60% addition of waste glass increased VeBe time by 19%.

The poor geometry of waste glass retards the placing period of fresh concrete when there is a high proportion of waste glass addition.

5.3.4 Flow Table

Topcu and Canbaz (2004) reported the flow table results of concrete containing various percentages of waste glass, and the results are given in Table 5.7. Test results revealed that the flow table values of concrete containing waste glass were between 350 and 370 mm. Waste glass addition increased workability and flow table values by as much as 4% due to the fact that waste glass does not absorb water and that the water layer over the surface of waste glass is thinner.

5.3.5 Compaction Factor

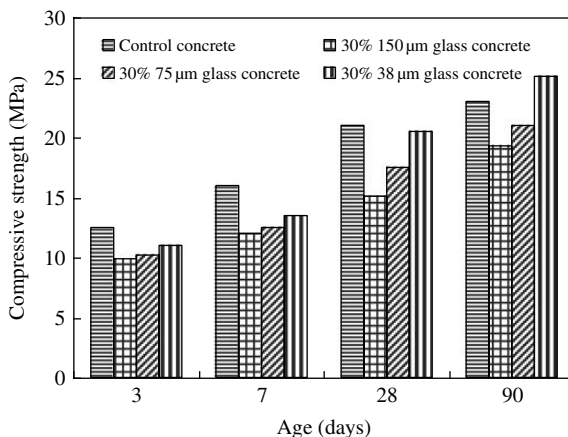
Park et al. (2004) conducted test to determine the compaction factor of concrete containing various percentages of waste glass. They concluded that the concrete containing waste glass aggregates, regardless of their color, with an input ratio of 30%, 50% and 70%, recorded 1.1–2%, 2.5–3.7% and 3.6–5.4% decrease in compacting factor, respectively, compared to plain concrete containing no waste glass. One factor for this tendency of compacting factor decrease may be due to the fact that the grain shape of waste glass aggregate were irregularly angled, which resulted in a fluidity drop parallel with an increase in the amount of waste glass aggregate & subsequent decrease in compacting factor of the concretes.

5.4 Properties of Hardened Concrete Containing Waste Glass

5.4.1 Compressive Strength

Shao et al. (2000) used ground waste glass (soda lime glass) as partial replacement of cement. Ground waste glass having three different particles (150 μm , 75 μm , and 38 μm) was used. The cement replacement by the ground waste glass was 30% by volume. Tests were conducted for compressive strength of concrete containing ground waste glass up to the age of 90 days. The concrete containing ground waste glass was compared to the concrete having the same percentage of silica fume and fly ash. Tests revealed that all the batches of glass concrete had lower strengths than the control concrete at the age of 3, 7, 28 and 90 days except that the strength of the concrete containing 38 μm glass exceeded that of control by 8% after 90 days of curing as shown in Fig. 5.2. Thus, the size effect was observed indicating that the smaller the size of glass, the higher the strength of glass concrete. Again, the 38 μm glass concrete exhibited strength higher than the fly ash concrete at all ages, but only half of that in silica fume concrete. The results are shown in the Fig. 5.3. It was also

Fig. 5.2 Compressive strength of concretes containing 30% ground glass (Shao et al., 2000)



observed that the activity index of 150 μm glass was less than 75%, which is the minimum as specified by ASTM C 618 (1994). However, the 75 μm and 38 μm glasses were not only very suitable, but directly comparable to fly ash concrete at all ages.

Shao et al. (2000) also tested hybrid concrete batches with 15% ground glass and 15% silica fume and compared the results with a reference batch containing only 15% silica fume. The results of the compressive strength tests are shown in the Fig. 5.4. It was observed that at early ages (3 and 7 days); all the hybrid batches had lower strengths than the reference batch. However, as the hydration progressed the strength of hybrid concretes approached that of the reference (15% silica fume concrete) but never exceeds that value even at 90 days. It was also observed that at 3 and 7 days, the activity indices were about the same as or even lower than that of the 30% glass concrete without silica fume. This was indicative of the low activity of glass at early ages in presence of silica fume. The activity index of concrete

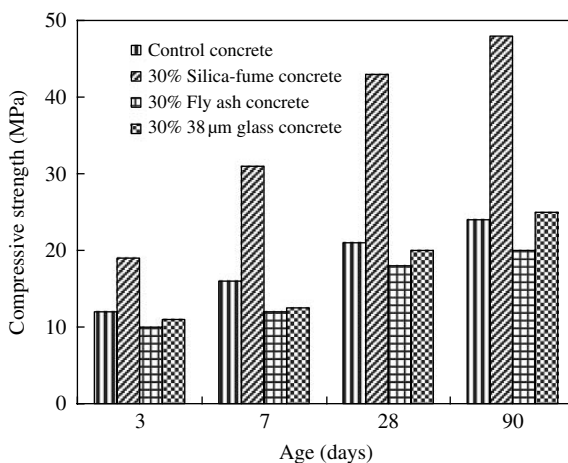
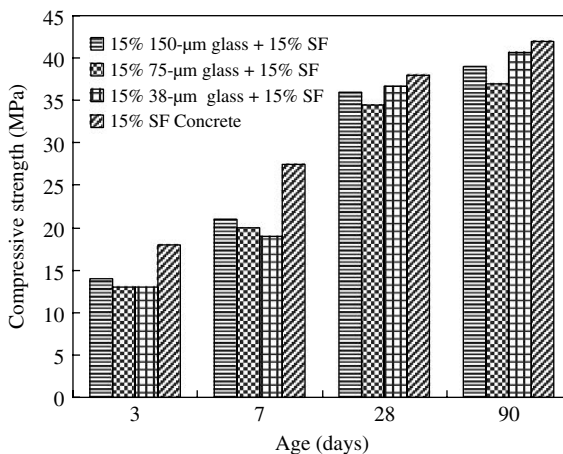


Fig. 5.3 Comparison of 38 μm glass concrete with silica fume concrete and fly ash concrete (Shao et al., 2000)

Fig. 5.4 Compressive strength of concretes containing 15% glass and 15% silica fume (Shao et al., 2000)



containing 15%, 38 μm glass was 95% at 28 days (higher than 30% glass concrete) and 96% at 90 days (lower than 30% glass concrete). The size effect of ground glass in hybrid concretes was not as apparent as that observed in glass concrete. The hybrid concrete with 150 μm glass exhibited an increased activity index which was close to 38 μm glass, which implied that the activity of ground glass has not been enhanced substantially by the highly reactive silica fume and that the strength gain in the hybrid concrete is attributed mainly to the Silica fume and not to ground glass.

Shayan and Xu (2004) investigated the effect of cement and sand replacement by glass powder (GLP) on the strength of mortar cubes (aggregate/ cement ratio of 2.25 and water/ cement ratio of 0.47). GLP had particle size less than 10 μm and specific surface area of 800 m^2/kg . In case of cement replacement, compressive strength of the mortar decreased with the increase in GLP replacement percentage as shown in Fig. 5.5.

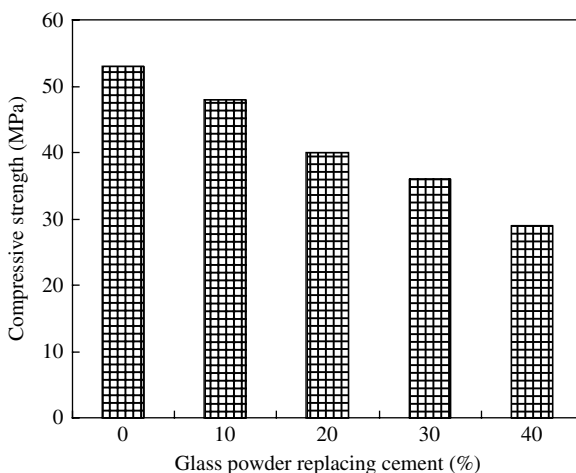


Fig. 5.5 Effect of glass powder (GLP) replacing cement on 28-day strength of mortar made with 100% sand (Shayan and Xu, 2004)

Long term strength development was studied in comparison to silica fume (SF). This series consisted of control specimens in which the fine aggregate was a reactive greywacke and other specimens contained 10% SF, 20% GLP and 30% GLP, each replacing corresponding amount of cement. In one case 30% GLP replaced the aggregate. Figure 5.6 shows the strength development of each combination over 270 days. These results indicated that 10% SF replacement produced higher strength than the GLP replacements but they also showed that mortar specimens containing GLP continued to develop further strength with time, indicating pozzolanic reactivity. It could be observed that when 30% sand was replaced by GLP, the 90 day strength was same as that of the SF bearing specimens.

To verify the positive effects on strength of aggregate replacement by GLP, Shayan and Xu (2004) conducted two additional tests on mortar cubes, cured for up to 270 days. In one set of specimens, 20% cement was replaced by GLP and in the other set; in addition, 10% of aggregate was also replaced by GLP. They confirmed that this replacement is beneficial, probably due to the improvement in the particle packing as well as the pozzolanic reaction. It could be observed that the strength achieved with 30% GLP replacing 20% cement and 10% aggregate exceeds that of the SF containing mix. Similar results are obtained when GLP is used in concrete.

Topcu and Canbaz (2004) conducted compressive strength tests on concrete containing waste glass. They used crushed green soda glass as coarse aggregate in concrete. Unit weight and specific gravity of the waste glass were 1493 kg/m^3 and 2400 kg/m^3 , respectively. Waste glass (WG) was used as 0, 15, 30, 45 and 60% of the aggregate mixtures in place of calcareous crushed stone aggregates of size 4–16 mm. Based on the test results, they reported the compressive strength decreased with the increase in the proportion of waste glass (Table 5.8). In case of using 15% of waste glass, there was decrease of 17% in compressive strength, while there was a decrease of 15% in the compressive strength of concrete with 30% of waste glass. When the proportion of waste glass was 45%, a decrease of 31% was

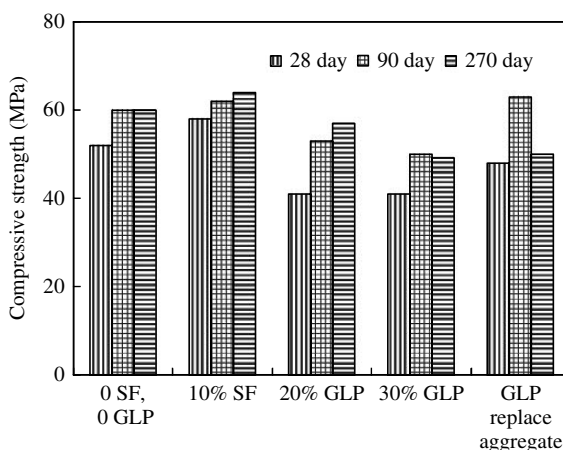


Fig. 5.6 Strength development of mortar with reactive aggregate (Shayan and Xu, 2004)

Table 5.8 Hardened concrete properties of concrete with WG (Topcu and Canbaz, 2004)

Waste Glass (%)	Compressive strength (MPa)	Tensile strength (MPa)	Flexural strength (MPa)	Dynamic modulus of elasticity (GPa)
0	23.5	2.59	4.5	37
15	21.67	2.34	5.27	59.98
30	19.55	2.29	3.97	25
45	16.12	2.35	5.24	27
60	12.04	1.63	3	22.58

observed. However, when this proportion increased to 60%, 49% of decrease in compressive strength was found.

Park et al. (2004) determined compressive strength of concretes containing waste glasses from (size between 6–20 mm) soda-lime series as fine aggregate. Waste glasses were collected and sorted into three different colors – amber (A), emerald (EG), and flint (F). They prepared concrete mixtures with water-cement ratio of 0.50, sand-coarse aggregate ratio of 0.47. Fine aggregate were replaced at 30, 50, and 70% with waste glass aggregates. They revealed that the compressive strength results for the concretes containing waste glass fine aggregates of different color were very similar to each other. Figure 5.7 shows test results for emerald green waste glass. Four week old concretes containing emerald green waste glass fine aggregates, regardless of their color and with mixing ratios of 30, 50 and 70% displayed reduction in compressive strength, each showing 99.4, 90.2 and 86.4% compressive strength of the plain concrete respectively. The tendency towards a decrease in compressive strength with an increase in the mixing ratios was repeated for concretes of 13 weeks of age. This inclination may be due to the decrease in adhesive strength between the surface of waste glass aggregates and the cement paste as well as the increase in the fineness modulus of the fine aggregates and the

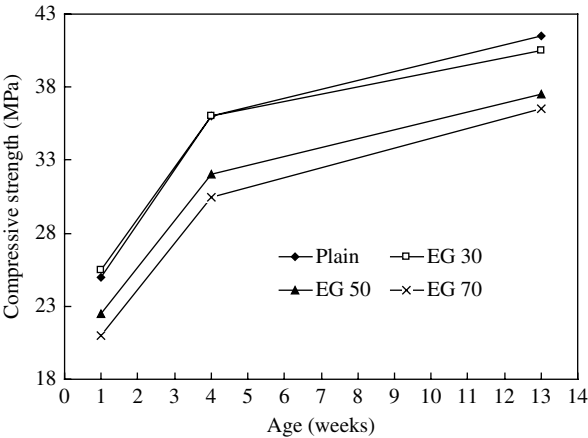


Fig. 5.7 Compressive strength of concrete containing emerald green waste glass (Park et al., 2004)

decrease in the compacting factor in accordance with the increase in mixing ratios of waste glasses (Robert, 1989).

Figure 5.8 shows the test result of compressive strength depending on the changes in the mixing rate of waste glass and polymer (SBR latex). It was observed that with the increase of waste glass content, the strength of the concrete decreased. For each mixing rate of the waste glass (0, 30, 50 and 70%), as the mixing rate of the polymer increased by 5–10%, the compressive strength increased by 12.1–22.3, 12.7–19.5, 14.4–25.4 and 4.8–13.6%, respectively.

Park and Lee (2004) reported the compressive strength of mortar containing waste glass of brown color. Waste glass content was 10, 20, 30, 50 and 100% of the weight of sand. Mortar specimens of size 50 mm cubes were treated in accordance with ASTM C 1260-01 (2003) and then immersed in NaOH solution at 80°C for 14 days. Between 2 to 49% loss in compressive strength (Fig. 5.9) was observed.

Corinaldesi et al. (2005) conducted tests for compressive strength of mortar made with waste glass as aggregate. They used three different fractions of the waste glass characterized by grain size distributions: labeled as glass A, particle size up to 36 μm ; labeled as glass B, particle size ranging from 36 μm to 50 μm and labeled as glass C, particle size ranging from 50 μm to 100 μm . Seven mortars were prepared; one was reference mortar (labeled as Ref) containing natural sand at a ratio of 3:1 with respect to the cement dosage. Three mortars were prepared with waste glass replacing 70% of the whole aggregate dosage (labeled A-70, B-70 and C-70), each containing a different waste glass fraction with a different grain size distribution (respectively, glass A, glass B and glass C). Moreover, other three mortars were prepared with waste glass replacing 30% of the whole aggregate dosage (labeled A-30, B-30 and C-30), each one containing one of the three different waste glass fractions. Compressive strength results are shown in Fig. 5.10. It can be seen that with the increase in glass content, compressive strength of mortar has increased.

Terro (2006) investigated the compressive strength of concrete made with fine waste glass (FWG), coarse waste glass (CWG), and fine and coarse waste glass

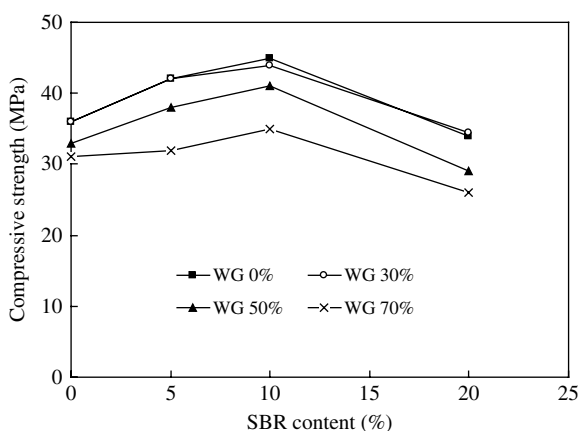
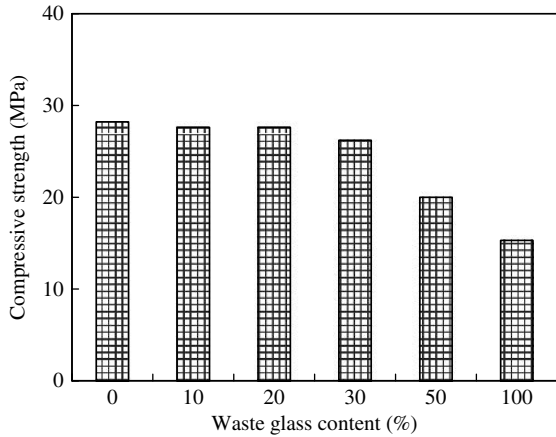


Fig. 5.8 Compressive strength of concrete containing emerald green waste glass and SBR (Park et al., 2004)

Fig. 5.9 Compressive strength of mortar containing brown waste glass (Park and Lee, 2004)



(FCWG) at ambient and elevated temperatures up to 700°C. Waste glass was used as replacement of aggregates in proportions of 10, 25, 50, and 100%. Compressive strength results are given in Table 5.9. He concluded that compressive strength of concrete decreased with increasing temperatures. At 10% replacement of aggregates with FWG, CWG and FCWG, the compressive strength of concrete was higher than that of the control mix up to 700°C. Although, at ambient temperatures, the control concrete possessed a slightly higher compressive strength comparing to the concretes with glass aggregates. This is due to the fact that the free water retained in the mix is dissipated at elevated temperatures much readily in mixes containing glass than the control concrete since glass does not absorb water, thus making concrete mixes made with waste glass more compact after the evaporation of the free water around 150°C. With higher replacement percentages of aggregates, concrete made with FCWG exhibited lower compressive strength at elevated temperatures. This could be attributed to the weaker initial strength of concrete made with FCWG

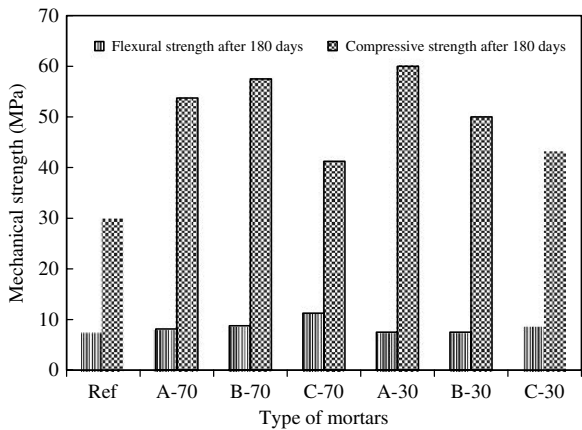


Fig. 5.10 Compressive and flexural strengths of mortars after 180 days of curing (Corinaldesi et al., 2005)

Table 5.9 Compressive strength of concrete made with waste glass in MPa (Terro, 2006)

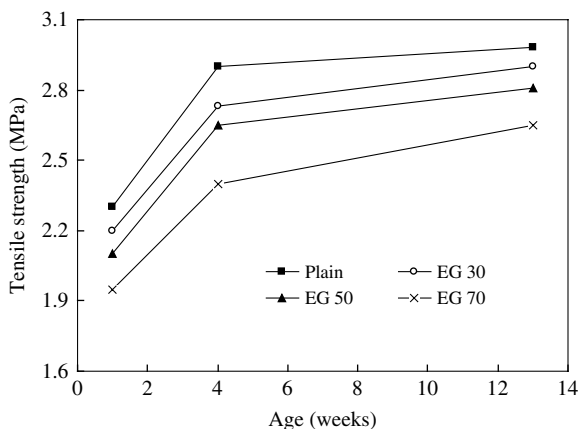
Temperature (°C)	Percentage of aggregate replacement with glass				
	0%	10%	25%	50%	100%
(FWG)					
20	39.5	40.5	37.0	36.0	23.5
60	44.5	35.0	37.5	38.0	24.5
150	40.0	55.0	41.0	37.0	21.0
300	38.0	42.0	36.5	36.0	26.5
500	22.0	34.5	34.0	28.5	18.0
700	11.0	22.0	11.0	10.0	8.0
(CWG)					
20	39.0	43.0	39.0	33.0	30.5
60	44.5	43.5	38.0	30.0	29.0
150	40.0	47.0	48.0	37.5	34.0
300	38.0	51.5	38.0	22.0	22.0
500	22.0	34.5	12.5	17.0	10.0
700	11.0	22.0	10.0	6.0	6.0
(FCWG)					
20	39.5	36.5	26.0	15.0	12.5
60	44.5	38.5	20.0	16.0	11.5
150	40.0	43.5	29.0	16.0	12.5
300	38.0	46.5	19.0	10.0	8.0
500	22.0	35.0	19.5	10.0	9.5
700	11.0	22.0	10.5	6.0	4.5

due to a combination of factors including lack of cohesion between fine and coarse aggregates on one side and the cement matrix on the other side. However, when approaching the temperature of 700°C, the compressive strength of the three types of concretes made with waste glass converges to very close values. This could be attributed to the approach of the glass to its melting threshold (700–800°C for soda-lime glass), where the microstructure of glass undergoes large physical and mechanical transformations. These transformations at the neighborhood of 700°C caused the softening of the glass introduced in the mix.

5.4.2 Tensile Strength

Park et al. (2004) conducted tensile strength tests for concretes containing waste glasses from (size between 6–20 mm) soda-lime series as fine aggregate. Waste glasses of three colors; amber (A), emerald (EG), and flint (F) were used. Concrete mixtures with water-cement ratio of 0.50, sand-coarse aggregate ratio of 0.47 were prepared. Fine aggregate were replaced at 30, 50, and 70% with waste glass aggregates. They concluded that four week old concretes containing emerald green waste glass fine aggregate at a 30, 50 and 70% mixing ratio showed a slight decrease in the tensile strength, the values being 96.6, 90.8 and 85.0% of plain concrete, respectively as shown in Fig. 5.11.

Fig. 5.11 Tensile strength of concrete containing emerald green waste glass (Park et al., 2004)



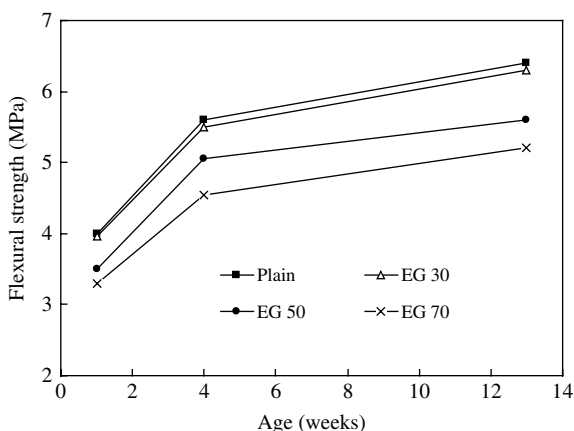
Park et al. (2004) also showed that tensile strength of concrete depends upon the changes in the mixing rate of WG and polymer (SBR latex). For each mixing rate of waste glass (0%, 30%, 50% and 70%), as the mixing rate of the polymer increased by 5–10% the tensile strength increased by 16.1–20.8%, 16.6–18.6%, 20–18.7% and 18.6–17.2% respectively.

Topcu and Canbaz (2004) investigated the effect of waste glass on the indirect tensile strength of concrete. They used crushed green soda glass as coarse aggregate in concrete. Unit weight and specific gravity of the waste glass were 1493 kg/m^3 and 2400 kg/m^3 , respectively. Waste glass (WG) was used as 0, 15, 30, 45 and 60% of the aggregate mixtures in place of calcareous crushed stone aggregates of size 4–16 mm. Results of tensile strength are given in Table 5.8. Strength decreased with the increase in waste glass content. Indirect tensile strength showed a decrease of 37% as a result of 60% of waste glass addition. Park et al. (2002) reported a decrease of 5% in the indirect tensile strength with 30% ground waste glass, while Tuncan et al. (2001) reported an increase of 6% in case of 15% addition of ground waste glass due to amorphous structure, as fine as cement and easily reacted hydration product. Kisacik (2002) observed a decrease of 2% in the indirect tensile strength of concrete with waste glass, in comparison to that of normal concrete.

5.4.3 Flexural Strength

Park et al. (2004) investigated the flexural strength of concretes made with waste glass aggregate of different colors according to their age. The results are presented in Fig. 5.12 for the emerald green waste glass, because the results were very similar to each other. It is evident from this figure that increase in the waste glass content has decreased flexural strength of concrete substantially; however decrease was not significant in case of concrete containing 30% waste glass.

Fig. 5.12 Flexural strength of concrete containing emerald green waste (Park et al., 2004)



For the variations in flexural strength depending upon the changes in mixing rate of waste glass and polymer (SBR latex), it was observed that with the increase in waste glass content, the strength of concrete decreased. For each mixing rate of waste glass (0, 30, 50 and 70%), as the mixing rate of polymer increased by 5–10%, the flexural strength increased by 12.3–14.9%, 12.8–12.9%, 17.2–19.2%, and 20.0–21.5% respectively.

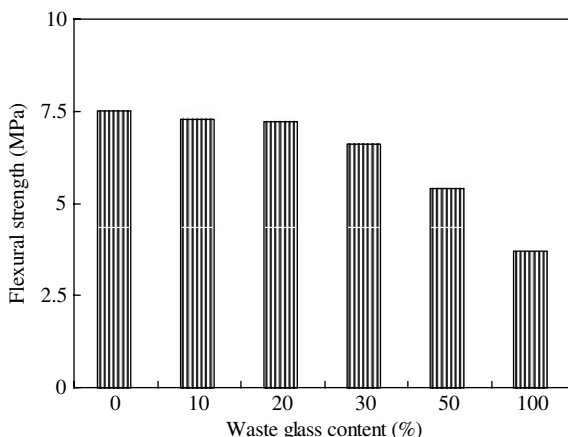
Topcu and Canbaz (2004) determined the effect of waste glass on the flexural strength of concrete. They used crushed green soda glass as coarse aggregate in concrete. Unit weight and specific gravity of the waste glass were 1493 kg/m^3 and 2400 kg/m^3 , respectively. Waste glass (WG) was used as 0, 15, 30, 45 and 60% of the aggregate mixtures in place of calcareous crushed stone aggregates of size 4–16 mm. Results of flexural strength are given in Table 5.8. Flexural strength was found to be consistent between 3.00 MPa and 5.27 MPa and also as the proportion of waste glass increased, this level decreased as much as 17%. Flexural strength was observed to decrease as much as 3% in the case of 15% addition in the study undertaken by Park et al. (2002). Kisacik (2002) found that when waste glass was used, flexural strength decreased as much as 8%.

Park and Lee (2004) studied the flexural strength of mortar containing waste glass of brown color. Waste glass content was 10, 20, 30, 50 and 100% of the weight of sand. Mortar specimens ($40 \times 40 \times 160 \text{ mm}$) were treated in accordance with ASTM C 1260-01 (2003) and then immersed in NaOH solution at 80°C for 14 days. They reported 3–51% loss in flexural strength (Fig. 5.13).

5.4.4 Dynamic Modulus of Elasticity

Topcu and Canbaz (2004) investigated the dynamic modulus of elasticity of concrete made with waste glass. They used crushed green soda glass as coarse aggregate in concrete. Unit weight and specific gravity of the waste glass were 1493 kg/m^3 and 2400 kg/m^3 , respectively. Waste glass (WG) was used as 0, 15, 30, 45 and 60% of the

Fig. 5.13 Flexural strength of mortar containing brown waste glass (Park and Lee, 2004)



aggregate mixtures in place of calcareous crushed stone aggregates of size 4–16 mm. Results of dynamic modulus of elasticity are given in Table 5.8. Dynamic modulus of elasticity of concrete varied between 59.98 and 22.58 GPa. With addition of waste glass (WG) addition into concrete, the dynamic modulus of elasticity was observed to decrease. When the amount of WG addition was 60%, the dynamic modulus of elasticity of normal concrete decreased as much as 39%. Tuncan et al. (2001) reported increase in dynamic modulus as much as 10% with 15% ground WG addition, because of finely divided WG effect to bond properties. In a study by Kisacik (2002), the dynamic modulus of elasticity of concrete increased as much as 36% as content of WG increased.

5.4.5 Alkali-Silica Reaction

The excessive expansion and disintegration of some concrete made of cements of relatively high alkali content and of certain silica-containing aggregates can be explained by the alkali-silica reaction (ASR). ASR is a chemical reaction of the alkalis with the hydrous forms of the silica present in the mineral constituents, discovered in 1940 by Stanton (1940) and described early by Blanks (1941) and Meissner (1941). The ASR produces a soft viscous substance called the ASR gel, which has been observed to appear in pop-outs or to exude from cracks in concrete structures. The chemistry of ASR has been reported by Dron and Brivot (1992, 1993), Gartner and Jennings (1987), Glasser (1992), Glasser and Kataoka (1981), Poole (1992), Swamy [1992a, 1992b], Swenson (1957) and Vivian (1951).

Jin et al. (2000) studied the effect of glass particle size on concrete, and reported that in the tests using opaline silica as the reactive constituent, it was found that the expansion increased as the reactive particle size was reduced to 50 μm but below that particular size no abnormal expansion was observed. However, based on a test with

opal aggregate in which large expansion were detected for particles as fine as $20\text{ }\mu\text{m}$ and $30\text{ }\mu\text{m}$, Diamond and Thaulow (1979) suggested that fineness of aggregate size has no guarantee against expansion.

Jin et al. (2000) investigated the effect of glass color on concrete and found that the effectiveness of green glass as an ASR suppressant was found to strongly correlate with the amount of Cr_2O_3 in the glass. Cr_2O_3 added straight to the concrete mixture was found to increase the expansion considerably (Fig. 5.14). But if added as chemically bound grit, it can serve as an ASR inhibitor. This ASR suppressing mechanism of Cr_2O_3 seems to support the hypothesis of Prezzi et al. (1997) that the expansion pressure resulting from electrical double-layer repulsion is inversely proportional to the ionic valence.

Shao et al. (2000) used ground waste glass (soda lime glass) as partial replacement of cement. Ground waste glass having three different particles ($150\text{ }\mu\text{m}$, $75\text{ }\mu\text{m}$, and $38\text{ }\mu\text{m}$) was used. The cement replacement by the ground waste glass was 30% by volume. Tests were conducted to study the effects of glass on expansion. They found that batches with 30% cement replaced by mineral additives had expansion less than that of control concrete. Of the three mineral additives, viz., SF, FA and GLP, SF mortar had the least expansion, followed by FA. While both the $150\text{ }\mu\text{m}$ and $75\text{ }\mu\text{m}$ glass batches experienced a similar amount of expansion, the $38\text{ }\mu\text{m}$ glass reduced the expansion to half of the control. All the batches had expansion below 0.01% and therefore according to ASTM C 1260-01 (2003) specifications, the expansions were within the permissible limits. The expansion tests showed that not only was the ground glass not expansive as was expected due to the possible alkali silica reaction, but it actually helped hinder the expansion as compared to control. This is also an indication of pozzolanic activity. The size effect of ground glass was also observed. The finer the particle size, the lesser was the expansion. This was in agreement with the studies conducted by Johnson (1974) and Meyer et al. (1996).

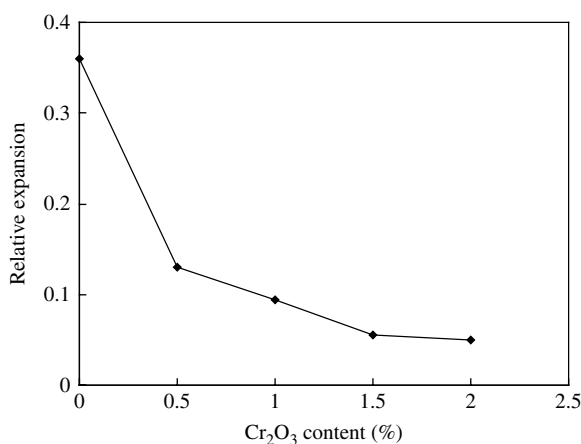


Fig. 5.14 Effect of Cr_2O_3 content in green glass on expansion (Jin et al., 2000)

Shayan and Xu (2004) found that particles size of glass can cause deleterious ASR expansion particularly at high glass contents. Six sets of mortar bars were made to contain 80% glass particles in the aggregate phase as the reactive component. The control set contained the aggregate and plain cement and in the other five sets, the cement was replaced by 5% SF, 10% SF, 10% GLP, 20% glass powder (GLP), and 30% GLP. GLP had particle size less than $10\mu\text{m}$ and specific surface area was $800\text{m}^2/\text{kg}$. Figures 5.15 and 5.16 show that the expansion results for these combinations and indicated that SF and GLP are effective in suppressing ASR expansion when used in sufficient amounts (10%SF AND $> 20\%$ GLP). These results indicated the efficiency of 20% and 30% GLP in suppressing ASR expansion to be better than 10% SF.

Shayan and Xu (2004) also conducted long term mortar bar expansion tests in combination with non-reactive and reactive aggregates and with the same levels of cement replacements as mentioned above. The cement alkali level used was 0.63% Na_2O equivalent in the case of reactive aggregate to find out whether the GLP would release sufficient amounts of alkali to cause deleterious ASR expansion greater than 0.1%. Expansion less than 0.1% at 1 year indicated innocuous combinations. The tests also indicated that GLP itself does not cause any expansion when the aggregate is non-reactive. Moreover, even when the aggregate is reactive, the presence of even 30% GLP does not release sufficient amounts of alkali to trigger the reactivity of the very sensitive aggregate used. This indicates that GLP could be used without fear of harmful effects.

The efficiency of GLP was also assessed in concrete expansion tests with reactive aggregates. Expansions are considered to be deleterious if they exceed 0.03% or 0.04% at 1 year. The tests conducted indicate that even 40% GLP, which has the potential to release more alkali than 30% GLP, has effectively suppressed the enormous expansion of the very reactive aggregate in the concrete (80% reduction). For less reactive aggregates, the expansion would have been completely suppressed.

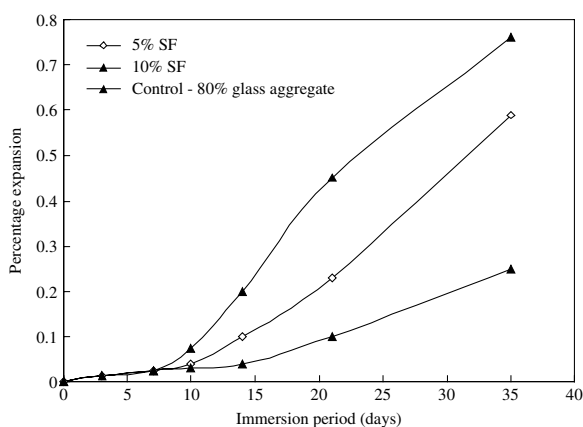
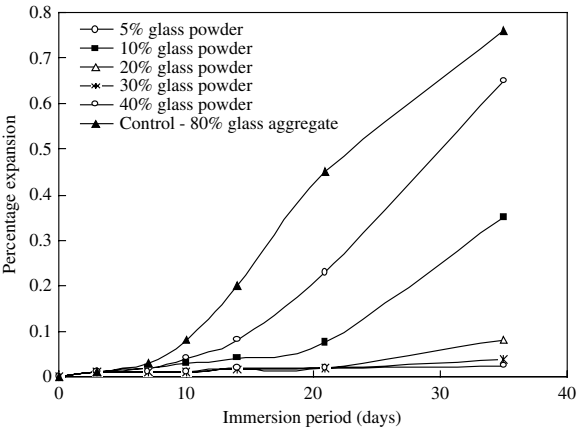


Fig. 5.15 Effects on SF expansion of mortar bars containing reactive aggregates (Shayan and Xu, 2004)

Fig. 5.16 Effects of GLP on expansion of mortar bars containing reactive aggregates (Shayan and Xu, 2004)



This confirms the beneficial effects of GLP in improving the durability properties of concrete.

Park and Lee (2004) reported that mortar bars with waste glasses display a relatively higher expansion rate than plain bars with no waste glass. Mortar bars containing brown waste glass showed higher expansion rates than base containing green glass. All mortar bars except 10% brown waste glass exceeded an expansion rate of 0.2% as required by ASTM C 1260-01 (2003), while the bars containing green waste glass showed an expansion rate within 0.2% up to 30% of its content. Figure 5.17 show expansion rates for mortar bars according to the contents of green and brown glass respectively. The expansion rates noticeably increased with an increase in waste glass content regardless of the types of waste glass used. The expansion rate of mortar bars containing brown glass was 2.5–10.3 times higher than that of plain mortar bars having no waste glass. The bars containing green

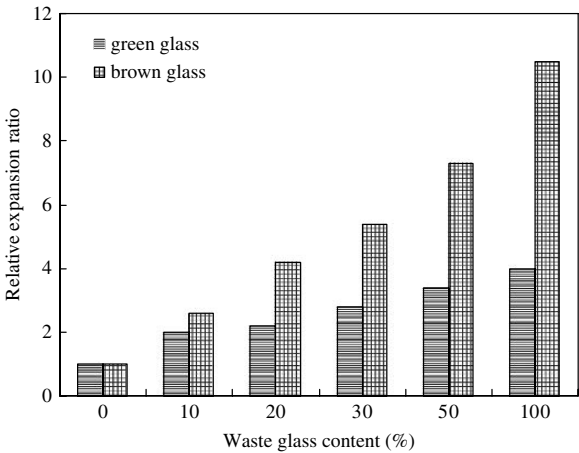


Fig. 5.17 Expansion ratio for mortar bars (Park and Lee, 2004)

glass showed an expansion rate of 1.8–3.9 times than plain mortar bars, which is less than that of the mortar bars with brown glass. This may be due to Cr_2O_3 , which is generally added to the glass to create a greenish hue and is considered to repress the expansion. This ASR suppressing mechanism of Cr_2O_3 seems to support the hypothesis of Prezzi et al. (1997) that the expansive pressure resulting from electrical double-layer repulsion is inversely proportional to the ionic valence. Thus the gel containing Cr^{3+} appears to be less expansive.

Park and Lee (2004) studied the effect of waste glass on expansion by testing mortar bars having different contents of steel fiber (0.5–1.5% by volume) and polypropylene (PP) fiber (0.1–0.5 vol. %) respectively with the content of brown glass fixed at 20%. It was observed that the ASR expansion decreased with an increase in the contents of both fibers. With a steel fiber content of more than 1.0%, the relative expansion rate defined by ASTM C 1260-01 (2003) was suppressed under 0.2%. The PP fibers did not bring the expansion rate down below 0.2%, which necessitated additional suppressive measures such as adding extra PP fiber, blast furnace slag or fly ash when using PP fibers.

In case of mortar bars containing 20% green glass in combination with steel or PP fibers, the expansion rate decreased with an increase in the contents of both fibers, but showed a lower expansion suppression effect than the brown glass. Figure 5.18 shows the comparison of expansion rates of mortar bars containing both waste glasses and fibers to those of mortar bars containing only waste glass. The expansion suppression effect of the reinforcing fiber was more prominent in the brown glass than in the green glass. With its content increasing, the steel fiber achieved 13–40% of expansion suppression rate when mixed with brown glass and 8–19% when mixed with green glass. In the PP fiber, expansion was suppressed by 5–18% when mixed with brown glass, and by 2–9% when mixed with green glass.

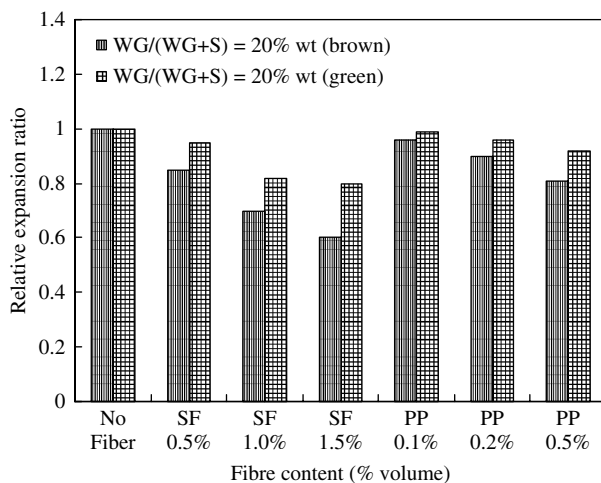


Fig. 5.18 Expansion ratio according to fiber content (Park and Lee, 2004)

Topcu and Canbaz (2004) conducted ASR tests, and concluded that the expansion of the mortar bar specimen containing 100% waste glass was more than 0.2% before 3 days. When the WG content was 0%, expansions were more than 0.2% after 4 days. For this reason, alkali-silica reactions slow down with decreasing WG content. ASR occurred on mortar bars with 0% WG due to very effective curing conditions. After 9 days of experiment, it is seen that white glass causes more dilatation than green and brown glass and ASR limit value exceed.

Shi et al. (2005) studied the effect of glass powder and fly ash on AAR expansion. They used four glass powders; one (GP-fine) from the screening of crushed glass, one (GP-dust) from a dust collector for the glass crushing process and two (GP-4000 and GP-6000) consist mainly of angular particles. It was evaluated by ASTM C1260 – an accelerated mortar bar method. They concluded that replacement of Portland cement with 20% glass powder or Class F fly ash significantly reduced expansion. The control batch exhibited an expansion of 0.50% at 14 days. The replacement of cement with 20% GP-4000 reduced the expansion to around 0.20%, which is considered to be the upper limit of expansion for “potentially reactive” aggregate, whereas the replacement of cement with 20% fly ash decreased the expansion to less than 0.2% at 14 days. It is obvious that use of the fly ash is more effective in reducing the AAR expansion than GP-4000. Results have indicated 20% replacement of cement with coal fly ash is usually not enough to control deleterious expansion with reactive aggregate (Shon et al., 2002), but a minimum of 30% Class F fly ash is generally required (Fournier et al., 2000). Detailed laboratory studies (Shi et al., 2004) have confirmed that a minimum of 50% cement replacement with GP-4000 is required to control deleterious expansion of mortars with reactive aggregates.

Bazant and Steffens (2000) presented a model for the kinetics of alkali-silica reaction in concrete. There are two basic problems for a comprehensive model; (i) the kinetics of the chemical reaction with the associated diffusion processes and (ii) fracture mechanics of the damage process. Only the former is addressed here. The analysis is focused on the attempts by C. Meyers and W. Jin to incorporate ground waste glass (mainly, bottle glass) into concrete. With minor adjustments, though, the model can be applied to ASR in natural aggregates as well. A characteristic unit cubic cell of concrete containing one spherical glass particle is analyzed. A spherical layer of basic ASR gel grows radially inward into the particle, controlled by diffusion of water toward the reaction front. Modification of the solution for the case of mineral aggregates with veins of silica is also indicated. Imbibitions of additional water from the adjacent capillary pores, which causes swelling of the gel was described as a second diffusion process, limited by the development of pressure due to resistance of concrete to expansion. The water used up to form the basic ASR gel and imbibed to cause its swelling appears as a sink term in the non-linear diffusion equation for the global water transport through a concrete structure. The differential equations are integrated numerically. The study of the effects of various parameters provides improved understanding of the ASR, and especially the effect of glass particle size. Full prediction will require measurements of some parameters of the reaction processes.

5.5 Use of Waste Glass in Asphalt Concrete

Crushed and screened waste glass can be used as a portion of fine aggregate in asphalt paving mixes. Satisfactory performance has been obtained from hot mix asphalt pavements incorporating 10–15% crushed glass in wearing surface mixes.

When used in *asphalt concrete*, glass processing must include the removal of ferrous and nonferrous metal, plastic, and paper. Gradation, specific gravity and durability of glass are very important when glass is used as fine aggregate in asphalt paving.

Waste glass used in asphalt surface pavements should be processed to a fine aggregate size (less than 4.75 mm) and blended with conventional aggregates to conform to gradation requirements in accordance with AASHTO T27-84 (1986a). Larger top sizes ranging from 9.5 mm to 15.3 mm should be suitable for use in base course mixes. Since specific gravity is approximately 10–15% below that of the conventional aggregates, waste glass can be expected to provide a greater yield (more volume of asphalt concrete per ton). Glass particles greater than 4.75 mm in size can be expected to break down during handling. Therefore, it is preferable to process (crush and screen) waste glass into a fine aggregate size (less than 4.75 mm) to its use in surface course asphalt paving mixes.

The angular shape and high friction angle (approximately 50°) of well-crushed glass contributes to good lateral stability.

Glass is not absorptive and bonds poorly to asphalt binder. Anti-stripping agents such as hydrated lime introduced as 2% of the aggregate mix by weight have been used in previous demonstrations to reduce potential stripping problems. Poor immersion-compression test results (retained stability) which is a measure of the potential for stripping problems, can also be expected where a high percentage of oversized glass particles are introduced into a mix (Petrarca, 1988).

Large percentages of glass in a surface pavement (greater than 15% by weight) produce a noticeable increase in the reflectivity of the pavement. Depending on the size of the glass particles, this could produce a noticeable glare, particularly on wet pavements. Smaller glass particles and lower percentages of glass can help to reduce reflective glare problems.

5.5.1 Mix Design

Asphalt mixes containing crushed glass can be designed using standard laboratory procedures. Conventional fine hot mix aggregate gradations, as specified in AASHTO M29-83 (1986b) may be used. It is recommended that mix design testing include stripping potential evaluations as outlined in AASHTO T283-85 (1986c). Generally, highway departments allow the use of 5–10% glass in their asphalt mixes.

Most data indicated that larger gravel-sized glass particles will reduce pavement performance, and that optimum performance can best be achieved by using crushed glass as a sand or fine aggregate substitute (less than 4.75 mm). When waste glass

is used as a fine aggregate substitute material, glass performance in hot mix asphalt should be comparable to conventional mixes (Slater, 1995). Base course applications, being less susceptible to stripping, rutting and skid resistance, could tolerate the introduction of glass particles up to 15.3 mm (5/8 in) in size, resulting in substitution of both coarse and fine aggregates in the mix.

5.6 Use of Waste Glass in Granular Base

Crushed and screened waste glass has the potential for use as a granular base material. Glass having fine aggregate size fraction less than 4.75 mm in size, exhibits properties similar to that of a fine aggregate. It has relatively high stability due to the angular nature of crushed glass particles.

Waste glass should be crushed and screened prior to use to produce a material that will be free of sharp edges and glass slivers, and that will meet the requirements of a fine aggregate material, as defined by AASHTO M29-83 (1986b). Waste glass should be free of ferrous and nonferrous metal, and the level of inorganic and organic debris should be reduced as much as practical. It has been recommended that levels of debris in the waste glass should be limited to 5% as determined by the American Geophysical Institute (American Geophysical Institute, 1982) test method.

Waste glass should be crushed and screened to produce a material that satisfied the grading requirements of granular base specifications, such as AASHTO M147-70 (1986d). Crushed glass has a unit weight of approximately 1120 kg/m³ which is lower than that of conventional aggregate. The compacted density of crushed glass will vary with the size and grading of the glass as well as the degree of contamination (extraneous debris, such as paper, plastic caps, and soil). Crushed glass exhibits a relatively flat moisture-density curve, which indicates that the compacted density is insensitive to moisture content. Relatively high angles of internal friction (compared with conventional aggregates) of greater than 50 degrees have been reported for crushed glass with top sizes of 19 mm and 6.4 mm. California Bearing Ratio (CBR) test results of crushed glass blended with conventional aggregate were found to exhibit values ranging from 42 to 125% for blends of 50% glass with crushed rock. Lower glass additions of 15% were found to exhibit values almost identical to that of the crushed rock used in the tests (approximately 133%) (WSDTED, 1993). Larger size glass particles have marginal durability, as measured by the Los Angeles Abrasion test, with values of approximately 40–45%. This suggests that additional processing (crushing) of the waste glass would be desirable to eliminate the larger, less durable glass fraction. Crushed glass is a free-draining material that exhibits permeabilities ranging from 10⁻¹ to 10⁻² cm/sec, depending on the glass gradation.

5.6.1 Mix Design

Crushed waste glass (cullet) used in granular base applications should be limited to the replacement of fine aggregate sizes. Fine crushed glass contains durable

sand-like particles and exhibits consistent properties. Recommended gradations are presented in Table 5.10. Crushed glass in this size range will perform as a highly stable (angular) fine aggregate material. It has been recommended that maximum cullet content should be limited to 15% in granular base applications and 30% in sub base applications (WSDTED, 1993).

Table 5.10 Recommended cullet gradation for use as a structural fill or granular base material (WSDTED, 1993)

Size	% Finer
1/4-inch	10–100
No. 10	0–50
No. 40	0–25
No. 200	0–5

References

- AASHTO (1986a) Standard method of test, sieve analysis of fine and coarse aggregates. AASHTO Designation: T27-84, Part II Tests, 14th Edition.
- AASHTO (1986b) Fine aggregate for bituminous paving mixtures. AASHTO Designation: M29-83, Part I Specifications, 14th Edition.
- AASHTO (1986c) Resistance of compacted bituminous mixtures to moisture induced damage. AASHTO Designation: T283-85, Part II Testing, 14th Edition.
- AASHTO (1986d) Aggregate and soil-aggregate subbase, base and surface courses. AASHTO Designation: M147-70 (1980), Part I Specifications, 14th Edition.
- Ahmed I (1991) Use of waste materials in highway construction. Purdue University, FHWA/INJHRP-91/3.
- American Geophysical Institute (1982) AGI Data Sheet 15.1 and 15.2, Comparison chart for estimating percent composition.
- ASTM C 618 (1994) Standard specifications for coal ash and raw or calcined natural pozzolan for use as a mineral admixture in concrete, Cement; Lime; Gypsum. Annual book of ASTM Standards. Vol. 01, American Society for Testing and Materials, Philadelphia.
- ASTM C 1260-01(2003) Standard test method for potential alkali reactivity of aggregates (mortar-bar method), Aggregates and Concrete, Vol. C04-02, American Society for Testing and Materials, West Conshohocken, PA.
- Bazant ZP, Steffens A (2000) Mathematical model for kinetics of alkali-silica reaction in concrete. Cement and Concrete Research 30: 419–428.
- Blanks RF (1941) Concrete deterioration at Parker Dam. Eng News-Rec 126, pp. 462–465.
- Chesner WH (1992) Waste glass and sludge for use in asphalt pavement. Utilization of Waste Materials in Civil Engineering Construction. Inyang H, Bergeson K, (Eds.), American Society of Civil Engineers.
- Chesner WH, Petrarca RW (1988) The ecosphere recycling system and the use of glass as a construction aggregate material. Proceedings of the 1988 Conference on Solid Waste Management and Materials Policy. Legislative Commission on Solid Waste, New York, USA.
- Corinaldesi V, Gnappi G, Moriconi G, Montenero A (2005) Reuse of ground waste glass as aggregate for mortars. Cement and Concrete Research 25: 197–201.
- Diamond S, Thaulow NA (1979) A study of expansion due to Alkali-Silica reaction as conditioned by grain size of reactive aggregates. Cement and Concrete Research 31: 591–607.

- Dickson P (1973) Cold weather paving with glassphalt. Albuquerque Symposium on Utilization of Waste Glass in Secondary Products, Albuquerque, USA.
- Dron R, Brivot F (1992) Thermodynamic and kinetic approach to the alkali-silica reaction: Part I. Cement and Concrete Research 22 (5): 941–948.
- Dron R, Brivot F (1993) Thermodynamic and kinetic approach to the alkali-silica reaction: Part II. Cement and Concrete Research 23 (4): 1001–1002.
- Egosi NG (1992) Mixed broken glass processing solutions. Utilization of Waste Materials in Civil Engineering Construction. Inyang H, Bergeson K, (Eds.), American Society of Civil Engineers.
- Fournier B, Berube MA, Roge CA (2000) Canadian Standard Association (CSA) standard practice to evaluate potential alkali-aggregate reactivity of aggregates and to select preventive measures against AAR in new concrete structures. Proceedings of the 11th International Conference on Alkali-Aggregate Reaction in Concrete, Quebec City, pp. 633–642.
- Gartner EM, Jennings HM (1987) Thermodynamics of calcium-silicate hydrates and their solutions. Journal of American Ceramic Society 70 (10): 743–749.
- Glasser FP (1992) Chemistry of the alkali aggregate reaction. Swamy RN, (Ed.), The Alkali-Silica Reaction in Concrete, Blackie, Glasgow and London, and Van Nostrand-Reinhold, New York, pp. 30–53.
- Glasser LSD, Kataoka N (1981) Alkali-aggregate-reaction in concrete. Paper S 252/23, CSIR, Pretoria.
- Jin W, Meyer C, Baxter S (2000) Glasscrete – Concrete with glass aggregate. ACI Material Journal 97 (2): 208–213.
- Johnson CD (1974) Waste glass as coarse aggregate for concrete. Journal of Testing and Evaluation 2 (5): 344–350.
- Kisacik IE (2002) Using glass in concrete. B.S. Thesis, Osmangazi University, Faculty of Engineering and Architecture, Department of Civil Engineering, Turkey, p. 52.
- Meissner HS (1941) Cracking in concrete due to expansion reaction between aggregate and high-alkali cement as evidenced in Parker Dam. Proceedings of the American Concrete Institute 37: 549–568.
- Meyer C, Baxter S, Jin W (1996) Alkali-silica reaction: concrete with waste glass as aggregate. Chong KP (Ed.), Materials for a New Millennium, Proceedings of ASCE Materials Engineering Conference, Washington DC, pp 1388–1394.
- Park SB, Lee BC (2004) Studies on expansion properties in mortar containing waste glass and fibers. Cement and Concrete Research 34: 1145–1152.
- Park SB, Lee BC, Kim JH (2002) Studies on mechanical properties of concrete containing waste glass aggregate. Ninth Annual International Conference on Composites Engineering, D. Hui (Ed.), Sponsored by International Community for Composite Engineering and College of Engineering, University of New Orleans, California, pp. 603–604.
- Park SB, Lee BC, Kim JH (2004) Studies on mechanical properties of concrete containing waste glass aggregate. Cement and Concrete Research 34: 2181–2189.
- Petrarca, R. (1988) Use of Glassphalt. Paper presented to the Long Island Society of Asphalt Technologists, USA.
- Phillips JC, Cahn DS, Keller GW (1972) Refuse glass aggregate in Portland cement concrete. Proceedings of the Third Mineral Waste Utilization Symposium, US Bureau of Mines, Chicago, Illinois.
- Poole AB (1992) Introduction to alkali-aggregate reaction in concrete. Swamy RN (Ed.), The Alkali-Silica Reaction in Concrete, Blackie, Glasgow and London, and Van Nostrand-Reinhold, New York, pp. 1–29.
- Prezzi M, Monteiro PJM, Sposito G (1997) The alkali-silica reaction: Part 1: Use of double layer theory to explain behavior of reaction product gels. ACI Material Journal 94 (1): 10–17.
- Reindl J (1998) Report by recycling manager. Dave County, Department of Public Works, Madison, USA
- Robert LR (1989) Micro silica in concrete. Material Science of Concrete, American Ceramic Society, Westerville, OH, pp. 197–222.

- Samtur H (1974) Glass recycling and reuse. University of Wisconsin, National Science Foundation, NTIS PB239674.
- Shao Y, Lefort T, Movas S, Rodriguez D (2000) Studies on concrete containing ground waste glass. *Cement and Concrete Research* 30: 97–100.
- Shayan A, Xu A (2004) Value-added utilization of waste glass in concrete. *Cement and Concrete Research* 34: 81–89.
- Shi C, Wu Y, Riefler C, Wang, H (2005) Characteristics and pozzolanic reactivity of glass powders. *Cement and Concrete Research* 35: 987–993.
- Shi C, Wu Y, Shao Y, Riefler C (2004) Alkali-aggregate reaction of mortar bars ground glass powder. Proceedings of the 12th International Conference on AAR in Concrete, Beijing.
- Shon CS, Zollinger DG, Sarkar SL (2002) Evaluation of modified ASTM 1260 accelerated mortar bar test for alkali-silica reactivity. *Cement and Concrete Research* 32: 1981–1987.
- Slater, W. (1995). New York City Hamilton Avenue Asphalt Plant Manager, Telephone Communication, USA.
- Stanton TH (1940) Expansion of concrete through reaction between cement and aggregate. *Proceedings American Society of Civil Engineers* 66: 1781–1811.
- Swamy RN (1992a) Testing for alkali-silica reaction. R.N. Swamy (Ed.), *The Alkali-Silica Reaction in Concrete*, Blackie, Glasgow and London, and Van Nostrand-Reinhold, New York, pp. 54–95.
- Swamy RN (1992b) *The Alkali-Silica Reaction in Concrete.*, (Ed.) Blackie, Glasgow and London, and Van Nostrand-Reinhold, New York.
- Swenson EG (1957) A reactive aggregate undetected by ASTM tests. *ASTM Bull* 226: 48–57.
- Terro MJ (2006) Properties of concrete made with recycled crushed glass at elevated temperatures. *Building and Environment* 41 (5): 633–639.
- Topcu IB, Canbaz M (2004) Properties of concrete containing waste glass. *Cement and Concrete Research* 34: 267–274.
- Tuncan M, Karasu B, Yalcin M (2001) The suitability for using glass and fly ash in Portland Cement Concrete. Proceedings of the 11th International Offshore and Polar Engineering Conference (ISOPE 2001), Stavenger, Norway 4: 146–152.
- Vivian HE (1951) Studies in cement aggregate reaction: XVI. The effect of hydroxyl ions on the reaction of opal. *Austrian Journal of Applied Science* 2: 108–113.
- WSDTED (1993) Washington State Department of Trade and Economic Development Glass Feedstock Evaluation Project., USA.

Chapter 6

Coal Fly Ash

Introduction

Coal Fly ash (FA) is a by-product of the combustion of pulverized coal in thermal power plants. It is removed by the dust collection systems from the exhaust gases of fossil fuel power plants as very fine, predominantly spherical glassy particles from the combustion gases before they are discharged into atmosphere. The size of particles is largely dependent on the type of dust collection equipment. Diameter of fly ash particles ranges from less than $1\text{ }\mu\text{m}$ – $150\text{ }\mu\text{m}$. It is generally finer than Portland cement. The chemical composition of fly ash is determined by the types and relative amounts of incombustible material in the coal used. The major chemical constituents in fly ash are silica, alumina and oxides of calcium and iron. Because of its fineness and pozzolanic and sometimes self-cementitious nature, fly ash is widely used in cement and concrete.

Depending upon the collection system, varying from mechanical to electrical precipitators or bag houses and fabric filters, about 85–99.9% of the ash from the flue gases is retrieved in the form of fly ash. Fly ash accounts for 75–85% of the total coal ash, and the remainder is collected as bottom ash or boiler slag. Fly ash because of its mineralogical composition, fine particle size and amorphous character is generally pozzolanic and in some cases also self cementitious whereas bottom ash and boiler slag are much coarser and are not pozzolanic in nature. Therefore, It is important to note that all the ash is not fly ash and the fly ashes produced by different power plants are not equally pozzolanic and, therefore, are not always suitable for use as mineral admixture in concrete.

Fly ash generated in coal burning power plants is an inherently variable material because of several factors. Among these are the type and mineralogical composition of the coal, degree of coal pulverization, type of furnace and oxidation conditions including air-to-fuel ratio, and the manner in which fly ash is collected, handled and stored before use. Since no two utilities or plants may have all of these factors in common, fly ash from various power plants is likely to be different. The fly ash properties may also vary within the same plant because of load conditions over a twenty four hour period. Non-uniformity of fly ash is a serious disadvantage and sometimes is the main hurdle.

6.1 Classification of Fly Ash

As per ASTM C 618 (1993) specification for “Fly ash and raw or calcined natural pozzolan for use as mineral admixture in Portland cement concrete,” pozzolans are defined as “silicious and aluminous materials which in themselves possess little or no cementitious value but will, in finely divided form and in the presence of moisture, chemically react with $\text{Ca}(\text{OH})_2$ at normal temperatures to form compounds possessing cementitious properties.”

ASTM C 618 (1993) categorizes natural pozzolans and fly ashes into the following three categories.

Class N: Raw or calcined natural pozzolans such as some diatomaceous earths, opaline chert and shale, stuffs, volcanic ashes and pumice are included in this category. Calcined kaolin clay and laterite shale also fall in this category of pozzolans.

Class F: Fly ash normally produced from burning anthracite or bituminous coal falls in this category. This class of fly ash exhibits pozzolanic property but rarely, if any, self hardening property.

Class C: Fly ash normally produced from lignite or sub-bituminous coal is the only material included in this category. This class of fly ash has both pozzolanic and varying degree of self-cementitious properties. (Most Class C fly ashes contained more than 15% CaO. But some Class C fly ashes may contain as little as 10% CaO).

Table 6.1 Requirements for fly ash and natural pozzolans for use as mineral admixtures in Portland cement concrete (ASTM C 618, 1993)

Requirements	Fly ash classification		
	N	F	C
Chemical requirements	70.0	70.0	50.0
$\text{SiO}_2 + \text{Al}_2\text{O}_3 + \text{Fe}_2\text{O}_3$, min (%)			
SO_3 , max (%)	4.0	5.0	5.0
Moisture content, max (%)	3.0	3.0	3.0
Loss on ignition, max (%)	10.0	6.0	6.0
Physical requirements	34	34	34
Amount retained when wet sieved on 45 μm sieve, max (%)			
Pozzolanic activity index, with Portland cement at 28 days, min (%) of control	75	75	75
Pozzolanic activity index, with lime, at 7 days, min (MPa)	5.5	5.5	—
Water requirement, max (%) of control	115	105	105
Autoclave expansion or contraction, max (%)	0.8	0.8	0.8
Specific gravity, max variation from average	5	5	5
Percentage retained on 45 μm sieve, max variation, percentage points from average	5	5	5

Table 6.1 presents chemical and physical requirements for fly ash and natural pozzolans for use as a mineral admixture in Portland cement concrete.

6.2 Properties of Fly Ash

6.2.1 Physical Properties

6.2.1.1 Particle Morphology

Generally, the fly ash particles consist of clear glassy spheres and a spongy aggregate. Diamond (1985), Joshi (1970), Joshi and Lam (1987) and Mehta (1988) have done morphological studies on particle shape and surface characteristics of various types of fly ashes using scanning electron microscope (SEM) and energy dispersive x-ray analysis (EDXA). Scanning electron micrographs of different fly ashes show the typical spherical shape of fly ash particles, some of which are hollow. The hollow spherical particles are known as cenospheres or floaters as they are very light and tend to float on water surface. Sometimes fly ashes may also contain many small spherical particles within a large glassy sphere, called pherospheres. The exterior surfaces of the solid and hollow spherical particles of low calcium oxide fly ashes are generally smooth and better defined than those of high calcium oxide fly ashes which may have surface coatings of material rich in calcium.

6.2.1.2 Fineness

Fineness of fly ash is one of the important physical properties and is related to its pozzolanic activity. ASTM C 618 (1993) limits the maximum amount of fly ash retained on the 45 μm (#325) mesh sieve on wet sieving as 34%. Generally, a large fraction of ash particle is smaller than 3 μm in size. In bituminous ashes, the particle sizes range from less than 1 to over 100 μm . Joshi (1970) reported that average size lies between 7–12 μm .

6.2.1.3 Specific Gravity

Joshi (1970) has reported that, in general, specific gravity of fly ash may vary from 1.3 to 4.8. The specific gravity of fly ash is related to shape, color as well as chemical composition of fly ash particle. Canadian fly ashes have specific gravity ranging between 1.94 and 2.94, whereas American ashes have specific gravity ranging between 2.14 and 2.69.

6.2.1.4 Pozzolanic Activity

The property of fly ashes, possessing little or no cementing value to react with calcium oxide in the presence of water and produce highly cementitious water insoluble products, is called pozzolanic reactivity. The meta-stable silicates present in

self-cementitious fly ash react with calcium ions in the presence of moisture to form water insoluble calcium-alumino-silicate hydrates. The pozzolanic activity of a fly ash depends upon many parameters such as fineness, amorphous matter, chemical and mineralogical composition, and the unburned carbon content or loss on ignition of the fly ash (Joshi, 1979). Several investigators have reported that when fly ash is pulverized to increase fineness, its pozzolanic activity increases significantly. However, the effect of increase in specific surface area beyond $6000 \text{ cm}^2/\text{g}$ is reported to be insignificant.

6.2.1.5 Moisture

To prevent caking and packing of the fly ash during shipping and storage and to control uniformity of fly ash shipments, a 3.0% limit on moisture content is specified in ASTM C618. Any amount of moisture in Class C fly ash will cause hardening from hydration of its cementitious compounds. Even surface spraying may cause caking. Therefore, it is important that such ashes have to be kept dry before being mixed with cement.

Physical properties of fly ashes reported by Electric Power Research Institute (1987) are given in Table 6.2.

6.2.2 Chemical Composition

Chemical constituents in fly ash reported in terms of oxides include silica (SiO_2), alumina (Al_2O_3), and oxides of calcium (CaO), iron (Fe_2O_3), magnesium (MgO), titanium (TiO_2), sulfur (SO_3), sodium (Na_2O), and potassium (K_2O). Unburned carbon is another major constituent in all the ashes. Amongst these SiO_2 and Al_2O_3 together make up about 45–80% of the total ash. The sub-bituminous and lignite coal ashes have relatively higher proportion of CaO and MgO and lesser proportions of SiO_2 , Al_2O_3 and Fe_2O_3 as compared to the bituminous coal ashes. Table 6.3 presents the chemical analysis of different fly ashes as reported by EPRI (1987).

6.2.2.1 Total Oxides

For class F fly ashes, the sum of silica, alumina and iron oxide ($\text{SiO}_2 + \text{Al}_2\text{O}_3 + \text{Fe}_2\text{O}_3$), must be at least 70.0%, whereas for Class C the required minimum is 50.0%. For fly ash to act as a pozzolan, it is necessary to have chemical constituents

Table 6.2 Physical properties of fly ashes (EPRI, 1987)

Parameter	Range
Specific gravity	2.14–2.69
Moisture content (%)	0.0–0.38
Retained on #325 sieve (%)	3.55–36.90
Blaine fineness (cm^2/g)	1579–5550

Table 6.3 Chemical analysis of fly ashes (EPRI, 1987)

Parameter	Range
Silicon dioxide (%)	30.92–62.76
Aluminum oxide (%)	12.30–26.95
Iron oxide (%)	2.84–24.43
Calcium oxide (%)	1.10–30.53
Magnesium oxide (%)	0.69–6.69
Sulfur trioxide (%)	0.31–3.85
Sodium oxide (%)	0.20–2.04
Potassium oxide (%)	0.22–3.03
Available alkalies (as equivalent Na ₂ O) (%)	0.23–1.54
Loss on ignition (%)	< 0.01–16.60

capable of reacting with lime in the presence of water. Therefore, a minimum proportion of total $\text{SiO}_2 + \text{Al}_2\text{O}_3 + \text{Fe}_2\text{O}_3$ are specified to ensure that sufficient reactive constituents are present.

6.2.2.2 Sulfur Trioxide (SO_3)

As per ASTM C618, the maximum SO_3 content in fly ash is 5.0%. The SO_3 content has been reported to affect to some degree the early age compressive strength of mortar and concrete specimens. The higher the SO_3 content, the higher is the resultant strength.

6.2.2.3 Carbon Content (Loss on Ignition)

The need for low carbon content in fly ash is related to requirements for proper air entrainment. More air entraining agent is required to entrain a specified amount of air in fly ash concrete than is required for a similar concrete without fly ash. The loss on ignition is related to the amount of carbon or unburned coal in the fly ash. For some of the fly ashes, there is a significant difference in carbon content and loss on ignition (LOI). Yet the specification restricts the LOI and not the unburned carbon. ASTM C618 sets the limit on loss on ignition at 6.0% for Class F and Class C fly ashes.

6.2.3 Mineralogical Characteristics

X-ray diffraction study of the crystalline and glassy phases of a fly ash is known as mineralogical analysis of fly ash. Mineralogical characterization is important in determining the crystalline phases that contain the major constituents of fly ash. Generally, fly ashes have 15–45% crystalline matter. The high calcium ashes (Class C) contain larger amounts of crystalline matter ranging between 25 and 45%. Table 6.4 presents crystalline phases in fly ashes identified by XRD analysis (McCarthy et al., 1988)

Table 6.4 Crystalline phases in fly ashes from North America (McCarthy et al., 1988)

Class of fly ash and code	Name	Nominal composition
Low-calcium/Class F		
Hm	Hematite	Fe_2O_3
Mu	Mullite	$\text{Al}_6\text{Si}_2\text{O}_{13}$
Qz	Quartz	SiO_2
Sp	Ferrite spinel	$(\text{Mg,Fe})(\text{Fe,Al})_2\text{O}_4$
High-calcium/Class C		
Ah	Anhydrite	CaSO_4
AS	Alkali sulfate	$(\text{Na,K})_2\text{SO}_4$
C_2S	Dicalcium silicate	Ca_2SiO_4
C_3A	Tricalcium aluminate	$\text{Ca}_3\text{Al}_2\text{O}_6$
Hm	Hematite	Fe_2O_3
Lm	Lime	CaO
MI	Melilite	$\text{Ca}_2(\text{Mg,Al})(\text{Al,Si})_2\text{O}_7$
Mu	Mullite	$\text{Al}_6\text{Si}_2\text{O}_{13}$
Mw	Merwinite	$\text{Ca}_3\text{Mg}(\text{SiO}_4)_2$
Pc	Periclase	MgO
Qz	Quartz	SiO_2
So	Sodalite structure	$\text{Ca}_2(\text{Ca,Na})_6(\text{Al,Si})_{12}\text{O}_{24}(\text{SO}_4)_{1-2}$
Sp	Ferrite spinel	$(\text{Mg,Fe})(\text{Fe,Al})_2\text{O}_4$

Although high calcium Class C ashes may have less glassy or amorphous material, they do contain certain crystalline phases such as anhydrite (CaSO_4), tricalcium aluminate ($3\text{CaOAl}_2\text{O}_3$), calcium sulpho-aluminate (CaSAI_2O_3) and very small amount of free lime (CaO) that participate in producing cementitious compounds. Also, glassy phase in Class C ashes is usually more reactive. The glassy particles in Class C fly ashes contain large amount of calcium which possibly makes the surface of such particles highly strained, and probably, it is because of this Class C fly ashes are highly reactive.

Anhydrite (CaSO_4) is formed from the reaction of CaO , SO_2 and O_2 in the furnace or flue. Quantity of anhydrite increases with the increase in SO_3 and CaO contents. It plays a significant role in fly ash hydration behavior because it participates along with tricalcium aluminate and other soluble aluminates to produce ettringite and calcium sulphotoaluminate hydrate.

Periclase is the crystalline form of magnesium oxide (MgO). This form of MgO present in fly ash affects the soundness of the resulting concrete through its expansive hydration to brucite, $\text{Mg}(\text{OH}_2)$.

Crystalline iron oxide, ferrite spinel and/or hematite are generally found in all fly ashes. In most of the fly ashes, about 0.33–0.50% of iron is present as crystalline oxide. The reactivity of fly ash is, however, dependent on the glassy phases of Fe_2O_3 .

Tricalcium aluminate ($3\text{CaOAl}_2\text{O}_3$) is one of the most important crystalline phases to identify and quantify in fly ash because it contributes to ettringite formation, and also in self-hardening reactions as well as disruptive sulfate reactions in hardened concrete.

6.3 Utilization of Fly Ash in Cement and Concrete

Coal fly ash can be utilized in following ways.

6.3.1 High Volume Uses

High volume utilization of fly ash includes

- as structural fills in embankments, dams, dikes and levees, and
- as sub-base and base courses in road way construction.

6.3.2 Medium Volume Uses

This includes the use of fly ash

- as raw material in cement production
- as an admixture in blended cements and
- as replacement of cement or as a mineral admixture in concrete
- in addition coal ash including fly ash may be used as partial replacement of fine aggregate in concrete
- for production of light weight aggregates for concrete and many other applications.

6.3.3 Low Volume Uses

This includes the coal ash utilization

- in high value added applications such as metal extractions. High value metal recovery of Aluminum (Al), Gold (Au), Silver (Ag), Vanadium (Va) and Strontium (Sr) fall in this category
- Fly ash has potential uses for producing light weight refractory material and exotic high temperature resistant tiles
- Cenospheres or floaters in fly ash are used as special refractory material and also as additives in forging to produce high strength alloys.

6.3.4 Miscellaneous Uses

Based upon its physical properties, coal ash is used

- as land fill for land reclamations for residential, commercial and recreational development projects
- as filler in asphalt, plastics, paints and rubber products
- in water treatment and as absorbent for oil and chemical spills.

6.4 Fresh Properties of Concrete Containing Fly Ash

Fresh concrete is a concentrated suspension of particulate materials of different densities, particles sizes and chemical composition in a solution of lime and other compounds. In fresh concrete, fly ash plays an important role in the fluidity of concrete. Fresh concrete properties include workability, air-entrainment, bleeding and segregation, pumpability, compactability, and finishability. Addition of fly ash has significant effect on the rate of hydration reactions as well as on the effectiveness of the chemical admixtures, particularly air entraining agent, and water reducer or superplasticizer.

Low calcium Class F fly ash normally acts as a fine aggregate of spherical form in early stages of hydration whereas high calcium Class C fly ash may contribute to the early cementing reactions in addition to its presence as fine particulate in the concrete mix. Hydration of cement is an exothermic reaction and the released heat causes a rise of temperature of fresh concrete.

6.4.1 Water Requirement and Workability

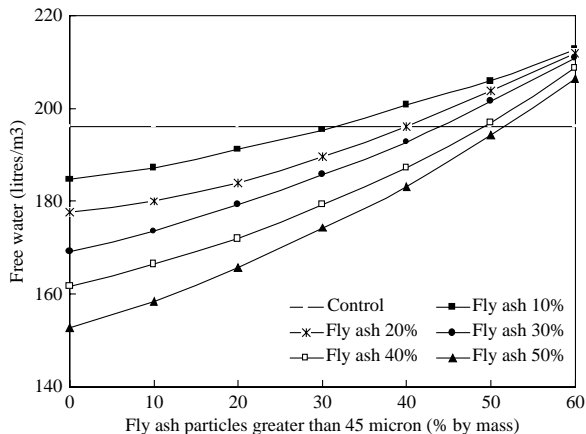
Workability is one of the governing factors of concrete mix design. In most cases, the fluidity of concrete is termed as workability and is defined as the ease with which concrete can be mixed, placed, handled, compacted and finished. Workability is determined by the rheological behavior of fresh concrete. Water content of concrete plays a dominant role in controlling workability. The spherical shape and glassy surface of most fly ash particles, usually finer than cement, permit greater workability or slump for equal water-cement ratios.

Several investigations have been conducted to study the role of Class F fly ash on the rheology of fresh concrete (Hobbs, 1983). Brown (1982) conducted several studies with fly ash replacing cement and fine aggregate at levels of 10–40% by volume. He concluded that for each 10% of ash substituted for cement, the compacting factor or workability changed to the same order as it would by increasing the water content of the mix by 3–4%. When fly ash was substituted for sand or total aggregate, workability increased to reach a maximum value at about 8% ash by volume of aggregate. Further substitution caused rapid decrease in workability.

Owens (1979) reported that with the use of fly ash containing large fraction of particles coarser than $45\mu\text{m}$ or a fly ash with high amount of unburned carbon, exhibiting loss on ignition more than 1%, higher water demand was observed. Water demand was noticeably increased to maintain the desired level of fluidity. Figure 6.1 shows the effects of coarse fly ash particles on the water demand of concrete mixtures.

To develop a theoretical understanding of the rheology of fresh fly ash concrete, Tattersall and Benfill (1983) suggested mathematical expressions relating the yield value (τ) and the plastic viscosity (μ) varied with volumetric parameters of concrete, in terms of Bingham model. Yield stress and plastic viscosity varied with

Fig. 6.1 Influence of coarse particulate of fly ash on the water required for equal workability in concrete (Owens, 1979)



volumetric parameters of concrete, water to cement ratio, replacement levels of cement/aggregates by fly ash, and fineness of fly ash. An increase in the volume of the paste at a constant ratio of ash to total cementitious material resulted in an increase in plastic viscosity. Apparently because of fine particle size and smooth glassy texture as well as spherical shape, fly ash acts to plasticize concrete at given water content when used as partial replacement of cement or fine aggregate.

6.4.2 Segregation and Bleeding

Utilization of fly ash in concrete significantly reduces the bleeding and segregation. The lubricating effect of the glassy spherical fly ash particles and the increased ratio of solids to liquid make the concrete less prone to segregation and increase concrete pumpability. Figure 6.2 shows the bleeding rate of fly ash concrete compared to that of control concrete without fly ash.

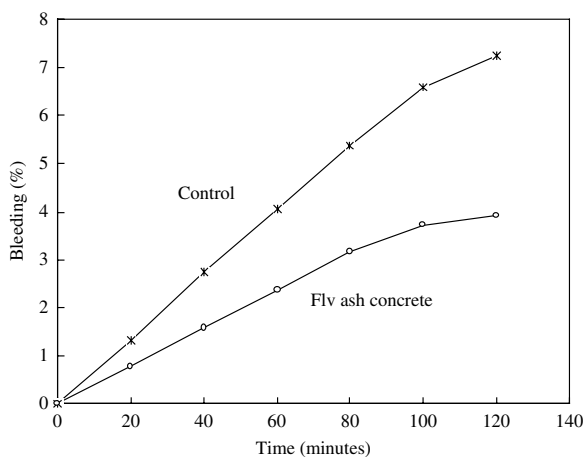
Joshi and Lohtia (1993) used Alberta fly ashes in making high volume fly ash concrete mixes. They reported that fly ash concrete mixes were more cohesive than control mixes. During the slump test, the fly ash concrete mixes sub-sided more slowly and gradually than the control mixes which exhibited abrupt fall or subsidence.

6.4.3 Time of Setting

With the addition of water to concrete, hydration reaction start and the cement paste begins to stiffen accompanied by heat release. The rate of stiffening of cement paste is expressed in terms of setting time.

Investigations have revealed that the addition of low calcium Class F fly ashes generally show some degree of retarding effect on cement setting. Generally, the

Fig. 6.2 Relative bleeding of control and fly ash concretes (Central Electricity Generating Board, 1967)



effect of fly ash on the time of setting depends on the characteristics and amount of fly ash used. The interacting effects of fly ash with other chemical and mineral admixtures used in concrete may also influence the setting of concrete. It has been observed that all Class F fly ashes, especially low calcium fly ashes with high carbon content or LOI, increase the setting time.

High calcium fly ashes, generally low in carbon and high in reactive and/or cementitious components sometimes exhibit opposite behavior of reduced setting time. Not all Class C fly ashes cause rapid setting. Ramakrishan et al. (1981) reported an increase in setting time with the use of high calcium fly ash in concrete.

Lane and Best (1982) reported the retarding influence of fly ash on setting of concrete as function of the proportion, fineness and chemical composition of the fly ash. They concluded that the influence of fly ash on setting time is less than the influence due to cement fineness, the water content of the paste, and the ambient temperature.

Joshi et al. (1993) used three different sub-bituminous Alberta coal ashes at replacement levels of 40–60% by cement weight to produce superplasticized and air entrained concretes. They observed that fly ash concrete achieved an initial setting time of 5–11 hours as compared to about 5 hours for non-fly ash concrete. The final setting time varied from 10 to 13 hours as against 7 hours for control mixes containing on fly ash.

Carette and Malhotra (1984) studied the effect of Canadian fly ashes on the fresh concrete properties. Fly ashes were from 11 different sources. Cement was replaced with 20% fly ash in all the mixes. Chemical properties of fly ashes are given in Table 6.5. Fresh concrete properties are given in Table 6.6.

Rodway and Fedriko (1989) made concretes with varying percentages of Alberta fly ash. Four percentages (0, 56, 68, and 76%) of fly ash of the total cementitious material were used. Superplasticizer and air entraining admixture was used to maintain constant slump and air content within specified limits. High fly ash concrete mixes exhibited increasingly greater initial setting times of 22–42.5 hours with

Table 6.5 Properties of some Canadian fly ashes (Carette and Malhotra, 1984)

Fly ash source	Type of coal	Major chemical compounds (% by weight)					
		SiO ₂	Al ₂ O ₃	Fe ₂ O ₃	CaO	MgO	LOI
1	Bituminous	47.1	23.0	20.4	1.21	1.17	2.88
2	Bituminous	44.1	21.4	26.8	1.95	0.99	0.70
3	Bituminous	35.5	12.5	44.7	1.89	0.63	0.75
4	Bituminous	38.3	12.8	39.7	4.49	0.43	0.88
5	Bituminous	45.1	22.2	15.7	3.77	0.91	9.72
6	Bituminous	48.0	21.5	10.6	6.72	0.96	6.89
7	Sub- Bituminous	55.7	20.4	4.61	10.7	1.53	0.44
8	Sub- Bituminous	55.6	23.1	3.48	12.3	1.21	0.29
9	Sub- Bituminous	62.1	21.4	2.99	11.0	1.76	0.70
10	Lignite	46.3	22.1	3.10	13.3	3.11	0.65
11	Lignite	44.5	21.1	3.38	12.9	3.10	0.82

increasing fly ash content from 56 to 76% compared to 7.6 hours for the control mix without fly ash. The observed delays appeared to be related to the problem of compatibility between cementitious materials and surperplasticizer to maintain workability.

Sivasundram et al. (1990) determined the setting time of high volume fly ash concrete mixes, and reported that the initial setting time of 7.50 hours was comparable to that of the control concrete, whereas the final setting time was extended by about 3 hours as compared to that of the control concrete.

6.4.4 Air Entrainment

Minute air bubbles are entrained in concrete by using air entraining agent (AEA) in order to improve the freezing and thawing resistance of concrete. For entraining a specified amount of air content, approximately 6% more air entraining agent

Table 6.6 Properties of concrete incorporating Canadian fly ashes (Carette and Malhotra, 1984)

Mix No.	Cement (kg/m ³)	Slump (mm)	Air (%)	Bleeding (%)	Setting time (hr:min)	
					Initial	Final
Control	295	70	6.4	2.9	4 : 10	6 : 00
F1	236	100	6.2	3.1	4 : 50	8 : 00
F2	237	105	6.2	4.6	7 : 15	10 : 15
F3	237	100	6.2	5.1	5 : 20	8 : 10
F4	238	110	6.3	4.3	: 20	8 : 25
F5	237	65	6.4	2.7	5 : 15	8 : 55
F6	238	75	6.5	2.6	4 : 30	6 : 50
F7	239	100	6.1	2.9	4 : 15	6 : 20
F8	236	115	6.2	5.6	5 : 10	7 : 30
F9	236	100	6.4	4.4	5 : 25	9 : 00
F10	237	130	6.5	2.5	4 : 45	7 : 00
F11	237	140	6.6	0.6	4 : 00	6 : 05

is required in fly ash concrete than for a similar concrete containing no fly ash. This increase in the requirement of the quantity of AEA is: (i) because of the greater surface area of the fly ash in concrete. Fly ash is generally finer than cement and the volume of fly ash added is normally more than the volume of the cement replaced. Due to this, a greater volume of air entraining agent is needed to provide the same surface concentrations of the air entraining agent; and (ii) secondly, the main reason leading to the increased demand of AEA is related to the carbon content, expressed in terms of loss on ignition of fly ash. Since 1980, loss on ignition limit in ASTM C618 has been reduced to 6.0% from the earlier permitted limit of 12% for the effective use of fly ash in air entrained concrete.

Gebler and Klieger (1983) investigated the requirements of AEA for Class C and Class F fly ashes. They reported that: (i) concretes made with Class C fly ash generally require less AEA than those made with Class F fly ashes; and (ii) for 6% air content in concrete, the AEA varied from 126 to 173% for fly ashes having more than 10% CaO, whereas it was in the range of 177–553% for fly ashes containing less than 10% CaO.

Joshi et al. (1993) reported that for some Class F fly ashes replacing about 50% cement, the average requirement of AEA was found to be more than double that of the equivalent plain concrete. A wide range of AEA demand was reported by Carette and Malhotra (1984) from the study of concretes made with Canadian fly ashes to entrain about 6% air content.

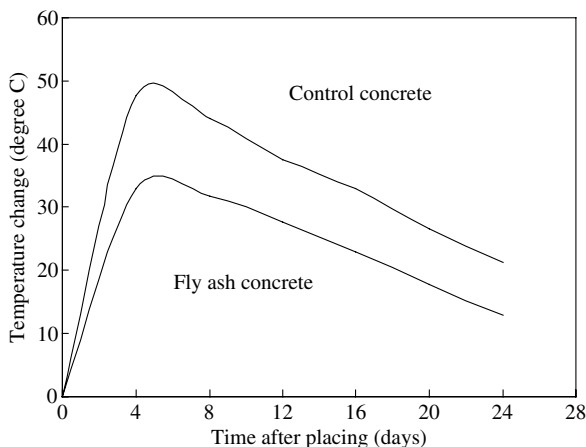
Fly ash addition affects both air content and loss of air content with time in plastic or fresh concrete depending upon the type of fly ash. Gebler and Klieger (1983) suggested that increase in both total alkalies and SO_3 contents in fly ash affect the air entrainment favorably. A concrete containing a Class F fly ash that has relative high CaO content and less organic matter or carbon tends to be less vulnerable to loss of air.

Burns et al. (1982) made attempts to neutralize the absorption characteristics of activated carbon in fly ash by using chlorine gas, calcium hypochlorite and some other surface active agents to resolve the problem of increased AEA demand. However, these studies need to be substantiated for practical use. The deactivating agents used for carbon in fly ash should not interfere with air entrainment and concrete durability on their own. Economy is another important factor to be considered in developing suitable remedial additives for solving the problem of AEA demand in concrete.

6.4.5 Temperature Rise

Hydration of Portland cement paste is accompanied by evolution of heat that causes temperature rise in concrete. Since pozzolanic reactions are slower, partial replacement of cement by fly ash results in release of heat over a longer period of time and the concrete temperature remains lower because heat is dissipated as it is evolved.

Fig. 6.3 Temperature rise curve for fly ash and plain concrete test sections (Compton and Macinnis, 1952)



Compton and Macinnis (1952) reported temperature-time curves, shown in Fig. 6.3 for control and fly ash concretes. In fly ash concrete, cement was replaced with 30% fly ash. This particular phenomenon is very useful in mass concreting, where cooling following a significant temperature rise due to the generation of the heat of hydration occurs, stresses can develop and cause cracking. Temperature rise, in fact, depends upon more factors than the rate of heat generation associated with hydration and pozzolanic reactions, including the rate of heat loss and the thermal properties of the concrete and the surrounding medium.

Sivasundram et al. (1989) and Langley et al. (1989) reported favorable effect of fly ash incorporation in concrete on temperature rise of not only massive concrete dams, but also in concrete mat foundations and massive columns in lower storey of the tall buildings. Low calcium Class F fly ashes generally tend to reduce the rate of temperature rise more as compared to high calcium Class C fly ashes (Crow and Dunstan, 1981). Some high calcium Class C fly ashes with self cementitious properties may react very rapidly with water, thus releasing excessive heat just like normal Portland cement hydration.

Bamforth (1980) investigated the temperature rise in large size foundation made with concrete containing fly ash and slag. Three types of concretes were used. They were: (i) control concrete with a Portland cement content of 400 kg/m^3 ; (ii) mix with 75% of the Portland cement replaced by GGBS; and (iii) mix with 30% of the Portland cement replaced by a bituminous fly ash. It was observed that with an increase in the quantity of cement replaced by fly ash and slag, the rate of heat release was slowed down and as a result the maximum temperature reached at any point in the concrete mass was lower than the control concrete.

ACI committee 211.1.81 (1984) estimated that on equivalent mass basis fly ash contributes to early age heat liberation in the range of 15–30% compared to normal Portland cement. Low calcium bituminous fly ash was successfully used to control the rise of temperature at early age in the construction of concrete structures, particularly dams. In general, incorporation of fly ash as replacement of normal Portland

cement exhibits less temperature rise than concrete without fly ash. Where early age strength is not the main design consideration, large quantities of cement replaced by fly ash are anticipated to reduce the rate and also amount of heat hydration significantly.

Atis (2002) studied the heat evolution of high-volume fly ash (HVFA) concrete. Heat evolution of concrete was studied by measuring the temperature increase in concrete under adiabatic curing condition. They concluded that: (i) characteristic of heat evolution of fly ash concrete was found to be strongly dependent on the replacement level of fly ash and dosage of superplasticizer; (ii) use of fly ash as cement replacement resulted in a reduction on the maximum temperature rise. Increasing the replacement level of fly ash caused lower temperature rise in concrete; and (iii) superplasticizer caused a delay in peak temperature rise time; this is taken as an indicator that high-dosage superplasticizer used in concrete caused retardation in hydration of cement. Concretes having similar ingredients showed similar peak temperature rise whether they are superplasticized or not.

6.5 Properties of Hardened Concrete Containing Fly Ash

6.5.1 Strength Development

Rate of strength development depends upon many factors such as: (i) fly ash characteristics such as its chemical and mineralogical composition, fineness, pozzolanic reactivity; (ii) type of cement; (iii) replacement level of cement with fly ash; (iv) mixture proportions; (v) ambient temperature; and (vi) curing environment.

The highly pozzolanic fly ashes start their contribution to strength development almost from the onset of Portland cement hydration. But the low calcium fly ashes do not exhibit significant pozzolanic activity to affect strength until about two weeks after hydration. However, some high calcium fly ashes, with calcium oxide content more than 15%, may start contributing to strength development as early as 3 days after mixing because of their self hardening and pozzolanic properties.

Because of its fineness as well pozzolanic reactivity, fly ash in cement concrete significantly improves the quality of cement paste and the micro-structure of the transition zone between the binder matrix and the aggregate. As a result of the continual process of pore refinement, due to the inclusion of fly ash hydration products in concrete, a gain in strength development with curing age is achieved. When high calcium Class C fly ash is used, the strength development with time is likely to be different from the one using Class F fly ash. The self-hardening reactions in the Class C fly ashes are likely to occur within the same time frame as the normal Portland cement hydration reactions, giving equal or sometimes greater strengths at early ages. The pozzolanic activity of such cementitious fly ashes further enhances strength at later ages.

Raba et al. (1981) determined the compressive strength of concrete made with bituminous fly ash (CaO 20%). In the mixes, fine aggregate was replaced with fly ash by volume, and mass of cement and coarse aggregate was kept constant for each series. Results are given in Table 6.7.

Cook (1982) conducted investigations using a high calcium fly ash with CaO content of 30.3% at 25% replacement level to develop concrete mixes with 28-day strength in the range of 55–75 MPa. He reported that as cement factor was increased, sand content and the water to cementitious material ratio was reduced. To maintain workability around 100 mm; water reducing admixture was used in all the mixes. The 180 day strength of the mixes ranged between 68 MPa and 86 MPa.

Joshi et al. (1993) tested a large number of fly concrete mixes made by using three different Alberta fly ashes containing about 10% calcium oxide. The replacement level varied between 40 to 60% by weight of cement. The mixes were superpalasticized and air entrained to obtain 100–120 mm slump and $6 \pm 1\%$ air content. The cementitious material content varied from 380 to 466 kg/m³, water to cementitious material ratio from 0.27 to 0.37, coarse aggregate ranged from 1012 to 1194 kg/m³, and fine aggregate or sand varied from 712 to 643 kg/m³. They reported that: (i) at 7 days, the fly ash concretes obtained strength between 27.9 MPa and 41.0 MPa compared to 44.1 MPa of control concrete. However at 28 days, the fly ash concretes developed strength varying from 37.6 to 50.7 MPa against 58.7 MPa for control concrete. At 120 days, strength of fly ash concrete ranged from 54.8 MPa to 74.6 MPa whereas it was 74.6 MPa of control concrete.

Class F bituminous fly ash contributes to the long term strength gain of concrete more than Class C sub-bituminous or lignite fly ash despite its relatively slower rate of strength development at early age. Swamy and Mahmud (1986) reported that concrete containing 50% low calcium bituminous fly ash as partial replacement of cement replacement developed 20–30 MPa compressive strength at 3 days, 60 MPa at the age of 28 days.

Table 6.7 Compressive of high-calcium fly ash concrete (Raba et al., 1981)

Cement (kg/m ³)	Fly ash (kg/m ³)	Compressive strength (kg/m ²)		
		% of control		% gained from 28 to 56 days
		28 days	56 days	
91	50	318	354	15.2
	59	352	393	16.0
	68	401	435	13.6
	77	471	494	10.5
136	50	210	228	10.2
	59	231	256	11.8
	68	245	269	11.1
	77	253	274	10.3
182	50	149	155	8.2
	59	153	167	12.4
	68	163	177	12.0
	77	187	190	6.2

For a typical low calcium fly ash, it was found that the pozzolanic reaction started at 11 days after hydration at 20°C and the significant effect on compressive strength appeared to occur after 28 days of curing. Mehta (1994) have reported that no significant contribution to strength development was noticed up to 7 days with the use of low calcium fly ash in concrete. At 28 days and beyond most fly ashes at the replacement levels of up to 30% by cement weight exhibited strength gain in concrete and the strength generally equaled that of control concrete.

Carette and Malhotra (1984) studied the effect of Canadian fly ashes on the compressive strength and flexural strength of concrete mixes. Chemical composition of fly ashes collected from 11 different sources has already been given in Table 6.5. Cement was replaced with 20% fly ash in all the mixes. Cylinders of size 150 × 300-mm were cast for compressive strength and prisms of size 75 × 100 × 400-mm for flexural strength. Compressive strength was measured up to the age of 365 days, and flexural strength up to the age of 91 days. Results are given in Table 6.8. It can be seen from the table that both compressive and flexural strength continued to increase with age, indicating pozzolanic action of fly ashes.

Haque et al. (1988) reported that Class F bituminous fly ashes from Alberta power plants can be used under proper curing conditions to produce concrete at 35–50% cement replacement having 80–100% of the strength of an equivalent plain concrete after being cured for 90 days.

Haque et al. (1988) concluded that for concrete mixes with 40–75% bituminous fly ash replacing cement, the increase in flexural strength was slightly less than the increase in compressive strength between 28 days and 91 days of curing.

Erdoğan and Türker (1998) studied the effect of particle size of high and low calcium fly ash on the compressive strength of mortar. Major chemical compounds in High calcium ash were 19.43% Al_2O_3 , 46.45% SiO_2 , 12.69% CaO and 9.32% Fe_2O_3 , whereas low calcium fly ash had 27.72% Al_2O_3 , 57.30% SiO_2 , 2.24% CaO and 5.72% Fe_2O_3 . Fly ashes were sieved from the 125, 90, 63, and 45 μm sieve by a sieve-shaker. Six different size groups, including the all-in ash, were obtained for both the ashes and the materials retained on each sieve. They were; material

Table 6.8 Properties of hardened concrete (Carette and Malhotra, 1984)

Mixture No.	Compressive strength (MPa)				Flexural strength (MPa)		
	7 days	28 days	91 days	365 days	14 days	28 days	91 days
Control	23.4	30.6	34.9	39.2	4.9	5.4	5.9
F1	18.4	25.7	31.4	38.3	4.4	4.4	5.4
F2	16.9	25.2	34.8	37.0	3.9	4.8	5.5
F3	14.4	21.0	27.6	34.4	4.0	5.0	5.3
F4	17.8	23.3	32.3	36.9	4.1	4.4	5.2
F5	20.1	28.0	33.9	44.3	3.5	4.4	5.3
F6	18.4	24.8	31.8	39.2	3.5	4.6	5.6
F7	16.7	24.1	29.1	35.7	3.9	4.5	5.4
F8	17.9	27.7	29.0	40.4	4.6	5.0	6.1
F9	16.7	24.9	31.1	35.6	4.3	4.2	5.7
F10	19.2	28.5	33.7	39.7	4.1	5.1	5.8
F11	21.1	29.4	35.3	40.1	4.8	5.3	6.6

retained on 125 μm sieve, material having 125–90, 90–63, and 63–45, and material passing 45 μm sieve. For strength tests, mixtures composed of 25% fly ash and 75% Portland cement, by weight, were prepared. Tests were conducted up to the age of 90 days, and results are given in Table 6.9. It is evident from these results that: (i) high-calcium ash incorporated mortars exhibited higher strength than mortars with low-calcium ash at all ages; and (ii) for both of the ashes, the finer the size of a fraction, higher was the compressive strength.

Siddique (2003a) investigated the effect of partial replacement of fine aggregate (sand) with varying percentages of Class F fly ash on the strength properties of concrete. Fine aggregate (sand) was replaced with five percentages (10, 20, 30, 40, and 50%) of Class F fly ash by weight. A control mix without fly ash was proportioned to have a 28-day cube compressive strength of 26.4 MPa. 150-mm concrete cubes were cast for compressive strength, 150 \times 300 mm cylinders for splitting tensile strength, and 101.4 \times 101.4 \times 508 mm beams for flexural strength. Tests were performed up to the age of 365 days. Compressive strength, splitting tensile and flexural strength results are shown in Figs. 6.4, 6.5 and 6.6, respectively. Based on the results, he concluded that: (i) compressive strength, splitting tensile strength, and flexural strength of fine aggregate (sand) replaced fly ash concrete specimens was higher than the plain concrete (control mix) specimens at all the ages. The strength differential between the fly ash concrete specimens and plain concrete specimens became more distinct after 28-days; (ii) all the three strengths continued to increase with age for all fly ash percentages; (iii) The maximum compressive strength occurs with 50% fly ash content at all ages. It was 40.0 MPa at 28-day, 51.4 MPa at 91-day, and 54.8 MPa at 365-day; (iv) at all the ages, the maximum splitting tensile strength was observed with 50% fly ash content. It was 3.5 MPa at 28-day, 4.3 MPa at 91-day, and 4.4 MPa at 365-day; (v) maximum flexural strength was found to occur with 50% fly ash content at all ages. It was 4.3 MPa at 28-day, 5.2 MPa at 91-day, and 5.4 MPa at 365-day; and (vi) results of this investigation suggests that Class-F fly ash could be very conveniently used in structural concrete.

Table 6.9 Compressive strength results of the mortars (Erdoğan and Türker, 1998)

		2 day (N/mm ²)	7 days (N/mm ²)	28 days (N/mm ²)	90 days (N/mm ²)
25% High + 75% PC 32.5	All-in ash	27.6	36.7	46.7	55.7
	Above 125 μm	19.2	26.6	31.2	33.2
	125–90 μm	22.6	27.6	35.0	38.4
	90–63 μm	24.8	31.3	35.4	42.6
	63–45 μm	26.6	35.1	41.4	47.5
25% Low + 75% PC 32.5	Under 45 μm	32.0	43.0	55.8	64.6
	All-in ash	23.5	33.2	39.6	47.4
	Above 125 μm	17.9	24.4	26.7	29.9
	125–90 μm	21.6	29.2	32.0	37.1
	90–63 μm	22.6	29.6	34.9	40.6
100% PC 32.5	63–45 μm	23.8	33.5	37.4	46.8
	Under 45 μm	26.6	37.3	43.4	57.2
		38.0	44.4	51.6	58.2

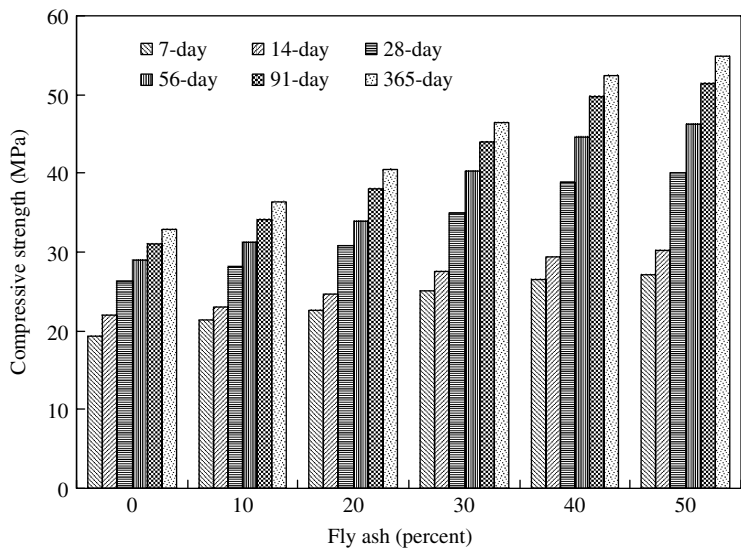


Fig. 6.4 Compressive strength versus fly ash percentage (Siddique, 2003a)

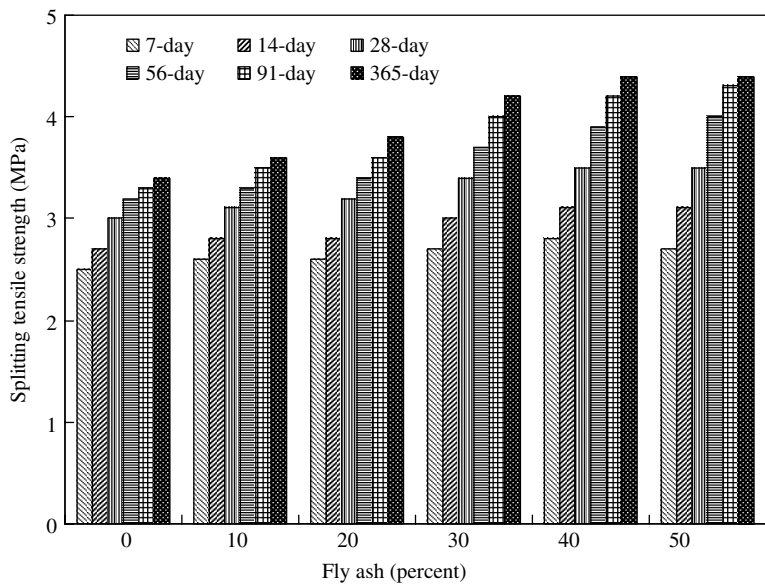


Fig. 6.5 Splitting tensile strength versus fly ash percentage (Siddique, 2003a)

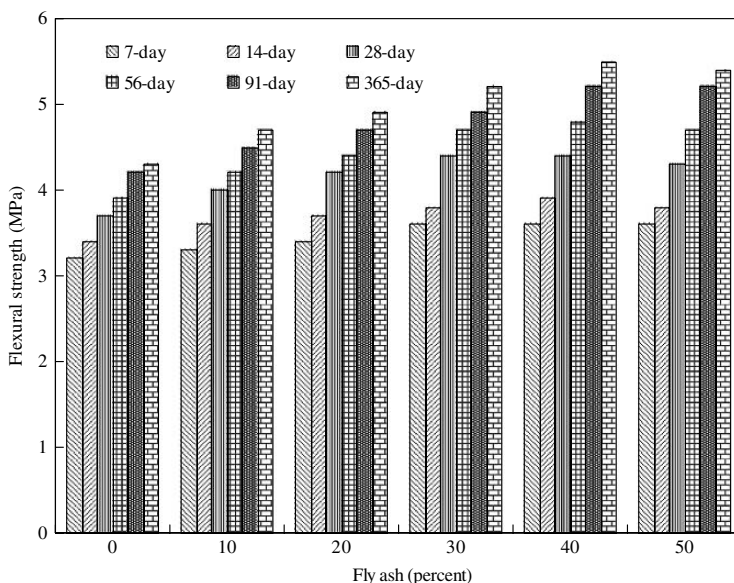


Fig. 6.6 Flexural strength versus fly ash percentage (Siddique, 2003a)

Saraswathy et al. (2003) investigated the influence of activated fly ash on the compressive strength of concrete. Various activation techniques, such as physical, thermal and chemical were adopted. Concrete specimens were prepared with 10, 20, 30, and 40% of activated fly ash replacement levels with cement. Compressive strength was determined at the age of 7, 14, 28, and 90 days. They concluded that: (i) activation of fly ash improved the strength of concrete. However, the compressive strength of fly ash concrete was less than that of OPC even after 90 days of curing; and (ii) among the activation systems studied, chemically activated fly ash (CFA) system improved the compressive strength to a certain extent, only 10% and 20% replacements. Since the CFA surface layer is etched by a strong alkali to facilitate more cement particles to join together and also the addition of CaO which is further promoting the growth of CSH gel and Ca(OH)_2 which is more advantageous to enhance the strength development.

Chindaprasirt et al. (2007) studied the effect of fly ash fineness on the compressive strength of concrete. Three fly ash finenesses: coarse, medium and fine were used. The coarse fly ash was 100% original fly ash (100FA). The medium fly ash was the 45% fine portion of the original fly ash (45FA). The fine fly ash was the 10% fine portion of the original fly ash (10FA). Three concrete mix series viz. a low, normal and a high strength concrete mix series were made. For the low and normal strength concrete, the water-to-cement ratios of 0.540 and 0.480, respectively, were used for PC mixes. For the high strength concrete, the water-to-cement ratio was 0.250 with the use of superplasticizer. The fly ash dosage of 30% by weight of binder was used for all fly ash concrete mixes. Compressive strength of concrete mixes was

Table 6.10 Compressive strength of concrete (Chindapasirt et al., 2007)

Mix	Compressive strength (MPa)		
	7 days	28 days	90 days
PC1	24.5	33.5	35.2
100FA1	24.5	41.0	47.0
45FA1	32.5	40.5	49.0
10FA1	31.0	46.5	51.5
PC2	33.0	48.5	53.0
100FA2	31.0	46.0	55.0
45FA2	32.5	44.0	57.5
10FA2	35.5	52.0	61.5
PC3	62.5	79.5	85.5
100FA3	51.5	84.0	88.5
45FA3	50.5	72.5	83.5
10FA3	59.5	71.0	82.5

determined up to the age of 90 days, and results are given in Table 6.10. It can be seen from this table that the strength of fly ash concrete were higher than those of the PC concrete in the same group. For the normal strength concrete, the 28 day strength of the PC2 concrete was 48.5 MPa, whereas those of fly ash concretes were between 44.0 and 52.0 MPa. For the high strength concrete, the strength of the PC3 concrete was 79.5 MPa, whereas those of the fly ash concretes were between 71.0 and 84.0 MPa. For the low strength concrete series, the strength of PC1 concrete was lower than the fly ash concrete owing to a very large reduction in the water content of the fly ash concrete. The reduction in the water content, the good dispersing and the filling effect of the fly ash contribute to the relatively good strength development of the fly ash concrete in this series. With the use of finer fly ash, the water content was further reduced and the strength of concrete enhanced further.

Demirboğa et al. (2007) investigated the role of high-volumes of Class C fly ash on the compressive strength of concrete. Cement was replaced with 0, 50, 60, and 70% fly ash. Compressive strength of concrete mixtures was determined at the age of 3, 7, 28, and 120 days. Based on the investigation, they reported that: (i) FA reduced compressive strength of concrete at all levels of replacement at 3, 7, 28, and 120 days; (ii) reductions were very high at early ages, but with increase in curing period the reduction percent decreased. Reductions at 3-day curing period were 69, 84, and 91% for 50, 60, and 70% FA replacement of PC, respectively. At 28-days curing period, these values reduced to 52, 68, and 78% for 50, 60, and 70% FA replacement of PC, respectively. At 120-days curing periods, reductions were 36, 43, and 50% for 50, 60, and 70% FA replacement of PC, respectively; and (iii) that cement paste containing FA showed a steady reduction in strength at 3, 7, 28, and 120 days as a function of replacement percentage. This can be directly related to the properties of FA that decrease the heat of hydration of cement and required long curing period. Results of numerous studies have indicated that FA slows the rate of hardening and reduces the early age compressive strength of concrete.

6.5.1.1 Effects of Curing Conditions

Gifford et al. (1987) studied the effect of dry curing on unprotected concrete specimens at 0 and 5°C made with 40% cement replacement with fly ash. They found that within 50 hours after casting, about 30 and 60% of the mixing water was lost through evaporation from unprotected surfaces on curing at 50 and 10% relative humidity, respectively. In addition to strength loss due to evaporation of water, it was reported that the combination of low curing temperature and the cooling effect of concomitant evaporation of water at low humidity would significantly retard the rate of hydration and thereby strength development. The importance of curing concrete in an enclosed environment particularly at low temperatures is therefore stressed in order to mitigate the effect of water evaporation during the initial hours after the placing of concrete.

Based on the satisfactory level of strength development at 28 days for a high volume fly ash concrete, made with Class F fly ash that had been moist cured for 3 days, Langley et al. (1989) reported that minimum duration of moist curing for fly ash concrete was 3 days after which normal curing practices as for ordinary plain concrete might be employed without any significant adverse effects. They also pointed out that long term strength development in mass fly ash concrete was less influenced by dry curing than much smaller test specimens used in the laboratory.

Swamy and Mahmud (1986) examined the effect of curing regime on strength development of high volume fly ash concrete mixes (Table 6.11). They reported 50–100% increase in strength over the 28-day strength of fly ash concrete after one year under-continuous moist or fog curing compared to only 18–25% increase for the control or plain concrete under similar curing conditions. Under the other two curing regimes, one with 7 day moist curing followed by air drying and the other with continuous dry curing, the corresponding increase in strength of fly ash concrete after one year varied between 6 to 22% of the 28 day strength of the reference concrete.

Haque et al. (1988) reported that mixes with Alberta fly ashes replacing up to 50% cement showed smaller reduction in strength at lower ash contents when curing were done at 50% relative humidity at room temperature of about 23°C.

Gopalan (1996) studied of effect of curing conditions on the compressive strength of concretes made with fly ash. Compressive strength was determined for three

Table 6.11 Rate of strength development of 28-day strength (Swamy and Mahmud, 1986)

Age (days)	Strength (MPa)								
	20			40			60		
	FOG	DRY	7F+D	FOG	DRY	7F+D	FOG	DRY	7F+D
1	19	–	–	25	–	–	34	–	–
7	55	71	–	67	80	–	68	79	–
28	100	100	100	100	100	100	100	100	100
150	176	125	104	140	119	105	135	123	117
270	197	114	110	150	125	116	140	113	121
365	209	118	106	162	122	107	146	116	118

7f+d = 7 days fog followed by air dry curing.

grades (designated as M1, M2 and M3) of cement concrete having water cement ratios of 0.53, 0.62 and 0.88. Each grade of concrete was then incorporated with two levels (20 and 40%) of fly ash replacement with cement by weight. Cylinders of size 200×100 mm were cast. Samples were subjected to standard fog curing at $23^{\circ}\text{C} \pm 2^{\circ}\text{C}$ and relative humidity of $95 \pm 3\%$ for seven days. Samples were also cured (dry curing) at $23^{\circ}\text{C} \pm 2^{\circ}\text{C}$ and relative humidity of $50 \pm 3\%$. Compressive strength results are given in Table 6.12. It is evident from these results that fly ash replacements up to 20% did not have a significant impact on the long term strength of fog cured mixes. The results from the fog cured samples showed that the rate of loss of strength was higher for richer mixes. Under drying conditions, there was no noticeable increase in strength after 91 days and strength development pattern did not depend upon the grade of the mix.

6.5.1.2 Effect of Curing Temperature at Early Age on Strength Development

The rate of pozzolanic reaction of fly ash in cement concrete is significantly influenced by curing temperatures at early ages as is the case of cement hydration reactions. Pozzolanic reactions are highly temperature dependent. The higher the curing temperature, higher is the rate of the pozzolanic reactions. When concrete made with Portland cement is cured at temperatures in excess of 30°C , an increase is seen in strength at early ages but a marked decrease in strength is observed in mature concrete (Neville, 1973)

William and Owens (1982) reported that concrete containing fly ash concrete behaved significantly different than concrete made with Portland cement as shown in Fig. 6.7. In contrast to the loss of strength that occurred with ordinary Portland cement concrete, fly ash concretes exhibited strength gains as a consequence of heating. The favorable effects of fly ash in concrete cured at moderately elevated temperatures can be advantageously used in the construction of mass concrete or concrete construction at elevated temperatures.

Ravina (1981) concluded that fly ash concrete subjected to high temperature at an early age of curing exhibited increased rate of strength gain possibly due to the

Table 6.12 Compressive strength of fly ash concretes (Gopalan, 1996)

Mix	Age of concrete (days)					
	28		91		180	
	Fog	Dry	Fog	Dry	Fog	dry
M1-00	49.9	45.1	58.8	61.2	51.9	
M2-00	33.1	31.1	40.2	37.0	42.6	34.3
M3-00	18.9	15.4	21.0	18.6	20.8	16.9
M1-20	36.2	32.1	44.0	40.2	53.9	41.1
M2-20	25.2	22.4	33.1	26.6	42.4	27.4
M3-20	13.6	11.3	17.2	14.0	22.0	13.5
M1-40	20.4	16.7	28.3	21.5	35.8	20.9
M2-40	19.2	16.6	27.5	20.8	35.5	19.6
M3-40	10.3	7.5	13.1	9.5	18.1	9.2

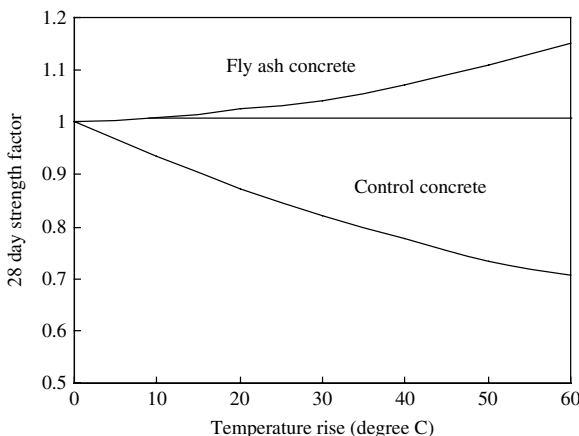


Fig. 6.7 Effect of temperature rise during curing on the compressive strength development of concretes (William and Owens, 1982)

higher rate of pozzolanic reactions. It was suggested that when concrete was cured at elevated temperatures, large quantities of fly ash may be incorporated with a significant improvement in strength compared to the rather limited contribution under normal curing conditions up to 28 days.

Ozer and Ozkul (2004) reported the influence of initial water curing on the strength development of ordinary Portland cement and pozzolanic cement concretes. They concluded that poor curing conditions more adversely affects the strength of concrete made from pozzolanic cement than that of ordinary Portland cement. Atis (2005) worked on strength properties of high-volume fly ash roller compacted and workable concrete, and the influence of curing condition. He reported that fly ash–cement concrete was more sensitive to dry curing conditions than conventional concrete.

Yazici et al. (2005) investigated the effect of curing conditions on the compressive strength of high-volume fly ash concrete mixtures. Cement was replaced with up to 70% fly ash, and concrete mixtures with 360 kg/m^3 cementitious content and a constant water/binder ratio of 0.4 were made. The curing conditions were standard curing in water and steam curing. Compressive strength of concrete mixtures was determined up to the age of 90 days. Based on the test results, they concluded that: (i) under standard curing conditions, the 1-day compressive strength decreased sharply with increasing fly ash content. However, at later ages (beyond 3 days), this difference diminished. The strength of 30% fly ash mixture was approximately equal to control mix strength at 3 days. At 7 days, 40% fly ash mixture exceeded the control mix strength, while the 50% and 60% fly ash mixtures reached the control mix strength at 28 days and 56 days, respectively. Strength was approximately 10 MPa at 1-day and 20 MPa at 3 days with 50% and 60% fly ash content, which is quite satisfactory for most cast-in place structural elements; and (ii) under steam curing, with increasing amount of fly ash content, compressive strength at early ages decreased. However, application of steam curing increased the 1-day compressive

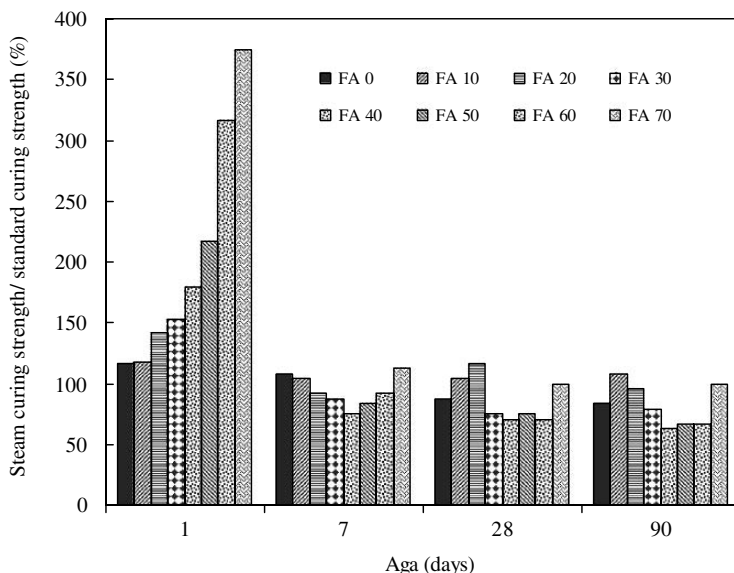


Fig. 6.8 The effectiveness of steam curing (Yazici et al., 2005)

strength of 50% FA concrete to 20 MPa, which is adequate for formwork removal, and therefore, beneficial for fabrication of precast products. Application of steam curing did not improve the later-age compressive strength of high volume fly ash concrete as much as standard curing. For example, steam-cured high-volume fly ash concrete mixture containing 50% fly ash showed only 40 MPa strength at 90 days compared to 60 MPa for the standard-cured mixture at the same age. Figure 6.8 shows the effectiveness of steam-curing versus standard curing for different ages. It is evident from this figure that the high-volume fly ash systems containing 40% or more fly ash, steam-curing may be of interest only when 1-day strength is the sole consideration.

Termkhajornkit et al. (2006) studied the effect of water curing condition on compressive strength of fly ash–cement paste. Replacement ratios of fly ash were 0%, 25% and 50% of total powders. The water to binder ratio was 0.80 and 1.00 by volume. Mix proportion and curing condition details are given in Table 6.13. Compressive strength of fly ash–cement paste is given in Table 6.14. Based on the results, they reported that: (i) for the samples prepared with water curing condition, the compressive strength of 0% FA increased until 91 days but suddenly dropped at 182 days. The compressive strength of 25% FA and 50% FA continually increased until 182 days. At 182 days, the compressive strength of 25% FA was higher than that of the cement paste. For the samples prepared under 7 days initial curing condition, the compressive strength of 0% FA was almost constant. The compressive strength of 50% FA increased until 28 days and after that became nearly constant. In contrast, the compressive strength of 25% FA constantly increased until 56 days. At this age, its compressive strength became close to that of cement paste; and (ii) regarding the

Table 6.13 Mix proportion and curing condition (Termkhajornkit et al., 2006)

Water/binder (W/B)	FA (%)	Curing condition	Code
0.8	0	In water	0.8-0-W
0.8	25	In water	0.8-25-W
0.8	50	In water	0.8-50-W
1.0	0	In water	1.0-0-W
1.0	25	In water	1.0-25-W
1.0	50	In water	1.0-50-W
1.0	0	In water 7 days	1.0-0-W7
1.0	25	In water 7 days	1.0-25-W7
1.0	50	In water 7 days	1.0-50-W7
1.0	0	In water 3 days	1.0-0-W3
1.0	25	In water 3 days	1.0-25-W3
1.0	50	In water 3 days	1.0-50-W3

effect of curing condition on the compressive strength, for 0% FA, the compressive strength of samples cured in water was higher than others except at 182 days. In contrast, there was no significant difference among compressive strength of samples cured in water 7 days and 3 days. As for 25% FA and 50% FA, the effect of water curing condition is small, especially for 25% FA.

6.5.2 Elastic Properties

Several investigators (Ghosh and Timusk, 1981; Lane and Best, 1982; Langley et al., 1989; Lohtia et al., 1977; Nasser and Marzouk, 1983) have observed that the effect of fly ash addition as cement replacement on modulus of elasticity of concrete is almost the same as on compressive strength. The modulus of elasticity of fly ash concrete is generally lower at an early age and is slightly higher at late ages.

Lohtia et al. (1977) observed that as compared to compressive strength gain, the increase in modulus of elasticity was less with the incorporation of 15–25% Class F

Table 6.14 Compressive strength of fly ash-cement paste (Termkhajornkit et al., 2006)

Mix/curing condition code	Compressive strength (MPa)				
	7 days	28 days	56 days	91 days	182 days
0.8-0-W	117.03	150.91	145.99	129.91	150.11
0.8-25-W	80.89	113.36	115.06	116.7	163.29
0.8-50-W	41.45	65.42	69.41	83.72	104.81
1.0-0-W	91.84	114.71	127.24	128.63	90.19
1.0-25-W	55.39	78.58	88.72	94.2	94.7
1.0-50-W	29.93	44.7	46.51	55.69	69.24
1.0-0-W7	91.84	95.89	94.97	96.68	97.94
1.0-25-W7	55.39	71.54	69.37	84.75	89.51
1.0-50-W7	29.93	42.84	48.45	48.29	46.77
1.0-0-W3	85.02	95.47	94.61	97.04	94.01
1.0-25-W3	65.17	71.82	87.68	77.18	98.51
1.0-50-W3	30.78	40.19	46.9	45.04	48.55

fly ash in concrete at the age of 90 days. In general, fly ash increased the modulus of elasticity of concrete when concretes of the same strength with and without fly ash are compared. Ghosh and Timusk (1981) reported that for all strength levels, the modulus of elasticity of fly ash concrete was generally equivalent to that of the corresponding reference concrete. They also found that the observed modulus exceeded the value given by the ACI formula, $E_c = 0.043 W(fc)^{3/4}$ MPa, where W is unit weight of concrete in kg/m^3 and f_c is compressive strength in MPa.

Normally fly ash properties affecting the compressive strength of concrete also influence the modulus of elasticity but to a lower extent. Crow and Dunstan (1981) reported that like Portland cement concrete, fly ash concrete had increased modulus of elasticity with age concomitant with the compressive strength development. The modulus of elasticity ranged from a low of 18.8 GPa at 28 days to a high of 39.6 GPa at 365 days. The majority of the fly ash concrete had a 28 day Poisson's ratio ranging from 0.14 to 0.25. At elevated temperatures, the modulus of elasticity of fly ash concrete using Saskatchewan lignite fly ash decreased in a similar way as that of plain concrete. Nasser and Marzouk (1983) reported that when fly ash concrete was heated from 21 to 232°C in the sealed containers to prevent loss of moisture, the modulus of elasticity was reduced up to 40%.

Langley et al. (1989) found that at the age of 28 days, the modulus of elasticity of concretes made with 50% fly ash constituting the cementitious material varied between 27.9 GPa and 36.1 GPa compared to 31.5–36.8 GPa for control concrete mixes. However, at 365 days, fly ash concrete mixes exhibited significant increase in modulus of elasticity compared to control concrete mixes.

Siddique (2003a) studied the effect of partial replacement of fine aggregate (sand) with varying percentages of Class F fly ash on the modulus of elasticity of concrete. Fine aggregate (sand) was replaced with five percentages (10, 20, 30, 40, and 50%) of Class F fly ash by weight. A control mix without fly ash was proportioned to have a 28-day cube compressive strength of 26.4 MPa. 150 × 300 mm cylinders were cast for modulus of elasticity. Tests were performed up to the age of 365 days. Results of modulus of elasticity are shown in Fig. 6.9. He concluded that: (i) Modulus of elasticity of fine aggregate (sand) replaced fly ash concrete specimens was higher than the plain concrete (control mix) specimens at all the ages. The differential between the fly ash concrete specimens and plain concrete specimens became more distinct after 28-days; (ii) modulus of elasticity of fine aggregate (sand) replaced fly ash concrete continued to increase with age for all fly ash percentages; and (iii) at all ages, the maximum value of modulus of elasticity occurs with 50% fly ash content. It is 24.5 GPa at 28-day, 28.0 GPa at 91-day, and 29.0 GPa at 365-day.

6.5.3 Porosity

Shafiq and Cabrera (2004) investigated the influence of curing conditions on the porosity and degree of saturation of normal concrete (100% OPC) and blended cement concrete (OPC/FA). Three different concrete mixes were prepared using 0, 40,

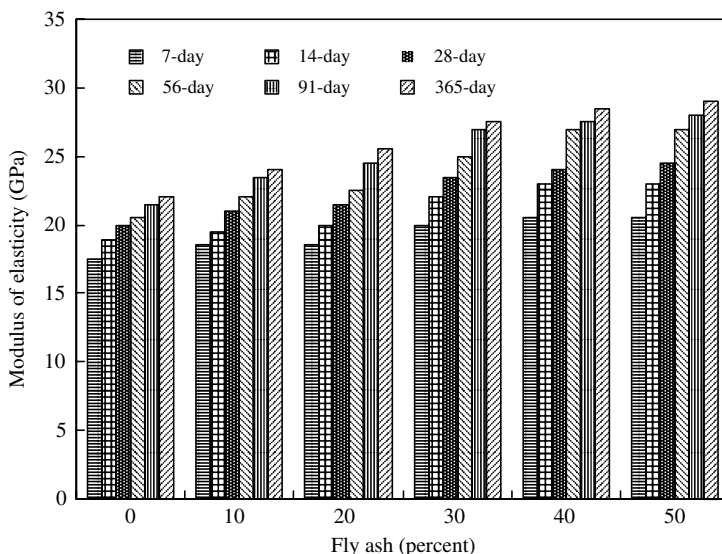


Fig. 6.9 Modulus of elasticity versus fly ash percentage (Siddique, 2003a)

and 50% fly ash content as partial substitution for cement. Mix proportion of control concrete was 1:2.33:3.5. Concrete slabs of dimensions 400 mm long, 250 mm wide, and 40 mm thick, were cast in a wooden mould. After 24 h the moulds were stripped and slabs were cured for 28 days under two different curing conditions, wet cured (in the fog room) and dry cured (at 65% RH at 20°C). At the end of this initial curing, 50 mm diameter cylindrical discs were cored out from the slabs. After initial curing, samples were exposed to different climatic conditions (75, 65, 40, and 12% relative humidity at a constant temperature of 20°C) until the equilibrium moisture condition was achieved. Total porosity and degree of saturation was determined using vacuum saturation technique (RILEM CP113, 1984). Porosity of concrete samples is shown in Fig. 6.10. Degree of saturation results are given in Table 6.15. They concluded that: (i) initial curing conditions affect the total porosity of concrete mixes. For OPC concrete, total porosity of dry cured samples was 5–10% higher than that of their corresponding wet cured samples. For 40 FA concrete, the total porosity of dry cured samples was increased by 9–20% as compared to that of wet cured samples, whereas a significantly higher porosity value of dry cured 50 FA concrete samples was obtained with respect to the corresponding wet cured samples, it ranged from 23% to 40% higher porosity value; (ii) average value of the degree of saturation of wet cured samples equilibrated at 75% RH was obtained as 68%, whereas for the corresponding dry cured samples it was determined as 56%. Similarly, an average value of 15% and 13% was determined respectively for wet cured and dry cured samples, those were equilibrated at 12% RH; and (iii) initial curing condition is one significant factor that controls the porosity and pore network formation of different types of concrete.

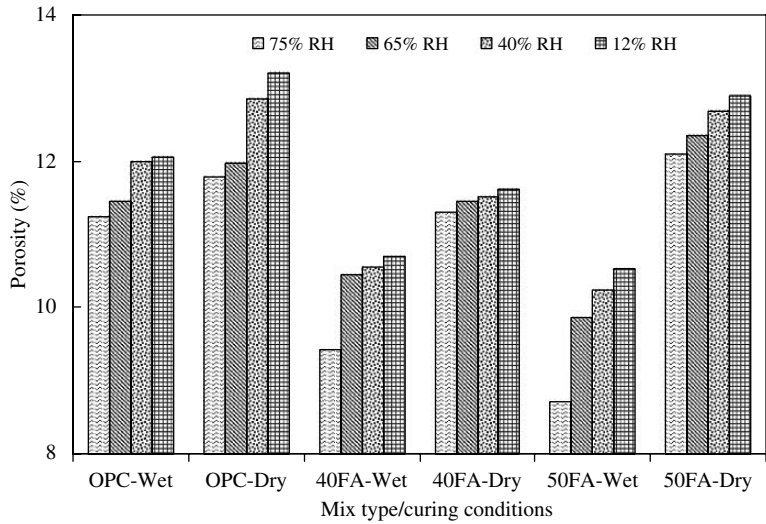


Fig. 6.10 Total porosity of different concrete mixes (Shafiq and Cabrera, 2004)

6.5.4 Sorptivity

Gopalan (1996) studied the sorptivity of concretes made with fly ash. Sorptivity measurements based on capillary movement of water were made on three grades (designated as M1, M2 and M3) of cement concrete having water cement ratios of 0.53, 0.62 and 0.88. Each grade of concrete was then incorporated with two levels (20 and 40%) of fly replacement with cement by weight. 100 × 25 mm discs were made for absorption tests. Samples were subjected to standard fog curing at 23°C ± 2°C and relative humidity of 95±3% for seven days. Samples were also cured (dry curing) at 23°C ± 2°C and relative humidity of 50±3%. Measured sorptivity results are given in Table 6.16. Based on the results obtained, he concluded that: (i) addition of fly ash influenced the sorptivity of the hardened concrete which strongly depended on the curing conditions. When fog cured concretes of identical strengths were considered, sorptivity of the fly ash concretes was found to be lower than that of cement concrete. Under drying curing conditions, the fly ash concrete

Table 6.15 Degree of saturation of OPC and FA blended cement concrete cured in wet and dry conditions (Shafiq and Cabrera, 2004)

RH (%)	Measured degree of saturation (%)					
	OPC		40 FA		50 FA	
	Wet	Dry	Wet	Dry	Wet	Dry
75	68.87	59.07	70.24	53.23	66.04	51.45
65	59.34	53.01	61.54	49.04	53.03	47.15
40	34.98	29.97	29.59	28.29	27.97	24.54
12	14.71	13.20	11.69	11.61	15.52	12.89

Table 6.16 Sorptivity (mm/hr^{1/2}) of fly ash concretes (Gopalan, 1996)

Mix	Age of concrete (days)					
	28		91		180	
	Fog	Dry	Fog	Dry	Fog	dry
M1-00	10.4	12.1	10.1	10.6	10.5	10.9
M2-00	10.5	12.8	9.7	11.3	11.4	12.1
M3-00	12.0	14.1	10.4	13.2	12.2	15.2
M1-20	11.0	15.3	9.0	11.7	8.0	12.4
M2-20	11.6	15.6	10.0	14.0	10.2	17.1
M3-20	13.4	15.9	9.7	16.9	9.6	18.2
M1-40	8.5	13.3	5.9	16.7	8.9	18.0
M2-40	9.6	18.9	8.0	17.0	9.3	22.0
M3-40	11.4	17.2	7.9	22.2	9.4	21.5

had higher sorptivity than cement concrete; (ii) addition of fly ash up to 20% did not change the sorptivity characteristics substantially, but for high fly ash concretes, sorptivity was lower than cement concrete of identical strength; under drying conditions, sorptivity increased by an average of 22%; (iii) for 20% fly ash replacement of 20%, there was no noticeable difference between fog cured fly ash and cement concretes; (iv) for samples under drying conditions, the increase in sorptivity was 19%; and (v) Thus, inadequate curing for a 20% fly ash concrete resulted in an increase of 20% in sorptivity. The corresponding value for 40% fly ash concrete was 60%.

6.5.5 Creep

Creep is the time dependent strain due to sustained loading. The effects of fly ash on creep of concrete are limited primarily to the extent to which fly ash influences the ultimate strength and rate of strength gain. Because of the increase in strength with age due to pozzolanic reactivity, concrete with fly ash proportioned to have the same strength at the age of testing as concrete without fly ash would produce less creep strain at all subsequent ages.

Lohtia et al. (1976) reported the results of creep and creep recovery stress-strength ratios of 20 and 35% of plain and fly ash concretes made by replacing cement with equal weights of fly ash varying from 0 to 25%. Based on their work, they concluded that: (i) replacement of 15% of cement with fly ash was found to be optimum with respect to strength, elasticity, shrinkage and creep of fly ash concrete; (ii) creep-time curves for plain and fly ash concretes were similar with creep linearly related to the logarithm of time; (iii) Increase in creep with fly ash content up to 15% was negligible. However, slightly higher creep occurred with fly ash contents more than 15%; (iv) creep coefficients were similar for the materials with fly ash contents in the range of 0–25%; and (v) creep recovery was found to vary from 22 to 43% of the corresponding 150-day creep. For replacement beyond 15%, the creep recovery

was smaller. No definite trend of creep recovery as a function of stress-strength ratio was observed.

Ghosh and Timusk (1981) found that fly ash concrete proportioned for equivalent 28-day strength of plain concretes ranging from 20 to 55 MPa showed less creep than the plain concrete. The probable reason for the observed behavior was the favorable effect of pozzolanic reactions due to fly ash which caused higher rate of strength gain after the time of loading than for the plain concrete. The results of the investigations by Yuan and Cook (1983) on high strength concretes containing 20–50% high calcium fly ash showed opposite trend in that fly ash concrete containing 30–50% ash had more creep than control concrete. However, the 20% fly ash concrete exhibited about the same creep as control concrete.

Nasser and Marzouk (1983) had also observed that creep of concrete with 20% fly ash under sealed conditions showed a continuing reduction with an increase in temperature except at 177°C, while that of unsealed specimens increased with temperature up to 71°C and decreased thereafter within the range of temperature between 21.4 and 232°C.

Nasser and Al-Manasser (1986) conducted creep tests on superplasticized and air entrained concretes containing 20–50% lignite fly ash from Saskatchewan. They concluded that concrete containing 20% of fly ash in unsealed conditions had on average 72% greater creep than the equivalent sealed concrete for stress-strength rates varying from 10 to 60%. However concrete with 50% fly ash had 13% less creep for unsealed specimens and 39% less for sealed ones. Similar behavior was reported by Carette and Malhotra (1987) with various types of Canadian fly ashes including Saskatchewan fly ash. In the study, concrete with 20% fly ash produced consistently lower creep compared to that of control concrete.

6.5.6 Drying Shrinkage

Volume changes in concrete due to hydration reactions, drying, wetting and drying, and thermal variation occur even without application of any loads. Under normal field conditions, drying shrinkage is an important phenomenon which induces time dependent deformations and is sometimes called creep under zero loads.

Ghosh and Timusk (1981) concluded that for the same maximum size of aggregate and for all strength levels, the shrinkage of concrete containing fly ash was lower than that of concrete without fly ash. Munday et al. (1982) reported that incorporation of fly ash did not significantly affect the shrinkage and expansions due to drying, wetting/drying and thermal changes in concrete.

Yuan and Cook (1983) reported that fly ash concrete containing 30 and 50% fly ash exhibited more creep than either the control concrete or concrete containing 20% fly ash, as shown in Fig. 6.11.

Nasser and Al-Manasser (1986) reported that up to 20% replacements of cement with fly ash did not have significant effect in drying shrinkage of concrete. Increase in drying shrinkage with fly ash addition may occur from increase in the

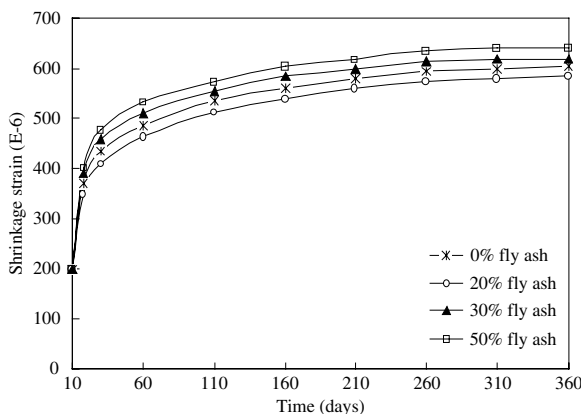


Fig. 6.11 Drying shrinkage of concretes incorporating high-calcium fly ash (Yuan and Cook, 1983)

paste volume if water content is the same. However, if water content is reduced, shrinkage was minimal.

Haque et al. (1988) investigated the shrinkage of concrete made by 40–75% cement replacement with a bituminous fly ash containing 10% calcium oxide. They concluded that drying shrinkage of concrete decreased with increase in fly ash content.

6.5.7 Thermal Conductivity

Thermal conductivity (TC) and other thermal transport properties of construction materials are essential in predicting the temperature profile and heat flow through the material. Mineralogical character of the aggregate greatly influences the TC of concrete (Neville, 1973). Aggregate type can cause nearly twice an increase in TC of concrete and this depends not only on the aggregate composition but also on its degree of crystallization. Aggregate with crystalline structure shows higher heat conduction than amorphous and vitreous aggregate of the same composition. Porosity and moisture content are other important factors that influence the TC of concrete.

Demirboğa (2007) investigated the effect of partial replacement of cement with fly ash on the thermal conductivity of concrete. Cement was replaced with 0, 15, and 30% fly ash. For each mixture, three samples of $110 \times 160 \times 40 \text{ mm}^3$ prisms were prepared. The specimens were dried at the age of 28 days in an oven at $110 \pm 10^\circ\text{C}$ and weighed at 24-h intervals until the loss in weight did not exceed 1% in a 24-h (ASTM C 332) for TC. The specimens' surfaces were sandpapered before measuring their thermal conductivities. A Quick TC Meter (QTM 500) based on ASTM C 1113 (1990) Hot Wire Method was used to measure the TC. Variation of thermal conductivity with fly ash is shown in Fig. 6.12. It can be seen from this figure that TC decreased with the increase in fly ash content. For 15% and 30% FA replacement,

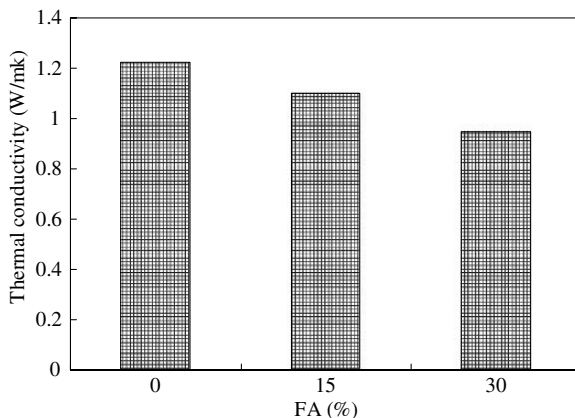


Fig. 6.12 Thermal conductivity of concrete with fly ash (Demirboğa, 2007)

the reductions were 12% and 23%, respectively, compared to the corresponding control specimens.

Demirboğa et al. (2007) studied the thermal conductivity (TC) of concrete incorporating high-volumes of Class C fly ash. Cement was replaced with 0, 50, 60, and 70% fly ash. Thermal conductivity test was conducted at the age of 28 days. They concluded that TC of concrete decreased to 32, 33, and 39% for 50, 60 and 70% fly ash replacement, respectively.

6.6 Durability Properties of Concrete Containing Fly Ash

6.6.1 Permeability

Movement of aggressive solutions into concrete or the removal of the dissolved reaction products out of concrete play an important role in determination of the rate of progress of concrete deterioration caused by chemical attack. Permeability of concrete is very important in determining the rates of mass-transport relevant to destructive chemical action. Therefore, concrete should be relatively impervious so as to enable it to withstand the service conditions for which it has been designed, without serious deterioration over the life span of the structure. The loss of concrete durability may be caused by the severity of the environment to which it is exposed or by internal changes within the mature concrete itself. The external causes may be physical, chemical or mechanical such as weathering, extremes of temperatures, abrasion and erosion, chemical action, and attack by natural or industrial aggressive liquids and gases. Some of the internal causes include alkali-silica reaction and incompatible dimensional changes due to the differences in the thermal properties of aggregate and cement paste. Less permeability generally means more durability.

The permeability of concrete primarily depends on the size, distribution and continuity of the pores of the hydrated paste of the concrete. The important factors

which control the pore structure of the paste are degree of hydration and water cement ratio.

The addition of fly ash results in considerable pore refinement. It transforms bigger pores into smaller ones due to the formation of pozzolanic reaction products concomitant with the progress of cement hydration. Since strength and impermeability are inversely related to the volume of pores larger than 100 Å in the hydrated paste, the phenomenon of pore refinement in fly ash concrete leads to the improvement in these characteristics.

In ordinary Portland cement concrete, calcium hydroxide formed during hydration of Portland cement can be leached out over a period of time. This creates channels available for the ingress of water and deleterious salt solutions. However, when fly ash is incorporated, it reacts with the calcium hydroxide in the water filled capillary channels to produce calcium silicate and aluminate hydrates of the same or similar type that are formed in the normal hydration of cement. Thus the calcium hydroxide is consumed in the pozzolanic reactions and converted to water insoluble hydration products. The reactions reduce the risk of leaching calcium hydroxide. The reaction products also tend to fill capillaries, thereby reducing permeability to aggressive fluids such as chloride or sulfate solutions.

Diffusion of ions, such as chlorides in cured concrete is generally represented by Fick's diffusion law:

$$dc/dt = D_c d^2c/dx^2,$$

Where c is the chloride ion concentration at a distance x after time t , and D_c is the diffusion coefficient of chloride ions in concrete. The values of D_c may vary from 1.0×10^{-9} to $50 \times 10^{-9} \text{ cm}^2/\text{s}$ for high and normal strength concrete, respectively. Short and Page (1982) reported that D_c value for paste with fly ash Portland cement was $14.7 \times 10^{-9} \text{ cm}^2/\text{s}$ compared to $44.7 \times 10^{-9} \text{ cm}^2/\text{s}$ for normal Portland cement paste.

Kasai et al. (1983) studied the air/gas permeability of mortar made with blended cements containing fly ash and blast furnace slag. The study was important from durability aspects of concrete with respect to carbonation. Up to the age of 7 days, blended cement mortars exhibited more permeability than plain cement mortars. However, with increased curing age, the permeability of blended cement mortars decreased. In general terms, the permeability was found to be directly related to the compressive strength development of the mortars.

Rodway and Fedriko (1989) investigated the permeability of concrete incorporating Class C fly ash for 68% cement replacement. They reported a permeability value of the fly ash concrete of about $3.65 \times 10^{-12} \text{ m/s}$. Ellis et al. (1991) observed decrease in permeability of concrete with increase in both either Class C or Class F fly ash contents for a fixed amount of cement. They concluded that: (i) concrete containing Class F was more effective than concrete with Class C fly ash in reducing concrete permeability; and (ii) permeability values of Class F fly ash concrete were either comparable to or superior to those achieved by using either silica fume or GGBS.

Bilodeau and Malhotra (1992) measured water and chloride permeability of concretes having 55–60% cement replacement with various sources of fly ash. They reported coefficient of water permeability of fly ash concretes in the range of 1.6×10^{-14} to 5.7×10^{-13} m/s. The values of chloride were less than 650 coulombs at 91 days. Thomas and Matthews (1992) investigated oxygen permeability of fly ash concrete. Concrete mixtures were made with 15, 30 and 50% fly ash as cement replacements, exhibited reduction in the permeability values by 50, 60 and 86%, respectively, compared to concrete with out fly ash.

Naik et al. (1994) evaluated the influence of addition of large amounts (50 and 70% cement replacement) of Class C fly ash on the chloride permeability of concrete. Concrete mixtures were designated as C-3 (0% fly ash), P4-7 (50% fly ash) and P4-8 (70% fly ash). Cylinders of size 100×200 mm were made. Chloride permeability was determined in accordance with ASTM C1202. Chloride permeability results are shown in Fig. 6.13. Chloride permeability decreased with age. At the age of 2 months, all concrete mixtures except the 70% fly ash mixture exhibited moderate (2000–4000 coulombs) permeability in accordance with ASTM C 1202 specifications. The 50% fly ash concrete mixture showed lower permeability relative to the no-fly ash concrete at all ages. The 70% fly ash mixture also performed better than that of the no-fly ash concrete after 3 months.

Shafiq and Cabrera (2004) investigated the effect of curing conditions on the oxygen permeability and water permeability of normal concrete (100% OPC) and blended cement concrete (OPC/FA). Concrete mixes were made with 0, 40, and 50% fly ash content as partial substitution for cement. Mix proportion of control concrete was 1:2.33:3.5. Concrete slabs of dimensions 400 mm long, 250 mm wide, and 40 mm thick, were cast, and were cured for 28 days under two different curing conditions, wet cured (in the fog room) and dry cured (at 65% RH at 20°C). 50 mm diameter cylindrical discs were cored out from the slabs after the initial curing. Samples were then exposed to different climatic conditions (75, 65, 40, and 12%

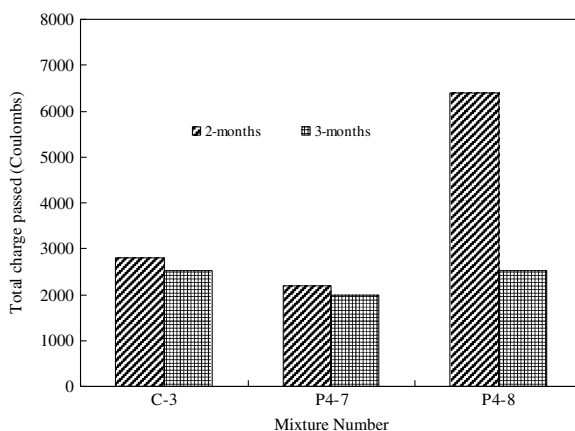


Fig. 6.13 Effect of fly ash addition on chloride permeability of concrete (Naik et al., 1994)

relative humidity at a constant temperature of 20°C) until the equilibrium moisture condition was achieved. Equilibrated concrete samples were tested in sequence for oxygen diffusion, oxygen permeability, and water permeability. The gas permeameter developed by Cabrera and Lynsdale (1988) was used to measure the oxygen permeability of cylindrical concrete samples of 50 mm diameter and 40 mm thick. Water permeability of concrete was determined by a penetration method. Coefficients of oxygen and water permeability are given in Tables 6.17 and 6.18, respectively. Based on the test results, they concluded that: (i) oxygen and water permeability ratios as calculated for OPC and FA blended concrete followed a similar trend but on different scales. For initially dry cured OPC concrete, the coefficients of oxygen and water permeability were 2–19 times higher than the coefficients obtained for the initially wet cured concrete samples. In contrast, the coefficients of oxygen and water permeability of dry cured FA blended cement concrete were 16–210 times greater than the coefficients of the corresponding wet cured concrete samples; (ii) a large difference in the coefficient of fluid permeability and/or diffusion between the dry cured and wet cured concrete was observed when concrete samples were equilibrated at 75% RH. In contrast a small difference between the fluid transport coefficients of dry cured and wet cured concrete samples was observed when they were equilibrated at 40% and 12% RH; and (iii) there was approximately 12% difference was calculated between the average degree of saturation of dry cured concrete samples equilibrated at 75% RH and the average degree of saturation of the corresponding wet cured concrete samples, which resulted in the much higher values of the fluid permeability and diffusion coefficients of dry cured samples relative to wet cured samples. This is probably due to the fact that the wet cured concrete samples when equilibrated at higher RH, have a tight pore network with small pore diameters and exhibit very high degree of saturation.

Chindaprasirt et al. (2007) examined the effect of fly ash fineness on the chloride permeability of concrete. Three fly ash finenesses: coarse, medium and fine were used. The coarse fly ash was 100% original fly ash (100FA). The medium fly ash was the 45% fine portion of the original fly ash (45FA). The fine fly ash was the 10% fine portion of the original fly ash (10FA). Three concrete mix series viz. a low, normal and a high strength concrete mix series were made. For the low and normal strength concrete, the water-to-cement ratios of 0.540 and 0.480, respectively, were used for PC mixes. For the high strength concrete, the water-to-cement ratio was 0.250 with

Table 6.17 Coefficient of oxygen permeability, K_o ($\times 10^{-19} \text{ m}^2$) and permeability ratio of OPC and FA blended cement concrete cured in wet and dry conditions (Shafiq and Cabrera, 2004)

RH (%)	Concrete type/curing condition								
	OPC			40 FA			50 FA		
	Wet	Dry	Dry/Wet	Wet	Dry	Dry/Wet	Wet	Dry	Dry/Wet
75	13.3	230.0	17.3	2.5	518.0	208.9	4.1	906.0	220.4
65	62.1	308.0	5.0	18.2	665.0	36.5	31.8	1070.0	33.6
40	192.0	486.0	2.5	104.0	1720.0	16.5	91.8	2270.0	24.7
12	337.0	772.0	2.3	136.0	2210.0	16.3	117.0	2690.0	23.0

Table 6.18 Coefficient of water permeability, $K_o (\times 10^{-19} \text{ m}^2)$ and permeability ratio of OPC and FA blended cement concrete cured in wet and dry conditions (Shafiq and Cabrera, 2004)

RH (%)	Concrete type/curing condition								
	OPC			40 FA			50 FA		
	Wet	Dry	Dry/ Wet	Wet	Dry	Dry/Wet	Wet	Dry	Dry/ Wet
75	11.0	210.0	19.1	2.8	442.0	157.9	10.0	3080.0	309.5
65	35.0	305.0	8.7	11.4	468.0	41.1	20.9	5140.0	245.9
40	166.0	658.0	3.9	22.8	678.0	29.7	62.0	12300.0	198.4
12	764.0	3870.0	5.1	425.0	6830.0	16.1	231.0	13300.0	57.6

the use of superplasticizer. Rapid chloride permeability (Coulomb charge) test was conducted at the age of 28 days as per ASTM C1202, and test results are shown in Fig. 6.14. Based on the test results they concluded that: (i) coulomb charge for the PC concrete was higher than those of the fly ash concrete in the same group; (ii) for low strength concrete, the coulomb charge of the PC1 concrete was 5800 indicating a rather poor chloride penetration characteristic. The incorporation of all fly ashes resulted in drastic reductions in the coulomb charges. The Coulomb charge of the original fly ash concrete (100FA1) was reduced to 2700, indicating moderate chloride penetration resistance. The charge was further reduced with the increase in the fly ash fineness. The charges of the 45FA1 and 10FA1 concrete are reduced to 2300 and 700, respectively; (ii) for the normal strength concrete, the coulomb charge of the PC2 concrete was 4200 and the charges of the fly ash concrete were 1250, 800 and 500 for the 100FA2, 45FA2 and 10FA2 mixes, respectively; and (iii) for the high strength concrete group, the coulomb charge of the PC3 concrete was slightly higher than 1000 and the charges of the fly ash concrete were only 500, 250 and 240 for the 100FA3, 45FA3 and 10FA3 mixes, respectively. Even at this high strength level, the reduction in the coulomb charge owing to the incorporation of the fly ash especially with the fine fly ashes was quite evident.

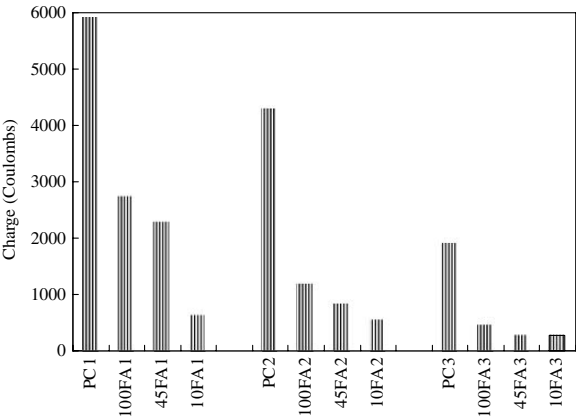


Fig. 6.14 Coulomb charge of concrete at the age of 28 days (Chindaprasirt et al., 2007)

6.6.2 Freezing and Thawing Resistance

Freezing-thawing resistance of fly ash concrete depends on the adequacy of air void system, the soundness of aggregate, degree of hydration and strength of binding paste, maturity and moisture content of concrete. Freeze-thaw durability is evaluated using the test procedure ASTM C666.

Air entrainment has the greatest influence on freeze-thaw durability of both fly ash and plain concrete mixes. Gebler and Klieger (1983) conducted tests to investigate the influence of air entrainment on the air-void parameters of hardened concretes made with both Class C and Class F fly ashes. The concretes were cast after 30, 60 and 90 minutes of initial mixing. They found that air void spacing factors were almost constant for the majority of concretes containing fly ash which were cast after 90 minutes. At early periods of casting concretes with Class F fly ash exhibited greater variability in air void parameters than concretes with Class C fly ash.

Yuan and Cook (1983) studied freeze-thaw performance of both air-entrained and non-air-entrained concretes made with high calcium fly ash at 0, 20, 30 and 50% levels of substitution for cement by weight. They concluded that (i) freeze-thaw resistance significantly improved by air entrainment in both plain and fly ash concretes; and (ii) concrete with 20% fly ash exhibited better frost resistance than the control concrete. However, when fly ash level in air entrained concrete was increased to 50%, more scaling damage was observed after 400 cycles of freezing and thawing.

Carette and Malhotra (1984) conducted freeze-thaw durability tests on concrete mixes with a wide range of Canadian fly ashes. Chemical composition of fly ashes has already been given in Table 6.5. Durability factor for fly ash concrete mixes was determined at 300 cycles and results are given in Table 6.19. It can be seen that with constant air content around 6.4%, all the fly ash concretes had about the same durability factor as control concretes.

Virtanen (1983) compared the freezing and thawing resistance of fly ash, condensed silica fume, and slag concretes. They concluded that: (i) air content has the

Table 6.19 Freeze-thaw durability factors for fly ash concretes Carette and Malhotra, 1984)

Mix No.	Cement (kg/m ³)	Air (%)	Durability factor
Control	295	6.4	98.1
F1	236	6.2	96.4
F2	237	6.2	98.8
F3	237	6.2	96.8
F4	238	6.3	98.8
F5	237	6.4	97.2
F6	238	6.5	96.8
F7	239	6.1	97.6
F8	236	6.2	96.9
F9	236	6.4	97.6
F10	237	6.5	97.2
F11	237	6.6	95.8

greatest influence on the freeze-thaw resistance of concrete; (ii) addition of fly ash had no major influence on the freeze-thaw resistance of concrete if the strength and air content are kept constant; and (iii) addition of blast furnace slag might have a negative effect on the freeze-thaw resistance of concrete when major part of cement was replaced.

Joshi (1987) conducted freeze-thaw tests on concrete made with 50% cement replacement with Alberta fly ash. It exhibited relative dynamic modulus of elasticity values in excess of 60% after 300 cycles. No significant differences were observed in freeze-thaw performance of air-entrained high volume fly ash concrete and the concrete containing both air-entraining and water-reducing agents. However, the test specimens without air entrainment failed at less than 50 freeze-thaw cycle indicating a low level of durability. They also reported that fly ash concrete mixes showed some scaling after 150–200 freeze thaw cycles and exhibited about 2% weight loss at the end of the 300 cycles. Malhotra et al. (1990) examined the durability of high volume Class F fly ash concretes and concluded that superplasticized and air entrained HFCC showed satisfactory durability against freeze-thaw attack.

Joshi et al. (1993) carried out freeze-thaw tests on air-entrained and superplasticized concretes made with 40–60% Alberta fly ash as cement replacement to produce high strength concrete mixes at water-to-cementitious material ratios of 0.28–0.36. The specimens were moist cured for 14 days prior to freeze-thaw tests. The air content of the mixes was maintained at $6 \pm 1\%$. The use of fly ash in concrete increased the air entraining agent demand to maintain constant air content. They concluded that most of the mixes had relative dynamic modulus of elasticity values in excess of 60% after 300 freeze-thaw cycles. In general, all the concrete mixes containing Alberta fly ash and with air content more than 5% exhibited acceptable freeze-thaw durability performance.

Schiepl and Hardtle (1994) reported that the main effect of pozzolanic reactions due to fly ash addition is to change the pore size distributions, the total porosity remaining mostly uncharged. In particular, the capillary water along with calcium hydroxide liberated during cement hydration is largely consumed in pozzolanic reactions. The phenomenon of pore refinement as a result of pozzolanic reactions leads to the breaking of continuity of the capillary pore structure. Malhotra et al., (1982) reported that the pozzolanic reactions alter the pore structure of the cement paste and thus densify the transition zone between the paste and aggregates.

6.6.3 Resistance to Aggressive Chemicals

Loss in durability of concrete by chemical attack can occur either due to the decomposition of cement paste or due to the disruptive internal expansion caused by chemical reactions in the paste or by combination of both the actions. Deleterious chemicals can react with Ca(OH)_2 to form water soluble salts that can be leached out of the concrete over a period of time, thereby increasing the permeability of concrete and aggravating the damage by increased and faster ingress of harmful chemicals.

Sulfates react with $\text{Ca}(\text{OH})_2$ and calcium aluminate compounds in concrete to form gypsum and calcium sulpho-aluminate, ettringite that can cause internal disruption of the concrete by concomitant volume increase of the paste.

6.6.3.1 Resistance to Sulfate Attack

Use of fly ash in concrete increases its resistance to sulfate attack and potentially corrosive salts that penetrate into the concrete and cause steel corrosion with accompanying cracking and spalling of the concrete. It is well established that the reaction of fly ash with calcium hydroxide released during cement hydration results in the formation of additional calcium aluminosilicate hydrates and accompanying reduction in permeability of the concrete.

Larsen (1985) reported that the change in the pore structure of cement paste as a result of fly ash addition can not be the sole reason for the observed favorable performance of fly ash concrete subject to chemical attack, particularly sulfate attack. He observed the favorable effect of the fly ash on sulfate resistance of concrete mixes even at ages when the pozzolanic reaction of fly ash was still not particularly high. Accordingly, it is suggested that additional chemical-mineral interaction including the reduction in tricalcium aluminate (C_3A) and calcium hydroxide content contribute to sulfate resistance. The fly ash may combine with some alumina phases such as C_3A in the cement during the first few days of cement hydration to form primary ettringite, thus reducing the potential for expansive sulfate-alumina reactions responsible for sulfate attack. With the increased conversion of C_3A in the initial stages, less of the aluminate containing phase is available for reaction during subsequent sulfate attack.

Dunstan (1976, 1980) investigated the sulfate resistance of concrete mixes made with lignite and sub-bituminous fly ashes. He concluded that lignite and sub-bituminous Class C fly ash generally reduced sulfate resistance when used in normal proportion. Dunstan reported that as the calcium oxide in the fly ash increased above a lower limit of 5% and the ferric oxide (Fe_2O_3) decreased, sulfate resistance was reduced. He proposed the use of an indicator 'R' defined as $R = \% \text{CaO} - 5/\% \text{Fe}_2\text{O}_3$.

For the fly ashes used by Dunstan (1980), those having 'R' values of 1.5 or less generally improved sulfate resistance while those with higher values did not. The general applicability of the 'R' factor to predict sulfate resistance of all fly ashes is further required to be investigated. With the use of fly ash at 25% cement replacement level, the sulfate resistance of concrete made with ASTM Type II cement at 0.45 water cement ratio has been related to the 'R' factor as follows:

<u>R limits</u>	<u>Sulfate resistance</u>
<0.75	greatly improved
0.75 – 1.5	moderately improved
1.5 – 3.0	no significant change
>3.0	reduced

Joshi (1987) reported that with the incorporation of Alberta fly ash at 15% replacement level by weight of cement, the sulfate resistance of cement-sand mortar

was significantly improved when exposed to sodium sulfate and magnesium sulfate solutions of concentration below 10%. For higher sulfate concentrations, the mortars made with Type-V cement and 15% Alberta fly ash developed adequate sulfate resistance.

Fay and Pierce (1989) conducted a study on air entrained fly ash. They used three fly ashes from the United States, representing a range of CaO contents of 11–28.8% and used 10–100% fly ash by weight of the total cementitious material as fly ashes were themselves quite cementitious. The specimens were cured for 14 days in a 100% humidity room and for another 14 days in a 50% humidity room before they were immersed in 10% Na₂SO₄ solution or subjected to cyclic soaking and drying phases in 2.1% Na₂SO₄ solution to generate data by accelerated test. The test results showed that: (i) both low-calcium Class C and Class F fly ashes can be effective cement replacements in controlling sulfate expansion; (ii) Class F fly ash was the most effective in reducing sulfate expansion at the lower cementitious content (251.5 kg/m³). Likewise at the higher cementitious content (387 kg/m³), Class F fly ash at 30% replacement level was found to be the most effective; (iii) high calcium Class C fly ash concrete mixes, with fly ash replacement levels blow 50%, generally exhibited more expansion than the control mixes, opposite to the behavior observed with low calcium class F concrete mixed; (iv) for low-calcium Class C fly ash replacement levels were suggested to be greater than 30% and for high calcium Class C fly ashes the corresponding suggested levels were greater than 75% to achieve the most improved sulfate durability; (v) the replacement level for a particular type of fly ash was found to depend on cementitious material content of the mix. With lower cementitious material content, 50% or more, while for richer mixes 50% or less Class C was suggested for improving the sulfate resistance of concrete; and (vi) Class F fly ash at replacement level of 30% significantly improved the sulfate durability for the cementitious levels tested and appeared to be optimum for both test conditions employed in the investigation. The high calcium Class C fly ash concretes generally performed much worse than the control mix under sulfate attack indicating the least effectiveness of these types of ash in reducing expansion.

Mehta (1993) concluded that fly ashes are amongst the group of pozzolans that significantly increase the life expectancy of concrete exposed to sulfate attack. In general, Class F type fly ash meeting the specification requirements will improve the sulfate resistance of any concrete/mortar mix in which it is included, although the degree of improvement may vary with either the cement used or the fly ash. The situation with Class C fly ash is different. A few studies indicated that some Class C fly ashes may rather reduce sulfate resistance when used in normal proportions.

6.6.3.2 Resistance to Sulfuric Acid

Sulfuric acid is a very aggressive acid that reacts with the free lime Ca(OH)₂, in cement paste forming gypsum (CaSO₄ · 2H₂O). This reaction is associated with an increase in volume of the concrete by a factor of 2.2 (Attigbo and Rizkalla, 1988). Another destructive action is the reaction between calcium aluminate present in cement paste and gypsum crystals. These two products form the less soluble

reaction product, ettringite ($3\text{CaO} \cdot \text{Al}_2\text{O}_3 \cdot 3\text{CaSO}_4 \cdot 32\text{H}_2\text{O}$). These very expansive compounds cause internal pressure in the concrete, which leads to the formation of cracks. The reacted surface becomes soft and white. Because of these, concrete structure loses its mechanical strength. Another important phenomenon where sulfuric acid is responsible for concrete corrosion is biogenic sulfuric acid corrosion, which occurs often in sewer systems. Due to different chemical and microbiological reactions, hydrogen sulfide releases into the atmosphere of sewer structures above the water level. This gas reacts with oxygen to form elemental sulfur, which is deposited on the walls of the sewer structures. In the slime layer coating these walls, aerobic sulfur-oxidizing bacteria (*Thiobacillus* sp.) metabolize the sulfur to sulfuric acid. Repair and sometimes complete replacement of the damaged structures becomes necessary after this acid attack. Pozzolans combine and stabilize the calcium hydroxide liberated during the hydration of cement in concrete, to form additional cementitious compound, mainly in the form of calcium silicate hydrate (CSH). The resultant binder matrix is more chemically resistant, by virtue of its denser microscopic pore structure.

Roy et al. (2001) investigated the acid resistance of silica fume, metakaolin and low-calcium FA-incorporated mortars. It was found that; the best performance in terms of chemical resistance was obtained by the incorporation of silica fume.

Aydin et al. (2007) investigated the effect of Class C fly ash on the sulfuric acid resistance of concrete. Cement was replaced with fly ash up to 70%. Cylinders (100×200 mm) and cubes (71 mm) were cast for mechanical properties and acid resistance. After 28 days curing in water, specimens were immersed in a 5% sulfuric acid (H_2SO_4) solution for 60 days in a plexiglass container. These specimens were kept covered throughout the testing period to minimize evaporation. Similar samples from each mixture were kept in water up to 88 days to compare strength values. After 60 days of exposure, acid-attacked surfaces of the specimens were cleaned with distilled water. Chemical resistance was evaluated by determining the weight loss (WL) and compressive strength loss (SL) of the specimens. Based on the results, they concluded that: (i) compressive loss was related with the FA content. The FA replacement seemed to improve the acid resistance of the steam-cured samples since loss percentages dropped to 21% (FA70) from 58% (FA0); (ii) negligible differences in loss were observed for standard cured concrete with increasing FA content. Similar trends have been observed in terms of weight loss for both curing cases. Weight loss dropped from 5% (FA0) to 3.3% (FA70) for standard curing and 8.3% (FA0) to 1.1% (FA70) for SC conditions; and (iii) strength loss and weight loss of Portland cement concrete cured in water were lower than that of steam-cured ones due to somewhat higher permeability of steam-cured samples. However, over 30% and 40% FA replacement levels, weight and strength losses of steam-cured concrete were lower than water-cured ones, respectively. In other words, sulfuric acid resistance of steam-cured concrete could be improved significantly by incorporation of FA. The positive effect of FA on acid resistance may arise from pozzolanic reaction between FA and calcium hydroxide liberated during the hydration of cement, which forms additional cementitious compound, mainly CSH.

6.6.3.3 Thaumasite Form of Sulfate Attack

In conventional sulfate attack, it is commonly believed that chemical reactions between ions and certain constituents (especially monosulfate hydrate (C_4ASH_{12}), calcium aluminate hydrates (C–A–H) and calcium hydroxide (CH)) in the hydrated cement paste, that result in the formation of ettringite and gypsum can cause excessive expansion, cracking and strength loss. Concrete deterioration due to conventional sulfate attack is often associated with the expansion of ettringite; however, the mechanism by which ettringite formation causes expansion still remains unexplained. Exertion of pressure by growing ettringite crystals, and swelling due to adsorption of water in alkaline environment by poorly crystalline ettringite, are two of the hypotheses that are supported by most researchers.

The formation of thaumasite is generally attributed to a consequence of the evolution of ettringite when it incorporates Si^{4+} (in octahedral coordination) in its structure, substituting for Al^{3+} ions in the presence of CO_3^{2-} . Another hypothesis on thaumasite is associated with the interaction between sulfates and carbonates present in the aqueous phase of the cement and C–S–H gel. This involves the destruction of the resistant structure of hydrated cement without volume alteration or without ettringite participation. A break up of the material may occur due to C–S–H gel destruction

Mulenga et al. (2003) investigated the formation of thaumasite in concrete and mortars containing fly ash. Type of cement was one German sulfate resisting (SRPC CEM I 42.5R-HS) and a Portland limestone cement (PLC) CEM II/A-L 32.5R. Amount of fly ash was varied at 0, 20, 30, 40, 50% of fly ash by mass of cement. Concrete specimens of size $40 \times 40 \times 160$ mm and mortar specimens of size $10 \times 40 \times 160$ mm were kept in sodium sulfate solutions at 8 and 20°C. The assessment of damage and deterioration of the specimens due to sulfate attack was conducted using the newly developed MNS-test method (Mulenga et al., 1999), employing direct tension test on concrete prisms and cores and the Wittekindt-test method (Wittekindt, 1960) by measuring the linear expansion of flat prisms immersed in 4.4% sodium sulfate solution. Direct tensile strength and length changes have been recorded over a period of 120 days. According to the MNS-Test Method the relative transverse tensile strength of at least 0.80 after 84 days and not less than 0.70 after 120 days of exposure to sulfate attack is required for a given concrete to be considered sulfate resistant. Figures 6.15 and 6.16 present a summary of the tensile strength results for concretes with 0, 30 and 50% fly ash contents.

The results showed that concrete employing the sulfate resisting cement CEM I 42.5R-HS performed very well and exhibited a high sulfate resistance despite the addition of fly ash and early exposure to sulfate attack. At both temperatures, the concrete mixtures with 50% fly ash recorded the lowest tensile strength but yet fulfilled the criteria for a sulfate resisting concrete. This strength loss can be attributed to the ettringite (at 20°C) and thaumasite formation (mainly at 8°C exposures) which was detected in these mixtures within 84 days of sulfate attack. All specimens of concretes employing PLC exhibited lower tensile strength values in the sulfate solutions than in distilled water and severe loss of strength after 120 days of

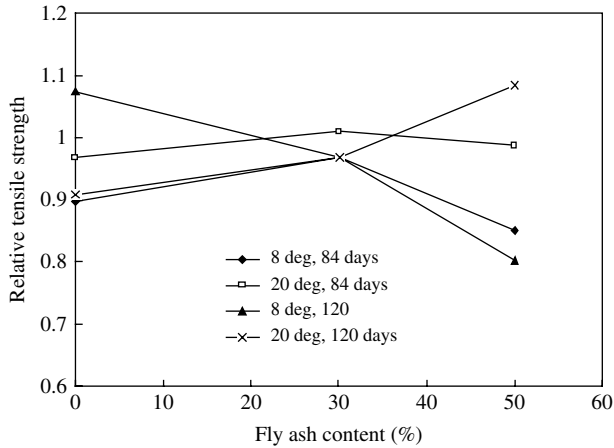


Fig. 6.15 Relative direct tensile strength of SRPC concrete prisms after immersion in 5% sodium sulfate solutions for 84 and 120 days (Mulenga et al., 2003)

sulfate attack at 8°C. The strength loss was accompanied by pronounced thaumasite formation. However, the addition of fly ash seemed to improve the sulfate resistance of these concretes when they are exposed to sulfates at 20°C. This can be attributed to the effects of the pozzolanic reaction taking place at a higher rate at 20°C as compared to its retardation at 8°C. In terms of tensile strength the performances of the plain SRPC as well as PLC specimens examined were considerably poorer than those of the PC/fly ash specimens. At 20°C all binders except those with 0% fly ash showed higher strength retention than at 8°C.

They further reported that visual appearance of the concrete specimens did not show any visible signs of deterioration even after 120 days exposure to 5% Na₂SO₄

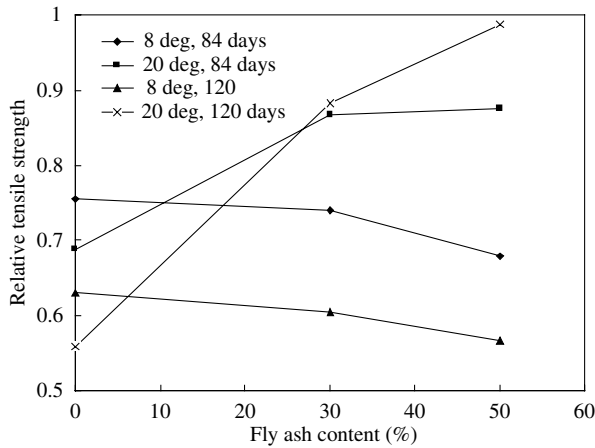


Fig. 6.16 Relative direct tensile strength of PLC concrete prisms after immersion in 5% sodium sulfate solutions for 84 and 120 days (Mulenga et al., 2003)

solutions. However, most of the specimens incorporating the PLCs showed signs of deterioration within 84 days of exposure to 5% Na₂SO₄ solutions. Some exfoliation of the corners and edges as well as cracks occurred on these specimens after 84 and 120 days respectively. At 8°C, signs of attack on fly ash specimens were somewhat more pronounced with edge and corner corrosion appearing than at 20°C. On the contrary, the specimens containing 30% and 50% fly ash were still in sound condition at 20°C. The plain PC specimens showed a greater rate of corrosion at 20°C than at 8°C.

Linear expansion results are given in Figs. 6.17 and 6.18. All SRPC mortar specimens did not show any significant expansion and proved to be sulfate resistant. However, thaumasite formation was evident in fly ash mixtures. On the other hand, the PLC specimens, including those stored in distilled water, gradually expanded throughout the period of experiment. However, after approximately 90 days all specimens in distilled water did not show any further expansion. Generally, all PLC/fly ash binder combinations tested as flat mortar prisms at 20°C exhibited lower expansions compared to the plain PLC specimens. According to the Wittekintd method they all proved not to be sulfate resistant as the average expansions of prisms exceeded 0.5 mm/m after 56 days. The sulfate attack at 8°C was stronger and caused more deterioration than at 20°C. The expansion results of mortar prisms corresponded to the visual assessment made by observing the physical appearance of specimens. All mortar prisms exhibited deterioration just after 56 days of immersion in sodium sulfate solution by developing cracks, softening and popouts. While this process continued at 20°C for even more than 120 days without causing total destruction of the specimens, the mortar prisms at 8°C were totally transformed into a mushy and in cohesive mass within 120 days of sulfate attack. In this case the thaumasite formation appeared to have played a major role in the deterioration of the specimens as compared to that of 20°C where mainly ettringite was formed.

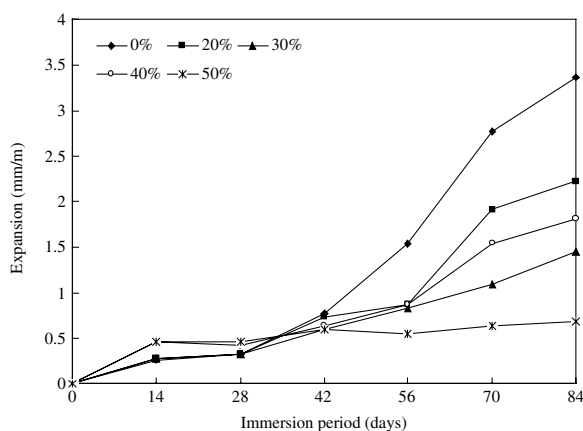


Fig. 6.17 Expansion of mortar prisms containing fly ash after immersion in 4.4% sodium sulfate solution, sulfate attack at 20°C (Mulenga et al., 2003)

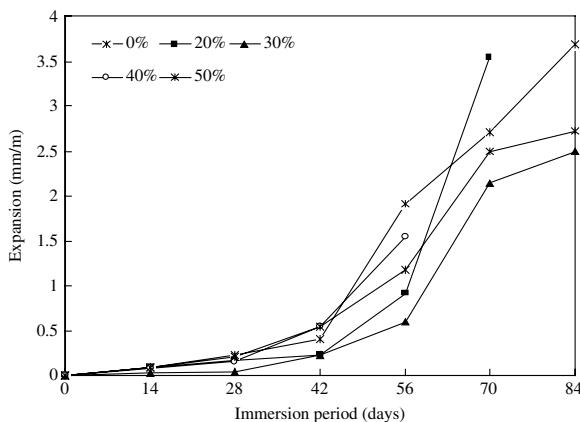


Fig. 6.18 Expansion of mortar prisms containing fly ash after immersion in 4.4% sodium sulfate solution, sulfate attack at 8°C (Mulenga et al., 2003)

6.6.4 Alkali-Silica Reaction

This deleterious chemical reaction occurs when certain acidic aggregates, containing reactive silica in the form of silicate, react with alkali metal ions such as sodium and potassium, present in a highly alkaline solution, resulting from the hydration of a high alkali Portland cement. As a result, alkali-silica gel is formed which can cause considerable expansion on water absorption. The gel is of the unlimited swelling type, it imbibes water with a consequent increase in volume. Since the gel is confined by the surrounding cement paste internal pressures are built up, which eventually lead to expansion, cracking and disruption of the cement paste. It is also believed that it is the swelling of hard reactive aggregate particles that is most harmful to concrete. Some of the relatively soft gel is leached out by water over a period of time and deposited in the cracks already formed due to the swelling of aggregates.

Alkali-silica reaction (ASR) also known as alkali-aggregate reaction (AAR) is influenced by the type and characteristics of aggregates, available alkali content, presence of moisture, temperature, type of admixture (organic and inorganic) and the alkali to silica ratio of the concrete mix. Numerous early studies suggested the effectiveness of fly ash in inhibiting or reducing expansion resulting from ASR (Stanton, 1942; Pepper and Mather, 1959).

Stanton (1942) was the first to recognize the deterioration of concrete as a result of reaction between the alkaline hydroxyl ions in the pore water of concrete and certain forms of silica occasionally present in the aggregate including opaline chert and siliceous magnesium lime stone. The studies were conducted using aggregates containing opaline material and cement with acid soluble alkali content of more than 0.6%. They reported that deleterious expansion due to the alkali-silica reaction could be reduced or eliminated by the addition of finely divided mineral admixtures including fly ash containing siliceous material.

Dunstan (1981) identified aggregates and their mineralogical constituents that can react with alkalis in concrete. They are: (i) silica materials- opaline or chalcedonic cherts, tridymite, cristobalite, siliceous limestone; (ii) glassy to cryptocrystalline rhyolites, dacites, and their tuffs; (iii) zeolite and neulandite; and (iv) certain phylites.

The reactivity of aggregate is affected by its particle size and porosity as these influence the area over which the reaction can take place. The greater the surface area of the reactive aggregates, the lower the quantity of alkalis available per unit area, and thus the less alkali silica gel can form. Furthermore, because of the low mobility of calcium hydroxide liberated during cement hydration, only that present near the surface of the aggregate is available for reaction, so that the quantity of $\text{Ca}(\text{OH})_2$ per unit area of aggregate is independent of the magnitude of the total surface area of the aggregate. With the addition of fly ash, containing pozzolanic silica in fine size fractions, the reactive surface area of the aggregate exposed to given alkaline pore water increases and this results in an increase of calcium hydroxide/alkali ratio of the reactive solution at the boundary of the aggregate. Under such circumstances a non-expansive calcium alkali silica gel is produced with favorable effects.

An effect of cement alkalis and fly ash on alkali-aggregate reaction as reported by Dunstan (1981) is shown in Fig. 6.19.

Hobbs (1981) studied the effect of different Class F fly ashes and blast furnace slag on alkali silica reactivity of mortars made with opaline aggregates and high alkali cement. Based on the test results, he concluded that: (i) partial replacement of a high-alkali cement by fly ash reduced the long-term expansion due to alkali-silica reactivity but, even when 30% or 40% of the cement was replaced, most of the blended cement mortars cracked at earlier or similar ages as compared to the Portland cement mortars; (ii) where part of the cement was replaced by fly ash, the lowest mortar alkali content, expressed as equivalent Na_2O , at which cracking was

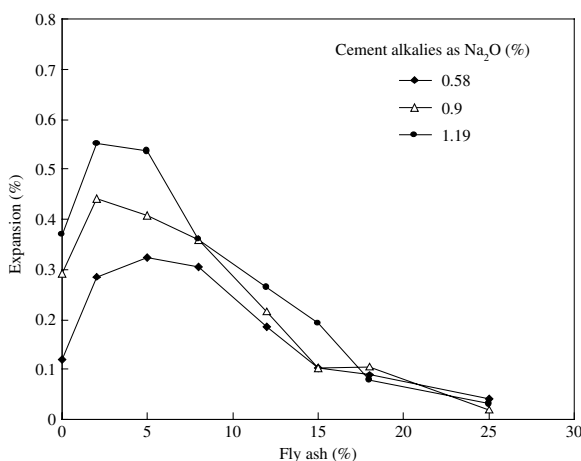


Fig. 6.19 Effects of cement alkalis and fly ash on alkali-aggregate reaction (Dunstan, 1981)

observed was 2.85 kg/m^3 . This related only to the acid soluble alkalis contributed by the Portland cement and compares with a figure of 3.5 kg/m^3 for a Portland cement mortar; (iii) if it is assumed that fly ash acts effectively like a cement with an alkali content of 0.2% by weight, the lowest alkali content at which cracking was observed was 3.4 kg/m^3 ; and (iv) both fly ash and granulated blast furnace slag act as alkali diluters, slag being more effective in reducing damage due to alkali-silica reactivity than fly ash.

Oberholster and Westra (1981) studied the effect of adding mineral admixtures, including fly ash, to mortar and concrete made with Malmesbury group aggregates in order to examine how effective they were in reducing expansion. They observed that fly ash addition effectively suppressed expansion at cement replacement levels of 20% or more on an equal volume basis.

Mehta (1983) concluded that alkali-silica reaction progresses slowly and the continuous formation of swelling type gel causes internal disruption and cracking of concrete. The damage to concrete due to this reaction is appreciably aggravated when other causes of deterioration such as weathering effects of freeze-thaw, sulfate attack, and other aggressive physical and chemical processes are concurrently active.

Perry et al. (1987) studied the alkali-aggregate reaction with 12 different Canadian fly ashes replacing 20–40% cement by weight in mortar mixes made with reactive opaline aggregate. They concluded that reduction in expansion after one year ranged from 5 to 81% at 20% replacement level, 34–89% at 30% replacement level, and 47–92% at 40% replacement level, respectively, compared to that of control mortar mix with no fly ash. The alkali content of fly ashes studies varied over wide limits. However, the alkalies present in fly ashes were less susceptible to reactive aggregate form unlike the free and water soluble alkalies of Portland cement.

Idorn (1991) reported that in field cases of deleterious silica reaction, the cement paste is chemically unaffected while the reacting aggregate particles are internally fractured and/or partially dissolved. High alkaline Portland cements generally having more than 0.6% sodium equivalent alkali content is highly vulnerable to attack by aggregates containing reactive amorphous as well as crystalline silica such as chalcedony, crypto-crystalline fibrous, and tridymite. Alkalies in most cases are derived from Portland cement itself, but they can also be augmented by their presence in the mixing water, admixtures, salt contaminated aggregate and deicing salts used on concrete.

6.6.5 Carbonation

Calcium hydroxide (Ca(OH)_2) and to lesser extent the hydrated cement compounds in Portland cement react in moist conditions with carbon dioxide (CO_2) from atmosphere to form calcium carbonate (CaCO_3). This process is called carbonation. The rate at which concrete carbonates depends up on: (i) (its permeability; (ii) degree of saturation with water; and (iii) mass of calcium hydroxide available for reaction.

Gebauer (1982) reported that an increase in water cement ratio of concrete mix resulted in an increase in the depth of carbonation. Kasai et al. (1983) studied the carbonation of mortar specimens made with different types of cement and fly ash after 7 days of moist curing. They concluded that: (i) carbonation was observed to progress rapidly up to three months and after that it slowed down; and (ii) greater the coefficient of permeability of the specimen, the greater was its susceptibility of CO_2 attack manifested in terms of increased depth of carbonation. The specimens made with fly ash cement exhibited greater carbonation effect than ordinary Portland cement specimens.

Ho and Lewis (1983) investigated the rates of carbonation of three types of concrete mixes: (i) plain concrete; (ii) the second containing a water reducing admixture; and (iii) third in which fly ash was used to replace part of the cement. Accelerated carbonation was induced by storing specimens in an enriched CO_2 atmosphere (4%) at 20°C and 50% RH for eight weeks. One week under these conditions was approximately equivalent to one year in a normal atmosphere (0.003% CO_2). They concluded that: (i) concretes having the same strength and water-to-cement ratio do not necessarily carbonate at the same rate; (ii) concrete containing fly ash showed significant improvement in quality when curing was extended from 7 to 90 days. This improvement was much greater than that achieved for the plain concrete; and (iii) depth of carbonation is a function of the cement content for concretes moist-cured for 7 days. However, with further curing to 90 days, concrete containing fly ash showed a slower rate of carbonation as compared to plain and water-reduced concretes.

Buttler et al. (1983) studied the carbonation behavior of cement sand mortars made with 25% pulverized fuel ash or fly ash replacing cement and at water cement ratios of 0.35–0.55. They concluded that more carbonation occurred at lower water contents when the fly ash concrete was desiccated with calcium chloride (CaCl_2). However, in the case of non-desiccated specimens, the effect of fly ash on carbonation at lower water contents was insignificant. Of course in non-desiccated specimens, more carbonation was observed at high water cement ratios.

Nagataki et al. (1986) reported a direct relationship between 28-day compressive strength and depth of carbonation irrespective of fly ash replacement in concrete, and also mentioned that the extent of carbonation decreased with an increase in compressive strength.

Joshi et al. (1994) found that up to about 7 days, the extent of carbonation measured by the affected depth from the outer surface in concrete, after subjecting the specimen to 4% CO_2 at 20°C and 50% R.H., was more in concrete containing fly ash than the control concrete without fly ash. However, after 90 days curing, the trend reversed in that the fly ash concrete exhibited less carbonation than the control concrete.

6.6.6 Corrosion Resistance

Corrosion of reinforcing steel embedded in fly ash concrete has great cause of concern for applications of concrete in the construction of reinforced and prestressed

concrete structures, particularly, those subject to chloride induced corrosion of steel caused by the use of deicing salts or sea water exposure of structures in a marine environment. The bond between the surrounding concrete and steel reinforcement and the high alkalinity of the concrete provide protection from corrosion.

In a hydrated Portland cement paste, about 20% Ca(OH)_2 by weight of the hydration products is present to provide the reserve basicity for steel protection. Diamond (1981) reported that the high alkalinity of the pore solution in cement paste primarily results from the presence of sodium and potassium ions rather than from the presence of calcium hydroxide alone. In the two fly ash systems examined, he reported that pH of pore solution was reduced from 13.75 in a control system to about 13.55 in the presence of fly ash. Under highly alkaline conditions i.e. pH larger than 11.5 of pore solution in concrete, a protective iron oxide film forms on the surface of reinforcing steel that makes it passive against further corrosion. This passive iron oxide layer is susceptible to the attack by chloride ions in concrete or to carbonation when the pH of the surrounding concrete is reduced below 11.0. Once this passive layer is destroyed, a galvanic cell can form between different areas on reinforcing bars causing reduction at anodic area. Furthermore, the rate and extent of corrosion of embedded steel depends on the electrical conductivity of the surrounding concrete and the permeation of moisture and air through the concrete. In practice, adequate cover of high quality and impervious concrete over the reinforcing steel has been found to provide adequate protection against corrosion.

Andrade (1986) tested concrete mixes with and without fly ash for corrosion using polarization resistance techniques where the intensity of corrosion of the steel reinforcement was measured and compared to safe values of corrosion. The addition of fly ash promoted the corrosion of steel in mortars but had no effect on concrete specimens. The decrease in the alkalinity due to introduction of fly ash was reported to have a major effect in promoting corrosion in fly ash mortar mixes.

Schiepl and Raupach (1992) studied the electrolytic resistance of fly ash concrete made with 20% cement replaced with fly ash compared with that of other concretes. They found that after one month, the fly ash concrete had equal electrolytic resistance to that of plain concrete. After one year, the fly ash concrete exhibited values of the same order of magnitude as blast furnace slag cement concrete containing 74 wt% slag.

Saraswathy et al. (2003) investigated the influence of activated fly ash on the corrosion resistance of concrete. Various activation techniques, such as physical, thermal and chemical were adopted. Corrosion-resistance of fly ash cement concrete was studied by using anodic polarization technique. Mild steel rods were embedded in cylindrical mortar (1:3) specimens of size 58 mm diameters and 60 mm height using w/c ratio of 0.45. The mortar specimens with 0, 10, 20, 30, 40 and 50% fly ash as replacement of cement were subjected to anodic polarization studies using a three electrode system which consists of embedded steel in mortar as anode, stainless steel ring electrode as cathode and saturated calomel electrode as reference electrode (Muralidharan et al., 2000). Anodic polarization studies have been carried out in 3% NaCl solution. The current flowing at +300 and +600 mV were recorded for mild steel embedded in OPC and OPC replaced by various fly ash systems at 10,

20, 30, 40 and 50% replacement levels and the corresponding magnitude of current for a fixed duration of 12 h are given in Table 6.20. From the table it was found that for OPC, the current measured was found to be 0.43 and 1.04 mA. For AFA the current measured at 30% replacement level was found to be 0.34 and 0.99 mA. On the other hand TFA and CFA systems showed superior properties even up to 50% replacement level. For example in the case of CFA system, the current measured was found to be 0.40 and 0.56 mA at 50% replacement level. These data clearly illustrated that activated fly ashes improved the corrosion-resistance properties even up to 50% replacement level.

Chalee et al. (2007) studied the effect of W/C ratio on covering depth required against the corrosion of embedded steel of fly ash concrete in marine environment up to 4-year exposure. Fly ash was used to partially replace Portland cement type I at 0, 15, 25, 35, and 50% by weight of cementitious material. Water to cementitious material ratios (W/C) of fly ash concretes were varied at 0.45, 0.55, and 0.65. The 200-mm concrete cube specimens were cast and steel bars with 12-mm diameter and 50 mm in length were inserted in the concrete with the covering depth of 10, 20, 50, and 75 mm. The specimens were cured in water for 28 days, and then placed to the tidal zone of marine environment in the Gulf of Thailand. Tests were conducted for the compressive strength, chloride penetration profile and corrosion of embedded steel bar after being exposed to tidal zone for 2, 3, and 4 years. Based on the tests, they concluded that: (i) cement concrete had higher rate of chloride penetration than fly ash concrete. The chloride penetration was comparatively low and decreased with the increase of fly ash replacement; (ii) use of fly ash to replace cement, the covering depth required for the initial corrosion of embedded steel bar in concrete could be reduced; (iii) decrease in W/C ratio resulted in reducing the covering depth

Table 6.20 Anodic polarization test parameters for OPC and various activated fly ash blended cement concrete in 3% NaCl solution (Saraswathy et al., 2003)

System	As-received fly ash (AFA)		Physically activated fly ash (PFA)		Thermally activated fly ash (TFA)		Chemically activated fly ash (CFA)	
	+300 mV shift current (mA)	+600 mV shift current (mA)	+300 mV shift current (mA)	+300 mV shift current (mA)	+300 mV shift current (mA)	+300 mV shift current (mA)	+300 mV shift current (mA)	+300 mV shift current (mA)
OPC (100%)	0.43	1.04	0.43	1.04	0.43	1.04	0.43	1.04
OPC + 10% FA	0.24	0.55	0.16	0.40	0.06	0.08	0.05	0.07
OPC + 20% FA	0.27	0.75	0.21	0.62	0.09	0.14	0.07	0.10
OPC + 30% FA	0.34	0.99	0.30	0.83	0.18	0.26	0.11	0.15
OPC + 40% FA	0.46	1.08	0.38	0.99	0.24	0.40	0.19	0.20
OPC + 50% FA	1.26	2.50	1.00	1.50	0.40	0.66	0.40	0.56

required for initial corrosion, and generally affected to the cement concrete rather than the fly ash concrete; (iv) fly ash concretes with 35% and 50% replacements and W/C ratio of 0.65, provided the result of corrosion resistance at 4-year exposure as good as cement concrete with W/C ratio of 0.45; and (v) concrete with compressive strength of 30 MPa could reduce the covering depth from 50 to 30 mm by using fly ash to replace Portland cement of 50%.

6.6.7 Abrasion Resistance

Abrasion of concrete occurs due to scraping, rubbing, skidding or sliding of objects on its surface. Abrasion resistance of concrete is influenced by number of factors such as compressive strength, surfacing finish, aggregate properties, types of hardeners, and curing. Abrasion resistance of concrete is primarily dependent on the compressive strength of concrete. Therefore, air-entrainment, water-cement ratio, and types of aggregates and their properties, which have influence on compressive strength of concrete, should also have their effect on the abrasion resistance of concrete. In general, hardened paste has low abrasion resistance. The use of hard aggregates and low water to cement ratio has been found to be quite effective in increasing abrasion/erosion resistance of both types of concrete, i.e., with and without fly ash. With the use of fly ash in concrete the quality of cement paste is improved, and the leachability of calcium hydroxide is impeded with age. Because of the dense structure of cement paste and good bonding characteristics of fly ash concrete, it is believed that the tendency of coarse aggregate to be plucked out of the binding matrix by abrasive action is reduced. At equal compressive strengths, properly cured and finished concrete with and without fly ash will exhibit essentially equal resistance to abrasive-erosive forces. Use of fly ash thus affects this aspect of durability only to the extent that it usually improves compressive strength of concrete due to its pozzolanic activity with time.

Liu (1981) compared the abrasion resistance of non-fly ash concrete with a fly ash concrete with 25% cement replacement. He concluded that abrasion of concrete with or without fly ash was similar up to 36 hours of abrasion testing, but after 72 hours of testing, the fly ash concrete lost about 25% more weight than the concrete without fly ash. Tikalsky et al. (1988) concluded that concrete containing Class C fly ash possessed superior abrasion resistance compared to either ordinary Portland cement concrete or concrete containing Class F fly ash. Nanni (1989) investigated the abrasion resistance of roller-compacted concrete using both laboratory and field specimens made by replacing cement with 50% Class C fly ash. He concluded that: (i) testing under air-dry conditions produced 30–50% less wear than under wet conditions; addition of steel or synthetic fibers did not cause any appreciable change in the abrasion resistance of concrete; and (iii) improper moist-curing conditions produced more negative effects on the surface quality than the compressive strength of concrete.

Langan et al. (1990) investigated the influence of compressive strength on the durability of concrete containing 50% fly ash as replacement of cement, and concluded that the presence of fly ash at high levels of cement replacement increased the weight loss due to abrasion at all ages relative to concrete without fly ash. Bilodeau and Malhotra (1992) investigated the abrasion resistance of concrete incorporating high volumes of Class F fly ash. Superplasticized mixtures were developed with 55–60% fly ash of total cementitious materials. Test results showed that fly ash concrete had poorer abrasion resistance than concrete without fly ash. Naik et al. (1995) evaluated the abrasion resistance of concrete proportioned to have five levels of cement replacements (15, 30, 40, 50, and 70%) with one source of Class C fly ash. Test results showed that abrasion resistance of concrete having cement replacement up to 30% was comparable to the reference concrete with out fly ash, but beyond 30% cement replacement, fly ash concrete exhibited slightly lower resistance to abrasion relative to non-fly ash concrete.

Ghafoori and Diawara (1999) investigated the abrasion resistance of concrete incorporating four percentages of fine aggregate replacement (5, 10, 15, and 20%) with silica fume. They concluded that the resistance to wear of concrete containing silica fume as a fine aggregate replacement was consistently better with increasing amounts of silica fume up to 10%. Naik et al. (1998) reported that blending of Class C fly ash with Class F fly ash showed either comparable or better abrasion resistance results than either the control mixture with out fly ash or the unblended Class C fly ash.

Siddique (2003b) studied the abrasion resistance of concrete proportioned to have four levels of fine aggregate replacement (10, 20, 30 and 40%) with Class F fly ash. A Control mixture with ordinary Portland cement was designed to have 28 days compressive strength of 26 MPa. Concrete specimens of size $65 \times 65 \times 60$ mm were made for the purpose. The abrasion resistance of concrete mixtures was determined at the ages of 28, 91, and 365 days in accordance with Indian Standard Specifications (IS: 1237, 1980). It was measured in term of depth of wear. Figure 6.20 shows the variation of depth of wear versus percentage of fine aggregate replacement with Class F fly ash, at 60 minutes of abrasion time. It is evident that with the increase in percentage of fine aggregate replacement with fly ash, depth of wear decreased, which indicated that the abrasion resistance of concrete increased with the increase in fly ash content. After 60 minutes of abrasion, depth of wear for Control Mixture M-1 (0% fly ash) was 2.8 mm at 28 days, 2.52 mm at 91 days, and 2.3 mm at 365 days, whereas depth of wear was 2.45 mm at 28 days, 2.14 mm at 91 days, and 1.92 mm at 365 days for Mixture M-2 (10% fly ash), 2.2 mm at 28 days, 1.98 mm at 91 days, and 1.75 mm at 365 days for Mixture M-3 (20% fly ash), 1.92 mm at 28 days, 1.71 mm at 91 days, and 1.56 mm at 365 days for Mixture M-4 (30% fly ash), 1.7 mm at 28 days, 1.56 mm at 91 days, and 1.32 mm at 365 days for Mixture M-5 (40% fly ash). This showed that for a particular percentage of fine aggregate replacement with fly ash, depth of wear decreased with increase in age, which means that abrasion resistance increased with age. This could be primarily attributed to the increase in compressive strength resulting from increased maturity of concrete with age.

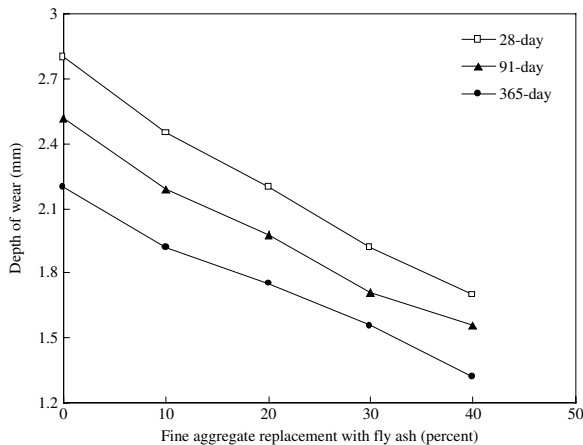


Fig. 6.20 Depth of wear @ 60 minutes of abrasion versus fine aggregate replacement with fly ash (Siddique, 2003b)

References

- ACI committee 211.1.81 (1984) Standard practice for selecting proportions for normal, heavy weight and mass concrete. ACI Manual of Concrete Practice.
- Andrade C (1986) Effect of fly ash in concrete on the corrosion of steel reinforcement. ACI SP – 91: 609–620.
- ASTM C 1113 (1990), Test method for thermal conductivity of refractories by hot wire (Platinum Resistance Thermometer Technique).
- ASTM C 618 (1993) Standard specification for coal fly ash and raw or calcined natural pozzolan for use as a mineral admixture in concrete, Annual Book of ASTM Standards, Philadelphia, USA.
- Atis CD (2002) Heat evolution of high-volume fly ash concrete. Cement and Concrete Research 32: 751–756.
- Atis CD (2005) Strength properties of high-volume fly ash roller compacted and workable concrete, and influence of curing condition. Cement and Concrete Research 35: 1112–1121.
- Attigbo EK, Rizkalla SH (1988) Response of concrete to sulfuric acid attack. ACI Materials Journal 84 (6): 481–488.
- Aydin S, Yazici H, Yiiter H, Baradan B (2007) Sulfuric acid resistance of high-volume fly ash concrete. Building and Environment 42: 717–721.
- Bamforth PB (1980) In-situ measurement of the effect of partial cement replacement using either fly ash or ground granulated blast furnace slag on the performance of mass concrete. Proceedings, Institution of Civil Engineering 69: 777–800.
- Bilodeau A, Malhotra VM (1992) Concrete incorporating high volumes of ASTM Class F fly ashes: mechanical properties and resistance to deicing salt scaling and to chloride-ion penetration. ACI Special Publication SP-132: 319–349.
- Brown JH. (1982) The strength and workability of concrete with PFA substitution. Proceedings International Symposium on the Use of PFA in Concrete, University of Leeds, England, pp. 151–161.
- Burns JS, Guarnaschelli C, McAskill, J (1982) No controlling the effect of carbon in fly ash on air entrainment. Proceedings, 6th International Symposium on Fly Ash Utilization, Reno, Nevada, DOE/METC, pp. 294–313.

- Buttler FG, Dector MH Smith GR (1983) Studies on the desiccation and carbonation of systems containing Portland cement and fly ash. ACI SP – 79 (1): 367–383.
- Cabrera JG, Lynsdale CJ (1988) A new gas permeameter for measuring the permeability of mortar and concrete. Magazine of Concrete Research 40: 77–82.
- Carette GG, Malhotra VM (1984) Characterization of Canadian fly ashes and their performance in concrete. Division Report MRP/MSL 84 - 137, CANMET, Energy, Mines and Resources, Canada.
- Carette GG, Malhotra VM (1987) Characterization of Canadian fly ashes and their relative performance in concrete. Canadian Journal of Civil Engineering 14: 267–282.
- Central Electricity Generating Board (CEGB) (1967) PFA data book. London.
- Chalee W, Teekavanit M, Kiattikomol K, Siripanichgorn A, Jaturapitakkul C (2007) Effect of W/C ratio on covering depth of fly ash concrete in marine environment. Construction and Building Materials 21: 965–971.
- Chindaprasirt P, Chotithanorm C, Cao, HT, Sirivivatnanon (2007) Influence of fly ash fineness on the chloride penetration of concrete. Construction and Building Materials 21: 356–361.
- Compton FR, Macinnis (1952) Field trial of fly ash concretes. Ontario Hydro Research News, pp. 18–21.
- Cook JE (1982) Research and application of high strength concrete using class C fly ash. Concrete International 4: 72–80.
- Crow RD, Dunstan ER (1981) Properties of fly ash concrete. Proceedings of Symposium on Fly Ash Incorporation in Hydrated Cement Systems, Edited by Sidney Diamond, materials research society, Boston, pp. 214–225.
- Demirboğa R (2007) Thermal conductivity and compressive strength of concrete incorporation with mineral admixtures. Building and Environment 42: 2467–2471.
- Demirboğa R, Türkmen, I, Karakoc MB (2007) Thermo-mechanical properties of concrete containing high-volume mineral admixtures. Building and Environment 42: 349–354.
- Diamond S (1981) Effects of two Danish fly ashes on alkali contents of cement fly ash pastes. Cement and Concrete Research 11: 383–394.
- Diamond S (1985) Selection and use of fly ash for high way concrete. Joint Highway Research Project, Purdue University, Indiana.
- Dunstan ER (1976) Performance of lignite and sub-bituminous fly ash in concrete. A progress Report REC - ERC - 76 - 1, USBR.
- Dunstan ER (1980) A possible method for identifying fly ashes that - will improve sulfate resistance of concretes. ASTM Cement, Concrete and Aggregate 2: 20–30.
- Dunstan ER (1981) The effect of fly ash on concrete alkali-aggregate reaction. ASTM Cement, Concrete and Aggregate 3: 10–104.
- Electric Power Research Institute (1987) Classification of fly ash for use in cement and concrete. CS-5116, Project 2422-10.
- Ellis WE Jr, Rigs EH, Butler WB (1991) Comparative results of utilization of fly ash, silica fume and GGBS in reducing the chloride permeability of concrete. Proceedings of the 2nd CAN-MET/ACI International Conference on Durability of Concrete, Montreal, Canada, ACI SP-126 (1): 443–457.
- Erdoğan K., Türker P (1998) Effects of fly ash particle size on strength of Portland cement fly ash mortars. Cement and Concrete Research 28 (9): 1217–1222.
- Fay K F V, Pierce JS (1989) Sulfate Resistance of concretes with various fly ashes. ASTM Standardisation News, pp. 32–37.
- Gebauer J (1982) Source observations on the carbonation of fly ash concrete. Silicate Industrials 6: 155–159.
- Gebler SH, Klieger P (1983) Effect of fly ash on the air void stability of concrete. Proceedings of the 1st International Conference on the Use of Fly Ash, Silica Fume, Slag and Other Mineral by Products in Concrete. ACI SP 79: 103–142.
- Ghafoori N, Diawara H (1999) Abrasion resistance of fine aggregate replaced silica fume concrete. ACI Materials Journal 96 (5): 559–567.

- Ghosh RS, Timusk J (1981) Creep of fly ash Concrete. *ACI Journal* 78 (5): 351–387.
- Gifford PM, Langan BW, Day RL, Joshi RC, Ward MA (1987) A study of fly ash concrete in curb and gutter construction under various laboratory and field curing regimes. *Canadian Journal of Civil Engineering* 14 (5): 614–620.
- Gopalan MK (1996) Sorptivity of fly ash concretes. *Cement and Concrete Research* 26 (8): 1189–1197.
- Haque MN, Langan BW, Ward MA (1988) High fly ash concretes. *ACI Materials* 8 (1): 54–60.
- Ho DWS, Lewis RK (1983) Carbonation of concrete incorporating fly ash or a chemical admixture. *ACI SP* – 79: 333–346.
- Hobbs DW (1981) The Alkali silica reaction: A model for predicting expansion in mortar. *Magazine of Concrete Research* 33:208–220.
- Hobbs DW (1983) Influence of fly ash on the workability and early strength of concrete. *Proceedings of the 1st International Conference on the Use of Fly Ash, Silica Fume, Slag and Other Mineral By-Products in Concrete, ACI SP 79*: 289–306.
- Idorn GM (1991) Concrete durability and resource economy. *Concrete International* 13 (7): 18–23.
- IS: 1237 (1980) Method for testing abrasion resistance of concrete, Bureau of Indian Standards (BIS), New Delhi, India.
- Joshi RC (1970) Experimental production of synthetic fly ash from kaolinite. MS Thesis, Iowa State University.
- Joshi RC (1979) Sources of pozzolanic activity in fly ashes – A Critical Review. *Proceedings of the 5th International Fly Ash Utilization Symposium, Atlanta, Georgia, USA*, pp. 610–623.
- Joshi RC (1987) Effect of a sub-bituminous fly ash and its properties on sulfate resistance of sand cement mortars. *Journal of Durability of Building Materials* 4: 271–286.
- Joshi RC, Lam DT (1987) Sources of self-hardening properties of fly ashes. *Materials Research Proceedings, Vol. 86, MRS. Pittsburgh, USA*, pp. 183–184.
- Joshi RC, Lohtia RP (1993) Effects of premature freezing temperatures on compressive strength, elasticity and microstructure of high volume fly ash concrete. *Third Canadian Symposium on Cement and Concrete, Ottawa, Canada*.
- Joshi RC, Lohtia RP, Salam MA (1993) High strength concrete with high volumes of Canadian sub-bituminous coal ash. *Third International Symposium on Utilization of High Strength Concrete, Lillachhammer, Norway*.
- Joshi RC, Lohtia RP, Salam MA (1994) Some durability related properties of concretes incorporating high volumes of sub-bituminous coal fly ash. *Proceedings, 3rd CANMET/ACI International Conference on Durability of Concrete, Nice, France*, pp. 447–464.
- Kasai Y, Matsui I, Fukushima U, Kamohara, H (1983) Air permeability of blended cement mortars. *Proceedings of the 1st International Conference on the Use of Fly Ash, Silica-Fume, Slag and Other Mineral By-Products in Concrete. ACI SP 29*: 435–451.
- Lane RO Best GF (1982) Properties and use of fly ash in Portland cement concrete. *Concrete International* 4: 81–92.
- Langan BV, Joshi RC, Ward MA (1990) Strength and durability of concrete containing 50% Portland cement replacement by fly ash and other materials. *Canadian Journal of Civil Engineering* 17 (1): 19–27.
- Langley WS, Caratte GG, Malhotra VM (1989) Structural concrete incorporating high volumes of ASTM class F fly ash. *ACI Materials Journal* 86 (5): 507–514.
- Larsen TD (1985) Use of fly ash in structural concrete in Florida, Presented at fly ash in high way construction seminar, Atlanta, Georgia.
- Liu TC (1981) Abrasion resistance of concrete. *ACI Journal Proceedings* 78 (5): 341–350.
- Lohtia RP, Nautiyal BD, Jain OP (1976) Creep of fly ash concrete. *ACI Journal* 73: 469–472.
- Lohtia RP, Nautiyal BD, Jain KK, Jain OP (1977) Compressive strength of plain and fly ash concrete by non-destructive testing methods. *Journal of the Institution of Engineers (India)* 58 a – 1: 40–45.
- Malhotra VM, Caratte GG, Bilodeau A, Sivasundram V (1990) Some aspects of durability of high volume ASTM class F (Low calcium) fly ash concrete. *Mineral Sciences Laboratories, Division Report MSL - 90 - 20 (OP & J)*.

- Malhotra VM, Carrette GG, Bremmer TW (1982) Durability of concrete containing granulated blast furnace slag or fly ash or both in Marine environment, Report 80 - 18E, CANMET, EMR, Canada.
- McCarthy GJ, Johansen DM, Steinwand SJ (1988) X-ray diffraction analysis of fly ash. Vol. 31, Barrett CS et al. (Eds.), *Advances in x-Ray Analysis*, Plenum Press, New York.
- Mehta PK (1983) Pozzolan and cementitious by-products as mineral admixtures for concrete – a critical review. *Proceedings of the 1st International Conference on the Use of Fly Ash, Slag and Silica Fume in Concrete*, Montebello, Canada, ACI SP 79: 1–46.
- Mehta PK (1988) Standard specifications for mineral admixtures – an overview. ACI SP 91: 637–658.
- Mehta PK (1993) Sulfate Attack on concrete – a critical review. *Materials science of concrete – Part: III*, Skalny J (Ed.), American Ceramic Society, pp. 105–130.
- Mehta PK (1994) Symposium on Durability of Concrete. Khayat IH, Aitcin PC (Eds.), Nice, France, pp. 99–118.
- Mulenga DM, Stark J, Nobst P (1999) Praxisnahes Prüfverfahren zum Sulfatwiderstand von Beton und Mörtel mit und ohne Flugasche. In: *Beiträge zum DafStb—Forschungskolloquium*, Bauhaus-Universität Weimar 37: 197–207.
- Mulenga DM, Stark J, Nobst P (2003) Thaumassite formation in concrete and mortars containing fly ash. *Cement & Concrete Composites* 25: 907–912.
- Munday JGL, Ong LT, Wong LG, Dhir RK (1982) Load independent movements in OPC/PFA concrete. Cabreva JA, Cusens RR (Eds.), *Proceedings, International Symposium on the Use of PFA in Concrete*, University of Leeds, England, pp. 243–246.
- Muralidharan S, Saraswathy V, Thangavel K, Srinivasan S. (2000) Competitive role of inhibitive and aggressive ions in the corrosion of steel in concrete. *Journal of Applied Electrochem* 30: 1255–1259.
- Nagataki S, Ohga H, Kim EK (1986) Effect of curing conditions on the carbonation of concrete with fly ash and the corrosion of reinforcement in long term basic. ACI SP 91: 521–540.
- Naik TR, Singh SS, Hossain MM (1994) Permeability of concrete containing large amounts of fly ash. *Cement and Concrete Research* 24 (5): 913–922.
- Naik TR, Singh SS, Hossain MM (1995) Abrasion resistance of high-strength concrete made with class C fly ash. *ACI Materials Journal* 92 (6): 649–659.
- Naik TR, Singh SS, Ramme BW (1998) Mechanical properties and durability of concrete made with blended fly ash. *ACI Materials Journal* 95 (4): 454–462.
- Nanni A (1989) Abrasion resistance of roller-compacted concrete. *ACI Materials Journal* 86 (53): 559–565.
- Nasser KW, Al-Manasser AA (1986) Shrinkage and creep of concrete containing 50 percent lignite fly ash at different stress – strength ratios. *Proceedings of the 2nd International Conference on Fly Ash, Silica Fume, Slag and Natural Pozzolans in Concrete*, ACI SP 91 (1): 433–448.
- Nasser KW, Marzouk, HM (1983) Properties of concrete made with sulfate resisting cement and fly ash. *Proceedings First International Conference on the Use of Fly Ash, Silica Fume, Slag and Other Mineral By-Products in Concrete*, ACI SP 79: 383–395.
- Neville AM (1973) *Properties of concrete* (2nd Edition). John Wiley, New York, 382 p.
- Oberholster RE, Westra WB (1981) The effectiveness of mineral admixtures in reducing expansion due to alkali-aggregate reaction with malmesbury group aggregate. *Proceedings of the 5th International Conference on Alkali-Aggregate Reaction in Concrete*, Cape Town, South Africa.
- Owens PL (1979) Fly ash and its usage in concrete. *Concrete Society Journal*, England 13 (7): 21–26.
- Ozer B, Ozkul MH (2004) The influence of initial water curing on the strength development of ordinary Portland and pozzolanic cement concretes. *Cement and Concrete Research* 34: 13–8.
- Pepper L, Mather B (1959) Effectiveness of mineral admixtures in preventing excessive expansion of concrete due to alkali-aggregate reaction. *Proceedings, ASTM* 59: 1178–1202.
- Perry C, Day RL, Joshi RC, Langan BW, Gillot JE (1987) The effectiveness of twelve Canadian fly ashes in suppressing expansion due to alkali-silica reaction. *Proceedings of the 7th International Conference on Alkali-Aggregate Reaction*, Ottawa, pp. 93–97.

- Raba, F Jr, Smith SL, Mearing M (1981) Sub bituminous fly ash utilization in concrete. Diamond S (Ed.), Proceedings Symposium on Fly Ash Incorporation on Hydrated Cement Systems, Materials Research Society, Boston, pp. 296–306
- Ramakrishnan V, Coyle WV, Brown J, Tluskus A, Benkataramanyam P (1981) Performance characteristics of concrete containing fly ash. Diamond S (Ed.), Proceedings Symposium on Fly Ash Incorporation in Hydrated Cement Systems, Materials Research Society, Boston, pp. 233–243.
- Ravina D (1981) Efficient utilization of coarse and fine fly ash in precast concrete by incorporating thermal curing. *ACI Journal* 78 (3): 194–200.
- RILEM CP113 (1984) Absorption of water by immersion under vacuum. *Material Structures Research Testing* 101: 393–394.
- Rodway LE, Fedriko, WM (1989) Superplasticized high volume fly ash structural concrete. *ACI SP* 114 (1): 98–112.
- Roy DM, Arjunan P, Silsbee MR (2001) Effect of silica fume, metakaolin, and low-calcium fly ash on chemical resistance of concrete. *Cement and Concrete Research* 31 (12): 1809–1813.
- Saraswathy V, Muralidharan S, Thangavel K, Srinivasan S (2003) Influence of activated fly ash on corrosion-resistance and strength of concrete. *Cement and Concrete Composites* 25: 673–680.
- Schiepl P, Raupach M (1992) Influence of the type of cement on the corrosion behavior of steel in concrete. *Ninth International Congress on the Chemistry of Cement*, New Delhi, pp. 296–301.
- Schiepl P, Hardtle R (1994) Relationship between durability and fore structure properties of concretes containing fly ash. Khayat IH, Aitcin PC, (Eds.), P.K. Mehta Symposium on Durability of Concrete, Nice, France, pp. 99–118.
- Shafiq N, Cabrera JG (2004) Effects of initial curing condition on the fluid transport properties in OPC and fly ash blended cement concrete. *Cement & Concrete Composites* 26: 381–387.
- Short NR, Page CL (1982) The diffusion of chloride ions through Portland and blended cement pastes. *Silicate Industrials* 237–240.
- Siddique R (2003a) Effect of fine aggregate replacement with class F fly ash on the mechanical properties of concrete. *Cement and Concrete Research* 33 (4): 539–547.
- Siddique R (2003b) Effect of fine aggregate replacement with class F fly ash on the abrasion resistance of concrete. *Cement and Concrete Research* 33 (11): 877–1881.
- Sivasundram V, Carette GG, Malhotra VM (1989) Properties of concrete incorporating low quantity of cement and high volumes of low-calcium fly ash. *Proceedings of the 3rd International Conference on Fly Ash, Silica Fume, Slag and Natural Pozzolans in Concrete*, ACI SP 114: 45–71.
- Sivasundram V, Carette GG, Malhotra VM (1990) Selected properties of high volume fly ash concretes. *ACI Concrete International*, vol. 12, no. 10. 12 (10):47–50.
- Stanton TE (1942) Expansion of concrete through reaction between cement and aggregate. *Transactions ASCE Part 2*: 68–85.
- Swamy RN, Mahmud HB (1986) Mix proportions and strength characteristics of concrete containing 50% low-calcium fly ash. *Proceedings of the 2nd CANMET/ACI International Conference on Fly Ash, Silica Fume, Slag and Natural Pozzolans in Concrete*, ACI SP 91 (1): 413–432.
- Tattersall GH, Benfill PFG (1983) *The Rheology of Fresh concrete*. Pitman, London.
- Termkhajornkit P, Nawa T, Kurumisawa K (2006) Effect of water curing conditions on the hydration degree and compressive strengths of fly ash-cement paste. *Cement & Concrete Composites* 28: 781–789.
- Thomas MDA, Matthews JD (1992) The permeability of fly ash concrete. *Materials and Structures* 25 (151): 388–396.
- Tikalsky PJ, Carrasquillo PM, Carrasquillo RL (1988) Strength and durability considerations affecting mix proportions of concrete containing fly ash. *ACI Materials Journal* 85 (6): 505–511.
- Virtanen J (1983) Freeze-thaw resistance of concrete containing blast furnace slag, fly ash or condensed silica fume. *Proceedings of the 1st International Conference on the Use of Fly Ash, Silica Fume, Slag and Other Mineral By-Products*, ACI SP 79: 923–942.
- William JT, Owens PL (1982) The implications of a selected grade of United Kingdom pulverized fuel ash on the engineering design and use in structural concrete. *Proceedings of the International Symposium on the Use of PFA in Concrete*, University of Leeds, England, pp. 301–313.

- Wittekindt W (1960) Sulfatbeständige Zemente und ihre Prüfung. *Zement-Kalk-Gips* 13 (12): 565–72.
- Yazici H, Aydın S, Yiğiter H, Baradan B (2005) Effect of steam curing on class C high-volume fly ash concrete mixtures. *Cement and Concrete Research* 35: 1122–1127.
- Yuan RL, Cook JE (1983) Study of class C fly ash in concrete. *Proceeding of the 1st International Conference on the Use of Fly Ash, Silica Fume, Slag, and Other Mineral By-Products in Concrete*, ACI SP 79: 307–319.

Chapter 7

Rice Husk Ash

Introduction

Rice-husk (RH) is an agricultural by-product material. It constitutes about 20% of the weight of rice. It contains about 50% cellulose, 25–30% lignin, and 15–20% of silica. When rice-husk is burnt rice-husk ash (RHA) is generated. On burning, cellulose and lignin are removed leaving behind silica ash. The controlled temperature and environment of burning yields better quality of rice-husk ash as its particle size and specific surface area are dependent on burning condition. For every 1000 kg of paddy milled, about 200 kg (20%) of husk is produced, and when this husk is burnt in the boilers, about 50 kg (25%) of RHA is generated. Completely burnt rice-husk is grey to white in color, while partially burnt rice-husk ash is blackish.

The form of silica obtained after combustion of rice husk depends on the temperature and duration of combustion of rice husk. Mehta (1979) suggested that essentially amorphous silica can be produced by maintaining the combustion temperature below 500°C under oxidizing conditions for prolonged periods or up to 680°C with a hold time less than 1 min. However, Yeoh et al. (1979) reported that RHA can remain in the amorphous form at combustion temperatures of up to 900°C if the combustion time is less than 1 h, while crystalline silica is produced at 1000°C with combustion time greater than 5 min. Using X-ray diffraction, Chopra et al. (1981) observed that at burning temperatures up to 700°C, the silica was in an amorphous form. The effect of different burning temperatures and the chemical composition of rice husk (Taiwan RHA) were studied by Hwang and Wu (1989). It was observed that at 400°C, polysaccharides begin to depolymerize. Above 400°C, dehydration of sugar units occurs. At 700°C, the sugar units decompose. At temperatures above 700°C, unsaturated products react together and form a highly reactive carbonic residue. The X-ray data and chemical analyses of RHA produced under different burning conditions given by Hwang and Wu (1989) showed that the higher the burning temperature, the greater the percentage of silica in the ash. K, S, Ca, Mg as well as several other components were found to be volatile.

Rice-husk ash (RHA) is a very fine pozzolanic material. The utilization of rice husk ash as a pozzolanic material in cement and concrete provides several advantages, such as improved strength and durability properties, reduced materials costs

due to cement savings, and environmental benefits related to the disposal of waste materials and to reduced carbon dioxide emissions. Reactivity of RHA is attributed to its high content of amorphous silica, and to its very large surface area governed by the porous structure of the particles (Cook, 1984; Mehta, 1992). Generally, reactivity is favored also by increasing fineness of the pozzolanic material. However, Mehta (1979) has argued that grinding of RHA to a high degree of fineness should be avoided, since it derives its pozzolanic activity mainly from the internal surface area of the particles.

Della et al. (2002) reported that a 95% silica powder could be produced after heat-treatment at 700°C for 6 hours. And specific surface area of particles was increased after wet milling from 54 to 81 m²/g.

7.1 Properties of RHA

7.1.1 Physical Properties

RHA is a very fine material. The average particle size of rice-husk ash ranges from 5 to 10 µm. Physical properties values as reported by few authors are given in Table 7.1.

7.1.2 Chemical Composition

Rice husk ash is very rich in silica content. Silica content in RHA is generally more than 80–85%. Chemical composition of RHA as reported by few authors is given in Table 7.2. For RHA to be used as pozzolan in cement and concrete, it should satisfy requirements for chemical composition of pozzolans as per ASTM C618. The combined proportion of silicon dioxide (SiO₂), aluminium oxide (Al₂O₃) and iron oxide (Fe₂O₃) in the ash should be not be less than 70%, and LOI should not exceed 12% as stipulated in ASTM requirement.

Table 7.1 Physical properties of RHA

Property	Value			
	Mehta (1992)	Zhang et al. (1996)	Feng et al. (2004)	Bui et al. (2005)
Mean particle size (µm)	–	–	7.4	5
Specific gravity	2.06	2.06	2.10	2.10
Fineness: Passing 45 µm (%)	99	99	–	–

Table 7.2 Chemical composition of RHA

Constituents	Percentage		
	Mehta (1992)	Zhang et al. (1996)	Bui et al. (2005)
Silica (SiO ₂)	87.2	87.3	86.98
Alumina (Al ₂ O ₃)	0.15	0.15	0.84
Iron Oxide (Fe ₂ O ₃)	0.16	0.16	0.73
Calcium Oxide (CaO)	0.55	0.55	1.40
Magnesium Oxide (MgO)	0.35	0.35	0.57
Sodium Oxide (Na ₂ O)	1.12	1.12	0.11
Potassium Oxide (K ₂ O)	3.68	3.68	2.46
Sulfur Oxide (SO ₃)	0.24	0.24	—
LOI	8.55	8.55	5.14

7.1.3 Pozzolan Activity

Rice husk contains considerable amount of SiO₂. Well burnt and well-ground rice husk ash is very active and considerably improves the strength and durability of cement and concrete. This pozzolanic material with good and consistent properties can be obtained only by burning rice husk under well-defined conditions. The sensitivity of burning conditions is the primary reason that prevents the widespread use of this material as pozzolan (Hewlett, 1998; Real et al., 1996). It has been reported that acid leaching of the husk helps to obtain relative pure silica with high specific surface area (Inoue and Hara, 1996). It is possible to enhance the pozzolanic properties and decrease the sensitivity of burning conditions of this material.

Zhang et al. (1996) studied the effect of incorporation of RHA on the hydration, microstructure and interfacial zone between the aggregate and paste. Based on the investigation, they concluded that: (i) calcium hydroxide [Ca(OH)₂] and calcium silicate hydrates [C-S-H] were the major hydration and reaction products in the RHA paste. Because of the pozzolanic reaction, the paste incorporating RHA had lower Ca(OH)₂ content than the control Portland cement paste; and (ii) incorporation of the RHA in concrete reduced the porosity and the Ca(OH)₂ amount in the interfacial zone; the width of the interfacial zone between the aggregate and the cement paste compared with the control Portland cement composite was also reduced. However, the porosity of the rice-husk ash composite in the interfacial zone was higher than that of the silica fume composite.

Yu et al. (1999) reported that improvement of concrete properties up on addition of RHA may be attributed to the formation of more C-S-H gel and less portlandite in concrete due to the reaction between RHA and the Ca⁺, OH⁻ ions or Ca(OH)₂.

Cisse and Laquerbe (2000) concluded that pozzolanic activity of rice-husk ash was responsible for the better strength and performance of sandcrete blocks in comparison with classic mortar blocks. In addition, the use of rice-husk ash enabled production of lightweight sandcrete with insulating properties at reduced cost.

Jauberthie et al. (2000) reported that concentration of silica is high on the external face of the husk, much weaker on the internal face and practically non-existent within the husk. An analysis of these zones is given in Table 7.3. These results

Table 7.3 Analysis of rice husk (Jaubertie et al., 2000)

Element	Micro analysis of external surface of rice husk		Micro analysis of interior surface of rice husk		Micro analysis of internal surface of rice husk	
	% (by weight)	% (by atomic)	% (by weight)	% (by atomic)	% (by weight)	% (by atomic)
C	6.91	11.11	62.54	69.54	30.20	40.93
O	47.93	57.84	35.19	29.38	42.53	43.27
Si	45.16	31.05	2.27	1.08	27.27	15.80
Total	100	100	100	100	100	100

confirm that the presence of amorphous silica is concentrated at the surfaces of the rice husk and not within the husk itself. Amorphous silica concentrated on the interior and exterior surfaces of the uncalcinated husk promote a pozzolanic action on the surface of the husk and therefore enable its use in cement/concrete.

Feng et al. (2004) investigated the effect of hydrochloric acid pretreatment and heating course on the pozzolanic activity of rice husk ash. Three methods were used to estimate the pozzolanic activity: (i) Rapid evaluation method—conductivity measurement, the conductivity method proposed by Luxan et al. (1989). The greater the change in the conductivity of the saturated $\text{Ca}(\text{OH})_2$ solution added with rice husk ash, the more active rice husk ash is. This method is valid to evaluate the pozzolanic activity of rice husk ash (1996); (ii) measuring the rate of consumption of $\text{Ca}(\text{OH})_2$ that reacted with rice husk ash. Rice husk ash/ $\text{Ca}(\text{OH})_2 = 1:1$, $\text{W/C} = 1.0$, 20°C , the $\text{Ca}(\text{OH})_2$ used was analytical grade $\text{Ca}(\text{OH})_2$; and (iii) comparing the strength of mortar made with and without rice husk ash. Hydrochloric acid-treated rice husk was prepared by immersing rice husk in 1 N HCl aqueous solution. The husks were washed repeatedly with water until hydrochloric acid was undetected in the filtrate and then air-dried at room temperature. Two kinds of rice husk ash were obtained by heating rice husk in a batch furnace under oxidizing atmosphere by which rice husk ash can be produced about 300 g at a time. One kind of rice husk ash (ADR) was obtained by heating hydrochloric acid treated rice husk, and another kind of rice husk ash (RHA) was obtained by heating untreated rice husk. The heating temperature ranged from 350 to 1100°C and the maintaining time was 4 h, and then the rice husk ash was ground in a ball mill for 60 min by adding grinding agent. Based on the study, they concluded that: (i) with hydrochloric acid pretreatment of rice husks, the pozzolanic activity of rice husk ash was stabilized and enhanced as well; the sensitivity of the pozzolanic activity of the rice husk ash to burning conditions was reduced. The pozzolanic activity of ADR (pretreated) was slightly affected by the change of maintaining time, but the maintaining time had a great effect on the pozzolanic activity of RHA (no pretreatment); (ii) the two kinds of rice husk ashes had the same rate of lime consumption at a very rapid rate in the initial period of reaction. The mechanism of reaction was consistent with diffusion control and ADR had a faster reaction rate with lime than RHA. The main reaction product was a C-S-H gel; (iii) during the first 12 h, RHA and ADR showed similar

behavior in the increase of hydration heat of the cement. The pozzolanic activity of ADR is higher than that of RHA; and (iv) because of the high of amorphous SiO_2 content in ADR with high activity, a significant increase in the strength of ADR specimen was observed compared with the strength of control mortar and that made with RHA. The cement mortar added with ADR had lower Ca(OH)_2 content after 7 days. The pore size distribution of the mortar with ADR showed a tendency to shift towards the smaller pore size.

Agarwal (2006) studied the accelerated pozzolanic activity of various siliceous materials, like rice husk ash, silica fume, fly ash, quartz, precipitated silica, and metakaolin. The compressive strength of accelerated tests was compared with cubes cured in water at 7 and 28 days. Maximum activity was observed in case of RHA ($< 45 \mu\text{m}$), followed by quartz and silica fume.

7.2 Fresh Properties of Paste/Concrete Containing RHA

7.2.1 Workability

Ikpong and Okpala (1992) studied the variation in workability of concrete of designed strengths with the incorporation of RHA. Cement was partially replaced with 0, 20, 25, and 30% of RHA. 28-day designed strength of concretes was 20, 25, 30, and 40 N/mm^2 . Slump and compaction factor results are given in Table 7.4. Based on the results, they concluded that: (i) to attain the same level of workability, the mixes containing rice husk ash required higher water content than those containing only ordinary Portland cement as the binder. This was reflected in the water-cement ratios of the three mixes (0%, 30 and 40% RHA contents) for each design strength, which have been calculated on the assumption of a constant cement content by weight (using the cement content of the mix containing 0% RHA); and (ii) with minor

Table 7.4 W/C ratio, slump and compaction factor values of mixes (Ikpong and Okpala, 1992)

Design strength (N/mm^2)	RHA (%)	W/C ratio	Slump (mm)	Compacting factor
20	0	0.80	40	0.926
	30	0.83	33	0.93
	40	0.85	35	0.92
25	0	0.69	35	0.89
	30	0.72	35	0.87
	40	0.75	37	0.92
30	0	0.59	50	0.92
	30	0.64	55	0.90
	40	0.65	35	0.89
40	0	0.54	50	0.90
	30	0.57	45	0.87
	40	0.61	45	0.91

variations, this higher water content of mixes containing RHA when compared with the conventional mixes was found to increase with the design strength of the mixes. For the mixes having 30% RHA content the percentage increases were 3.2, 4.4, 8.5 and 5.6 for the design strengths of 20, 25, 30, and 40 N/mm² respectively. And for the mixes having 40% RHA content the percentage increases, were 6.3, 8.7, 10.2 and 13.0 for the corresponding design strengths.

Ismail and Waliuddin (1996) reported the effect of rice husk ash (RHA) passing #200 and #325 sieves as 10–30% partial replacement of cement on the workability of high-strength concrete (HSC). Control mixture had proportion of 1:1.07:1.90 with cement content of 571 kg/m³. Slump and density results are given in Table 7.5. It can be seen that slump and density values were reduced with the increase in RHA content. However, fineness of RHA did not have significant effect on both of these properties.

Bui et al. (2005) investigated the influence of rice husk ash on the slump of concrete mixtures. Two types (PC30 and PC40) of ordinary Portland cement were used. Cement PC 30 and PC 40 had Blain specific surface area of 2700 and 3759 cm²/g, respectively. Three water-to-binder ratios (0.30, 0.32, and 0.34) were used. Rice husk ash was used to replace 10%, 15% and 20% by mass of PC. The superplasticizer was added to all mixtures for obtaining high workability. In the mixtures with water to binder ratio of 0.34, the amount of superplasticizer was kept constant to investigate the influence of RHA on workability. Figure 7.1 shows the influence of RHA content on the slump of gap-graded mixtures made with water to binder ratio of 0.34. It is clear that slump decreased with the increase in RHA content for same level of superplasticizer.

7.2.2 Air-Entrainment

Zhang and Malhotra (1996) studied the effect of RHA on the AEA requirement of concrete mixtures. They used RHA as partial replacement of cement in varying percentages (0, 5, 8, 10 and 15%). Results are shown in Fig. 7.2. They concluded that AEA requirement increased with the increase in RHA content possibly because of high specific surface area of RHA in comparison to cement.

Table 7.5 Fresh concrete properties (Ismail and Waliuddin, 1996)

Mix type	RHA (%)		w/ (C+RHA)	Slump (mm)	Density (kg/m ³)
	#200	#325			
A	–	–	0.24	70	2425
Aa-10	10	–	0.31	30	2405
Aa-20	20	–	0.33	60	2400
Aa-30	30	–	0.36	30	2398
Ab-10	–	10	0.30	30	2403
Ab-20	–	20	0.32	45	2396
Ab-30	–	30	0.34	32	2390

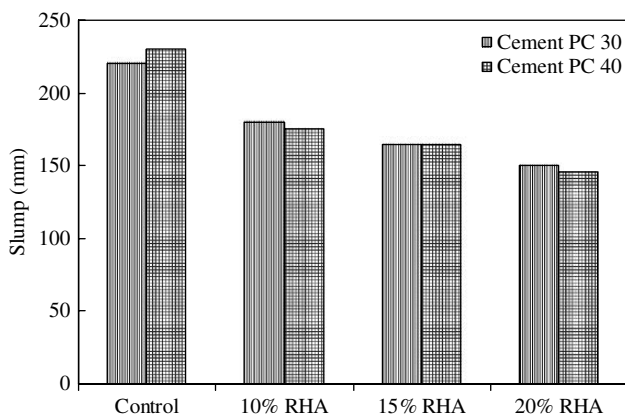


Fig. 7.1 Slump variation of gap-graded concretes made with different fineness at constant superplasticizer content (Bui et al., 2005)

7.2.3 Consistency and Setting Times

Singh et al. (2002) examined the effect of lignosulfonate (LS) and CaCl_2 on the setting times, consistence and pozzolanic reaction of blended cement made with RHA. Pastes of 10% RHA-blended Portland cement were made with the addition of 2% CaCl_2 , 1% LS, and (1% LS+ 2% CaCl_2). Both the initial and final setting times were enhanced considerably in the presence of 1% LS indicating that it prolonged the setting behavior. It showed that 1% LS acted as a retarder. The 2% CaCl_2 , on the other hand, reduced both initial and final setting times showing that it acted as an accelerator in the hydration of RHA-blended OPC. However, in the presence of

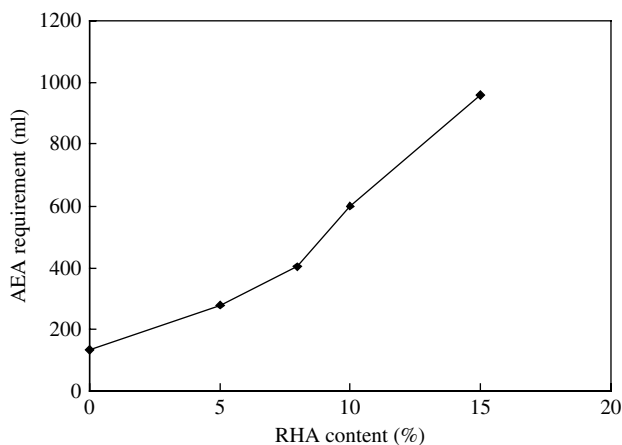


Fig. 7.2 Relationship between requirement of air-entraining admixture and RHA content (Zhang and Malhotra, 1996)

a mixture of 1% LS and 2% CaCl_2 , the setting time values were higher than that in the presence of 2% CaCl_2 and lower than that in the presence of 1% LS. The effect of admixtures on the consistency of 10% RHA-blended OPC is given in Table 7.6. From the table, it is clear that in the presence of 1% LS, the water/binder ratio was reduced considerably as is generally expected in the presence of a superplasticizer. In the presence of 2% CaCl_2 (an accelerator), the water/binder ratio was lower than that of control but higher than that in the presence of 1% LS. However, in the presence of a mixture of 1% LS and 2% CaCl_2 , the water/binder ratio was the lowest. This indicated that water reduction was enhanced in the presence of a mixture of a superplasticizer (1% LS) and an accelerator (2% CaCl_2).

Jaturapitakkul and Roongreung (2003) studied the normal consistency and setting times of cementing material made from rice husk ash (RHA) and calcium carbide residue (CCR). Calcium Carbide Residue (CCR) is a by-product of acetylene production process. CCR consists mainly of calcium hydroxide, $\text{Ca}(\text{OH})_2$, and is obtained in a slurry form. Chemical composition of CCR was 51.94% CaO , 3.36% SiO_2 , 2.56% Al_2O_3 , 0.33% Fe_2O_3 , 0.46% MgO , 0.03% K_2O , 0.22% SO_3 and 41.72% LOI. The major compound in RHA was SiO_2 (78.22%). The normal consistency of cement paste was 23.9% while those of CCR-RHA pastes were between 43.7% and 62.0%, depending on RHA content. Paste 80C20R (80% of CCR and 20% of RHA) had normal consistency of 43.7% and increased to 62.0% in paste 20C80R (20% of CCR and 80% of RHA). The normal consistency of CCR-RHA pastes needed more water than that of cement paste because of the high porosity of the two materials as well as the high LOI of CCR. The higher the RHA content in the paste, the higher was the water requirement to maintain the same normal consistency. Initial and final setting times of the cement paste were 107 and 195 min, respectively. For CCR-RHA pastes, the shortest setting time occurred in paste 50C50R and the longest setting time was paste 80C20R. The initial and final setting times of paste 50C50R were 345 and 635 min, respectively, while those of paste 80C20R, the longest setting times, were 502 and 680 min, respectively. The initial setting time of the new cementing material was about 3.2–4.6 times longer than that of the cement paste. The results suggested that the ratio of CCR to RHA of 50–50% by weight was the suitable ratio to obtain the highest pozzolanic reaction. In CCR-RHA paste, the $\text{Ca}(\text{OH})_2$ from CCR reacted with SiO_2 from RHA to form CSH while Portland cement reacted with water and formed CSH directly. The long setting times of calcium carbide residue-rice husk ash paste was because the pozzolanic reaction between pozzolan and lime was usually much slower than the hydration of cement.

Table 7.6 Variation of water consistency with admixtures (Singh et al., 2002)

Composition	Water-binder
90% OPC + 10% RHA	0.42
90% OPC + 10% RHA + 2% CaCl_2	0.40
90% OPC + 10% RHA + 1% LS	0.38
90% OPC + 10% RHA + 2% CaCl_2 + 1% LS	0.37

7.3 Properties of Hardened Concrete Containing RHA

7.3.1 Porosity and Water Absorption Capacity

Saraswathy and Song (2007) investigated the effect of partial replacement of cement with rice husk ash (RHA) on the porosity and water absorption of concrete. Cement was replaced with 0, 5, 10, 15, 20, 25, and 30% RHA. Proportion of control (with out RHA) mix was 1:1.5:3 with w/c ratio of 0.53. Porosity and water absorption test was carried out as per ASTM C642-97. For determination of effective porosity and coefficient of water absorption, specimens of size 83 mm diameter and 50 mm thick were cast with and without rice husk ash and cured for 28 days in distilled water. After the curing period was over the specimens were dried in an oven at $105 \pm 5^\circ\text{C}$ for 48 h in order to evaporate the moisture content present in the concrete. Table 7.7 shows the results of porosity and coefficient of water absorption. Based on the results, they concluded that: (i) porosity values decreased with the increase in RHA content because small RHA particles improved the particle packing density of the blended cement, leading to a reduced volume of larger pores; and (ii) coefficient of water absorption for rice husk ash replaced concrete at all replacement levels was found to be less when compared to control concrete.

7.3.2 Compressive and Tensile Properties

Ikpong and Okpala (1992) studied the variation in strength of medium workability concrete with the incorporation of RHA. Cement was partially replaced with 0, 20, 25 and 30% of RHA. 28-day designed strength of concretes was 20, 25, 30 and 40 N/mm^2 . Compressive strength results up the age of 90 days, are given in Table 7.8. The compressive strength continued to increase with age for each of the mixes. The control mix (0% RHA) attained a higher strength than the OPC/RHA mixes at all age. At the age of 28 days all the OPC/RHA concretes, except the designed mix of 40 N/mm^2 , had attained their 28-day design strengths. For the designed mix of 40 N/mm^2 , the mix having 30% RHA content reached 98.5% of its design strength, while the one having 40% RHA content reached 86.5%. Furthermore

Table 7.7 Porosity and water absorption of rice husk replaced Concrete (Saraswathy and Song, 2007)

RHA (%)	Porosity (%)	Water absorption coefficient (m^2/s)
0	18.06	3.5571×10^{-10}
5	18.18	6.7587×10^{-11}
10	13.82	1.0320×10^{-11}
15	13.80	1.0644×10^{-11}
20	13.54	1.2122×10^{-10}
25	13.04	1.4548×10^{-10}
30	11.89	1.3030×10^{-10}

Table 7.8 Compressive strength development with age (Ikpong and Okpala, 1992)

Design strength (N/mm ²)	RHA (%)	Compressive strength (N/mm ²)			
		7-day	14-day	28-day	90-day
20	0	17.5	23.9	33.1	37.8
	30	15.8	18.2	29.1	36.1
	40	13.27	15.2	27.2	33.9
25	0	22.9	27.2	35.4	39.2
	30	18.7	23.8	31.1	37.5
	40	14.8	21.0	28.6	34.0
30	0	28.4	37.6	43.5	46.3
	30	22.6	32.0	38.3	43.2
	40	16.7	27.5	31.8	37.1
40	0	32.4	38.8	44.2	47.6
	30	24.0	33.5	39.4	44.9
	40	1.5	29.3	34.6	38.9

even at the early age of 7 days most of the OPC/RHA concretes had attained over 60% of their 28-day design strengths. The worst case which was the designed mix of 40 N/mm² containing 40% RHA, attained 46% of its 28-day design strength.

Zhang and Malhotra (1996) investigated the influence of 10% RHA inclusion as partial replacement of cement on the compressive strength of concrete and compared it with the compressive strength of concrete containing 10% silica fume (SF). Water-to-cementitious material ratio was maintained at 0.40. Compressive strength results up to the age of 730 days are shown in Fig. 7.3. It can be seen that RHA concrete, in general, achieved higher strength than control concrete mixture but lower than that of silica fume concrete. At 28 days, the RHA concrete had a compressive strength of 38.6 MPa compared with 36.4 MPa for the control concrete and 44.4 MPa for SF concrete. At 180 days, RHA concrete exhibited compressive strength of 48.3 MPa compared with 44.2 MPa for the control concrete and 50.2 MPa for SF concrete.

Ismail and Waliuddin (1996) examined the effect of rice husk ash (RHA) passing #200 and #325 sieves as 10–30% partial replacement of cement on the compressive strength of high-strength concrete (HSC). Control mixture had mixture proportion of 1:1.07:1.90 with cement content of 571 kg/m³. Strength tests were conducted up to the age of 150 days, and results are given in Table 7.9. Based on the test results, they concluded that: (i) it is possible to get high strength concrete economically using RHA; (ii) optimum replacement of cement by RHA was around 10% to 20% with finely ground RHA; (iii) rate of hydration in concrete made with part replacement of cement by RHA was slow as compared to concrete with OPC. This fact was very dominant during the initial three days of age of concrete. This rate of slow hydration also affects the 150 day strength of concrete made by part replacement of cement by RHA in the mix; and (iv) the lower strength of concrete made with part replacement of cement by RHA was because of higher w/c ratios. Though the w/c ratio for samples Ab-10 and Ab-20 was 23 and 28% higher than w/c ratio in

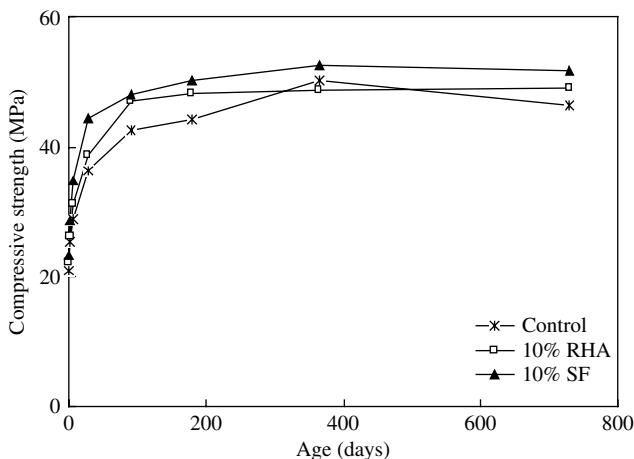


Fig. 7.3 Development of compressive strength of concrete with RHA and silica fume (Zhang and Malhotra, 1996)

specimen-A, the 28 day strength was 98% and 97% of the concrete of Mix-A where no replacement was made.

Zhang and Malhotra (1996) studied the mechanical properties of concrete made with 10% RHA and 10% silica fume (SF). Tests were conducted at the age of 28 days, and results are given in Table 7.10. These results indicated that splitting tensile strength, flexural strength and modulus of elasticity of control and concrete incorporating RHA and SF were comparable.

Wada et al. (1999) demonstrated that RHA mortar and concrete exhibited higher compressive strength than the control mortar and concrete. They have further reported excellent strength development at the early stages even without steam curing for RHA mortar and concrete.

Singh et al. (2002) investigated the effect of lignosulfonate (LS) and CaCl_2 on the compressive strength of blended cement made with RHA. Pastes of 10% RHA-blended Portland cement were made with the addition of 2% CaCl_2 , 1% LS, and (1% LS+ 2% CaCl_2). Compressive strength was determined at the age of 7 and 28 days, and results are shown in Fig. 7.4. The figure shows that in the presence of 2%

Table 7.9 Compressive strength of RHA concrete (Ismail and Waliuddin, 1996)

Mix type	RHA (%)		w/(C+ RHA)	Compressive strength (MPa)			
	#200	#325		3-day	7-day	28-day	150-day
A	—	—	0.24	54.3	62.3	72.4	85.0
Aa-10	10	—	0.31	46.2	56.0	68.1	71.1
Aa-20	20	—	0.33	35.3	46.8	57.3	57.4
Aa-30	30	—	0.36	31.5	39.3	47.7	48.8
Ab-10	—	10	0.30	47.0	61.0	71.0	72.4
Ab-20	—	20	0.32	46.7	56.0	70.2	70.3
Ab-30	—	30	0.34	43.1	51.7	63.0	63.2

Table 7.10 Mechanical properties of concrete mixtures Zhang and Malhotra (1996)

Mix	RHA (%)	SF (%)	W/Cm ratio	Splitting tensile strength (MPa)	Flexural strength (MPa)	Modulus of elasticity (GPa)
1	0	0	0.40	2.7	6.3	29.6
2	10	–	0.40	3.5	6.8	29.6
3	–	10	0.40	2.8	7.0	31.1

CaCl_2 , compressive strength was higher at 7 days and lower at 28 days of hydration than that of the control. In the presence of 1% LS, the values were lower than that of control on all days of hydration. However, in the presence of a mixture of 1% LS and 2% CaCl_2 , the compressive strength was maximum at 28 days of hydration. The results exhibited very clearly that when a mixture of a superplasticizer (1% LS) and an accelerator (2% CaCl_2) was added to the RHA blended OPC, the superplasticizer reduced the water demand and the accelerator enhanced the compressive strength. Thus the role of the two admixtures becomes supplementary to each other.

Nehdi et al. (2003) made a comparative study of the compressive strength of concrete mixtures made with: (i) 0% rice husk ash; (ii) Egyptian rice husks tested in a Torbed reactor at combustion temperatures between 750 and 830°C plus external jet of air. These were categorized as EG-RHA (A), EG-RHA (B) and EG-RHA (C); (iii) a raw rice husk ash (RAW-US-RHA) and a high quality RHA (US-RHA) from USA, produced using fluidized bed technology; and (iv) silica fume (SF). Physical properties of cementitious materials are given in Table 7.11. Three different percentages (7.5, 10, and 12.5%) of Egyptian and US rice husk ashes, SF, and two

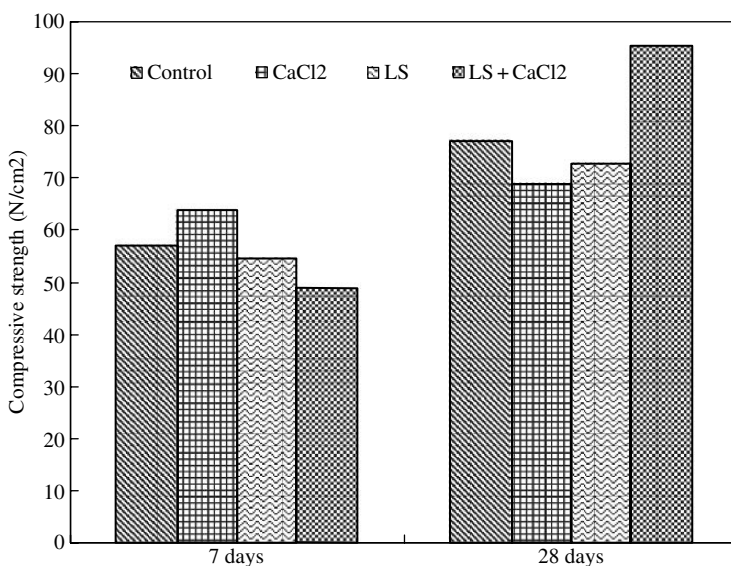
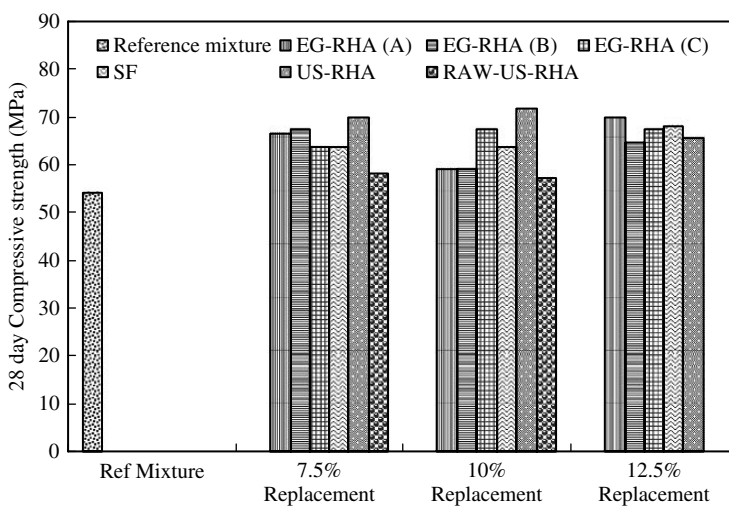
**Fig. 7.4** Effect of admixtures on the compressive strength of blended cement and 28 days (Singh et al., 2002)

Table 7.11 Physical properties of cementitious materials (Nehdi et al., 2003)

Property	Type I cement	RHA-A (750°C)	RHA-B (830°C)	RHA-A (750°C) + air	US-RHA	SF
Specific gravity	3.17	2.05	2.05	2.05	2.06	2.16
Passing 45 μm (%)	83.9	98.2	97.7	97.9	98.4	97.2
Mean particle size (μm)	13.4	7.15	7.63	7.41	6.8	0.16
Water requirement (%)	–	99	95	100	104	114
Pozzolanic activity index (%) at 7 days		88	105	117	114	94
Pozzolanic activity index (%) at 28 days		122	117	144	109	102

percentages (7.5 and 10%) of raw US rice husk ashes were used. Compressive strength test results at the age of 28 days are shown in Fig. 7.5. It can be seen from this figure that the strength of all mixtures incorporating RHA and SF additions outperformed that of the reference mixture.

Jaturapitakkul and Roongreung (2003) determined the compressive strength of mortar made with a cementing material (combination of rice husk ash and calcium carbide residue). Calcium Carbide Residue (CCR) is a by-product of acetylene production process. CCR consists mainly of calcium hydroxide, $\text{Ca}(\text{OH})_2$, and is obtained in a slurry form. Chemical composition of CCR was 51.94% CaO , 3.36% SiO_2 , 2.56% Al_2O_3 , 0.33% Fe_2O_3 , 0.46% MgO , 0.03% K_2O , 0.22% SO_3 and 41.72% LOI. The major compound in RHA was SiO_2 (78.22%). Control mixture was made using Portland cement Type I as cementitious material. The rest of the mortars were made with a mixture of CCR and RHA as cementitious material. The mortar

**Fig. 7.5** Compressive strength for various concrete mixtures made with rice husk ashes from Egypt and US (Nehdi et al., 2003)

contained 1.0 part of cementitious material to 2.75 parts of river sand by weight. The water-cementitious material ratio was kept at a constant of 0.65 in all mixtures. Superplasticizer was employed in order to maintain the flow of mortar between 110 ± 5 since the mixture of CCR-RHA mortars required more water to achieve the target flow. Compressive strengths of mortars were determined at the age of 1, 3, 7, 14, 28, 60, 90, and 180 days of curing. They concluded that: (i) mortar 50C50R gave the highest compressive strength. Its strength was 0.9, 10.0, 15.6, 18.6, and 19.1 MPa, respectively, at the age of 1, 7, 28, 90, and 180 days. Mortar 50C50R had lower compressive strength than that of the control mortar at the same testing age; (ii) difference of compressive strength of mortar 50C50R and control mortar at an early age was very high and reduced to about two times after 28 days. It is important to mention the mix proportion of the mortar 50C50R did not contain Portland cement and the strength of mortar was solely contributed from the pozzolanic reaction of the two materials; and (iii) mortar 50C50R contained 50% of CCR and 50% of RHA as cementitious material gave the highest compressive strength. Increasing or decreasing of CCR content from 50% of the total cementitious material resulted in lower compressive strength of mortar.

Bui et al. (2005) investigated the compressive strength of concrete mixtures made with two types (PC30 and PC40) of ordinary Portland cement having Blain specific surface area of 2700 and 3759 cm^2/g , respectively. Three water-to-binder ratios (0.30, 0.32, and 0.34) were used. Rice husk ash was used to replace 10%, 15% and 20% by mass of PC. Strength measurements were made up to the age of 90 days. Based on the results, they concluded that: (i) rice husk ash (RHA) can be used as a highly reactive pozzolanic material to improve the microstructure of the interfacial transition zone (ITZ) between the cement paste and the aggregate in high-performance concrete; (ii) in addition to the pozzolanic reactivity of RHA (chemical aspect), the particle grading (physical aspect) of cement and RHA mixtures exerted significant influences on the blending efficiency; (iii) relative strength increase (relative to the concrete made with plain cement, expressed in %) was higher for coarser cement; and (iv) simulation results demonstrated that the favorable results for coarser cement (i.e., the gap-graded binder) reflected improved particle packing structure accompanied by a decrease in porosity and particularly in particle spacing.

Rodriguez de Sensale (2006) studied the compressive and splitting tensile strength of concretes with rice-husk ashes (RHA). Two sources of ash were considered; a residual RHA from rice paddy milling industry in Uruguay and another produced by controlled incineration from the USA. Two (10 and 20%) replacement percentages of cement by RHA, and three water/cementitious material ratios (0.32, 0.40, and 0.50) were used. The median particle size of the two ashes was the same, and the activity index was similar. X-ray diffraction analysis indicated that the USA RHA can be considered to be non-crystalline RHA; but the UY RHA showed crystalline materials, which were identified as cristobalite. The percentage of reactive silica contained in the USA RHA was 98.5% and in the UY RHA was 39.55%. $100 \times$ 200-mm cylinders were used for compressive and splitting tensile strength measurement. Compressive strength was measured at the age of 7, 28, and 91 days and splitting tensile strength at the age of 28 days. Test results of strengths are given

Table 7.12 Compressive and splitting tensile strength results of RHA concretes (Rodriguez de Sensale, 2006)

w/(c+RHA)	RHA		Compressive strength (MPa)			Splitting tensile strength (MPa)
	Type	%	7-day	28-day	91-day	
0.32	—	0	48.4	55.5	60.6	3.63
	UY	10	51.1	60.4	64.3	3.57
		20	44.3	54.8	62.7	3.54
	USA	10	39.5	51.4	64.5	3.62
		20	30.5	47.4	68.5	3.54
0.40		0	35.8	42.3	45.6	—
	UY	10	41.1	50.4	54.9	—
		20	27.9	40.7	51.4	—
	USA	10	29.7	40.8	51.5	—
		20	23.6	39.4	57.3	—
0.50		0	24.6	32.9	35.9	2.85
	UY	10	24.1	31.5	35.5	2.32
		20	24.9	34.9	37.9	2.63
	USA	10	22.7	34.5	44.4	2.92
		20	20.8	35.9	52.9	3.00

in Table 7.12. Based on the results obtained, he concluded that: (i) at lower age (7 days), concretes with UY-RHA exhibited higher compressive strength than concretes with USA-RHA; (ii) at higher age (91 days), the RHA concrete had higher compressive strength in comparison with that of concrete without RHA, and the highest values of compressive strengths were achieved in concretes with 20% USA-RHA; (iii) long term compressive strength of the concretes with UY-RHA was not as high as the one obtained with USA-RHA, which also increased with the increase in RHA content; and (iv) the results of splitting tensile revealed the significance of the filler and pozzolanic effect for the concretes with RHA. On the one hand, the results were consistent with the compressive strength development at 28 days for the USA-RHA. On the other hand, in the concretes with UY-RHA, lower splitting tensile strengths were observed, which can be due to the fact that with residual RHA, the filler effect of the smaller particles in the mixture was higher than the pozzolanic effect.

The results are compared with those of the concrete without RHA, with splitting tensile strength and air permeability. It is concluded that residual RHA provides a positive effect on the compressive strength at early age, but the long term behavior of the concretes with RHA produced by controlled incineration was more significant. Results of splitting tensile and air permeability reveal the significance of the filler and pozzolanic effect for the concretes with residual RHA and RHA produced by controlled incineration.

Sakr (2006) examined the role of RHA inclusion as partial replacement of cement, on the mechanical properties of heavyweight concrete. The aggregates used were special natural heavy weight mineral ores, mainly ilmenite and baryte. They were used as the fine and coarse aggregates for the heavy weight concrete. Gravel

and sand were used as the coarse and fine aggregate for the gravel concrete. The RHA had a specific surface area of $5.6 \times 10^6 \text{ mm}^2/\text{g}$, and the unit weight was $2.06 \times 10^3 \text{ kg/m}^3$. The chemical composition of the RHA was 87.0% SiO_2 , 1.75% Al_2O_3 , 2.5% Fe_2O_3 , 2.5% CaO , 2.3% MgO , and 2.5% K_2O . Percentage replacement of RHA was 0, 5, 10, 15, and 20% by weight of cement. Tests were conducted for compressive strength, indirect tensile strength, flexural strength, bond strength, and modulus of elasticity at the age of 28 days. They concluded that: (i) with the increase in RHA content up to 15%, generally, all the mechanical properties increased. Beyond 15%, decrease in strength properties values was observed. This may be due to the high specific surface areas of RHA, which consume more water to have the same workability; (ii) ilmenite concrete had the highest compressive strength when compared to the corresponding barite concrete or gravel concrete. This increase may be attributed to the shape, specific surface area, and hardness of the ilmenite aggregates. It may also be due to the effect of titanium oxide (TiO_2) in ilmenite, which may be combined with water to form a gelatinous material that fills the voids in the cement matrix, consequently increasing bonding between the cement particles and thus increasing its compressive strength; and (iii) 15% of RHA mixed with baryte concrete showed a higher tensile strength when compared to gravel concrete but a lower tensile strength than ilmenite concrete mixed with 15% of RHA. The ilmenite concrete exhibited the highest flexural strength, bond strength, and static modulus of elasticity in compression as compared to the baryte or gravel concrete.

Saraswathy and Song (2007) reported the compressive, splitting tensile and bond strength of concrete in which cement was partially replaced with RHA. Proportion of control (with out RHA) mix was 1:1.5:3 with w/c ratio of 0.53. Percentage replacements were 0, 5, 10, 15, 20, 25, and 30%. 100 mm cubes and 150×300 mm cylinders were cast for compressive and splitting tensile strength, respectively. For bond strength measurement, cold twisted deformed bars of 12 mm diameter and 450 mm long were used. The rod was placed centrally along with helical reinforcement provided in the centre of the concrete cube of size $100 \times 100 \times 100$ mm. 28-day results of compressive strength, splitting tensile strength and bond strength are given in Table 7.13. Based on the results obtained, they concluded that: (i) compressive strength increased with increase in RHA contents. Blending percentage and with age. At 28 days, all the rice husk ash replaced concretes exhibited higher compressive strength than the control concrete; (ii) inclusion of RHA (up to 25%) as partial replacement of cement did not affect the splitting tensile strength of concrete. After 25% replacement level, a slight decrease in split tensile strength was observed; and (iii) all the rice husk replaced concretes showed higher bond strength values than the conventional concrete, indicating that replacement of rice husk ash does not affect the bond strength properties.

Gastaldini et al. (2007) studied the effect of chemical activators (K_2SO_4 , Na_2SO_4 , Na_2SiO_3) on the compressive strength of concrete made with 20% of rice husk ash as partial replacement of cement. Water/binder ratios used were 0.35, 0.50 and 0.65 and binder/aggregate ratios were 1:3.75, 1:5.25 and 1:6.9. Potassium sulfate (K_2SO_4), sodium sulfate (Na_2SO_4) and sodium silicate (Na_2SiO_3) were used as chemical activators in concentrations of 1% by weight of cement. Compressive strength was measured at the age of 7, 28, and 91 days, and results are given in

Table 7.13 28-day strengths of RHA concretes (Saraswathy and Song, 2007)

RHA (%)	Compressive strength (MPa)	Splitting tensile strength (MPa)	Bond strength (MPa) at 0.25 mm slip
0	36.45	4.49	3.32
5	36.49	4.57	4.11
10	37.43	4.65	4.31
15	37.38	4.92	3.79
20	37.71	4.60	3.43
25	39.55	4.58	4.07
30	37.80	3.67	3.87

Table 7.14. From the results, it was concluded that: (i) mixture with 20% rice husk ash and w/b ratio = 0.50 showed compressive strength values equal to that of the reference mixture (REF) at 7 days. The same mixture with different w/b ratios (0.35 and 0.65) showed lower strength when compared with the reference mixture. At 28 and 91 days, compressive strength values were higher than those of the reference samples for all w/b ratios; (ii) the three activators yielded a huge increase in strength at 7 days. The mixture activated with K_2SO_4 showed the highest increase when compared with the sample without activator. The percentage increases were 21%, 30% and 63% at 7 days, 11%, 13% and 44% at 28 days and 9%, 33% and 44% at 91 days for the mixtures with w/b ratio = 0.35, 0.50 and 0.65, respectively. When compared with the reference sample, the increases for the same w/b ratios and age ranged from 13% to 52%; and (iii) significant growth in the samples with w/b = 0.65, mainly in the sample activated with K_2SO_4 , can be attributed to the increase in pH and the changes in the RHA structure caused by the activator, which improved the hydration. In addition, more space is available for the deposition of hydration

Table 7.14 Compressive strength of RHA concretes (Gastaldini et al., 2007)

Mixture	w/b ratio	Compressive strength (MPa)		
		7 day	28 day	91 day
REF (Control)	0.35	58.3	64.2	76.1
	0.50	36.4	47.7	53.5
	0.65	24.6	28.0	31.9
20 RHA	0.35	54.2	69.7	83.4
	0.50	36.4	48.1	53.9
	0.65	17.7	27.0	33.6
20 RHA 1% Na_2SO_4	0.35	59.2	73.3	82.8
	0.50	39.5	50.7	56.5
	0.65	25.3	36.8	42.5
20 RHA 1% K_2SO_4	0.35	65.9	77.4	91.0
	0.50	47.2	54.3	71.8
	0.65	28.9	38.9	48.3
20 RHA 1% Na_2SiO_3	0.35	54.2	74.4	77.5
	0.50	37.4	48.7	53.8
	0.65	29.1	40.3	45.1

Table 7.15 Compressive strength of blended cements (Chindaprasirt et al., 2007)

Mix	w/b ratio	Compressive strength (MPa)			
		7 day	28 day	90 day	180 day
OPC	0.55	44	51	57	60
FA20	0.53	32	45	57	57
FA40	0.51	29	46	62	77
RHA20	0.68	31	54	61	62
RHA40	0.80	17	32	43	53

products when compared with lower w/b ratios. This composition showed higher strength at 7 days (28.9 MPa) when compared with the sample without activator (17.7 MPa) and the reference sample (24.6 MPa), which illustrates the benefits of the activator.

Chindaprasirt et al. (2007) determined the compressive strength development of blended cements containing rice husk ash and fly ash. Class F lignite fly ash and RHA were used at replacement dosages of 20 and 40% by weight of cement. The combined amount of SiO_2 , Al_2O_3 , and Fe_2O_3 in FA was 78.1%, indicating that fly ash was a class F fly ash. The Blaine fineness of the FA was $2600 \text{ cm}^2/\text{g}$, which was coarser than PC ($2900 \text{ cm}^2/\text{g}$). RHA contained high silica content of 90% and low loss on ignition (LOI) of 3.2%. The Blaine fineness of RHA was $14,000 \text{ cm}^2/\text{g}$. Mortars were made with sand-to-binder ratio of 2.75 and adjusted water contents to achieve similar flow of $110 \pm 5\%$. Compressive strength was determined at 7, 28, 90 and 180 days using 50 mm cubes. Table 7.15 shows water-to-binder (W/B) ratios and compressive strengths of the mortar mixes. The addition of fly ash resulted in a reduction in the water requirement of the mortar for similar flow, whereas incorporation of RHA resulted in significant increase probably due to the high surface area of RHA.

Use of fly ash and RHA resulted in a reduction of 7 and 28 day compressive strength. The reduction of early strength is typical of the fly ash mixes. For RHA mixes, the low initial strength was due to the high water-to-binder of the mixes. For 20% RHA replacement level, although the W/B ratio was increased, the strength at 28 days was higher than that of PC mix, suggesting that RHA was quite reactive. Although possessing high fineness, RHA contribution to the strength development was limited by the high water demand associated with its high surface areas.

7.3.3 Drying Shrinkage

Zhang and Malhotra (1996) studied the drying shrinkage strain of concretes made with 10% RHA and 10% silica fume (SF). Tests were conducted up the age of 448 days. Figure 7.6 shows the drying shrinkage strain of concretes after 7 days of initial curing in lime-saturated water. These results indicated that RHA concrete had a drying shrinkage of 638×10^{-6} after 448 days, which was similar to the strains for the control and silica fume concretes.

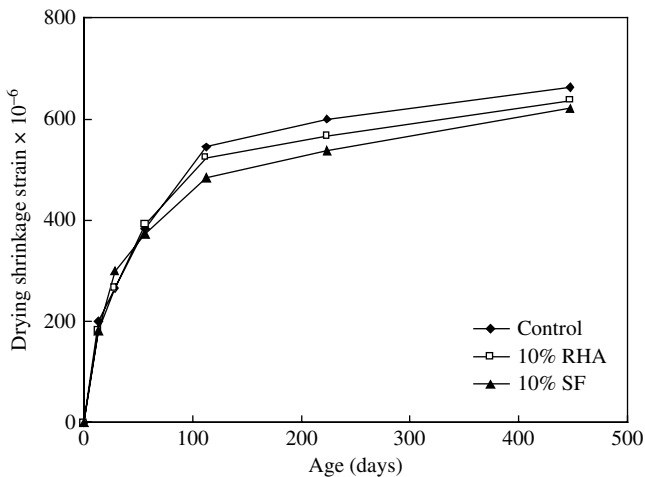


Fig. 7.6 Drying shrinkage of RHA and SF concretes (Zhang and Malhotra, 1996)

7.4 Durability Properties of Concrete Containing RHA

7.4.1 Permeability

Zhang and Malhotra (1996) investigated the chloride-ion penetration resistance of concretes made with 10% RHA and 10% silica fume (SF). Details of the concrete mixture along with the chloride-ion penetration test conducted as per ASTM C1202 are given in Table 7.16. It can be seen from these results that use of RHA and SF has drastically reduced the chloride-ion penetration at both the age. These values were less than 1000. As per ASTM C1202, when charge passed through concrete is less than 1000 coulombs, the concrete has very high resistance to chloride-ion penetration.

Nehdi et al. (2003) made a comparative study of the rapid chloride permeability of concrete mixtures made with: (i) 0% rice husk ash; (ii) Egyptian rice husks; EG-RHA (A), EG-RHA (B) and EG-RHA (C); (iii) a raw rice husk ash (RAW-US-RHA) and a high quality RHA (US-RHA) from USA, produced using

Table 7.16 Test results of resistance of concrete to chloride-ion penetration (Zhang and Malhotra, 1996)

Mix No.	Type of concrete	W/Cm	Unit weight (kg/m ³)	Compressive strength (MPa)	Chloride-ion resistance (Coulombs)	
					28 days	90 days
CO-D	Control	0.40	2320	36.5	3175	1875
R10-D	10% RHA	0.40	2340	45.5	875	525
SF10-D	10% SF	0.40	2310	42.8	410	360

fluidized bed technology; and (iv) silica fume (SF). Physical properties of cementitious materials have already been given in Table 7.11. Three different percentages (7.5, 10, and 12.5%) of Egyptian and US rice husk ashes, SF, and two percentages (7.5 and 10%) of raw US rice husk ashes were used. Chloride permeability tests were carried out as per ASTM C1202. As per ASTM, permeability categorization is as: Very Low (0–1000 Coulombs); Low (1000–2000 Coulombs); Moderate (2000–3500 Coulombs). 28 days results are shown in Fig. 7.7. Based on the results, they concluded that: (i) non-ground RHA did not significantly change the rapid chloride penetrability classification of concrete; and (ii) finely ground RHA reduced the rapid chloride penetrability of concrete from a moderate rating to low or very low ratings depending on the type and addition level of RHA. Such reductions are comparable to those achieved by SF.

Coutinho (2003) determined the rapid chloride permeability of concrete with partial replacement of RHA in various percentages (10, 15, and 20%) and when using controlled permeability formwork (CPF). Controlled permeability formwork (or CPF) is one of the few techniques developed recently for directly improving the concrete surface zone. This technique reduces the near-surface water/binder ratio and reduces the sensitivity of concrete to poor site curing. CPF consists of using a textile liner on the usual formwork, allowing air bubbles and surplus water to drain out but retaining the cement particles and so enabling the water–cement ratio of the outer layer to become very low and the concrete to hydrate to a very dense surface skin as the filter makes enough water available at the right time to activate optimum hydration. So CPF enhances durability by providing an outer concrete layer which

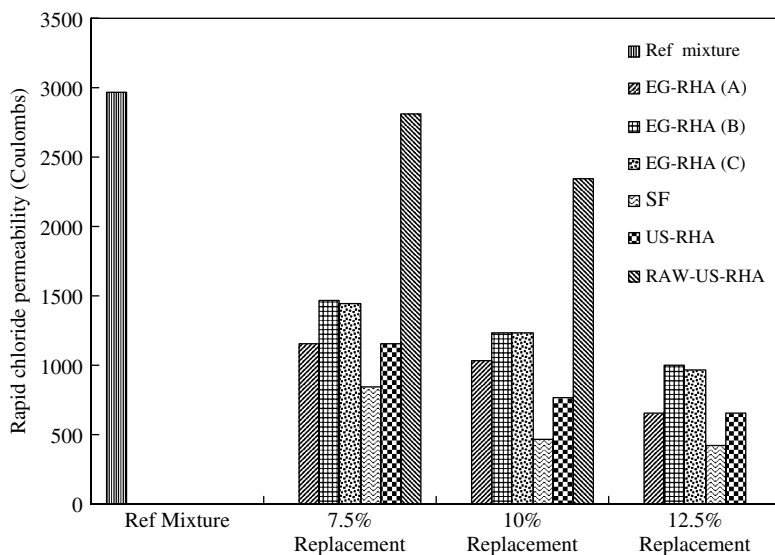


Fig. 7.7 Rapid chloride permeability at 28 days for various concrete mixtures made with rice husk ashes from Egypt and US (Nehdi et al., 2003)

Table 7.17 Rapid chloride permeability results (Coutinho, 2003)

Type of mixture	Average charge passed (Coulombs)
Control	2349.3
Control + CPF	1916.3
10% RHA	435.0
10% RHA + CPF	384.7
15% RHA	322.0
15% RHA + CPF	245.0
20% RHA	260.0
20% RHA + CPF	202.0

is richer in cement particles, with a lower water/binder ratio, less porous and so much less permeable than when ordinary formwork is used. Resistance to chloride penetration was assessed with the AASHTO T277-83 test method up to the age of 100 days. Table 7.17 shows the average of 3 test specimens for each series. It is evident from these results that inclusion of RHA significantly reduced the charge passed. Further more, when CPF was used, it greatly reduced the permeability of concrete mixtures.

Rodriguez de Sensale G (2006) studied the air-permeability of concretes with two sources of rice-husk ash; a residual RHA from rice paddy milling industry in Uruguay and another produced by controlled incineration from the USA. Two (10 and 20%) replacement percentages of cement by RHA, and two water/cementitious material ratios (0.32 and 0.50) were used. The percentage of reactive silica contained in the USA RHA was 98.5% and in the UY-RHA was 39.55%. Air-permeability for concrete was determined with the “Torrent permeability tester” method (Torrent, 1999; Torrent and Frenzer, 1995). 150 × 300-mm cylinders were used for measurement of air-permeability at the age of 28 days. The particular features of the Torrent method are a two-chamber vacuum cell and a pressure regulator, which ensures that air flows at right angles to the surface and is directed towards the inner chamber; this allows the calculation of the permeability coefficient K_t on the basis of a simple theoretical model. By comparing the results (Torrent and Frenzer, 1995) of gas permeability measured by the Torrent permeability tester (K_t) and oxygen permeability obtained for the Cembureau method (K_o), the following relation is presented: $K_o = 2.5 K_t^{0.7}$ where K_o and K_t are expressed in 10^{-16} m^2 . Permeability results of RHA concretes are given in Table 7.18. It can be seen from the table that: (i) for a particular water-cementitious ratio, Permeability of UY-RHA concrete was more than that USA-RHA concrete; and (ii) with the increase in water-cementitious ratio, permeability increased for both types of RHA. The results of air permeability revealed the significance of the filler and pozzolanic effect for the concretes with RHA. On the one hand, the results are consistent with the compressive strength development at 28 days for the USA RHA. On the other hand, in the concretes with UY RHA, lower air permeability was observed, which can be due to the fact that with residual RHA, the filler effect of the smaller particles in the mixture is higher than the pozzolanic effect.

Table 7.18 Permeability results of RHA concretes (Rodriguez de Sensale, 2006)

w/(c+RHA)	RHA		Permeability coefficient (m ²)
	Type	%	
0.32	—	0	1.08×10^{-16}
	UY	10	0.23×10^{-16}
		20	0.05×10^{-16}
	USA	10	0.08×10^{-16}
		20	0.03×10^{-16}
0.50		0	28.20×10^{-16}
	UY	10	71.82×10^{-16}
		20	49.10×10^{-16}
	USA	10	26.36×10^{-16}
		20	14.20×10^{-16}

Saraswathy and Song (2007) investigated the effect of partial replacement of cement with rice husk ash (RHA) on the chloride permeability of concrete. Proportion of control (with out RHA) mix was 1:1.5:3 with w/c ratio of 0.53. Cement was replaced with 0, 5, 10, 15, 20, 25, and 30% RHA. Test was conducted as per ASTM C1202-94. Concrete specimens of size 85 mm diameter and 50 mm thickness with and without rice husk ash were cast and allowed to cure for 28 days. Rapid chloride permeability (charge passed) through concretes made with 0, 5, 10, 15, 20, 25, and 30% RHA were 1161, 1108, 653, 309, 265, 213, and 273 coulombs, respectively. It can be seen that replacement of rice husk ash drastically reduced the Coulomb values. As the replacement level increased, the chloride penetration decreased. As per ASTM C1202, RHA reduced the rapid chloride penetrability of concrete from a low to very low ratings from higher to lower replacement levels.

Gastaldini et al. (2007) studied the influence of chemical activators (K_2SO_4 , Na_2SO_4 , Na_2SiO_3) on the chloride-ion permeability of concrete made with 20% of rice husk ash as partial replacement of cement. Water/binder ratios used were 0.35, 0.50 and 0.65 and binder/aggregate ratios were 1:3.75, 1:5.25 and 1:6.9. Potassium sulfate (K_2SO_4), sodium sulfate (Na_2SO_4) and sodium silicate (Na_2SiO_3) were used as chemical activators in concentrations of 1% by weight of cement. Chloride-ion penetration was measured according to ASTM C1202 (2000) at the age of 28 and 91 days. Results of chloride-ion penetration are given in Table 7.19. Based on the results they concluded that: (i) at 28 days, RHA concrete exhibited significant reduction in the total charge passed. This reduction amounted to 42%, 51% and 27% for w/b = 0.35, 0.50 and 0.65, respectively. At 91 days, the same w/b ratios showed reductions of 65%, 68% and 59%; (ii) concrete mixtures with activators showed lower total charge passed values when compared with the mixture without activator. The mixtures activated with K_2SO_4 showed the best results. At 28 days, the mixture activated with Na_2SiO_3 showed the lowest charge passed values. Overall, the best results at 91 days were seen in the sample activated with K_2SO_4 ; and (iii) at 91 days, all mixtures with chemical activators showed very low charge passed values

Table 7.19 Chloride-ion permeability of RHA concretes (Gastaldini et al., 2007)

Mixture	w/b ratio	Total charge passed (C)	
		28 day	91 day
REF (Control)	0.35	1727	1288
	0.50	3166	2136
	0.65	3681	2866
20 RHA	0.35	999	452
	0.50	1557	692
	0.65	2677	1176
20 RHA 1% Na ₂ SO ₄	0.35	933	515
	0.50	1393	630
	0.65	2004	760
20 RHA 1% K ₂ SO ₄	0.35	820	326
	0.50	1312	552
	0.65	2242	818
20 RHA 1% Na ₂ SiO ₃	0.35	704	342
	0.50	914	578
	0.65	1470	732

(100–1000 C), even for w/b ratios as high as 0.65 which can be rated as very low as per ASTM C1202.

7.4.2 Corrosion Resistance

Saraswathy and Song (2007) investigated the corrosion performance of concrete made with 0, 5, 10, 15, 20, 25, and 30% RHA as partial replacement of cement. Proportion of control (with out RHA) mix was 1:1.5:3 with w/c ratio of 0.53. Corrosion performance was evaluated by impressed voltage test and open circuit potential measurements. For impressed voltage test, cylindrical concrete specimens of size 50 mm diameter and 100 mm height were cast with centrally embedded rebar of 12 mm diameter and 100 mm height. After 28 days of curing, the specimens were subjected to impressed voltage test. In this technique, the concrete specimens were immersed in 5% NaCl solution and embedded steel in concrete was made anode with respect to an external stainless steel electrode serving as cathode by applying a constant positive potential of 12 V to the system from a DC source. The variation of current was recorded with time. For each specimen, the time taken for initial crack and the corresponding maximum anodic current flow was recorded. For open circuit potential test, specimens of size 100 × 100 × 100 mm were cast. 12 mm diameter rebar of 120 mm length were embedded at a cover of 25 mm from one side of the specimen. After casting the specimens were subjected to water curing for 28 days. After 28 days of curing the cubes were taken out and dried for 24 h and subjected to alternate wetting and drying in 3% NaCl solution. One cycle consisted of seven days immersion in 3% NaCl solution and seven days drying in open atmosphere. The tests were

continued over a period of 200 days. Open circuit potential measurements were monitored with reference to saturated calomel electrode (SCE) periodically with time as per ASTM C876. Impressed voltage results were expressed in terms of time to cracking in hours. Time of cracking were 42, 72, and 74 hours for concretes made with 0, 5, and 10% RHA. However, no cracking was observed for concretes with 15, 20, 25, and 30% RHA ever after 144 hours of exposure. It can be observed from the results that there was no in concretes made with 15, 20, 25 and 30% rise husk even after 144h of exposure. Whereas in ordinary Portland cement concrete, the specimen was cracked even after 42h of exposure in 5% NaCl solution. The concrete specimens containing 5 and 10% rise husk also failed within 72 and 74 hours of exposure. This indicated that the replacement of rice husk ash refined the pores and thereby the permeability and corrosion gets reduced.

Open circuit potential measurements values (OCP) as per ASTM C876-97 were lesser than -275 mV vs. saturated calomel electrode (SCE), was considered to be passive in condition. They concluded that all the rice husk ash replaced concretes had shown less negative potential than -275 mV even up to 100 days of exposure indicating the passive condition of the rebars. Beyond 100 days of exposure all the systems showed a more negative potential than -275 mV vs SCE irrespective of the replacement ratio showing the active condition of rebars.

7.4.3 Carbonation

Gastaldini et al. (2007) examined the role of chemical activators on the carbonation of concrete containing 20% of rice husk ash as partial replacement of cement. Water/binder ratios used were 0.35, 0.50 and 0.65 and binder/aggregate ratios were 1:3.75, 1:5.25 and 1:6.9. Potassium sulfate (K_2SO_4), sodium sulfate (Na_2SO_4) and sodium silicate (Na_2SiO_3) were used as chemical activators in concentrations of 1% by weight of cement. Specimens of size 100×100 mm were cured for 28 days. Their top surface was sealed and they underwent a preconditioning cycle as required by RILEM TC116-PCD (1999). They were then placed in a controlled atmosphere chamber with 5% CO_2 , at $23 \pm 1^\circ C$ and $RH\ 65 \pm 1\%$. The carbon dioxide penetration depth was measured at different exposure times, 4, 8 and 12 weeks by means of the phenolphthalein test carried out on the transversely split section of the cylinders specimens using the RILEM CPC18 (1988) method. Figure 7.8 shows the changes in these coefficients for the w/b ratios used. For all mixtures investigated, Kc increased with the increase in w/b ratio because of the increase in concrete porosity and the lower concentration of cement. For the same w/b ratio (0.35, 0.50 and 0.65), the lowest carbonation coefficients were seen in the mixture with RHA and 1% K_2SO_4 showed. The values obtained were lower than those in the reference concrete.

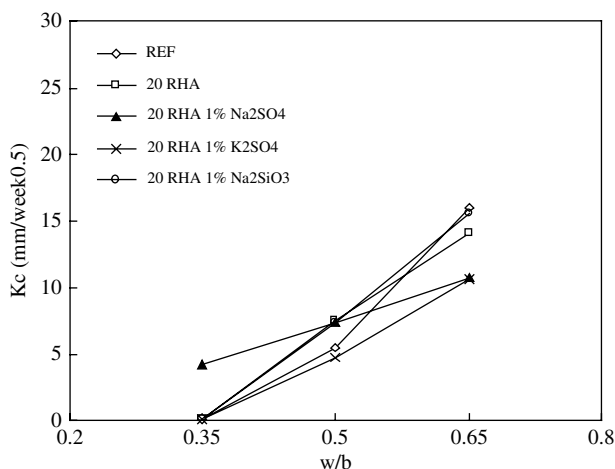


Fig. 7.8 Carbonation coefficients with reference to the w/b ratios (Gastaldini et al., 2007)

7.4.4 Freezing and Thawing Resistance

Zhang and Malhotra (1996) studied the freezing and thawing resistance of concretes made with 10% RHA and 10% silica fume (SF) as per ASTM C666 Procedure A. Details of the concrete mixture along with the results of freezing/thawing are given in Table 7.20. The control, RHA, and silica fume concretes showed excellent performance in the freezing and thawing test. The RHA concrete had a durability factor of 98.3 and very small changes in length, mass, pulse velocity, and resonant frequency after 300 cycles of freezing and thawing.

7.4.5 Sulfate Resistance

Sakr (2006) investigated the role of RHA on the sulfate resistance of heavyweight concrete. The aggregates used were special natural heavy weight mineral ores,

Table 7.20 Test results of concrete to freezing and thawing cycles (Zhang and Malhotra, 1996)

Mix No.	Type of concrete	Compressive strength (MPa)	Change at the end of 300 freezing/thawing cycles				Durability factor (%)
			Weight	Length	Pulse velocity	Resonant frequency	
CO-D	Control	36.5	0.08	0.006	-0.55	-0.84	98.0
R10-D	10% RHA	45.5	0.02	0.001	0.01	-0.86	98.3
SF10-D	10% SF	42.8	0.12	0.001	0.19	0.47	101.0

mainly ilmenite and baryte. They were used as the fine and coarse aggregates for the heavy weight concrete. Gravel and sand were used as the coarse and fine aggregate for the gravel concrete. Ilmenite, barite and gravel concrete mixtures were made with 0 and 15% RHA. For the sulfate resistance test, 100 mm cubes were immersed in a 5% MgSO_4 solution for different periods (1, 3, and 6 months) and the loss in compressive strength due to sulfate attack was determined. They concluded that: (i) reductions in compressive strength of the gravel, baryte, and ilmenite control mixtures 8.5, 7.0, and 8.0%, respectively, after immersion in 5% MgSO_4 for 28 days, while the reductions after 90 days of immersion were 16, 14, and 14%, respectively; (ii) reduction percentages of the compressive strength of gravel, baryte and ilmenite concrete incorporating 15% of RHA when immersed in a sulfate solution for 28 days were 5, 6, and 6%, respectively; and (iii) decrease rate of the effect of sulfate ions on compressive strength was generally increased as the immersion time in the sulfate solution increased.

Chindaprasirt et al. (2007) determined the sulfate resistance of mortars made from ordinary Portland cement containing fly ash and ground rice husk ash (RHA). Class F fly ash and RHA were used at replacement dosages of 20 and 40% by weight of cement. The Blaine fineness of PC, FA, and RHA was $2900 \text{ cm}^2/\text{g}$, $2600 \text{ cm}^2/\text{g}$, and $14,000 \text{ cm}^2/\text{g}$, respectively. Mortars were made with sand-to-binder ratio of 2.75 and adjusted water contents to achieve similar flow of $110 \pm 5\%$. The test for sulfate-induced expansion was done following the procedures described in ASTM C1012 with 5% sodium sulfate solution. The expansion of the PC prism was much larger than those made with the blended cements. The accelerating expansion pattern of the PC mortar was observed from 120 days onward. There was no obvious accelerating expansion pattern shown by blended cement mortar prisms. FA20, FA40 and RHA20 mixes show a “linear” pattern of expansion after about 120 days in sulfate solution. RHA40 mix, however, shows a very small expansion even after immersion for 360 days. Figure 7.9 shows the pH levels of the sodium sulfate solution. The highest level of the pH of sulfate solution was approximately 12.5 for all the mortars and was observed within the first 7 days of immersion, indicating that a substantial amount of the calcium hydroxide was leached out and thus increased the pH of the solution. The fresh solution pH was 7.0–7.5. After one day of immersion, the pH level was found to be more than 12. Even Khatri et al. (1997) have reported that the pH of 12–12.5 was obtained within a few hours of immersion. The pH of the solution increased slightly as the immersion period continued until the solution was replaced by a fresh solution. At 90 and 180 days, the pH levels of the sulfate solutions were significantly lower and different. The pH value of the solution with PC mortar was the highest of 11.0 followed by those of FA20, FA40, RHA20 and RHA40 with 10.7, 10.5, 10.1 and 9.5, respectively. The expansion of the mortar bar is sensitive to the pH level of the solution (Cao et al., 1997). At pH 12–12.5 only ettringite formation can take place and at pH of 8.0–11.5 gypsum formation and decalcification occur (Khatri et al., 1997). (Shi and Stegemann, 2000) have reported that dissolution of $\text{Ca}(\text{OH})_2$ and calcium sulfoaluminate, and the decalcification of CSH with a high C/S ratio in hardened PC paste results in a very porous layer whereas the decalcification of the low C/S CSH

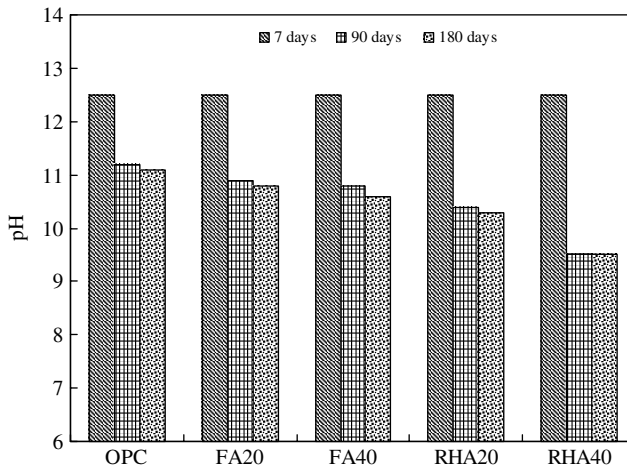


Fig. 7.9 pH level of the sodium sulfate solutions immersed with mortar bars (Chindaprasirt et al., 2007)

results in a protective layer of silica gel. For FA and RHA blended cement, C/S ratio of CSH would have been lower as a result of the pozzolanic reaction. FA and RHA mortars thus showed better resistance to the sulfate attack in comparison to PC mortar with RHA, being more reactive and showing better resistance to sulfate attack.

7.4.6 Deicing Salt Scaling Resistance

Zhang and Malhotra (1996) reported the scaling resistance of concretes made with 10% RHA and 10% silica fume (SF) as per ASTM C 672. Scaling resistance results are given in Table 7.21. The visual evaluation of test slabs showed that the performance of the RHA concrete was similar to that of the control concrete but marginally better than SF concrete. For both control and RHA concrete, no coarse aggregate was visible after 50 cycles whereas for SF concrete some coarse aggregates were visible. All the three concretes had a total mass of scaling residue of equivalent to or less than 0.8 kg/m^3 after 50 cycles in the presence of deicing salts. The control, RHA, and silica fume concretes showed excellent performance in the

Table 7.21 Test results of deicing salt scaling (Zhang and Malhotra, 1996)

Mix No.	Type of concrete	W/C ratio	Compressive strength (MPa)	Visual rating	Total scaling residue (kg/m^3)
CO-D	Control	0.40	36.5	2	0.3
R10-D	10% RHA	0.40	45.5	2	0.6
SF10-D	10% SF	0.40	42.8	3	0.8

Table 7.22 Expansion of mortar bars containing RHA (Hasparyk et al., 2000)

Replacement (%)	Expansion (%)			
	Quartzite		Basalt	
	16 days	30 days	16 days	30 days
0	0.28	0.53	0.84	1.10
4	0.16	0.36	0.76	0.99
8	0.21	0.45	0.32	0.81
12	0.09	0.25	0.08	0.33
15	0.06	0.15	0.04	0.25

freezing and thawing test. The RHA concrete had a durability factor of 98.3 and very small changes in length, mass, pulse velocity, and resonant frequency after 300 cycles of freezing and thawing.

Nehdi et al. (2003) investigated the effect of RHA and SF on the deicing scaling resistance of concrete. Concrete mixtures were made with 10% RHA and 10% SF as partial replacement of cement. Tests were conducted up to 50 cycles as per ASTM C672. Results showed that RHA concrete specimens (visual rating 2) performed similar to the control concrete mixture (visual rating 2) but little better than SF concrete mixtures (visual rating 3). These results were in agreement with those reported by Zhang and Malhotra (1996).

7.4.7 Alkali-Silica Reaction

Hasparyk et al. (2000) studied the expansion of mortar bars made with different levels of cement replacement with rice husk ash (RHA). Two types of reactive aggregates (quartzite and basalt) were used. Percentages of RHA were 0, 4, 8, 12, and 15%. Tests were conducted as per ASTM C 1260. Expansion at 16 and 30 days are given in Table 7.22. It can be seen from these results that inclusion of RHA was very effective in controlling the expansion of mortar bars at the age of 16 and 30 days.

References

- Agarwal SK (2006) Pozzolan activity of various siliceous materials. *Cement and Concrete Research* 36 (9): 1735–1739.
- ASTM C1202 (2000) Electrical indication of concrete's ability to resist chloride ion penetration. *Annual Book of American Society for Testing Materials Standards*, C04.02.
- Bui DD, Hu J, Stroeve P (2005) Particle size effect on the strength of rice husk ash blended gap-graded Portland cement concrete. *Cement & Concrete Composites* 27: 357–366.
- Cao HT, Bucea L, Ray A, Yozghatlian S (1997) The effect of cement composition and pH of environment on sulfate resistance of Portland cements and blended cements. *Cement Concrete Composites* 19: 161–171.
- Chindaprasirt P, Kanchanda P, Sathonsaowaphak A, Cao HT (2007) Sulfate resistance of blended cements containing fly ash and rice husk ash. *Construction and Building Materials* 21 (6): 1356–1361.

- Chopra SK, Ahluwalia SC, Laxmi S (1981) Technology and manufacture of rice-husk ash masonry (RHAM) cement, Proceedings of ESCAP/ RCTT Workshop on Rice-Husk Ash Cement, New Delhi.
- Cisse IK, Laquerbe M (2000) Mechanical characterization of filler sandcretes with rice husk ash additions: Study applied to Senegal. *Cement and Concrete Research* 30: 13–18.
- Cook DJ (1984) Development of microstructure and other properties in rice husk ash—OPC systems. Proceedings of the 9th Australasian Conference on the Mechanics of Structures and Materials, University of Sydney, Sydney, pp. 355–360.
- Coutinho JS (2003) The combined benefits of CPF and RHA in improving the durability of concrete structures. *Cement & Concrete Composites* 25: 51–59.
- Della VP, Kuhn I, Hotza D (2002) Rice husk ash as an alternate source for active silica production. *Materials Letters* 57: 818–821.
- Feng Q, Yamamichi H, Shoya M, Sugita S (2004) Study on the pozzolanic properties of rice husk ash by hydrochloric acid pretreatment. *Cement and Concrete Research* 34: 521–526.
- Gastaldini ALG, Isaia GC, Gomes NS, Sperb JEK (2007) Chloride penetration and carbonation in concrete with rice husk ash and chemical activators. *Cement & Concrete Composite* 29: 176–180.
- Hasparyk NP, Monteiro PJM, Carasek H (2000) Effect of silica fume and rice husk ash on alkali-silica reaction. *ACI Materials Journal* 97 (4): 486–491.
- Hewlett PC (1998) *Chemistry of Cement and Concrete*, Wiley, New York, pp. 471–601.
- Hwang CL, Wu DS (1989) Properties of cement paste containing rice husk ash. *American Concrete Institute SP*, 114: 733–765.
- Ikpong AA, Okpala DC (1992) Strength characteristics of medium workability ordinary Portland cement-rice husk ash concrete. *Building and Environment* 27 (1) 105–111.
- Inoue K, Hara N (1996) Thermal treatment and characteristics of rice husk ash. *Inorganic Materials* 3: 312–318.
- Ismail MS, Waliuddin AM (1996) Effect of rice husk ash on high strength concrete. *Construction and Building Materials* 10 (7): 521–526.
- Jaturapitakkul C, Roongreung B (2003) Cementing material from calcium carbide residue-rice husk ash. *Journal of Materials in Civil Engineering* 15 (5): 470–475.
- Jauberthie R, Rendell F, Tamba S, Cisse I (2000) Origin of the pozzolanic effect of rice husks. *Construction and Building Materials* 14: 419–423.
- Khatri RP, Sirivivatnanon V, Yang JL (1997) Role of permeability in sulfate attack. *Cement Concrete Research* 27: 1179–89.
- Luxan MP, Mndruga M, Seavedra J (1989) Rapid evaluation of pozzolanic activity of natural products by conductivity measurement. *Cement and Concrete Research* 19: 63–68.
- Mehta PK (1979) The chemistry and technology of cement made from rice husk ash. Proceedings UNIDO/ESCAP/RCTT Workshop on Rice Husk Ash Cements, Peshawar, Pakistan, January 1979. Regional Centre for Technology Transfer, Bangalore (India), pp. 113–22.
- Mehta PK (1992) Rice husk ash – a unique supplementary cementing material. Proceedings of the International Symposium on Advances in Concrete Technology, Athens, Greece, pp. 407–430.
- Nehdi M, Duquette J, Damatty A El (2003) Performance of rice husk ash produced using a new technology as a mineral admixture in concrete. *Cement and Concrete Research* 33: 1203–1210.
- Real C, Alcala MD, Criado JM (1996) Preparation of silica from rice husks. *Journal of American Ceramic Society* 79 (8): 2012–2016.
- RILEM CPC18 (1988) Measurement of hardened concrete carbonation depth. *Materials and Structures* 21 (126): 453–5.
- RILEM Recommendations of TC116-PCD (1999) Tests for gas permeability of concrete. *Materials and Structures* 32 (217): 163–79.
- Rodriguez de Sensale G (2006) Strength development of concrete with rice-husk ash. *Cement & Concrete Composites* 28: 158–160.
- Sakr K (2006) Effects of silica fume and rice husk ash on the properties of heavy weight concrete. *Journal of Materials in Civil Engineering* 18 (3): 367–376.

- Saraswathy V, Song Ha-Won (2007) Corrosion performance of rice husk ash blended concrete. *Construction and Building Materials* 21 (8): 1779–1784.
- Shi C, Stegemann JA (2000) Acid corrosion resistance of different cementing materials. *Cement Concrete Research* 30: 803–808.
- Singh NB, Singh VD, Rai S, Chaturvedi S (2002) Effect of lignosulfonate, calcium chloride and their mixture on the hydration of RHA-blended Portland cement. *Cement and Concrete Research* 32: 387–392.
- Torrent R (1999) Gas permeability of high-performance concretes-site and laboratory test. High-performance concrete and performance and quality of concrete structures, Gramado. In: *Proceedings Second CANMET/ACI Int.* pp. 291–308.
- Torrent R, Frenzer GA (1995) A method for rapid determination of the coefficient of permeability of the covercrete. *Proceedings of the International Symposium on Non-Destructive Testing in Civil Engineering, (NDT-CE)*, pp. 985–92.
- Wada I, Kawano T, Mokotomaeda N (1999) Strength properties of concrete incorporating highly reactive rice-husk ash. *Transaction of Japan Concrete Institute* 21 (1): 57–62.
- Yeoh AK, Bidin R, Chong CN, Tay CY (1979) The relationship between temperature and duration of burning of rice-husk in the development of amorphous rice-husk ash silica, *Proceedings of UNIDO/ESCAP/ RCTT, Follow-up Meeting on Rice-Husk Ash Cement*, Alor Setar, Malaysia.
- Yu Q, Sawayama K, Sugita S, Shoya M, Isojima Y (1999) The reaction between rice-husk ash and Ca(OH)_2 solution and the nature of its product. *Cement and Concrete Research* 29 (1): 37–43.
- Zhang MH, Lastra R, Malhotra VM (1996) Rice-husk ash paste and concrete: some aspects of hydration and the microstructure of the interfacial zone between the aggregate and paste. *Cement and Concrete Research* 26 (6): 963–977.
- Zhang MH, Malhotra VM (1996) High-performance concrete incorporating rice husk ash as a supplementary cementing material. *ACI Materials Journal* 93 (6): 629–636.

Chapter 8

Municipal Solid Waste Ash

Introduction

Municipal solid waste ash (MSWA) is the by-product produced during the combustion of municipal solid waste. Incineration is the commonly used practice for managing the increasing production of municipal solid waste (MSW). Two widely used processes of incinerating MSW are the refuse-derived fuel (DRF) process and the mass-burning process. The refuse-derived fuel process consists of first separating metals and glass from the MSW. The MSW is then shredded and incinerated, and the generated heat is recovered to produce electricity. The mass-burning process consists of burning the MSW as it is received in the plant without waste separation or shredding.

Major portions of the MSW are then transformed physically and chemically as a result of incineration. The by-product of the incineration process is ash. Ash is typically 1–30% by wet weight and 5–15% by volume of the wet MSW depending upon the nature of the incineration plant. Two types of the ashes are produced as a result of the incineration process; bottom ash and fly ash. Bottom ash residues are large and heavy particles which are removed from the bed of the incinerator whereas fly ash residues are very fine particles entrained in exhaust gases. In some plants, fly ash is saturated with water and combined with bottom ash into a mixture, and then, is disposed off. In the United States, typically all of the ash streams are combined. This combined stream is referred to as combined ash. In Europe, most facilities separate and separately manage the bottom ash and fly ash streams.

Out of the total MSW ash, bottom ash constitutes 75–80% of the total combined ash stream. Majority (approximately 90%) of the bottom ash consists of grate ash, which is the ash fraction that remains on the stoker or grate at the completion of the combustion cycle. It is similar in appearance to porous, grayish, silty sand with gravel, and contains small amounts of unburnt organic material and chunks of metal. The grate ash stream consists primarily of glass, ceramics, ferrous and nonferrous metals, and minerals.

Boiler ash, scrubber ash, and precipitator or baghouse ash consist of particulates that originate in the primary combustion zone area and are subsequently entrained in the combustion gas stream and carried into the boiler and air pollution control

system. As the combustion gas passes through the boiler, scrubber, and precipitator or baghouse, the entrained particulates stick to the boiler tubes and walls (i.e., boiler ash) or are collected in the air pollution control equipment (i.e., fly ash), which consists of the scrubber, electrostatic precipitator, or baghouse. Ash extracted from the combustion gas consists of very fine particles, with a significant fraction measuring less than 0.1 mm (No. 140 sieve) in diameter. The baghouse or precipitator ash comprises approximately 10–15% of the total combined ash stream.

8.1 Properties of MSW Ash

8.1.1 Physical Properties

MSW ash is a grey to black amorphous, glasslike material that contains high levels of several toxic metals such as lead and cadmium and organic compounds (such as dioxins). The nature and quality of MSW ash depends greatly on the nature of the waste, type of combustion unit, and nature of the air-pollution-control device. Physical properties of MSW ash are given in Table 8.1. Municipal solid waste combustor ash is a relatively lightweight material compared with natural sands and aggregate. The bulk specific gravity values ranges from 1.5 to 2.2 for sand-size or fine particles and 1.9–2.4 for coarse particles, compared with approximately 2.6–2.8 for conventional aggregate materials.

Combustor ash is highly absorptive with absorption values ranging from 5 to 17% for fine particles and from about 4–10% for coarse particles. Conventional aggregates typically exhibit absorption values of less than 2%. Combustor ash is primarily a sandy material with the major fraction passing a 4.75 mm (No. 4) sieve. Ash also contains a relatively high minus 0.075 mm (No. 200 sieve) silt fraction.

Bethanis et al. (2002) determined the (i) effect of milling on the particle size distribution of incinerated municipal bottom ash with a particle size less than 8 mm; and (ii) properties of sintered milled incinerator bottom ash samples. Ash samples were milled for 2, 8, and 16 hours and then were sintered. They reported that: (i) 50% of the volume (d_{50} value) of the as-received ash was 295 μm , and this decreased to 15 μm after 2 h milling. Corresponding d_{50} values for 8 and 16 h-milled ash were 6.2 and 3.9 μm , with d_{95} values of 0.8 and 0.7 mm respectively; and (ii) extensively milled ash samples had higher sintered densities and higher shrinkage. Increasing the sintering temperature to 1080°C increased densification for 8 and 16-h milled samples and maximum densities of 2.6 g/cm^3 were achieved with 20% shrinkage. Firing above 1080°C resulted in a rapid decrease in density and sample expansion. The coarser particle size distribution of the 2 h-milled samples produced much lower sintered densities (1.3 g/cm^3) and increase in density with sintering temperature was greatly reduced.

Filipponi et al. (2003) examined the physical properties of three municipal solid waste incineration bottom ashes (MBA) and one hospital waste incineration bottom

Table 8.1 Selected properties of MSW ash

Property	Bottom ash	Combined ash
Bulk specific gravity		
Fine (< No. 4 sieve)	1.70–1.81 (Koppelman and Tanenbaum, 1993) 1.50–2.22 (Eighmy and Gress, 1996)	1.86–2.03 (Koppelman and Tanenbaum, 1993)
Coarse (> No. 4 sieve)	2.11–2.23 (Chesner et al., 1986) 1.93–2.44 (Koppelman and Tanenbaum, 1993)	1.96–2.24 (Koppelman and Tanenbaum, 1993)
Absorption (%)		
Fine (< No. 4 sieve)	12.0–17.0 (Chesner et al., 1986)	4.8–14.8 (Koppelman and Tanenbaum, 1993)
Coarse (> No. 4 sieve)	4.1–4.7 (Chesner et al., 1986)	3.6–10.0 (Koppelman and Tanenbaum, 1993)
Moisture content (% dry weight)	29–66 (Chesner et al., 1986) 22–62 (Koppelman and Tanenbaum, 1993)	17–76 (Koppelman and Tanenbaum, 1993)
Unit weight (kg/m ³)	960–1400 (Chesner et al., 1986)	990–1170 (Koppelman and Tanenbaum, 1993)
LOI (%)	6.4 Koppelman and Tanenbaum, 1993 3.7 (Chesner et al., 1986)	2.5–13.5 Koppelman and Tanenbaum, 1993)
Gradation (% passing)		
Fine fraction, < 4.75 mm No. 4 sieve)	50–70 (Chesner et al., 1986) 42–62 (Koppelman and Tanenbaum, 1993) 60 (Eighmy and Gress, 1996)	50–70 (Koppelman and Tanenbaum, 1993)
Silt fraction, < 0.075 mm (< No. 200 sieve)	9–16 (Chesner et al., 1986) 2–16 (Koppelman and Tanenbaum, 1993) 2 (Eighmy and Gress, 1996)	15–20 (Koppelman and Tanenbaum, 1993)
Maximum density (kg/m ³)	1260–1570 (Chesner et al., 1986)	1260–1730 (Koppelman and Tanenbaum, 1993)

ash (HBA) coming from different Italian incineration facilities. Physical properties of bottom ashes are given in Table 8.2.

Aubert et al. (2006) evaluated the physical properties of MSWI fly ashes subjected to two types of stabilization processes. The first one, the conventional process, called “A”, was based on the washing, phosphation and calcination of the ash, and a modified process, called “B”, intended to eliminate metallic aluminum and sulfate

Table 8.2 Physical properties of bottom ashes (Filipponi et al., 2003)

Property	HBA	MBAMO	MBARE	MBABO
Bulk density (kg/m ³)	1511	1138	1365	1425
Specific gravity	2.56	2.43	2.46	2.44
Water content (%)	13.65	21.68	39.28	24.71
Loss on Ignition (%)	5.55	3.47	8.47	2.94

contained in the ash. The first process (A) has following steps: (i) washing of fly ash as it removes the soluble salts (especially chlorides) contained in the ash, so as to improve its behavior in cement-based materials and allows the sodium contained in halite (NaCl) to be recovered for use in technical soda plants; (ii) phosphation with phosphoric acid to stabilize heavy metals; and (iii) calcination to eliminate organic compounds. In the second process (B), the only difference was the washing step of the treatment. It was modified in order to eliminate metallic aluminum and calcium sulfate. Sodium carbonate (Na_2CO_3) was added to the washing water for two reasons: – this addition increased the pH value during washing, which enabled metallic aluminum to be dissolved; - Na_2CO_3 reacts with CaSO_4 to form Na_2SO_4 , which is very soluble, and calcite CaCO_3 , which is inert in cement-based products. Physical properties of treated fly ashes (TFA) by two processes are given in Table 8.3. It can be seen that modifications in the stabilization process significantly increased the surface area of the TFA. The values in the comparison of bulk density and specific gravity confirm this result. The TFA-B particles were more porous than TFA-A. Moreover TFA-B contained particles of neo-formed calcite, which were small. This could also explain the increase in surface area.

8.1.2 Chemical Composition

Major elements in MSW ash are silica, calcium, and iron. Ash composition can be expected to vary from facility to facility. Chemical composition as reported by Koppelman and Tanenbaum (1993) are given in Table 8.4.

Clozel-Leloup et al. (1999) and Zevenbergen and Comans (1994) reported that the most common phases in incinerator bottom ashes include silicates (quartz), alumino-silicates of Ca and Na (plagioclase, ghelenite, piroxene, olivine, alite, belite), metal oxides, hydroxides (portlandite), sulfates (anhydrite), carbonates (calcite, siderite), as well as metals and alloys.

Rémond et al. (2002) carried out the characterization of MSWI fly. The oxide components of fly ash were SiO_2 (27.23%), CaO (16.42%), Al_2O_3 (11.72%), Na_2O (5.86%), K_2O (5.8%), MgO (2.52%), Fe_2O_3 (1.8%), TiO_2 (0.84%), P_2O_5 (0.34%), SO_3 (3.0%), Cl (7.2%). The loss on ignition at 975°C was also very high (13%). In addition, the ash has high chlorine, sodium and potassium contents. The most abundant heavy metals were zinc and lead. The total quantity of heavy metal represented approximately 2% of the total mass of the ash. They further reported that XRD analysis of MSWI fly ash indicated that main crystalline compounds, in order

Table 8.3 Physical characteristics of MSWI fly ashes (Aubert et al., 2006)

Property	TFA-A	TFA-B
Bulk density (g/cm^3)	2.81	2.71
Specific gravity (g/cm^3)	2.95	2.86
BET specific surface area (m^2/g)	2.26	18.6

Table 8.4 Chemical properties of MSW ash (Koppelman and Tanenbaum, 1993)

Constituent	Bottom ash	Combined ash
Silica	16.8–20.6	13.8–20.5
Calcium	7.15–7.69	5.38–8.03
Iron	2.11–9.35	2.88–7.85
Magnesium	1.05–1.18	0.90–1.84
Potassium	0.84–1.02	0.84–1.15
Aluminium	4.77–5.55	3.26–5.44
Sodium	3.51–4.10	2.00–4.62

of Size were: quartz (SiO_2), sylvite (KCl) and halite (NaCl), anhydrite (CaSO_4), calcite (CaCO_3) and lime (CaO).

Rémond et al. (2002) studied the backscattered electron images of the MSWI fly ash for the two fields of observation, FA1 and FA2. They concluded that: (i) MSWI fly ash has various forms, unlike coal fly ash that is composed of spherical particles ; (ii) some MSWI fly ash particles are spherical (full or hollow) and a relatively large fraction of the ash appears to have a vitreous form; and (iii) there are also obverse elongated, angular, very porous particles and clusters of sintered particles.

Bethanis et al. (2002) studied the effect of milling on the chemical composition of incinerated municipal bottom ash with a particle size less than 8 mm. They reported that: (i) approximately 75–85% of the milled bottom ash consisted of silica (SiO_2), alumina (Al_2O_3), iron (Fe_2O_3) and calcium oxides (CaO). Sodium, potassium, magnesium, phosphate and titanium were also present; (ii) heavy metals of environmental concern at high concentrations were Zn (>2000 mg/kg), Ni (80–120 mg/kg), Cu (650–800 mg/kg) and Cr (300–350 mg/kg); (iii) loss on ignition of dried milled ash ranged from 11.8 to 12.3% indicating that a significant fraction of un-burnt organic carbon remained in the ash; and (iv) main minerals present in the milled ash were quartz (SiO_2) and calcite (CaCO_3).

Filipponi et al. (2003) analyzed the chemical composition of three municipal solid waste incineration bottom ashes (MBA) and one hospital waste incineration bottom ash (HBA) coming from different Italian incineration facilities. Chemical composition of bottom ashes is given in Table 8.5. It can be seen that the bottom ashes were mainly composed of Si, Al and Ca oxides, accounting for 79–82% of the material on a dry weight basis. In particular, the Si and Al oxides content ranged from 52 to 70%.

Song et al. (2004) studied the characteristics of ashes from different locations at a municipal solid waste incinerator (MSWI) equipped with a water spray tower (WST) as a cooling system, and a spray dryer adsorber (SDA), a bag filter (BF) and a selective catalytic reactor (SCR) as air pollution control devices (APCD). The amount of bottom ash generated from the incinerator was about 16% of incinerated waste, and that of fly ash collected from different air pollution control devices, was 1.2% of incinerated waste. Chemical composition results from XRD analysis are given in Table 8.6. The quantity of oxide material is estimated with the total amount of analyzed element and basicity of ash calculated from the ratio of CaO and SiO_2 . They concluded that: (i) SiO_2 was a major compound in bottom ash and showed

Table 8.5 Oxides composition of bottom ashes (Filipponi et al., 2003)

Oxide (%)	HBA	MBAMO	MBARE	MBABO	OPC
SiO ₂	59.62	47.76	41.13	56.99	25.94
TiO ₂	1.09	0.79	1.23	0.49	0.33
Al ₂ O ₃	10.68	10.55	11.35	9.20	5.01
Fe ₂ O ₃	1.95	8.61	6.77	3.97	4.85
MnO	0.07	0.13	0.11	0.08	0.07
MgO	2.74	3.67	3.85	3.46	2.27
CaO	12.22	16.45	19.77	13.22	52.23
Na ₂ O	7.04	3.51	2.84	5.87	0.32
K ₂ O	0.58	1.41	1.57	1.35	1.98
P ₂ O ₅	0.36	1.29	1.84	0.70	0.12

the least amount in the ash from BF; (ii) Only a small amount of Cl was found in bottom ash and a large amount in the ash from BF and SDA. From these results, it can be inferred that the air pollution control devices removed a significant portion of metal and organic chlorides with deposition into solid particles; (iii) CaO was found in almost the same amount in both the bottom ash and the ash from WST, but larger amount of CaO in the ash from SDA was shown due to injected lime solution to remove acid gas; (iv) most of the metal oxides, having low volatility such as Fe₂O₃ and CuO, were found with large amounts in the bottom ash. The basicity of bottom ashes ranged from 0.08 to 1.46; and (v) bottom ash had different chemical compound concentrations and contents of heavy metals with particle sizes. Metal oxide and basicity were increased as the particle size of bottom ash decreased, with the exception of SiO₂, Na₂O and CuO. The ash from WST was indicating higher basicity than bottom ash. The ash from SDA showed the highest basicity due to injected lime solution and the basicity of the ash from BF was also high.

Aubert et al. (2006) determined the chemical characteristics of MSWI fly ashes subjected to two types of stabilization processes. The first one, the conventional process, called “A”, was based on the washing, phosphation and calcination of the ash, and a modified process, called “B”, intended to eliminate metallic aluminum and sulfate contained in the ash. Details of the two processes have been described in physical properties of the fly ashes reported by Aubert et al., (2006). On chemical composition, they reported that: (i) chemical compositions of the two ashes were comparable. They contain large amounts of calcium, silicon, phosphorus (due to the stabilization process) and aluminum. The washing step of both processes dissolved the chlorides contained in the ash. The addition of Na₂CO₃ in process-B was efficient: TFA-B was free of sulfates as expected. The minor elements content of the two ashes was comparable. Large amounts of heavy metals can be seen, especially zinc, lead, chromium and cadmium. Table 8.7 indicates the proportions of calcite and metallic aluminum in each TFA. TFA-B contained a large amount of calcite due to the reaction between calcium sulfate and sodium carbonate. Moreover, the increase of pH value during the washing step enabled metallic aluminum to be dissolved. The amount of residual aluminum in TFA-B was below the

Table 8.6 XRD analysis of ashes from different locations (Song et al., 2004)

Element	Bottom ash (% dry weight)				Fly ash (% dry weight)		
	> 5 mm	2–5mm	0.85–2 mm	< 0.85 mm	WST	SDA	BF
pH	3.46	11.7	12.2	12.3	5.5	12.3	11.6
SiO ₂	53.16	34.82	33.10	25.3	16.61	5.83	4.73
TiO ₂	0.18	0.90	1.55	2.08	4.06	1.94	1.17
Al ₂ O ₃	3.98	8.58	10.32	10.77	8.82	2.79	1.77
Fe ₂ O ₃	1.40	5.99	5.75	4.49	3.63	2.36	0.95
Cr ₂ O ₃	0.13	0.14	—	—	0.16	0.07	0.20
K ₂ O	0.94	1.93	2.29	2.19	1.98	1.53	10.57
Na ₂ O	6.67	2.24	1.94	2.07	1.44	—	10.92
P ₂ O ₅	5.00	10.07	7.02	6.45	4.75	1.42	1.20
CaO	19.13	27.88	30.43	37.04	33.96	52.90	25.16
MgO	1.49	2.17	2.27	3.30	6.02	2.55	1.25
CuO	1.48	0.76	0.45	0.33	0.11	0.07	0.20
PbO	0.08	0.11	0.16	0.15	0.15	0.12	0.49
ZnO	0.67	1.70	1.32	0.95	1.04	0.54	0.85
SO ₃	5.27	1.51	1.95	2.84	7.02	6.69	7.98
Cl	0.41	1.20	1.45	2.03	8.58	20.32	31.72
Basicity CaO/SiO ₂	0.36	0.08	0.92	1.46	2.04	9.07	5.36

measurement threshold ($< 0.07\%$). These results showed that the modifications made to the process gave the desired results: TFA-B was free of metallic aluminum and sulfate.

8.1.3 Elemental Analysis

Bethanis et al. (2002) investigated the mineralogy of milled and sintered municipal bottom ash. The major crystalline phases identified in the milled ash were quartz (SiO₂) and calcite (CaCO₃), ghelenite (Ca₂Al₂SiO₇) and hematite (Fe₂O₃). Analysis of the milled ash sintered at the maximum density temperature revealed that diopside (CaMgSi₂O₆) was the principal crystalline phase, with significant amounts of clinoenstatite (MgSiO₃) and wollastonite (CaSiO₃), and minor amounts of albite (NaAlSi₃O₈) and hematite. The quartz and calcite peaks decreased on sintering and had completely disappeared by 1080°C, due to the formation of crystals of the pyroxenoids group, such as diopside and wollastonite. Diopside is an important rock forming mineral in several metamorphic and basic to ultra-basic igneous rocks. It

Table 8.7 Calcite (CaCO₃) and metallic aluminum contents (Aubert et al., 2006)

	TFA-A	TFA-B
Calcite (%)	1	17
Metallic aluminum (%)	0.13–0.35	< 0.07

Table 8.8 Elemental composition of bottom ash (Filipponi et al., 2003)

Element	Concentration (mg/kg dry wt)			
	HBA	MBABO	MBAMO	MBARE
Al	8393	55317	30279	27919
Ca	22985	133270	103389	246441
Cd	< 8	< 8	< 8	< 8
Cr	168	79	182	80
Cu	1084	2660	2231	1526
Fe	4659	11238	33814	28746
K	3264	3073	4221	3788
Mg	3177	12542	8798	31016
Mn	72	61	151	83
Ni	332	61	151	83
Pb	< 80	1287	1197	1473
Zn	201	1443	1709	21344
Chloride (% dry wt)	< 0.01	0.12	0.24	0.35
Sulfate (% dry wt)	0.09	0.76	0.65	0.77

is reported to form the major crystalline phase in glass-ceramics formed of vitrified municipal incinerator fly ash, filter dusts and industrial waste (Barbieri et al., 2000; Boccaccini et al., 1995; Boccaccini et al., 1997).

Filipponi et al. (2003) evaluated the municipal solid waste incineration bottom ashes (MBA) and one hospital waste incineration bottom ash (HBA) coming from different Italian incineration facilities for elemental analysis. Elemental composition of the bottom ashes are presented in Table 8.8. With respect to the anion content of bottom ash, low chloride and sulfate ion concentrations were detected, thus reassuring about the occurrence of possible detrimental effects on cement setting and hardening. Among the trace elements, the major concentrations were detected in HBA for Cu and Ni; are commonly recognized as lithophilic elements, meaning that at the combustion temperatures typical of waste incineration, they are not able to form gaseous species. Conversely, the major concentrations in MBAs were measured for Pb and Zn.

Song et al. (2004) also reported the distribution characteristic of the remaining metals in bottom ash and fly ash. The concentration of heavy metals increased with the decrease in bottom ash particle size (Park and Hu, 1996) as shown in Table 8.9. It is because coarser particles have a longer retention time so that the metal has more thermal volatilization; on the other hand, the fine particles do not have sufficient retention time to become volatile and are soon dropped down to the bottom ash pit. In case of fly ash, most of the heavy metal concentrations were higher than those in bottom ash. This could be explained by the fact that the vaporized metals were condensed and aggregated on the surface of fly ash due to the temperature in flue gas cooling system. The highest metal concentration was observed at the bag filter, which collected the particles having large specific surface area.

Müller and Rübner (2006) determined the composition of municipal waste incinerator bottom ash by XRD in conjunction with the microscopic analysis. They reported that bottom ash components were essentially divided into six different

Table 8.9 Metal concentration in bottom ash and fly ash from MSW (Song et al., 2004)

Element	Bottom ash (mg/kg)					Fly ash (mg/kg)			
	> 5 mm	2–5 mm	0.85–2 mm	< 0.85 mm	Mixture	WST	SDA	BF	
Ba	11.246	36.66	61.568	66.133	43.405	63.780	41.980	33.983	
Na	436.126	5118.00	7414.517	10348.965	5739.613	9028.0	6178.0	37122.58	
Mg	552.179	3029.00	5290.942	7662.234	4115.366	11030.0	8851.0	6681.66	
Al	1800.175	31696.83	37182.56	45110.00	28055.94	25690.0	10240.0	6430.71	
Ca	28628.55	77110.00	91581.69	119188.08	78013.11	57720.0	117100.0	65206.96	
V	9.973	10.43	10.499	19.662	12.985	10.160	6.993	4.166	
Cr	0.343	80.373	408.078	536.186	355.721	115.10	169.070	183.303	
Mn	166.633	875.90	889.000	978.902	703.075	803.10	580.300	314.437	
Fe	8906.0	12048.0	25050.0	23860.450	17521.31	3427.0	2006.00	761.848	
Co	1.311	2.294	2.354	5.282	2.824	6.975	3.275	1.874	
Cu	682.391	1196.32	2367.197	4597.282	2246.780	70.570	406.700	601.880	
Zn	578.900	1935.00	4918.016	9879.000	4405.403	4516.0	9036.00	12813.44	
Sr	41.303	134.500	153.269	220.278	135.299	121.80	138.300	108.978	
Cd	3.875	5.431	19.069	25.346	13.667	14.190	15.690	190.162	
Sn	72.901	448.90	922.416	972.003	597.957	447.00	366.700	767.147	
Sb	30.508	22.800	54.159	59.194	42.498	46.570	75.420	157.768	
Pb	53.808	325.80	1542.691	1596.840	888.567	227.90	254.00	2053.589	
Hg	0.001	0.034	0.005	0.047	0.021	0.021	11.443	48.445	

groups of components: (i) crystalline silicates in a glass matrix: hedenbergite (Fig. 8.1); (ii) ferrohedenbergite, melilite, wollastonite, quartz, feldspar (both as well as rounded grains with many fissures and cracks); (iii) oxides, sometimes in siliceous glass matrix: magnetite (Fig. 8.2), hematite, periclase; (iv) bottle glass, mostly composed of Na_2O , CaO and SiO_2 sometimes fused with quartz and feldspar; (v) metals: aluminium, brass, steel, copper, zinc; (vi) ceramic fragments: china, brick, plaster, mortar; and (vii) components of organic origin: apatite (bone fragments), charcoal, plant fibers, polymers.

8.1.4 Hydration Characteristics of MSW Ash with C_3S and C_2S

Portland cement is a mixture with four principal constituents: C_3S (Ca_3SiO_5) 50–70 wt%, C_2S (Ca_2SiO_4) 20–30 wt%, C_3A ($\text{Ca}_3\text{Al}_2\text{O}_6$) 5–12 wt% and C_4AF ($\text{Ca}_4\text{Al}_2\text{Fe}_2\text{O}_{10}$) 5–12 wt% (Lin et al., 1997).

Lin et al. (2003a) studied the hydration characteristics of C_3S and that of MSWI fly ash slag incorporated into C_3S . The MSW fly ash slag was prepared by melting MSW ash in electric-heated melter at 1400°C for 30 min. The melts were water-cooled to obtain fine slag, which was then ground in a ball mill until fine enough to pass through a #200 sieve. The resultant pulverized slag had Blaine fineness of $500\text{ m}^2/\text{kg}$, with a specific gravity of 2.7. Anhydrous C_3S was provided by the Construction Technology Laboratories, Skokie, IL, USA. Chemical composition of MSW fly ash slag and C_3S are given in Table 8.10.

Slag blended C_3S pastes (C_3S -slag) consisting of 80% C_3S and 20% pulverized slag were compared to a blend of 100% C_3S . Water to binder ratio of 0.38 was used



Fig. 8.1 Hedenbergite crystals in a MSWI bottom ash aggregate (Müller and Rübner, 2006)

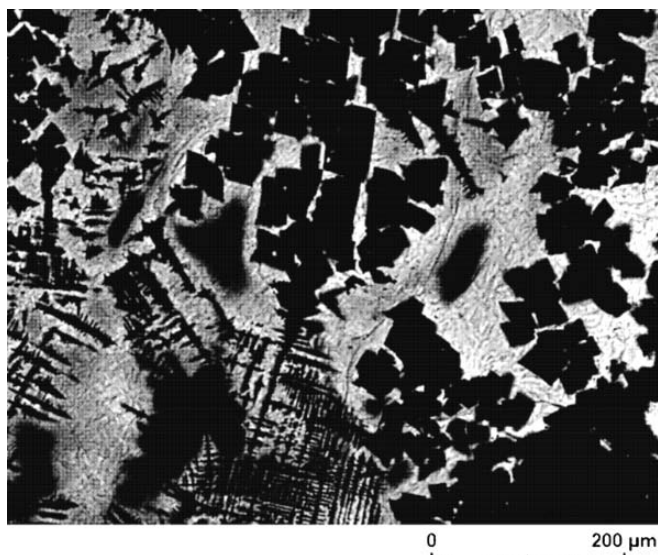


Fig. 8.2 Magnetite embedded in a siliceous glass matrix (Müller and Rübner, 2006)

for both mixtures. Test cubes of 25.4 mm were prepared according to STM-305, followed by demoulding (ASTM C31-69), then cured in an environmental chamber, maintained at 25°C with a relative humidity >98%, for periods ranging from 1 to 90 days. After curing for 1, 3, 7, 14, 28, 60 or 90 days, the samples were subsequently crushed and the hydration reactions were stopped with absolute alcohol, filtrated in vacuum, washed with acetone several times and dried, then subjected to XRD,

Table 8.10 Chemical composition of C_3S and MSWI fly ash and slag (Lin et al., 2003a)

Composition	C_3S	MSWI fly ash	MSWI fly ash slag
CaO (%)	72.3	16	27.3
SiO ₂ (%)	25.2	34.3	38.9
Al ₂ O ₃ (%)	0.08	4.3	23.3
Fe ₂ O ₃ (%)	0.02	3.6	5.4
MgO (%)	< 0.01	0.5	3.6
SO ₃ (%)	< 0.01	8.8	0.2
Na ₂ O (%)	< 0.01	5.3	1.3
K ₂ O (%)	< 0.01	3.0	< 0.01
TiO ₂ (%)	0.01	4.2	—
P ₂ O ₅ (%)	< 0.01	3.9	—
Mn ₂ O ₃ (%)	0.01	—	—
SrO (%)	< 0.01	—	—
Zn (mg/l)	—	7115	6480
Pb (mg/l)	—	1284	295
Cu (mg/l)	—	1409	604.4
Cr (mg/l)	—	811	695.3
Cd (mg/l)	—	80	5.8

DTA/TGA and ^{29}Si nuclear magnetic resonance analyses. Based on the hydration characteristics of pure C_3S pastes and C_3S -slag pastes, they concluded that: (i) C_3S -slag pastes had lower CSH and $\text{Ca}(\text{OH})_2$ values than the pure C_3S pastes at all stages of hydration, possibly due to the partial replacement of C_3S by slag with less activity; (ii) as the hydration precedes, the C_3S peaks decreased, up to 90 days, due to the activation of the slag by liberated $\text{Ca}(\text{OH})_2$ and the amounts of hydration products ($\text{Ca}(\text{OH})_2$) produced from the C_3S -slag pastes were smaller than from the pure C_3S pastes; and (iii) ^{29}Si MAS/NMR techniques indicated that the hydration degree of pure C_3S pastes increased with time; also C_3S -slag pastes showed that the hydration degree values at all ages were lower.

Wang et al. (2004) reported the hydration characteristics with C_2S being present in MSWI fly ash slag. Based on the results obtained they concluded that: (i) lower CSH and $\text{Ca}(\text{OH})_2$ amounts in C_2S samples incorporated in MSWI slag were observed, possibly due to the partial replacement of the mineral constituents by less active slag; (ii) incorporation of C_2S into slag decreased the initial hydration reaction, whereas it increased the pozzolanic reaction at a later stage, by consuming $\text{Ca}(\text{OH})_2$ to form CSH; and (iii) ^{29}Si MAS/NMR techniques indicated that C_2S -slag pastes showed lower degree of hydration for all hydration ages. This might be due to the sluggish behavior of slag formation by an acidic film on the grains of slag, retarding hydration process, which occurred as the $\text{Ca}(\text{OH})_2$ broke down the silica framework.

8.2 Utilization of MSW Ash

Following are the potential uses of MSW fly ash. Ferreira et al. (2003) published various uses of MSW fly ash, that included: (i) construction materials; (ii) geotechnical applications; (iii) agriculture; and (iv) miscellaneous applications.

8.2.1 Cement Production

MSW fly ash contains 24–27% of lime, some silicates and alumino-silicates. Mangialardi et al. (1999) reported that it could potentially be used for the production of cement powder. Beretka et al. (2002) have reported that for MSW fly ash could be used in low energy cements, also called calcium sulfo-aluminate cements. These are special cements that can be synthesized at low temperatures and which present high strength and rapid hardening.

8.2.2 Concrete

MSW fly ash could be used as partial replacement for cement in concrete mixes as a supplementary cementitious material as it contains some quantities of typical

cement minerals, although in lesser quantity than cement clinker. Hamernik and Frantz (1991) reported that MSW fly ash is similar to class C pozzolans, as defined in the ASTM standard and could be possibly used as partial replacement of cement even though they failed to comply with one or more criteria of the standard.

MSW fly ash can also be used in concrete as aggregate: MSW fly ash could be processed into pellets and used as lightweight aggregates. Rebeiz and Mielich (1995) have advocated the possible use of MSW ash in construction applications including the innovative use in the production of polymer concrete (PC). Results have shown that good quality PC can be produced with MSW ash.

8.2.3 Ceramics

Ceramic industry is a high consumer of silicate-based natural raw materials and this fact makes it a potential candidate for MSW fly ash applications. GEC (1996) reported the application of MSW combined ash in the production of ceramic tiles. Tiles contained 50% incinerator ash and presented good results in durability, with a fracture load of 76.20 kgf/cm² in bending which is higher than the reported JIS standard for floor tiles (12.24 kgf/cm²). Absorption coefficient values lay within normal range for ceramics. Leaching tests showed minimum releases for some of the tested heavy metals and organics. Produced tiles were applied in outside and inside pavement and exterior facing of walls.

8.2.4 Glass and Glass-Ceramics

MSW fly ash could be converted into a glasslike substance by melting, at high temperatures (above 1300°C). This process is called vitrification. During vitrification high temperatures destroy organic contaminants, like dioxins, with efficiencies over 99.9%, while heavy metals are either encapsulated in the silicate matrix or separated from the product by evaporation or differential precipitation.

Potential uses of vitrified fly ash are: road base materials; embankments; blasting grit; partial sand replacement in concrete; in monolith blocks for coastal protection and, in the production of construction and decorative-materials, like water-permeable blocks, ceramic tiles, pavement bricks and decorative stones for gardens.

8.2.5 Road Pavement

MSW fly ash's possible application in road pavement could be as a substitute for sand and/or cement in cement stabilized bases and sub-bases. Environmental issues related with this application are the contamination of the underlying soil and groundwater by substances leached from the road base.

8.2.6 Embankment

One of the potential applications for MSW fly ash is in soil stabilization as a substitute of lime or cement because of its pozzolanic characteristics. MSW fly ash's density is less than other fill materials used in the construction of embankments: typical values for MSW fly ash are 1.7–2.4 while for sand is 2.65 (Tay and Goh, 1991).

Tay and Goh (1991) examined the possibility of using MSW fly ash in geotechnical applications as a substitute for filler. They report that fly ash displays the prerequisite properties for this type of application with high strength and free-draining, typical of granular material, and lower compacted densities than conventional earth fills. They also assessed the possibility of using fly ash in soil stabilization (instead of lime or cement) finding that soil-fly ash mixtures presented improved shear strengths and lower compressibility than other non-treated soils.

8.3 Properties of Cement Containing MSW Ash

8.3.1 Compositional Effects

Shih et al. (2003) investigated the replacement of raw mix in cement production by municipal solid waste incineration ash. MSWI ash was sieved from 0.074 to 2 mm. Magnet-repelled (MR) ash was prepared by passing the MSWI ash through a magnetic separator to remove its metallic content. Both the MSWI and MR ashes were ground to 74 μm size with a centrifugal ball mill. Major chemical compounds in raw cement mix were of 63.8% CaO, 19.8% SiO₂, 5% Al₂O₃, 3.5% Fe₂O₃, 2.1% MgO. MSWI ash had 27.2% CaO, 29.4% SiO₂, 18% Al₂O₃, 13.3% Fe₂O₃, 1.6% MgO. MR ash had 27.4% CaO, 46.4% SiO₂, 9.5% Al₂O₃, 7.1% Fe₂O₃, 1.7% MgO. They studied the calcination and compositional effects of ash replacement.

For compositional effect of ash replacement on the calcination, two parameters in cement chemistry were examined. The first one is hydraulic modulus (H.M) given as $\text{CaO}/(\text{SiO}_2 + \text{Al}_2\text{O}_3 + \text{Fe}_2\text{O}_3)$ which gives the evaluation of hydraulic activity for strength development. The second one is lime saturation factor (LSF) given as $\text{CaO}/(2.8\text{SiO}_2 + 1.2\text{Al}_2\text{O}_3 + 0.65\text{Fe}_2\text{O}_3)$ which governs the ratio of alite to belite and also indicates whether the clinker is likely to contain free lime. Table 8.11 gives HM and LSF results of the effect of ash replacement. H.M. and LSF all decreased with increase in MR ash replacement. At replacement level of (< 3%), there was no significant change in HM and LSF values. But at a large amount of ash replacement, especially cement with 15% ash replacement, H.M. was significantly lowered to about 28% indicating the hydraulic activity for strength development to be weak. In addition, the low LSF supports this point that calcium oxide content might not be enough to produce calcium silicates in the calcinations and hence causes the decrease of the hydraulic activity. Therefore, insufficient calcium oxide might be the predominant reason causing the poor strength development of specimens made from the MR ash replaced clinkers.

Table 8.11 Effect of ash replacement on HM and LSF (Shih et al., 2003)

	Without ash replacement	3% ash replacement	10% ash replacement	15% ash replacement	Conditioned cement
HM	2.25	2.14	1.91	1.76	2.31
LSF	1.00	0.95	0.84	0.77	1.01

Goh et al. (2003) studied the properties of municipal fly ash (MFA) for use as blended cement. They reported that: (i) major elements in MFA were Ca, K, Na, Si, Al, and Mg; (ii) specific gravity of the ash varied between 2.12–2.58, generally lower than that of OPC (3.2); (iii) BET surface area of the MFA was found to be 6.03 m²/g, about six times higher than OPC (1.03 m²/g); (iv) compressive strength results indicated that up to 10% by weight of OPC could be replaced by MFA, with higher mortar strength being achieved than in the control cubes; (v) seven-day strength activity index of 123.6% achieved by the MFA, which is almost 50% higher than the requirement of 75%, suggests its contribution toward the strength development of the blended cements; and (vi) Mercury porosimetry performed on hardened cement pastes indicated a reduction in the average pore diameter with an increasing percentage of cement replacement, indicating a pore refining capability of MFA particles.

Krammart and Tangtermsirikul (2004) determined the chemical composition of cement made by replacing cement raw materials with 5 and 10% of municipal solid waste incinerator bottom ash (MSWI) and calcium carbide waste (CCW). Calcium carbide waste (CCW) is a by-product from production of acetylene gas (C₂H₂). Chemical composition of major oxides cements containing MSWI and CCW are shown in Fig. 8.3. From this figure it is evident that chemical compositions of

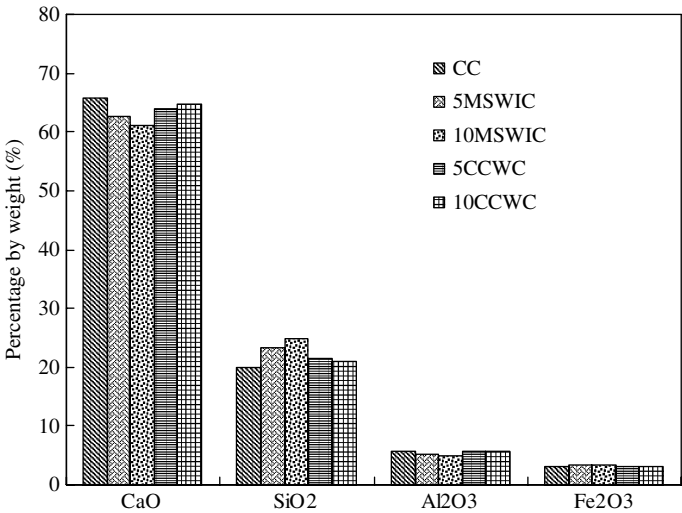


Fig. 8.3 Comparison of four major oxides of the cements (Krammart and Tangtermsirikul, 2004)

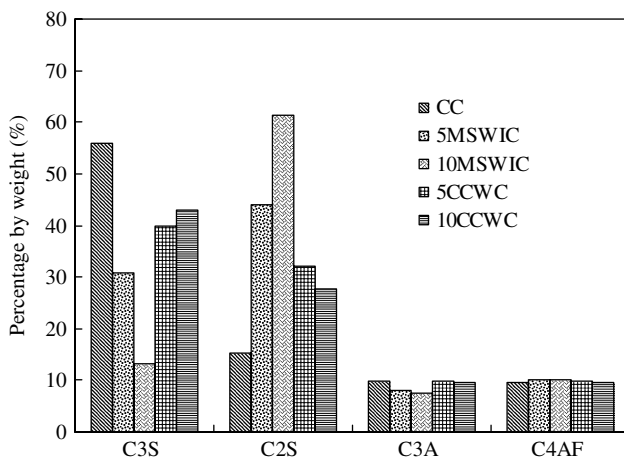


Fig. 8.4 Comparison of oxide compound compositions of cements (Krammart and Tangterm-sirikul, 2004)

MSWI cements and CCW cements were similar to those of the control cement (CC), except the SiO_2 contents, of which 5MSWIC and 10MSWIC are respectively equal to 23.34% and 24.85%, as higher than that of the CC (20.03%). On the other hand, CaO content of CC (65.88%) was higher than those of 5MSWIC (62.75%) and 10MSWIC (61.13%). All MSWI and CCW cements, except for 10CCWC, contained lower free lime. The excess free lime usually hydrates very slowly, causing unsoundness of the cement paste in hardened state. So, the reduction of free lime content results in not only the burnability improvement of the cement but also the volume stability of the concrete. Figure 8.4 shows the comparison of four major oxides compounds composition in cements containing MSWI and CCW. C_3S calculated from Bogue's equation of 5MSWIC (30.80%) and 10MSWIC (13.17%) were considerably lower than that of CC (56.02%), whereas C_2S were significantly higher (43.89% for 5MSWIC, 61.44% for 10MSWIC and 15.24% for CC).

Lin et al. (2004a) studied the composition of slag blended cement pastes. Synthetic slag samples were prepared by melting CaO-modified and Al_2O_3 -modified municipal solid waste incinerator (MSWI) fly ash. MSWI fly ash was mixed with 5% CaO and 5% Al_2O_3 (by weight), respectively, resulting in two fly ash mixtures. These mixtures were then melted at 1400°C for 30 min to produce two types of slag with different contents, designated as C-slag and A-slag. The major components observed in the composition-modified fly ash slag were SiO_2 (32–33%), CaO (24–32%), and Al_2O_3 (15–23%). The next most abundant components were Fe_2O_3 (3–4%), Na_2O (2–3%) and K_2O (1–2%). They further reported that the pozzolanic activity index reached 97.1 and 91.4% for the C-slag and A-slag, respectively, as compared with 79.2% for the unmodified slag. Thus, both the modified slag samples exhibited a pozzolanic activity index higher than the unmodified slag sample, suggesting that the Ca and Al modifications contributed to the early pozzolanic activity (at 28 days).

Saikia et al. (2007) evaluated the properties of cement clinkers containing a fraction of MSW ash. They observed that: (i) high amounts of MSW fly ash (more than 44%) together with CaCO_3 and very small amounts of SiO_2 and Fe_2O_3 can be used to produce cement clinkers. The amount of CaCO_3 use for the production of clinkers (approximately 50%) was lower than the required amount for production of conventional cement clinkers (more than 70%). This 20% reduction in CaCO_3 is significant because it can partly reduce the emission of CO_2 into the atmosphere; (ii) if collection of the alkali metal salts and some of the volatile elements by controlling their volatilization behaviors is made possible, then MSW ash can be used to produce cement clinkers without any pretreatment; and (iii) water washing of the ash may be a pretreatment method, as it can reduce the major part of the chloride salt (from approximately 15% to less than 1%), which offers some advantages to overcome the chloride related problem during the kiln operation, as well as during ultimate application of the produced cement clinkers.

8.3.2 Degree of Hydration

Lin et al. (2004b) researched on the degree of hydration of different types of cements mixed with municipal solid waste incinerator fly ash slag. MSWI fly ash slag was prepared by first melting the MSWI fly ash at 1400°C for 30 min in an electrically heated furnace. Slag samples were then obtained. The resultant slag samples were water-quenched, then further pulverized with a ball mill, passing through a No. 200 sieve. Major composition of The MSWI fly ash slag was of SiO_2 (38.9%), CaO (27.2%), and Al_2O_3 (23.3%). The three types of Portland cements used were Type I (ASTM Type I ordinary Portland cement), Type III (high early strength Portland cement) and Type V (sulfate resistant Portland cement) having pozzolanic activity index of 103, 102 and 104, respectively. The degree of hydration of the SBC pastes was determined by thermal analysis (Jazairi and Illston, 1980). Differential thermal and thermogravimetric analysis were performed on pastes prepared with water to cement weight ratio of 0.38, at various curing ages. The degree of hydration was determined using this formula:

$\alpha = \{(W_{105} - W_{580}) + 0.41(W_{580} - W_{1007})\} / nW_{1007} \times 100\%$, where α is the degree of hydration (%); n the fixed water in completely hydrated cement pastes, 0.24 for the OPC paste; W_{105} , W_{580} , W_{1007} the sample weights in grams at 150, 580 and 1007°C , respectively; 0.41 the conversion factor for molar ratio of CaCO_3 -derived CO_2 to H_2O . Table 8.12 lists all the degrees of hydration for the OPC and SBC pastes. The slag was blended with various types of cement at different ratios. There was significant decrease in the degree of hydration of SBC pastes with the increase in replacement ratio of slag. The Type I cement paste, incorporating 10% of MSWI fly ash slag, showed a degree of hydration similar to that of the plain cement after 90 days of curing time because the hydration reactions from the slag, and C_3S and C_2S in Type I Portland cement were significant. On the other hand, in the SBC samples of the Type I cement paste incorporating 40% of MSWI fly ash slag, the dilution greatly

Table 8.12 Effect of amount of fly ash slag on the degree of hydration (Lin et al., 2004b)

Replacement ratio (wt %)		Degree of hydration (%)					
Cement	Fly ash slag	1 day	3 days	7 days	28 days	60 days	90 days
Type I							
100	0	43.6	51.8	59.8	70.0	75.4	83.2
90	10	42.5	42.8	59.1	67.7	70.8	81.1
80	20	38.0	39.1	53.4	62.0	66.0	78.6
60	40	29.0	30.4	43.8	51.9	53.6	61.0
Type III							
100	0	56.9	57.5	62.7	69.4	72.1	74.8
90	10	45.3	54.2	59.8	66.9	69.8	72.5
80	20	44.9	52.7	57.4	66.5	69.2	71.4
60	40	30.7	38.7	47.7	55.3	57.6	59.2
Type III							
100	0	55.7	61.8	65.2	70.6	72.2	73.7
90	10	44.0	52.7	59.5	66.1	70.5	72.1
80	20	39.5	48.0	54.6	63.3	67.4	68.4
60	40	25.7	32.8	41.9	50.8	53.2	54.3

reduced the C_3S , C_3A and C_2S content in the cement, which delayed the hydration process during the early stages of curing, as well as the degree of hydration.

For the SBC samples of the Type III cement paste incorporating 10% of MSWI fly ash slag, the degree of hydration of the sample, after 90 days of curing time, although close, was still 2.3% less than plain cement. The SBC samples of the Type III cement paste incorporating 20% of MSWI fly ash slag, presented a late acceleration of the hydration process, with a degree of hydration after 60 days that was 3.4% less than plain cement. The SBC samples of the Type III cement paste, incorporating 40% of MSWI fly ash slag, showed slowed hydration, since at 7 days the hydration of Type III cement was comparatively greater than other types of cement and a larger portion of pulverized slag had been added, which greatly reduced the amount of C_3S , C_3A , and C_2S .

In the SBC samples of the Type V cement paste incorporating 10% of MSWI fly ash slag, the degree of hydration in the pastes was 1.6% less than plain cement. In the SBC samples of the Type V cement paste, incorporating 20% of MSWI fly ash slag, the degree of hydration of the paste exceeded plain cement by 5.3%, for a curing time of 90 days. In the SBC samples of the Type V cement paste incorporating 40% of MSWI fly ash slag, the degree of hydration was reduced as the hydration of V cement is also slow, and the addition of a large amount of pulverized slag would greatly reduce the quantity of C_3S , C_3A , and C_2S . In addition, it was found that the degree of hydration generally increased with the curing age, but decreased with the blend ratio.

Bentur (1980) determined the degree of hydration based on the loss-on-ignition. He regarded the degree of hydration to be a result of gels that formed in the pastes.

Müller and Rübner (2006) reported that three types of different reactions were observed in the concrete containing MSW bottom ash: (i) alkali-silica reaction (ASR) of bottle glass fragments and glassy compounds of other siliceous

components of the bottom ash; (ii) reaction of aluminium to form aluminium hydroxide and calcium aluminate hydrate (CAH); and (iii) reaction of aluminate with calcium sulfate to form ettringite and monosulfate.

8.3.3 Consistency and Setting Times

Rémond et al. (2002) studied the influence of 0, 5, 10, 15 and 20 replacement of cement with MSWI fly ash on the flow and setting times of the mortars. Flow time and setting times results are shown in Figs. 8.5 and 8.6. They concluded that: (i) flow time increased with the increase in ash content; and (ii) incorporating ash in the mortars considerably increased the initial and final setting times. There was a dramatic increase in setting times when the ash content was increased from 10% to 15%. (Taylor, 1997) has reported that zinc and lead are setting retarders, or may even inhibit setting. These two components are the most abundant heavy metals found in the MSWI ash used.

Lin et al. (2003b) investigated the effect of varying percentages of MSWI fly ash slag on the fluidity and setting times of cement. The MSWI fly ash slag was prepared by the melting of the cyclone ash at 1400°C for 30 min. The melts were water quenched to obtain fine slag, which was then ground in a ball mill until fine enough to pass through a #200 sieve. The resultant pulverized slag had a fineness of 500 m²/kg and specific gravity ranging from 2.7 to 2.9, close to that of ordinary Portland cement (OPC). The major components in the MSWI ash slag were SiO₂(38.9%), CaO (27.2%), and Al₂O₃(23.2%). The proportion of cement

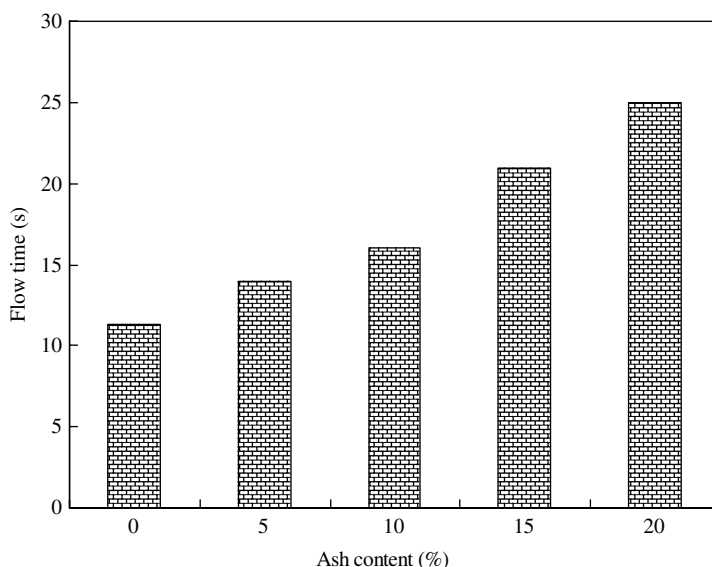


Fig. 8.5 Flow times of the M0, M5, M10, M15 and M20 mortars (Rémond et al., 2002)

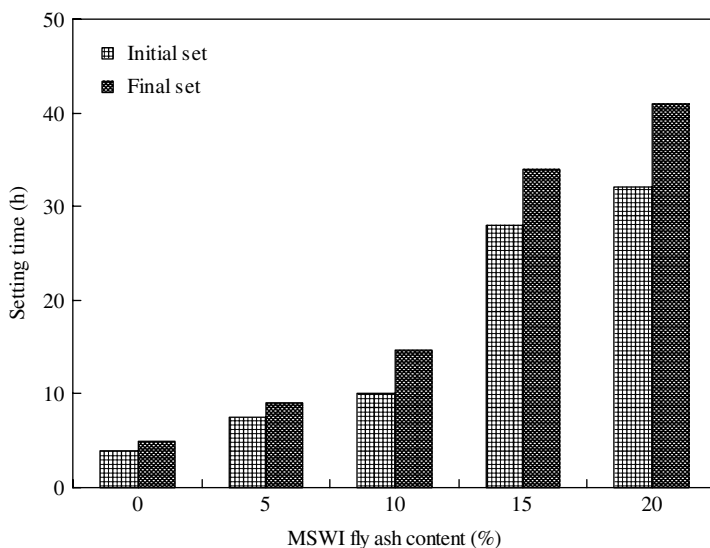


Fig. 8.6 Initial and final setting times for M0, M5, M10, M15 and M20 mortars (Rémond et al., 2002)

substitution was 10, 20, and 40%, with 0% substitution being the control group. The W/C ratio was 0.38 while the cement to sand ratio was 1:2.75. Fluidity and setting time test were conducted as ASTM C143 and ASTM C191, respectively. Fluidity values were 100, 110, 135 and >150 for 0, 10, 20, and 40% cement substitution, respectively. For 0, 10, 20, and 40% cement substitution, initial setting time were 3.68, 3.97, 4.15, and 4.87 hours, respectively, where was final setting time were 7.25, 7.75, 8.37, 9.7 hours. They concluded that: (i) fluidity value increased with the increase in MSWI fly ash content. This was possible because the fly ash slag is a glassy material with less water absorptivity; and (ii) setting times of cement pastes increased with the increase in MSWI fly ash slag content.

Krammart and Tangtermsirikul (2004) determined the normal consistency, setting times and flow value of cement made by replacing cement raw materials with 5 and 10% of municipal solid waste incinerator bottom ash (MSWI) and calcium carbide waste (CCW). Test results of normal consistency, setting times and flow value are given in Table 8.13. Based on the test results, they concluded that: (i) flow values of 5CCWC and 10CCWC cements were very close to that of CC. While 5MSWIC and 10MSWIC cements had lower flow values than CC, especially when increasing MSWI percentage in the raw material; (ii) that times of setting were slightly different when MSWI and CCW were replaced as a raw material in cement. 5MSWIC, 10MSWIC, 5CCWC and 10CCWC cement exhibited longer setting time than CC due to the lower C_3S and higher C_2S than those in CC; and (iii) flow values are in good agreement with results of normal consistency of all cements. The higher the flow values of the cements were, the lower the normal consistency of the cement pastes obtained.

Table 8.13 Normal consistency and setting time of paste (Krammart and Tangtermsirikul, 2004)

Type of cement	Flow value	Normal consistency	Setting time (Hr: min)	
			Initial	Final
CC	105	0.245	2:25	3:05
5MSWIC	93	0.265	3:00	3:50
10MSWIC	88	0.290	2:25	3:20
5CCWC	105	0.240	2:40	3:35
10CCWC	106	0.230	2:25	3:20

Lin et al. (2004b) investigated the setting times of different types of cements mixed with municipal solid waste incinerator fly ash slag. Major composition of The MSWI fly ash slag was of SiO_2 (38.9%), CaO (27.2%), and Al_2O_3 (23.3%). The three types of Portland cements used were Type I (ASTM Type I ordinary Portland cement), Type III (high early strength Portland cement) and Type V (sulfate resistant Portland cement) having pozzolanic activity index of 103, 102 and 104, respectively. Cements were replaced with 10, 20, and 40% of MSWI fly ash slag. Setting times for various replacement levels of MSWI fly ash slag are presented in Table 8.14. They concluded that: (i) for ordinary Type I, Type III and Type V Portland cement, the setting time decreased in the following sequence Type III > Type V > Type I. The sequence corresponding to that of the Type III cement had greater Blaine fineness; and (ii) the three types of cement containing 40% fly slag had a significantly retarded setting time compared to the 10 or even the 20% slag replacement.

8.3.4 Compressive Strength

Lin et al. (2003b) reported the results of the compressive strength of mortars made with cement containing varying percentages of MSWI fly ash slag. The major components in the MSWI ash slag were SiO_2 (38.9%), CaO (27.2%), and Al_2O_3 (23.2%). The proportion of cement substitution was 0, 10, 20, and 40%. The W/C ratio was 0.38 while the cement to sand ratio was 1:2.75. Compressive strength was determined up to the age of 90 days, and results are shown in Fig. 8.7. Mortar with a 10% substitution showed strength that was 1–2 MPa higher than the control after 60 and 90 days. At 28 days, mortar with a 20% substitution showed strength 6 MPa lower than that of the control group mortar. However, the strength became close to

Table 8.14 Setting times of MSWI fly ash slag-blended cement (SBC) (Lin et al., 2004b)

Cement	Setting time (h)							
	OPC		10% MSWI		20% MSWI		40% MSWI	
	Initial	Final	Initial	Final	Initial	Final	Initial	Final
Type I	3.68	7.25	3.97	7.75	4.15	8.37	4.86	9.76
Type III	1.63	4.00	2.15	4.75	2.63	5.33	4.02	6.67
Type V	5.67	8.08	6.16	8.50	6.32	8.83	6.62	8.95

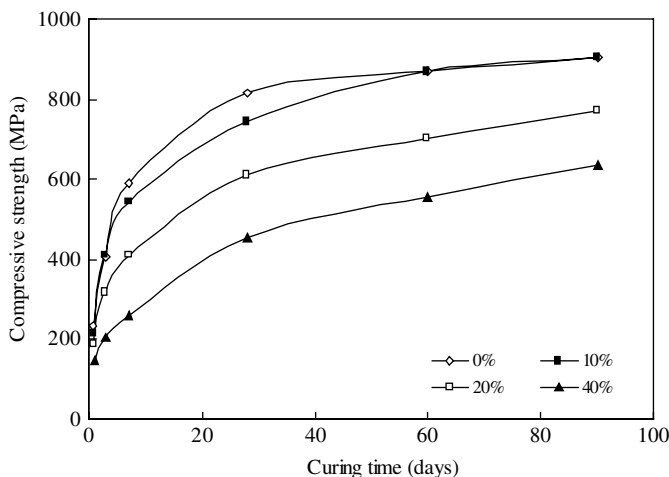


Fig. 8.7 Compressive strength of mortar with MSWI fly ash slag substitution (Lin et al., 2003b)

that of the control group after 60 days. The compressive strength increased with longer curing ages and lower substitution percentages.

Shih et al. (2003) studied the effect of ash replacement of raw mix in cement production by municipal solid waste incineration ash on the unconfined compressive strength (UCS). MSWI ash was sieved from 0.074 to 2 mm. Magnet-repelled (MR) ash was prepared by passing the MSWI ash through a magnetic separator to remove its metallic content. Both the MSWI and MR ashes were ground to 74 μm size with a centrifugal ball mill. Major chemical compounds in raw cement mix were of 63.8% CaO, 19.8% SiO₂, 5% Al₂O₃, 3.5% Fe₂O₃, 2.1% MgO. MSWI ash had 27.2% CaO, 29.4% SiO₂, 18% Al₂O₃, 13.3% Fe₂O₃, 1.6% MgO. MR ash had 27.4% CaO, 46.4% SiO₂, 9.5% Al₂O₃, 7.1% Fe₂O₃, 1.7% MgO. Figure 8.8 shows the influence of MR ash replacement on the UCS development at various curing ages. Up to 5% replacement level, there was no significance influence of ash on UCS. However, beyond 5% replacement, UCS dropped dramatically. With MR ash replacement above 10%, specimens fail to meet the standard regardless of the curing age. The reasons might be due to the alternation of chemical composition in raw mix or interferences that existed in MR ash restraining the formation of crystalline phase caused by large amount of replacement. The effect of large ash replacement was examined by XRD analysis. The formation of alite (Ca₃Al₂O₆) in cement clinkers was deducted as cement raw mix was replaced by large amount of ash. In addition, the insufficiencies of calcium oxide for the crystalline formation might be the major inducement of the deduction of alite phase.

Krammart and Tangtermsirikul (2004) determined the compressive strength of mortar of cement made by replacing cement raw materials with 5 and 10% of municipal solid waste incinerator bottom ash (MSWI) and calcium carbide waste (CCW). Figure 8.9 shows development of the compressive strengths with respect to age. For mortar specimens with 5CCWC and 10CCWC cement, compressive strength was

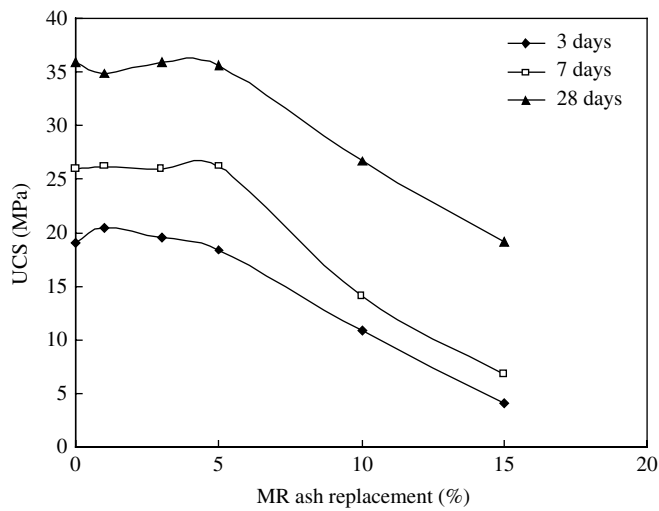


Fig. 8.8 UCS of specimens with MR ash replacement (compression pelletization at 49 MPa) (Shih et al., 2003)

equivalent to that of CC cement. On the contrary, compressive strengths of 5MSWIC and 10MSWIC were lower than that of CC mortar, especially when MSWI percentage in the raw material was increased. This is because MSWI cements had lower CaO and higher SiO₂ than those in CC, and thus C₃S content was lower than CC.

Lin et al. (2004b) compared the compressive strength of various types of cements incorporating municipal solid waste incinerator fly ash slag. Major composition of The MSWI fly ash slag was of SiO₂ (38.9%), CaO (27.2%), and Al₂O₃ (23.3%). The

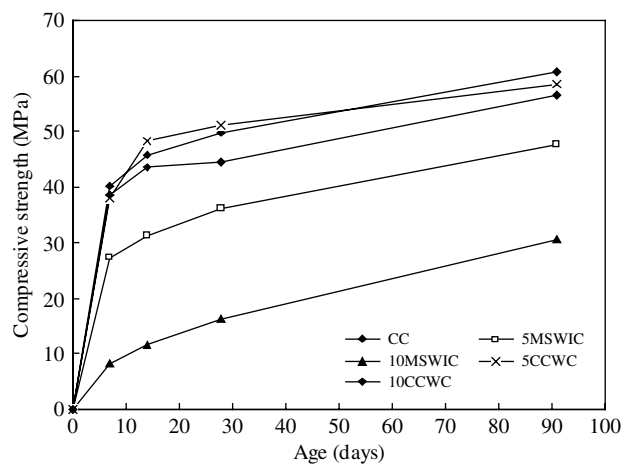


Fig. 8.9 Compressive strength development of mortars made from various cements (Krammart and Tangtermsirikul, 2004)

Table 8.15 Effect of amount of fly ash slag on the compressive strength (Lin et al., 2004b)

Replacement ratio (wt %)		Compressive strength (MPa)					
Cement	Fly ash slag	1 day	3 days	7 days	28 days	60 days	90 days
Type I							
100	0	50	67	81	95	97	98
90	10	45	59	70	91	96	100
80	20	30	44	60	80	92	95
60	40	21	34	47	59	67	79
Type III							
100	0	59	67	68	73	73	75
90	10	53	59	63	73	76	81
80	20	44	54	59	69	75	83
60	40	34	37	42	55	58	67
Type V							
100	0	56	75	87	96	99	102
90	10	49	70	81	93	97	104
80	20	40	55	63	86	93	98
60	40	25	37	44	78	81	85

three types of Portland cements used were Type I (ASTM Type I ordinary Portland cement), Type III (high early strength Portland cement) and Type V (sulfate resistant Portland cement) having pozzolanic activity index of 103, 102 and 104, respectively. Table 8.15 shows the compressive strength of the Type I, Type III and Type V cement pastes incorporating MSWI fly ash slag. They concluded that: (i) for plain Type I, Type III and Type V Portland cement, the 1 day compressive strength development increased in the following sequence Type III > Type V > Type I. The sequence corresponded to that of the Type III Portland cement with greater Blaine fineness. However, the compressive strength development of plain Type I, Type III and Type V cement pastes increased in the following sequence: Type V > Type III > Type I after 3–90 days; and (ii) compressive strength of the slag-blended cement pastes in the early stages (1–28 days) was reduced when the cement replacement levels increased. However, at a later stage, the compressive strength of the slag-blended cement paste samples incorporating 10 and 20% of slag, varied from 95 to 110% of that developed by the plain cement pastes. On the other hand, the SBC samples that incorporated 40% of slag exhibited a decline in the compressive strength. The results indicated that the SBC pastes had a slower compressive strength development in the early stages, but the strength obviously increased at later ages.

8.3.5 Pore Size Distribution

Lin et al. (2003b) studied the pore size distribution of mortars made with cement containing MSWI fly ash slag. The major components in the ash were SiO₂(35.8%), CaO (14.7%), and Al₂O₃(9.8%). The proportion of cement substitution was 0, 10, 20, and 40%. The W/C ratio was 0.38 while the cement to sand ratio was

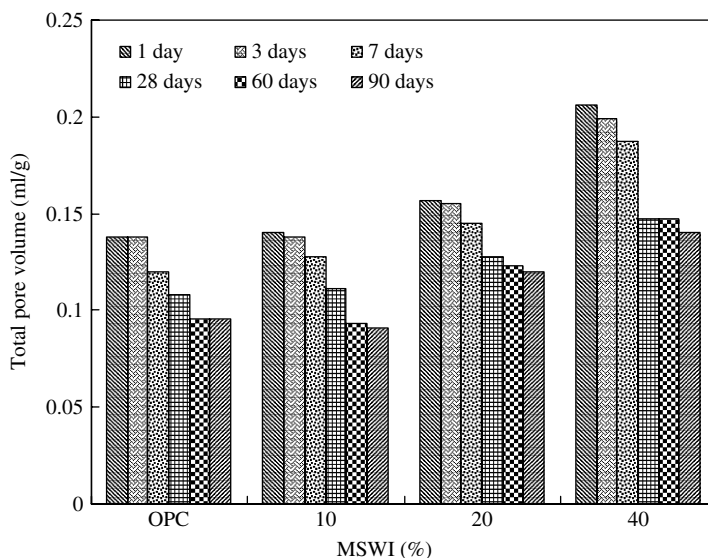


Fig. 8.10 Pore size distribution (total pore) in mortar with MSWI fly ash slag substitutions (Lin et al., 2003b)

1:2.75. Figure 8.10 shows the total pore volume of cement mortars. They concluded that: (i) addition of MSWI fly ash slag increased the total porosity of the mortar; (ii) porosity decreased in all the samples with the hydration period, due to the gradual filling of large pores by the hydration products of the cementitious materials; (iii) at the age of 7 days, the porosity of cement mortar mixed with fly ash was found to be slightly higher than that of OPC, and the pore size distribution had shifted toward a larger pore size (>10 nm). This was probably due to voids around the fly ash particles, which caused the number of pores greater than 10 nm to increase; and (iii) at 28 days, porosity and pore size distribution in MSWI cement was greater than in the OPC. However, at 60 days and later, for mortar with 10% substitution, the interspaces were gradually filled up due to the formation of more pozzolanic reaction products, and the porosity approached the values of the OPC control samples. The tendency was more pronounced for an increased blend ratio, due to pores being filled with C-S-H (Tobermorite) formed by the pozzolanic reaction. This resulting densification, which enhanced the later strength, was caused by the shifting of the pore size distribution to a smaller diameter range.

Lin et al. (2004a) investigated the pore size distribution of slag blended cement (SBC) pastes. Synthetic slag samples were prepared by melting CaO-modified and Al_2O_3 -modified municipal solid waste incinerator (MSWI) fly ash. MSWI fly ash was mixed with 5% CaO and 5% Al_2O_3 (by weight), respectively, resulting in two fly ash mixtures. These mixtures were then melted at 1400°C for 30 min to produce two types of slag with different contents, designated at C-slag and A-slag. SBC

was prepared by mixing cement and modified slag. Both C-slag and A-slag were used to partially replace the cement, at ratios of 10, 20, and 40% (w/w) respectively. Pore size distribution was measured by MIP. They concluded that: (i) SBC pastes made with C-slag developed finer pores with the increase in curing age and blend ratio. The percentage of fine pores by volume (< 10 nm), in C1, C2 and C3 pastes at 90 days, was 51, 56, and 73%, respectively, for corresponding blend ratios of 10, 20, and 40%. C-slag blended cement pastes had increased numbers of fine pores with increased curing times, showing that the C-slag enhanced the pozzolanic reactions by filling the pores; and (ii) fine pores in the A1, A2 and A3 pastes had different patterns. The percentage of the volume of the fine pores (< 10 nm) increased for the A1, A2, and A3 pastes as the curing time and the blend ratio increased.

Lin et al. (2004b) reported the porosity distribution in various types of cements incorporating municipal solid waste incinerator fly ash slag. Major composition of the MSWI fly ash slag was of SiO_2 (38.9%), CaO (27.2%), and Al_2O_3 (23.3%). The three types of Portland cements used were Type I (ASTM Type I ordinary Portland cement), Type III (high early strength Portland cement) and Type V (sulfate resistant Portland cement) having pozzolanic activity index of 103, 102 and 104, respectively. They concluded that: (i) pore size distribution varies with slag replacement levels and curing time. In general, for all the three types of ordinary Portland cement and the fly ash-slag blended cement (SBC) pastes, the pore volume in general decreased with curing time. For plain Type I, Type III and Type V cement pastes, dramatic variations occurred from 1 to 28 days, but little variation was observed from 60 to 90 days, implying that active hydration reactions took place during the early ages; and (ii) for SBC pastes incorporating slag at different replacement levels, for a larger blend ratio ($> 20\%$), the difference in the pore volume from 1 to 28 days was insignificant. The pore volume in the SBC paste samples shifted to the gel pores at later ages. The tendency was for this to be more pronounced for an increased blend ratio, due to the pores being filled with C–S–H gels that formed via pozzolanic reactions. This resulting densification and enhanced later strength was caused by the shifting of the gel pores.

8.3.6 Shrinkage/Expansion Characteristics

Rémond et al. (2002) investigated the effect of 0, 10, and 20 replacement of cement with MSWI fly ash on shrinkage and mass loss of mortars. Specimens of size $20 \times 40 \times 160$ mm, $40 \times 40 \times 160$ mm were used for measuring the shrinkage and mass loss respectively. These tests were carried out on specimens of size up to the age of 35 days. Results are presented in Figs. 8.11 and 8.12. They concluded that: (i) shrinkages of the two mortars containing ash (M10 and M20) were almost same. Up to 7 days, shrinkage of the two mortars containing ash is approximately twice of that of the control mortar M0. Beyond that, their respective evolution is comparable;

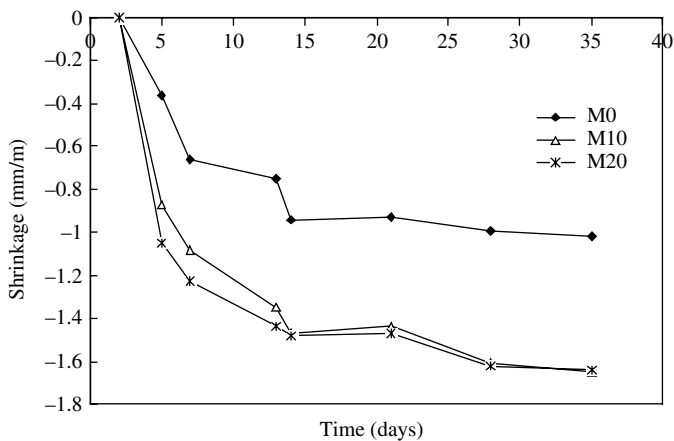


Fig. 8.11 Size variation of the M0, M10, and M20 mortars (Rémond et al., 2002)

and (ii) mass variations of M10 and M20 mortars are lower than those of the control mortar M0.

The lower shrinkage values of M0 mortar cannot be explained by drying shrinkage. Indeed, mortars containing ash lose less water than the M0 mortar (Fig. 8.12). The increase in shrinkage of these two mortars would therefore seem to be due to an increase in autogenous shrinkage. The lower water loss of these mortars in relation to the M0 mortar can be explained by the immobilization of water due to hydration product formation. Thus, the high chloride and sulfate content of the MSWI fly ash may result in the formation of high quantities of ettringite and chloroaluminates chloroaluminates (hydrates which mobilize a large number of water molecules). The

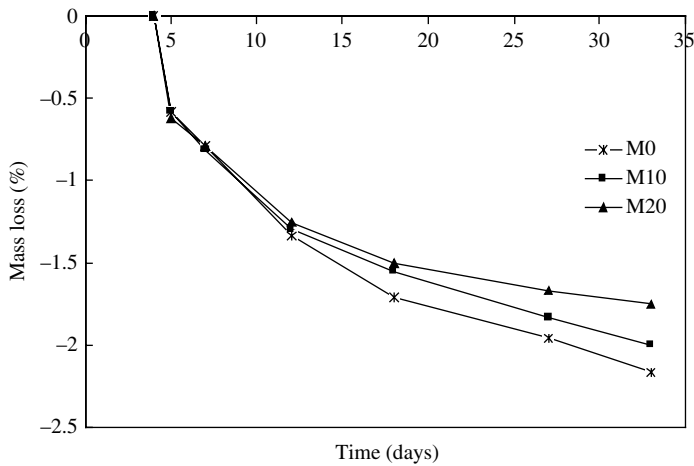


Fig. 8.12 Mass variation of the M0, M10, and M20 mortars (Rémond et al., 2002)

early formation of these two hydrates could explain the high shrinkage of mortars containing fly ash observed in early stages.

Krammart and Tangtermsirikul (2004) measured the sulfate expansion of mortar made by replacing cement raw materials with 5 and 10% of municipal solid waste incinerator bottom ash (MSWI) and calcium carbide waste (CCW). Sulfate expansion of mortar bar specimens were conducted as per ASTM C 1012. Sodium sulfate was used to prepare the test solution. The concentration of SO_4^{2-} in the test solution was 3.38%. All mortar bar specimens were prepared with w/c of 0.53 and initially cured in water for 28 days and then exposed to the prepared solution in plastic tanks for 392 days. They concluded that: (i) expansion was almost similar in all cement mortar specimens up to about 60 days. After that, however, the expansion was observed to be higher for CC cement mortar specimens than for the other cements; and (ii) the expansions of MSWI and CCW cements were lower than that of the control cement. MSWI cements showed the lowest expansion.

8.4 Properties of Concrete Containing MSW Ash

Berg and Neal (1998) studied the possibility of using municipal solid waste bottom ash (MSWBA) from a refuse-derived fuel facility as potential Portland cement concrete ingredient. Portland cement-related ASTM methods and other analytical techniques such as X-ray diffraction were used. They concluded that: (i) MSWBA sample was found to be a marginal concrete aggregate. The sample met most ASTM C331 standards for size gradation, but high angularity and brittle nature of aggregate could significantly affect the workability; (ii) sulfate and chloride concentrations were also high enough to create potential sulfate attack and reinforcing steel corrosion problems; and (iii) suggested that iron removal and aggregate processes such as size control offer cost-effective methods to improve MSWBA for use as an aggregate.

Mangialardi (2001) studied the sintering process of municipal solid waste (MSW) fly ash in order to manufacture sintered products for reuse as concrete aggregates. Four types of fly ash resulting from different Italian MSW incineration plants were studied. A modification of the chemical composition of MSW fly ash — through a preliminary four-stage washing treatment of this material with water—was attempted to improve the chemical and mechanical characteristics of sintered products. The sintering treatment of untreated or washed fly ash was performed on cylindrical compact specimens (15 mm in diameter and 20 mm in height) at different compact pressures, sintering temperatures and times. He concluded that: (i) sintering process of untreated MSW fly ashes proved to be ineffective for manufacturing sintered products for reuse as a construction material, because of the adverse chemical characteristics of these fly ashes in terms of sulfate, chloride, and vitrifying oxide contents; (ii) a preliminary washing treatment of MSW fly ash with water greatly improved the chemical and mechanical characteristics of sintered products and, for all the types of fly ash tested, the sintered products sat-

ified the Italian requirements for normal weight aggregates for use in concretes having a specified strength not greater than 12 and 15 N/mm², when measured on cylindrical and cubic specimens, respectively; and (iii) a compact pressure of 28 N/mm², a sintering temperature of 1140°C, and a sintering time of 60 min were the best operating conditions for manufacturing sintered products of washed MSW fly ash.

8.4.1 Compressive Strength

Pera et al. (1996) examined the use of municipal solid waste incinerator (MSWI) bottom ash as alternative aggregate for concrete having a characteristic 28-day compressive strength of 25 MPa. The aggregates passing the 20 mm sieve and retained on the 4 mm sieve having density of 2.21 and water absorption capacity for 2.36%. Three series concrete mixtures were made. First was control mixture with 290 kg/m³ cement, 930 kg/m³ natural sand, 970 kg/m³ natural gravel, and 190 kg/m³ water. In second series (C1), concrete was made using natural sand, 50% natural gravel (in volume) and 50% treated bottom ash (in volume). In third series (C2) natural gravel was entirely replaced by treated bottom ash. Compressive strength testes were carried out up to the age of 90 days and results are given in Table 8.16. They concluded that concrete with 50% bottom ash satisfy the requirements to be used as a building concrete presenting a characteristic 28-day strength of 25 MPa. When the gravel is entirely replaced by bottom ash the strength decreases due to the softness of aggregates.

Collivignarelli and Sorlini (2002) assessed the feasibility of concrete production using stabilized MSW (municipal solid waste) incineration fly ashes in addition to natural aggregates. The fly ashes were washed, milled, and then stabilized by a cement-lime process and were reused as a “recycled aggregate.” Natural aggregate was partially substituted by 200 or 400 kg of stabilized waste (respectively about 11 and 22% of total natural aggregate), and a slump of 200 mm was maintained. They concluded that: (i) MSWI fly ashes showed good chemical and physical quality for the production of concrete mixtures, and they could be reused as construction materials and represent an interesting alternative to final landfill disposal; and (ii) although concrete mechanical characteristics were worsened by waste addition, the minimum compressive resistance of 15 MPa, required for concrete structural utilization, was attained by most of the concrete mixtures after 28 days of curing.

Table 8.16 Compressive strength of concrete made with MSWI bottom ash (Pera et al., 1996)

Compressive strength (MPa)	Type of Concrete		
	Control	C1	C2
7 days	28.0 ± 2.4	20.8 ± 1.7	17.0 ± 1.7
28 days	32.9 ± 2.4	29.9 ± 1.3	22.3 ± 2.0
90 days	41.80 ± 2.1	34.6 ± 0.8	28.4 ± 1.0

Bertolini et al. (2004) researched the effect of replacing part of Portland cement with MSWI fly ash and bottom ash on the compressive strength of concrete. Control concrete was made with 440 kg/m^3 of Portland, water/cement ratio of 0.50 and 1700 kg/m^3 of crushed limestone aggregate. In control concrete, 30% cement was replaced with washed MSWI fly ash, dry ground MSWI bottom ash, and wet ground MSWI bottom ash. Two concrete mixtures with replacement of 30% by mass of cement with traditional coal FA and ground limestone were also cast. Tests were conducted up to the age of 180 days. They concluded that: (i) 28-day compressive strength of concrete with 30% wet ground MSWI bottom ash was 64.5 MPa whereas it was 51.7 MPa and 20.1 MPa for 30% washed MSWI fly ash and 30% dry ground MSWI bottom ash, respectively; (ii) 28-day compressive strength of concrete with 30% wet ground MSWI bottom ash was similar to that of the concrete with 100% Portland cement (63.5 MPa). It was even higher than that of the concrete with coal FA (53.4 MPa). This showed that wet ground MSWI bottom ash has hydraulic properties; and (iii) at longer curing (180 days), the concrete with wet ground MSWI bottom ash achieved a strength (90 MPa) fairly higher than that of the concrete made with only Portland cement or with the use of FA (75 MPa).

8.4.2 Chloride Penetration/Resistance

Bertolini et al. (2004) investigated the effect of partial replacement of Portland cement with MSWI fly ash and bottom ash on the chloride penetration of concrete. Control concrete was made with 440 kg/m^3 of Portland, water/cement ratio of 0.50 and 1700 kg/m^3 of crushed limestone aggregate. In control concrete, 30% cement was replaced with washed MSWI fly ash, dry ground MSWI bottom ash, and wet ground MSWI bottom ash. Two concrete mixtures with replacement of 30% by mass of cement with traditional coal FA and ground limestone were also cast. To study the resistance to chloride penetration, 150-mm cubes were exposed to drying–wetting cycles with a 3.5% by mass sodium chloride solution. Only one surface of the cube was exposed to the chloride solution, because the other faces of the cube were covered by an epoxy coating, and chloride profiles were analyzed after different times of exposure. Cores, 30 mm in diameter, were taken from the exposed surface and they were cut at depth increments of 5 or 10 mm. The chloride content was determined by potentiometric titration after grinding and digestion in nitric acid, and it was expressed as percentage of the dry mass of the sample. Figures 8.13 and 8.14 show chloride profiles measured on cube specimens after 6 months of exposure to chloride wetting and drying cycles. Based on the results, they concluded that: (i) concrete with wet ground MSWI bottom ash, together with the concrete with the addition of PFA, showed the lowest penetration of chloride ions. This behavior can be related to the well-known pore refinement and decrease in permeability produced by pozzolanic reaction; (ii) bottom ash from MSWI treated by a wet grinding process can be advantageously used as an additional ingredient in the production of cement mixes with improved resistance to aggressive agents and water penetration;

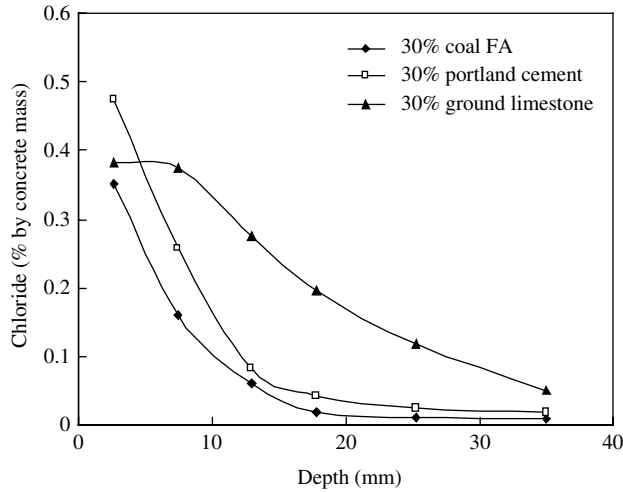


Fig. 8.13 Chloride profiles after 6 months of exposure to chloride cycles (1-day immersion in 3.5% NaCl solution and 2-day drying) of reference concretes (Bertolini et al., 2004)

and (iii) MSWI bottom ash is more attractive as a potential mineral addition for concrete than MSWI FA. MSWI FA did not induce such remarkable improvement of the concrete properties and, furthermore, it required onerous washing treatments to reduce the content of chlorides and hazardous species (with the consequent necessity of proper treatment and disposal of liquid residues).

Aubert et al. (2004) evaluated the influence of the treated MSWI fly ash (TFA) on the gas permeability and porosity of concrete. (MSWI) fly ashes were treated by

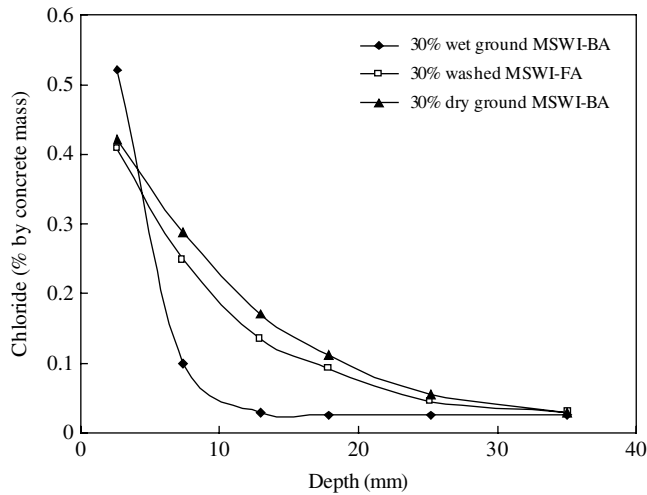


Fig. 8.14 Chloride profiles after 6 months of exposure to chloride cycles (1-day immersion in 3.5% NaCl solution and 2-day drying) concretes with MSWI ashes (Bertolini et al., 2004)

Table 8.17 Physical properties of Concrete (Aubert et al., 2004)

Mixture	Slump (cm)	Gas permeability (10^{-16} m^2)	Water porosity (%)	Total porosity (%)
R	12	3.3–4.6	14.2–15.1	14.2–16.7
S12	6.5	1.9–5.1	12.7–14.2	14.5–16.2
A12	6.5	1.6–4.6	13.4–16.9	15.9–17.2
S50	5	35.8–68.0	18.5–20.7	21.5–25.4
A50	7.5	17.9–35.6	18.1–22.5	22.7–25.0

physicochemical treatment, known as Revasol process (This process allows reducing the soluble fraction, fixing heavy metals and eliminating dioxins). Five mixtures were made; reference concrete (R); two compositions A12 and A50 in which cement was replaced by TFA in the proportions of 12.5% and 50%, respectively; two compositions S12 and S50 in which 12.5% and 50% of cement were replaced by sand. Cement and sand content in control concrete was 300 kg/m³ and 724 kg/m³, respectively. The permeability was measured with a Cembureau permeameter at the age of 28 days. The pressure head was set at 1 bar and the measurements were made when the steady state had been reached. The porosity of the concrete was obtained from the difference between the mass of the same sample dry and saturated with water. The total volume of the sample was determined by hydrostatic weighing, and it was thus possible to calculate the porosity accessible to water. The total porosity of the concrete was calculated starting from the bulk and absolute densities measured on concrete. Table 8.17 presents the results of gas permeability and porosity. The physical properties of hardened concrete (gas permeability, porosity accessible to water and total porosity) control the transport properties of concrete and so its durability. These properties are not significantly modified by the introduction of TFA.

8.4.3 Shrinkage

Pera et al. (1996) determined shrinkage after drying-wetting cycles of concrete made with municipal solid waste incinerator (MSWI) bottom ash as alternative aggregate. The MSWI had density of 2.21 and water absorption capacity for 2.36%. Three series concrete mixtures were made. First was control mixture with 290 kg/m³ cement, 930 kg/m³ natural sand, 970 kg/m³ natural gravel, and 190 kg/m³ water. In second series (C1), concrete was made using natural sand, 50% natural gravel (in volume) and 50% treated bottom ash (in volume). In third series (C2) natural gravel was entirely replaced by treated bottom ash. They were subjected to drying-wetting cycles: 14 days at 20°C, 50% R.H., followed by 14 days in water at 20°C. During the drying period, control and C1 concretes reached a maximum shrinkage of 330 µm/m, whereas it was 250 µm/m for concrete C2. After the immersion period, these values were 100 µm/m for the control and C1 concretes, and 50 µm/m for C2. These results show that bottom ash had no negative effect on the durability of concrete, when all the reactions due to metallic aluminum were avoided.

8.5 Leachate Analysis

Collivignarelli and Sorlini (2002) carried out leaching tests for concrete samples made with stabilized MSW (municipal solid waste) incineration fly ashes in addition to natural aggregates. The fly ashes were washed, milled, and then stabilized by a cement-lime process and were reused as a “recycled aggregate.” Leachate tests were conducted for concrete samples after 28 days of curing, and results showed that metal concentrations were lower than the maximum limits, with the exception for mercury.

Lin et al. (2003b) conducted leaching concentrations test toxic characteristics leaching procedure (TCLP) of MSWI fly ash and slag and that of the mortars made with cement containing MSWI fly ash slag. The major components in the MSWI fly ash were SiO_2 (35.8%), CaO (14.7%), and Al_2O_3 (9.8%) whereas the major components in the MSWI ash were SiO_2 (35.8%), CaO (14.7%), and Al_2O_3 (9.8%). The proportion of cement substitution was 0, 10, 20, and 40%. The W/C ratio was 0.38 while the cement to sand ratio was 1:2.75. Table 8.18 shows the leaching concentrations of heavy metals in MSWI fly ash. There was high leachability of the targeted metals, Zn, Cr, and Cd. In particular, the leaching concentration of Cd reached 1.8 mg/l, a hazardous level.

Table 8.19 shows the results of TCLP analysis. As can be seen, the TCLP concentrations that leached from the mortar samples with a 10–40% cement substitution by MSWI fly ash slag were all lower than the regulatory standard for hazardous substances. They also met the regulatory effluent standard.

Aubert et al. (2004) studied the leaching behavior of crushed and monolithic concrete made with treated MSWI fly ash (TFA). MSWI fly ashes were treated by physicochemical treatment, known as Revasol process (This process allows reducing the soluble fraction, fixing heavy metals and eliminating dioxins). Five mixtures were made; reference concrete (R); two compositions A12 and A50 in which cement was replaced by TFA in the proportions of 12.5% and 50%, respectively; two compositions S12 and S50 in which 12.5% and 50% of cement were replaced by sand. Cement and sand content in control concrete was 300 kg/m³ and 724 kg/m³, respectively. Table 8.20 shows the total concentrations of the most harmful elements leached. These results are compared with threshold values allowed for leachates from MSWI bottom ashes to be reused in road works in France. It can be seen that: (i) except for Cr and As, the results obtained on the TFA containing concrete were

Table 8.18 TCLP leaching concentrations of heavy metals in MSWI fly ash and slag (Lin et al., 2003b)

Heavy metal (mg/l)	MSWI fly ash	Slag	Regulatory limit
Cd	1.8±0.03	–	1.0
Cr	4.3±0.13	0.27±0.01	5.0
Pb	0.7±0.02	0.36±0.02	5.0
Cu	0.6±0.01	3.21±0.05	–
Zn	162±0.3	9.10.8±0.33	–

Table 8.19 Heavy metal concentrations for mortar with MSWI fly ash slag substitution (Lin et al., 2003b)

Cement substitution	Heavy metal concentration (mg/l)				
	Pb	Cr	Cd	Cu	Zn
0	0.34	0.03	–	0.04	0.12
10	0.31	0.33	–	0.05	0.13
20	0.35	0.03	–	0.05	0.15
40	0.36	0.04	–	0.05	0.14
Regulatory standard	5.0	5.0	1.0	–	–

very similar to those of the reference; (ii) only chromium exceeded the legal thresholds in the case of the crushed concrete; all concentrations were satisfactory for the monolithic concrete; (iii) the concentrations of heavy metals obtained on monolithic concrete were always much lower than those obtained on crushed concrete except in the case of arsenic; and (iv) leaching of arsenic was influenced by the pH of the solution: the lower the pH (10.6–11.5 in monolithic concrete versus 11.8–12 in crushed one), the higher the amount of arsenic leached.

Aubert et al. (2006) examined the leaching behavior of MSWI fly ashes subjected to two types of stabilization processes. The first one, the conventional process, called “A”, was based on the washing, phosphation and calcination of the ash, and a modified process, called “B”, intended to eliminate metallic aluminum and sulfate contained in the ash. Details of the two processes have been described in physical properties of the fly ashes reported by Aubert et al., (2006). The results of the leaching tests are given in Table 8.21. Based on the results obtained and comparison with European standards, they concluded that: (i) process TFA-A did not efficiently stabilize chromium, and its efficiency was poor for antimony and cadmium. In the case of chromium, the calcinations during the process led to the oxidation of some Cr (III) to Cr (VI) which is the soluble form of chromium. This could explain why the release of chromium was so high. Some experiments are in progress to try to reduce the chromium during the calcinations step of the process; (ii) the main differences in the behavior of the two ashes to leaching was the release of chromium, selenium and antimony (higher for TFA-B) and the release

Table 8.20 Comparison of total concentration leached for crushed and monolithic concrete (Aubert et al., 2004)

Elements	Crushed concrete			Monolithic concrete			Threshold for bottom ashes
	R	A12	A50	R	A12	A50	
Cr (µg/kg)	435	809	2304	69	90	182	1500
Zn (µg/kg)	272	393	373	251	161	289	
Pb (µg/kg)	15	35	47	3	5	10	10000
Cd (µg/kg)	11	15.6	3.3	0.7	0.4	0.5	1000
As (µg/kg)	< 1.3	2.5	9.3	2.8	2.8	22	2000
FS (µg/kg)	30.6	30.8	14.0	3.5	2.7	2.2	50
SO ₄ (µg/kg)	< 300	< 348	776	< 300	< 300	512	1000

Table 8.21 Concentrations of leached elements (Aubert et al., 2006)

Elements	Concentrations of leached elements		European landfill directive		
	TFA-A	TFA-B	Inert	Non-hazardous	Hazardous
As (mg/kg)	0.169	0.032	0.5	2	25
Ba (mg/kg)	1.741	0.113	20	100	300
Cd (mg/kg)	0.203	0.03	0.04	1	5
Cr (mg/kg)	1.112	33.384	0.5	10	70
Cu (mg/kg)	0.012	0.007	2	50	100
Mo (mg/kg)	0.269	0.200	0.5	10	30
Ni (mg/kg)	0.553	< 0.0001	0.4	10	40
Pb (mg/kg)	0.004	0.008	0.5	10	50
Sb (mg/kg)	0.091	2.390	0.06	0.7	5
Se (mg/kg)	0.098	0.670	0.1	0.5	7
Zn (mg/kg)	7.628	0.057	4	50	200
P (mg/kg)	9.837	< 0.100	—	—	—
SF (g/kg)	11.0	5.4	4	60	100
SO ₄ (g/kg)	7.578	0.826	1	20	50
pH	6.6	10.3	—	> 6	—

of zinc, nickel and cadmium (higher for TFA-A). Na_2CO_3 is often used to extract the chromium (with or without NaOH) (Potgieter et al., 2003). So, the addition of Na_2CO_3 during the washing step of process B could transform the insoluble chromium in a soluble form, which could explain the high mobility of chromium in TFA-B; and (iii) TFA-A would have to be sent to landfills for non-hazardous waste because of the significant release of zinc, cadmium and antimony, which are above the limit values for waste acceptable at landfills for inert waste. The values of nickel and selenium are slightly higher than those recommended by the directive. TFA-B would have to be disposed of in landfills for hazardous waste because of its significant release of chromium, selenium and antimony.

8.6 Use of MSW Bottom Ash in Road Base

Forteza et al. (2004) evaluated the physical and chemical composition of MSW bottom ash towards its utilization as pavement element. They studied physical (moisture content, apparent and bulk densities, crystallinity, etc.) and engineering properties (particle size distribution, abrasion and impact resistance, etc.), full chemical characterization of the bottom ash and the study of leaching as a function of aging time. The results obtained indicated that the metal content of both the raw bottom ash and its leachates fulfilled the environmental regulations provided that the bottom ash is stored for at least one month. Engineering properties of the bottom ash are close to those of natural aggregates and, thus, road-construction use of these residues seems to be feasible.

References

- Aubert JE, Husson B, Sarramone N (2006) Utilization of municipal solid waste incineration (MSWI) fly ash in blended cement, Part I: Processing and characterization of MSWI fly ash. *Journal of Hazardous Materials B136*: 624–631.
- Aubert JE, Husson B, Vaquier A (2004) Use of municipal solid waste incineration fly ash in concrete. *Cement and Concrete Research* 34: 957–963.
- Barbieri L, Bonamartini AC, Lancellotti I (2000) Alkaline and alkaline-earth silicate glasses and glass-ceramics from municipal and industrial wastes. *Journal of the European Ceramic Society* 20: 2477–2483.
- Bentur B (1980) Effect of curing temperature on the pore structure of tricalcium silicate pastes. *Journal of Colloid and Interfaces Science* 74 (2) 26–37.
- Berg ER, Neal JA (1998) Municipal solid waste bottom ash as Portland cement concrete ingredient. *Journal of Materials in Civil Engineering* 10 (3): 168–173.
- Bertolini L, Carsana M, Cassago D, Curzio AQ, Collepari M (2004) MSWI ashes as mineral additions in concrete. *Cement and Concrete Research* 34: 1899–1906.
- Bethanis S, Cheeseman CR, Sollars CJ (2002) Properties and microstructure of sintered incinerator bottom ash. *Ceramics International* 28: 881–886.
- Beretka J, Vito B de, Santoro L, Sherman N, Valenti GL (1993) Utilization of industrial wastes and by-products for the synthesis of special cements. *Resources, Conservation and Recycling* 9 (3): 179–190.
- Boccaccini AR, Kopf M, Stumpfe W (1995) Glass-ceramics from filter dusts from waste incinerators. *Ceramics International* 21: 231–235.
- Boccaccini AR, Petitmermet M, Wintermantel E (1997) Glass-ceramics from municipal incinerator fly ash. *Ceramic Bulletin* 76 (11): 75–78.
- Chesner WH, Collins RJ, Fung T (1986) The characterization of incinerator residue in the city of New York. Proceedings of the 1986 National Waste Processing Conference. ASME Solid Waste Processing Division, USA
- Clozel-Leloup B, Bodéan, F, Piantone P (1999). Bottom ash from municipal solid waste incineration. Mineralogy and distribution of metals. *Proc. STAB & ENV* 99 46.
- Collivignarelli C, Sorlini S (2002) Reuse of municipal solid wastes incineration fly ashes in concrete mixtures. *Waste Management* 22: 909–912.
- Eighmy TT, Gress DL (1996) The Iaconia, New Hampshire bottom ash paving project: Vol. 3, physical performance testing report. Environmental Research Group, University of New Hampshire, USA.
- Ferreira C, Ribeiro A, Ottosen L (2003) Possible applications for municipal solid waste ash. *Journal of Hazardous Materials B96*: 201–216.
- Filipponi P, Poletti A, Pomi R, Sirini P (2003) Physical and mechanical properties of cement-based products containing incineration bottom ash. *Waste Management* 23: 145–156.
- Forteza R, Far M, Seguí C, Cerdá V (2004) Characterization of bottom ash in municipal solid waste incinerators for its use in road base. *Waste Management* 24: 899–909.
- GEC (1996) Waste treatment technology in Japan, Committee for Studying Transfer of Environmental Technology, Global Environment Centre Foundation.
- Goh CC, Show KY, Cheong HK (2003) Municipal solid waste fly ash as a blended cement material. *Journal of Materials in Civil Engineering*. 15 (6): 513–523.
- Hamernik JD, Frantz GC (1991) Physical and chemical properties of municipal solid waste fly ash. *ACI Materials Journal* 88 (3): 294–300.
- Jazairi BE, Illston JM (1980) The hydration of cement paste using the semi-isothermal method of derivative thermogravimetry. *Cement and Concrete Research* 10: 361–366.
- Koppelman LE, Tanenbaum EG (1993) The potential for beneficial use of waste-to-energy facility ash: Vol. 4, engineering properties. New York State Energy Research and Development Authority, USA.

- Krammart P, Tangtermsirikul S (2004) Properties of cement made by partially replacing cement raw materials with municipal solid waste ashes and calcium carbide waste. *Construction and Building Materials* 18: 579–583.
- Lin CK, Chen JN, Lin CC (1997) An NMR, XRD and EDS study of solidification/stabilization of chromium with Portland cement and C3S. *Journal of Hazardous Materials* 56: 21–34.
- Lin KL, Wang KS, Tzeng BY, Lin CY (2003b) The reuse of municipal solid waste incinerator fly ash slag as a cement substitute. *Resources, Conservation and Recycling* 39: 315–324.
- Lin KL, Wang KS, Lee TY, Tzeng BY (2003a) The hydration characteristics of MSWI fly ash slag present in C₃S. *Cement and Concrete Research* 33: 957–964.
- Lin KL, Wang KS, Ten BY, Lin CY (2004a) The hydration characteristics and utilization of slag obtained by the vitrification of MSWI fly ash. *Waste Management* 24: 199–205.
- Lin KL, Wang KS, Lin CY, Lin CH (2004b) The hydration properties of pastes containing municipal solid waste incinerator fly ash slag. *Journal of Hazardous Materials B109*: 173–181.
- Mangialardi T (2001) Sintering of MSW fly ash for reuses as a concrete aggregate. *Journal of Hazardous Materials B87*: 225–239.
- Mangialardi T, Paolini AE, Poletti A, Sirini P (1999) Optimization of the solidification/stabilization process of MSW fly ash in cementitious matrices. *Journal of Hazardous Materials* 70 (1–2): 53–70.
- Müller U, Rübner K (2006) The microstructure of concrete made with municipal waste incinerator bottom ash as an aggregate component. *Cement and Concrete Research* 36: 1434–1443.
- Park YY, Hu CG (1996) A study on behavior of heavy metals during waste incineration. *Journal of Korean Environmental Science Society* 5 (6): 785–799.
- Pera J, Coutaz L, Ambroise J, Chababbet M (1996) Use of Incinerator bottom ash in concrete. *Cement and Concrete Research* 27 (1): 1–5.
- Potgieter SS, Panichev N, Potgieter JH, Panicheva S (2003) Determination of hexavalent chromium in South African cements and cement-related materials with electrothermal atomic absorption spectrometry. *Cement and Concrete Research* 33: 1589–1593.
- Rebeiz KS, Mielich KL (1995) Construction use of municipal-solid-waste ash. *Journal of Energy Engineering* 121 (1): 2–13.
- Rémond S, Pimienta P, Bentz DP (2002) Effects of the incorporation of municipal solid waste incineration fly ash in cement pastes and mortars 1. experimental study *Cement and Concrete Research* 32: 303–311.
- Saikia N, Kato S, Kojima T (2007) Production of cement clinkers from municipal solid waste incineration (MSWI) fly ash. *Waste Management*. 27 (9): 1178–1189.
- Shih P-H, Chang J-E, Chiang L-C (2003) Replacement of raw mix in cement production by municipal solid waste incineration ash. *Cement and Concrete Research* 33: 1831–1836.
- Song G-u, Kim K-h, Seo Y-C, Kim S-C (2004) Characteristics of ashes from different locations at the MSW incinerator equipped with various air pollution control devices. *Waste Management* 24: 99–106.
- Taylor HFW (1997) *Cement Chemistry*. Thomas Telford, London.
- Tay JH, Goh ATC (1991) Engineering properties of incinerator residues. *Journal of Environmental Engineering* 117 (2): 224–235.
- Wang KS, Lin KL, Lee TY, Tzeng BY (2004) The hydration characteristics when C₂S is present in MSWI fly ash slag. *Cement and Concrete Composites* 26: 323–330.
- Zevenbergen C, Comans RNJ (1994) “Zevenbergen C, Comans RNJ (1994)”. *Geochemical factors controlling the mobilization of major elements during weathering of MSWI bottom ash. Environmental Aspects of Construction with Waste Materials*. Elsevier Science, BV, Amsterdam.

Chapter 9

Wood Ash

Introduction

Wood ash (WA) is the residue generated due to combustion of wood and wood products (chips, saw dust, bark, etc.). It is the inorganic and organic residue remaining after the combustion of wood or unbleached wood fiber. The physical and chemical properties of wood ash vary significantly depending on many factors. The physical and chemical properties of wood ash, which determine its beneficial uses, are dependent upon the species of the wood and the combustion methods that include combustion temperature, efficiency of the boiler, and supplementary fuels used. Ash content yield decreases with increasing combustion temperature (Etiegni and Campbell, 1991).

Hardwoods usually produce more ash than softwoods and the bark and leaves generally produce more ash than the inner woody parts of the tree. On the average, the burning of wood results in about 6–10% ashes. When ash is produced in industrial combustion systems, the temperature of combustion, cleanliness of the fuel wood, the collection location, and the process can also have profound effects on the nature of the ash material. Therefore, wood ash composition can be highly variable depending on geographical location and industrial processes. This makes testing the ash extremely important.

Typically, wood ash contains carbon in the range of 5–30% (Campbell, 1990). The major elements of wood ash include calcium (7–33%), potassium (3–4%), magnesium (1–2%), manganese (0.3–1.3%), phosphorus (0.3–1.4%), and sodium (0.2–0.5%). Density of wood ash decreases with increasing carbon content. The chemical and physical properties depend upon the type of wood, combustion temperature, etc. (Campbell, 1990; Mishra et al., 1993). An elemental metal and other analysis for various types of wood are shown in Table 9.1.

Typical wood burnt for fuel at pulp and paper mills and wood products industries may consist of saw dust, wood chips, bark, and saw mill scraps, hard chips rejected from pulping, excess screenings such as sheaves and primary residuals without mixed secondary residuals. Physical and chemical properties of wood ash are important in determining their beneficial uses. These properties are influenced by species of tree, tree growing regions and conditions, method and manner of combustion

Table 9.1 Elemental metals and other analyses for ash from wood (mg/kg)

Elemental metal	Regulatory limits (U.S.EPA)	Normal wood fuel	Particle/plywood	Creosote treated	Pentachlorophenol treated	Construction/ demolition wood	CCA treated
Aluminum	N/A	4000–4500	4400–4800	3600–5000	3600–4200	4900–5800	3900–4500
Arsenic	41/75	42–53	22.5–26.9	51–64	24.3–27.7	78–98	8570–9390
Barium	N/A	220–300	280–400	200–280	220–270	480–590	220–280
Cadmium	39/85	5.5–6.1	7.3–7.9	5.1–5.7	8.7–10.1	7.1–8.1	10.7–11.7
Chromium	1200/3000	12–14	12–15	14–17	19–23	34–39	1710–1850
Copper	1500/4300	41–46	50–59	49–52	52–61	71–93	2610–2820
Iron	N/A	5900–6100	3700–4300	14900–17100	5000–5100	6900–7400	6400–6900
Lead	300/840	29–35	73–78	47–50	198–235	920–1010	58–73
Manganese	N/A	2440–2750	2430–2740	2040–2140	2020–2230	2030–2230	2610–2720
Mercury	17–57	0.05–0.08	0.06–0.10	0.12–0.14	0.09–0.16	0.36–0.52	0.03–0.32
Molybdenum	18/75	5.6–6.7	7.6–8.2	4.0–5.4	4.8–6.1	6.9–8.0	8.6–11.4
Nickel	420/420	6–8	6–7	8–10	9–9	7–10	6–8
Selenium	36/100	0.53–0.64	0.55–0.64	0.74–0.81	0.55–0.65	0.84–0.97	1.18–1.45
Silver	N/A	0.2–0.4	0.3–0.4	0.4–0.4	0.1–0.2	0.1–0.1	0.7–0.8
Zinc	2800/7500	380–420	530–610	450–510	540–590	1420–1520	520–620
PH		11.31–11.67	10.64–10.85	10.69–11.09	10.18–10.39	10.76–11.12	10.68–10.84
Alkalinity (%)		12.0–13.2	13.4–14.6	10.2–11.6	9.1–11.3	11.7–12.5	11.1–12.2

including temperature, other fuel used with wood fuel, and method of wood ash collection (Etiegni, 1990; Etiegni and Campbell, 1991; National Council for Air and Stream Improvement, Inc., 1993) Further quality variation in the wood ash properties occur when wood is co-fired with other supplementary fuels such as coal, coke, gas, and the relative quantity of wood versus such other fuels NCASI (1993).

9.1 Properties of Wood Ash

9.1.1 Physical Properties

Etiegni and Campbell (1991) studied the effect of combustion temperature on yield and chemical properties of wood ash. For this investigation, lodge-pole pine saw dust collected from a saw-mill was combusted in an electric furnace at different temperatures for 6–9 hours or until the ash weight became constant. The results showed that wood ash yield decreased by 45% when combustion temperature were increased from about 550–1100°C. The average particle size of the wood ash was found to be 230 μm . The concentration of potassium, sodium, zinc, and carbonate decreased while concentrations of other metal ions remained constant or increased with increasing temperature. The pH of wood ash was found to vary between 9 and 13.5.

Naik (1999) determined the physical and chemical properties of wood ashes derived from different mills. Scanning Electron Microscopy (SEM) was used to determine shape of wood ash particles. The SEM micrographs showed wood ashes as a heterogeneous mixture of particles of varying sizes, which were generally angular in shape. The wood fly ash consisted of cellular particles, which were unburned, or partially burned wood or bark particles. The average moisture content values for the wood ash studied were about 13% for fly ash and 22% for bottom ash. The average amount of fly ash passing sieve # 200 (75 μm) was 50%. The average amount of fly ash retained on sieve No. 325 (45 μm) was about 31% for wood fly ash. Test results for unit weight or bulk density (ASTM C 29) exhibited average density values of 490 kg/m^3 for fly ash and 827 kg/m^3 for bottom ash. Wood fly ash had an average specific gravity value of 2.48. Specific gravity for bottom ash showed an average of 1.65. The average saturated surface dry (SSD) moisture content values were 10.3% for fly ash and 7.5% for bottom ash. The average cement activity index at the age of 28 days for fly ash was about 66% of the control. The average water requirement for fly ash exhibited a value of 116%. Autoclave expansion tests for fly ash exhibited a low average expansion value of 0.2%.

Naik et al. (2003) evaluated the wood ashes from five different sources for possible use in making controlled low-strength materials (CLSM). They used wood ashes from five different sources in Wisconsin (USA) and were designated as W1, W2, W3, W4, and W5. ASTM standards do not exist for wood ash. The nearest ASTM standard (ASTM C 618, 1994), available is for coal ash and volcanic ash, was used for analysis of its properties. Physical properties of all the five sources of

wood ash are presented in Table 9.2. Each source of wood ash exhibited different physical properties. Fineness of the wood ash (% retained on 45 μm sieve) varied from 23 to 90%. Source W1 and W5 met the ASTM requirement for fineness (34% maximum), while sources W2, W3 and W4 exceeded the ASTM limit. The strength activity index of the wood ash is a comparison of the compressive strength development of 50 mm mortar cubes that have 20% (by mass) replacement of cement with wood ash, with compressive strength of standard cement mortar. Wood ashes W1 and W3 met the strength activity index requirement of ASTM (75% minimum at either 7 or 28 days), while wood ashes W2, W4 and W5 did not meet the requirement. Water requirement of all wood ashes also exceeded the maximum water requirement for coal ash specified by ASTM C 618 (105%); however, sources W1 and W3 satisfied the requirement for natural pozzolan (Class N). The higher water requirement indicated that for concrete and CLSM containing wood ash, more water would be required to produce same slump or flow as compared with the control mixture. Unit weight values of the wood ashes W1, W2, W4, and W5 were 545, 412, 509, and 162 kg/m^3 , respectively. These unit weights are significantly less than the unit weight of a typical ASTM Class C or Class F fly ash (approximately 100 to 1300 kg/m^3). Source W3 had a unit weight of 1376 kg/m^3 . Specific gravity of wood ash sources ranged from 2.26 to 2.60. Specific gravity of wood ash source W1 and W5 was lower than that of a typical coal fly ash (approximately 2.40–2.60). The low unit weight and specific gravity of some wood ashes indicate that adding these wood ashes into CLSM would lower the unit weight of the CLSM. This may be useful for obtaining lighter-weight CLSM.

Udoeyo et al. (2006) reported the physical properties of waste wood ash (WWA), used as additive in concrete. They used wood waste collected from a dump site at the timber market in Uyo, Akwa Ibom State of Nigeria. The waste was subjected to a temperature of 1000°C in an oven to incinerate it into ash before it was used as an additive in concrete. The WWA had a specific gravity of 2.43, a moisture content of

Table 9.2 Physical properties of wood ash used (Naik et al., 2003)

Test	Source					ASTM Requirement C 618 for coal fly ash		
	W1	W2	W3	W4	W5	Class C	Class F	Class N
Retained on No. 325 sieve (%)	23	60	90	40	12	≤ 34	≤ 34	≤ 34
Strength Activity Index	88	38	102.0*	53.8	112.3	≥ 75	≥ 75	≥ 75
with Cement, % of	84	39	83.3*	59.3	72.0	≥ 75	≥ 75	≥ 75
Control	88	34	78.7*	59.4	67.0			
3 days								
7 days								
28 days								
Water Requirement, % of Control	115	155	115	126	130	≤ 105	≤ 105	≤ 115
Autoclave Expansion, %	0.2	0.5	-0.6*	-0.22	0.12	± 0.8	± 0.8	± 0.8
Unit Weight, kg/m^3	545	412	1376	509	162	—	—	—
Specific Gravity	2.26	2.41	2.60	2.26	2.33	—	—	—

*When material passing 150 μm (N. 100) sieve (25% of wood ash W3) was used.

1.81%, and a pH value of 10.48. The average loss on ignition of the ash was found to be 10.46.

Abdullahi (2006) determined the properties of wood ash to be used as partial replacement of cement. The wood ash used was powdery, amorphous solid, sourced locally, from a bakery. The wood ash was passed through BS sieve 0.075 mm size. The specific gravity of wood ash was found to be 2.13. The bulk density of wood ash was found to be 760 kg/m³.

9.1.2 Chemical Composition

Etiegni (1990) and Etiegni and Campbell (1991) obtained X-ray diffraction data to determine the presence of various compounds in dry and wet ash, which was then dried for 24 hours. The major oxides detected in the wood ash were lime (CaO), calcite (CaCO₃), portlandite (Ca(OH)₂) and calcium silicate (Ca₂SiO₄). The authors reported that swelling of wood ash occurred due to the possible hydration of silicates and lime present in the ash.

Naik et al. (2003) studied the chemical composition of wood ashes from five different sources for their possible use in making controlled low-strength materials (CLSM). Wood ashes from five different sources designated as W1, W2, W3, W4, and W5 were used. ASTM standards do not exist for wood ash. The nearest ASTM standard (ASTM C 618, 1994) available is for coal ash and volcanic ash, was used for analysis of its properties. Chemical composition of all the five sources of wood ash is presented in Table 9.3. All wood ashes did not meet all the chemical requirements of ASTM C 618, particularly for the amount of carbon as shown by LOI test results. The LOI obtained for the wood ashes ranged from 6.7 to 58.1%. These high LOI ashes probably will present some difficulties when developing air-entrained

Table 9.3 Chemical composition of wood ash used (Naik et al., 2003)

Analysis parameter	Source					ASTM requirement C 618 for coal ash		
	W1	W2	W3	W4	W5	Class C	Class F	Class N*
Silicon Dioxide, SiO ₂ , (%)	32.4	13.0	50.7	30.0	8.1	—	—	—
Aluminum Oxide, Al ₂ O ₃ (%)	17.1	7.8	8.2	12.3	7.5	—	—	—
Iron Oxide, Fe ₂ O ₃ (%)	9.8	2.6	2.1	14.2	3.0	—	—	—
SiO ₂ + Al ₂ O ₃ + Fe ₂ O ₃ (%)	59.3	23.4	61.0	56.5	18.6	≥ 50	≥ 70	≥ 70
Calcium Oxide, CaO (%)	3.5	13.7	19.6	2.2	25.3	—	—	—
Magnesium Oxide, MgO (%)	0.7	2.6	6.5	0.7	4.5	—	—	—
Titanium Oxide, TiO ₂ (%)	0.7	0.5	1.2	0.9	0.3	—	—	—
Potassium Oxide, K ₂ O (%)	1.1	0.4	2.8	2.0	2.7	—	—	—
Sodium Oxide, Na ₂ O (%)	0.9	0.6	2.1	0.5	3.3	—	—	—
Sulfite, SO ₃ (%)	2.2	0.9	0.1	2.1	12.5	≤ 5	≤ 5	≤ 4
LOI (1000°C)** (%)	31.6	58.1	6.7	35.3	32.8	≤ 6	≤ 6	≤ 10
Moisture (%)	2.4	0.5	0.2	0.4	3.3	≤ 3	≤ 3	≤ 3
Available Alkali, Na ₂ O (%)	0.9	0.4	0.8	1.1	4.2	≤ 1.5	≤ 1.5	≤ 1.5

* Volcanic ash. ** LOI means Loss on Ignition.

Table 9.4 Chemical composition of wood ash (Abdullahi, 2006)

Constituent	SiO ₂	Al ₂ O ₃	Fe ₂ O ₃	CaO	MgO	K ₂ O	NaO	L.O.I
Composition (%)	31.8	28	2.34	10.53	9.32	10.38	6.5	27

concrete mixtures. The high carbon content tends to reduce the amount of air entrained in the concrete mixture and thus requires higher dosages of air-entraining admixtures. However, the higher carbon contents of the wood ashes should not affect the performance of these ashes in CLSM. Wood ash W-2 showed a very low value of SiO₂ + Al₂O₃ + Fe₂O₃ (23.4% most likely due to its high LOI).

Udoeyo et al. (2006) reported the chemical composition of waste wood ash (WWA). The results of the oxide concentrations of the ash, measured using an X-ray diffraction (XRD) test, showed that its major oxide components are: CaO, SiO₂, Al₂O₃, K₂O, Fe₂O₃, MgO, SO₃, TiO₂, and P₂O₅. Other substances, such as Na₂O, ZnO, Cl, MnO, SrO, Cr₂O₃, CuO, ZrO₂, and Rb₂O, were found in trace amounts. The chemical analysis showed that the ash has silicon dioxide (SiO₂), aluminum oxide (Al₂O₃), and iron oxide (Fe₂O₃) values of 20.8, 11.6, and 5.37, respectively. A combination of the percentage masses of these three oxides gives a total of 37.8%, which is less than the 70% limit specified for pozzolan in ASTM C 618 (1994).

Abdullahi (2006) determined the chemical composition of wood ash to be used as partial replacement of cement. The results of chemical analysis of wood ash are shown in Table 9.4. The total percentage composition of Iron oxide (Fe₂O₃ = 2.34%), aluminium oxide (Al₂O₃ = 28.0%) and silicon dioxide (SiO₂ = 31.80%) was found to be 62.14%. This is less than 70% minimum required for pozzolana (ASTM C 618, 1994). This reduces the pozzolanic activity of the wood ash. The loss on ignition obtained was 27%. The value is more than 12%; the maximum as required for pozzolana (ASTM C 618-94). This means that the wood ash contain appreciable amount of un-burnt carbon which reduces its pozzolanic activity. The un-burnt carbon is not pozzolanic and its presence serves as filler to the mixture. The alkali content (Na₂O) was found to be 6.5%. This value is higher than the maximum alkali content of 1.5% required for pozzolana. The alkali content is important where the wood ash is to be used with reactive aggregate (Neville, 1995). Wood ash will not be suitable for construction work where reactive aggregate is to be used.

9.1.3 Elemental Analysis

Mishra et al. (1993) investigated the elemental and molecular composition of mineral matters in ash from five types of wood and two types of barks as a function of temperature. The mass loss occurred in the range of 23 to 48% when the combustion temperature was increased from 500 to 1300°C. This was attributed to decreased elemental mass concentrations of K, S, B, Na, and Cu resulting from increased temperature.

Steenari and Lindqvist (1998) characterized fly ashes derived from co-combustion of wood chips and fossil fuels, and compared their properties with those obtained

from combustion of wood ash alone. In their work, wood fly ash samples were obtained by the co-firing of wood chips with coal, oil, and peat in utility boilers in Sweden. The fly ashes derived from the co-combustion of wood with coal or peat exhibited lower concentrations of calcium, potassium, and chlorine, and higher concentrations of aluminum ion and sulfur relative to pure wood ash. The pH of leachates obtained from the co-combustion ashes were lower compared to pure wood ash. The concentrations of trace metals in these ashes were similar to those observed in pure wood ashes.

Naik et al. (2002) studied the elemental analysis of wood obtained from Rothschild, Wisconsin in United States, and compared it with that of the Type-I cement. Analysis was done using Instrumental Neutron Activation Analysis. The neutron activation analysis method exposes the sample to neutrons, which results in an activation of many elements. This activation consists of radiation of various elements. For the ash and cement utilized in this project, gamma-ray emissions were detected. Many different elements may be detected simultaneously based on the gamma-ray energies and half-lives. The results of the elemental analysis of wood ash are given in Table 9.5. The elemental composition of the cement and wood ash differed considerably. The predominate elements contained in the wood ash (>5000 ppm) were Aluminum, Cadmium, Calcium, Iron, Magnesium, Manganese, Potassium, Sodium, and Titanium. Primary elements in the cement were Aluminum, Calcium, Iron, and Potassium. The wood ash had much higher amounts of Magnesium, Manganese, Potassium, Aluminum, and Sodium than the cement. The total elemental composition of these materials gives some indication of the potential for leaching.

9.1.4 Mineralogical Analysis

Campbell (1990) presented data on major and trace elements in wood ash. The major elements were calcium (7–33%), potassium (3–4%), magnesium (1–2%), phosphorus (0.3–1.4%), manganese (0.3–1.3%), and sodium (0.2–0.5%). The trace elements were zinc, boron, copper, molybdenum, and others at parts per million levels. Carbon content in wood ash was found to vary between 4 and 34% by mass.

Naik et al. (2002) studied the mineralogical analysis of wood ash obtained from Rothschild in Wisconsin in United States. Major mineral species (crystalline phases) that were found in the wood ash are shown in Table 9.6. The predominant crystalline phase present in the wood ash sample was quartz (SiO_2). Additional trace amounts of crystalline phases detected in wood ash included gypsum ($\text{CaSO}_4\text{H}_2\text{O}$), magnetite (Fe_3O_4), microcline (KAlSi_3O_8), mullite ($\text{Al}_2\text{O}_3\cdot\text{SiO}_2$), periclase (MgO), and plagioclase (NaCa). The mineralogical analysis also indicated large amounts of amorphous material present in the wood ash (46.9%). The calcite, hematite, magnetite, microcline, mullite, plagioclase, and quartz present in the wood ash are generally not reactive when used in concrete. Generally, cement had predominant phases of tricalcium aluminate, amorphous, dicalcium silicate, tetracalcium aluminoferrite, and tricalcium silicate.

Table 9.5 Elemental analysis of cement and wood ash (Naik et al., 2002)

Elemental (Bulk chemical analysis)			Elemental (Bulk chemical analysis)		
Element	Type I cement (ppm)	Wood ash (ppm)	Element	Type I cement (ppm)	Wood ash (ppm)
Aluminum	18104.0	27478.3	Palladium	< 616.0	< 905.5
Antimony	12.7	3.6	Potassium	6148.2	44220
Arsenic	95.2	148.3	Praseodymium	< 13.6	< 32.5
Barium	< 94.9	291.5	Rubidium	< 21.7	< 100.4
Bromine	< 0.4	2.7	Rhenium	< 61.5	100.1
Cadmium	< 1322.0	< 1375.9	Samarium	4.0	5.1
Calcium	< 116255.4	17043.1	Scandium	3.3	2.6
Cerium	16.1	43.3	Selenium	< 72.7	< 75.7
Cesium	< 0.3	1.0	Silver	< 7.2	< 7.2
Chlorine	< 146.1	416.7	Sodium	637.2	6036.1
Chromium	20.5	31.4	Strontium	64.9	< 285.9
Cobalt	4.9	3.8	Tantalum	0.5	1.1
Copper	< 265.1	< 241.6	Tellurium	0.2	< 0.3
Dysprosium	< 4.3	< 7.5	Terbium	< 0.2	< 0.3
Europium	0.3	0.3	Thorium	2.3	3.7
Gallium	< 357.4	< 660.8	Thulium	< 0.4	8.3
Gold (Au)	< 0.0	< 0.0	Tin	< 198.4	< 194.6
Hafnium	1.0	2.7	Sodium	637.2	6036.1
Holmium	< 3.7	< 6.5	Silver	< 7.2	< 7.2
Indium	< 0.4	< 0.6	Strontium	64.9	< 285.9
Iodine	< 10.9	< 16.1	Tantalum	0.5	1.1
Iridium	< 0.0	< 0.0	Thorium	2.3	3.7
Iron	19601.2	17519.9	Thulium	< 0.4	8.3
Lanthanum	14.8	29.4	Tin (Sn)	< 198.4	< 194.6
Lutetium	0.5	0.7	Titanium	1241.0	2971.2
Magnesium	4581.0	6216.0	Tungsten	< 2.0	11.6
Manganese	4329.5	17605.6	Uranium	9.0	6.2
Mercury	1.1	0.4	Vanadium	59.7	32.1
Molybdenum	< 65.0	< 65.3	Ytterbium	2.7	3.8
Neodymium	17.2	26.1	Zinc	< 10.2	< 18.2
Nickel	< 1265.1	< 1206.2	Zirconium	60.7	< 103
Ruthenium	6.3	22.9			

9.2 Uses of Wood Ash

Approximately 70% of the wood ash generated is landfilled; an additional 20% is applied on land as a soil supplement [2–14]. The remaining 10% has been used for miscellaneous applications (Campbell, 1990; Etiegni, 1990; Etiegni and Campbell, 1991; NCASI, 1993) including construction materials, metal recovery, and pollution control. NCASI (1993) has estimated that of the total wood ash produced in the US, only about 28% is being utilized NCASI (1993). In Europe, wood ash is used as a feedstock for cement production and road base material (Greene, 1988). Landfilling is becoming very restrictive due to shrinking landfill space and strict environmental regulations. The use of wood ash as a soil supplement is becoming more limited due to the presence of heavy metals and high alkalinity, as well as

Table 9.6 Mineralogy of wood ash (Naik et al., 2002)

Analysis parameter	%
Amorphous	46.9
Calcite (CaCO_3)	3.6
Quartz (SiO_2)	34.5
Microcline (KAlSi_3O_8)	7.9
Mullite ($\text{Al}_2\text{O}_3\text{SiO}_2$)	—
Albite ($\text{NaAlSi}_3\text{O}_8$)	5.7
Portlandite (Ca(OH)_2)	1.4
Syngenite ($\text{K}_2\text{Ca(SO}_4\text{)2H}_2\text{O}$)	—

reduced availability of land for application. Due to these reasons, many attempts are being made to develop high-volume use technologies for wood ash, especially for use in construction materials (Meyers and Kopecky, 1998).

9.2.1 Land Application

Planning for wood ash application requires several considerations. Before planting any crop the soil's nutrient level and pH must be determined through proper soil testing. Wood ash applications should be limited to a level that maintains the soil pH within the optimum range for the intended crop growth. The liming ability of wood ash is generally estimated by using a laboratory measured parameter called the calcium carbonate equivalent (CCE). The CCE indicates how well the wood ash will raise the soil pH compared to lime (calcium carbonate). As with the nutrient composition of wood ash, the CCE of different wood ash may vary considerably, however, most are within the range of 25–60%. With proper soil tests and the lime equivalency of the wood ash, application rates for wood ash are calculated by dividing the recommended lime application rate by the lime equivalency of the wood ash.

During application of wood ash to the soil, special care needs to be taken to prevent the ash from entering any surface or ground water. Wood ash should be land applied as soon as possible to avoid the need for on-site storage. One of the major obstacles to land spreading of wood ash is the undesirable handling and spreading characteristics of ash. Most ash has a low density and small particle size and consequently creates dust problems during transport and application. Wood ash should always be covered during transport to prevent losses in route to the application sites. Studies have indicated that the handling characteristics of ash generally improve with increasing relative humidity, so efforts should be made to avoid spreading on extremely dry days. Moisture can be added to improve the handling characteristics of ash; however, if too much moisture is added, the ash will cake and become difficult to spread uniformly. Ash can be spread with conventional manure spreading or lime application equipment and is either top dressed or incorporated. To get the maximum benefit, incorporate the wood ash throughout the root zone whenever possible as the benefits only occur where the ash and soil are in contact. It is also essential

to calibrate the spreader to insure that the target application rate is met. Due to the physical characteristics of ash, it is often difficult to obtain uniform application, but calibration and knowledge of the application distribution of the spreader can help to minimize non-uniformity.

Etiegni and Campbell (1991) reported the use of wood ash as an agricultural soil supplement and liming material. For that investigation, two types of plants (winter wheat and poplar) were grown in a greenhouse on six different Idaho (United States) soils amended with varying amounts of wood ash. The results indicated a substantial increase in the wheat biomass and in the diameter and height of the poplar at ash concentrations of up to 2% (16 tons/acre). Based on the results obtained, the author indicated that wood ash could be used as a low-grade fertilizer containing potassium and as a liming agent. Meyers and Kopecky (1998) evaluated the effects of land spreading of wood ash on the yield and elemental composition of forage crops and soil nutrient levels using both greenhouse and field investigations. The use of wood ash resulted in a higher yield compared to those obtained with limed and fertilized control treatments. No adverse effects were noted at wood ash application rates of up to 20 tons/acre.

Nguyen and Pascal (1997) measured tree growth responses using two sources of wood ash as a forest soil amendment. Four different application rates (0, 2, 4, and 8% by mass) were used. The tree growth responses were measured using greenhouse and microcosm approaches. The addition of wood ash affected all the measured growth responses (height, diameter, and total leaf area) within the tested range. However, 2% (i.e., 16 tons/acre) application rate was found to be optimum.

Bramryd and Frashman (1995) reported a decrease in acidity and aluminum concentration when wood ash was applied to the soil having 35-year old pine trees in Sweden. Except Cu, no significant increase in heavy metal concentrations was found due to the addition of wood ash. However, the concentration of extractable Mn was found increased.

Naylor and Schmidt (1986) evaluated wood as a fertilizer and liming material. In their study, wood ash was mixed with two acidic soils at rates of 0, 0.4, 1.8, and 2.4 tons/acre to assess changes in extractable nutrients and soil pH. Generally, concentrations of extractable P, K, and Ca increased with increasing ash application rate. The same trend was also noticed for soil pH. The neutralizing capability of the ash was found to be half of that achieved by using agricultural limestone.

9.2.2 Pollution Control

Wood ash has been used as a replacement of *lime or cement kiln dust* in the solidification of hazardous wastes (NCASI, 1993). It has also been used for odor as well as pH control of hazardous and non-hazardous wastes. Wood ash has been added to compost as a color and odor control. Wood ash has been found to capture several water borne contaminants (NCASI, 1993).

9.2.3 Construction Materials

Not much work has been reported relating to the applications of wood ash as a construction material, particularly in cement-based materials. Due to high carbon content in wood ash, its use is limited to low- and medium-strength concrete materials. In Europe, wood ash has also been used as a feedstock in the manufacture of Portland cement (Etiegni, 1990).

Based on the measured physical, chemical, morphological properties, Naik (1999) reported that wood ash has a substantial potential for use as a pozzolanic mineral admixture and an activator in cement-based materials. He further indicated that wood ash has significant potential for use in numerous other materials including Controlled Low Strength Materials (CLSM), low- and medium-strength concrete, masonry products, roller-compacted concrete pavements (RCCP), materials for road base, and blended cements.

Naik (2000) investigated the use of wood ash as a major ingredient in the manufacture of CLSM. A total of 31 CLSM mixtures were proportioned using three sources of wood fly ash to obtain a range of compressive strengths from 0.34 to 1.0 MPa at the age of 28 days. All CLSM mixtures consisted of wood fly ash, water, and cement. Each CLSM mixture was tested for its fresh/rheological and hardened properties. Fresh CLSM properties included unit weight, amount of bleedwater, settlement, and setting and hardening characteristics. Hardened CLSM properties included compressive strength, density, and permeability. Several CLSM mixtures containing high volumes of wood fly ash were found to be appropriate for backfill of excavations, and/or for making low- to medium-strength concrete (Naik, 1999; Naik and Kraus, 2000). Fehrs (1996) also reported that wood ash can be used in manufacture of low-strength concrete and controlled low-strength materials.

Mukherji et al. (1995) conducted experiments to explore the use of wood ash in the ceramic industry. They reported that wood ash derived from the “Neem” (Margosa) tree could be used as a substitute for CaCO_3 in the manufacture of glaze. A series of color stains was also manufactured using the “Neem” wood ash and other ingredients. These stains were calcined at 1250°C . The glazes and colors developed using this wood ash were tested and evaluated for the desired properties for these materials. The authors concluded that the glazes and colors developed in their investigation are suitable for use in both green and baked ware.

9.3 Properties of Concrete Containing Wood Ash

9.3.1 Batch Leaching of WWA

Udoeyo et al. (2006) reported the leachate results of waste wood ash (WWA) used in varying percentages (5, 10, 15, 20, 25, and 30%), by weight, of cement as additive in concrete. Analysis of leachate from WWA, showed the presence of chromium,

Table 9.7 Slump test results of wood ash concrete (Abdullahi, 2006)

Replacement of OPC by WA (%)	0	10	20	30	40
Water/Binder Actual Ratio	0.6	0.66	0.67	0.68	0.69
Slump (mm)	30	35	40	40	35

copper, iron, zinc, and arsenic in the leachates at almost all pH values. As evident in the results, arsenic exhibited the highest leachability, while iron exhibited the lowest leachability. It was further noted that apart from leaching of chromium, leaching of all other metals from WWA showed significant dependence on pH. The leachability of the metals increased with decrease in pH. Apparently, the mineralogical phase of the metal oxides present in the ash affected their susceptibility to attack by H⁺ ions present in the leachant. At a lower pH, there was an increase in the intensity of attack of these ions on WWA mineral phases containing these elements, thus the increase in leachability. A similar trend has been observed by other researchers (Fytianos and Tsaniklidi, 1998; Karuppiyah and Gupta, 1997). Their results also indicated that a pH of 5 does not provide enough concentration of H⁺ to attack iron oxide phases that are produced during incineration of wood waste. The leachate concentrations of almost all the metals were higher than the EPA fresh water acute criteria. Considering that wood ash would not normally contain high concentrations of these metals, the recorded high concentrations in the leachate are attributable to the wood preservatives used. It is therefore important to screen wood waste as part of their selection process for use in concrete.

9.3.2 Slump

Udoeyo et al. (2006) reported slump test results of concrete containing varying percentages (5, 10, 15, 20, 25, and 30% by weight of cement) of waste wood ash (WWA) used as additive in concrete. The values of slump were 62, 8, 5, 2.5, 0, 0, 0 mm for concrete containing 0, 5, 10, 15, 20, 25, and 30% WWA, respectively. It is evident from the results that WWA concrete mixes exhibited less workability than that of plain concrete of the same water-cement ratio, and it increased with higher content of WWA ash. At 20, 25, and 30% additive levels the concrete was insensitive to slump.

Abdullahi (2006) studied the influence of wood ash (WA) on the slump of concrete. He used wood ash as partial replacement of cement in varying percentages (0, 10, 20, 30, and 40%) in concrete mixture proportion of 1:2:4. The result for the slump test is given in Table 9.7. Test result showed that mixtures with greater wood ash content require greater water content to achieve a reasonable workability.

9.3.3 Water Absorption Capacity

Udoeyo et al. (2006) evaluated the water absorption capacity of concrete made with varying percentages (5, 10, 15, 20, 25, and 30% by weight of cement) of waste wood

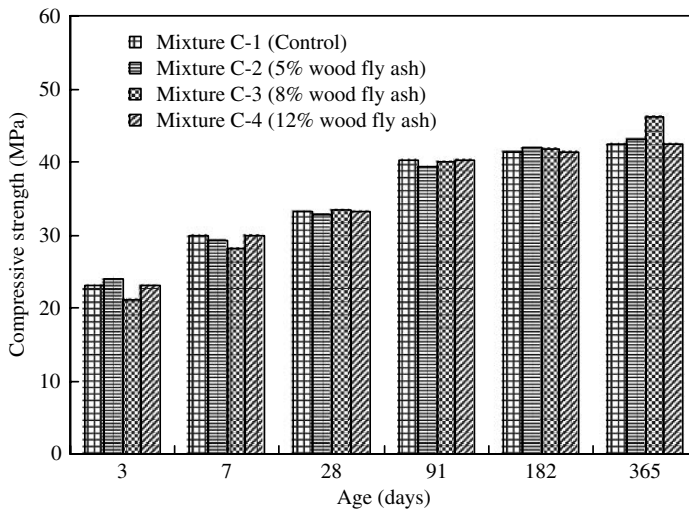


Fig. 9.1 Compressive strength of concrete mixtures containing wood fly ash (Naik et al., 2002)

ash (WWA) as additive. Concrete specimens absorbed more water as the ash content increased. The water absorption at 5% WWA content was 0.4% and increased to 1.05% at 30% WWA content. However, these values are less than 10% which is the percentage water absorption value accepted for most construction materials.

9.3.4 Compressive Strength

Naik et al. (2002) investigated the compressive strength of concrete mixtures made with wood ash up to the age of 365 days. Wood ash content was 5, 8, and 12% of the total cementitious materials. Figure 9.1 shows the compressive strength results. Based on the results, they concluded that: (i) control mixture (without wood fly ash) achieved strength of 34 MPa at 28 days and 44 MPa at 365 days; (ii) strength of concrete mixtures containing wood fly ash ranged from 33 MPa at 28 days and between 42 and 46 MPa at 365 days; and (iii) inclusion of wood fly ash contributed to the strength development of concrete mixtures, even as the cement content was decreased by about 15%. This indicates contribution of wood fly ash to pozzolanic activity.

Udoeyo et al. (2006) determined the compressive strength of concrete made with varying percentages (5, 10, 15, 20, 25, and 30 by weight of cement) of waste wood ash (WWA). They reported that compressive strength generally increased with age but decreased with the increase in the WWA content. Comparisons of the strength of WWA concrete with those of the control (plain) concrete of corresponding ages showed that the strength of WWA concrete was generally less than that of the plain concrete. A possible explanation for this trend is that the WWA acts more like filler

in the matrix than as a binder. Thus, increasing the ash content led to an increase in the surface area of the concrete filler to be bonded by the same amount of cement as that of the control. To further establish if there was a significant enhancement in strength due to a longer duration of curing, Udoeyo et al. (2006) performed a *t*-test with alpha values equal 0.05 and 0.01 selected as the significant and highly significant levels, respectively, to compare the strength of WWA concretes at 28 days and at 90 days. The test results showed that there were significant differences at 5, 10, 15, and 20% additive levels between the 28-day and 90-day strengths. However, when the ash content increased beyond 20%, there existed no statistical difference between both strengths. The improvement in the later-age (90-day) strength up to the 20% additive level may be due to fine-filler effect and the weak pozzolanic activity of the WWA in the concrete, as it is a known fact that strength contribution due to OPC hydration is quite negligible at a later age. The pozzolanic activity of WWA in the concrete entails the formation of additional calcium silicate hydrate (CSH) binder, through the reaction of amorphous silica (SiO_2) content of the ash with the free lime (CaOH_2) from OPC hydration and from the chemical reaction of the high CaO content of the ash with water. The reason for no significant differences between both strengths at 25 and 30% additive levels could be due to inadequate water in the mix for the continuation of the weak pozzolanic activity of the ash in the concrete since self-desiccation may have taken place much earlier at these additive levels.

Abdullahi (2006) reported the compressive strength test results of wood ash (WA) concrete. He used wood ash as partial replacement of cement in varying percentages (0, 10, 20, 30, and 40%) in concrete mixture proportion of 1:2:4. Tests were conducted at the age of 28 and 60 days. Results are given in Table 9.8. The results showed that the specimens containing 0% wood ash had the highest compressive strength. The mixture containing 20% wood ash had higher strength than that containing 10% wood ash at 28 and 60 days. This was due to the fact that the silica provided by 10% wood ash was inadequate to react with the calcium hydroxide produced by the hydration of cement. Increase in wood ash content beyond 20% resulted in a reduction in strength at 28 and 60 days. In this case, the silica present in the mix was in excess of the amount required to combine with the calcium hydroxide from the hydrating cement. The excess silica had no pozzolanic value but only served as filler. At 60 days hydration period, the compressive strength of concrete containing 20% wood ash increased considerably indicating that greater strength can be obtained at later ages. The optimum replacement of cement by wood ash was 20%.

9.3.5 Splitting Tensile Strength

Naik et al. (2002) investigated the influence of wood ash on the splitting tensile strength of concrete. Wood ash content was 5, 8, and 12% of the total cementitious materials. Figure 9.2 shows the splitting tensile strength results. They concluded that: (i) control mixture (without wood fly ash) achieved a strength of 3.8 MPa at 28

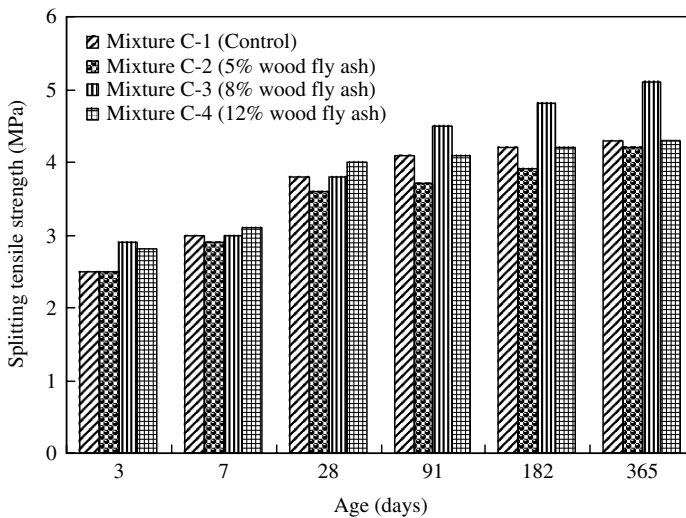


Fig. 9.2 Splitting tensile strength of concrete mixtures containing wood fly ash (Naik et al., 2002)

days and 4.3 MPa at 365 days; (ii) strength of concrete mixtures containing wood fly ash varied between 3.6 and 4.0 MPa at 28 days and between 4.2 and 5.1 MPa at 365 days; and (iii) splitting tensile strength generally followed a similar pattern as for the compressive strength.

9.3.6 Flexural Strength

Naik et al. (2002) studied the effect of wood ash on the flexural strength of concrete. Three percentages (5, 8, and 12) of wood ash of the total cementitious materials were used. Flexural strength results of concrete mixtures are shown in Fig. 9.3. Based on the investigation, they concluded that: (i) control mixture (without fly ash) achieved a strength of 4.1 MPa at 28 days and 4.4 MPa at 365 days; (ii) strength of concrete mixtures containing wood fly ash varied between 3.9 and 4.4 MPa at 28 days and between 4.3 and 5.3 MPa at 365 days; and (iii) test results indicated that inclusion of

Table 9.8 Compressive strength of wood ash concrete (Abdullahi, 2006)

WA content (%)	Compressive strength (N/mm ²)	
	28-day	60-day
0	23.96	24.15
10	13.09	14.06
20	14.13	18.60
30	9.02	7.91
40	8.59	7.82

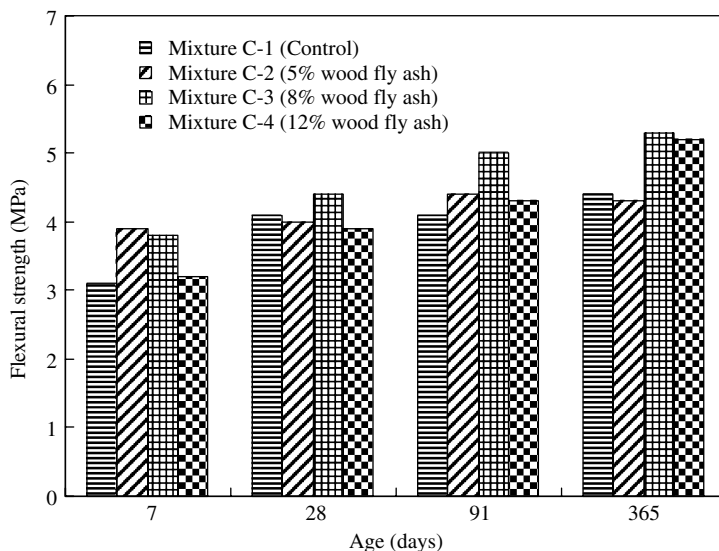


Fig. 9.3 Flexural strength of concrete mixtures containing wood fly ash (Naik et al., 2002)

wood fly ash enhanced the flexural strength of concrete mixtures due to pozzolanic contribution of the wood fly ash.

Udoeyo et al. (2006) reported flexural strength results of concrete made with varying percentages (5, 10, 15, 20, 25, and 30% by weight of cement) of waste wood ash (WWA), used as additive in concrete. The flexural strength decreased with the increase in WWA content but at a slower rate than that of compressive strength. The 28-day flexural strength of samples containing 5% WWA was 5.20 N/mm², and it decreased to 3.74 N/mm² at 30% WWA content. The flexural strength magnitudes of WWA concrete ranged between 67% and 93% of the control concrete at corresponding ages and additive levels.

9.3.7 Drying Shrinkage

Naik et al. (2002) investigated the drying shrinkage of concrete mixtures made with wood fly ash. Wood ash content was 5, 8, and 12% of the total cementitious materials. They reported that: (i) shrinkage of control mixture (with out wood ash) was -0.0092% at 7 days and -0.052% at 232 days; (ii) shrinkage of concrete mixture with 5% wood ash, ranged from 0.012% at 7 days to -0.027% at 232 days; (iii) shrinkage for mixture with 8% wood ash was 0.014% at 7 days and -0.013% at 232 days; and (iv) mixture with 12% wood ash had shrinkage between -0.0051% at 7 days and -0.044% at 232 days.

9.3.8 Freezing and Thawing Resistance

Naik et al. (2002) studied the influence of wood ash on the freezing and thawing resistance of concrete. It was evaluated by testing for changes in relative dynamic modulus, pulse velocity, and change in length. Wood ash content was 5, 8, and 12% of total cementitious materials.

The results of the relative dynamic modulus of concrete mixtures are shown in Fig. 9.4. There is no significant effect of freezing-thawing cycles (300 cycles) on the relative dynamic modulus of the concrete mixtures. The inclusion of wood ash in concrete mixtures did not make a significant difference in relative dynamic modulus.

For control mixture (without wood ash), relative dynamic modulus was 97.7% and it was 95.7% for mixture (with 5% wood ash), 97.8% for mixture (8% wood ash), and 95.7% for mixture (with 12% wood ash).

The pulse velocity of concrete mixtures is shown in Fig. 9.5. There is no significant effect from inclusion of wood ash on the pulse velocity of concrete mixtures. At 300 cycles, the pulse velocity of concrete mixtures (without wood ash) was 5425 m/sec, 5480 m/sec for mixture (5% wood ash), 5560 m/sec for mixture (8% wood ash), and 5435 m/sec for mixture (12% wood ash).

Percent change in length of concrete mixtures is shown in Fig. 9.6. For control mixture (with out wood ash), percent change in length was 0% at 32 cycles and -0.00556% at 360 cycles.

The percent change in length for mixture (with 5% wood ash) was -0.003273% at 32 cycles and 0.01113% at 300 cycles, 0.002942% at 32 cycles and 0.00903% at 300 cycles for mixture (with 8% wood ash), -0.000417% at 32 cycles and 0.01156% at 213 cycles for mixture (with 12% wood ash).

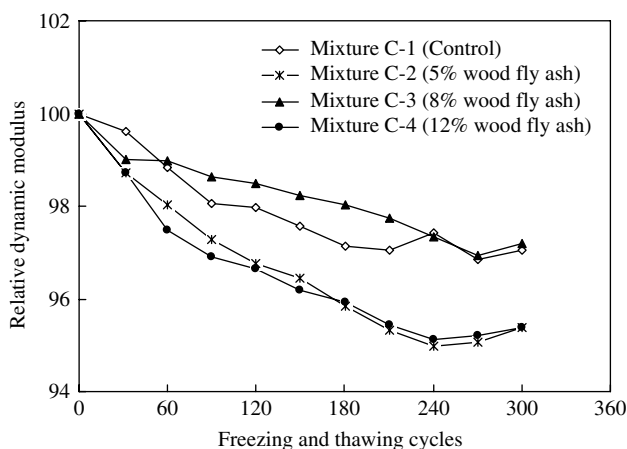


Fig. 9.4 Relative dynamic modulus of concrete mixtures containing wood fly ash (Naik et al., 2002)

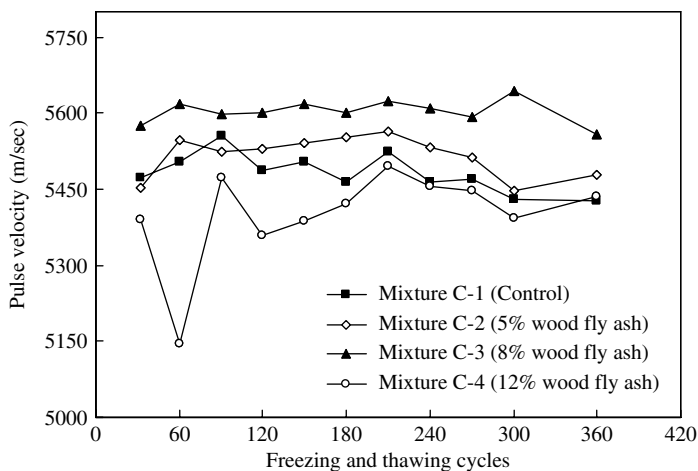


Fig. 9.5 Pulse velocity of concrete mixtures containing wood fly ash (Naik et al., 2002)

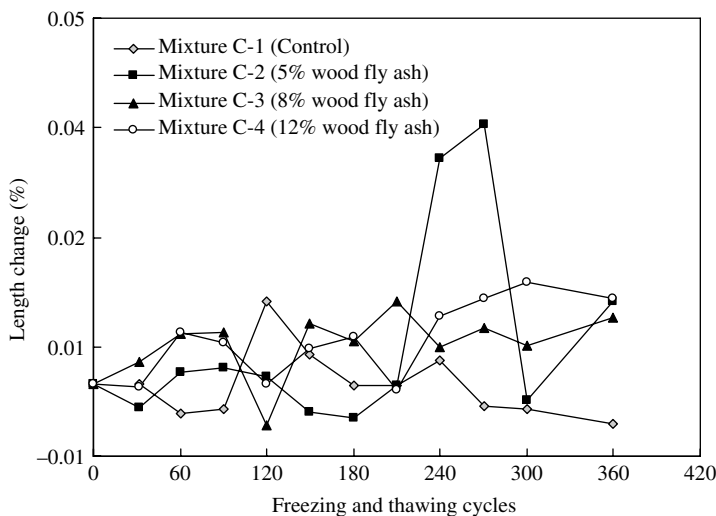


Fig. 9.6 Length change (%) of concrete mixtures containing wood fly ash (Naik et al., 2002)

References

- Abdullahi M (2006) Characteristics of wood ash/OPC Concrete. *Leonardo Electronic Journal of Practices and Technologies* 8: 9–16.
- ASTM C 618 (1994) Standard specification for coal fly ash and raw or calcined natural pozzolan for use in concrete. ASTM, Philadelphia, USA.
- Bramryd T, Frashman B (1995) Silvicultural use of wood ashes – effects on the nutrient and heavy metal balance in a pine (*pinus sylvestris*, l.) forest soil. *Water, Air and Soil Pollution Proceeding of the 1995 5th International Conference on Acidic Deposition: Science and Policy, Acid Reign '95, Part II*, Kluwer Academic Publishers, Dordrecht Netherland, 85 (2): 1039–1044.

- Campbell AG (1990) Recycling and disposing of wood ash. *TAPPI Journal* 73 (9): 141–143.
- Etiegni L (1990) Wood ash recycling and land disposal. Ph.D. Thesis, Department of Forest Products, University of Idaho at Moscow, Idaho, USA, pp. 174.
- Etiegni L, Campbell AG (1991) Physical and chemical characteristics of wood ash. *Bioresource Technology*, Elsevier Science Publishers Ltd. 37 (2): 173–178.
- Fehrs JE (1996) Ash from the combustion of treated wood: characterization and management options. Presented at the National Bioash Utilization Conference, Portland, ME, pp. 20.
- Fytianos K, Tsaniklidi B (1998) Leachability of heavy metals in Greek fly ash from coal combustion. *Environment International* 24 (4): 477–486.
- Greene TW (1988) Wood ash disposal and recycling source book. Prepared for the Coalition of Northeast Governors by OMNI environmental Sources, Beaverton, Oregon.
- Karuppiiah M, Gupta G (1997) Toxicity of metals in coal combustion ash leachate. *Journal of Hazardous Materials* 56: 53–58.
- Meyers NL, Kopecky MJ (1998) Industrial wood ash as a soil amendment for crop production. *TAPPI Journal* 81 (4): 123–130.
- Mishra MK, Ragland KW, Baker AJ (1993) Wood ash composition as a function of furnace temperature. *Biomass and Bioenergy*, Pergamon Press 4 (2): 103–116.
- Mukherji SK, Dan T K, Machhoya BB (1995) Characterization and utilization of wood ash in the ceramic industry. *International Ceramic Review* 44 (1): 31–33.
- Naik TR (1999) Tests of wood ash as a potential source for construction materials. Report No. CBU-1999-09, UWM Center for By-Products Utilization, Department of Civil Engineering and Mechanics, University of Wisconsin-Milwaukee, Milwaukee, pp. 61.
- Naik TR (2000) Flowable slurry incorporating wood fly ash from the Weyerhaeuser company. Report No. CBU-2000-01, Rep-367, UWM Center for By-Products Utilization, University of Wisconsin-Milwaukee, pp. 37.
- Naik TR, Kraus RN (2000) Use of wood ash for structural concrete and flowable CLSM. Report No. CBU-2000-31, UWM center for By-products Utilization, University of Wisconsin-Milwaukee, Final Report Submitted to The University of Wisconsin System, Solid Waste Management and Research Program, pp. 121.
- Naik TR, Kraus RN, Siddique R (2002) Demonstration of manufacturing technology for concrete and CLSM utilizing wood ash from Wisconsin. Report No. CBU-2002-30, Report for Year 1 activities submitted to the Wisconsin Department of Natural Resources, Madison, WI, for Project # 01-06 UWM Center for By-Products Utilization, Department of Civil Engineering and Mechanics, University of Wisconsin-Milwaukee, Milwaukee, pp. 124.
- Naik TR., Kraus RN, Siddique R (2003) CLSM containing mixtures of coal ash and a new pozzolanic material. *ACI Materials Journal* 100 (3): 208–215.
- National Council for Air and Stream Improvement, Inc. (NCASI) (1993) Alternative management of pulp and paper industry solid wastes. Technical Bulletin No. 655, NCASI, New York, NY, pp. 44.
- Naylor LM, Schmidt EJ (1986) Agricultural use of wood ash a fertilizer and limiting material. *TAPPI Journal* 114–119.
- Neville A. M. (1995) Cementitious materials of different types. Pearson Education Asia Pte. Ltd..
- Nguyen P, Pascal KD (1997) Application of wood ash on forestlands: ecosystem responses and limitations. Proceeding of the Conference on Eastern Hardwoods, Resources, Technologies, and Markets, Forest Product Society, Madison, WI, April 21–23, pp. 203.
- Steenari BM, Lindqvist O (1998) Co-combustion of wood with coal, oil, or peat-fly ash characteristics. Department of Environmental Inorganic Chemistry, Chalmers University of Technology, Goteborg, Sweden, Report No. ISSN 0366-8746 OCLC 2399559, 1372: 1–10.
- Udeoyo FF, Inyang H, Young DT, Oparadu, EE (2006) Potential of wood waste ash as an additive in concrete. *Journal of Materials in Civil Engineering* 18 (4): 605–611.

Chapter 10

Volcanic Ash

Introduction

Volcanic ash (VA) is formed during volcanic eruptions. Ash is created when solid rock shatters and magma (molten rock) separates into minute particles during explosive volcanic activity. The usually violent nature of an eruption involving steam (phreatic eruption) results in the magma and solid rock surrounding the vent is torn into particles of clay to sand size.

The plum that is generally seen above an erupting volcano is composed primarily of ash and steam. The very fine particles maybe carried away for miles together, settling out as a dust-like layer across the landscape. This is known as ‘ash fall’. The commonly used term for any material explosively thrown out from a vent is tephra, also known as pyroclastic debris. If liquid magma is ejected as spray, the particles will solidify in the air to small fragments of volcanic glass. Tephra particles of gravel are termed cinders. The ejection of large quantities of ash will produce an ash cone. A layer of volcanic ash tends to become cemented together to form a solid rock called ‘tuff’.

The average grain-size of rock fragments and volcanic ash erupted from an exploding volcanic vent varies largely amongst eruptions and also during a single explosive eruption, lasting from hours to days. Heavier, large-sized rock fragments typically fall back to the ground on or close to the volcano and progressively smaller and lighter fragments are blown farther from the volcano by wind. Volcanic ash, the smallest particles (2 mm in diameter or smaller, even less than 0.001mm), can travel hundreds to thousands of kilometers downwind from a volcano depending on wind speed, volume of ash erupted, and height of the eruption column.

The size of ash particles, which fall on the ground decreases exponentially with increasing distance from a volcano. Also, the range in grain size of volcanic ash typically diminishes downwind from a volcano. The distribution of ash particle sizes can vary widely. The particle size distribution in case of Mount St. Helens 1980 (Johnston, 1997) eruptions is given in Table 10.1. Volcanic ash is not the product of combustible materials, like the soft fluffy material generated by burning wood, leaves, or paper. Volcanic ash is hard and abrasive, and does not dissolve in water. It conducts electricity when wet.

Table 10.1 Particle size variation with distance of Mount St. Helens (Johnston, 1997)

Distance from the volcano (km)	Mean particle diameter (mm)
0	4.0
54	0.10
150	0.0625
235	0.0380
414	0.0466
621	0.034

10.1 Volcanic Ash Particles Component

Volcanic ash typically consists of tiny particles composed of varying proportions of: (i) Volcanic glass; and (ii) minerals or crystals; and other rock fragments (lithics).

10.1.1 Volcanic Glass

Volcanic glass shards are the fragments of the molten part of magma that cools down and solidifies during eruption. Glass shards are remnants of tiny gas bubbles that develop and grow in size during the final ascent toward the surface. Such shards may consist of many gas bubbles or only a portion of a single gas bubble. During eruption, the expanding gas breaks the bubbles and surrounding glass into shards of various sizes and shapes. Shards formed by phreatomagmatic eruptions often have a particularly angular shape resulting from the violent explosive interaction between magma and water. Glass is relatively hard (5 on Moh's scale), and the more angular the glass shards, the more abrasive the ash. Scanning electron micrograph (SEM) of a highly vesicular glass shard of ash measuring just over 0.1 mm long erupted during the 18 May 1980 eruption of Mount St. Helens is shown in Fig. 10.1, whereas Fig. 10.2 shows the SEM image of phreatomagmatic glass shards > 0.064 mm (Cas and Wright, 1988).

10.1.2 Minerals or Crystals (Phenocrysts)

Minerals within volcanic ash are primarily derived from the magma. These minerals crystallized and grew within the magma while it was below the earth's surface. The type of minerals within an ash deposit depends upon the chemistry of the magma from which it was erupted. Fine minerals may also grow on the walls of expanding gas bubbles in the magma prior to fragmentation into ash-sized particles. Cristobalite is a type of silica crystal that forms in this way. Cristobalite is known to cause silicosis in humans, which is typically contracted by people working for prolonged periods in industries that expose workers to fine rock dust.

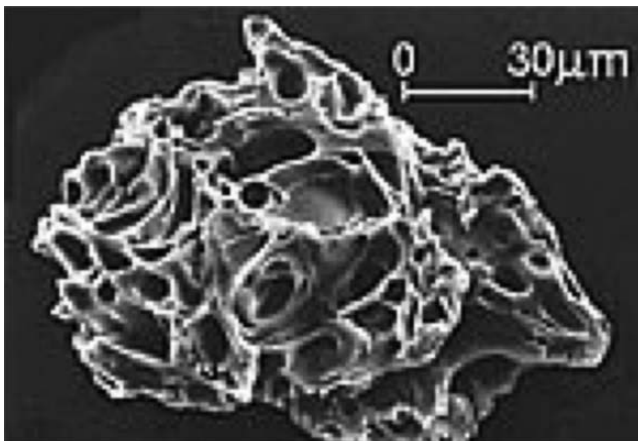


Fig. 10.1 Scanning electron micrograph (SEM) of a highly vesicular glass shard of ash measuring just over 0.1 mm long, erupted during 18 May 1980 eruption of Mount St. Helens (Johnston, 1997)

10.1.3 Other Rocks (Often Called Lithics)

Rising magma will incorporate pieces of different types of rocks through which it moves including rocks located deep beneath a volcano and within the volcano itself. The rapid ascent of magma during explosive eruption often rip fragments from the walls of the magma conduit, which are ejected and fragmented further by the explosive expansion of volcanic gases. These non-magmatic rock fragments are found in varying abundances within ash deposits and often have a shape and texture distinctly different than glass shards.

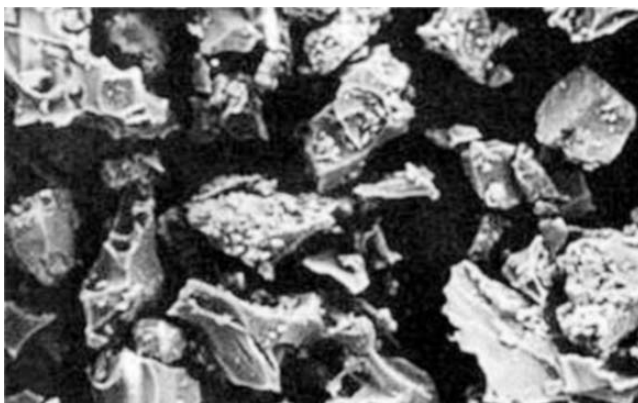


Fig. 10.2 SEM image of phreatomagmatic glass shards > 0.064 mm (Cas and Wright, 1988)

10.2 Properties of Volcanic Ash

Physical and chemical properties of a volcanic ash could be referenced with ASTM C618-93, a Standard Specification for ‘Fly Ash and Raw or Calcinated Natural Pozzolan for Use as a Mineral Admixture in Portland Cement Concrete’.

10.2.1 Density

The density of individual particles vary between 700 and 1200 kg/m³ for pumice, 2350–2450 kg/m³ for glass shards, 2700–3300 kg/m³ for crystals, and 2600–3200 kg/m³ for lithic particles, as shown in Table 10.2. Pumice fragments may form temporary mats of floating material if deposited on water. Since coarser and denser particles are deposited close to source, fine glass and pumice shards are relatively enriched in ash fall deposits at distal locations.

The bulk density of any ash fall deposit can be variable, with reported dry bulk densities of newly fallen and slightly compacted deposits ranging between 500 and 1500 kg/m³; (Moen and McLucas, 1980; Scott and McGimsey, 1994). Both increasing and decreasing bulk densities with distance from source have been reported (Scasso et al., 1994), but distal ash falls most commonly show slight increases in bulk density with distance from a volcano. Bulk density of wet ash ranges between 1,000 and 2,000 kg/m³. Grain-size, composition (proportions of crystal, lithics, glass shards and pumice fragments), particle shape, and moisture content determine the bulk density of ash deposits. Less spherical particles (more irregular) will pack relatively poorly resulting in higher porosity and lower bulk densities. Particle aggregation prior to deposition will result in higher particle packing and therefore higher densities.

10.2.2 Hardness

The abrasiveness of volcanic ash is a function of the hardness of the material forming the particles. Hardness values for the most common particles are shown in Table 10.3. Ash particles commonly have sharp broken edges, which make them a very abrasive material.

Table 10.2 Density of volcanic ash particles (Shipley and Sarna-Wojcicki, 1982)

Type of ash particle	Density of particle (kg/m ³)
Pumice fragments	700–1,200
Volcanic glass shards	2,350–2,450
Crystals and minerals	2,700–3,300
Other rock fragments	2,600–3,200

Table 10.3 Moh's scale of hardness (mineral hardness from Deer et al., 1978)

Scale number	Mineral	Metal	Minerals in volcanic ash and their hardness
1	Talc		
2	Gypsum	Aluminum Copper	Mica (H 2-3)
3	Calcite	Brass	
4	Fluorite	Iron	
5	Apatite	Steel	volcanic glass, pyroxene, amphibole (H 5-6)
6	Orthoclase (Feldspar)		plagioclase, alkali-feldspar (H 6-6.5)
7	Quartz		
8	Topaz		
9	Corundum	Chromium	

Typical physical properties of volcanic ash, as reported by Hossain (2003) are given in Table 10.4.

10.2.3 Chemical Composition

Chemical composition and chemistry of volcanic ash is directly related to the chemistry of the source magma. Volcanic glass is relatively high in silica compared to mineral crystals, but relatively low in non-silica elements (especially Mg and Fe). Generally, both glass and most minerals always contain Si, Al, K, Na, Ca, Mg and/or Fe. Typical chemical composition of volcanic ash as reported by Hossain (2003) are given in Table 10.5.

Hossain (2005a) carried out the quantitative XRD analysis of Portland cement (PC) and blended cements with 20% volcanic ash (VA) and 20% volcanic pumice powder (VPP) as cement replacement. The fineness of VA and VPP were 285 and 298 m²/kg, respectively. Both VA and VPP satisfy the requirement of Class F fly ash as per ASTM C618. The phase composition of these materials is presented in Table 10.6.

10.2.3.1 Soluble Components

Freshly fallen volcanic ash particles have surface coatings of soluble components (salts) and/or moisture. These components make volcanic ash a bit corrosive and

Table 10.4 Physical properties of volcanic ash (Hossain, 2003)

Physical properties	Volcanic ash
Fineness (m ² /kg)	242
Residue on 75 μ m sieve (%)	42
Bulk density (kg/m ³)	2450

Table 10.5 Chemical properties of volcanic ash (Hossain, 2003)

Chemical compounds	Amount (%)
Calcium oxide (CaO)	6.10
Silica (SiO ₂)	59.32
Alumina (Al ₂ O ₃)	17.5
Iron oxide (Fe ₂ O ₃)	7.06
Sulfur trioxide (SO ₃)	0.71
Magnesia (MgO)	2.55
Sodium oxide (Na ₂ O)	3.80
Potassium Oxide (K ₂ O)	2.03
Loss on ignition	1.0

potentially conductive. These soluble coatings are derived from the interactions in an eruption column between ash particles and volcanic-gas aerosols, which may be composed of sulfuric and hydrochloric acid droplets with absorbed halide salts. The amount of available aerosols varies greatly between eruptions of similar size and volume.

Volcanic eruptions inject water vapor (H₂O), carbon dioxide (CO₂), sulfur dioxide (SO₂), hydrochloric acid (HCl), hydrofluoric acid (HF) and ash into the atmosphere. HCl and HF will dissolve in water and fall as acid rain whereas most SO₂ is slowly converted to sulfuric acid (H₂SO₄) aerosols. Ash particles may absorb these aerosol droplets onto their surfaces. When ash falls to the ground, the soluble components (leachates) can be washed away by water, potentially resulting in changes to local water chemistry and hence quality. Chemical changes in the underlying soil can occur as a result of leaching of the aerosols coating individual grains and longer term from unstable glass particles (Cronin et al., 1996). Table 10.7 shows concentrations of leachable constituents in ash fall from historic eruptions (all concentrations in mg/kg).

Table 10.6 Potential phase composition of the cementing materials from X-ray diffraction (Hossain, 2005a)

Phase	PC (%)	PVAC (PC blended with 20% VA) (%)	PVPC (PC blended with 20% VPP) (%)
C ₃ S	68.1	46.3	46.8
C ₂ S	14.1	9.5	9.6
C ₃ A	5.9	5.1	5.3
C ₄ AF	9.2	6.4	6.4
Other	2.4	5.2	5.1
Total	99.7	72.5	73.2
Glassy fraction	0.3	27.5	26.8

Table 10.7 Concentrations of leachable constituents (mg/kg) in ash fall from historic eruptions (http://en.wikipedia.org/wiki/Volcanic_ash)

	Fuego, Costa Rica		Pacaya, Guatemala		Santiaguito, Guatemala		Mt. St. Helens, USA		Ruapehu, New Zealand	
Element	Mean	Max	Mean	Max	Mean	Max	Mean	Max	Mean	Max
Al	5.2	26.8	12.8	21.2	5.2	19.6	—	—	42.8	1160
B	0.088	0.044	0.06	0.108	1.08	3.92	—	—	—	—
Ba	0.296	1	0.68	1.12	0.132	0.348	0.152	0.24	—	—
Br	—	—	—	—	—	—	—	—	1.6	13.6
Ca	400	1040	196	304	600	2240	440	800	1890	6760
Cd	0.008	0.04	0.056	0.128	0.056	0.256	0.0052	0.025	—	—
Cl	124	232	204	840	440	1400	392	668	248	2020
Co	0.0036	0.0328	0.0072	0.024	0.132	0.6	0.0196	0.072	—	—
Cu	0.324	2.52	1.24	2.36	1.56	2.8	0.164	0.48	—	—
F	21.2	88	28.8	44	14.4	23.2	7.2	12	25.8	95.6
Fe	2.08	22.4	2.8	9.2	1.56	3.6	0.376	0.48	5.74	92.8
K	—	—	—	—	—	—	—	—	36.1	253
Li	0.044	0.116	0.0036	0.064	0.4	1.88	0.208	0.52	0.5	1.45
Mg	22	44	19.6	52	96	400	48	84	235	1200
Mn	1.48	3.12	1	2.88	19.6	92	7.6	13.2	—	—
Na	128	184	156	440	400	1760	264	440	292	1150
Pb	0.104	0.96	0.014	0.044	0.0096	0.048	0.0092	0.072	—	—
Si	7.2	12.4	9.2	15.2	7.6	11.2	40	56	—	—
Sr	2	5.2	1.64	2.6	1.48	4.4	1.76	2.88	—	—
U	0.00108	0.0028	0.00008	0.00048	0.0012	0.006	0	0	—	—
V	0.06	0.128	0.0248	0.068	0.0364	0.08	0.0012	0.0264	—	—
Zn	0.144	0.56	5.6	18.8	2.04	8.4	2.04	26.8	—	—
Nitrate									21.9	88.9
Sulfate							1000	1800	5190	24530

10.3 Uses of Volcanic Ash

Uses of volcanic ash are based on its physical properties of fine size, angularity of particles, friability, light color, and chemical or pyrochemical properties.

10.3.1 As Abrasive

Because of its fineness, angularity, and moderate hardness (5.5–6.0 on Mohs scale), Volcanic ash could be used as an abrasive for use as a polishing, scouring, and cleansing agent. Processing of volcanic ash for abrasive uses generally includes only drying and the screening out of coarser particles and incidental contaminants.

10.3.2 In Ceramics

Volcanic ash, or pumicite, is composed of minute shards of volcanic glass corresponding roughly to a frit composed of feldspar and quartz and, therefore, could be suitably used in ceramics.

10.3.3 In Ceramics Glazes and Bodies

The substitution of volcanic ash for equivalent amounts of other materials in ceramic glazes does not affect the final glaze, although the firing temperature may be slightly lower due to the surprisingly low fusion temperature of the ash. In ceramic bodies, however, the results are not so predictable. Number of test bodies with different types of clays and shale and with varying amounts of volcanic ash indicated that 7–15% volcanic ash additions to shale or red-firing clay body lowers the vitrification temperature, increasing the firing range for a matured body, and producing a greater rigidity in the ware at the maximum temperature. These qualities produced by the volcanic ash additions permit economy in use of fuel, and reduce losses in the kiln due to the less critical temperature range requirements and the ability of the ware to stand up under its own weight at the maximum temperatures attained in the kiln.

10.3.4 In Glass and Vitreous Enamels

Volcanic ash has the same function in glass and vitreous enamel as it has in case of ceramic glazes. Because of the lower content of the iron oxide, the use of volcanic ash in glass and vitreous enamels products is limited. Volcanic ash could be an important ingredient in fiber glass and foam glass where the slight darkening of color is not very important.

10.3.5 In Light Weight Aggregates, Cellular Blocks, and Concrete

Volcanic ash could be used for making lightweight aggregates. The Oklahoma Geological Survey has investigated the possibility of producing light-weight aggregates, cellular blocks and concrete. Besides having cementing properties, volcanic ash can also serve the purpose of a fine aggregate that fills the voids between the fine sand aggregate and the cement. It can be used in concrete as partial replacement of cement.

10.3.6 Miscellaneous Uses

Volcanic ash could be used as the main ingredient in some sweeping compounds, as insulation in packing water and steam pipes, lagging boilers, and as loose fill insulation in walls and ceilings. It can also be used as filler or diluents in paint and as a carrier for insecticides. Volcanic ash has been used for the purification and clarification of oils by filtration.

10.4 Effect of Volcanic Ash on Soil Properties

Naji (2002) conducted a study on natural volcanic ash in order to assess the performance of lime-stabilized mixture (lime-volcanic ash and fine materials). The natural volcanic ash was collected from the vicinity of Sana'a city, Yemen. The samples were collected from a hole one meter below the natural surface level. Volcanic ash used in this investigation neither had clay content nor plasticity index, therefore, fine soils that has some clay content and plasticity index needed to be added to the ash to enhance the gradation of the ash to produce desirable reaction between the lime and ash. For this purpose, two different types of fine soils were used each at different proportions of dry weight of mixture samples, specifically at 15 and 25% of dry weight of samples. Properties of volcanic ash and that of two types of soils are given in Table 10.8. Tests were performed for materials characterization, compaction, deformation properties and strength characteristics.

10.4.1 Maximum Dry Density

Figure 10.3 shows the effect of lime content on the maximum dry density. The maximum dry density and optimum moisture content for treated volcanic ash with 25%

Table 10.8 Properties of volcanic ash and fine soils (Naji, 2002)

Property	Value		
	Volcanic ash	Soil-1 (silty)	Soil-2 (clayey)
Specific gravity	2.21	2.67	2.72
Liquid limit (%)	NP	26	38
Plasticity Index (%)	NP	7	15
Organic matters (%)	Nil	0.42	0.53
Passing #200 sieve (%)	Nil	75	94
Clay content (%)	Nil	3	12
Sulfate content (%)	Nil	0.005	0.003
Unified classification	GW	ML	CL
AASHTO classification	A-1-a	A-4	A-6
Coefficient of uniformity	5.6	—	—
Coefficient of curvature	1.15	—	—
Wearing (%)	53	—	—

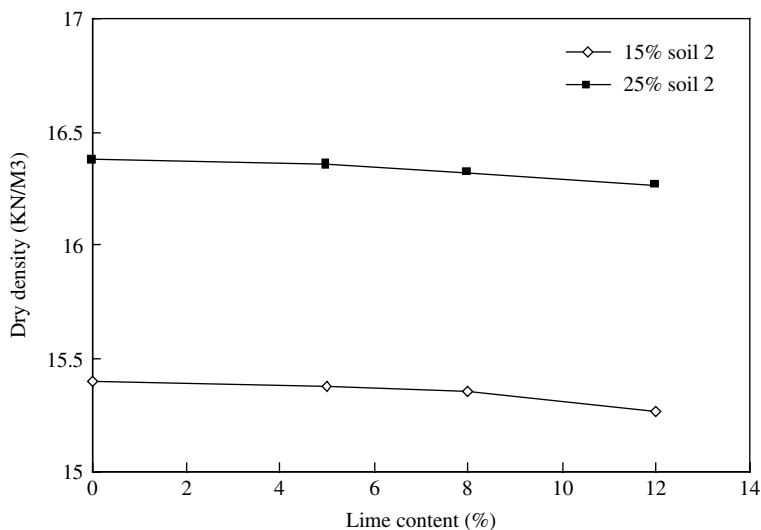


Fig. 10.3 Effect of lime content on maximum dry density (Naji, 2002)

soil-2 were greater than those of the corresponding cases of the volcanic ash with 15% soil-2 due to the high percentage of soil-2 which has higher specific gravity and plasticity. Similar results were obtained for ash-soil1 mixtures but the maximum dry density and optimum moisture content for untreated and treated ash with soil-1 are less than those of the corresponding cases of ash with soil-2 due to the lower specific gravity and plasticity of soil-1.

10.4.2 Deformation Properties

Samples prepared at optimum moisture content for various volcanic ash-lime-soil combinations, were tested for stress-strain behavior. Figure 10.4 shows that, in general, with increased curing time, failure stress increased and the corresponding ultimate strain decreased for ash-soil-lime mixture and this could be attributed to allowing a longer time for lime to hydrate and forming a strong skeleton structure throughout the material binding the ash grains together.

10.4.3 Compressive Strength Characteristics

Strength properties were studied using unconfined compressive strength. From stress strain curves the maximum compressive strength was obtained. As expected, results revealed that compressive strength of lime soil mixtures is dependent on lime content added, soil type, soil content and curing time.

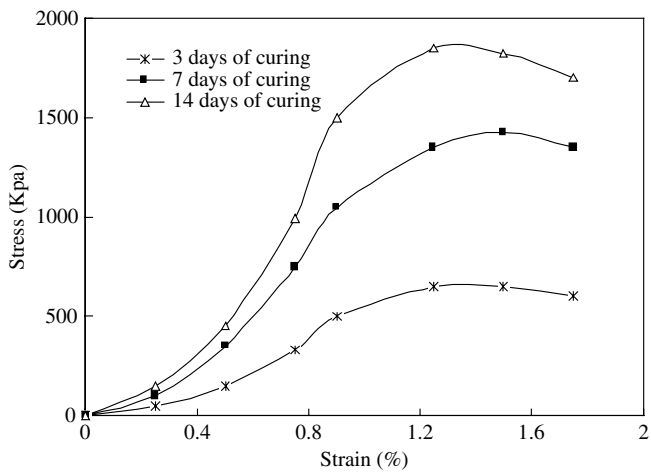


Fig. 10.4 Typical stress-strain curves (Naji, 2002)

10.4.3.1 Effect of Lime Content

The effect of lime content on the unconfined compressive strength of volcanic ash mixed with soil-1 and soil-2 at the age of 7 days is shown in Fig. 10.5. It is clear from the figure that there was substantial increase in compressive strength with the increase in lime content. This trend continued until 8% lime content. After that the increase in strength became insignificant with increasing lime until a content of 12%. The reason behind such behavior may be attributed to the degree to which the soil-lime pozzolanic reaction had proceeded. Because the soil content

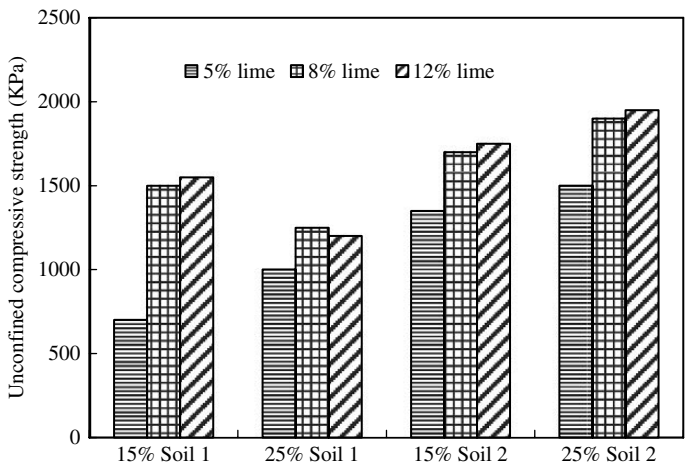


Fig. 10.5 Effect of lime content on unconfined compressive strength at 7 days of curing (Naji, 2002)

was limited only to 15 and 25% of the mixture, adding lime will cause cation exchange and flocculation-agglomeration with soil particles and results in increase of strength. Such reactions will continue until reaching the optimum value, in this case was about 8% of lime content. After this stage any more lime content might be redundant and will cause less reaction and therefore, marginal strength will be gained. In general, strength of volcanic ash with soil-2 for various lime content was higher than the strength of the volcanic ash with soil-1 under same conditions. This could be attributed to the fact that soil-2 had higher percentage of clay and plasticity. Since the fine particles are a good source of silica and alumina, the extent of soil-lime pozzolanic reaction is higher in case of soil-2 and this led to better results.

10.4.3.2 Effect of Soil Content

Effect of the soil content on the unconfined compression strength is shown in Fig. 10.6. Irrespective of soil type, it is evident from this figure that as the amount of the added soil increased, the compressive stress increased. Strength gained with the addition of soil-2 was higher than that gained with soil-1. This is true for all samples regardless of lime content or curing duration.

10.4.3.3 Effect of Soil Type

Figure 10.7 shows the effect of soil type on strength of samples with 8% lime content and 7 days curing time. The figure indicates that samples containing soil-2 generally had higher strengths than samples with soil-1. This might be due to the fact that lime reacts better with clayey soils rather than silty soils. Clay soils have high plasticity, higher surface area and contain higher percentage of silica and alumina. Thus,

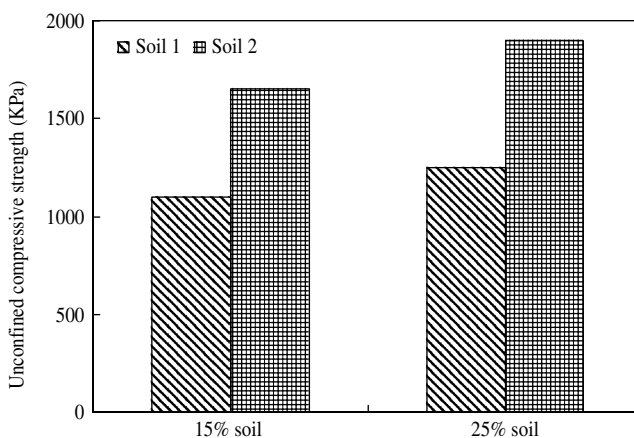


Fig. 10.6 Effect of soil content on unconfined compressive strength, 8% lime and 7 days of curing (Naji, 2002)

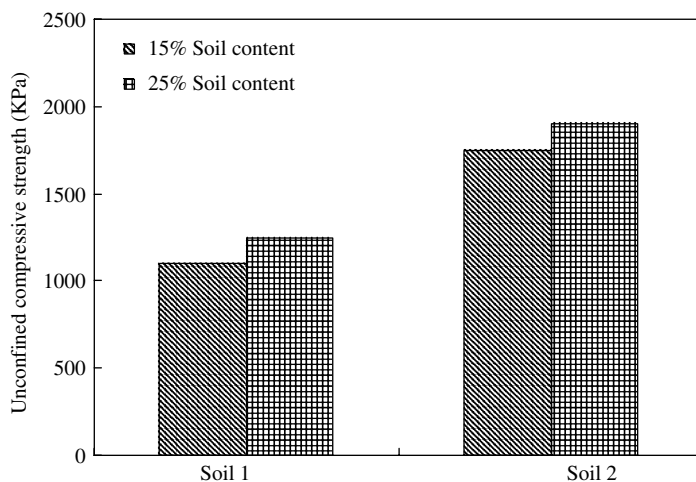


Fig. 10.7 Effect of soil type on unconfined compressive strength, 8% lime and 7 days of curing (Naji, 2002)

efficiency of reaction associated with soil-2 was higher than that associated with soil-1 and this led to high strength gained for mixes with soil-2 when other variables are kept constant. Moreover, clay particles have the ability to act as a cementation agent in the mixture with the presence of water. When compacted mixtures were cured, the clay particles seem to crystallize and form a kind of bonding between ash particles, which resulted in additional increase in compressive strength for samples that contained soil-2. However, this kind of bond might be affected if samples are subjected to soaking in water.

10.4.3.4 Effect of Curing Time

The effect of curing period on the unconfined compressive strength is presented in Fig. 10.8. The figure shows the effect of curing time for ash mixed with 15% of soil-1 and soil-2 individually and with 8% lime content. The figure indicates that the strength of ash-soil-lime mixture is time dependent where strength gained gradually due to the formation of cementation agent that produced due to the reaction of lime with fine soil particles. This agent crystallizes slowly into an interlocking matrix and increased the samples strength. Longer curing period allowed longer time for lime to react and form a strong skeleton structure throughout the material binding the ash grains together. For short curing time the reaction of lime did not reach advanced stages and this resulted in remaining of soil of the molding water between ash grains, which loosened the mixture. For longer curing period, more efficient lime reaction took place and may be utilizing all the water within the mixture.

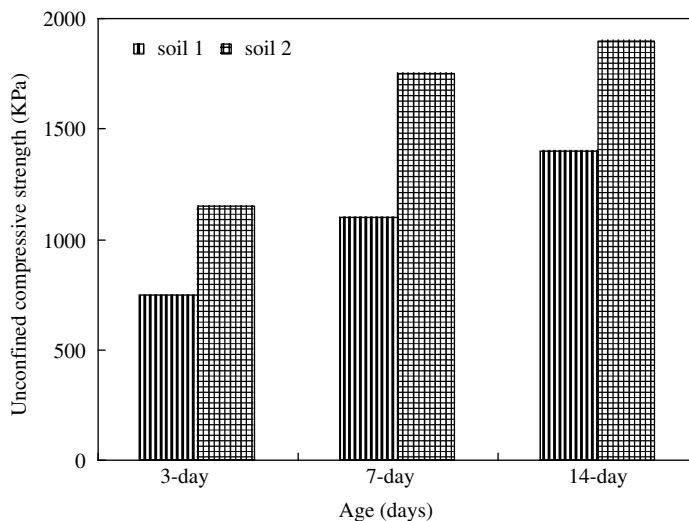


Fig. 10.8 Effect of curing time on unconfined compressive strength, 8% lime and 15% soil content (Naji, 2002)

10.5 Properties of Blended Cement Containing Volcanic Ash

10.5.1 Consistency and Setting Times

Hossain (2003) investigated the effect of partial replacement of cement by volcanic ash (VA) and pumice powder (VP) on the consistency and setting times of blended cement. Percentage replacement varied from 0 to 50%. Volcanic ash (VA), pumice powder (VP) and cement were chemically analyzed. Chemical analysis indicated that the VA and VP had very similar compositions and had silica content of about 60%, while silica in cement was 65%. Both VA and VP had compounds such as calcium oxide, alumina and iron oxide (total about 31%). The amount of oxides of sodium and potassium known as 'alkalies', was higher in VA (5.83%) and VP (7.69%) than that in cement (2.6% maximum). Variation in normal consistency and setting times with different percentages of VA and VP are presented in Table 10.9.

Normal consistency decreased by 13.8% for VA and by 12.4% for VP when the VA or VP content was varied from 0 to 50%. The normal consistency decreased by 3.79% when the VP content was increased from 0 to 25% compared to 5.17% in the case of VA. The decrease in normal consistency was due to the reduction of cementitious binder in the fresh mixture with the increase of VA or VP content. On the other hand, specific gravity of VA or VP was less than that of cement, which resulted in the larger volume of VA or VP compared to the volume of cement replaced as the replacement was made by mass. As a result, the overall volume was increased needing more water to form a paste of same consistency for different % of VA and VP in the mixture.

Table 10.9 Effect of volcanic ash and pumice powder on consistency and setting times of cement (Hossain, 2003)

Mixture details	Normal consistency (%)		Setting times (hours)			
			Initial		Final	
	VA	VP	VA	VP	VA	VP
100-0	29.0	29.0	3.15	3.15	3.15	5.15
98-2	29.0	28.6	3.15	3.16	3.16	5.15
96-4	29.0	28.8	3.15	3.18	3.18	5.15
94-6	28.8	28.7	3.20	3.20	3.20	5.15
90-10	28.5	28.6	3.30	3.20	3.20	5.20
85-15	28.0	28.5	3.45	3.30	3.30	5.20
80-20	28.0	28.2	3.45	3.40	3.40	5.25
75-25	27.5	27.9	3.80	3.60	3.60	5.80
65-35	26.0	26.7	4.25	4.15	4.15	6.20
50-50	25.0	25.4	6.00	6.10	6.10	8.20

Setting times results showed an increase in both setting times with the increase in VA or VP content. Initial setting time increased by 90% (compared to 93.7% in VP) where as increase in final setting time was 58% (compared to 59.2% in VP) with the increase in VA content from 0 to 50%. For the case of VP, initial setting time increased by 14.28% (compared to 20.6% in VA) and final setting time increased by 12.62% (compared to 16.5% in VA) when VP content was increased from 0 to 25%. This was reasonable as the increase of VA or VP content reduced the cement content in the mixture and also decreased the surface area of the cement. As a result, the hydration process slowed down causing setting time to increase. The slow hydration means low rate of heat development. This is of great importance in mass concrete construction, for which Portland volcanic ash cement (PVAC) or Portland volcanic pumice cement (PVPC) can be mostly used, besides other general uses.

10.5.2 Compressive Strength

Hossain (2003) studied the effect of partial replacement of cement with volcanic ash (VA) and pumice powder (VP) on the compressive strength of cement mortar. Percentage replacement varied from 0 to 50%. Tests were conducted up to the age of 28 days and results are given in Table 10.10. Based on the results, he concluded that: (i) compressive strength decreased with the increase in VA or VP content. This was due to the reduction of cement content in the mix with the increase of VA or VP content. The finely divided silica (61%) in VA or VP can combine with calcium hydroxide (liberated by the hydrating PC) in the presence of water to form stable compounds such as calcium silicates, which have cementitious properties. Such pozzolanic action of VA or VP contributed to the enhancement of strength and long-term durability although the reduction of strength in blended cement due to cement replacement by VA or VP was not compensated; (ii) strength got reduced by

Table 10.10 Effect of volcanic ash and pumice powder on the compressive strength of cement mortar (Hossain, 2003)

Mixture details	Compressive strength of mortar (MPa)							
	Volcanic ash (VA)				Pumice powder (VP)			
	Age (days)				Age (days)			
	1	3	7	28	1	3	7	28
100-0	10.6	21.6	28.6	37.5	10.6	21.6	28.6	37.5
98-2	10.0	19.9	27.1	36.0	9.9	18.6	26.4	34.5
96-4	9.4	19.3	27.2	35.6	9.7	18.4	26.7	34.9
94-6	9.0	18.9	26.5	34.7	9.5	18.6	26.6	34.8
90-10	9.1	18.4	26.6	35.1	9.3	18.3	26.1	34.2
85-15	8.7	18.1	24.2	29.6	8.9	18.0	25.6	33.2
80-20	8.3	17.8	25.9	33.9	8.4	16.7	22.9	30.0
75-25	7.9	17.0	22.4	26.7	8.0	15.9	22.1	28.4
65-35	7.1	15.5	21.3	23.9	7.5	15.1	21.1	24.3
50-50	4.2	6.4	8.1	16.5	5.1	7.4	9.2	16.4

21% (1-day), 18% (3-days) and 9.5% (7 and 28-days) when VA content varied from 0 to 20%. Strength reductions at 35% VA were 19% (7-days) and 31% (28-days) while at 50% VA, the reductions were 70% (7-days) and 52% (28-days); (iii) VP mixtures also showed a similar pattern of strength variation. Strength was reduced by 26% (1-day strength), 26.4% (3-days), 22.7% (7-days) and 24.2% (28-days) when VP content was varied from 0 to 25%; and (iv) it was possible to obtain a mortar having a strength of 21 MPa (7-days) and 24 MPa (28-days) using locally available sand and replacing 35% of cement by VA or VP.

10.5.3 Microstructure of Hydration Products

Escalante-Garcia and Sharp (2004) examined the microstructure of hydration products of blended cements. Pastes of neat and blended Portland cement (incorporating either 60% ground granulated blast furnace slag, or 30% pulverized fuel ash, or 22% volcanic ash) were cured for one year at temperatures ranging from 10°C to 60°C. Microstructure of backscattered electron images (BEI) of the OPCS-VA blended cement after curing for 1 year at 10 and 60°C are shown in Fig. 10.9. The microstructure observed after curing at 10°C indicated a high degree of hydration of the anhydrous phases in the cement and low porosity (Escalante-garcia and Sharp, 1998; Escalante-Garcia and Sharp, 2001), whereas the porosity after curing at 60°C was appreciably greater. The apparent porosity of the pastes increased with increasing curing temperature. Chemical analysis data for the hydration products in ternary composition diagrams indicated that in the presence of the replacement materials the composition of the C-S-H shifted towards higher Si (from 0.31 for OPC to 0.35 for OPC-VA paste) and Al contents (0.031 for OPC to 0.045 for OPC-VA paste), whereas that of Ca was lower (0.66 for OPCS to 0.61 for OPCS-VA paste).

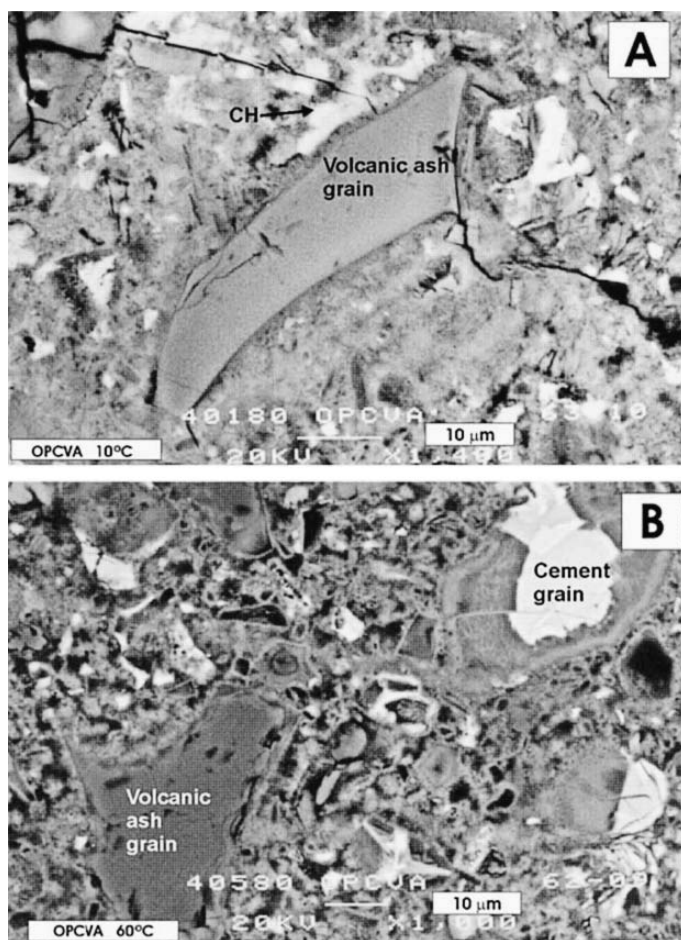


Fig. 10.9 BEI of OPCVA-VA cured for 1 year at (A) 10°C and (B) 60°C (Escalante-Garcia and Sharp, 2004)

10.5.4 Alkali-Silica Reaction and Autoclave Expansion

Hossain (2005b) investigated the alkali-silica reaction, autoclave expansion, and strength activity index of Portland cement were volcanic ash (VA) and pumice powder (VP) were used as additives. Cement was replaced in varying percentages by VA and VP (0–40%). Alkali-silica reaction and strength activity index tests were conducted as per ASTM C 311 (2000), and autoclave expansion tests as per ASTM C 151 (2000). Results of alkali-silica reaction are given in Table 10.11, and that of autoclave expansion and strength activity index (SAI) in Table 10.12, respectively. Based on the test results, he concluded that: (i) for the effectiveness in the alkali-silica reactions as per ASTM C 618, the expansion (the ratio between the length change of the test mix and that of the control mix) at day 14 should have a

Table 10.11 Effect of volcanic ash (VA) and pumice powder (VP) on the alkali-silica reaction (Hossain, 2005b)

VA or VP content (%)	VP		VA	
	Length change (mm)	Expansion (%)	Length change (mm)	Expansion (%)
0 (Control)	0.089	—	0.089	—
10	0.115	129	0.101	113
20	0.095	105	0.088	99
30	0.087	98	0.082	92
40	0.081	91	0.075	84

maximum value of 100%. Mix with 10% VP or VA content showed the maximum length change and the highest reduction in length value. Mixes with 30 and 40% VP or VA content, on the other hand, satisfied the ASTM C 618 requirement; (ii) the autoclave expansion of the paste mixes decreased with the increase in VP and VA content. All mixes containing up to 40% VP or VA, satisfied the ASTM C 618 requirement of 0.8% maximum; and (iii) the strength activity index (SAI), which is the ratio between the strength of the tested samples and the strength of the control samples, is calculated at 7 and 28 days. The SAI value ranged between 78% and 100% at 7 days and between 67% and 100% at 28 days. SAI values for mixes with 10%, 20%, and 30% VA or VP content are more than 75% as required by ASTM C 618 (1993).

10.5.5 Electrical Resistivity

Hossain and Lachemi (2004a) reported the results of the electrical resistivity of volcanic ash blended cement mortar. The mortars had 20% and 40% VA as cement replacement and water/binder ratio of 0.55. The electrical resistivity was measured with an automatic LCR meter by applying a 10-mV AC at 1 kHz across saturated specimens (50 mm in diameter and 50 mm thick) using copper plate electrodes.

Table 10.12 Effect of volcanic ash (VA) and pumice powder (VP) on the autoclave expansion and strength activity index (SAI) (Hossain, 2005b)

VA or VP content (%)	Autoclave expansion (%)		Strength activity index (SAI)			
	VP	VA	VP		VA	
			7 days	28 days	7 days	28 days
0 (Control)	0.40	0.40	—	—	—	—
10	0.28	0.25	96	94	100	100
20	0.24	0.21	85	83	96	94
30	0.19	0.17	81	78	81	75
40	0.16	0.14	78	67	78	67

The instrument gave value of the electrical resistance. The value of the resistance measured was then used to calculate the electrical resistivity. The tests were conducted at 7, 28, 91, and 180 days of moist curing. Variation of electrical resistivity of volcanic ash blended cement mortar with curing time is shown in Fig. 10.10. They concluded that electrical resistivity of the cement-VA mortars increased rapidly with the curing time. The 40% VA mortars had shown substantially higher resistivity than 20% VA mortars whereas the resistivity of the control mortar (0%VA) did not increase with the curing time especially in the long term and remained lower than the VA mortars. Electrical current through hydrating cement mortar is electrolytic (i.e., mainly due to the flow of ions through the pore spaces). Hence, the electrical resistivity is an indirect measurement of porosity and diffusivity (Ping et al., 1995). In reinforcement of concrete structures, at the onset of corrosion of the bars, the corrosion current and hence the rate of corrosion is influenced by the electrical resistivity of VA blended cement mortars. It would enhance the overall resistivity of VA blended concrete and hence a lower degree of bar corrosion after the breakdown of passivity.

10.5.6 Total Pore Volume (TPA)

Hossain and Lachemi (2004a) studied the total pore volume of volcanic ash blended cement mortar. The mortars had 20% and 40% VA as cement replacement and water/binder ratio of 0.55. The mercury intrusion porosimetry was used to measure the TPV of the cement and cement-VA mortars. The tests were conducted at 7, 28, 91, and 180 days of moist curing. The TPV decreased with the increase of curing time as shown in Fig. 10.11. The increase of VA contents increased TPV. Mortar specimens with 40% VA showed higher TPV than the specimens with 0% and 20% VA.

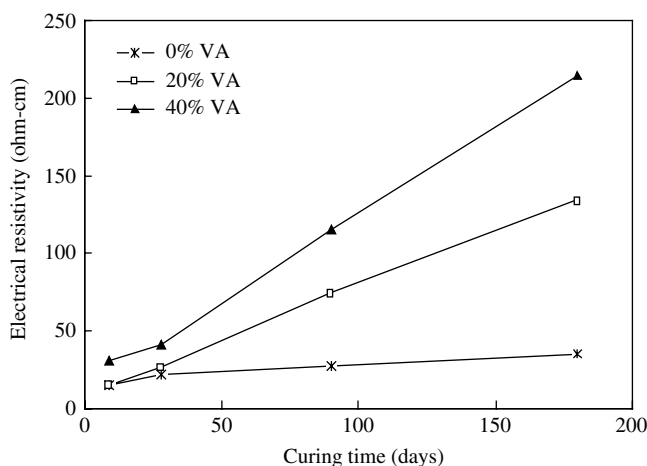


Fig. 10.10 Variation of electrical resistivity with curing time and % VA (Hossain and Lachemi, 2004a)

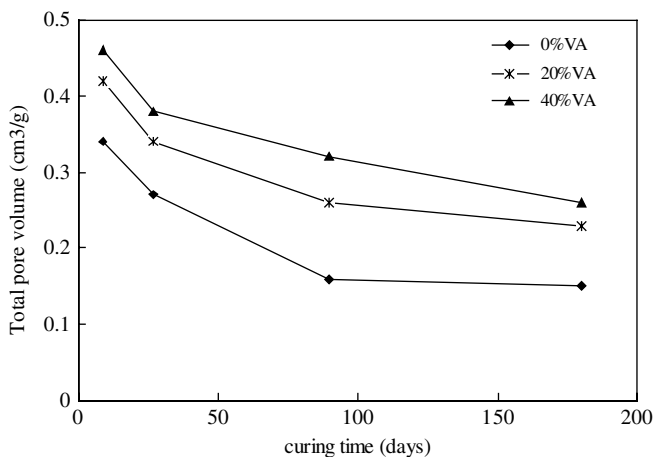


Fig. 10.11 Total pore volume (TPA) as function of curing time and VA content (Hossain and Lachemi, 2004a)

10.6 Properties of Concrete Containing Volcanic Ash

10.6.1 Compressive Strength

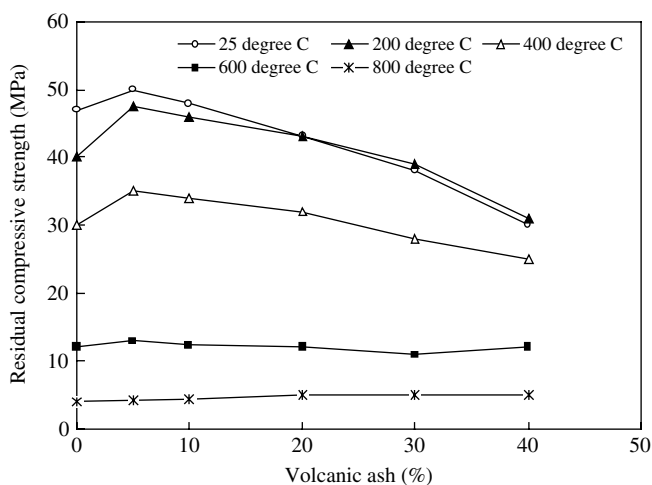
Hossain and Lachemi (2004b) investigated the residual compressive strength of concretes made with 0–40% of volcanic ash (VA) as cement replacement by mass, subjected to high temperatures up to 800°C. Volcanic ash had Calcium Oxide (6.1%), Silica (59.3%), Alumina (17.5%), Iron Oxide (7%), Sulfur Trioxide (0.7%), Magnesia (2.6%), Sodium Oxide (3.8%), LOI (1%), and its fineness was 285 m²/kg. Initial tests for air content, slump and 28-days compressive strength were conducted and the results are given in Table 10.13. 100-mm concrete cubes were subjected to high temperatures and residual compressive strength results of volcanic ash concrete (VAC) are shown in Fig. 10.12. They concluded that: (i) from 25 to 200°C, the VAC with 20 to 40% VA showed an increase in strength. The strength gain was probably due to the formation of tobermorite, which was formed by reaction between unhydrated VA particle and lime at high temperature (Nasser and Marzouk, 1979). The strength of control OPC however was decreased by about 14%. No visible cracking or spalling was absorbed at this temperature range; (ii) from 200 to 400°C, a significant decrease was observed in VAC, which was 19–33% of the original strength. This reduction was due to the pore structure coarsening in such concretes (Chan et al., 1996); (iii) severe loss in strength was observed in 400–600°C temperature range. The strength loss was within the range of 59–73%. The VAC performed better and showed no cracking except hairline cracks. The better performance of VAC in temperature was due to reduced amount of $\text{Ca}(\text{OH})_2$, which otherwise resulted in strength loss and disintegration (Chan et al., 1999); (iv) at 800°C all the concrete showed severe deterioration due to the decomposition of C-S-H gel

Table 10.13 Mixture details of volcanic ash concrete (Hossain and Lachemi, 2004b)

Mixture ID	VA (%)	w/b	Cement (kg/m ³)	Aggregates (kg/m ³)		Air content (%)	Slump (mm)	28-days compressive strength (MPa)
				FA	CA			
VA-0	0	0.45	400	760	1020	2.5	80	41.4
VA-05	5	0.45	380	755	1020	2.5	80	42.9
VA-10	10	0.45	360	751	1020	2.6	90	40.8
VA-20	20	0.45	320	743	1019	2.8	110	35.2
VA-30	30	0.45	280	734	1019	2.9	86	30.7
VA-40	40	0.45	240	725	1018	3.1	85	25.2

(Lin et al., 1996); and (iv) generally, strength loss decreased with the increase of VA content when the temperature was varied from 200–800°C. This was an indication of better performance of VAC in retaining the strength at evaluated temperature as compared to control OPC concrete. The deterioration of strength at evaluated temperature for such concretes were due to the coarsening of pore structure and increase in pore diameter. The beneficial effect of pozzolanic VA was more pronounced at temperatures below 600°C. Spalling was observed in 10% of controlled OPC concrete specimens while VAC only showed visible network of fine structure cracks.

Hossain (2005c) examined concrete specimens made with different plain (ASTM I, II, and V) and blended cements incorporating different percentages of volcanic ash (VA) up to 30% as cement replacement. The specimens were exposed to marine environment for a period of 1 year. A set of combinations with mixing water and initial curing conditions were studied such that cast in situ and precast conditions of concrete in marine environment were simulated. Tests were conducted for

**Fig. 10.12** Residual compressive strength as function of volcanic ash for different temperature levels (Hossain and Lachemi, 2004b)

compressive strength under three different curing conditions. Curing conditions were; ordinary water ordinary water (OWOW), sea water sea water (SWSW), and ordinary water sea water (OWSW). Based upon the experimental study, he concluded that: (i) compressive strength of concrete decreased in a marine environment and the strength loss increased with the age of exposure; (ii) use of Types I and II blended cements with VA (between 10 and 20%) increased concrete resistance against sea-water attack; (iii) use of VA in combination with Portland cements with very low C_3A content such as ASTM Type V, did not result in a level of resistance equal to or greater than that of Types I or II Portland cements in marine environments; (iv) precasting is beneficial in marine environments in all three types of plain and blended cements. In some cases, the loss in strength has been reduced to even more than 35% in simulated precast situations; and (v) the blending of VA in Type I cement was observed to be more beneficial than the blending in Types II or V cements against marine environments in both simulated precast and cast in situ situations.

10.6.2 Chloride-Ion Resistance and Porosity

Hossain and Lachemi (2004b) reported the chloride-ion resistance and porosity of concretes made with 0–40% of volcanic ash (VA) as cement replacement. Details of the mixture proportions are given in Table 10.13. Chloride permeability tests were conducted as per ASTM C 1202 (1997) whereas porosity was measured by using MIP on specimens subjected to 25°C, 600°C, and 800°C temperatures. Chloride-ion resistance and porosity results of volcanic ash concrete (VAC) are shown in, Figs. 10.13 and 10.14 respectively. Based on the results, they reported: (i) a clear relationship between the residual compressive strength and concrete permeability, as more permeable specimens showed more pronounced loss of compressive strength. As the temperature was increased, a severe loss in impermeability was observed, possibly due to loss ranged from 500 to 2000%. The ASTM C 1202 (1997) specifies the concrete as highly permeable if the charge that passes through it is more than 4000 Coulombs. Because all the specimens showed values higher than 4000 Coulombs after fire, such concretes can be considered as no durable depending upon the situation, even if they retain a higher proportion of their compressive strength; and (ii) MIP test results clearly indicated an increase in porosity with the increase in temperature. This effect can be related to the coarsening of pore structure possibly due to micro cracks formed due high temperature (Chan et al., 1996) and was responsible for the strength and permeability loss. A significant decrease in porosity was observed in VAC by the addition of pozzolanic VA as compared with the control OPC concrete even at elevated temperatures.

Hossain (2005c) studied the porosity of concrete mixtures made with different plain (ASTM I, II, and V) and blended cements incorporating different percentages of volcanic ash (VA) up to 30% as cement replacement. The specimens were exposed to marine environment for a period of 1 year. Tests were conducted for

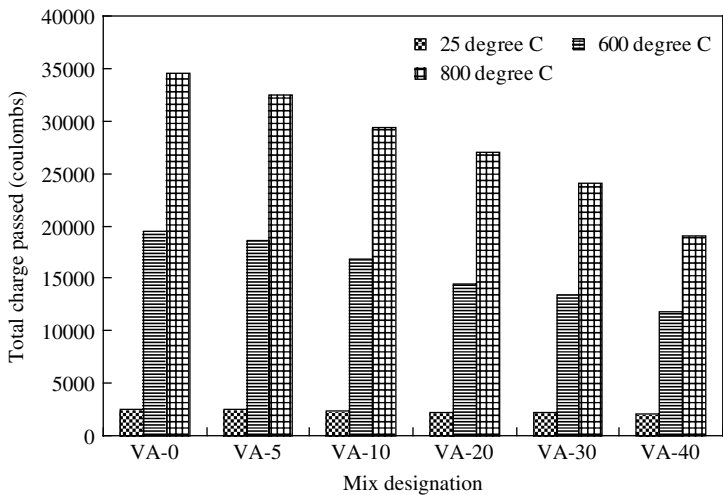


Fig. 10.13 Effect of high temperature on chloride-ion resistance of volcanic ash concretes (Hossain and Lachemi, 2004b)

porosity and rapid chloride permeability under three different curing conditions. Curing conditions were; ordinary water ordinary water (OWOW), sea water sea water (SWSW), and ordinary water sear water (OWSW). Based upon the experimental study, he concluded that blending Type I cements with 20% VA produced the best performance showing lower porosity and higher chloride ion resistance under both OWSW (precast) and SWSW (cast in situ) situations. This indicated that a Type I blended VA cement is a potential choice for the construction of marine structures. In view of the high chloride combining capacity of high C_3A Type I cement; and (vii)

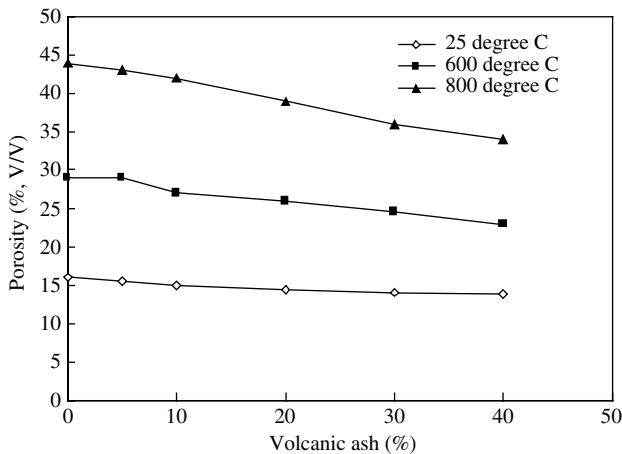


Fig. 10.14 Porosity of volcanic ash concrete as function of volcanic ash content for different temperature levels (Hossain and Lachemi, 2004b)

the use of precasting in place of casting in situ will further increase the resistance of concrete against marine environments.

Hossain and Lachemi (2006) evaluated the performance of volcanic ash (VA) and finely ground volcanic pumice (VP) based ASTM Type I and Type V (low C_3A) blended cement concrete mixtures. 0 and 20% VA or VP were used in blended cement for preparing concrete mixtures with two (0.35 and 0.45) water-to-binder ratio. Tests were conducted for density, compressive strength and rapid chloride permeability, and porosity. Table 10.14 summaries strength and density (at 28 days) of concrete mixtures as well as test results of RCP and, MIP tests conducted at 56 day. They concluded that (i) 28-day density of concrete mixtures varied between 2360 and 2410 kg/m^3 ; (ii) Type I/V VA/VP based blended concrete showed lower strength, higher chloride ion resistance and lower porosity/average pore diameter than Type I/V plain concrete: this can be attributed to the fact that the strength gain of VA/VP based pozzolanic concrete is not merely related to lowering of porosity; (iii) concrete mixtures with higher W/B showed lower strength, lower chloride ion resistance and higher porosity/ average pore diameter; and (iv) use of type V cements showed slightly better chloride ion resistance and lower porosity with no visible strength gain compared to Type I; and (iv) VP based concrete showed lower chloride ion resistance and higher porosity compared with VA based concrete with no significant 28-day strength difference.

10.6.3 Sulfate Resistance

Hossain and Lachemi (2006) compared the performance of volcanic ash (VA) and finely ground volcanic pumice (VP) based ASTM Type I and Type V (low C_3A)

Table 10.14 Strength, durability and micro-structural properties of concrete (Hossain and Lachemi, 2006)

Mixtures	28-day density (kg/m^3)	28-day compressive strength (MPa)	RCPT (C) at 56 days	Porosity (%)	Average pore diameter (μm)
W/B = 0.45					
Type I	2401	38	2850	16.46	0.0464
Type V	2403	37	2805	16.39	0.0461
20VA-I	2384	32	2210	14.95	0.0435
20VP-I	2380	31	2186	14.89	0.0428
20VA-V	2365	31	2321	15.40	0.0444
20VP-V	2360	30	2316	15.35	0.0438
W/B = 0.35					
Type I	2410	49	2350	15.10	0.0432
Type V	2408	48	2306	15.03	0.0427
20VA-I	2401	41	1920	13.20	0.0402
20VP-I	2398	40	1905	13.11	0.0395
20VA-V	2372	42	1985	13.60	0.0413
20VP-V	2370	41	1966	13.51	0.0403

blended cement concrete mixtures. 0 and 20% VA or VP were used in blended cement for preparing concrete mixtures with two (0.35 and 0.45) water-to-binder ratio. Concrete mixtures were immersed in magnesium–sodium sulfate solution for period up to 48 months. They determined weight loss and corrosion resistance. Results are given in Table 10.15. They concluded that: (i). Type I/V VA/VP based blended cement concrete specimens showed higher and faster rate of deterioration than those of Type I/V plain cement concrete specimens. The higher deterioration in Type I and Type V VA/VP based blended cement concretes in sulfate environment compared to Type I and Type V plain Portland cement concretes can be attributed to the presence of Mg^{2+} cations associated with $MgSO_4$. The consumption of portlandite ($Ca(OH)_2$) by the pozzolanic reaction in VA and VP blended cements causes Mg^{2+} cations to react directly with the calcium silicate hydrate (C–S–H) gel converting it to cohesion less, porous, reticulated magnesium silicate hydrate (M–S–H) gel; (ii) use of Type V cements reduced the deterioration of VA/VP based concrete specimens compared with those of Type I possibly due to lower C_3A content. However, Type I/V VA/VP based blended cement concrete specimens exhibited weight loss which were more than the 2.5% failure criterion; (iii) Type I/V VA/VP based blended cement concretes showed inferior performance compared with Type I/V plain cement concretes in terms of corrosion resistance. This could be attributed to the advance stage of deteriorations (in Type I/V VA/VP based blended concretes) at this period whereby a weight loss that ranged between 7.47% and 15.4% which is higher than 2.5%, was observed. High degree of deterioration in blended cement concrete mixtures could not preserve the integrity of the internal structure and enabled the SO_4 ions to diffuse to the steel, leading to corrosion of reinforcing steel; (iv) on the contrary, the specimens made with plain Type I/V cements exhibited better resistance to sulfate attack, especially specimens with W/B of 0.35 where reinforcing steels were not found to be in active state of corrosion (polarization

Table 10.15 Weight loss, corrosion potential and polarization resistance after 48 months of exposure (Hossain and Lachemi, 2006)

Mixtures	Concrete weight loss (%)	Corrosion potential, SCE (mV)	Polarization resistance ($k\Omega\text{ cm}^2$)	Corrosion initiation (months)
W/B = 0.45				
Type I	1.34	-434	51	44
Type V	1.51	-372	69	44
20VA-I	15.4	-749	22	44
20VP-I	14.6	-704	22	44
20VA-V	11.1	-738	8	44
20VP-V	10.9	-701	8	44
W/B = 0.35				
Type I	5.7	-245	630	No corrosion
Type V	3.3	-203	347	No corrosion
20VA-I	11.6	-784	25	44
20VP-I	11.0	-753	26	44
20VA-V	7.7	-736	40	44
20VP-V	7.5	-707	41	44

resistance $N87 \text{ k}\Omega\text{cm}^2$) after 48 months of exposure. This might be attributed to the mechanism of MgSO_4 attack as well as to the diffusion of SO_4 ions; and (v) Initial polarization resistance on steel in various concrete mixtures was very high (ranging between 5200 and 6400 $\text{k}\Omega \text{ cm}^2$ for concrete mixtures with w/b 0.45; between 3600 and 5600 $\text{k}\Omega\text{cm}^2$ for concrete mixtures with w/b .35). The polarization resistance decreased significantly (rate of decrease seems to be higher in Series A with W/B of 0.45 compared to Series B with W/B of 0.35) in an immersion period of 48 months.

References

- ASTM C 618 (1993) Standard specification for coal fly ash and raw or calcined natural pozzolan for use as a mineral admixture in concrete, Annual Book of ASTM Standards, Philadelphia, USA.
- ASTM C 1202 (1997) Test method for electrical indication of concrete's ability to resist chloride ion penetration. ASTM International, West Conshohocken, Philadelphia, USA, 6 pp.
- ASTM C 151 (2000) Standard test method for autoclave expansion of Portland cement, Annual Book of ASTM Standards, Philadelphia, USA.
- ASTM C 311 (2000) Standard test methods for sampling and testing fly ash or natural pozzolans for use as a mineral admixture in Portland cement concrete, Annual Book of ASTM Standards, Philadelphia, USA.
- Cas RAF, Wright JV (1988) Volcanic successions: modern and ancient, Chapman & Hall, London, p. 528.
- Chan SYN, Peng GF, Anson M (1999) Residual strength and pore structure of high strength concrete and normal strength concrete after exposure to high temperature. *Cement and Concrete Composites* 21: 23–27.
- Cronin S, Hedley M, Smith G, Turner M (1996) Impacts on soil and pasture chemical composition, in impacts of October 1995 Ruapehu ash fall on soil fertility: Department of Soil Science and Fertilizer and Lime Research Centre, Massey University, 33 p.
- Deer WA, Howie RA, Zussman J (1978) An introduction to rock forming minerals, Longman, London, 528 pp.
- Escalante-Garcia JJ, Sharp JH (1998) Effect of temperature on the hydration of the main clinker phases in Portland cements: Part II, Blended cements. *Cement and Concrete Research* 28: 1259–74.
- Escalante-Garcia JJ, Sharp JH (2001) The microstructure and mechanical properties of blended cements hydrated at various temperatures. *Cement and Concrete Research* 31: 695–702.
- Escalante-Garcia JJ, Sharp JH (2004) The chemical composition and microstructure of hydration products in blended cements, *Cement and Concrete Composites* 26: 967–976.
- Johnston DM (1997) Physical and social impacts of past and future volcanic eruptions in New Zealand, Unpublished Ph.D. Thesis, University of Canterbury, Christchurch, 288 p.
- Hossain, KMA (2003) Blended cement using volcanic ash and pumice. *Cement Concrete Research* 33: 1601–1605.
- Hossain KMA, Lachemi M (2004a) Corrosion resistance and chloride diffusivity of volcanic ash blended cement mortar. *Cement Concrete Research* 34 (4): 695–702.
- Hossain KMA, Lachemi M (2004b) Residual strength and durability of volcanic ash concrete exposed to high temperature. *ACI Materials Journal* 101 (6): 493–500.
- Hossain, KMA (2005a) Chloride induced corrosion of reinforcement in volcanic ash and pumice based blended concrete. *Cement and Concrete Composite* 27: 381–390.

- Hossain, KMA (2005b) Volcanic ash and pumice as cement additives: pozzolanic, alkali-silica reaction and autoclave expansion characteristics. *Cement Concrete Research* 35: 1141–1144.
- Hossain, KMA (2005c) Performance of volcanic ash based precast and in-situ blended cement concretes in marine environment. *ASCE Materials Journal* 17 (6): 694–702.
- Hossain KMA, Lachemi M (2006) Performance of volcanic ash and pumice based blended cement concrete in mixed sulfate environment. *Cement and Concrete Research* 36: 1123–1133.
- Lin WM, Lin TD, Powers-Couche LJ (1996) Microstructures of fire damaged concrete. *ACI Materials Journal* 93 (3): 199–205.
- Moen WS, McLucas GB (1980) Mount St. Helens ash: properties and possible uses. Washington Department of Natural Resources, Division of Geology and Earth Resources, Report of Investigations 24, 60 p.
- Naji JA (2002) The use of lime to stabilize granular ash materials for road construction. *Journal of Science & Technology* 7 (7).
- Nasser KW, Marzouk HM (1979) Properties of mass concrete containing fly ash at high temperatures. *ACI Journal, Proceedings* 76 (4): 537–551.
- Ping G, Ping X, Yan F, Beaudoin JJ (1995) Micro structural characterization of cementitious materials: Conductivity and impedance method. *Materials Science of Concrete IV*, American Ceramic Society, Westerville, OH, pp. 201–262
- Scasso RA, Corbella H, Tiberi P (1994) Sedimentological analysis of the tephra from 12–15 August 1991 eruption of Hudson volcano. *Bulletin of Volcanology* 56: 121–132.
- Scott WE, McGimsey RG (1994) Character, mass, distribution, and origin of tephra-fall deposits of the 1989–1990 eruption of Redoubt volcano, south-central Alaska. *Journal of Volcanology and Geothermal Research* 62: 251–272.
- Shipley S, Sarna-Wojcicki AM (1982) Distribution, thickness, and mass of Late Pleistocene and Holocene tephra from major volcanoes in the northwestern United States: a preliminary assessment of hazards from volcanic ejecta to Nuclear reactors in the Pacific Northwest: US Geological Survey Miscellaneous Field Studies Map MF-1435.

Chapter 11

Cement Kiln Dust

Introduction

Cement kiln dust (CKD) is a by-product of cement manufacturing. It is a fine powdery material similar in appearance to Portland cement. It is composed of micron-sized particles collected from electrostatic precipitators during the production of cement clinker. Fresh cement kiln dusts can be classified as belonging to one of the four categories, depending upon the kiln process used and the degree of separation in the dust collection system (Collins and Emery, 1983). There are two types of cement kiln processes: wet-process kilns, which take feed materials in a slurry form; and the dry process kilns, which accept feed materials in dry-ground form. In both of these processes, cement kiln dust can be collected in two ways: (i) part of the dust can be separated and returned to the kiln from the dust collection system (cyclone) close to the kiln, or (ii) the total quantity of dust generated can be recycled or discarded.

The chemical composition of CKD depends both on the raw materials used to produce the clinker, and on the type and source of carbon-based fuel to heat the material in the rotary kiln. Free lime can be found in CKD and its concentration is typically highest in the coarser particles collected closest to the kiln. Finer particles tend to exhibit higher concentrations of sulfates and alkalis. If the coarser particles are not separated out and returned to kiln, then the dust will contain higher free lime, as it contains some coarser particles. CKD from wet-process kilns also tends to be lower in calcium content than the dust from dry-process kilns. The X-ray diffraction analysis of the kiln dust indicates that it consists mainly of limestone as a main component, small quantity of quartz together with CaSO_4 , NaCl , K_2SO_4 , spurite $[\text{2}(\text{C}_2\text{S}).\text{CaCO}_3]$ and sulphospurite $[\text{2}(\text{C}_2\text{S}).\text{CaSO}_4]$.

11.1 Properties of Cement Kiln Dust (CKD)

11.1.1 Physical Properties

CKD is fine powdery material of relatively uniform size. Table 11.1 lists some typical physical properties of CKD (Collins and Emery, 1983).

Table 11.1 Typical physical properties of CKD (Collins and Emery, 1983)

Property	Value
Gradation (75% passing)	0.030 mm (No. 450 sieve)
Maximum particle size	0.300 mm (No. 50 sieve)
Specific surface (cm ² /g)	4600–14000
Specific gravity	2.6–2.8

Table 11.2 Typical chemical composition of CKD (Collins and Emery, 1983)

Parameter	Cement kiln dust (CKD)		
	Fresh	Stockpiled	
		Sample 1	Sample 2
CaO	40.5	31.4	44.2
SiO ₂	14.5	11.7	11.9
Al ₂ O ₃	4.10	3.18	3.24
MgO	1.55	0.97	1.73
Na ₂ O	0.44	0.13	0.27
K ₂ O	4.66	1.65	2.92
Fe ₂ O ₃	2.00	2.16	1.45
SO ₃	6.50	8.24	2.40
LOI (105°C)	22.9	40.4	30.2

11.1.2 Chemical Composition

CKD has similar chemical composition to that of the conventional Portland cement. The major constituents are compounds of lime, iron, silica, and alumina. Table 11.2 gives the typical chemical composition for fresh and stockpiled CKD (Collins and Emery, 1983). The pH of CKD water mixtures is generally around 12. It contains significant alkalies, and is considered to be caustic. Trace constituents in CKD including certain trace metals such as cadmium, lead, selenium, and radio nuclides are generally found in concentrations less than 0.05% by weight.

11.2 Uses of CKD

Approximately 15 million tons of CKD is produced annually in United States (Environmental Protection Agency, US, 1993a). Cement kiln dust has the potential for reuse in many different ways, but the best way to reuse this byproduct material is to reciprocate it in cement making process. This is always not feasible in some kiln facilities. Approximately 60–67 (8–8.4 million tons) percent of the total CKD generated in United States is used in this way (EPA, 1993a). The most common beneficial uses of CKD are soil stabilization, waste treatment, cement replacement, asphalt pavement and other uses.

11.2.1 Soil Stabilization

Cement kiln dust (CKD) can be used for soil stabilization as an alternative to lime, which is sometimes used in road construction. Utilization of CKD is not only effective for improving soils strength, but also helps in minimizing work time and cost. When lime is used, the soil is remixed and compacted 48 hours after the lime is applied. Cement kiln dust, on the other hand, gets rid of extra step, as the initial mixing and compacting is enough to stabilize the material sufficiently (Miller and Zaman, 2000). Cement is often used for soil stabilization in transportation construction. Cement kiln dust is an effective alternative to cement, which is more expensive than finer CKD. In United States, 10% of the CKD that is beneficially used is utilized for soil stabilization (Corish and Coleman, 1995).

11.2.2 Waste Treatment

CKD is also used for stabilization and solidification of wastes. Its absorptive capacity and alkaline nature reduces the moisture content in wastes, thereby increasing the bearing capacity. Furthermore, CKD is cheap, yet effective, alternative to other conventional waste treatment materials like cement and lime. Cement kiln dust has been successfully used to treat numerous types of waste materials. Everything from coal-mine waste effluents (Haynes and Kramer, 1982) and industrial wastewater, to sewage and oil sludge (Morgan et al., 1984) has been stabilized using kiln dust.

11.2.3 Cement Replacement

CKD's cement like properties also makes it a potential replacement for Portland cement in utilization in concrete and flowable slurry, etc.

11.2.4 Highway Uses

CKD has been used as mineral filler in asphalt concrete mixes. The blending of CKD into asphalt cement binder prior to incorporation with the hot mix aggregate results in a binder (mastic) that can significantly reduce asphalt cement requirements (between 15 and 25% by volume) (Kraszewski and Emery, 1981). CKD provides stripping resistance for the pavement. CKD can also be used as a replacement for Portland cement or hydrated lime in slurry seals (mix of fine aggregate and emulsified asphalt. Slurry seal mixes with 2% CKD using a stripping fine aggregate gave excellent results in abrasion testing (Emery, 1981).

CKD can be added to asphalt binder to produce low ductile mastic asphalt. Mastic asphalt is a mixture of asphalt binder and fine material. When mastic asphalt is produced using CKD mixed 50/50 with an asphalt cement binder, potentials exist

for a relatively large volume replacement of asphalt cement (between 15 and 25% by volume). CKD can be used as a cementitious material or a pozzolan activator in stabilized base or flowable fill applications.

11.3 Properties of Cement Mortar/Concrete Containing CKD

11.3.1 Compressive Strength

EL-Sayed et al. (1991) investigated the effect of cement kiln dust (CKD) on the compressive strength of cement paste and corrosion behavior of embedded reinforcement. They reported that up to 5% substitution of CKD, by weight of cement had no adverse effect on the strength of the cement paste and on reinforcement passivity. Batis et al. (2002) also reported the increase in compressive strength and corrosion resistance of the mix when CKD and blast furnace slag were added in proper ratio in ordinary Portland cement.

Shoaib et al. (2000) studied the effect partial substitution of ordinary Portland cement (OPC) and blast furnace slag cement (BFSC) with cement kiln dust (CKD) on the compressive strength of concrete and also determined the optimum quantity of CKD which could be recycled in the manufacture of these types of cements. The CKD contained the mixture of raw feed, partially calcined cement clinker, and condensed volatile salts. Two mixes with two types of cements (OPC and BFSC) were used. Percentages of replacement of CKD as ratio to cement used were 0, 10, 20, 30, and 40%. The mixes have same mix proportion (1 Cement: 1.9 Sand: 3.52 Gravel and 0.5 W/C ratio), and the cement content used in the mixes was 350 Kg/m³. Compressive strength was determined at the age of 1, 3, and 6 months. Based on the test results, they reported that: (i) control mix (0% CKD) achieved compressive strength of 27, 28.5 and 32.0 MPa at the age of 1, 3, and 6 months, respectively. Compressive strengths of concrete mixes decreased with the increase in CKD percentage at all ages (Fig. 11.1). At all age (1, 3, and 6 months), approximately 44% reduction in strength was observed at 40% CKD content. However, with 10% CKD content, the percentage reduction in compressive strength was 15, 3.5, and 1.6% at 1, 3, and 6 months. This was due to the replacement of cement clinker, which is mainly responsible for the strength development.

In addition, the large amounts of alkalies present in CKD caused a sort of crystallization of hydration products, which resulted in opening of pore system of the hardened samples leading to the reduction of the compressive strength; and (ii) substitution of blast furnace slag cement (BFSC) enhanced the compressive strength with curing time due to the formation, precipitation, and accumulation of hydrated products in water-filled pores to form a more compact body. Compressive strength of control mix (0% CKD) was 32.5, 35.0, and 37.5 MPa at the age of 1, 3, and 6 months, respectively. At all ages, compressive strength of mixes decreased with increase in CKD percentage. Maximum reduction (44 to 46%) in strength occurred with 40% CKD content. However, at 10% CKD content, reduction in strength at

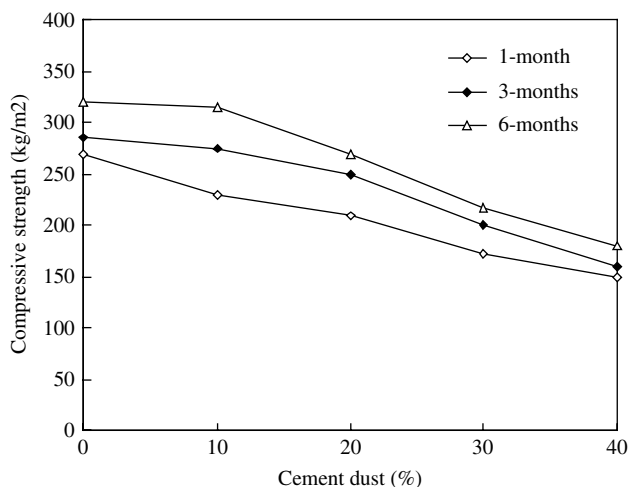


Fig. 11.1 Effect of cement dust percentage on the compressive strength of concrete made by OPC (Shoaib et al., 2000)

the age of 1, 3, and 6 months was 17%, 16%, and 13%, respectively. Generally, the addition of CKD reduced the compressive strength of concrete mixes especially with a high value of substitution, but some of the enhancement in strength for mixes containing 10% and 20% CKD in comparison to strength evaluated due to 90% or 80% free cement. This may be due to the accelerating effect of alkalis and lime containing dust in the activation of slag observed at 3 and 6 months, wherever alkalis increased the solutions of the silicates and consumption of the hydrated lime by the activated slag to form calcium hydro-silicate or calcium aluminate hydrate with dense structure. Reduction in compressive strength of hardened concrete mixes with high values of dust due to the increase of the alkalis, sulfates and chlorides, and also due to the decrease of slag and clinker values affecting the amount of CSH and aluminates hydrates, led to the formation of considerable amounts of hydrated sulpho-aluminates and chloro-aluminates which helps expansion and softening.

Al-Harthy et al. (2003) investigated the influence of CKD on the compressive strength of concrete mixtures at the age of 3, 7, and 28 days. Seven different concrete mixtures were made by replacing cement with 0 (control), 5, 10, 15, 20, 25, and 30% CKD by total weight of the cement. For each of the mixtures, three water-to-binder ratios of 0.50, 0.60, and 0.70, by weight were used. Details of the mixture and fresh concrete properties are given in Table 11.3.

Compressive strength test results of mixtures with water-to-binder ratio 0.7 and 0.5 are shown in Figs. 11.2–11.3. Based on the investigations, they reported that: (i) there was generally a decrease in compressive strength with an increase in CKD replacement for cement. More reduction in compressive strength was observed in mixtures with higher water-to-binder ratio (0.7) than in mixtures with low water-to-binder ratio (0.5). For all blends, the control mixture (no CKD) generally produced the highest compressive strength. At the age of 28 days, control mixtures (no CKD)

Table 11.3 Mixture proportion and fresh concrete properties (Al-Harthy et al., 2003)

Blend type	Water/binder ratio by weight					
	0.70		0.60		0.50	
	Slump (mm)	Unit weight (g/cm ³)	Slump (mm)	Unit weight (g/cm ³)	Slump (mm)	Unit weight (g/cm ³)
Control	55	2.51	80	2.51	90	2.50
95% C + 5% D	50	2.51	70	2.49	80	2.52
90% C + 10% D	50	2.52	65	2.48	70	2.51
85% C + 15% D	50	2.54	65	2.48	60	2.52
80% C + 20% D	45	2.51	60	2.47	50	2.51
75% C + 25% D	45	2.50	55	2.47	50	2.52
70% C + 30% D	40	2.51	55	2.48	45	2.51

with water-to-binder ratio of 0.70, 0.60, and 0.50 achieved compressive strengths of 34.4, 37.5, and 55 MPa, respectively. However, small amounts of replacements up to 5% did not seem to have an appreciable adverse effect on the compressive strength, especially at low water-to-binder ratio (0.50). At 5 and 10% CKD substitution for Portland cement, the reductions in the 28-day compressive strength values were 1.8 and 4.5%, respectively. At water-to-binder ratio (0.60), 28-day strength reductions were 12.4 and 18% for 5 and 10% CKD replacement for Portland cement, whereas at water-to-binder ratio (0.70), strength reductions were 8 and 13% for 5 and 10% CKD replacement. At maximum level (30%) of CKD substitution, the reductions in strengths were 31, 29, and 22% for water-to-binder ratios of 0.70, 0.60, and 0.50,

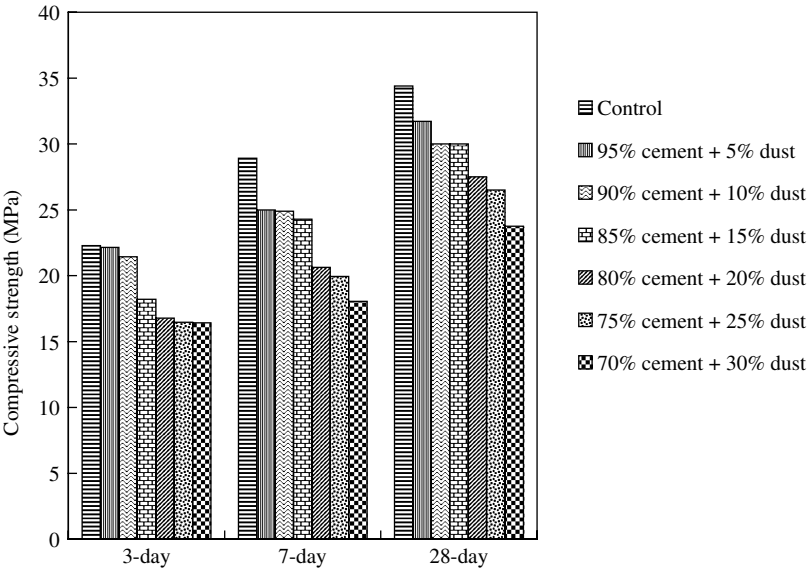


Fig. 11.2 Effect of CKD on the compressive strength for water-binder ratio 0.70 (Al-Harthy et al., 2003)

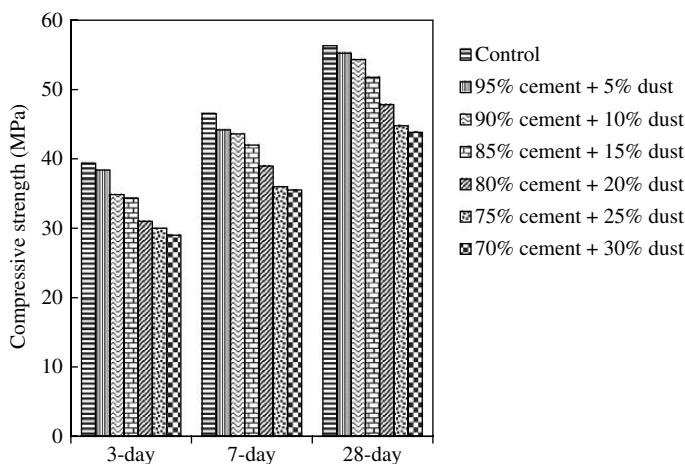


Fig. 11.3 Effect of CKD on the compressive strength for water-binder ratio of 0.50 (Al-Harthy et al., 2003)

respectively; and (ii) concrete mixtures containing lower percentages (5%) of CKD produced close compressive strength values to the control mix, especially at a water-to-binder ratio of 0.50.

Konsta-Gdoutos and Shah (2003) examined use of CKD as an activator for ground granulated blast furnace slag (GGBFS) to create non-conventional cementitious binders for concrete. CKD's high alkali and sulfate content makes it an excellent activator for pozzolanic materials. Four different ('E', 'P', 'A', and 'X') types of CKDs and a granulated blast furnace slag were used. CKDs (E) and (P) were generated from wet-process kilns and collected by electrostatic precipitators and bag houses, respectively. They contained large amounts of calcite, expressed as high LOI, and small amounts of lime. CKD (X) was a dolomitic dust obtained from a dry-process kiln with a pre-calciner and a pre-heater, and collected by a bag-house. CKD (A) was removed from a long dry kiln with electrostatic precipitators. The compressive strength of cylindrical mortar specimens (75×150 mm) was determined at the age of 7, 28, and 56 days, and results are presented in Fig. 11.4. Based on the test results they conclude that: (i) development of compressive strength for the CKD-slag blends up to 56 days showed that compressive strength of all four CKD-slag blends increased with curing time indicating slag activation by the CKD and the formation, precipitation, and accumulation of calcium silicate hydrates as products of hydration. Strength of all CKD-slag blends was always lower compared to OPC and OPC-slag mixes, at all ages. The slag blend activated with CKD (P) had the lowest early and late strength of all the mixes, ranging between 12.1 MPa at 7 days and 17.2 MPa at 56 days. CKD (P) lacked adequate quantities of lime for a pozzolanic reaction, and its water-soluble Na_2O equivalent content (1.69%) was much lower than the optimum quantity of 3% by mass of slag. Therefore, it was reasonable to assume that the activation of slag with CKD (P) was more the

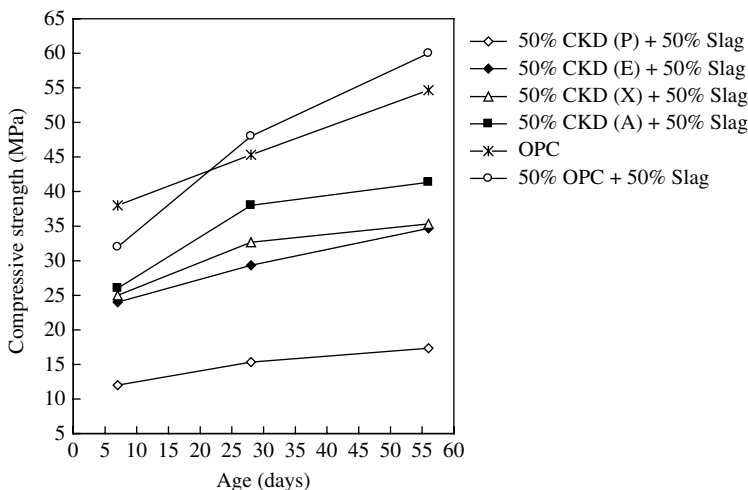


Fig. 11.4 Rate of compressive strength development of slag mortar blends activated with CKDs P, E, A, and X, compared with OPC and OPC-slag blends (Konsta-Gdoutos and Shah, 2003)

case of a weak effect of alkali activation, and that without the optimum supply of $\text{Ca}(\text{OH})_2$ the pozzolanic reaction cannot be sustained; and (ii) slag blends activated with CKDs (A), (E), and (X) had almost the same 7-day strength of approximately 25 MPa, indicating a high degree of slag activation. After 56 days of hydration, compressive strength of the three slag blends with CKDs (E), (A) and (X) ranged from 34.4 to 41.2 MPa, with the highest strength achieved by the blend activated by CKD (A), followed by the two slag blends with CKD (E) and CKD (X). The fine and uniform size distribution of the CKD (A) provided a higher specific surface and promoted a more intense reaction. The lower rate of strength development of the blend with CKD (X) at later ages, when compared with CKD (E), may be attributed to the more than optimum amount of $\text{Ca}(\text{OH})_2$ for the pozzolanic reaction. The remaining unreacted $\text{Ca}(\text{OH})_2$ weakens the hardened matrix. This was in agreement with the results of Shi (2001) from studies in lime–pozzolan cements. Higher rate of strength development were determined by the availability of Ca^{+2} provided by the free lime content of the CKD. Compressive strength of all the four CKD–slag blends increased with curing time.

Wang et al. (2004) determined the compressive strength of pastes made with 50% CKD, 50% fly ash (FA) having 0, 2, and 5% NaOH addition, cured at 24, 38, and 50°C. Water-to-solid ratio of 0.52 was maintained for all pastes to obtain a desirable flow. Figure 11.6 demonstrates the effect of NaOH addition on binder strength development. As can be seen from Fig. 11.5(a) and 11.5(b), when curing temperature was 24 and 38°C, addition of 2% NaOH increased the binder strength. The binder made with 50% CKD–50% FA–2% NaOH and cured at 38°C had the highest strength of all pastes, approximate 27 MPa at the age of 56 days. Addition of 5% NaOH tends to increase binder strength at an early age (before 7 days) but decreased binder strength at a later age. Gebauer (1981) also indicated that excessive NaOH addition

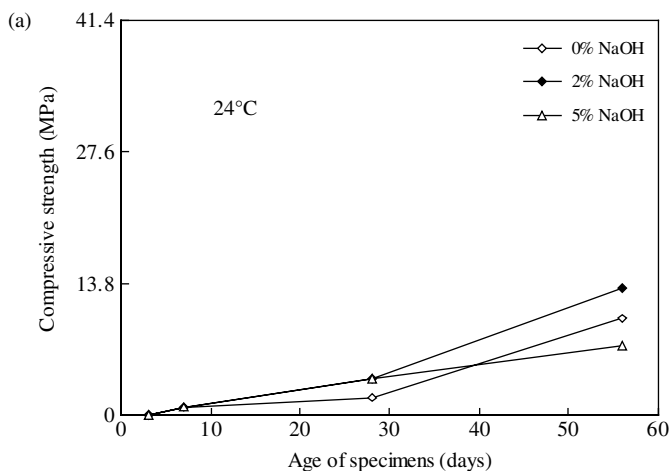


Fig. 11.5(a) Effect of NaOH addition on binder strength (Wang et al., 2004)

may result in undesirable morphology and non-uniformity of hydration products in the pastes, thus reducing binder strength. When the curing temperature was 50°C, addition of even 2% NaOH into the system had caused reduction of binder strength at both early and later ages. Elevated curing temperature also accelerates ion dissolution and binder hydration, resulting in the non-uniform microstructure. Thus, the combination of NaOH addition and a high curing temperature (50°C) may not be preferred for the CKD-FA binder strength development.

The effect of curing temperature on compressive strength of the CKD-FA pastes is presented in Fig. 11.6. General observation indicated that the effectiveness of

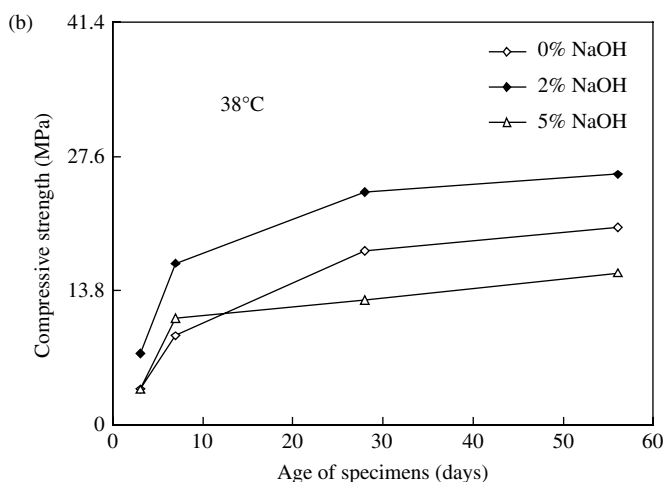


Fig. 11.5(b) Effect of NaOH addition on binder strength (Wang et al., 2004)

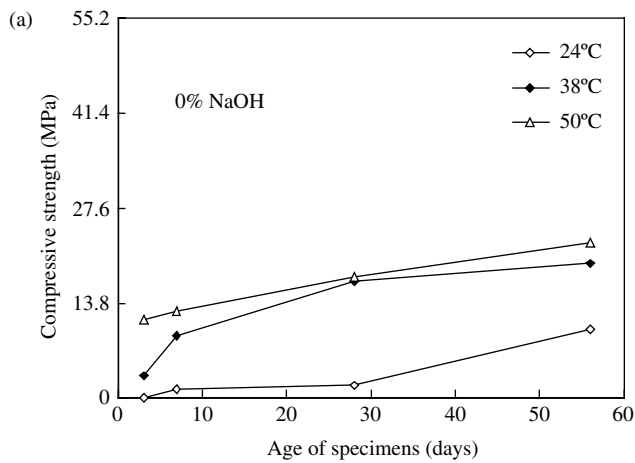


Fig. 11.6(a) Effect of curing temperature on binder strength (Wang et al., 2004)

activation, in terms of strength improvement, resulting from elevated curing temperature was much higher than that from NaOH addition. When a proper CKD-to-FA ratio and activation method are employed (such as a binder made with 50% CKD-50% FA-2% NaOH and cured at 38°C , the compressive strength of the CKD-FA binder is comparable with that of OPC.

As can be seen from the Fig. 11.6, when cured at 24°C, CKD-FA pastes had 28- and 56-day strength lower than 6.9 MPa and 13.8 MPa, respectively. While cured at an elevated temperature (38°C), the strength of CKD-FA pastes was doubled. However, strength of OPC pastes increased only 15% when the curing temperature

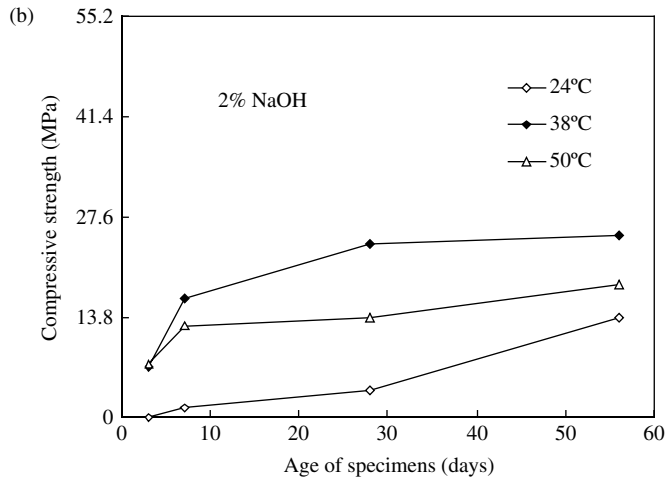


Fig. 11.6(b) Effect of curing temperature on binder strength (Wang et al., 2004)

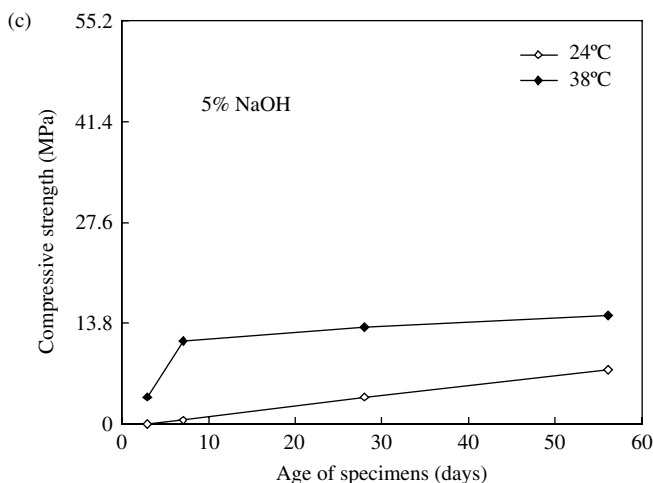


Fig. 11.6(c) Effect of curing temperature on binder strength (Wang et al., 2004)

was increased from 24 to 38°C. This implies that curing at elevated temperature has more significant contribution to pozzolanic reaction than that to OPC hydration. However, further increase in curing temperature from 38 to 50°C appears not to improve (sometimes even reduce) the strength of CKD-FA pastes. This may be attributed to the effect of hydration temperature on the microstructure of binder pastes (Kjellsen et al., 1992; Verbeck and Helmuth, 1968). Because of low solubility and diffusibility, cement hydration products rapidly formed at an elevated temperature may not be able to diffuse to a significant distance from the binder grain, thus resulting in a highly non-uniform distribution of the solid phases. The dense hydration products around the cement grains would serve as diffusion barriers, slowing or even remarkably preventing further hydration. As a result, although binder hydration proceeds more rapidly with increasing temperature at early age, the ultimate strength of concrete cured at a high temperature may not increase significantly (Kjellsen et al., 1992). Bhatti (1984, 1985, 1986) also observed that the addition of FA into a CKD-OPC system lowered the alkali content and resulted in improved strength.

11.3.2 Tensile Strength Properties

Shoaib et al. (2000) investigated the effect partial replacement of ordinary Portland cement (OPC) and blast furnace slag cement (BFSC) with cement kiln dust (CKD) on the tensile strength of concrete mixes at the age of 1, 3, and 6 months. Percentages of replacement of CKD as ratio to cement used were 0, 10, 20, 30, and 40%. Two mixes with two different types of cement were used. The mixes had same mix proportion (1 Cement: 1.9 Sand: 3.52 Gravel and 0.5 W/C Ratio), and the cement content used in three mixes was 350 Kg/m³. Based on the test results,

they concluded that: (i) tensile strength of concrete mixes decreased with increase in CKD percentage due to poor bond between aggregate and cement mortar-like free OPC hydration phases (Fig. 11.7). Maximum reduction in tensile strength occurred at 40% CKD, and it was 39, 41 and 41% at the age of 1, 3, and 6 months. However, at 10% CKD, reduction in strength was nominal (13% at 1 month, 12% at 3 months, and 13% at 6 months); and (ii) tensile strength of concrete mixes decreased with the substitution of blast furnace slag cement (BFSC) with CKD. Strength of mixes also decreased with curing time. Control mix (0% CKD) achieved the strength of 34.4, 30.0, and 28.2 MPa at the age of 1, 3, and 6 months. Strength continued to decrease with increase in CKD percentage, and the maximum reduction (27% at 1 month, 35% at 3 months, and 38% at 6 months) in strength occurred with 40% CKD substitution. However, at 10% CKD percentage, reduction in splitting tensile strength was nominal (13% at 1 month, 5% at 3 months, and 23% at 6 months).

Al-Harthy et al. (2003) studied the role of CKD on the flexural strength and toughness of concrete mixtures at the age of 3, 7, and 28 days. Mixtures were made by replacing cement with 0 (control), 5, 10, 15, 20, 25, and 30% CKD by total weight of the cement, with three water-to-binder ratios of 0.50, 0.60, and 0.70. Details of the mixture and fresh concrete properties are given in Table 11.3. Effect of CKD addition on the flexural strength is shown in Fig. 11.8. Test results indicated that: (i) at 28 days, control mixtures (no CKD) with water-to-binder ratio of 0.70, 0.60, and 0.50 achieved flexural strengths of 3.80, 3.85, and 4.7 MPa, respectively. At water-to-binder ratio of 0.50, reduction in flexural strength was up to 6% for CKD substitution levels up to 25%, whereas it was 20% for 30% CKD substitution. Similarly, at water-to-binder ratio of 0.60, there was significant decrease (3%) in flexural strength for up to 10% CKD substitution, whereas 13 to 29% reduction in flexural strength was observed for CKD sub-

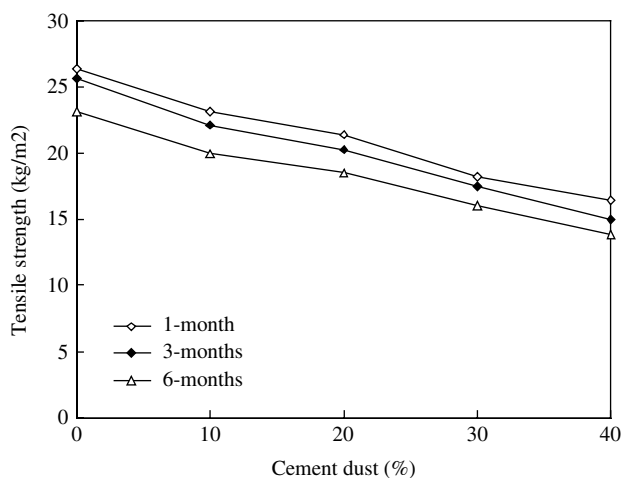


Fig. 11.7 Effect of cement dust percentage on the tensile strength of concrete made by OPC (Shoaib et al., 2000)

stitution levels beyond 10%. At water-to-binder ratio (0.70), there was significant reduction in flexural strengths (26–37%) for CKD substitution levels of 5 to 30%; (ii) Reduction in concrete toughness was also observed at the age of 28 days. Control mixtures (no CKD) with water-to-binder ratio of 0.70, 0.60, and 0.50 achieved concrete toughness of 3.68 E-04, 4.0 E-04, and 4.31 E-04 N/mm², respectively. At water-to-binder ratio of 0.50, reduction in toughness was 16% for 5% CKD substitution, but beyond 5% CKD substitution, reduction in toughness was up to 45% for 30% CKD level. Similar trends were also observed for water-to-binder ratios of 0.60 and 0.70. At water-to-binder ratio of 0.60, there was 16% reduction in toughness at 5% CKD level, and then it decreased to 47% for 30% CKD level. At water-to-binder ratio of 0.70, reduction in toughness varied between 27 and 55% depending upon the CKD substitution; and (iii) concrete mixtures containing lower percentages (5%) of CKD produced close flexural strength and toughness values to the control mix, especially at a water-to-binder ratio of 0.50.

11.3.3 Hydration Properties

Bhatty (1984, 1985, 1986) studied binary, ternary, and quaternary mixes using ordinary Portland cement (OPC), five different CKDs, two different types of FA (Class C and Class F), and slag. He concluded that cements containing CKD alone had reduced setting time, strength and workability. Dyer et al. (1999) examined ternary blends containing two types of CKD, pulverized fuel ash (PFA), and OPC, and they found that CKD accelerated the binder hydration. Taylor (1997) reported that low

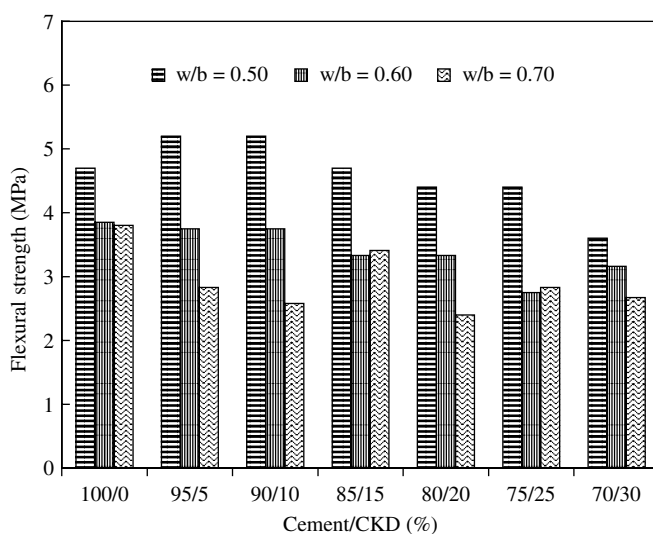


Fig. 11.8 Effect of CKD addition on the flexural strength (Al-Harthy et al., 2003)

chemical reactivity caused by the high degree of polymerization at which tetrahedral silicate is bridged with oxygen, most fly ashes, especially Class F fly ash, react with water very slowly at a room temperature. As a result, chemical and hydrothermal activations are often used to accelerate hydration of FA in cements (pozzolanic reaction). However, even under the conditions of alkaline activation, FA hydrates relatively slowly. Research has indicated that if the two materials are appropriately blended, the alkalis from CKD may activate hydration of FA and the blends may create a cementitious material in which the waste material deficiencies will be converted into benefits.

Amin et al. (1995) examined the effect of kiln dust content and the calcination temperature on the hydration of granulated slag. They concluded that activation of slags increased with increasing content calcinations-temperature of CKD. El-Didamony et al. (1997) evaluated the effect of washed and calcined kiln dust with anhydrite. They found that the activation of the slag increased with firing temperature of kiln dust and amount of added anhydrite. Kiln dust calcined at 1300°C with 15% anhydrite was found to be suitable for the production of supersulfated cement.

Konsta-Gdoutos and Shah (2003) studied the heat of hydration aspect on the utilization of cement kiln dust (CKD) as an activator for ground granulated blast furnace slag (GGBFS) to create non-conventional cementitious binders for concrete. Four different ('E', 'P', 'A', and 'X') types of CKDs and a granulated blast furnace slag were used. The finest material used was CKD (A) with a specific surface of 8270 cm²/g and a mean equivalent spherical diameter of 9 µm, and also the most uniform (57%) falling into the narrow range of 1–10 µm. CKD (E) was the coarsest one with a mean diameter of 60 µm and was evenly divided between 45 and 100 µm. In CKDs (P) and (X), 75% of their particles were in the range between 1 and 45 µm. Both had mean particle size of approximately 18 µm, and specific surfaces of 5410 and 6140 cm²/g. The heat of hydration of CKD–slag pastes was measured using an adiabatic DSS Qdrum calorimeter. XRD was employed to identify the phases present in hydration products.

From the heat evolution curves of the slag activated in mixes with 50% CKD (E) and CKD (P), it was observed that the trend of heat evolution of both blends was similar to that of the Portland cement–slag blend. One initial peak appeared before the induction period, which was attributed to the rapid dissolution of alkali sulfates and aluminates. One lower peak also appeared after the induction period for both blends, indicating a lower degree of slag activation. The dissolution process of slag activated with CKD (E) was initially much slower because of slow rate supply of K⁺ and SO₄²⁻. Heat evolution curves of blends activated with CKDs (A) and (X) showed that the very strong initial peak, which appeared before the dormant period was attributed to the combined effect of the hydration of high free lime content and the dissolution of alkali sulfates. The dormant period appeared very short, indicating a vigorous dissolution of ions and an accelerated initial formation of hydration products. The rate of deceleration period was higher for the blend with CKD (A) indicating a more intense and more continuous formation of hydration products when compared to both the OPC–slag blend and the CKD (X)–slag blend.

XRD was used to identify the phases formed during hydration. For slag activated with CKD (P), calcite peaks remained constant, indicating that carbonate particles were inert and did not participate in any hydration reaction releasing Ca^{+2} . It should be noted that it was not possible to identify any $\text{Ca}(\text{OH})_2$ peaks up to 28 days of hydration. The slag activated with CKD (E) unexpectedly exhibited a very long setting time. The subsequent release of sufficient sulfate ions from the dissolution of syngenite and favorable ratio of SO_4^{-2} to $\text{Al}(\text{OH})_4^-$ caused the formation of well-crystallized ettringite. No $\text{Ca}(\text{OH})_2$ could be detected after 7 days of hydration indicating that whole of available lime was consumed. The diffractogram of the blend with CKD (A) showed that ettringite was formed within the first hour of mixing. For slag activated with CKD (X) release of aluminum from the decomposition of Friedel's salt caused the formation of ettringite. Unreacted $\text{Ca}(\text{OH})_2$ can be detected in the mix even after 28 days.

Wang et al. (2004) studied the effect of curing temperature and NaOH addition on hydration of cement kiln dust (CKD) and fly ash (FA) binders. Reaction products and degree of hydration of the mixes were studied by X-ray diffraction (XRD) and thermogravimetric analysis (TGA). They reported that: (i) XRD pattern of CKD-FA pastes showed that major crystalline hydration product of CKD-FA binders was ettringite. While in a CKD-FA system, sulfate content was high due to composition of CKD, and aluminate content may be low due to slow hydration of the Class F FA. Therefore, the ettringite formed in a CKD-FA system was quite stable at the age of 28 days or even at 120 days. It was observed that alkali (sodium/potassium) sulfate crystals were often found in the pastes having NaOH addition. When 2% NaOH was added in a CKD-FA binder, the intensity of ettringite of the paste decreased at both 7 and 28 days. NaOH addition may accelerate chemical dissolution but depressed crystal (both ettringite and CH) formation during the binder hydration, and (ii) TGA test results of CKD-FA pastes with different amounts of NaOH were consistent with XRD result. The major crystalline hydration product of CKD-FA binder was ettringite. Curing at elevated temperature had more significant influence on CKD-FA binder strength development than on OPC strength development and appeared more effective for CKD-FA binder strength improvement than NaOH addition. Ettringite formation in a CKD-FA binder was slightly reduced when curing temperature increased from 38°C to 50°C. With an increased amount of NaOH addition, the ettringite formed in CKD-FA pastes decomposed at a reduced temperature. Binder made with 50% CKD-50% FA-2% NaOH and cured at 38°C had satisfactory strength.

11.3.4 Setting Times

Ramakrishnan (1986) undertook a comparative study of concrete properties made with cement blended with kiln dust versus the properties of corresponding concrete made with plain Portland cement. The blended cement was produced by blending 5% cement kiln dust with 95%, by weight of regular Type I cement. Test results

indicated that addition of cement kiln dust slightly retarded the setting times of cement and fresh concrete properties of blended cement concrete mixes were almost the same as those of plain concrete mixes.

Heikal et al. (2002) determined the setting times, electrical conductivity and fluidity of three blends of slag cement, namely, 70/30, 50/50, and 30/70% by mass of Portland cement clinker and granulated slag. Each blend was mixed with 2.5, 5.0, 7.5 and 10% by mass of CKD. Test results indicated that cement kiln dust affected the rheological properties of Portland cement clinker/granulated slag composites and depended on its amount as mix composition. The increase in CKD content increased the water requirement for normal consistency. The addition of 2.5% CKD by mass to mixes (70% Portland clinker, 30% granulated slag) and (50% Portland clinker, 50% granulated slag) retarded the initial and final setting time, whereas it accelerated the final setting time of mix (30% Portland clinker, 70% granulated slag).

Konsta-Gdoutos and Shah (2003) determined the time of initial setting of CKD-slag pastes. They found that: (i) OPC reached initial setting in 4.5 hrs, whereas for the OPC-slag blend, it was extended to 50 minutes. Time of setting was much shorter than the control blends for the blend with CKD (A), which may be due to the formation of ettringite; CKD (A) contained a very high amount of sulfate ($\approx 17\%$). Significant retardation was observed for the slag blends activated with CKDs (E), (P), and (X). Initial setting times for the blends with CKD (P) and (X) were very similar, around 7 hrs and 30 minutes for the CKD (P)-slag blend, and almost 9 hrs for the blend with CKD (X). Slag activated with CKD (E) took more than 14 hrs to reach the initial set.

11.3.5 Sorptivity

Al-Harthy et al. (2003) used sorptivity and initial surface absorption test (ISAT) to measure the absorption characteristics of different mortar samples containing CKD. They concluded that sorptivity of mortar decreased with the incorporation of CKD (up to 30%) in the mixtures. Without affecting strength, addition of CKD improved absorption properties of mortars and thus, can enhance their durability. The mortar mixtures containing CKD produced lower sorptivity values than the mixture containing no CKD (control). This was attributed to the very fine particle sizes of CKD.

11.3.6 Electrical Conductivity

Salem and Ragai (2001) measured the electrical conductivity of granulated slag cement kiln dust-silica fume blended hardened pastes. For this purpose, they prepared a blended cement pastes containing granulated slag and CKD with and without silica fume. The water-to-solid (w/s) ratios used were 0.30, 0.40, and 0.50 to produce low-normal and high- porosity respectively. The variation of electrical conductiv-

ity with hydration time was measured at 30° and 50°C. Five dry mixtures were prepared using slag: CKD (raw or washed) of 80:20 (by weight) and containing 0%, 2%, 5%, 10%, and 20% active silica fume as a partial substitute of slag. For conductivity measurements, the blended cement pastes were made with different initial porosities using w/s ratios of 0.30, 0.40 and 0.50 by weight. The changes in the electrical conductivity for each phase were measured at time intervals from 3.5 minutes up to 24 h (during setting and hardening) at two constant temperatures of 30°C and 50°C. Based on the test results they reported that: (i) the electrical conductivity of pastes with raw CKD for various blends showed only-one conductivity maximum. The increase of electrical conductivity in the initial stage of hydration was mainly attributed to the initial hydrolysis of raw CKD and increase of ionic concentration and mobility of ions (Ca^{2+} , OH^- , Na^+ , and K^+). These ions were, however, readily absorbed by the formation of a thin layer of hydration products, which formed an envelope. This envelope consisted of electrical double layers of absorbed Ca^{2+} , Na^+ , and K^+ ions and counter-ions that led to a decrease in conductivity values after maximum. Further, there appeared a notable increase in the rate of initial hydrolysis of CKD with increasing addition of silica fume, (ii) by increasing the water-to-solid (w/s) from 0.30 up to 0.50, the conductance increased and the location of conductivity peaks of higher w/s appeared somewhat later than those of lower ones. This was attributed to the increase of the degree of the hydrolysis of raw CKD constituents by increasing the w/s ratios of the pastes. Also the increase in temperature of hydration led to an increase in the rate of hydrolysis of CKD. The location of the conductivity peaks occurred at shorter times with increasing rate of hydration; (iii) washed CKD showed notable lowering in the conductivity maxima of the pastes. This was mainly attributed to the reduction of alkali contents (Na^+ and K^+ ions) in washed CKD, which led to decrease in the rate of its hydrolysis. Also, the rate of decrease in conductivity values with time of hydration beyond the maxima was less in pastes with washed CKD than those of pastes of raw CKD. This was mainly due to the decrease rate of activation of granulated slag and silica fume by the washed CKDs compared with the pastes made with raw CKD; and (iv) increasing the w/s ratio facilitated the pozzolanic interaction of silica fume with the liberated free $\text{Ca}(\text{OH})_2$ during CKD hydration. This resulted in shortening of the time required for the conductivity peaks to develop with increasing w/s ratio of the paste. The effect of increasing the hydration temperature showed the same trend as obtained for the specimens containing unwashed CKD.

Heikal et al. (2002) studied the electrical conductivity of three blends of slag cement, namely, 70/30, 50/50, and 30/70% by mass of Portland cement clinker and granulated slag. Each blend was mixed with 2.5, 5.0, 7.5, and 10% by mass of CKD. Test results indicated that presence of CKD affected the location and height of the conductivity peaks. By increasing the CKD from 2.5 to 7.7%, the conductivity maximum increased. With further addition (10%), the height of the conductivity maximum decreased.

11.3.7 Durability Properties

Ramakrishnan and Balaguru (1987) reported freezing and thawing durability of concretes containing 5% CKD as replacement for cement. Three types of cements, namely, Type I, II, and III were investigated. Six sets of concrete with cement contents of 332 kg/m³ and 386 kg/m³ were tested. Water-cement ratio was 0.52 for lower cement content and 0.45 for the higher water-cement content. Air contents of the concrete mixtures ranged from 3.1 to 8.4%. Weight loss, fundamental resonant transverse frequency, and pulse velocity were measured at 30-cycles interval. The freeze-thaw testing was stopped at 300 cycles. The durability behavior of the concretes was evaluated by using relative dynamic modulus, durability factor, and absorption coefficient. The analysis of test results indicated that 5% replacement of cement with CKD does not appreciably affect the freeze-thaw durability of concrete.

11.3.8 Alkali-Silica Reaction (ASR)

Alkali-Silica Reaction (ASR) is a chemical reaction between the alkalis in cement paste and certain siliceous aggregates. These aggregates, when placed in a highly alkaline solution and in the presence of water and calcium, will expand and a gel will begin to form. As the aggregate particle expands, it causes the concrete to crack. As the concrete deteriorates, more water enters to fuel the reaction. This cycle continues until the concrete deteriorates past the point of serviceability.

The basic reaction procedure is well known. In highly alkaline solutions, the reactive silica of the aggregate is converted into a sellable alkali-silicate gel. The particles of aggregate absorb water, creating within them a swelling pressure which, if it exceeds the tensile strength of the aggregate, leads to cracking. One of the parameters determining the effect of the gel is porosity of aggregates. In porous aggregates, the reaction products are initially laid down on the pores. In dense aggregates, even small amount of gel may cause cracking. Pressure starts to build up when all of the pore volume has been filled. However, it is not only the amount of gel but also its viscosity, which varies with composition and storage temperature, which influence the course of the reaction. The pore solution of hardened cement comprises a highly concentrated alkali metal hydroxide solution with pH of more than 13. The alkalis originate predominantly from the cement. However, additives, admixtures, and external factors such as de-icers and to a smaller extent the aggregate as well, may contribute to the alkali content of the pore solution. The contribution made by the individual cement components depends primarily on their reactivity and on the way in which the alkalis they contain are bonded. In Portland cement clinker, typically between 60% and 80% of the alkalis are in the form of sulfates, this being referred to as the degree of sulfation of the alkalis. The remainder is incorporated in the clinker phases. While the alkali sulfates dissolve very quickly after batching, the alkalis present in the clinker minerals may not be released until the minerals react.

The conditions required for ASR to occur are: (i) a sufficiently high alkali content of the cement; (ii) a reactive aggregate, such as chert; and (iii) water – ASR will not occur if there is no water in the concrete, since alkali-silica gel formation requires water. Alkali silica reaction is diagnosed primarily by four main features: (i) Presence of alkali silica reactive aggregates; (ii) Crack pattern; (iii) Presence of alkali silica gel in cracks and/or voids; and (iv) $\text{Ca}(\text{OH})_2$ depleted paste.

11.3.8.1 Mitigating ASR

Once ASR begins, it is very difficult to halt/control. Two strategies that have been used are to limit the ingress of water into the concrete, or to draw lithium down into the concrete. Limiting the ingress of water into concrete is extremely difficult and usually proves impractical. The use of lithium has been found to be effective but is very costly. The best way to mitigate ASR is to prevent its occurrence through the proper use of materials in the concrete mixture. There are several ways to mitigate ASR. One option is to use cements with alkalis of less than 0.60%. Another solution is to limit or prohibit the use of reactive aggregates. In reality, sources of both low alkali cements and non-reactive aggregates are limited, so it is often impractical to specify either of these options. A third alternative is to specify slag cement when concrete contains reactive aggregates.

11.3.8.2 Role of Slag Cement in Mitigating ASR

The use of mineral admixture such as fly ash, GGBS, silica fume reduce the potential of ASR occurring by: (i) reducing the total alkalis in the system thus reducing the alkali-silica ratio; (ii) consuming alkalis in the hydration process, making them unavailable for the alkali silica reaction; (iii) reducing pore size and mobility of the alkali; and (iv) reducing the pore liquid that reacts with the aggregate.

11.3.8.3 Effect of CKD on ASR

When using CKD with high alkali content, fly ash or blast furnace slag should be incorporated to prevent alkali-silica reaction problem. Dyer et al. (1999) reported that for a given Portland cement content, optimum strength was achieved in blends containing approximately 10% cement kiln dust for Portland cement levels up to 80%. Beyond this level a CKD/PFA ratio (of one) was optimal. Isothermal conduction calorimetry results and measurements of calcium hydroxide levels indicated that this was due to acceleration of the reactions of the blend constituents by the dust. Additionally, the chemical composition of the optimal blends promoted the production of calcium aluminates and ferrite hydrates of a type conducive to maintaining the integrity of the cementitious matrix.

Malvar et al. (2004) assessed the various alkali silica reaction (ASR) mitigation techniques and developed a set of recommended mitigation procedures, which require not only the use of low alkali cement, but replacement of part of it by Class F fly ash (or Class N pozzolan) (25%–40% by weight), or ground granulated blast

furnace slag (GGBFS). The Class F fly ash (or Class N pozzolan) should also have a maximum of 1.5% available alkali, a maximum 6% loss on ignition, and a maximum of 8% CaO (lime). In addition to mitigating ASR, these recommendations are expected to: (i) reduce concrete costs; (ii) enhance the durability of concrete; and (iii) increase fly ash and GGBFS recycling.

11.4 Properties of Controlled Low-Strength Materials Containing CKD

Pierce et al. (2003) evaluated the fluid and hardened properties of controlled low-strength materials (CLSM) with cement kiln dust (CKD) as the primary binding agent. The low-strength property of CKD can be advantageous when used in CLSM because most applications require future excavatability. Since CLSM is often produced with fly ash (FA), it inherently mitigates the higher water demand of CKD. Laboratory mixtures were prepared with CKD: FA ratios of 1:12, 1:6, and 1:1. The w/b of 0.95, 1.0, 1.05, and 1.10 were tested for each of the CKD: FA ratio. Table 11.4 provides the mixture proportions for the three CKD: FA ratios at a w/b of 0.95. They studied flowability, bleeding, setting time, mass density, and 28-day unconfined compressive strength (UCS).

Based on the investigations, they reported their findings about following properties.

(i) Flowability: In general, the flowability increased with the increase in w/b ratio. This trend was expected because the water content increases proportionally with the w/b, making the material more fluid. However, this was not true for the 1:1 CKD: FA mixture. In this case, flowability decreased considerably when the w/b increased from 0.95 to 1.00 and decreased again when the w/b increased from 1.05 to 1.08. This observation suggested that there is less control of flowability when the percentage of CKD in the mixture is high. When the percentage of CKD is relatively low, flowability does not significantly change with the CKD amount, but when percentage of CKD is relatively high (1:1 CKD: FA mixture), flowability gets significantly affected. Based on the series of mixtures investigated herein, CLMS produced with a CKD: FA ratio of 1:6 or 1:12 yielded acceptable flow (according to ACI Committee 229, 1999, range of acceptable flow is between 200 and 300 mm) between w/b of 1.00 and 1.08. This finding also confirms earlier results by Gassman

Table 11.4 Mixture proportions for CKD-CLSM at w/b of 0.95 (Pierce et al., 2003)

Constituents	CKD:FA = 1.2		CKD:FA = 1.2		CKD:FA = 1.2	
	Mass	% of total mass	Mass	% of total mass	Mass	% of total mass
CKD (g)	160	1.3	298	2.5	1013	8.65
Fly ash (g)	1926	16	1788	14.8	1043	8.65
Sand (g)	8027	66.3	8027	66.3	8027	66.3
Water (ml)	1982	16.4	1982	16.4	1982	16.4
Total mass (g)	12095	100	12095	100	12095	100

et al. (2001); (ii) bleeding: As w/b ratio was increased, it was expected that bleeding would increase, but the test results, in the case, showed that Mixtures 1:12 and 1:1 CKD: FA demonstrated both increase and decrease in bleeding levels consistently between 6 and 7%, irrespective of w/d ratio. For all the mixtures, bleeding ranged between 4 to 8%, which is more than the acceptable limit of 2% (Hoopes, 1988); (iii) density: The average mass density of all mixtures was within 2052 to 2129 kg/m³. These results fall well within the range (1840–2320 kg/m³) prescribed by ACI Committee 229 (1999). Since Specific gravity of CKD as 2.6 and that of fly ash as 2.26, there was not much difference in the density of these mixtures; (iv) compressive strength : 28-day compressive strength increased with the increase in CKD content, but decreased with w/b ratio. This occurs to a lesser degree between 1:12 and 1:6 mixtures, and to a much greater degree between 1:6 and 1:1 mixtures. The average strength for the 1:12, 1:6, and 1:1 CKD: FA mixtures were 45, 71, and 365 kPa. It could also be concluded that mixtures 1:12 and 1:6 would easily allow for manual excavation, as their strength was less than 100 kPa. Mixture 1:1 attained strength from 300 to 400 kPa, which fall within the lower range of a typical CLSM mixture (0.3 to 0.7 MPa, according to ACI Committee 229). The average strength for the 1:12, 1:6, and 1:1 CKD: FA mixtures were 45, 71, and 365 kPa. These values of the strength are representative of soft, medium and very stiff clay; and (v) modulus of elasticity: Like compressive strength, modulus of elasticity also increased with the increase in CKD content. The average modulus of elasticity for mixtures with CKD content 1.3% (1:12 CKD: FA), 2.5% (1:6 CKD: FA), and 8.65% (1:1 CKD: FA) was 3.3, 4.9, and 70 MPa, respectively.

Katz and Kovler (2004) investigated the use of five types of industrial by-products for the production of controlled low-strength materials (CLSM). They used cement kiln dust (CKD), asphalt dust (AD), coal fly ash (FA), coal bottom ash (BA) and quarry waste (QW). Ordinary Portland cement (OPC) (with up to 10% of coal fly ash) was used in all the mixes. Water content was adjusted to provide a constant flow of 200 mm. Based on the study, they concluded that: (i) fly ash, asphalt dust and cement kiln had very fine particle size, where as bottom ash and quarry wastes were coarser. The shape of the particles affected the water-demand, as smaller quantity of water was needed for the rounded particles. Increasing the fine waste content significantly increased the water required for the constant flow. Increasing the cement content was accompanied by an equivalent reduction in crushed sand content. The increased amount of water was needed for BA due to its porous nature and rough surface. The large amount of fines in the QW was the direct reason for the increased amount of water. High bleeding values were observed with mixes containing FA (2 times more than AD mixes and 3 times more than CKD mixes) due to its spherical shape and its delayed setting; (ii) cementing capacity of CKD enhanced the thickening of the mix at an early age, helping to reduce the bleeding in these mixes; (iii) increasing the amount of the fine waste slightly increased the setting time of FA and CKD mixes, but significantly increased the setting time of AD mixes due to its being completely inert material. Replacing the CS with BA reduced the setting time of mixes due to contribution of BA to the chemical process involved in setting. However when QW was used, the setting time significantly increased due

to high concentration of fine materials. CaCl_2 was used as an accelerator at 2% and 5%, by weight of cement, the reductions in the setting time were 14% and 35% respectively; (iv) only a few fine cracks were detected in the base mixes containing FA and AD. Wider cracks were observed in CKD mixes exhibiting somewhat larger shrinkage; (v) doubling the fine waste (FW) content increased the volume changes and tendency to crack; the shrinkage of the mixes containing FA and AD increased by almost 75%, but that of the CKD mix increased by almost 300%; and (vi) in all the mixes, increasing the cement content reduced the shrinkage and tendency to cracking: while increasing the fine content by using the QW significantly increased the shrinkage probably due to clay present in the fines of that waste. It was observed that the early age shrinkage was inversely proportional to the bleeding of the mix. The CKD mixes with relatively very little bleeding exhibited the largest shrinkage since the water dried out from the bulk of the material rather than from the surface. As long as there was enough water available for the evaporation from the surface, shrinkage was small as in the FA and AD mixes; and (vii) Parameters that led to the increased water demand also influenced the total absorption, which significantly increased as the amount of fines were increased (QW fines) or by using a porous material (BA).

11.5 Use of CKD as Soil Stabilizer

CKD represents a potentially useful and cost-effective alternative to other soil stabilizers such as lime, fly ash and Portland cement. Kamon and Nontananandh (1991) suggested that a cementitious stabilizer should have a hydration modulus between that of Alite and Belite. CKD satisfied this requirement and thus, having self-cementing characteristics, reacted with soil in a manner similar to Portland cement. Typically, CKD had approximately one-third of the amount of cement oxides (CaO , Al_2O_3 , SiO_2 , Fe_2O_3) present in Portland cement.

Baghdadi (1990) reported that: (i) after 28 days of curing kaolinite samples mixed with 16% (by weight) CKD, the unconfined compressive strength (UCS) was increased from 210 to 1115 kPa; (ii) addition of 8% CKD resulted in a reduction of the plasticity index (PI) from 513 to 326. This reduction in PI was found to increase with increasing CKD content. Fatani and Khan (1990) utilized CKD to stabilize dune sand and asphalt mixes used for pavement bases; they reported a 10-fold improvement in mix stability with the addition of 11% CKD. Zaman et al. (1992) found that, when added to highly expansive clay, CKD increased the UCS from 103 to 263 kPa after 28 days of curing, and the PI of the clay decreased from 64 to 46% after 2 hrs mixing. Baghdadi et al. (1995) found that CKD significantly increased the compressive strength of dune sand and that the compressive strength increased with increasing amount of CKD and curing duration.

Miller et al. (1997) found that CKD substantially reduced the collapse potential and compressibility of compacted shale. Three natural soils from Oklahoma were selected: (i) a high plasticity clay from Norman, OK; (ii) a medium plasticity clay from Atoka, OK; and (iii) a low plasticity silt from Shawnee, OK. Soils 1, 2, and 3 have Unified Soil Classification System designations of CH, CL and ML,

respectively. Miller and Azad (2000) conducted laboratory study to evaluate the effectiveness of cement kiln dust (CKD) as a soil stabilizer. A method based on pH measurement of soil–CKD mixtures was presented for rapidly assessing potential strength increase due to the addition of CKD. Based on the test results they concluded that: (i) addition of CKD to soil could substantially improve the unconfined compressive strength. The improvement was more significant for soils with low plasticity index (PI); (ii) CKD rapidly increased the unconfined compressive strength during the first 7–14 days after compaction, and thereafter more slowly. For similar CKD contents, the rate of increase was greater for low PI soils; (iii) unconfined compression stress–strain behavior of test soils was dramatically altered with the addition of CKD. The stiffness increased substantially and failure occurred at much smaller values of axial strain when compared to the untreated soil. The tangent modulus from UCT stress–strain curves increased approximately 10-fold with the addition of CKD. Brittle failure was exhibited by the treated soils at axial strains of approximately 1–3%, whereas untreated soils exhibited plastic; (iv) Optimum moisture content and maximum dry unit weight, increased and decreased, respectively, with increasing amounts of CKD; and (v) treatment with CKD reduced the PI of moderately to high plastic soil.

11.6 Use of CKD in Asphalt Pavement/Concrete

Ciesielski and Collins (1994), Kraszewski and Emery (1981), Parsons (1995), and Transportation Association of Canada (1996) reported the use of CKD as mineral filler in asphalt concrete in testing/field trials. AASHTO (1986) has suggested the specification requirements for mineral fillers, as given in Table 11.5. The grading requirements for mineral fillers are such that CKD can, with minimal screening, readily comply with the specification requirements.

Taha et al. (2002) investigated the use of cement bypass dust (CBPD) or CKD as filler in asphalt paving mixtures. Initially, the effect of adding either lime or CBPD (0, 3, 5, 7, 10, and 15%) on binder properties (penetration, ductility, and softening point) was investigated. Then, three different asphalt concrete mixtures were prepared using lime (control), and 5 and 13% CBPD substitution for lime or fine aggregate. The mixtures were subjected to Marshall testing. Results indicated

Table 11.5 AASHTO M17 specification requirements for mineral filler for use in bituminous paving mixtures (AASHTO, 1986)

Particle sizing		Organic impurities	Plasticity index
Sieve size	% Passing		
600 m (No. 30)	100	Mineral filler must be free from any organic impurities	Mineral filler must have plasticity index not greater than 4
300 m (No. 50)	95–100		
75 m (No. 200)	70–100		

that the substitution of 5% CBPD produced the same optimum asphalt binder content as the control mixture (4.5%, by weight of aggregate) without any negative effect on asphalt concrete properties (stability, flow, voids in total mix, voids in mineral aggregate, and voids filled with asphalt). However, the use of 13% CBPD for lime and fine aggregate would require a higher optimum asphalt binder content of 5.7%, by weight of aggregate. This will produce an uneconomical mix. Thus, 5% CBPD substitution for lime or cement would be the optimum used in asphalt paving mixtures.

Cold in-place recycling (CIR) is an on-site recycling process in which an asphalt pavement with structural failures is reconstructed using 100% RAP to a typical treatment depth of 2–5 inches, using a mobile train of equipment — tanker truck, milling machine, crushing and screening equipment, mixer, additives, and a paver. Typically, the pavement can be opened to traffic at the end of the work day. CIR recycling can treat rutting in subsurface layers, repair cracks, and also can be used for maintenance patching. It also may require a curing period, followed by application of a wearing surface. Its longer equipment train may need sufficient room to maneuver. Anil et al. (2005), Cross (1999), Cross and Fager (1995), Murphy and Emery (1996), Wood et al. (1988), and Zaman et al. (1999) reported studies on the cold in-place recycling of asphalt pavements.

Zaman et al. (1999) conducted laboratory study to examine the durability of CKD-stabilized aggregate base, as measured by resilient modulus, unconfined compressive strength and layer coefficient. Specifically, the effect of freezing/thawing and wetting/drying was evaluated. The Meridian limestone aggregate, which is considered to be of substandard quality and therefore unsuitable for highway base courses, was used as the raw material and also stabilized with cement-kiln-dust. A testing protocol was proposed to quantify the effect of freezing/thawing and wetting/drying. Based on the test results they concluded that RM values of the raw Meridian aggregate were in the range 49.42 MPa to 306.59 MPa, within the tested stress level. These values are low and may be inadequate for most applications. The data demonstrated that cement-kiln-dust is an effective stabilizing agent for strengthening the Meridian aggregate intended for base/subbase construction. With the addition of 15% CKD, the RM values increased manifold up to 499.51 MPa. Freezing/thawing and wetting/drying cycles had considerable adverse effect on the durability as measured by the resilient modulus of CKD-stabilized aggregate. Within a range of 8 cycles, the RM values decreased substantially with increasing number of freezing/thawing and wetting/drying cycles. The highest reduction in RM value due to freezing/thawing was 54.21%, 67.51%, and 65.11% for 4, 8, and 12 cycles, respectively. For wetting/drying actions, the highest reduction in RM value was 34.27%, 53.58%, and 61.88% for 4, 8, and 12 cycles, respectively. The layer coefficients of the stabilized aggregates were significantly higher than those of the raw aggregates. However, the layer coefficient of the stabilized aggregate base dropped significantly when the aggregate experienced freezing/thawing and wetting/drying cycles. When subjected to about eight cycles of freezing/thawing and wetting/drying, the layer coefficients of CKD-stabilized aggregate base assumed values close to or lower than those of the raw aggregate base. This investigation

points to the need to explore more in depth the durability studies and recommends a protocol of freeze/thaw, wet/dry testing methodology.

Anil et al. (2005) investigated the stabilization characteristics of Reclaimed Asphalt Base (RAB) with self-cementing class C fly ash in the laboratory and also as part of the demonstration project of full-depth cold in-place recycling of low-volume road asphalt pavement. On the basis of the results they concluded that: (i) the self-cementing fly ash is characterized by rapid hydration, and both compaction time and water content to be controlled carefully during construction; (ii) RAB-fly ash mixtures have higher unconfined strength and CBR at lower-than-optimum moisture content; and (iii) higher CBR values obtained by using Class C fly ash to stabilize recycled asphalt and base course may allow for thinner asphalt wear surfaces, thereby reducing construction costs.

11.7 Leachate Analysis

Cement kiln dust, like cement itself, is not considered to be a hazardous material under the Environmental Protection Agency (EPA)'s Resource Conservation and Recovery Act (RCRA) regulations. However, this does not mean that cement kiln dust doesn't contain anything that could pose a hazard to the environment. For CKD to remain a safe material it has to be handled properly to prevent environmental contamination and the toxicity of cement kiln dust must be determined on a case-by-case basis (Haynes and Kramer, 1982). Number of factors that affect the level of contaminants in cement kiln dust are: (i) material usually varies in content from facility to facility, and differences can even be apparent within a single cement kiln; (ii) finer particles contain higher concentrations of sulfates and alkalis, while coarser particles that are usually collected closer to the kiln have higher concentrations of free lime; (iii) waste fuels used in some cement kilns may increase the toxic metal content of CKD; and (iv) Dust recirculation can cause increased contaminant concentrations.

The composition of CKD is also dependant on how it is generated, but significant variability is possible even between kilns with relatively minor processing differences (EPA, 1993a). Bulk constituents found in both coal ash and CKD (that is, constituents that exceed 0.05% by weight in the sampled material) are similar and include aluminum, calcium, iron, magnesium, potassium, silicon, sodium, and titanium. In addition, CKD bulk constituents include manganese, sulfur, and chloride (EPA, 1993a). At individual ash disposal landfills, environmentally significant sulfur concentrations may be derived from co-disposal of pyrites (i.e., iron sulfide) with coal ash (Environmental Protection Agency, 1993b).

CKD is composed of an assemblage of oxidized, anhydrous phases, which include oxides, alumino-silicates, sulfates and chlorides. Many of these phases such as lime (CaO), arcanite (K_2SO_4) and sylvite (KCl), are unstable or highly soluble at earth surface conditions. When CKD contacts water, these phases will either dissolve completely or more stable and less soluble secondary phases will

precipitate. Thus, the concentration of some constituent elements in CKD leachate will be controlled by the solubility of the secondary precipitates, and the concentration of others will be controlled by their availability to the leachate solutions and by their diffusive flux into the solution from the leaching of primary phases over the time (Eary et al., 1990). To differentiate between these two classes of elemental behavior, Reardon et al. (1995) recommended conducting leaching test on a particular waste at least at two different solid/ waste ratios. They pointed out that if an element's concentration does not double when solid/ waste ratio is halved, there must be a solid phase control on its concentration in solution.

Representative ranges and median trace element concentrations for coal ash from three regions of the United States and for CKD are presented in Table 11.6. The data reveal that median concentrations of arsenic, barium, chromium, nickel and vanadium are lower in CKD than in coal ash, but medians generally lie within the range of concentrations found in coal ash. Cadmium, lead, selenium, and silver median concentrations are higher for CKD than for coal ash. Median concentrations of mercury and thallium in CKD are within the median ranges for coal ash, but the maximum values for mercury and thallium found in CKD exceed the coal ash maximum values. EPA's review of results from Toxicity Characteristic Leaching Procedure (TCLP) analyses on CKD samples concluded that trace metal constituents rarely exceed RCRA toxicity limits (Environmental Protection Agency, 1995). CKD and coal combustion wastes are generally alkaline and have very low concentrations of organic compounds. pH values for CKD leachate range from 6.11 to 12.98 standard units (EPA, 1993a).

The Portland Cement Association (1992) did an analysis of metal contaminants in cement kiln dust using the EPA's toxicity characteristic leaching procedure (TCLP). CKD samples from 79 plants in the United States and 10 in Canada were tested for concentrations of trace metals including mercury, selenium, thallium, cadmium, lead, antimony, silver, arsenic, nickel, barium, beryllium, and chromium. Out of all the kiln dust studied, CKD from only two plants had concentrations of any materials over an acceptable limit. One facility produced samples with excess lead, and another had excess selenium. The high levels of these contaminants were attributed to the fact that the cement kilns producing the overly contaminated CKD recirculated their dust.

Duchesne and Reardon (1998) conducted the study to determine whether the concentration of a given chemical constituent in cement kiln dust leachate was controlled by precipitation of a secondary mineral phase or whether its concentration depended upon its initial availability to the leachate solution and its subsequent diffusive flux from the hydrating particles with time. When CKD was brought in contact with water, high concentrations of potassium, sulfate and caustic alkalies were leached. Series of batch leaching experiments were performed by reacting samples of CKD at 3:1, 6:1, and 20:1 water: solid ratios in 60ml high density polyethylene containers. Each sample was slit into two portions. One portion was acidic with 1.0ml of 1:1 HCl for cation analysis and unacidified portion was reserved for anion analysis. Samples of reacted and non-reacted CKD were analyzed by a Siemens D5000 X-ray diffractometer. Based on the test results they concluded

Table 11.6 Trace metal concentration in CKD compared to three geographical sources in USA

Element	Eastern coal ash ^a			Midwestern coal ash ^a			Western coal ash ^a			CKD ^b		
	Range	Median		Range	Median		Range	Median		Range	Median	
Antimony	—	—		—	—		—	—		1.77–27.2	6.2	
Arsenic	2–279	75		0.5–179	54		1.3–129	18		2.1–20.3	4.9	
Barium	52–2200	892		300–4300	905		300–5789	2700		11–779	103	
Beryllium	—	—		—	—		—	—		0.158–1.6	0.59	
Boron	10–580	121		10–1300	870		41.9–1040	311		—	—	
Cadmium	0.1–8.24	1.59		0.5–18	2.6		0.1–14.3	1.01		0.89–80.7	4.6	
Chromium	34–437	165		70–395	172		3.4–265	45		11.5–81.7	18.1	
Cobalt	6.22–79	40.6		19–70	35.7		4.9–69	13		—	—	
Copper	3.7–349	136		20–330	125		29–340	74.8		—	—	
Fluorine	0.4–89	8.8		3.2–300	75		0.4–320	50.1		—	—	
Lead	1.3–222	18		3–252	149		0.4–250	26.1		5.1–1490	287	
Manganese	79–430	190		194–700	410		56.7–769	194		—	—	
Mercury	0.02–4.2	0.192		0.005–0.3	0.044		0.005–2.5	0.067		0.005–14.4	0.11	
Molybdenum	0.84–51	15		7–70	43		1.4–100	12		—	—	
Nickel	6.6–258	78		26–253	121		1.8–229	38		6.9–39	15.9	
Selenium	0.36–19	8.05		0.08–19	7		0.13–19	4.1		2.5–109	11.3	
Silver	0.25–8	0.695		0.1–1.2	0.39		0.04–6	0.26		1.1–22.6	3.7	
Strontium	59–2901	801		30–2240	423		931–3855	2300		—	—	
Thallium	7–28	25		2–42	16		0.1–3.5	1.06		0.99–108	3.5	
Vanadium	110–551	269		100–570	270		11.9–340	94		6.6–204	25.9	
Zinc	16–1420	163		20–2300	600		4–854	71		—	—	

All values are in milligram.

^a from Environmental Protection Agency, US, 1988. ^b from EPA, 1993a.

that: (i) leachates contained extremely high concentrations of leachable potassium, sulfate and caustic alkalinity: (ii) leachates exhibited high concentrations of Cr and Mo. Even for the high dilution leach test (20:1, water/CKD), CR concentrations were more than 40 times EPA's maximum contaminant level (MCL) value of 0.05 mg/l; and (iii) CKD leach results at different water-solid ratios provided evidence that there was no solubility control for the concentrations of Na, Cl, Cr, Mo, Se, and in most instances, K in solution. Evidence for solubility control, however, was found for Si, Ca, SO₄, Mg, Al, Zn, Ti, Sr, and Ba concentrations. Direct evidence by XRD or microscopy was found for portlandite, ettringite, C-S-H and gypsum.

References

- AASHTO (1986) Standard method of test. mineral filler for bituminous paving mixtures. AASHTO000 Designation: M17-83, Part I Specifications, 14th Edition.
- ACI Committee 229 (1999) Controlled low-strength materials. American Concrete Institute. Farmington Hills, USA, p. 15
- Al-Harthy AS, Taha R, Al-Maamary F (2003) Effect of cement kiln dust (CKD) on mortar and concrete mixtures. *Construction and Building Materials* 17 (5): 353–360.
- Amin AM, Ebied E, El-Didamony H (1995) Activation of granulated slag with calcined cement kiln dust. *Silicates Industrial* 60 (3–4): 109–115.
- Anil M, Upadhyaya S, Gustin F, Roohanirad A, Stokes J (2005) Full-depth cold in-place recycling of asphalt pavements with self-cementing fly ash: Field and laboratory studies. *World of Coal Ash 2005*; Lexington, Kentucky, USA.
- Baghdadi ZA (1990) Utilization of kiln dust in clay stabilization. *Journal of Abdulaziz University: Engineering Science* 2: 53–163.
- Baghdadi ZA, Fatani MN, Sabban NA (1995) Soil modification by cement kiln dust. *Journal of Materials in Civil Engineering* 7 (4): 218–222.
- Batis G, Rakanta E, Sideri E, Chaniotakis E, Papageorgiou A (2002) Advantages of simultaneous use of cement kiln dust and blast furnace slag. *International Conference on Challenges of Concrete Construction*. University of Dundee, Dundee, UK.
- Bhatty MSY (1984) Use of cement kiln dust in blended cements. *World Cement* 15 (4): 126–128 and 131–134.
- Bhatty MSY (1985) Use of cement kiln dust in blended cements – alkali-aggregate reaction expansion. *World Cement* 16 (10): 386–391.
- Bhatty MSY (1986) Properties of blended cements made with Portland cement, cement kiln dust, fly ash, and slag. *Proceedings of the International Congress on the Chemistry of Cement*. Communications Theme-3, 1 (4): 118–127.
- Ciesielski SK, Collins RJ (1994) Recycling and use of waste materials and by-products in highway construction. *National Cooperative Highway Research Program Synthesis of Highway Practice* 199, Transportation Research Board, Washington, DC.
- Collins RJ, Emery JJ (1983) Kiln dust-fly ash systems for highways bases and sub-bases. *Federal Highway Administration, Report No. FHWA/RD-82/167*, Washington DC.
- Corish A, Coleman T (1995) Cement kiln dust. *Concrete* 29 (5): 40–42.
- Cross SA (1999) Experimental cold in-place recycling with hydrated lime. *Transportation Research Record No. 1684*, pp. 186–193.
- Cross SA, Fager GA (1995) Fly ash in cold recycled bituminous pavements. *Transportation Research Record No. 1486*, pp. 49–56.
- Duchesne J, Reardon EJ (1998) Determining controls on element concentrations in cement kiln dust. *Journal of Waste Management* 18 (5): 339–350.

- Dyer TD, Halliday JE, Dhir RK (1999) An investigation of the hydration chemistry of ternary blends containing cement kiln dust. *Journal of Material Science* 18 (5): 4975–4983.
- Eary LE, Rai D, Mattioli SV, Ainsworth CC (1990) Geotechnical factors controlling the mobilization of inorganic constituents from fossil fuel combustion residues: Part II. Review of the minor elements. *Journal of Environmental Quality* 19: 202.
- El-Didamony H, Ali AH, Sharara AM, Amin AM (1997) Assessment of cement dust with anhydrite as an activator for granulated slag. *Silicates Industrial* 62 (1–2): 31–35.
- EL-Sayed HA, Gabr NA, Hanafi S, Mohran MA (1991) Reutilization of by-pass kiln dust in cement manufacture. International Conference on Blended Cement in Construction, Sheffield, UK.
- Emery JJ (1981) Potential uses for kiln dusts. Proceedings ORF/CANMET Symposium on Mineral Fillers, Ontario Research Foundation and Canada Center for Mineral and Energy Technology, Toronto, Canada.
- Environmental Protection Agency, US (1988) Report to congress: wastes from the combustion of coal by utility power plants. Office of Solid Waste and Emergency Response. EPA/530-SW-88-002.
- Environmental Protection Agency, US (1993a) Report to congress on cement kiln dust. EPA-530-R-94-001, USA.
- Environmental Protection Agency (1993b) Supplemental analysis on potential risks to human health and the environment from large-volume coal combustion waste.
- Environmental Protection Agency (1995) Regulatory determination on cement kiln dust; Final Rule. Federal Register 60 (25): 7366–7376, USA.
- Fatani MN, Khan AM (1990) Improvement of dune sand asphalt mixes for pavement bases. *Journal of Abdulaziz University: Engineering Science* 2: 39–47.
- Gassman SL, Pierce CE, Schroder AJ (2001) Effects of prolonged mixing and retempering on properties of controlled low-strength material (CLSM). *ACI Materials Journal* 98 (2): 194–199.
- Gebauer J (1981) Alkali in clinker: influence on cement and concrete properties. Proceedings of the 5th International Conference on Alkali-Aggregate in. Reaction in Concrete, Capetown, South Africa: 1–9.
- Haynes BW, Kramer GW (1982) Characterization of US cement kiln dust. Bureau of Mines Information Circular 8885, US Department of the Interior, Pittsburgh, Pennsylvania.
- Heikal M, Aiad I, Helmy MI (2002) Portland cement clinker, granulated slag and by-pass cement dust composites. *Cement and Concrete Research* 32 (11): 1805–1812.
- Hoopes RJ (1988) Engineering properties of air-modified controlled low-strength materials. The Design and Application of Controlled Low-Strength Materials (Flowable Fill), ASTM STP 1331: 87–101.
- Kamon M, Nontananandh S (1991) Combining industrial wastes with lime for soil stabilization. *Journal of Geotechnical Engineering* 117 (1): 1–17.
- Katz A, Kovler K (2004) Utilization of industrial by-products for the production of controlled low-strength materials. *Journal of Waste Management* 24 (5): 501–512.
- Kjellsen KO, Detwiler RJ, Gjorv OE (1992) Pore structure of plain cement pastes hydrated at different temperatures. *Cement and Concrete Research* 22 (1): 112–120.
- Konsta-Gdoutos MS, Shah SP (2003) Hydration and properties of novel blended cements based on cement kiln dust and blast furnace slag. *Cement and Concrete Research* 33 (8): 1269–1276.
- Kraszewski L, Emery J (1981) Use of cement kiln dust as filler in asphalt mixes. Proceedings ORF/CANMET Symposium on Mineral Fillers, Ontario Research Foundation and Canada Center for Mineral and Energy Technology, Toronto, Canada.
- Malvar IJ, Cline D, Burke DF (2004) Preventing alkali-silica reaction. ASCE Conference Proceedings, pp.378–389.
- Miller GA, Azad S (2000) Influence of soil type on stabilization with cement kiln dust. *Construction and Building Materials* 14 (2): 89–97.
- Miller GA, Azad S, Dhar B (1997) The effect of kiln dust on the collapse potential of compacted shale. Testing soil mixed with waste or recycled materials, ASTM STP-1275: 232–245.
- Miller GA, Zaman M (2000) Field and laboratory evaluation of cement kiln dust as a soil stabilizer. Transportation Research Record No. 1714: 25–32.

- Morgan DS, Novoa JI, Halif AH (1984) Oil sludge solidification using cement kiln dust. *Journal of Environmental Engineering*, 110 (5): 935–948.
- Murphy DT, Emery JJ (1996) Modified cold in-place asphalt recycling. *Transportation Research Record No. 1545*: 143–150.
- Parsons T (1995) Kiln-dust-antistripping additives for asphaltic concrete mixtures. Report, Newfoundland Department of Works, Services and Transportation, Materials Engineering Division.
- Pierce CE, Tripathi H, Brown TW (2003) Cement kiln dust in controlled low-strength materials. *ACI Material Journal* 100 (6): 455–462.
- Portland Cement Association (1992) 5420 Old Orchard Road, Skokie, IL 6–77, USA.
- Ramakrishnan V (1986) Evaluation of kiln dust in concrete. *ACI Special Publication (SP-91)*: 821–840.
- Ramakrishnan V, Balaguru P (1987) Durability of concrete containing cement kiln dust. *ACI Special Publication* 100 (4): 305–322.
- Reardon EJ, Czank CA, Warren CJ, Dayal R, Johnston HM (1995) Determining controls on element concentrations in fly ash leachate. *Waste Management and Research* 13:435.
- Salem TH, Ragai MSh (2001) Electrical conductivity of granulated slag cement kiln dust-silica fume pastes at different porosities. *Cement and Concrete Research* 31 (5): 781–787.
- Shi C (2001) Studies on several factors affecting hydration and properties of lime pozzolan cements. *Journal of Materials in Civil Engineering* 13 (6): 441–445.
- Shoaib MM, Balaha MM, Abdel-Rahman AG (2000) Influence of cement kiln dust substitution on the mechanical properties of concrete. *Cement and Concrete Research* 30 (3): 371–337.
- Taha R, Al-Rawas A, Al-Harthy A, Qatan A (2002) Use of cement bypass dust as filler in asphalt concrete mixtures. *Journal of Materials in Civil Engineering* 14 (4): 338–343.
- Taylor H.FW (1997) *Cement Chemistry*. 2nd Edition, Thomas Telford, London.
- Transportation Association of Canada (1996) Moisture damage of asphalt pavements and anti-stripping additives. Report Prepared by John Emery Geotechnical Engineering Limited for Transportation Association of Canada, Ottawa.
- Verbeck GJ, Helmuth RH (1968) Structures and physical properties of cement paste. *Proceedings of the 5th International Symposium on the Chemistry of Cements*, Tokyo, pp. 1–32.
- Wang K, Shah SP, Mishulovich A (2004) Effects of curing temperature and NaOH addition on hydration and strength development of clinker-free fly ash binders. *Cement and Concrete Research* 34 (2): 299–309.
- Wood LE, White TD, Nelson TB (1988) Current practice of cold in-place recycling of asphalt pavements. *Transportation Research Record No. 1178*: 31–37.
- Zaman M, Lagurous JG, Sayah A (1992) Soil stabilization using cement kiln dust. *Proceedings of the 7th International Conference on Expansive Soils*. Dallas, TX, pp. 347–351.
- Zaman M, Zhu JH, Laguros JG (1999) Durability effects on resilient moduli of stabilized aggregate base. *Transportation Research Record No. 1687*: 29–38.

Chapter 12

Foundry Sand

Introduction

A foundry produces metal castings by pouring molten metal into a preformed mold to yield the resulting hardened cast. The metal casts include iron and steel from the ferrous family and aluminum, copper, brass and bronze from non-ferrous family. Foundry sand is high quality silica sand with uniform physical characteristics. It is a by-product of ferrous and non-ferrous metal casting industries, where sand has been used for centuries as a molding material because of its thermal conductivity. Foundries successfully recycle and reuse the sand many times in a foundry. When the sand can no longer be reused in the foundry, it is removed from the foundry and is termed as foundry sand. The physical and chemical characteristics of foundry sand depend on the type of casting process and the industry sector from which it originates. In modern foundry practice, sand is typically recycled and reused through many production cycles. For example, in United States alone, Industry estimates that approximately 100 million tons of sand is used in production and approximately 6–10 million tons is discarded annually and is available to be recycled into other products and in industry. The automotive industries and its parts are the major generators of foundry sand. Foundries purchase high quality size-specific silica sands for use in their molding and casting operations.

The raw sand is normally of a higher quality than the typical bank-run or natural sands used in fill construction sites. The sands form the outer shape of the mold cavity. These sands normally rely upon a small amount of bentonite clay to act as the binder material. Chemical binders are also used to create sand “cores”. Depending upon the geometry of the casting, sand cores are inserted into the mould cavity to form internal passages for the molten metal. Once the metal has solidified, the casting is separated from the molding and core sands in the shakeout process. In the casting process, molding sands are recycled and reused multiple times. Eventually, however, the recycled sand degrades to the point that it can no longer be reused in the casting process. At that point, the old sand is displaced from the cycle as byproduct, new sand is introduced, and the cycle begins again. A schematic of the flow of sands through a typical foundry is shown in Fig. 12.1.

Although there are other casting methods, including die-casting and permanent mould casting, sand casting is the most prevalent and preferred mold casting

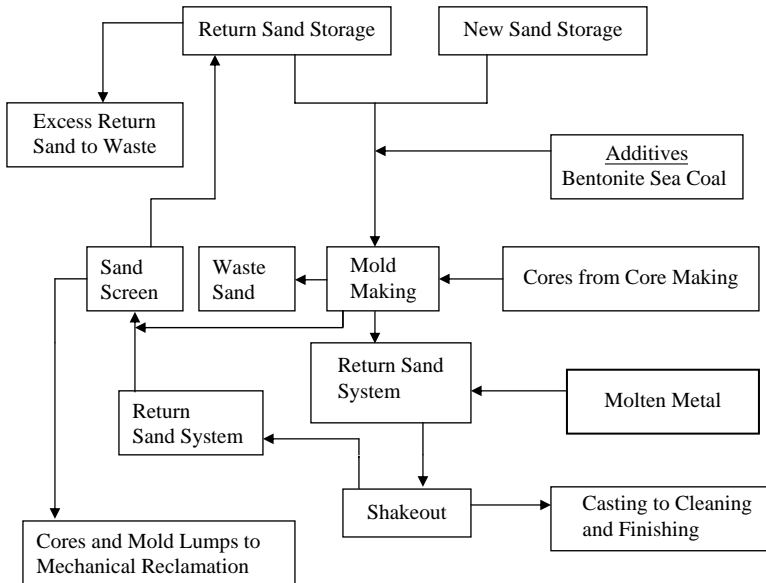


Fig. 12.1 Recycling of foundry sand

technique. Sand is used in two different ways in metal castings as a molding material, which focuses the external shape of the cast part and as cores that form internal void spaces in products such as engine blocks. Since sand grains do not naturally adhere to each other so binder is to be introduced to cause the sand to stick together and holds its shape during the introduction of molten metal into mould and cooling of casting. The sands from the brass, bronze and copper foundries are generally not reused (Foundry Industry Recycling Starts Today (FIRST), 2004).

12.1 Types of Foundry Sands

Classification of foundry sands depends upon the type of binder systems used in metal casting. Generally two types of binder systems are used and based on that foundry sands are classified as: clay-bonded systems (green sand) and chemically-bonded systems. Both types of sands are suitable for beneficial use but they have different physical and environmental characteristics.

12.1.1 Green Sand

Generally, green sand moulds are used to produce about 90% of casting volume. Green sand is composed of naturally occurring materials which are blended together; high quality silica sand (85–95%), betonies clay (4–10%) as a binder,

a carbonaceous additive (2–10%) to improve the casting surface finish and water (2–5%). Green sand is the most commonly used recycled foundry sand for beneficial reuse. It is black in color due to carbon content.

12.1.2 Chemically-Bonded Sand

Chemically bonded sands are used both in core making where high strengths are necessary to withstand the heat of molten metal, and in mold making. Most chemical binder systems consist of an organic binder that is activated by a catalyst although some systems use inorganic binders. Chemically bonded sands are generally light in color and in texture than clay bonded sands.

Foundries produce recycled foundry sand (RFS) generally in their overall production volume although there are different sand to metal ratios employed in different casting processes and products. Most foundries have two sand systems one feeding the external molding lines and the other feeding the internal core lines. After the metal is poured and the part is cooling, green sand is literally shaken off the castings, recovered and reconditioned for continual reuse. Used cores are also captured during this cooling and shake out process; these break down and are crushed and reintroduced into green sand systems to replace a portion of sand lost in the process. Depending on the projected end use, it may be important to segregate sand streams at the foundry as each stream can have different characteristics. Additionally, some sand is typically unrecoverable during shake off and finishing processes. These sands may be contaminated with metals or very large chunks of burnt cores and will need to undergo some type of segregation, crushing and screening before recycling.

12.2 Properties of Foundry Sand

12.2.1 Physical Characteristics

Foundry sand is typically sub-angular to round in shape. After being used in the foundry process, a significant portion of sand is of agglomeration form. When these are broken down, the shape of individual sand grains is apparent. Green sands are typically black, or gray, not green and chemically bonded sand is typically a medium tan or off-white color. Figures 12.2 and 12.3 show the unprocessed foundry sand and green sand respectively (FIRST, 2004). The typical physical properties of spent foundry sand from green sand systems are given in Table 12.1. The grain size distribution of spent foundry sand is uniform, with 85–95% of the material between 0.6 mm and 0.15 mm, 5–12% of foundry sand can be expected to be smaller than 0.075 mm. Waste foundries sand gradations have been found to be too fine to satisfy some specifications for fine aggregate.

Spent foundry sand has low absorption capacity and is non-plastic. The content of organic impurities (particularly from sea coal binder systems) can vary widely



Fig. 12.2 Unprocessed foundry sand (FIRST, 2004)

and can be quite high. This may preclude its use in applications where organic impurities could be important e.g., Portland cement concrete aggregate (MOEE, 1993). The specific gravity of foundry sand varies between 2.39 and 2.55. The variation in specific gravity values could be due to the variability in fines and additive contents in different samples (Javed and Lovell, 1994). In general, foundry sands are dry, with moisture contents less than 2%. A large fraction of clay lumps and friable particles are found, which are attributed to the lumps associated with the molded sand, which are easily disintegrated in the test procedure.

Its durability and soundness, chemical composition, and variability can quantify the quality of foundry sand. Various aspects of foundry sand production influence these three characteristics. Durability/soundness of foundry sand is important to ensure the long-term performance of civil engineering applications. Durability of the foundry sand depends on how the sand was used in the foundry. Successive

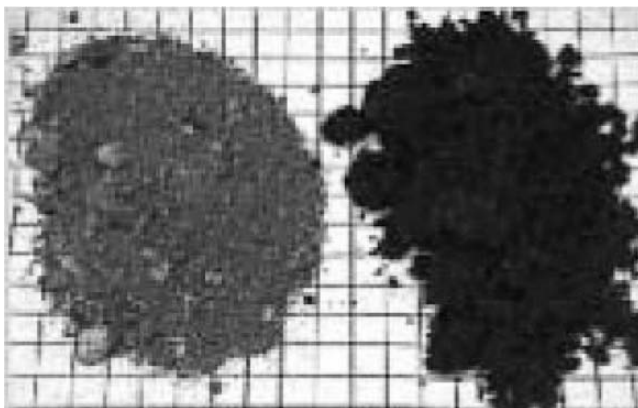


Fig. 12.3 Green sands from a gray iron industry (FIRST, 2004)

Table 12.1 Typical physical properties of spent green foundry sand

Property	Results	Test methods
Specific gravity (Javed and Lovell, 1994)	2.39–2.55	ASTM D854
Bulk relative density (kg/m ³) (Johnson, 1981)	2589	ASTMC48/ AASTHO T84
Absorption (%) (Javed and Lovell, 1994)	0.45	ASTM C128
Moisture content (%) (Javed and Lovell, 1994)	0.1–10.1	ASTM D2216
Clay lumps and friable particles (American Foundrymen's Society (AFS), 1991; Javed and Lovell, 1994)	1–44	ASTM C142/ AASTHO T112
Coefficient of permeability (cm/sec) (Javed and Lovell, 1994)	10^{-3} – 10^{-6}	AASTHO T215/ ASTM D2434
Plastic limit/plastic index (Johnson, 1981)	Non-plastic	AASTHO T90/ ASTM D4318

molding can cause the foundry sand to weaken due to temperature shock. At later stages of mould use, this can lead to the accelerated deterioration of the original sand particles. However, in civil engineering uses, the foundry sand will not normally be subjected to such severe conditions. In geotechnical applications, foundry sand often demonstrates high durability.

12.2.2 Chemical Composition

Chemical composition of the foundry sand relates directly to the metal molded at the foundry. Chemical composition of the foundry sand depends on the type of metal molded at the foundry, type of binder and combustible used. Generally, there is some variation in the chemical composition of the foundry sand and it varies from foundry to foundry. Sand produced by a single foundry, generally does not show significant variation over time. Moreover, blended sands produced by consortia of foundries often produce consistent sands. The chemical composition of the foundry sand may influence its performance. Spent foundry sand consists primarily of silica sand, coated with a thin film of burnt carbon, residual binder (bentonite, sea coal, resins) and dust. Table 12.2 lists the chemical composition of a typical sample of spent foundry sand as determined by x-ray fluorescence. Silica sand is hydrophilic and consequently attracts water to its surface. This property could possibly lead to moisture-accelerated damage and associated stripping problems in an asphalt pavement. Anti-stripping additives may be required to counteract such problems. Depending on the binder and type of metal cast, the pH of spent foundry sand can

Table 12.2 Chemical composition of foundry sand (AFS, 1991)

Constituent	Value (%)
SiO ₂	87.91
Al ₂ O ₃	4.70
Fe ₂ O ₃	0.94
CaO	0.14
MgO	0.30
SO ₃	0.09
Na ₂ O	0.19
K ₂ O	0.25
TiO ₂	0.15
Mn ₂ O ₃	0.02
SrO	0.03
LOI	5.15
TOTAL	99.87

vary between 4 and 8 (Johnson, 1981). It has been reported that some spent foundry sands can be corrosive to metals (MNR, 1992). Because of the presence of phenols in foundry sand, there is some concern that precipitation percolating through stockpiles could mobilize leachable fractions, resulting in phenol discharges into surface or ground water supplies. Foundry sand sources and stockpiles must be monitored to assess the need to establish controls for potential phenol discharges (Johnson, 1981; MOEE, 1993).

12.2.3 Mechanical Properties

Typical mechanical properties of spent foundry sand are listed in Table 12.3. Spent foundry sand has good durability characteristics as measured by low Micro-Deval abrasion (Ontario Ministry of Transportation, 1996) and magnesium sulfate soundness loss (AASHTO, 1986) tests. The Micro-Deval abrasion test is an attrition/abrasion test where a sample of the fine aggregate is placed in a stainless steel jar with water and steel bearings and rotated at 100 rpm for 15 minutes. The percent loss has been determined to correlate very well with magnesium sulfate soundness and other physical properties. Studies by Javed and Lovell (1994) revealed relatively high soundness loss, which may be due to the samples of bound sand loss and not a breakdown of individual sand particles. The angle of shearing resistance (also

Table 12.3 Typical mechanical properties of spent foundry sand

Property	Results	Test method
Micro-deval abrasion loss (%) (MNR, 1992)	< 2	—
Magnesium sulfate soundness loss (%) (MNR, 1992)	5–15 6–47	ASTM C88
Friction angle (deg)	33–40	—
California bearing ratio (%) (Javed and Lovell, 1994)	4–20	ASTM D1883

called friction angle) of foundry sand varies between 33 and 40 degrees, which is comparable to that of conventional sands (Javed and Lovell, 1994).

12.2.4 Potential Contaminants

Casting processes used in foundries involve a variety of sands, inorganic or organic binders and other additives, which generate residues in sand. The presence of these residues and the mixing of used sand with dust and other fine-grained foundry waste materials limit the reuse of foundry sand. Foundries use screening systems and magnetic separators to segregate reusable sand from other wastes and to separate particles of varying sizes. By carefully monitoring the casting process and used sand, foundries can ensure that their sand is largely free from excess contaminants and qualifies as a non-hazardous industrial by-product (FIRST, 2004). Several studies have been conducted to characterize the foundry sand and evaluate the environmental impacts of reusing the sand. These studies rely upon the tests of various constituents that leach out from sand, such as Toxicity Characteristics Leaching Procedure (TCLP), which measures constituent concentrations dissolved in an acidic solution having contact with sand.

12.2.4.1 Metal and Other Inorganic Contaminants

In general, TCLP results show that metal concentrations in foundry sand are below the regulatory thresholds, such as those specified for hazardous waste by the Resource Conservation and Recovery Act (RCRA) (Winkler and Bolshakov, 2000). Many of the leachate concentrations measured was lower than federal drinking water standards, indicating that it is generally safe to reuse these sands. Studies of foundry sand also indicated that metal contaminant concentrations are in the same order of magnitude as those in virgin sand and sandy soils. Mixed foundry by-products from non-ferrous foundries (which contain a combination of sand, dusts, and slag) have occasionally been found to have metal leachate concentrations above RCRA thresholds. For example, some foundry dusts have been found to have higher concentrations of metals relative to sand. Comparisons of the total metal content of sand to TCLP results found no direct correlation (Winkler and Bolshakov, 2000).

12.2.4.2 Organic Contaminants

The binder system is the primary source of organic contaminants in sand. Green sand casting, which generally does not involve the use of organic binders, has lower potential for leaching organic compounds than chemically bonded systems depending upon the curing and pouring process. The more reactive organic compounds commonly used in binders and resins are of special concern, because they can be transformed into new hazardous compounds under incomplete combustion conditions. Testing has not indicated that these reactive compounds are found at significant concentrations in sand (FIRST, 2004).

12.3 Management Options

12.3.1 Recycling

In foundry processes, sand from collapsed moulds or cores can be reclaimed and then reused. Some new sand and binder is then added to maintain the quality of the casting and to make up for sand lost during normal operations (Javed and Lovell, 1994). Foundry sand is produced by different foundry classes. The ferrous foundries (gray iron, ductile iron and steel) produce the most sand, and aluminum, copper, brass and bronze produce the rest. For example, there are 3,000 foundries in the United States generating 6–10 million tons of foundry sand per year. While the sand is typically used multiple times within the foundry before it becomes a byproduct, only 10% of the foundry sand was reused elsewhere outside the foundry industry in 2001. The sands from the brass, bronze and copper foundries are generally not reused. Little information is available regarding the amount of foundry sand that is used for purposes other than in-plant reclamation, but spent foundry sand has been used as a fine aggregate substitute in construction applications and as kiln feed in the manufacture of Portland cement.

12.3.2 Disposal

Most of the spent foundry sand from green sand operations is land-filled, sometimes being used as a supplemental cover.

12.3.3 Uses of Foundry Sand

12.3.3.1 In Embankments

Construction materials to be used in embankments are categorized on the basis of (i) soil type; (ii) grain size distribution, (iii) Atterbergs limits; (iv) shear strength; (v) compactability; (vi) specific gravity; (vii) permeability; and (viii) frost susceptibility. Foundry sand consists of uniform sand, with a coarse appearance. Generally, foundry sand without fines is nonplastic in nature. The plastic behavior can depend on the clay content. Foundry sand has 6–10% of clay, liquid limit (LL) greater than 20, and plastic index (PI) greater than 2. Foundry sands have good shear strength. For foundry sands without clay, friction angle varies between 30° and 36°, which is comparable to conventional sands. Its shear strength is superior to silts, clays or dirty sands, showing that foundry sand is acceptable for use as an embankment material. Moisture-density relationships have been developed for greensands with 0–5% fines, green sands with 5–12% fines, and chemically bonded sands. They show the optimal moisture content for maximum dry density for a specified level of compaction.

Foundry sand has specific gravity of 2.40–2.60. Green sands with fines less than 6% and chemically bonded sands have permeability values in the range of 6×10^{-4} – 5×10^{-3} cm/sec. The fine content of the foundry sand determines its frost susceptibility. Foundry sand without fines can have low to negligible frost susceptibility. Foundry sand has been used effectively in normal embankment construction with and without permeability and leachate control (FIRST, 2004).

12.3.3.2 In Barrier Layers Construction

Sand and bentonite are the two major components of foundry sands, and they are expected to have hydraulic properties similar to those of sand-bentonite mixtures. Sand-bentonite mixtures are being used as barrier layers throughout the US Foundry sands having liquid limit (LL) > 20 and/or a bentonite content > 6% are suitable for the construction of barrier layers (Foundry Industry Recycling Starts Today (FIRST, 2004).

12.3.3.3 In Flowable Fills

Flowable fill is engineered slurry backfill that can be used in place of conventional compacted soil backfill. Flowable fill is also known as controlled low strength material (CLSM), flowable mortar, lean-mix backfill, and controlled-density fill. Typical components of flowable fill include sand, fly ash, cement, and water. Flowable fill can be used for a variety of applications, such as trench backfill, pipe bedding, structural backfill, and underground void (abandoned pipelines, tunnels, underground storage tanks, etc.) filling. Flowable fill is an ideal application for beneficial reuse of spent foundry sands, because the sand represents a large fraction of the flowable fill mix. Research has shown that foundry sand is a viable component for flowable fill. The foundry sand does not have to meet ASTM C33 gradation specification requirements as a concrete fine aggregate to be suitable for use in flowable fill mixes. ACI 229R (1994) reports that foundry sand with up to 20% fines produced successful flowable fill mixtures. Since low-strength development is desirable in flowable fill, even foundry sand with organic binders may be suitable. Foundry sand for flowable fill can be used in a dry or moisture conditioned form (FIRST, 2004).

12.3.3.4 In Roadway Construction

Roadway structural fill applications provide an opportunity for high volume reuse of foundry sand. Foundry sand can be used in making strong durable road bases, but proper care has to be taken for mix design evaluation and the moisture content. The marketability of the sand depends on the availability of other fill material at or near the construction site. Foundry sand use is more advantageous when it is stockpiled close to the construction site FIRST, 2004 otherwise transportation costs may offset the low initial cost advantage of foundry sand.

12.3.3.5 As Soil Reinforcement

One application for foundry system sands is in earthwork construction, where large volumes can be beneficially re-used. Currently, earthwork projects consume large quantities of processed earth, which is costly and also detrimental to the environment. Thus, re-using foundry sands in earthwork projects can help solve waste disposal problem, and reduce the effect that processing earthen materials has on the environment (FIRST, 2004). Thus, if foundry sands are to be used in large-volume earthwork projects, their strength, compressibility, and material interaction should be characterized.

12.3.3.6 In Hot Mix Asphalt

Asphalt concrete is the most popular paving material used in highways and roadways. Foundry sand has been used successfully to replace a portion of the fine aggregate used in HMA. Studies have shown that foundry sand can be used to replace between 8 and 25% of the fine aggregate content. When mixes are properly designed using Superpave, Marshall, or Hveem techniques, foundry sand can be an effective sand alternative (FIRST, 2004).

Hot mix asphalt production requires that all constituent products; (i) have inherently good quality characteristics; (ii) come from consistent, reputable supply sources; (iii) meet all environmental requirements; and (iv) are economically competitive with similar materials.

Foundry sand has the potential to be a very high quality material in hot mix applications. However, it is important that the foundry sand should be cleaned of clay, dust, and other deleterious materials. Additionally, metals present in the sands should be removed either manually or magnetically. Then, it may be blended with other sands, at 8–25% replacement, to provide equal or possibly better results than normal sands.

12.3.3.7 In Portland Cement Concrete

Portland cement concrete (PCC) is a mixture of approximately 25% fine aggregate, 45% coarse aggregate, 20% cement and 10% water. Foundry sand can be used beneficially in concrete productions as fine aggregate replacement. Fine aggregate gradation as per ASTM C33 is recommended. Generally foundry sand is too fine to permit full substitution. The percentage of materials passing the No. 30, 50, and 100 sieves is too high. To meet the specification, it is necessary to remove the fines or to blend the spent foundry sand with coarser sands.

An American Foundry Society (AFS) study in Illinois investigated foundry sand as a substitute for fine aggregate in concrete (FIRST, 2004). When foundry sands without fines replaced a portion of the fine aggregate, the concrete produced had compressive strengths, tensile strengths and modulus of elasticity values comparable to mixtures composed of natural sand. On the other hand, when green foundry sands that had not been processed, replaced 33% of the fine aggregate, the resulting

concrete compressive strengths at 28 days were between 17.93 MPa and 27.58 MPa. These low strength concretes can be used in applications not requiring structural grade concrete, such as buried applications like sewer pipe or below grade concrete. The decrease in concrete compressive strength, as well as in tensile strength and modulus of elasticity, were attributed to too many fines and organic materials (clay and dust) in the foundry sand. Likewise, foundry sand has been used to make paving blocks and bricks. For these applications, foundry sand replaced 35% of the fine aggregate. If the fineness modulus was not exceeded, the concrete product was acceptable and provided compressive strength, absorption, and bulk density. It is suggested that proper testing be performed to establish the appropriate limits on foundry sand addition prior to using it in commercially produced products. As with regular concrete, trial mixtures should always be tested prior to production for any potential compatibility problems. Foundry sand is black. In some concretes, this may cause the finished concrete to have a grayish/black tint, which may not be desirable. A 15% fine aggregate replacement with foundry sand produces a minimal color change. Also, the foundry must be able to meet the quantity requirements of the pre-cast manufacturer.

12.3.3.8 In Other Engineering Applications

Other engineering applications of foundry sand are given below:

- Portland cement manufacturing,
- Mortars,
- Agricultural/soil amendments,
- Traction material on snow and ice,
- Vitrification of hazardous materials,
- Smelting,
- Rock wool manufacturing,
- Fiberglass manufacturing, and
- Landfill cover or hydraulic barriers.

Foundry Sand in Portland Cement Manufacturing

Portland cement reacts chemically with water when hydrating, causing it to set and harden. When mixed with fine and coarse aggregate, concrete is formed. There are several specifications for Portland cement, as designated by ASTM C150 and ASTM C1157. The requirements that must be met for foundry sand to be used in Portland cement production are: (i) its silica content equals or exceeds 80%; (ii) it is a low alkali material; (iii) a large quantity of sand is available; and (iv) it has uniform particle sizes.

Foundry sand may be one of the highest quality sources of silica available to the cement industry. The major chemical constituents of raw Portland cement available in foundry sand include silica and alumina and iron oxides. By using foundry sands to replace virgin sands, the quantity of mined virgin sands can be reduced. Blended

hydraulic cements are of particular interest in the beneficial use of foundry sand, since these cements are produced by blending together two or more types of fine materials. The cement manufacturer has to evaluate the foundry sand to confirm its compatibility with other raw materials.

Foundry Sand in Grouts and Mortars

Mortars primarily consist of sand, cement and other additives, and are used in masonry construction. Its primary uses are to joint and seal concrete masonry units, to strengthen masonry structures by bonding with steel reinforcing, and to provide architectural quality. The cement paste occupies the space between the sand particles and makes it workable. Sand used in masonry mortar mixes is generally specified based on grading ASTM C144. The color of the foundry sand can impart a dark shade into the mortar, so it should be deemed acceptable prior to its use in architectural projects.

Foundry Sand in Agricultural/Soil Amendments

Foundry sand can be used as an additive in topsoil and compost materials. It is ideal for topsoil manufacture because of its uniformity, consistency, and dark color. Since a high sand content is required for topsoil, it is an essential ingredient. In composting, foundry sand reduces the formation of clumps and prevents the mix from compacting. This allows to circulate through the material and to stimulate decomposition. For these applications, the presence of clay is beneficial, since it promotes the retention of nutrients.

Foundry Sand as a Traction Material on Snow and Ice

Another possible use of foundry sand is as an anti-skid material on roads covered with snow and ice. Its angular particles improve traction on highways in the winter. Likewise, its black color (ex. green sand) will hold the heat longer and will melt the ice faster. Typically, foundry sand is too fine to comply with anti-skid regulations, but when mixed with a coarser material, it does comply.

Foundry Sand for Smelting

Another potential use for foundry sand is as a raw material in zinc and copper smelting. Foundry sand can be used in place of virgin sand. Guidelines for using silica sands in zinc and copper smelting are that the sand should be relatively pure silica (minimum 99.0%), have a maximum particle size of 2 mm and a bulk phenol content of less than 2 mg/kg (ppm). The foundry should demonstrate to the smelting plant that the foundry sand meets these criteria and will produce quality zinc and copper.

Foundry Sand in Rock Wool Manufacturing

Foundry Sand is commonly used to reinforce other materials such as building material insulation, and is similar to fiberglass. Foundry sand can serve as a source of silica in the rock wool production process. They are produced by combining blast furnace slag with silica or alumina in a cupola furnace and then fiber zing the molten material. To be used in production, the foundry sand has to be pretreated and formed into briquettes.

Foundry Sand in Fiberglass Manufacturing

Foundry sand can be used in the manufacture of fiberglass. Fiberglass is produced by melting silica sand and straining it through a platinum sieve with microscopic holes, thereby forming the desired glass fibers. Manufacturers of fiberglass have specifications for silica content and particle size distribution, so to be used in this application, the foundry sand has to have the needed properties.

12.4 Properties of Controlled Low Strength-Materials (CLSM) Containing Foundry Sand

12.4.1 Plastic Properties

Naik et al. (2001) evaluated the performance and leaching characteristics of CLSM. For this purpose, they used one regular concrete sand and two types of foundry sands; clean foundry sand (FS1) and used foundry sand (FS2), and two fly ashes (F1 and F2) from two sources for making several CLSM mixtures. Fineness modulus of regular concrete sand, clean foundry sand and used foundry sand was 3.57, 2.33, and 2.32, respectively. Unit weight of regular concrete sand, clean foundry sand and used foundry sand was 1.840, 1.730, and 1.784 kg/m³, respectively.

Cement had a chemical composition of 20.3% SiO₂, 4.3% Al₂O₃, 2.6% Fe₂O₃, 63.6% CaO, 2.2% SO₃, 0.6% LOI. Fly ash F1 chemical composition was 48.4% SiO₂, 27.0% Al₂O₃, 6.6% Fe₂O₃, 8.5% CaO, 0.6% SO₃, 2.8% LOI, whereas fly ash F2 contained 6.1% SiO₂, 24.4% Al₂O₃, 21.6% Fe₂O₃, 3.26% CaO, 1.5% SO₃, 10.7% LOI.

Plastic properties investigated include; flow/spread, temperature, unit weight, settlement, bleed water, shrinkage cracks and condition of set. For each CLSM mixture, testing specimens of 150 mm × 300 mm cylinders were made to measure the plastic properties. They prepared a total of 18 different fly ash slurry mixtures. Of these, two were the control mixtures without foundry sand, and the remaining sixteen had four different replacement levels of fly ash (30, 50, 70, and 85%) with two types of foundry sand (clean and used). The replacement of fly ash by the foundry sand was on a mass basis. Based on the test results they concluded that: (i) unit weight of the slurry material varied between 1,570 and 2,115 kg/m³; (ii) mixtures made with fly ash F1 showed some bleed-water at the one hour age, and the bleed-water

decreased generally with time up to the age of 14 days. In the case of the fly ash F2 mixtures, all the mixtures except the 85% foundry sand mixtures exhibited absence of bleed-water even at the one-hour age. This may be attributed to the greater fineness of fly ash F2 and the lower amount of water used in these mixtures compared with the fly ash F1 mixtures; (iii) all the fly ash F2 mixtures became hard at the age of 5 days. Generally, because of setting and hardening of the mixtures, the depth of nail penetration decreased with age; and (iv) there was slight increase in settlement up to 3 days, thereafter, the settlement became approximately constant. In general, total settlement was found to be less than 18 mm for the F1 mixtures and 3.2 mm for the F2 mixtures with and without foundry sand up to 14 days. In order to have settlement less than or equal to 3 mm, the water content of the mixtures should be maintained so as to have a flow of 275 mm or less. All of the test specimens showed absence of shrinkage cracks up to the 14-day age.

12.4.2 Compressive Strength

Reddi et al. (1995) reported that compressive strength of stabilized foundry sands decreased with the increase in foundry sand content in the mixes. Cement and fly ash mixtures were prepared using 0, 25, 50, 75, and 100% levels of replacement of silica sand with foundry sand. The ratio of water to the cementitious binder was chosen as 1.0 in the case of Portland cement and 0.35 in the case of fly ash. The samples were founded in PVC pipes, 2.85 cm in dia and 5.72 cm long. The mixtures of sands and the binders were poured into these pipes and then vibrated on a vibrating table to minimize air pockets. For each of the replacement levels, compressive strengths were obtained after 3, 7, 14, 28, and 56 days in order to evaluate the difference due to curing time. The clay bonded foundry sand reduced the strength of the stabilized mixes more than the resin- bonded foundry sands. A similar observation was made in context of fly ash stabilization. The drastic reduction in strength with an increase in clay-bonded foundry sand replacement was apparent in the cases of both fly ash and cement. Cement-stabilized mixes acquired their strength considerably slower than fly ash stabilized mixes. After 7 days of curing the cement-stabilized RBS reached only 30% of peak strength whereas its fly ash counterpart achieved 80% of its peak strength.

Tikalsky et al. (2000) concluded that CLSM mixtures containing only Portland cements had compressive strength that exceeded the upper limit of acceptable compressive strength range i.e., 700 Kpa. This was found for all the four sands i.e., three from casting facilities and one from a commercial aggregate producer. Type 1 and 2 cements and class F fly ash was used. Text mixtures were prepared in accordance with mixing recommendations developed by ACI committee 229 (1994). Three specimens from each CLSM mixture were tested at 3, 7, 14 and 28 days. All the mixtures containing fly ash maintained a compressive strength below upper limit and one CLSM mixture did not reach the lower limit. The data supports the concept

that by-product foundry sand can be successfully used in CLSM. The foundry sand assists in keeping the strength from exceeding the upper compressive strength limit.

Naik et al. (2001) determined the compressive strength of CLSM mixtures. CLSM mixtures were made with one regular concrete sand and two types of foundry sands; clean foundry sand (FS1) and used foundry sand (FS2), and two fly ashes (F1 and F2) from two sources for making several CLSM mixtures. 150 mm \times 300 mm cylinders were used to measure the compressive strength of flowable slurry mixtures. Based on the investigation, they reported that: (i) compressive strength of all slurry mixtures made with and without foundry sand ranged between 0.17 and 0.4 MPa at the age of 7 days; (ii) compressive strength results of slurry mixtures made with founder sands and F1 fly ash increased with age. At 28-days, the compressive strength of slurry mixtures made with fly ash F1 ranged from 0.27 to 0.55 MPa, and from 0.3 to 0.6 to MPa with fly ash F2; and (iii) generally compressive strength increased with an increasing amount of foundry sand up to certain limit, and then decreased. The strength data revealed that excavatable flowable slurry with up to 85% fly ash replacement with clear and used foundry sand can be manufactured without significantly affecting the strength of the reference mixtures.

They further reported that in order to obtain a relatively high strength at the age of 28 days and beyond for mixtures tested, fly ash replacement with foundry sand should be maintained between 30 and 50%. The amounts of foundry sand corresponding to the maximum compressive strength values were 50% for clean and clear sand for fly ash F1 mixture, 30% for used sand for fly ash F1 mixture, 70% for clean sand for fly ash F2 mixture and 30% for used sand for fly ash F2 mixture at the age of 91 days. The maximum compressive strength for both fly ash mixtures were obtained at 30% fly ash replacement with the used foundry in spite of variation in the mixture design and source of fly ash.

12.4.3 Permeability

Naik et al. (2001) investigated the permeability of CLSM mixtures. CLSM mixtures were made with one regular concrete sand and two types of foundry sands; clean foundry sand (FS1) and used foundry sand (FS2), and two fly ashes (F1 and F2) from two sources for making several CLSM mixtures. 100 mm \times 125 mm cylinders were used for measuring the permeability. All specimen preparations were done in accordance with ASTM C192. The permeability of mixtures was evaluated in accordance with ASTM D 5084. They reported that the permeability for fly ash F1 slurry mixtures varied from 4×10^{-6} cm/s to 74×10^{-6} cm/s, and it was between 5×10^{-6} cm/s and 69×10^{-6} cm/s for fly ash F2 slurry mixture. The minimum permeability value was observed at 30% fly ash replacement level with foundry sand. The permeability for both the fly ash mixtures was not significantly affected by increasing foundry sand content up to 70% fly ash replacement at the age of 30 days. However, it increased abruptly when the replacement levels for the fly ashes with foundry sand were increased to 80% from 70%. The increase may be attributed to the increase in

voids produced by the increase in the amount of foundry sand and decrease in the amount of finer particles of fly ash in the mixture. There was no significant effect of foundry sands (clean or used) on the permeability values of mixtures tested. So the permeability of test mixtures was not significantly influenced by inclusion of foundry sand up to 70% fly ash replacement while, at 85% replacement of foundry sand a sharp increase in permeability was observed.

12.4.4 Leachate Analysis

Ham and Boyle (1981) evaluated the leaching characteristics of used foundry sand. They concluded that: (i) leaching potential was greatly influenced by the process temperature; and (ii) constituents of the leachates depended upon the type of foundry sand, which reflected the differences in the binder material present in the waste material.

Fero et al. (1986) determined the concentration of organic compounds in ground water leached from an iron foundry landfill. Test samples derived from all monitoring wells showed all measured organics were below their respective detection limits. Engroff et al. (1989) evaluated the leachate characteristics of foundry sands derived from nine common core binder systems using the toxicity characteristic leaching procedure (TCLP) test method. The test data showed the presence of a wide range of organic compounds, but their concentrations were low. Ham et al. (1993) summarized the results of the leachate investigations carried out at the University of Wisconsin-Madison.

Traeger (1987) investigated the leaching potential of foundry by-products material using both the TCLP and American Foundrymen's Society (AFS) leachate test techniques. For comparison, leach tests were also conducted on native soils from Wisconsin. In general, constituents leached from foundry sands were lower than the native soils. The concentrations of substances leached from native soil were either comparable to or higher than that of foundry sand. The results further indicated that foundry sand was non-hazardous per Resource Conservation and Recovery Act (RCRA) criteria.

Ham et al. (1990) compared the leachate quality in foundry landfills with samples taken from above the zone of saturation. Their results indicated that leachates from the unsaturated zone had relatively low concentrations of contaminants with respect to drinking water standards for all contaminants except, iron, manganese, and fluoride. A leach test conducted on auger waste samples was more accurate in predicting field leachate compositions than the leach test on a raw composite waste.

Tikalsky et al. (1998) reported that the swelling potential and instability of bentonite-stabilized mixes render the leachable quality unpredictable. The data on total phenolics obtained from leachability experiments were normalized to account for difference in volumes of leachates collected for each stabilized mix. In the experiments, cement and fly ash mixtures were prepared using 0, 25, 50, 70, and 100% levels of silica sand by foundry sand. This normalization was important for

unequal amounts of foundry sand used with each of four binders. To provide a basis for comparison among the four binders, treatment efficiencies were calculated representing the percentage of total phenolics immobilized due to stabilization process. The treatment efficiencies (TE) were used in the existing literature and involve normalizing the contaminants leached from stabilized product with respect to contaminant leached from untreated waste. The results showed that fly ash is more effective than cement in stabilizing the phenolics. Faster setting times were consistently observed for all mixtures of fly ash compared with corresponding mixtures of cement. Treatment efficiencies increased as the percentage replacement of foundry sands increased. In other words, the total phenolics leached from each stabilized gram of foundry sands decreased as higher proportions of clean sand were replaced by foundry sand. So the swelling potential and instability of bentonite-stabilized mixes render the leachate quality unpredictable.

Naik et al. (2001) conducted tests on various samples to determine the leachability of CLSM mixtures. For this purpose, the ASTM (ASTM D 3987), leach method was selected because it simulates mobility (leaching) of substances in CLSM that can occur through permeation of water under field conditions. In this method, an extract of each by-product materials and CLSM mixture was obtained. Each test sample, weighing about 70 grams, was prepared and added to a two-liter container having a watertight closure. A volume of test water equal to 20 times the weight of the waste sample (1400-mL) was added to the container. The container was continuously agitated for 18 hours at about 20°C. The sample was then allowed to settle for five minutes and the bulk of the aqueous phase was separated from the solid by filtration through a coarse filter paper. The liquid was filtered through a 0.45 mm filter. The resulting extract was analyzed for various constituents using Wisconsin Department of Natural Resources (WDNR) Approach. They concluded that these materials contained very little organics, leachate derived from each material was analyzed for inorganic constituents in accordance with WDNR requirements. The clean foundry sand met both the WDNR preventive action limits (PAL) and the enforcement standards (ES) of Ground Water Quality Standards (GWQS). The used foundry sand met all parameters of the ES, but it exceeded the PAL for lead and chromium. However, used foundry sand met all requirements, except for Fe, for public welfare-related GWQS.

Both foundry sands met all the requirements for the DWS. The fly ash sample (F2), except for arsenic, met all parameters of the ES. It exceeded the PAL for arsenic, chromium, lead, and selenium. With the exception of selenium, this fly ash also met all parameters of the DWS. The fly ash F2 met all parameters of the GWQS related to public welfare except for iron. The leachate data for various CLSM mixtures revealed that the reference mixture containing only fly ash F1 met all the requirements of the ES and most of the PAL of the GWQS. It also met all the parameters of the DWS. With fly ash F1, addition of clean foundry sand caused a slight reduction in selenium concentration of the CLSM mixture containing up to 70% clean foundry sand. Since the clean foundry sand showed absence of selenium, the detected selenium contribution in the CLSM is due to contributions from both fly ash and cement. All the CLSM mixtures met the ES and PAL parameters for

public welfare-related GWQS. The CLSM mixture containing fly ash F2 without foundry sand met all requirements of the ES of the GWQS. However, selenium concentration was above the PAL for the mixtures containing up to 70% foundry sand. Except for selenium, these mixtures satisfied the drinking water standards (DWS). Fly ash F2 and the cement contributed to the amounts of selenium in the CLSM mixtures. Generally, addition of both clean and used foundry sand caused reduction in the selenium concentration of the CLSM mixture. Therefore, addition of foundry sand appears to provide favorable environmental performance for the CLSM mixtures. American Engineering Testing (1992) reported leachate concentrations of coal combustion product materials in the same range as that observed in Portland cement and virgin soil.

12.5 Properties of Concrete Containing Foundry Sand

Utilization of foundry sand in concrete and concrete related products like bricks, blocks and paving stones has been reported by Khatib and Ellis (2001), Naik et al. (2003), Naik et al. (2004) and Siddique et al. (2007).

12.5.1 Compressive Strength

Khatib and Ellis (2001) investigated the properties of concrete containing foundry sand as a partial replacement of fine aggregate. Three types of sand used in foundries were considered, the white fine sand without the addition of clay and coal, the foundry sand before casting (blended), and the foundry sand after casting (spent). The standard sand (Class M) was partially replaced by (0, 25, 50, 75, and 100%) these types of sand. Thirteen concrete mixtures were made to conduct this study. Compressive strength of concrete mixture was determined up to the age of 90 days. Based on the test results they concluded that: (i) with the increase in the replacement level of standard sand with foundry sand, the strength of concrete decreased; (ii) the concrete containing white sand showed somewhat similar strength to those containing spent sand at all replacement levels; (iii) presence of high percentage of blended sand in the concrete mixture caused a reduction in strength as compared with concrete incorporating white sand or spent sand; and (iv) increase in strength was not observed at low replacement levels (less than 50%).

Naik et al. (2003) studied the utilization of Class F fly ash, coal-combustion bottom ash, and used foundry sand for manufacture of bricks, blocks, and paving stones. They made total of 18 mixture proportions with and without the by-products were developed. Replacement rates, by mass, for sand with either bottom ash or used foundry sand were 25 and 35%. Replacement rates, by mass, for Portland cement with fly ash were 25 and 35% for bricks and blocks, and 15 and 25% for paving stones. Nominal dimensions (width, length, and height) of bricks and paving stones were 90 mm × 190 mm × 60 mm. Dry-cast paving stones were produced using brick

moulds. The blocks were three web hollow blocks with nominal dimensions of 190 mm \times 400 mm \times 190 mm. Tests for compressive strength were performed according to ASTM C140 for each brick or paving stone mixture at 5, 28, 56, 91, and 288 days. Three compression specimens were tested for each block mixture at 7, 14, 28, and 91 days.

They reported that bricks with partial replacement of cement with fly ash (FA) showed slightly higher strength than the control while considerable reduction in strength was observed when a part of sand was substituted with bottom ash (BA). This was attributed to the lower strength of porous BA compared to sand. Substitution of part of the sand with used foundry sand (UFS) in brick mixtures caused a small reduction in strength. All mixtures, except for those with partial substitution of sand with BA, met the compressive strength requirement of ASTM C 55 for Grade N (24 MPa) bricks from about three to 18 days of age. Mixtures containing BA met the strength requirement for Grade S (17 MPa) bricks from the age of about 18 days. According to ASTM C 55, Grade N bricks are 'for use where high strength and resistance to moisture penetration and severe frost action are desired'. Grade S bricks are "for general use where moderate strength and resistance to frost action and moisture penetration are required.

In case of paving stones, they concluded that all the mixtures showed considerable strength gain with time. Paving stones with FA showed higher strength than the control mixture throughout the test. Partial replacement of sand with BA caused a large reduction in compressive strength. Unlike bricks and blocks, partial replacement of sand with UFS, as in paving stones caused considerable reduction in strength. Overall, none of the paving stones met the compressive strength requirement of ASTM C 936 for solid concrete paving units (55 MPa).

In case of blocks, they reported that all the mixtures except the one exceeded minimum compressive strength requirement of ASTM C 90 (13 MPa). The exception mixture blocks exceeded the requirement from about 17 days of age. Blocks containing FA showed a higher rate of strength gain than the control. Overall, partial replacement of cement with FA, sand with BA and sand with UFS resulted in considerable increase, considerable decrease and slight decrease respectively in the compressive strength of blocks. Since they meet the strength requirement of ASTM, they could still be used for construction of interior walls in cold regions. The results of this investigation showed that: (i) partial replacement of cement with FA consistently improved the strength and durability of concrete masonry units; and (ii) up to 25% of sand in blocks could be replaced with either BA or UFS in cold regions; and up to 35% of sand in bricks and blocks could be replaced with either BA or UFS for use where frost action is not a concern.

Naik et al. (2004) reported the compressive strength of pre-cast molded concrete products such as wet-cast concrete bricks and paving stones made with high volumes of fly ash, bottom ash and used foundry sand. ASTM class fly ash was used as a partial replacement (0, 25, and 35%) of Portland cement. Bottom ash combined with used foundry sand replaced 0, 50, and 70% of natural sand. Three wet-cast brick mixtures and three wet-cast paving stone mixtures were proportioned in which the proportions of cementitious material, fine aggregates and coarse aggregates

were approx. 1:3.4:1.4 for bricks and 1:2.9:1.2 for paving stones. Cylinders of size 100 mm \times 200 mm were cast as specimens for testing compressive strength. The wet-cast bricks were having size of 90 \times 190 \times 60 mm (width, length and height) while the dimensions for paving stones were 100 \times 190 \times 60 mm. Tests for compressive strength were done as per ASTM C 140. Based on the test results, they concluded that at the age of 3 days, the average compressive strength of wet-cast bricks made with control mixture was 32% higher than the compressive strength requirement of ASTM C 55 for Grade N bricks (min. 24 MPa). Overall the test showed that concrete with cylinder strength as low as 14 MPa can be used in producing wet-cast bricks that meet the ASTM requirements for Grade N bricks. Wet-cast bricks made from other mix proportions than control met the compressive strength requirement of ASTM C 55 for Grade S bricks at approx. 7 and 22 days, respectively. The cylinder strength and the brick strength are linearly related up to approximately 25 MPa cylinder strength and 40 MPa brick strength. Within this range brick strengths were almost twice of the equivalent cylinder strengths. After this level the brick strength did not increase as rapidly as equivalent cylinder strength.

While in case of paving stone, they reported that compressive strength development of cylinders followed the similar trend as in brick concrete mixtures. The compressive strength of paving stones continued to increase with age but fell short of the ASTM C 936 requirements (min. 55 MPa). For producing paving stones that meet the ASTM strength requirements, the increase in amounts of cementitious materials may be needed. For early age strength gain, the use of lower w/cm, HRWRA, and accelerating admixtures should be used for commercial production purposes. The paving-stone strength was higher than the corresponding cylinder strength, which was approx. 1.5 times the equivalent cylinder strength.

Siddique et al. (2007) investigated the effect on spent foundry sand as partial replacement of fine aggregate on the compressive strength of concrete. For this purpose, they made four concrete mixtures. First were control mix (without spent foundry sand) and the other three mixtures contained spent foundry sand. The proportions of fine aggregate replaced were 10, 20, and 30%. Mixture proportions are given in Table 12.4. The control mixture with out spent foundry sand was

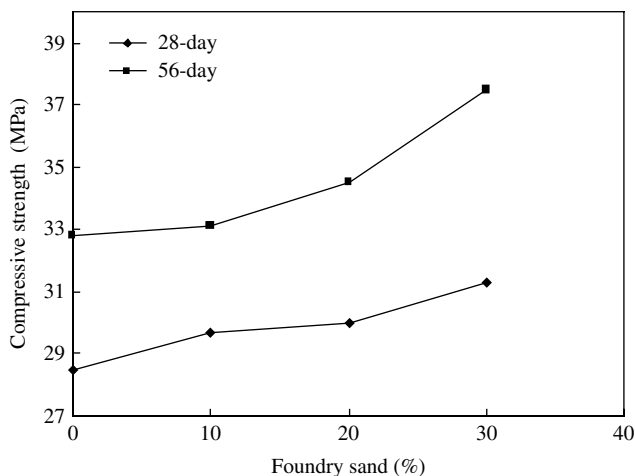
Table 12.4 Mixture proportions of concrete mixtures (Siddique et al., 2007)

Mixture No.	M-1	M-2	M-3	M-4
Cement (kg/m ³)	372	372	372	372
Foundry sand (percent)	0	10	20	30
Foundry sand (kg/m ³)	0	54	108	162
Water (kg/m ³)	186	186	186	186
W/C	0.5	0.5	0.5	0.5
Sand SSD (kg/m ³ +)	539	485	431	377
Coarse aggregate (10mm) (kg/m ³)	410	410	410	410
Coarse aggregate (20mm) (kg/m ³)	819	819	819	819
Superplasticizer (l/m ³)	4.5	5.9	5.9	5.9
Slump (mm)	90	85	85	80

Table 12.5 Strength properties results of concrete made with foundry sand (Siddique et al., 2007)

Mix type	Foundry sand content (%)	Compressive strength (MPa)		Split tensile strength (MPa)		Modulus of elasticity (GPa)	
		28 days	56 days	28 days	56 days	28 days	56 days
M-1	0	28.5	32.8	2.5	3.0	25.10	27.19
M-2	10	29.7	33.1	2.8	3.2	26.75	29.11
M-3	20	30.0	34.5	2.9	3.3	29.11	31.12
M-4	30	31.3	37.5	3.0	3.6	31.11	33.20

proportioned to have a 28-day cube compressive strength of 28.5 MPa. Compressive strength tests were carried out at the age of 28 and 56 days. The tests results are given in Table 12.5 and shown in Fig. 12.4. Based on the test results, it was concluded that compressive strength of concrete mixes with 10, 20, and 30% fine aggregate replacement with foundry sand fly ash, was higher than the control mix (M-1) at all ages. Figure 12.4 shows that compressive strength increased marginally with the increase in foundry sand. At the age of 28 days, compressive strength increased by 4.2, 5.2, and 9.8% when compared to ordinary mix without foundry sand, whereas increase was 1.0, 5.18, and 14.3% at the age of 56 days. Compressive strength at 56 days was 15, 12, 15, and 20% higher than the 28 days compressive strength for mixes containing 0, 10, 20, and 30% foundry sand. Increase in the compressive strength of concrete mixes incorporating spent foundry sand indicated that foundry sand could be successfully used in making concrete as partial replacement of fine aggregate.

**Fig. 12.4** Compressive strength versus spent foundry sand content (Siddique et al., 2007)

12.5.2 Splitting Tensile Strength and Modulus of Elasticity

Siddique et al. (2007) determined the effect of spent foundry sand as partial replacement of fine aggregate on the splitting tensile strength and modulus of elasticity of concrete. The proportions of fine aggregate replaced were 10, 20, and 30%. Tests were carried out at the age of 28 and 56 days.

The splitting tensile strengths of concrete mixes are given in Table 12.5 and shown in Fig. 12.5. From Table 12.5 and Fig. 12.5, it is evident that splitting tensile strength of all mixes continued to increase with the age. Figure 12.5 shows that splitting tensile strength increased with the increase in foundry sand. At the age of 28 days, splitting tensile strength increased by 12, 14, and 20% when compared to ordinary mix without foundry sand, whereas increase was 6.0, 10, and 20% at the age of 56 days. Splitting tensile strength at 56 days was 20, 14, 14, and 20% higher than the 28 days strength for mixes containing 0, 10, 20, and 30% foundry sand.

Modulus of elasticity test results of foundry sand concretes are given in Table 12.5 and shown in Fig. 12.6. Figure 12.6 shows the variation of modulus of elasticity with foundry sand content. From the test results, it can be seen that the modulus of elasticity of foundry sand fly ash concretes with 0, 10, 20, and 30% fine aggregate (sand) replacement was higher than the control mix (M-1) at all ages. It is also evident that modulus of elasticity of all mixes continued to increase with age.

12.5.3 Freezing and Thawing Resistance

Naik et al. (2003) conducted an investigation to determine the effect of freezing and thawing (F&T) on bricks and paving stones. Tests were performed according to

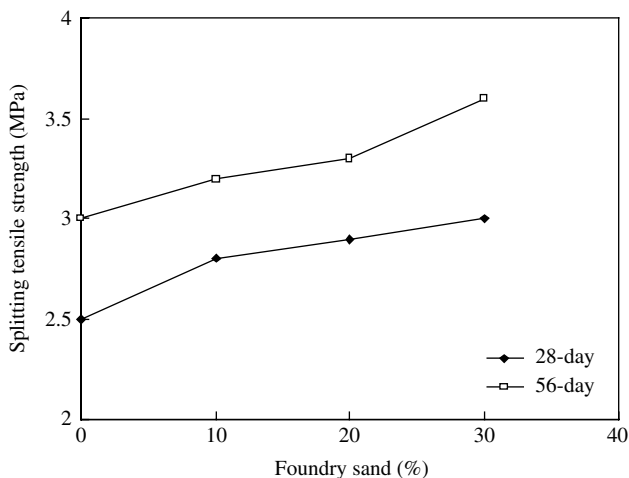


Fig. 12.5 Splitting tensile strength versus spent foundry sand (Siddique et al., 2007)

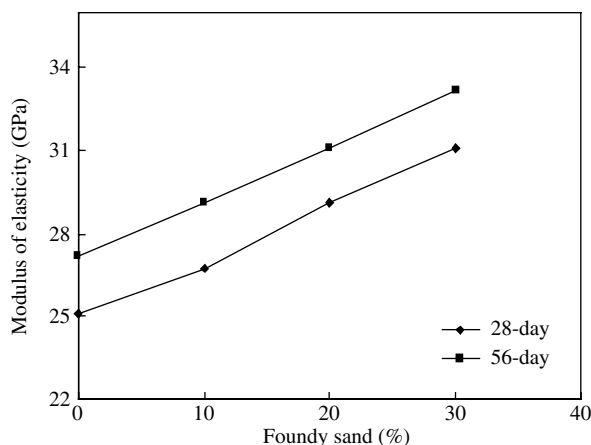


Fig. 12.6 Modulus of elasticity versus spent foundry sand (Siddique et al., 2007)

ASTM C 1262. Freezing and thawing tests on bricks and paving stones were started at the age of 74 days and for blocks, it was 154 days. In this work, a weight loss of approximately 0.2% based on the estimated initial oven-dry weight of bricks was taken as a critical value, after which the bricks in general showed rapid or sudden increase in weight loss leading to rupture. Based on the test results, they reported that bricks mixtures reached the critical value (0.2%) of weight loss at about 92, 150, 30, 18, 40, and 12 cycles of F&T, respectively. On the basis of these numbers, bricks with FA, showed about 1.6 times longer F&T life than the control. When BA was used as a partial substitution for sand in bricks, a sharp drop in F&T life was observed. Partial substitution of sand with UFS also caused a sharp drop in F&T life of bricks, in spite of its nearly negligible effect on strength, density, and absorption. This might have something to do with the nature of the UFS. Weight loss of roughly 0.2% based on estimated initial oven-dry weight of the paving stones was taken as a critical value.

In case of paving stone, all mixtures of paving stones reached the critical value of weight loss (0.2%) at about 190, 200, 150, 120, 95, and 45 cycles of F&T, respectively. Overall, the F&T life of the paving stones was about 2.3 times that of the bricks. This was attributed to the lower water-cementitious materials ratio (W/Cm) of paving stones, which resulted in higher values of compressive strength compared to bricks. Partial replacement of cement with FA, sand with BA, and sand with UFS resulted in slight increase, some reduction, and large reduction in F&T life of paving stones. The very large decrease in F&T life of paving stones containing UFS could be attributed to the plastic and slippery nature of moist UFS.

For blocks a weight loss of roughly 1.1% based on estimated initial oven-dry weight of specimens was taken as a critical value. Blocks of all mixtures reached the critical value of weight loss at about 250, 350 (estimated by extrapolation), 200, 10, 170, and 30 cycles, respectively. Partial replacement of cement with FA caused considerable increase in the F&T life of blocks. Blocks

with 25% replacement of sand with either BA or UFS showed a large reduction in F&T life compared to FA. Blocks with 35% replacement of sand with either BA or UFS showed a very sharp reduction in F&T life compared with FA. Although the strength of blocks containing UFS was considerably higher than that of blocks containing BA, the F&T lives of the two groups of blocks were about the same. This could again be attributed to the plastic and slippery nature of moist UFS.

Naik et al. (2004) conducted tests for freezing and thawing resistance of bricks and paving stones in accordance with ASTM C 140. The test procedure involved water saturated brick and paving stone specimens, each with a 10mm layer of one bearing surface immersed in H₂O subjected to cycles of freezing to -17°C and thawing to 24°C and the mass of each specimen. The resistance to cycles of freezing and thawing decreased with increasing amounts of the three byproduct materials (fly ash, bottom ash, and used foundry sand in case of bricks. In case of paving stones the wet-cast paving stones made with control mix showed a significant amount of mass loss due to surface spalling between 60 and 150 cycles of freezing and thawing.

12.5.4 Drying Shrinkage

Effect of foundry sand on the shrinkage of concrete has been reported by Khatib and Ellis (2001) and Naik et al. (2003).

Khatib and Ellis (2001) examined the effect of foundry sand as a partial replacement of fine aggregate on the drying shrinkage of concrete. Three types of sand used in foundries were considered, the white fine sand without the addition of clay and coal, the foundry sand before casting (blended), and the foundry sand after casting (spent). The standard sand (Class M) was partially replaced by (0, 25, 50, 75, and 100%) these types of sand. Thirteen concrete mixtures were employed to conduct this study. Concrete shrinkage up to 60 days was determined. Based on the test results they concluded that: (i) length change of concrete increased as the replacement level of standard sand with the three types of sand increased; (ii) drying shrinkage values were higher in concrete containing spent sand and lower in concrete containing white sand; and (iii) expansion was generally lower in concrete containing white sand as compared with the other two types (blended and spent) at a low sand replacement level of 25%; and, different trend was obtained at higher levels.

Naik et al. (2003) measured the drying shrinkage of bricks and blocks in accordance with ASTM C 426. The test started at the age of 300 days for bricks and at 270 days for blocks. The drying shrinkage values for all specimens (mixture proportions) of bricks were about 0.023, 0.041, 0.031, 0.034, 0.041, and 0.036%, respectively. Lower drying shrinkage of bricks implies less likelihood of development of drying shrinkage cracks in masonry brick walls. Bricks containing FA, BA, and UFS shrunk more than the control bricks upon drying. Overall, bricks with UFS shrunk more than those with BA. However, all the bricks met the maximum drying shrinkage requirement of ASTM C 55 (0.065%). While the drying shrinkage values for all

blocks (mixture proportions) were 0.023, 0.020, 0.031, 0.028, 0.038, and 0.040%, respectively, blocks containing either BA or UFS shrunk more than the control upon drying. As in the case of bricks, blocks with UFS shrunk more than those with BA. However, all the blocks met the maximum drying shrinkage requirement of ASTM C 90 (0.065%).

References

- AASHTO (1986) Standard method of test for soundness of aggregate by use of sodium sulfate or magnesium sulfate. AASHTO Designation: T104, Part II Tests, 14th Edition.
- ACI 229R (1994) Controlled low-strength materials. *Concrete International* 55–64.
- American Engineering Testing (1992) Coal ash utilization: A summary of current practices and economic, environmental, and energy impacts. Report Prepared for Northern States Power Co., Minneapolis, USA.
- American Foundrymen's Society (1991) Alternative utilization of foundry waste sand. Final Report (Phase I) Prepared by American Foundrymen's Society Inc. for Illinois Department of Commerce and Community Affairs, Des Plaines, Illinois.
- Engroff EC, Fero EL, Ham RK, Boyle WC (1989) Laboratory leachings of organic compounds in ferrous foundry process waste. Final Report to American Foundrymen's Society; Des Plaines, Ill, USA.
- Fero RL, Ham RK, Boyle WC (1986) An investigation of ground water contamination by organic compounds leached from iron foundry solid wastes. Final Report to American Foundrymen's Society, Des Plaines, Ill, USA.
- Foundry Industry Recycling Starts Today (FIRST) (2004) Foundry sand facts for civil engineers. Federal Highway Administration Environmental Protection Agency Washington, DC, USA.
- Ham RK, Boyle WC (1981) Leachability of foundry process solid wastes. *Journal of Environmental Division, ASCE* 107 (1): 155–170.
- Ham RK, Boyle WC, Blaha FJ (1990) Comparison of leachate quality in foundry waste landfills to leach test abstracts. *Journal of Hazardous and Industrial Solid Waste Testing and Disposal* 6: 29–44.
- Ham RK, Boyle WC, Engroff EC, Fero RL (1993) Organic compounds in ferrous foundry process waste leachates. *Journal of Environmental Engineering ASCE* 119 (1): 34–55.
- Javed S, Lovell CW (1994) Use of foundry sand in highway construction. Joint Highway Report No. C-36-50N, Department of Civil Engineering, Purdue University, Indiana, USA.
- Johnson CK (1981) Phenols in Foundry Waste Sand Modern Casting. American Foundrymen's Society.
- Khatib JM, Ellis DJ (2001) Mechanical properties of concrete containing foundry sand. *ACI Special Publication SP 200*: 733–748.
- MNR (1992) Mineral aggregate conservation – reuse and recycling. Report Prepared by John Emery Geotechnical Engineering Limited for Aggregate and Petroleum Resources Section, Ontario Ministry of Natural Resources, Queen's Printer for Ontario.
- MOEE (1993) Spent foundry sand – alternative uses study. Report Prepared by John Emery Geotechnical Engineering Limited for Ontario Ministry of the Environment and Energy and the Canadian Foundry Association, Queen's Printer for Ontario.
- Naik TR, Kraus RN, Chun YM, Ramme WB, Siddique R (2004). Precast concrete products using industrial by-products. *ACI Materials Journal* 101 (3): 199–206.
- Naik TR, Kraus RN, Chun YM, Ramme WB, Singh SS (2003) Properties of field manufactured cast-concrete products utilizing recycled materials. *Journals of Materials in Civil Engineering* 15 (4): 400–407.
- Naik TR, Singh SS, Ramme WB (2001) Performance and leaching assessment of flowable slurry. *Journals of Environmental Engineering* 127 (4): 359–368.

- Ontario Ministry of Transportation (1996) Resistance of fine aggregate to degradation by abrasion in the microduval apparatus. LS-619, Ontario Ministry of Transportation, Ontario, Canada.
- Reddi NL, Rieck PG, Schwab AP, Chou ST, Fan LT (1995) Stabilization of phenolics in foundry sand using cementitious materials. *Journals of Hazardous Materials* 45: 89–106.
- Siddique R, Gupta R, Kaur I (2007) Effect of spent foundry sand as partial replacement of fine aggregate on the properties of concrete. The 22nd International Conference on Solid Waste Technology and Management, Widener University, Philadelphia, USA. 1386–1396.
- Tikalsky PJ, Gaffney M, Regan R (2000) Properties of controlled low-strength material containing foundry sand. *ACI Material Journal* 97 (6): 698–702.
- Tikalsky PJ, Smith E, Regan R (1998) Proportioning spent casting sand in controlled low-strength materials. *ACI Material Journal* 95 (6): 740–746.
- Traeger PA (1987) Evaluation of the constructive use of foundry wastes in highway construction. MS Thesis, The University of Wisconsin-Madison, Madison, Wisconsin.
- Winkler ES, Bolshakov AA (2000) Characterization of foundry sand waste. Chelsea Center for Recycling and Economic Development, University of Massachusetts at Lowell, USA.
- Ham RK, Boyle WC, Engroff EC, Fero RL (1993) Organic compounds in ferrous foundry process waste leachates. *Journal of Environmental Engineering ASCE* 119 (1): 34–55.

Index

- a selective catalytic reactor (SCR), 269
- abrasion resistance, 118, 134, 227, 228
- absorption, 385
- absorption characteristics, 366
- absorption coefficient, 277
- absorption values, 266
- accelerated steel corrosion, 33
- acid resistance, 217
- activated fly ash, 195, 225
- activator, 11, 357
- activator concentration, 53
- activators, 256
- activity index, 14, 156, 290
- additive, 314, 392
- AEA requirement, 240
- aggregate, 277
- agricultural by-product, 235
- agricultural soil, 312
- air bubbles, 187
- air content, 126, 139, 153, 188
- air entrained concretes, 186
- air entrained fly ash, 216
- air entraining agent, 187
- air entrainment, 213
- air permeability, 22, 117
- air pollution control devices (APCD), 269
- air-cooled blast furnace slag, 1
- air-cured concrete, 61
- air-permeability, 255
- air-void system, 31
- alite, 286
- alkali activation, 53
- alkali silica reaction, 30, 165, 170, 223, 339, 368
- alkali silica reactive aggregates, 369
- alkali silica reactivity, 222
- alkali-silica reactivity, 30
- alkali-activated cementitious materials, 25
- alkali-aggregate reaction, 221, 223
- alkali-silicate gel, 368
- alkalies, 352
- alkalis, 30
- alumina, 41, 352
- amber, 153
- amorphous, 266
- amorphous material, 309
- amorphous silica, 236
- angularity, 329
- anhydride, 182
- anhydrite, 182
- anthracite, 178
- anti-stripping additives, 385
- applications of plastic, 96
- ash composition, 268
- asphalt binder, 124, 353
- asphalt concrete, 390
- asphalt concrete aggregate, 152
- asphalt dust, 371
- asphalt mixes, 171
- asphalt pavement, 352
- asphalt paving mixtures, 373
- asphalt surface pavements, 171
- asphaltic concrete, 121
- attrition/abrasion, 386
- autoclave expansion, 340
- automobile shredded residue, 97
- available alkali content, 221
- backscattered electron images, 269
- bag filter (BF), 269
- ball mill, 3
- baryte, 250
- bending strength, 71, 133
- bentonite, 389
- bentonite clay, 381
- betonies clay, 382
- binder hydration, 363
- binder systems, 382

- bituminous coal, 178
- blast furnace slag, 69, 209
- blast furnace slag cement, 354
- bleed-water, 393
- bleeding, 4, 5, 140, 371
- bleeding capacity, 4
- bleeding rate, 4
- blended cement, 26, 279, 365
- blended cements, 58, 252, 313, 338
- blocks, 398, 399
- boiler slag, 177
- bond strength, 250
- borosilicate glasses, 149
- bottom ash, 177
- bricks, 398
- brittle failure, 128
- bulk density, 3, 43, 104, 326
- bulk relative density, 385

- C-S-H gel, 43, 52
- calcination, 267
- calcination temperature, 364
- calcium, 309
- calcium aluminate hydrate, 355
- calcium hydro-silicate, 355
- calcium hydroxide, 50
- california Bearing Ratio, 172
- capillary movement, 204
- carbide waste, 279
- carbon content, 181, 308
- carbonate aggregates, 29
- carbonation, 35, 62, 223, 224, 258
- carbonation behavior, 224
- cement factor, 191
- cement hydration reactions, 198
- cement kiln dust, 351
- cement matrix, 72
- cement paste, 130, 190
- cement replacement, 352
- cement-based materials, 313
- cementitious efficiency, 12
- cenospheres, 179
- ceramic, 313
- change in length, 319
- characterization of MSWI fly, 268
- chemical activators, 250
- chemical attack, 214
- chemical composition, 308
- chemical constituents, 180
- chemical reactivity, 364
- chemically bonded sands, 383
- chloride, 95
- chloride binding capacity, 22, 77
- chloride concentrations, 22
- chloride diffusion, 77
- chloride diffusivity, 78
- chloride ingress, 78
- chloride ion resistance, 346
- chloride penetrability, 80
- chloride penetration, 77, 78, 294
- chloride penetration depths, 78
- chloride penetration resistance, 24
- chloride permeability, 210, 256
- chloride-ion penetration resistance, 253
- chloride-ion resistance, 344
- chopped tire, 122
- clean foundry sand, 393, 395
- CLSM, 394
- coal bottom ash, 371
- coal fly ash, 177
- coal-combustion bottom ash, 398
- coarse waste glass, 154, 160
- cocalcined kaolin–sludge mixtures, 48
- coefficient of permeability, 148, 385
- cold in-place recycling, 374
- color, 43
- combustor ash, 266
- compacting factor, 239
- compaction factor, 155
- compositional effect, 278
- compressive strength, 11, 12, 18, 28, 45, 65, 66, 68, 69, 108, 110, 128–130, 155, 158, 159, 191–193, 195–197, 200, 202, 228, 243, 244, 246–249, 285, 286, 293, 294, 315, 316, 337, 354, 355, 358, 371, 394, 395, 398, 399, 401
- concrete, 57, 353
- concrete expansion, 167
- concrete mixture, 398
- condensed silica fume, 213
- conductivity, 44, 367
- consistency, 6, 57, 242, 284
- construction material, 313
- contaminants, 396
- controlled Low Strength Materials, 313
- controlled low-strength material, 140
- controlled low-strength materials, 305, 307, 370
- corrosion, 31
- corrosion performance, 257
- corrosion resistance, 33, 87, 225, 347, 354
- corrosivity, 33
- covering depth, 226
- creep, 21, 87, 205
- crumb rubber, 123, 137, 140
- crumb tire rubber, 133

- crumbed fibers, 131
- crushed glass, 148, 172
- crystalline matter, 181
- crystalline phases, 271
- crystobalite, 324
- curing conditions, 68, 192, 197, 210
- curing period, 335
- curing regime, 197
- curing temperature, 52, 359

- degree of hydration, 45, 281, 365
- degree of pozzolanic reaction, 47
- degree of saturation, 202
- dehydroxylation, 55
- dehydroxylyzation, 41
- deicing salt resistance, 30
- deicing scaling resistance, 262
- density, 127, 240, 326, 346, 371
- depolymerization, 102
- depth of wear, 228
- depth-sensing indentation (DSI), 74
- deterioration, 32
- differential thermal analysis (DTA), 44
- diffusion, 77
- diffusion coefficients, 23
- diffusion rates, 78
- dilatancy, 56
- discrete reinforcement, 97
- dry process kilns, 351
- drying shrinkage, 21, 206, 252, 318, 404
- dust collection equipment, 177
- dying-wetting cycles, 296
- dynamic modulus of elasticity, 30, 136

- earthwork construction, 390
- efficiency factor, 13
- efficiency factor (k), 50
- efflorescence, 2
- electrical conductivity, 366
- electrical resistivity, 340
- electrolytic resistance, 225
- elemental analysis, 309
- elevated temperature, 361
- elevated temperatures, 67, 202
- emerald, 153
- energy absorption capacity, 135
- energy recovery recycling, 102
- environmental scanning electron microscope (ESEM), 48
- ettringite, 11, 69, 365
- evolution of heat, 188
- expanded, 95
- expansion, 82, 166, 262
- expansion rates, 168

- expansion tests, 30
- expansive gels, 30

- failure mode, 135
- fatigue, 136
- feedstock recycling, 102
- fertilizer, 312
- fiberglass, 393
- filler, 278
- fine aggregate, 193, 388, 398, 400
- fine waste glass, 154, 160
- fineness, 179, 306, 329
- fineness modulus, 391
- flexural strength, 17, 19, 132, 133, 163, 164, 192, 193, 245, 317, 318, 362
- flexural strengths, 53
- flint, 153
- flow, 283, 394
- flow table, 155
- flow value, 284
- flowability, 370
- flowable fill, 140, 389
- flowable slurry, 353
- flue gases, 177
- fluidity, 56, 154, 366
- fluidity of mortar, 6
- fluorogypsum, 69
- fly ash, 9, 100, 170, 209, 252, 358
- fly ash concrete, 184, 206
- fly ash fineness, 195, 211
- fly ashes, 395
- foundry sand, 381
- fracture mechanics, 170
- free chloride diffusion coefficient, 23
- freeze-thaw, 213
- freeze-thaw performance, 31
- freezing and thawing, 137, 368, 402
- freezing and thawing resistance, 187, 259, 319
- freezing-thawing resistance, 213
- freezing/thawing, 374
- fuel ash–metakaolin (PC–PFA–MK, 65

- gap-graded mixtures, 240
- gas permeability, 295
- GE Brightness, 43
- geotechnical applications, 278
- GGBS, 5, 189
- glass, 147
- glass particle size, 165
- glass powder, 157, 170
- gradation, 352
- grain size distribution, 383
- granular Base, 152
- granular base, 172

- granular process, 124
- granulate shape, 97
- green sand, 382
- green sands, 383
- green soda glass, 153
- ground granulated blast furnace slag, 1
- ground granulated blast-furnace slag, 11
- ground plastic, 108
- ground rubber, 123, 124
- ground tire rubber, 121

- hardened cement paste, 25
- hardened concrete, 21
- hardness, 326
- hazardous waste, 387
- hazardous wastes, 312
- heat evolution, 51, 190
- heat of hydration, 1, 364
- heavy particles, 100
- heavyweight concrete, 249
- high alkali, 357
- high calcium fly ashes, 186
- high density, 95
- high-performance concrete, 14
- high-performance concretes, 67
- high-reactivity metakaolin (HRM), 76
- high-strength concrete, 14, 139, 240
- high-volumes of class C fly ash, 196
- hospital waste incineration bottom ash, 267
- hot weather, 17
- hydrated phases, 52
- hydration, 237
- hydration characteristics, 276
- hydration characteristics of C_3S , 274
- hydration period, 44
- hydration product, 8
- hydration reaction, 44
- hydration temperature, 361
- hydrochloric acid pretreatment, 238
- hydrogarnet, 44
- hydroxide ion concentrations, 81

- ilmenite, 250
- image characteristics, 9
- impact resistance, 116, 136
- incinerated municipal bottom ash, 266, 269
- incineration, 100
- incineration process, 265
- incinerator bottom ash, 279
- incinerator fly ash slag, 285
- initial and final setting times, 242
- initial curing conditions, 25
- initial surface absorption, 62
- initial surface absorption test, 366

- interfacial transition zone, 11, 71
- interfacial zone, 237
- intrinsic permeability, 22
- inverted slump cone time, 106
- iron, 352

- kaolin clay, 41
- kaolinite, 41

- land-filled, 388
- landfilling, 310
- leachability, 397
- leachate, 100, 142, 313, 376
- leachate range, 376
- leaching, 309
- leaching behavior, 297
- leaching characteristics, 396
- leaching concentrations, 297
- leaching tests, 277
- lead glasses, 149
- lightweight aggregates, 330
- lignite, 178
- lime, 352
- lime content, 333
- lime-stabilized mixture, 331
- liming material, 312
- long term strength, 191
- low calcium class F fly ashes, 189
- low density, 95
- low energy cements, 276
- low-calcium fly ash, 65

- magma, 324
- magnesium, 309
- magnesium oxychloride, 129
- magnesium sulfate resistance, 83
- magnesium sulfate solution, 28
- manganese, 309
- mass loss, 290
- material, 172
- material recovery facilities, 148
- maximum dry density, 331
- mechanical properties, 14, 245, 249, 386
- mechanical recycling, 101
- melting point, 97
- mercury intrusion porosimeter (MIP), 60
- metakaolin, 15, 19, 41, 46, 50
- micro-hardness, 71
- micro-structure, 190
- microfiller, 64
- microscopic analysis, 272
- microsilica, 33
- microstructure, 7, 9, 52, 57, 237, 338
- microwave curing, 50

- mineral admixtures, 66, 223
- mineral aggregate, 374
- mineral filler, 353
- mineralogical analysis, 181, 309
- mineralogy of milled and sintered , 271
- mitigation techniques, 369
- modulus of elasticity, 113, 133, 164, 201, 202, 245, 371, 402
- moisture content, 180, 385
- moisture-density, 388
- molten iron, 1
- molten slag, 1
- mortar, 160
- mortar bar expansion, 167
- mortar bars, 168
- municipal bottom ash, 271
- municipal solid waste, 265
- municipal solid waste ash, 265
- municipal solid waste incineration, 278
- municipal solid wastes, 96
- municipal waste stream, 98

- natural pozzolan, 42
- natural pozzolans, 178
- natural sands , 381
- non-air-entrained concretes, 213
- non-ferrous foundries, 387
- non-plastic, 383
- normal consistency, 242, 336

- open circuit potential test, 257
- optimum moisture content, 331
- organic compounds, 396
- oxygen permeability, 210

- particle grading, 248
- particle shape, 179
- particle size, 236, 266, 352
- particle size distribution, 3, 4, 15, 148
- paving stones, 398, 399
- periclase, 182
- permeability, 1, 116, 208, 209, 389, 395
- personal computer (PC) scrap, 101
- petroleum effluent treatment plant, 48
- phenolics, 397
- phenols, 386
- phosphation, 267
- phosphorus, 309
- physical properties, 97, 266, 306
- plastic aggregates, 104, 108
- plastic bottle waste, 111
- plastic limit/plastic index, 383
- plastic viscosity, 184
- plastic waste management, 98

- plastic wastes, 93, 98
- plasticity, 332
- plasticized, 95
- plastics, 93
- plastics recycling, 100
- poisson's ratio, 202
- polarization resistance, 32
- polarization resistance techniques, 225
- polyethylene, 95
- polyethylene terephthalate, 104
- polymer, 160
- polymer concrete, 277
- polymer milling process, 104
- polypropylene, 95
- polypropylene fibers, 105
- polystyrene, 95
- polyvinyl, 95
- pore size distribution, 58, 59, 61, 288
- pore sizes, 7
- pore solutions, 23, 81
- pore structure, 215
- porosity, 58, 61, 202, 237, 243, 344
- porosity , 153
- porosity distribution, 290
- porous aggregates, 368
- portlandite (CH), 75
- post-consumer glass, 151
- post-consumer plastic, 101
- potassium, 309
- powder, 327
- pozzolan activator, 354
- pozzolanic action, 238
- pozzolanic activity, 236–238, 308, 316
- pozzolanic activity index, 280
- pozzolanic materials, 357
- pozzolanic reaction, 8, 11, 51, 241
- pozzolanic reactions, 47, 198, 214
- pozzolanic reactivity, 179, 190
- pozzolans, 178
- pre-cast, 399
- pressure-treated lumber, 96
- printed circuit board (PCB) scrap, 101
- pulse velocity, 319
- pulverized slag, 274
- pumice fragments, 326
- PVC floorings, 101
- pyrolysis, 104

- quarry waste, 371

- rapid chloride permeability, 253
- reactive aggregates, 167
- reactivity of aggregate, 222
- rebar, 32, 257

- reclaimed asphalt base, 375
- recycled asphalt pavement, 152
- recycled plastic, 97, 106
- recycled rubber, 139
- reflective properties, 150
- refuse-derived fuel (DRF) process, 265
- relative dynamic modulus, 319
- replacement ratios, 200
- residual compressive strength, 342
- resistance, 82
- rheology, 184
- rice-husk, 235
- rice-husk ash, 235
- road pavement, 277
- rubber aggregate, 143
- rubber concrete, 129
- rubber shreds, 135
- rubber-chips, 128
- rubberized mixtures, 125
- sandcrete, 237
- scaling resistance, 261
- scrap rubber, 125
- scrap tires, 121
- setting time, 6
- setting times, 56, 57, 241, 283, 285, 337, 366
- settlement, 394
- shredded, 122
- shrinkage, 22, 87, 135, 290
- shrinkage cracks, 394
- shrinkage of concrete, 206
- silica, 352
- silica content, 236
- silica fume, 24, 50, 65, 156
- silica sand, 385
- sintering process, 292
- size, 97
- slit tire, 122
- slump, 5, 56, 106, 108, 124, 125, 139, 154, 239, 240
- slump test, 314
- smelting, 392
- soda ash, 149
- soda lime glass, 166
- soda-lime, 149
- sodium, 309
- softening point, 97
- soil amendment, 312
- soil stabilization, 278, 352, 353
- soil stabilizers, 372
- soil supplement, 310
- solidification of wastes, 353
- sorptivity, 61, 204, 366
- spalling, 31, 139, 342
- specific gravity, 3, 43, 97, 127, 148, 153, 179, 236, 274, 306, 352, 385
- specific surface, 3, 352
- specific surface area, 70, 240, 250
- spent foundry sand, 383
- spherical glassy particles, 177
- spherical particles, 269
- spherical shape, 179
- splitting tensile strength, 18, 112, 132, 133, 193, 245, 248, 316
- spongy aggregate, 179
- spray dryer adsorber (SDA), 269
- stabilization processes, 267
- stabilized bases and sub-bases, 277
- steady-state diffusivity, 77
- steel beads, 138
- steel reinforcement, 32
- stratlingite, 44
- stratlingite (C_2ASH_8), 52
- strength, 64, 315
- strength activity index, 306, 340
- strength development, 190
- stress-strain relationship, 67
- stress-deformation curves, 66
- stress-strength ratios, 205
- structural fill, 389
- sub-bituminous, 178
- sulfate attack, 1, 25, 82, 84, 215
- sulfate content, 357
- sulfate expansion, 292
- sulfate resistance, 25, 27, 85, 86, 215, 259
- sulfate resisting cement, 218
- sulfuric acid, 216
- sulfuric acid resistance, 217
- surface area, 3, 6, 15, 59, 268
- swelling potential, 396
- temperature, 113
- temperature rise, 189
- tensile strength, 70, 162, 163, 361
- tephra, 323
- terephthalate, 95
- ternary blends, 24
- test, 386
- thaumasite, 86, 218
- thaumasite-type of sulfate attack (TSA), 85
- the mass-burning process, 265
- thermal activation, 43
- thermal and temperature-dependent mechanical properties, 115
- thermal conductivity, 150, 207, 381
- thermal reprocessing, 102

- thermal volatilization, 272
- thermo-mechanical recycling, 101
- thermogravimetric analysis, 75
- thermogravimetric analysis (TG), 44
- thermogravimetric analysis (TGA), 365
- thermoplastic polyolefin, 101
- threshold value, 59
- time of setting, 186
- tire rubber, 125
- tire-added latex concrete, 133
- tire-rubber ash, 138
- tobermorite, 44, 289, 342
- total chloride diffusion coefficient, 23
- total combined ash stream, 265
- total pore volume, 341
- toughness, 135, 362
- toxicity characteristics leaching procedure, 142
- trace element, 376

- ultra-fine GGBS, 14
- ultra-fine slag, 56
- unburned carbon, 184
- unconfined compressive strength, 141, 286, 333, 374
- unit weight, 127, 143, 153, 250, 306, 393
- unplasticised, 95
- used foundry sand, 395, 398

- vebe time, 154
- vibro-mill, 3
- virgin polypropylene, 97
- virgin resins, 103
- virgin sand, 392
- vittrification, 277

- volcanic ash, 323
- volcanic glass shards, 324
- volcanic pumice, 327

- waste glass, 147, 151, 158
- waste glasses, 153
- waste treatment, 352
- waste wood ash, 308
- water absorption, 62, 243, 314
- water absorption capacity, 293
- water absorption characteristics, 63
- water content, 394
- water demand, 58, 184
- water permeability, 24, 210
- water requirement, 306
- water-binder ratio, 22
- water-cementitious material ratio, 76
- water-to-binder ratio, 355
- water-to-binder ratio) (W/B, 27
- water-to-cementitious material ratio, 244
- water-to-solid (w/s) ratios, 366
- water/binder ratio, 5, 56, 341
- water/cementitious ratio, 28
- weight loss, 347, 403
- wet-cast concrete, 399
- wet-process kilns, 351
- window glasses, 149
- wood ash, 303
- workability, 1, 56, 57, 125, 184, 239, 314

- X-ray diffraction (XRD), 365

- yield value, 184